Aus dem Institut für Biochemie
Universität Freiburg (Schweiz)

The influence of light on the circadian clock of mice and men

INAUGURAL-DISSERTATION

zur Erlangung der Würde eines *Doctor rerum naturalium*
der Mathematisch-Naturwissenschaftlichen Fakultät
der Universität Freiburg in der Schweiz

vorgelegt von
Corinne JUD
aus
Schänis (SG)

Dissertations-Nr. 1625
UniPrint Fribourg
2009

Von der Mathematisch-Naturwissenschaftlichen Fakultät der Universität Freiburg in der Schweiz angenommen, auf Antrag von:

- Prof. Dr. Urs E. Albrecht, Abteilung Medizin, Einheit für Biochemie, Universität Freiburg, Schweiz
- Prof. Dr. Christian Cajochen, Abteilung Chronobiologie, Universitäre Psychiatrische Kliniken (PUK) Basel, Schweiz
- Prof. Dr. Zhihong Yang, Abteilung Medizin, Einheit für Physiologie, Universität Freiburg, Schweiz
- Jurypräsident: Prof. Dr. Eric M. Rouiller, Abteilung Medizin, Einheit für Physiologie, Universität Freiburg, Schweiz

Freiburg in der Schweiz, den 12. Februar 2009

Der Dissertationsleiter:

Prof. Dr. Urs Albrecht

Der Dekan:

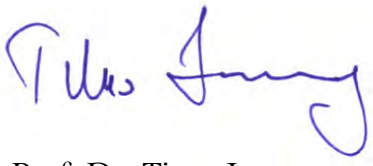

Prof. Dr. Titus Jenny

Hiermit versichere ich, die vorliegende Doktorarbeit selbständig und ohne Benutzung anderer als der im Literaturverzeichnis angegebenen Quellen und Hilfsmittel verfasst zu haben. Wörtlich oder inhaltlich übernommene Textpassagen sind als solche gekennzeichnet.

Freiburg in der Schweiz, den 18. Dezember 2008

Corinne Jud

Men love to wonder, and that is the seed of science.
Ralph Waldo Emerson

Acknowledgements

Now that I'm reaching the end of my PhD, I start to be sentimental about the time I spent in the laboratory of **Urs Albrecht**. It was a great time – a good mixture between excellent but also tough moments. During my PhD, I had the opportunity to meet many different people. Some of them were teaching me while others were trained by me.
All these memories would never have become real if my supervisor Urs Albrecht had not given me the chance to do my PhD in his lab. Hence I thank him for this opportunity and for his support. He was always ready to help me whatever the problem was. I'm grateful for everything I learned in his lab!
However, I would never have been able to finish this PhD without the friendship and the help of the other lab members. From my first day in the lab until now, **Antoinette Hayoz** and **Gabriele Hampp** kept on motivating me whenever it was necessary. I also would like to express my gratitude to **Isabelle Schmutz** and **Sonja Langmesser** for their advice and help. Moreover, I thank **Stéphanie Baeriswyl**, **Geneviève Bulgarelli**, **Jürgen Ripperger** and **Frédéric Stadler** for everything they did for me. Special thanks to **Céline Feillet** for critically reading my thesis draft and leaving me our shared computer during the writing period of my thesis. I will not forget all the challenging questions my diploma and master students were asking me. My knowledge increased by teaching **April Bezdek**, **Dirk-Jan Saaltink** and **Sylvie Chappuis** and I would like to thank them for this.

Thanks to all the people of the Unit of Biochemistry for their friendly integration and support, especially **Ila**, **Fred**, **VJ**, and **René**. I will never forget all the cheerful moments we spent together. Moreover, I express my gratitude to **Cathy**, **Jojo**, **Jean-Marc**, **Olga**, **Doudou**, **Cyrill**, **Ashot**, **Maria** and all the others who helped me in organizing all those additional things that are needed to accomplish a PhD.

I sincerely acknowledge **Christian Cajochen** and **Zhihong Yang** for accepting co-reference of my thesis, for their critical comments and for their fruitful collaborations.

Most of all I thank my **family** and my **friends** who are like sisters and brothers for me - all of them gave me the strength to reach the end of this thesis.

Table of contents

1 Summary 1

1.1 English 2

1.2 German 3

2 General Introduction 5

2.1 Historical background 6

2.2 Evolutionary relevance of having a clock 7

2.3 Definition of the term "biological clock" 8

2.4 The circadian clock in *Drosophila melanogaster* 11

2.5 The circadian clock in zebrafish (*Danio rerio*) 13

2.5.1 How to measure circadian rhythms in zebrafish 14

2.5.2 Molecular machinery of the circadian clock in zebrafish 15

2.5.3 Light signalling to the zebrafish clock 17

2.5.4 Concluding remarks 17

2.6 The circadian clock in mammals 18

2.6.1 The circadian pacemaker resides in the brain 18

2.6.2 Anatomy of the SCN and its neutrotransmitter content 19

2.6.3 Input pathways to the mammalian circadian clock 19

2.6.3.1 Photic input via the retinohypothalamic tract 19

2.6.3.2 Non-photic input via the geniculohypothalamic tract 21

2.6.3.3 Non-photic input via the serotonergic tract from the raphe nuclei 21

2.6.4 Output pathways from the mammalian circadian clock 22

2.6.4.1 Neuronal output 22

2.6.4.2 Humoral output 24

2.6.4.3 Peripheral oscillators and their hierarchical organization 26

2.6.5 Molecular machinery of the circadian clock in mammals 28

2.6.5.1 How everything started: chronology of clock gene discoveries 28

2.6.5.2 The core loop 31

2.6.5.3 The secondary loops 32

2.6.5.4 Timing of the loops via CK1 33

2.6.5.5 Multiple regulations of the molecular clock machinery 35

2.6.6 Association of clock genes and photic entrainment of the SCN 40

2.6.6.1 Light pulses can provoke phase shifts in behaviour 41

2.6.6.2 Phase shifts: the light-triggered signalling cascade 42

2.6.6.3 Phase shifts: perturbation of the transcription/translation feedback loop 45

2.7 Effects of the circadian clock on the human body 46

2.7.1 Melatonin and human chronobiology 50

2.7.2 Assessing circadian rhythms in humans 53

2.7.3 Entrainment of the human pacemaker to light 54

3 Aim of the thesis 57

4 Results 61

4.1 Development of circadian rhythms in murine pups 62

Publication: Jud & Albrecht, 2006

4.2 Light induced *Cry1* coincides with high amplitude phase resetting in *Rev-Erbα/Per1* double mutant mice 69

Manuscript: Jud & Albrecht

4.2.1 Additional data 94

4.2.1.1 Light induction of *Dec1, Per2,* and *cFos* 94

4.2.1.2 Might misregulated *Dexras1* cause the Type 0 PRC? 95

4.2.1.3 Other attempts to explain the Type 0 PRC 98

4.3 The effect of blue light on the human circadian system in the evening 100

Publication: Cajochen *et al.*, 2006

4.3.1 Additional data 106

4.4 The effect of blue light on the human circadian system in the morning 107

Submitted Manuscript: Jud *et al.*

4.4.1 Additional data 120

5 Discussion and Perspectives 123

5.1 Development of circadian rhythms 124

5.1.1 Discussion 124

5.1.2 Perspectives 126

5.2 Analysis of *Rev-Erbα/Per1* double mutant mice 126

5.2.1 Discussion 126

5.2.2 Perspectives 128

5.3 The influence of light on clock gene expression in humans 129

6 Materials and Methods 133

6.1 Materials 134

6.1.1 Chemicals and solvents 134

6.1.2 Kits and ready for use solutions 136

6.1.3 Radioactive chemicals 137

6.1.4 Ladders and enzymes 137

6.1.5 Cell lines 137

6.1.6 Cell culture products 138

6.1.7 Oligonucleotides 138

6.1.8 Antibodies 139

6.1.9 Bacteria and vectors used for cloning 139

6.1.10 Plasmids 140

6.1.11 Mouse strains 140
6.1.12 Computer programs and appliances 142
6.1.13 Consumer material 142
6.1.14 Appliances 143
6.2 Methods 145
6.2.1 Animals 145
6.2.1.1 Animal guidelines 145
6.2.1.2 Mouse breeding 145
6.2.1.3 Mouse activity recording 145
Publication Jud *et al.,* 2005**:** "A guideline for analyzing circadian wheel-running behaviour in rodents under different lighting conditions."
6.2.1.4 Genotyping of mice 162
6.2.2 Molecular biology applications 167
6.2.2.1 Solutions 167
6.2.2.2 Isolation of RNA 168
6.2.2.3 Spectrophotometric determination of nucleic acid concentration 168
6.2.2.4 Agarose gel electrophoresis 170
6.2.2.5 RT-PCR and cloning 171
6.2.2.6 Isolation and purification of recombinant DNA 174
6.2.2.7 Ligation in low-melting agarose 175
6.2.2.8 Ligation using oligonucleotide linkers 176
6.2.3 Processing of human buccal cells 178
6.2.3.1 SOP – Sampling human oral mucosa 178
6.2.3.2 SOP – Processing of human oral mucosa 179
6.2.3.3 Sampling human oral mucosa using the cytobrush 183
6.2.3.4 Processing of human oral mucosa sampled with the cytobrush 184
6.2.4 *In Situ* Hybridization 185
6.2.4.1 Solutions 185
6.2.4.2 Tissue Fixation, Embedding and Sectioning 186
6.2.4.3 Linearization of plasmids 187
6.2.4.4 *In vitro* Transcription 188
6.2.4.5 Dewaxing, Postfixation and Hybridization of Sections 189
6.2.4.6 Posthybridization Washes and Autoradiography 190
6.2.4.7 Emulsion Coating 191
6.2.4.8 Development and Hoechst Staining 191
6.2.4.9 Viewing and Photography 192
6.2.5 Cell culture 193
6.2.5.1 Solutions 193
6.2.5.2 Maintenance of cells 195
6.2.5.3 Counting of cells using a Neubauer hemacytometer 196
6.2.5.4 Preparation of mouse embryonic fibroblasts (MEFs) 197
6.2.5.5 Preparation of mouse dermal fibroblasts (MDFs) 199
6.2.5.6 Synchronization of cells via dexamethasone shock 201
6.2.5.7 Transfection 202
6.2.5.8 RNA isolation from cells 204

6.2.6 Protein methods 206
6.2.6.1 Cell fractionation for cytoplasmic and nuclear protein extracts 206
6.2.6.2 Determination of protein concentrations according to Bradford 207
6.2.6.3 Western blot 208
6.2.6.4 Corticosterone RIA 213
6.2.6.5 Immuncytochemistry 215

7 Abbreviations 217

8 References 221

9 *Curriculum Vitae* 241

10 Appendix 245

Preface to the appendix 246

Appendix I 247
Publication Zhang *et al.,* 2008**:** "Fragile X-related proteins regulate mammalian circadian behavioural rhythms."

Appendix II 264
Publication Cavadini *et al.,* 2007**:** "TNF-alpha suppresses the expression of clock genes by interfering with E-box-mediated transcription."

Appendix III 280
Publication Viswambharan *et al.,* 2007**:** "Mutation of the circadian clock gene Per2 alters vascular endothelial function."

Appendix IV 290
Corticosterone levels before and after stress in wild-type and *Per2*^{Brdm1} mice

Chapter 1

Summary

Abstract

The continuous light-dark cycles caused by the rotation of the Earth around its own axis facilitated the evolution of circadian clocks, which have a huge impact on our daily life. Deregulation of the internal clock can lead to sleeping disorders, depression and various other health problems. Thus it is important to understand the mechanisms which allow our clock to tick properly. Since circadian clocks are quite conserved between species, model organisms such as mice can be used for basic research on the molecular clock mechanisms and its impact on physiology. In spite of this, not all results obtained in mice can be extrapolated directly to humans.

The first aim of this thesis was to investigate whether the emergence of circadian rhythms in murine pups is dependent on a functional maternal clock. To elucidate this, wild-type males were crossed with arrhythmic *Per1*^{Brdm1}*Per2*^{Brdm1} or *Per2*^{Brdm1}*Cry1*$^{-/-}$ double mutant females in constant darkness. The heterozygous offspring developed normal circadian rhythms although they were reared without any external Zeitgeber. However, their clocks were less synchronized to each other as compared to wild-type controls. These findings indicate that development of circadian rhythms does not depend on a functional circadian clock in maternal tissue.

In a second part of this thesis, the role of *Per1* and *Rev-Erbα* in the circadian machinery was studied. Strikingly, mice mutant for these two genes showed high amplitude resetting in response to a brief light pulse at the end of their subjective night phase, which is rare in mammals. *cFos* was induced to comparable levels as those in wild-type mice, which indicates that the photosensitivity is normal in these animals. Surprisingly, the otherwise not light responsive gene *Cry1* was also induced under these conditions. Hence, *Rev-Erbα* and *Per1* may be part of a mechanism that evolved to prevent drastic phase shifts in mammals.

The last part of this thesis aimed at developing a non-invasive method to measure and quantify human circadian clock gene expression in oral mucosa. It was demonstrated that *PER2* was expressed in a circadian fashion in human buccal samples and that it was influenced by blue light in an age dependent manner. Hence this method may help shed more light onto the molecular mechanisms underlying disorders associated with the internal clock.

Taken together, this work provides new insights into the distinct role of clock genes and the influence of light on the circadian oscillator. Increasing knowledge in these domains will allow the development of better therapeutic approaches for human circadian disorders.

Zusammenfassung

Zirkadiane Uhren entstanden als Anpassung an den immer wiederkehrenden Wechsel von Tag und Nacht, welcher durch die Rotation der Erde um ihre eigene Achse hervorgerufen wird. Störungen der inneren Uhr können zu Depressionen, Schlafstörungen und vielen anderen Gesundheitsproblemen führen. Deswegen ist es wichtig zu verstehen, was es unserer inneren Uhr erlaubt, richtig zu funktionieren. Da zirkadiane Uhrwerke zwischen den Arten ziemlich konserviert sind, kann ihr molekularer Aufbau und ihr Einfluss auf die Physiologie in Modellorganismen wie z.B. Mäusen untersucht werden.

Ein erstes Ziel der vorliegenden Arbeit war es, zu untersuchen, ob es für die Entstehung von zirkadianen Rhythmen in jungen Mäusen eine funktionierende maternale Uhr braucht. Um diese Frage zu beantworten, wurden Wildtypmännchen mit arrhythmischen *Per1*^{Brdm1}*Per2*^{Brdm1} oder *Per2*^{Brdm1}*Cry1*$^{-/-}$ doppelt mutanten Weibchen in kompletter Dunkelheit gekreuzt. Die heterozygoten Jungen zeigten einen normalen zirkadianen Rhythmus, obwohl sie in der vollständigen Abwesenheit von Zeitgebern aufgewachsen waren. Die Uhren innerhalb eines Wurfes waren jedoch weniger miteinander synchronisiert als die von Wildtypen. Diese Ergebnisse deuten an, dass die Entstehung zirkadianer Rhythmen nicht von einer intakten Uhr im maternalen Gewebe abhängig ist.

In einem zweiten Teil wurden die Funktion von *Per1* und *Rev-Erbα* innerhalb des zirkadianen Uhrwerks untersucht. Mäuse, welchen diese zwei Gene fehlen, zeigten eine bei Säugetieren sehr seltene Phasenverschiebung mit einer hohen Amplitude als Antwort auf einen Lichtpuls am Ende ihrer Aktivitätsphase. Da *cFos* in Mutanten und Wildtypen vergleichbar induziert wurde, scheint die Photosensitivität in diesen Tieren normal zu sein. Überraschenderweise wurde das ansonsten nicht auf Licht reagierende Gen *Cry1* in den Mutanten induziert. Daher scheinen *Per1* und *Rev-Erbα* Bestandteil eines Mechanismus zu sein, welcher verhindert, dass die Phasenverschiebung in Säugetieren überschiesst.

Ziel des letzten Teils war es, eine nicht-invasive Methode zu entwickeln, um die zirkadiane Expression von humanen Uhrengenen in der Mundschleimhaut zu messen. Es wurde gezeigt, dass in diesem Gewebe *PER2* zirkadian transkribiert und durch blaues Licht am Abend induziert wird. Zudem wurde gezeigt, dass dieser Effekt altersabhängig zu sein scheint. Diese Ergebnisse deuten an, dass diese Methode hilfreich sein kann, um mehr über den zirkadianen Taktgeber im Menschen auf Ebene der Gene zu erfahren. Ausserdem könnte sie dazu beitragen, mehr über die molekularen Mechanismen zu lernen, welche Störungen der inneren Uhr hervorrufen.

Zusammengefasst gewährt diese Arbeit neue Einsichten in die unterschiedlichen Aufgaben von Uhrengenen und den Einfluss von Licht auf die zirkadiane Uhr. Mit wachsendem Wissen in diesen Gebieten wird die Entwicklung von neuen Therapieansätzen zur Behandlung von Störungen des zirkadianen Systems im Menschen voranschreiten.

Chapter 2

General Introduction

2 General Introduction

2.1 Historical background

Daily rhythms in animals and plants have been studied not only in recent times but also earlier in history. Alexander the Great's scribe Androsthenes (4th century B.C.) noted that the tree *Tamarindus indicus* opens its leaves during the day and closes them at night. The first known experiment on biological rhythms was carried out in 1729 by the French astronomer Jean-Jacques d'Ortous De Mairan. He observed that the leaves of the heliotrope plant *Mimosa pudica* open during the day and fold at night. The plants continued to open and fold their leaves regularly even when he put them in constant darkness. Thus, the daily rhythm was maintained even in the absence of daylight as an environmental cue. The famous Swedish taxonomist Carolus Linnaeus (1707-1778) even created a garden with flowers which opened their petals at various times so that he could tell the time of day by looking in his garden. Another important observation has been made by the French botanist De Candolle in 1883 who noticed that the period length of plants placed in constant light differed slightly from the expected 24 hours. In the early 1900's Karl von Frisch observed that bees visited flowers only at specific times of the day. Together with Ingeborg Beling he trained bees to visit a nectar feeding station between 4 and 6 PM. The bees visited only at these times, and continued to visit even when the nectar was removed. This behaviour, called "Zeitgedächtnis" (memory of time), even continued when outside cues such as light were removed in laboratory trials. Although von Frisch and Beling did not know it, the bees were following an internal clock.

The term “biological clock” was only coined in the 1950's by Gustav Kramer and Klaus Hoffmann who did prove its existence with their elegant bird experiments. The adjective *circadian* is taken from the Latin words *circa* and *dies* and means "around a day". Circadian rhythms are self-sustained biological rhythms, which persist with a period of approximately 24 hours in organisms placed in constant conditions. In the 1950's as well, Colin Pittendrigh demonstrated that circadian clocks are temperature compensated, which means that clocks have approximately the same period length when the temperature changes within physiological ranges. Contrary to most metabolic activities, the period of the biological clock does not increase with body temperature. He concluded this from experiments on *Drosophila pseudoobscura* where he placed eggs at different temperatures and recorded their delay to eclosion. The flies emerged in constant darkness on schedule regardless of the temperature. In fact, the name *Drosophila* means dew-loving, referring to its tendency to eclose in the morning.

2.2 Evolutionary relevance of having a clock

Any living organism on earth is subjected to rhythmic changes of its environment. The major rhythms influencing the biosphere are the daily cycle caused by the earth's rotation around its own axis and the seasonal cycle caused by the earth orbiting the sun. It is believed that circadian rhythms evolved due to these predictable rhythms and have been fine-tuned under selective pressure. One argument strengthening the idea that the circadian clock has emerged due to the organism's adaptation to these geophysical facts is its ubiquity. Any organism investigated from cyanobacteria to human beings passing through fungi, insects, reptiles, fish, birds, mice, and so forth show circadian rhythmicity. According to Pittendrigh's "escape-from-light" hypothesis it is thought that the first circadian rhythms originated in the earliest cells to protect the replication of DNA from high ultraviolet radiation during daytime. Having a clock allowed to schedule light-sensitive processes to the night to protect the organism from deleterious photo-oxidative effects occurring during the day (Pittendrigh, 1993).

Besides the periodic geophysical forces of the environment that influenced the evolution of the clock, the need to segregate incompatible metabolic processes has shaped it further. Fixation of nitrogen for example is unable to coexist with photosynthesis. On the other hand, some processes need to coincide to be of use. The availability of a receptor and the release of its corresponding hormone have to be synchronized to generate any endocrine effect. However, having an internal clock does not only provide an organism with intrinsic benefits but also with extrinsic advantages. For instance it is better for an animal to forage for food when it is available and predators are asleep or to search for individuals of the opposite sex at a time conducive for mating. Thus having a clock allows organisms to predict changes in the environment and to prepare their metabolism. Hence they do not only react to changes but they can anticipate them. This reduces energetic costs that would result from constant production of enzymes that are needed only at a certain time. Plants for example can prepare their photosynthetic machinery just before the light appears and thus make use of the first sunbeam. Although the set-up of circadian clocks varies enormously between organisms, their functions bear remarkable similarities. Today, the simplest known circadian clock is that of the prokaryotic cyanobacterium (photosynthetic eubacteria) *Synechococcus elongatus* who's central oscillator consists of only three proteins: KaiA, KaiB and KaiC (fig. 2-1). This circadian oscillator is so basic that it was even reconstituted *in vitro* with just these three proteins and some ATP (Nakajima *et al.,* 2005). Although the Kai proteins do not regulate a specific set of clock-controlled genes, they regulate genome wide gene expression turning on

about two thirds of the genome in the morning and switching them off in the evening. The rest of the genome is activated at dusk and switched off at dawn. It is noteworthy that none of the Kai proteins shares homologies with any known clock gene found in any other organism so far.

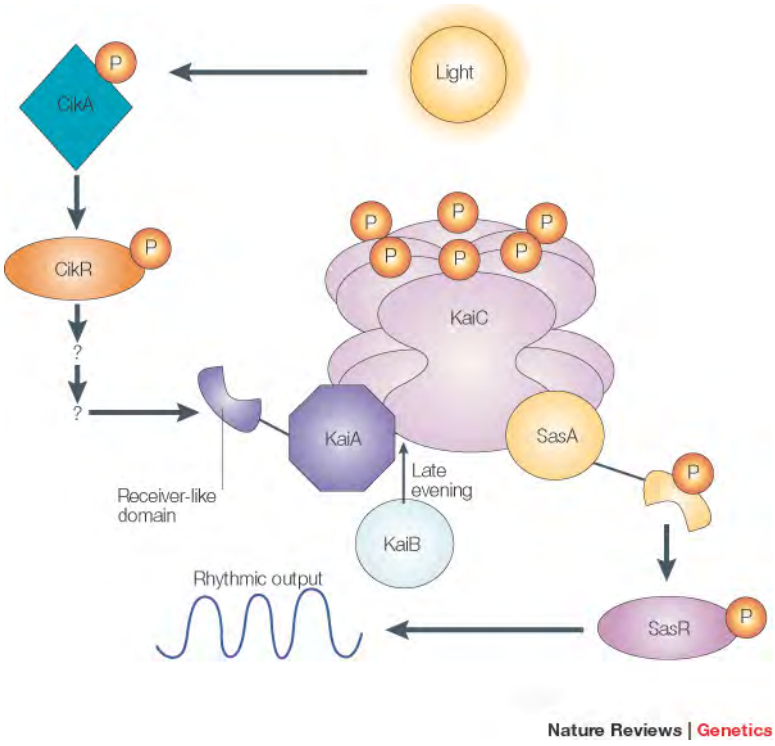

Fig.2-1: The cyanobacterial periodosome model. Environmental information, such as daylight is transduced through the phosphorylation and activation of Circadian input kinase A (CikA). CikA in turn phosphorylates and activates its predicted binding partner, Circadian input kinase R (CikR). Information is then transferred through protein-protein interaction to the receiver-like domain of the circadian-clock protein KaiA. KaiA interacts with KaiC and stimulates autophosphorylation of KaiC, which is hexameric. In the phosphorylated state, KaiC hexamers can form a complex with other clock components. *Synechococcus* adaptive sensor A (SasA) joins the complex and is thereby stimulated to phosphorylate its predicted binding partner, *Synechococcus* adaptive sensor R (SasR). Phosphorylated, active SasR sends temporal information from the periodosome to the rest of the cell to activate rhythmic gene expression, either directly or indirectly. Late in the evening, another protein, KaiB, binds KaiC and inhibits KaiA-stimulated phosphorylation of KaiC. The complex then dissociates into its individual components (not shown) and ends the cycle. The molecular events that reactivate the cycle in constant environmental conditions have not yet been described (Bell-Pedersen *et al.*, 2005).

2.3 Definition of the term “biological clock”

Looking up the word “clock” in an ordinary dictionary one finds something similar to the following definition (www.brainyquote.com): *“A machine for measuring time, indicating the hour and other divisions by means of hands moving on a dial plate. Its works are moved by a weight or a spring, and it is often so constructed as to tell the hour by the stroke of a hammer on a bell. It is not adapted, like the watch, to be carried on the person”*. This definition clearly describes what we understand being a clock in our daily life. However, for scientific purposes more sophisticated definitions are required because well defined terms are the basis to describe the outcome of any experiment. In this respect, a system has to meet the following characteristics to be called “clock” from a biological point of view:

1. The timing mechanism needs to be inherent.
2. The system needs to be able to perceive information from the environment.

3. In order to synchronize the system to the outside, incoming signals have to be integrated by the timekeeping device. However, this synchronization is only possible within a narrow range that is close to the endogenous frequency of the system.
4. The timing has to be sent to the receivers via one or several outputs.

Once a system has been defined as being a clock, it has to be decided whether the system oscillates independently or whether it depends on the oscillations of a superior system. In the former case one talks about pacemakers whereas the latter are called slaves.

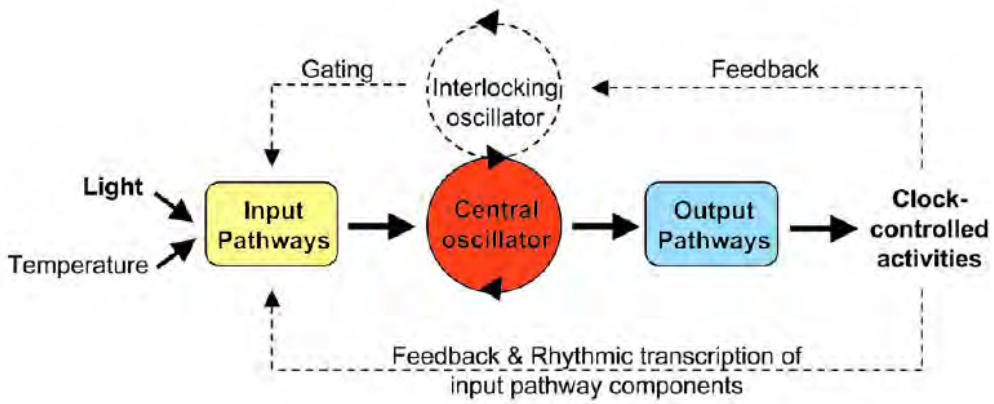

Fig. 2-2: Model of the circadian system.
The circadian system consists of three basic elements: an input pathway (yellow), an endogenous pacemaker generating circadian rhythms (red), and an output pathway (blue). Environmental signals, called Zeitgeber (German for "time giver"), are transduced to the master clock via input pathways. The Zeitgeber can be light, food intake, social factors, chemical or physical factors, etc. The input signals are received *via* receptors and then sent to the central pacemaker that generates oscillations. The output pathway finally translates the oscillation into rhythms such as genome transcription in cyanobacteria or sleep-wake cycles in animals. Some organisms contain more complex circadian clocks (shown as dotted line) that include multiple, interlocking oscillators and positive or negative feedback from clock-controlled activities to the pacemaker and/or input components (figure modified from Gardner *et al.*, 2006).

Definition of the term "circadian clock"

Clocks that are found within a living organism are called "biological clocks". Naturally occurring rhythms can be grouped into cycles that are shorter than a day, about a day or longer than a day. Short rhythms are called "ultradian" (e.g. circahoral = about an hour, circatidal) whereas long rhythms are called "infradian" (e.g. circalunar, circannual). The most exhaustively studied biological timekeeping devices are circadian clocks (fig. 2-2) that are distinguished from other biological oscillators by the following properties:

1. They are self-sustained because they persist under constant conditions with a period (duration between the occurrence of two peaks or troughs) of about 24 hours. Kept under constant conditions, the rhythm starts to free-run which means that it drifts out of phase from the original period dictated by the environment.

2. They can be synchronized by environmental cues - called Zeitgebers - allowing them to match local time. The phasing of the rhythm can be shifted by the same stimulus to which it entrains.
3. They are temperature compensated meaning that their period length is stable over a wide range of biological temperatures.
4. They send a timing signal to peripheral oscillators to set them to the prevailing Zeitgeber.

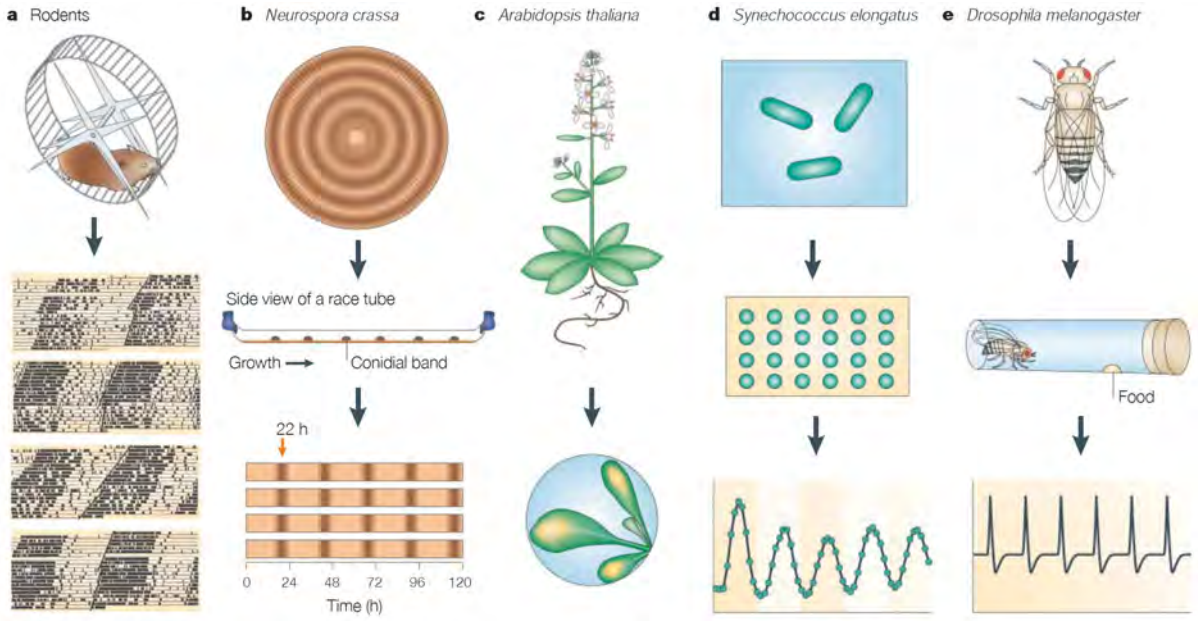

Fig. 2-3: Tools of the trade. Each model system for circadian research offers its own means on non-invasive or automatic ways of recording daily rhythms. **A** Daily wheel-running activity of rodents occurs in constant darkness and is recorded in the form of an actogram. Bouts of activity are seen in black and provide information about the period and phase of the mammal's clock. **B** The fungus *Neurospora crassa* produces asexual spores under the control of a biological clock. This process of conidiation can be measured using a specialized growth chamber called a race tube. **C** Plants show a daily rhythm of leaf movement. In *Arabidopsis thaliana*, rhythms of bioluminescence from luciferase fusions can be visualized for many days in constant light. **D** In the unicellular cyanobacterium, *Synechococcus elongatus*, luciferase fusions are used to monitor rhythms of promoter activity in high-throughput 96-well plates, allowing for saturation mutagenesis to determine components of the oscillator, as well as input and output pathways. **E** Daily flight movements of the model fly *Drosophila melanogaster* break an infrared beam in a specialized tube. The number of breaks can be monitored electronically to detect the circadian pattern of locomotor activity (Golden & Canales, 2003).

It is important to make a clear differentiation between circadian and daily rhythms. While the former are endogenous rhythms with a period close to 24 hours the latter are 24-hours rhythms that are driven by a recurrent Zeitgeber and disappear under constant conditions. Circadian rhythms can be studied quite easily by manipulating the environment (e.g. light cycles, food access) and observing subsequently the outputs (e.g. wheel-running behaviour, blood pressure, hormone secretion, temperature, fluorescence). Some organisms are rather

well established model systems for circadian research and their rhythmic outputs can be studied automatically (fig. 2-3), which is quite a relief for the otherwise sleep deprived chronobiologist.

2.4 The circadian clock in *Drosophila melanogaster*

In the modern era, the studies of Pittendrigh on fruit flies have been continued by Ron Konopka, a graduate student in Seymour Benzer's laboratory. He performed a phenotype-based screen of mutagen-exposed flies and isolated three period mutants in eclosion rhythm and locomotor activity: long (per^L, ± 29 h), short (per^S, ± 19 h) and arrhythmic (per^0), which all mapped to a single locus, called *period* (*per*), on the X-chromosome (Konopka & Benzer, 1971). In 1984, the same *Drosophila period* was the first clock gene ever isolated (Bargiello *et al.*, 1984; Reddy *et al.*, 1984) and it was shown to encode a large protein of more than 1200 amino acids.

Later on, it has been discovered that both PER protein and RNA are expressed rhythmically (Siwicki *et al.*, 1988; Hardin *et al.*, 1990; Zerr *et al.*, 1990). This observation led to the formulation of the negative autoregulatory feedback loop model (fig. 2-4) in which PER feeds back on its own transcription. Nowadays the Transcription-Translation Oscillator Model (TTO) is still the model of choice in chronobiology. However, this gold standard starts to be questioned slowly since the number of observations not fitting the model increases steadily (Lakin-Thomas, 2006).

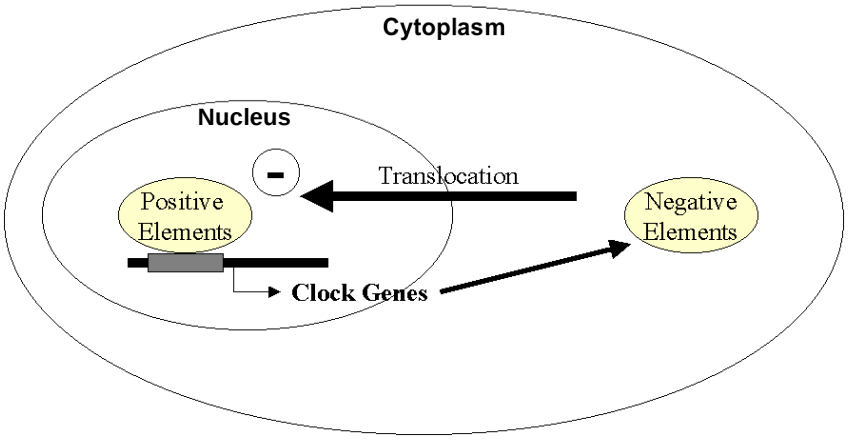

Fig. 2-4: The negative autoregulatory feedback loop within a cell.
Positive elements stimulate the transcription of clock genes. The translated products regulate the transcription of their own transcription negatively.

For a decade, *period* was the only known circadian gene in animals. Only after ten more years, the second fly clock gene *timeless* (*tim*) was discovered (Sehgal *et al.*, 1994) using genetic and biochemical screens. *Tim* protein and RNA levels undergo cycling similar to those of *per*. Today, a lot is known about the workings of the biological clock in the fruit fly

(fig. 2-5). Its negative autoregulatory feedback loop consists of a core system of four regulatory proteins, which create the daily rhythm of the fruit fly's clock. The cycle begins when the two positive elements, CLOCK (CLK) and CYCLE (CYC), bind together and increase the production of PER and TIM. The latter two proteins accumulate gradually over time and slow down their own production when they reach a critical concentration. It is of note, that the transcription factors CLK and CYC contain both a basic helix-loop-helix (bHLH) domain, which allows them to dimerize and to bind DNA. Additionally, they contain a PER-ARNT-SIM (PAS) dimerization domain. The CLK/CYC heterodimers activate *tim* and *per* transcription by binding directly to their E-box (a binding site for bHLH-PAS

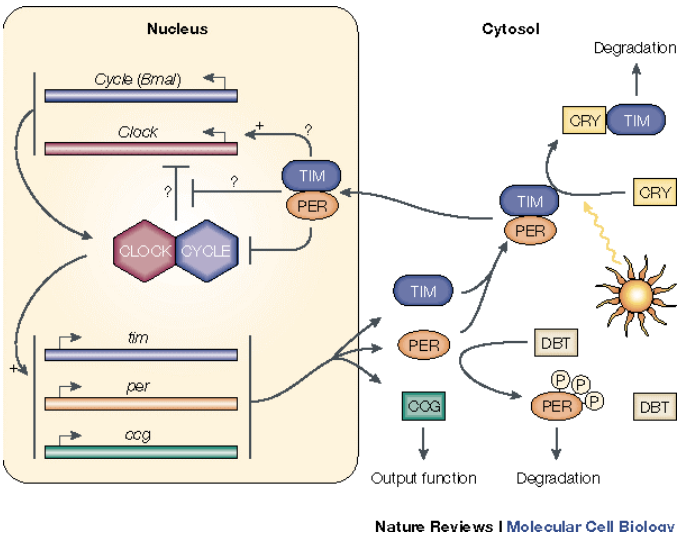

Fig. 2-5: Model for the circadian clockwork in *Drosophila melanogaster*. At least two interlocked feedback loops are involved in generating rhythms: a negative autoregulatory loop of PER and TIM proteins on their own genes (through inhibition of the transcriptional activator CLOCK-CYCLE), and a positive effect of these proteins on the expression of CLOCK, CRY and DBT proteins regulate the stability of the TIM and PER proteins, respectively. CLOCK-CYCLE also regulataes clock-controlled genes (ccg), and hence rhythmic output (Cermakian & Sassone-Corsi, 2000)

transcription factors: CACGTG) elements found in their promoters. Interestingly, *Clk*, but not *cyc*, RNA and protein levels cycle over a 24-h period with a phase almost opposite to that of PER and TIM. *Drosophila* genetics identified five additional circadian components, *cryptochrome* (*cry*), *doubletime* (*dbt*, a casein kinase I), *shaggy* (*sgg*), *Par domain protein 1ε* (*Pdp1ε*) and *vrille* (*vri*), which act to fine tune the simple transcriptional-translational feedback loop (Price *et al.*, 1998; Blau *et al.*, 1999; Martinek *et al.*, 2001; Cyran *et al.*, 2003). TIM-free PER protein is phosphorylated by DBT in the cytoplasm and thus marked for degradation. This fate can be neutralized by the dephosphorylation of PER by protein phosphatase 2A (PP2A; Harms *et al.*, 2004). Thanks to these opposing activities, PER stability can be altered precisely. As TIM progressively accumulates, it binds the PER-DBT complex and blocks the phosphorylation of PER by DBT. The nuclear entry of PER/DBT and TIM is independent of each other (Hall, 2003) and promoted by Casein Kinase 2 (CK2; Allada & Meissner, 2005) and Shaggy (SGG; Harms *et al.*, 2004), respectively. Once they

reach the nucleus, PER/DBT and PER/DBT/TIM complexes inhibit CLK function. The direct hyperphosphorylation of CLK by DBT releases the CLK/CYC heterodimer from the E-box promoter sequences which in turn leads to reduced *per* and *tim* (as well as *vri* and *Pdp1ε*) expression (Hardin, 2005). Following light exposure at dawn, TIM protein is rapidly degraded by CRY, which binds to TIM after a conformational change caused by light exposure (Ceriani *et al.*, 1999; Emery *et al.*, 2000; Ashmore & Sehgal, 2003). The interaction of TIM with the protein JETLAG (JET) targets it for ubiquitination and subsequent degradation by the proteasome pathway (Koh *et al.*, 2006). This degradation of TIM leads each day (or after a light pulse) to the resetting of the clock.

Although *Drosophila* has been studied for many years, not all components of its molecular clock have been first identified in the fly. Some of them have been discovered in mammals and only afterwards their homologues have been found in the fly. Through the years, fruitful information exchange has developed between the different model organisms used, due to the conserved characteristic of the clocks in "higher" eukaryotes.

Contrary to "higher" animals, the molecular oscillators found in many tissues of Drosophila seem to function autonomously and they can be directly reset by light (Plautz *et al.*, 1997). This observation indicates that each oscillator might function as a pacemaker (reviewed in Bell-Pedersen *et al.*, 2005). However, some studies indicate that the neuropeptide pigment-dispersing factor (PDF), which is secreted in the dorsal brain with a circadian pattern, might mediate communication among central oscillator neurons in the brain (Peng *et al*., 2003; Stoleru *et al*., 2004; Grima *et al*., 2004).

2.5 The circadian clock in zebrafish (*Danio rerio*)

In the past few years, the zebrafish has become one of the most valuable lower vertebrate models for studying circadian clock function. It is thought that the teleost (= "perfectly boned fish") circadian system might be the more ancestral vertebrate clock that became far more specialized in mammals due to selective pressure. There are several reasons for its "success" in the field. The most prominent ones are its utility in large-scale genetic screens and the transparency of the embryo. Furthermore, the eggs can be fertilized externally and the rapidly developing fish can be observed in a test tube. Hence maturation of the clock during early development can be studied quite easily, via *in vivo* imaging approaches for example. Another attractive property of the zebrafish is that its peripheral oscillators can be directly entrained to light independently of connections with the retina (Whitmore *et al.*, 2000) as it is also the case

for *Drosophila.* It seems that peripheral oscillators in both fishes and flies have a high degree of autonomy. Besides light, temperature cycles are also able to entrain the fish oscillators since *Danio rerio* is poikilotherm, which means that its internal temperature varies with external temperature. This property makes the fish a more accessible model to study how the circadian timing system responds to temperature changes. Consistent with other organisms, the zebrafish circadian clock is temperature compensated over a 10°C range (Lahiri *et al.*, 2005). Last but not least most tissues and also cell lines possess functional clocks that can be entrained to either light or temperature cycles *in vitro*.

2.5.1 How to measure circadian rhythms in zebrafish

Before zebrafish could ascend to be an excellent model for circadian studies, suitable rhythmic output parameters had to be found. Locomotor activity and pineal melatonin synthesis were soon identified displaying a robust circadian rhythm. The former can be monitored in larval zebrafish (5-18 days old) by a computerized video image analysis system (Cahill *et al.*, 1998). Larval swimming has proven to be a robust and reliable marker for circadian rhythms with peak activity during the day. Furthermore, the rhythm persists under constant conditions with an average free-running period of 25.5 hours. In contrast, measuring locomotor activity in adult fish turned out to be a rather bad marker due to high inter-individual variability in cycle robustness (Hurd *et al.*, 1998). Besides locomotor activity, pineal melatonin rhythms as the principal endocrine clock output turned out to be a robust marker. Cultured pineal glands continue to produce and secrete melatonin *in vitro* with a precise timing for one week or more (Cahill, 1996). At least in part, melatonin synthesis rhythm results from the control of arylalkylamine-*N*-acetyltransferase (AANAT) mRNA which encodes the rate limiting enzyme for melatonin synthesis. Two isoforms of this enzyme have been identified in zebrafish: AANAT1 is expressed exclusively in the retina and AANAT2 is expressed mainly in the pineal gland but small levels are also found in the retina. Measuring melatonin rhythms is a useful tool to confirm findings obtained in locomotor activity screens. Last but not least a third way has been developed to study the clock in fish. This method takes advantage of transgenic lines carrying luciferase reporter constructs (Kaneko & Cahill, 2005). The bioluminescence of these transgenes can be measured automatically using a scintillation counter.

2.5.2 Molecular machinery of the circadian clock in zebrafish

From studies in mammals and *Drosophila* it has been known that the molecular machinery of the clock is quite conserved between these two phylae. Due to this, it was not a big surprise that homologues of *Clock*, *Bmal*, *Per* and *Cry* have been identified in zebrafish, as it is the case for most other vertebrates (table 2-1). However, a big difference exists between teleosts and mammals as the fish has more clock genes. This peculiarity of having two paralogs of many mammalian single-copy genes appears to be the result of a whole-genome duplication occurring early during evolution in the teleost lineage (Postlethwait *et al.*, 1998).

Table 2-1: Zebrafish clock gene homologues (Vallone *et al.*, 2005)

Gene	Cloning	Known functions
Cry1a	Homology	Light inducible expression, blocked by protein synthesis inhibitors. Interacts with CLOCK-BMAL. Represses CLOCK1-BMAL3 activation by direct interaction in the nucleus. Does not affect CLOCK-BMAL binding to an E-box.
Cry1b	Homology	Represses CLOCK-BMAL activation.
Cry2a	Homology	Represses CLOCK-BMAL activation.
Cry2b	Homology	Represses CLOCK-BMAL activation.
Cry3	Homology	Does not interact with or repress CLOCK-BMAL activators.
Cry4	Homology	Does not interact with or repress CLOCK-BMAL activation.
Clock1	Homology	Interacts with BMAL and activates transcription by binding to E-boxes. Temperature influences strongly the amplitude of transcriptional activation and phosphorylation.
Clock2	Homology	Interacts with BMAL and activates transcription by binding to E-boxes. Temperature influences strongly the amplitude of transcriptional activation. Closest similarity with NPAS2.
Clock3	Homology	Interacts with BMAL and activates transcription by binding to E-boxes. Temperature influences strongly the amplitude of transcriptional activation.
Bmal1	Two Hybrid with Clock	Interacts with CLOCK1 and activates transcription by binding to E-boxes. Temperature does not influence strongly the amplitude of transcriptional activation.
Bmal2	Two Hybrid with Clock	Interacts with CLOCK1 and activates transcription by binding to E-boxes.
Bmal3	Homology	Interacts with CLOCK1 and activates transcription by binding to E-boxes.
Per1 (4)	Homology	Clock regulated. Light acutely down-regulates expression.
Per2	Homology	Light inducible expression involves MAPK pathway and is not blocked by protein synthesis inhibitors. Represses CLOCK1-BMAL3 activation by interacting in the cytoplasm and preventing nuclear import. mRNA maternally inherited. Tissue specific expression during early development. Required for maturation of rhythmic AANAT2 expression in the pineal gland.
Per3	Homology	Clock regulated. Tissue specific expression during early development. Transcript maternally inherited.
Rev-Erbα	Homology	Expression during early development appears first in pineal (44-48 hours post fertilization [hpf]), then the retina (68-76 hpf) and finally in the optic tectum (96 hpf).

The basics of the molecular oscillator in zebrafish appear to have much in common with the more extensively studied mammalian clock. However there are some small differences between the two that may be informative because there is evidence for specialization of clock gene function in fish. In accordance with many organisms, the molecular clockwork of *Danio*

rerio functions as an autoregulatory feedback loop. CLOCK-BMAL heterodimers function as positive elements that activate the transcription of clock genes and clock-controlled genes via binding to E-box motifs. The exact composition of these heterodimers changes as a function of time and depending on the tissue. Contrary to mammals, *Bmal* and *Clock* mRNA expression oscillates rhythmically peaking at the beginning of the night (fig. 2-6; Whitmore *et al*., 1998; Pando *et al*., 2001; Zhuang *et al.*, 2000). *Per* genes oscillate in anti-phase to *Bmal* and *Clock*, reminiscent to the situation in mammals (Oishi *et al.*, 1998), with *Per1* peaking at ZT0 (Zeitgeber time 0 = lights on, ZT12 = lights off) and *Per3* at ZT3. *Per1* and *Per3* continue to cycle under dark-dark (DD) conditions. *Per2* on the other hand, is strictly light-dependent and does not cycle under DD (Pando *et al.*, 2001). In mammals, all three *Per* genes are rhythmically expressed in constant conditions, and *Per1* and *Per2* are both light inducible (Shearman *et al.*, 1997).

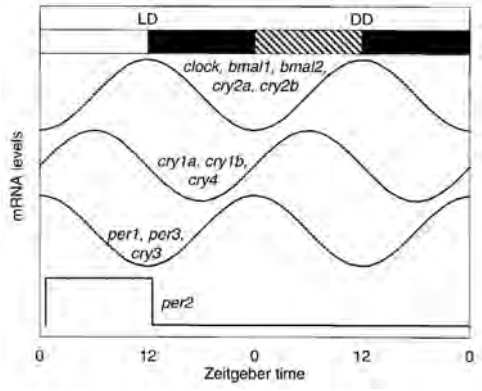

Fig. 2-6: Expression rhythms of zebrafish clock genes.
The approximate timing of mRNA rhythms in LD and DD is illustrated. The rhythm in *Per2* mRNA is driven by the LD cycle, whereas other rhythms persist in constant darkness (LD = light dark cycle, open bar = light phase, black bar = dark phase, DD = constant darkness, hatched bar = subjective day, black bar = subjective night) (Cahill, 2002).

The zebrafish clock contains six *Cry* genes (Kobayashi *et al.*, 2000). Four of them show high sequence homology to the mammalian *Cry genes* (*Cry1a*, *Cry1b*, *Cry2a*, *Cry2b*), two of them having higher similarity to *Drosophila Cry*. All zebrafish *Cry* genes are rhythmically expressed but with differing expression patterns. The mRNA of *Cry1a* and *Cry1b* peak during daytime whereas *Cry2a* and *Cry2b* peak in the evening. This difference in peak expression might indicate that they are not completely redundant within the oscillator. *Cry3* peaks in the morning in parallel with *Per1/3* whereas *Cry4* peaks during the day, like *Cry1a/b* do. *Cry* genes that are more similar to mammalian *Crys* have been shown to inhibit CLOCK-BMAL mediated transcription *in vitro* (Ishikawa *et al.*, 2002; Hirayama, Fukuda *et al.*, 2003). In contrast to the first set of genes, *Cry3* and *Cry4* are unable to suppress the potential to activate transcription of CLOCK-BMAL heterodimers (Ishikawa *et al.*, 2002; Kobayashi *et al.*, 2000; Hirayama, Nakamura *et al.*, 2003). Unlike the other *Per* and *Cry* genes in zebrafish, *Per2* and *Cry1a* are directly light inducible which suggest some specific regulation by the light input pathway (Pando *et al.*, 2001; Hirayama *et al.*, 2005, Cermakian *et al.*, 2002). Interestingly,

neither *Per2* nor *Cry1a* show rhythmic expression when temperature but not light is cycling (Lahiri *et al.*, 2005). However, both CRY1A and PER2 act as inhibitors of the CLOCK-BMAL heterodimers mediated transcription (Hirayama, Fukuda *et al.*, 2003). CRY1A appears to interact with the heterodimers in the nucleus without affecting E-box binding whereas PER2 sequesters newly synthesized CLOCK-BMAL in the cytoplasm (Ishikawa *et al.*, 2002; Hirayama, Fukuda *et al.*, 2003; Hirayama, Nakamura *et al.*, 2003).

2.5.3 Light signalling to the zebrafish clock

Recently, it has been shown that *Cry1a* acts as a light-signalling molecule in the zebrafish clock (Tamai *et al*., 2007) as its induction is critical for light-induced phase shifts. Overexpression of *Cry1a* in *Per1*-luminescent cell lines even led to a complete abolishment of the clock oscillations within the cells. This experiment indicates that *Cry1a* acts as a strong transcriptional repressor and as a possible light-induced repressor of clock function. Furthermore, *Cry1a* overexpression mimics exposure to constant light. It has also been shown that constant light conditions lead to a fall in *Per1* expression and subsequent tonic repression of its transcription. However, *Cry1a* seems not to be the only actor in the light input pathway to the zebrafish clock as light pulses also strongly induce *Per2*. Interestingly, an injection of *Per2* antisense morpholino into early-stage zebrafish embryos blocks subsequent synchronized rhythms in zebrafish *aanat2* expression in the pineal gland (Ziv *et al.*, 2005). The mechanism by which *Per2* might be involved in clock resetting still remains to be elucidated. Another study shows that distinct mechanisms seem to be involved in the induction of *Per2* and *Cry1a* by light (Hirayama *et al.*, 2005). They demonstrate that *Per2* continues being induced in the presence of protein synthesis inhibitors whereas *Cry1a* light induction requires *de novo* protein synthesis (especially the synthesis of AP-1).

2.5.4 Concluding remarks

As a summary of the zebrafish molecular clock, one can say that it is in general consistent with the mammalian model that will be described thereafter. The most important differences between the two systems lie in the number of *Cry* genes and in the regulation of *Per2*. The fact that *Clock* is cycling is also worth mentioning as well as the direct light sensitivity of central and peripheral oscillators in the zebrafish. The presence of two classes or groups of *Cry* genes, one similar to *Drosophila Cry* and one similar to mammalian *Crys*, suggests that the zebrafish circadian system may share characteristics with both the *Drosophila* and the

mammalian circadian system (Pando & Sassone-Corsi, 2002). This conjecture is also strengthened by the fact that *clock* expression oscillates in Drosophila while *cycle* (*Bmal1* homologue) expression is constant. Exactly the opposite is true for the mammalian system where *Clock* is constitutively expressed and *Bmal1* oscillates in a circadian fashion. In the zebrafish, both *Clock* and *Bmal* are rhythmically expressed.

Since the work presented in this thesis focuses on the mammalian circadian system, the following sections will only concentrate on the circadian clock in rodents and humans.

2.6 The circadian clock in mammals

2.6.1 The circadian pacemaker resides in the brain

As early as in 1948, Curt Richter discovered the approximate area where the principal circadian pacemaker is located in mammals. Performing a series of lesion experiments in the rat brain, he found only one area that had an effect on circadian rhythms when it was ablated. This region was the frontal part of the hypothalamus located at the base of the brain immediately above the optic chiasm. In 1972, two independent groups narrowed down this area to the suprachiasmatic nuclei (SCN, fig. 2-7), which consist of two clusters (Moore & Eichler, 1972; Stephan & Zucker, 1972). They ablated the SCN bilaterally and observed a loss in circadian rhythmicity of corticosterone rhythm, drinking behaviour and locomotor activity. Later transplantation experiments demonstrated that circadian behaviour can be restored in lesioned animals by SCN grafts (Lehman *et al.*, 1987; Ralph *et al.*, 1990; Sujino *et al.*, 2003). Similar studies have been performed in a number of other mammalian species and they confirmed that the circadian pacemaker resides in the SCN in all mammals.

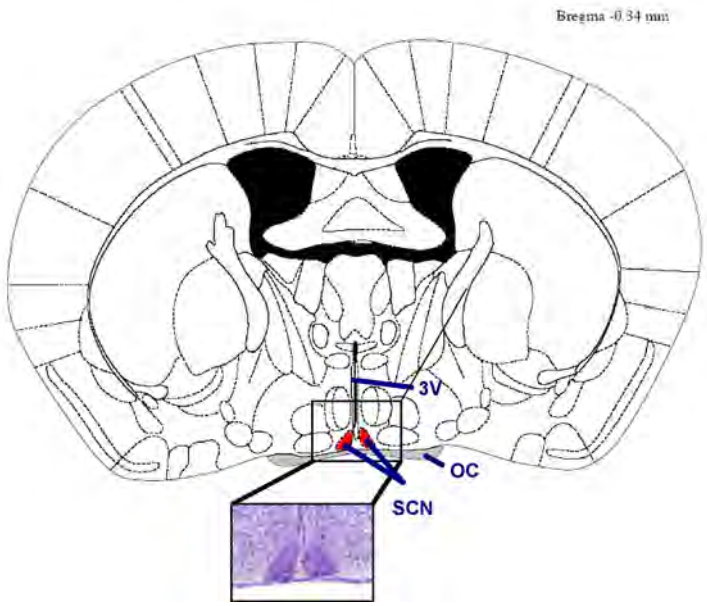

Fig. 2-7: Localization of the suprachiasmatic nuclei (SCN) in the mouse brain.
This coronal section of a mouse brain shows the position of the SCN (red) on top of the optic chiasm (OC, gray) on both sides below the third ventricle (3V). The enlarged panel shows the SCN stained with cresyl violet (adapted from Paxinos & Franklin, 2001).

2.6.2 Anatomy of the SCN and its neurotransmitter content

In mice, each of the two "pear-shaped" suprachiasmatic nuclei contains about 10'000 neurons and each is 300 μm wide, 350 μm high and 600 μm long (Abrahamson & Moore, 2001). The SCN can be subdived into two parts: a ventrolateral (vlSCN, or core) and a dorsomedian part (dmSCN, or shell). Although early studies suggested that all SCN neurons were cell autonomous clocks (Welsh *et al.*, 1995), recent studies demonstrated that they are not identical in function. The two SCN regions not only differ from the phenotypic point of view but also from the neuropeptides they express (fig. 2-8), their pacemaker ability and their response to environmental cues. Hence gene expression or firing in dorsal "shell" neurons peaks earlier in the day compared to ventral "core" neurons (Yamaguchi *et al.*, 2003; Schaap *et al.*, 2003). The shell mostly secretes arginine vasopressin (AVP) whereas the core predominantely expresses vasoactive intestinal peptide (VIP; Abrahamson & Moore, 2001) and gastrin-relesing peptide (GRP; Mikkelsen *et al*., 1991; Abrahamson & Moore, 2001). Interestingly, cultured SCN slices continue to secrete AVP and VIP rhythmically into the medium. Hence, they seem to play a crucial role in transducing signals from the SCN to the periphery (Gillette & Reppert, 1987; Shinohara *et al.*, 1994).

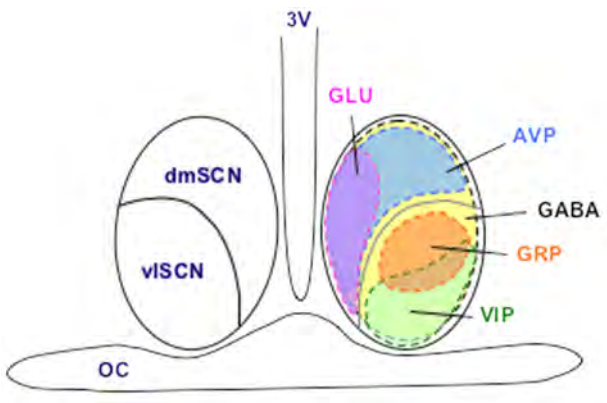

Fig. 2-8: Heterogeneity of the SCN.
The left nucleus represents the subdivision of the SCN into a dorsomedian (dm, shell) and a ventrolateral (vl, core) part. The nucleus on the right side shows the distribution of neuropeptide and neurotransmitter expression in the mouse SCN. 3V, third ventricle; AVP, arginine vasopressin (blue); GABA, γ-amino-butyric acid (yellow); GLU, glutamate (purple); GRP, gastrin-releasing peptide (orange); OC, optic chiasm; VIP, vasoactive intestinal peptide (green) (picture taken from the thesis of Mathieu Chansard, Université Louis Pasteur de Strasbourg, 2007)

Besides the neuropeptides already mentioned (and several others not cited here), the neurotransmitter γ-amino butyric acid (GABA) is expressed all over the SCN (Moore & Speh, 1993). Furthermore, some neurons in the shell are known to express glutamate (GLU; Csaki *et al.*, 2000).

2.6.3 Input pathways to the mammalian circadian clock

To be able to adapt the body to the environment, the pacemaker has to receive information from the outside, integrate it and send it to the peripheral oscillators. Hence, the SCN are

connected to a great number of afferent nervous fibers. There exist three major input pathways: the retinohypothalamic tract (RHT), the geniculohypothalamic tract (GHT) and the serotonergic input from the raphe nucleus (fig. 2-9).

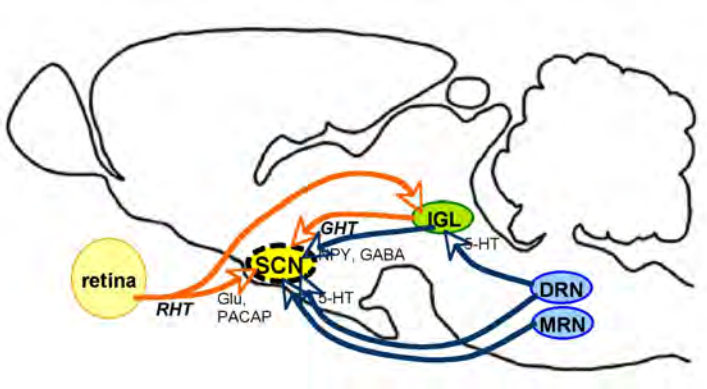

Fig. 2-9: Main afferent pathways to the SCN in rat.
Orange and dark blue arrows represent photic and non-photic inputs respectively. 5-HT, serotonin; DRN dorsal raphe nucleus; IGL, intergeniculate leaflets; GABA, γ-amino-butyric acid; GHT, geniculohypothalamic tract; GLU, Glutamate; MRN, median raphe nucleus; NPY, neuropeptide Y; PACAP, pituitary adenylate cyclase-activating peptide; RHT, retinohypothalamic tract; SCN, suprachiasmatic nuclei (adapted from the thesis of Mathieu Chansard, Université Louis Pasteur de Strasbourg, 2007).

2.6.3.1 Photic input via the retinohypothalamic tract

Mammals perceive external light information mainly via a subset of photosensitive retinal ganglion cells (pRGC; fig. 2-10) in the eye (Moore *et al.*, 1995; Provencio *et al.*, 1998; Berson *et al.*, 2002; Sekaran *et al.*, 2003). These cells express the photopigment melanopsin (a homologue of a photoreceptor in amphibian skin; Provencio *et al.*, 2000; Gooley *et al.*, 2001; Lucas *et al.*, 2001; Hattar *et al.*, 2002; Dacey *et al.*, 2005) and send the photic information directly to the SCN via the RHT (Moore & Lenn, 1972).

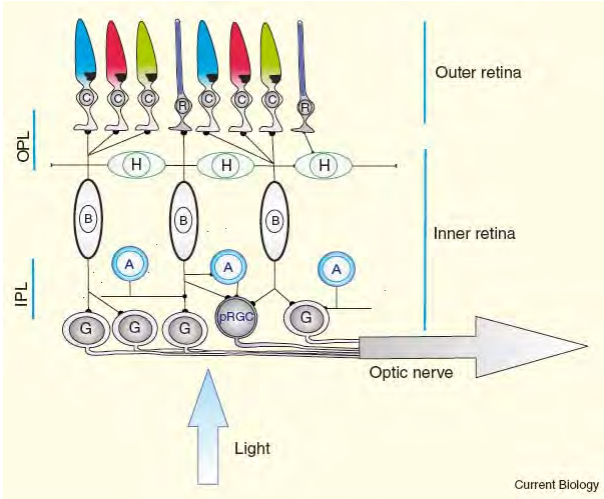

Fig. 2-10: Light detection in the vertebrate retina.
The rods (R) and cones (C) convey visual information to the ganglion cells (G) via the second order bipolar cells (B). At the outerplexiform layer (OPL), horizontal cells (H) facilitate lateral connectivity and feedback to the photoreceptors. At the inner plexiform layer (IPL) amacrine cells (A) allow lateral connections between bipolar and ganglion cells. The optic nerve is formed by the axons of all the ganglion cells. A subset of ganglion cells (pRGC) also detects light directly; for this, they require the photopigment melanopsin. Light, via melanopsin, activates a G-protein cascade in the cells that depolarizes their membrane. These cells also receive synpatic input in the IPL from bipolar cells and amacrine cells. Thus photodetection in the retina occurs both in the outer and inner retina. Counter-intuitively, light passes through the transparent ganglion layer to reach the rods and cones (Foster & Hankins, 2007).

The monosynaptic RHT fibers end directly on the VIP expressing neurons in the ventrolateral part of the nucleus (Ibata *et al*., 1989; Tanaka *et al*., 1993). The molecules implicated in the photic signalling are the excitatory neurotransmitter GLU (Castel *et al.,* 1993) and the neuropeptide pituitary adenylate cyclase-activating protein (PACAP; Hannibal *et al.,* 1997). Another interesting property of the RHT is that it is implicated exclusively in conveying circadian information to the SCN. This is based on the fact that RHT lesions only alter photic entrainment without affecting vision (Johnson *et al.,* 1988). Light is the strongest Zeitgeber for the SCN. Every day it resets the phase of the endogenous circadian clock and the linked oscillations in physiology and behaviour to exactly 24 hours. Strikingly, the effect of light on the SCN varies depending on the time at which it is perceived. The light response will be discussed later in section 2.6.7.

2.6.3.2 Non-photic input via the geniculohypothalamic tract

The second most important afferent pathway to the SCN comes from the intergeniculate leaflets (IGL) of the thalamus, located between the dorsal and ventral parts of the lateral geniculate nucleus. The IGL is connected to the retina (Hickey & Spear, 1976) and receives the same information as the SCN because each RGC that innervates the core region of the SCN also connects the IGL (Pickard, 1985; Moore & Card, 1994). The major signalling molecules within the IGL are the neuropeptide Y (NPY) and the neurotransmitter GABA (Harrington *et al.,* 1985; Moore & Speh, 1993; Moore & Card, 1994). It has been shown that NPY-immunoreactive cells of the IGL project to the SCN core (VIP neurons; Card & Moore, 1989; Morin *et al.,* 1992; Harrington *et al.,* 1997) where they form a dense plexus (Harrington *et al.,* 1985). Based on the fact that the IGL neurons projecting to the SCN receive information from the same RGC than those which directly connect to the SCN, it appears that the IGL constitute the integration point of a complex circuit. Furthermore, the IGL obtain additional information from structures like the dorsal raphe nuclei (Meyer-Bernstein & Morin, 1996). This indicates that this path allows the tight regulation of photic and non-photic entrainment of the circadian clock.

2.6.3.3 Non-photic input via the serotonergic tract from the raphe nuclei

The third most important afferent input pathway to the SCN comes from the median raphe nucleus in hamsters (Meyer-Bernstein & Morin, 1996; Leander *et al*., 1998) and both the median and the dorsal raphe nucleus in rats (Moga & Moore, 1997). These fibers end within

VIP-immunoreactive cells of the SCN core region (Kiss *et al.,* 1984; Bosler & Beaudet, 1985; Francois-Bellan & Bosler, 1992) where the retinal afferents also end (van den Pol & Tsujimoto, 1985).

An important fact is that the administration of agonists or chemical depletion of the serotonergic path affect locomotor activity both in LD and in DD (van Esseveldt *et al.,* 2000). Due to this it is thought that the serotonergic tract participates in a non-photic regulation of the entrainment of the circadian clock.

2.6.4 Output pathways from the mammalian circadian clock

Once the central pacemaker in the SCN has integrated the input signal, time cues have to be sent to peripheral oscillators (fig. 2-11). To synchronize behavioural and physiological rhythms, the signals are sent to the periphery via both neuronal pathways and diffusible molecules. The induction of clock-controlled genes (CCGs) orchestrates action potential firing rate, rates of cellular metabolism, hormone release, etc. (Reppert & Weaver, 2002).

2.6.4.1 Neuronal output

The SCN innervates several brain areas mostly located within the thalamus and the hypothalamus. The bulk of the SCN output innervates the subparaventricular zone (SPZ) and the dorsomedial nucleus of the hypothalamus (DMH). The SPZ is subdivided into a ventral part (vSPZ), just above the SCN, and a dorsal part (dSPZ), just below the paraventricular nucleus (Lu *et al.,* 2001). In addition to the anatomic discrimination of the SPZ, the two areas also differ in their physiological relevance. Lesions within the vSPZ disrupt the circadian rhythms of sleep and wakefulness, as well as locomotor activity, but have little effects on oscillations in body-temperature. By contrast, ablation of the dSPZ severely impairs circadian rhythms of body temperature whereas the sleep-wake cycle and locomotor activity remain unchanged (Lu *et al.,* 2001). From these experiments it can also be concluded that direct projections of the SCN to the ventrolateral preoptic nucleus (VLPO) or the orexin neurons, which are both involved in the sleep system, are not sufficiently strong to maintain circadian rhythms of precited functions. It seems that the relay neurons in the SPZ are predominantly required to preserve them. Furthermore, the SPZ also has efferents to the VLPO and the orexin neurons (Chou *et al.,* 2002; Sakurai *et al.,* 2005; Yoshida *et al.,* 2006; Watts *et al.,* 1987). However, the major output from the SPZ signals to the DMH, where the information received directly from the SCN is amplified (Lu *et al.,* 2001; Deurveilher & Semba, 2005).

The role of the DMH seems to be the regulation of sleep and wakefulness, as well as locomotor activity, corticosteroid secretion and feeding (Chou *et al.*, 2003). Moreover, lesion studies of the DMH implicate that its output is mainly activating. It is one of the largest sources of input to the VLPO and orexin neurons conveying SCN influence to the sleep-wake regulatory system (Chou *et al.*, 2003; Aston-Jones *et al.*, 2001; Chou *et al.*, 2002; Yoshida *et al.*, 2006; Thompson *et al.*, 1996).

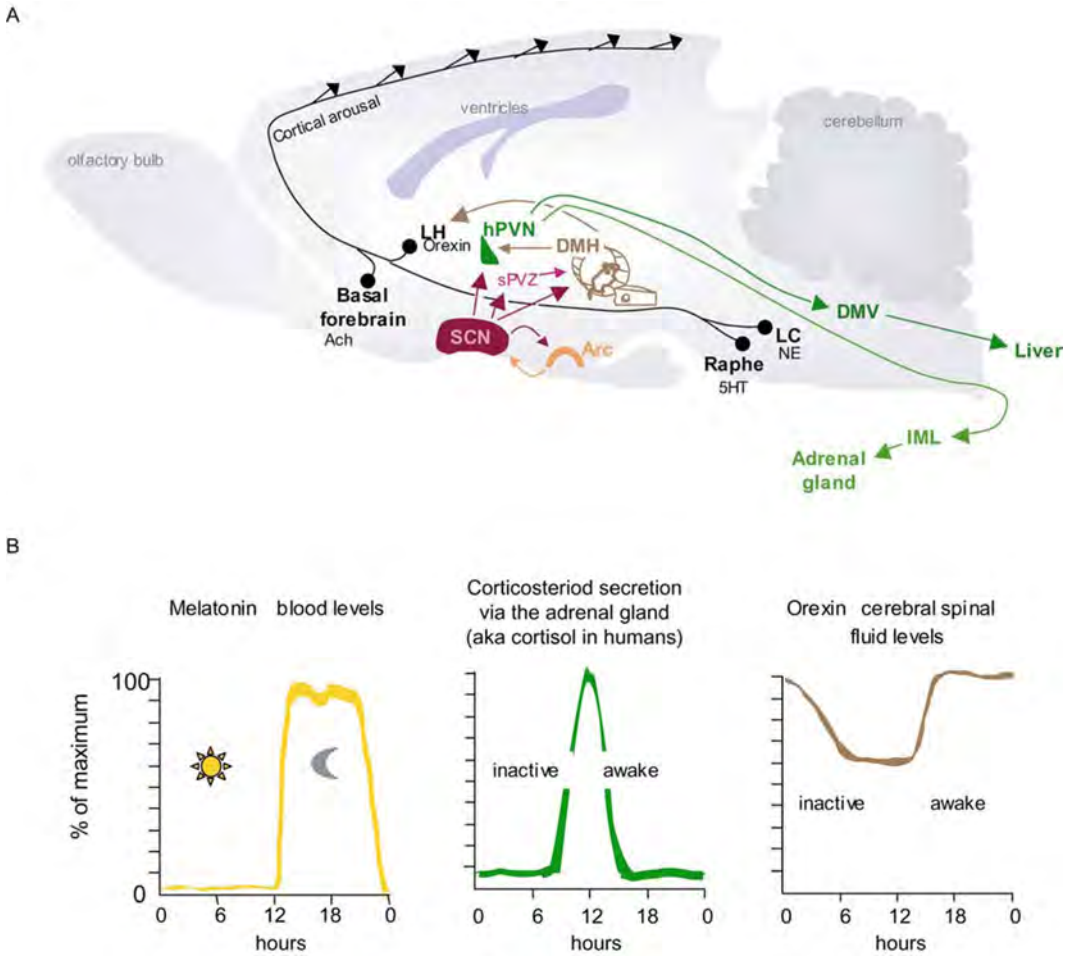

Fig. 2-11: Physiological significance of SCN output signals: coordination of internal physiology to optimize performance. A The SCN (red) sends extensive projections to the paraventricular nucleus of the hypothalamus (green, hPVN), subparaventricular zone (pink, sPVZ), and dorsal medial hypothalamus (brown, DMH). Internal physiology is "primed" for food intake via the SCN → sPVZ → DMH → hPVN circuit that ultimately regulates synthesis and secretion of corticosterone from the adrenal cortex and glucose production in the liver. Cortical arousal is regulated in part via the SCN → DMH → LH circuit. The SCN is reciprocally connected with the arcuate nucleus (Arc). The Arc contains receptors responsive to blood-born hormones, and therefore represents a key feedback pathway to the SCN. The SCN also receives input from other brain areas, and thus functions as an integrator of both environmental and internal signals. Ach, acetylchonline; DMV, dorsal motor nucleus of vagus; 5HT, serotonin; IML, intermediolateral column of spinal cord; LC, locus coeruleus; LH, lateral hypothalamus; NE, norepinephrine; Raphe, Raphe nucleus **B** Examples of various body rhythms controlled by the SCN. Melatonin is low during the day, and high at night. Corticosterone and orexin levels are coupled to the behavioural state of the animal, high during wakefulness and low during sleep. Note, the timing and shape of the waveforms are different. Distinct cell types and heterogeneity of phase within the SCN may serve to regulate the diverse timing of these targets. This figure and the figure legend are taken from the introductory workshop of the 72nd Cold Spring Harbor Laboratories Symposium (2007): Clocks & Rhythms (derived in part from Saper (2005) and Bujis (2001)).

The major role of the DMH seems to be the integration of clock information from the SCN and the SPZ for feeding, temperature, social and other cues. This allows the animals to be flexible enough to adapt their behavioural and physiological cycles to the environment, resulting in optimal survival conditions (Saper *et al.,* 2005). Interestingly, it seems that these complex three-stage pathways for circadian control of sleep and other behaviours have evolved to allow their different control within nocturnal and diurnal animals. In both kinds, the SCN firing is active during the light cycle whereas the VLPO is always active during the sleep cycle (Sherin *et al.,* 1996; Gaus *et al.,* 2002). This indicates that there must be an intervening set of circuitry that allows the circadian output to be set at opposite phases in nocturnal animals and diurnal animals despite an identical clock input and sleep-control system (Saper *et al.,* 2005).

Several groups have shown that the different parts of the SCN signal to distinct regions. The median preoptic area (MPOA) for example receives projections from the shell of the SCN, while SPZ is targeted by neurons of the core SCN. Besides, both core and shell project to the DMH, the paraventricular nuclei of the hypothalamus (PVN) and the paraventricular thalamic nucleus (Watts & Swanson, 1987; Watts *et al.,* 1987, Leak & Moore, 2001). AVP secreted from the PVN is primordial for the regulation of corticosterone (Buijs *et al.,* 1998). Furthermore, the PVN is also crucial for the rhythmic secretion of melatonin (Simonneaux & Ribelayga, 2003).

2.6.4.2 Humoral output

As mentioned above, the clock output is not only assured by neuronal projections but also by diffusible factors. This idea was born in 1987, when graft experiments were performed on SCN-lesioned hamsters placed in DD (Lehman *et al.,* 1987). The transplant was able to restore rhythmic locomotor activity but not photoperiodic response. Later on, other researches showed that luteinising hormone (LH) rhythm, oestrous cycle, corticosterone and melatonin rhythm could not be restored by grafts as well (Meyer-Bernstein *et al.,* 1999). These studies pointed to the existence of at least one diffusible factor implicated in synchronizing the body to the environment. In 1996, this hypothesis was confirmed by transplanting encapsulated SCN into the third ventricle of SCN-lesioned hamsters thereby restoring the circadian locomotor activity of these animals. The semipermeable polymeric capsule used in this experiment prevented the natural outgrow of neurones. However diffusion of hormones or other factors was not impaired by this membrane (Silver *et al.,* 1996). Similar results have been obtained by surgical isolation of the SCN *in vivo*, which disrupted the photoperiodic

response (e.g. gonad regression failure in hamsters in DD) but not the rhythmic locomotor activity (Hakim *et al.*, 1991). During the last few years, several diffusible signalling molecules of the circadian clock have been identified.

Rhythmic locomotor activity for example has been found to be inhibited by an injection of transforming growth factor α (TGFα) into the third ventricle. Thus TGFα seems to be an inhibitory factor for locomotor activity that is secreted by the SCN during the day. Furthermore, TGFα mRNA is expressed rhythmically in the SCN and peaks in the middle of the day in the Syrian hamster. This peptide exerts its action through binding on epidermal growth factor receptor (EGFR) localized in the SPZ. Indeed, a mutation in this receptor leads to increased daytime activity in mice. However, *waved-2* mutant mice (EGFR activity reduced by about 80-95 % compared to the wild-type; *Egfr*$^{-/-}$ mutant mice are not viable) only display increased daytime activity compared to the wild-type under light dark cycles but show normal activity patterns under DD conditions (Kramer *et al.*, 2001). This finding raises the question whether TGFα influences locomotor activity only under diurnal but not circadian conditions.

Besides TGFα, prokineticin 2 (*Pk2*), which is expressed in the SCN and peaks at the beginning of the day, is thought to be implicated in the regulation of locomotor activity. Similar to TGFα, injecting PK2 into the third ventricle during night-time abolishes locomotor activity (Cheng *et al.*, 2002). Moreover, a light pulse at night induces *Pk2* mRNA in the SCN, which leads to a subsequent block in locomotor activity (Cheng *et al.*, 2002; Cheng *et al.*, 2005). PK2 receptors are expressed in several brain regions like the PVN, the DMH and at high levels in the paraventricular thalamic nucleus. However, the role of PK2 in the regulation of locomotor activity is controversial: first of all, the PK2 receptor is absent in the SPZ (Cheng *et al.*, 2002) although this region is strongly implicated in the regulation of locomotor activity (Lu *et al.*, 2001). Second of all, expression levels of PK2 should be opposite in nocturnal versus diurnal animals if PK2 is a real inhibitor of locomotor activity. Yet this is not the case in the diurnal species *Arvicanthis niloticus* where *Pk2* also peaks during the day. But the possibility remains that PK2 acts as an activator of locomotor activity in diurnal animals whereas it is an inhibitor in nocturnal species. The fact that the PK2 receptor is absent in the SPZ of *Arvicanthis niloticus* as well, somehow weakens this hypothesis (Lambert *et al.*, 2005). Nevertheless, *Pk2* seems to be a CCG since it contains an E-box motif in its promoter, which allows its activation by binding of CLOCK-BMAL1 heterodimers (Cheng *et al.*, 2002). Time will help us learn more about the role of PK2 within the circadian clockwork.

Recently, another factor inhibiting daytime locomotor activity has been identified: cardiotrophin-like cytokine (CLC). It is expressed in a circadian fashion within AVP neurons in the SCN peaking at the end of the day and its receptors are located in the third ventricle. Like TGFα and PK2 its injection inhibits locomotor activity (Kraves & Weitz, 2006). Perhaps these three peptides may act together to influence locomotor activity.

2.6.4.3 Peripheral oscillators and their hierarchical organization

The current view is that most if not all cells of the body contain their own autonomous circadian clockwork (Balsalobre *et al.*, 2000). This allows tissue-based and even cell-specific interpretation of endocrine or neuronal signals sent by the SCN. In contrast to simpler animals such as *Drosophila* and zebrafish, peripheral oscillators of mammals are organized into a strict hierarchy (fig. 2-12). Time cues sent by the SCN are thought to coordinate peripheral oscillators and to impose cellular synchrony within a given tissue. To test this hypothesis, organs of SCN-lesioned animals were extracted and cultured. As expected, their oscillations were out of phase with one another. Surprinsingly, the oscillations within a given tissue were nicely synchronized suggesting the presence of organ-specific synchronizers (Yoo et al., 2004; Stratmann & Schibler, 2006). Nevertheless, the observed synchrony within a tissue could be a simple culture artefact because changing culture medium is sufficient to reset desynchronized oscillators (Yamazaki et al., 2000). Finally, Guo and colleagues (2006) showed that the capacity of tissues to oscillate *in vitro* does not implicate that they are also rhythmic *in vivo*. They studied *Per1, Per2* and *Bmal1* gene expression by *in situ* hybridization in SCN-lesioned versus control hamsters. Since *Pers* and *Bmal1* oscillate 180° out of phase from one another, the *Per:Bmal1* ratio in control animals should give a large peak during the course of a cycle. As expected this large peak could be observed in peripheral tissues of control but not SCN-lesioned animals indicating arrhythmicity among cellular oscillators. Summarizing this paragraph, one can say that there is much evidence for the SCN to be the coordinator for timing of peripheral oscillators and that it is the SCN as well that imposes cellular synchrony within a given tissue.

However, this relationship between the SCN and the periphery has been shown not to be as linear as it had been hypothesized some time ago. Restricted feeding for example has the power to uncouple circadian gene expression, especially in the liver (but also in other peripheral tissues), from the pacemaker (Damiola *et al.*, 2000; Stokkan *et al.*, 2001). This finding implies that metabolism and circadian clocks are tightly interwoven with each other via complex feedback mechanisms. Depending on the situation, circadian clocks either drive

the periphery or metabolic parameters affect the clock. To come back to the example of restricted feeding it is interesting to mention that the speed and the degree to which an organ changes its circadian rhythm vary between organs. The complex relationship between the pacemaker and the periphery in this context is underlined by the fact that tissues lacking glucocorticoid receptors shift their phases much faster compared to tissues carrying it. Furthermore, tissues of adrenalectomized animals also entrain faster when feeding time and photoperiod are shifted to opposite phases compared to sham operated animals (Le Minh *et al.*, 2001). This implicates that the clock phase is set differently *in vivo* by food availability and glucocorticoid secretion. Astonishingly, administration of glucose alone is able to shift clock gene expression in cultured cells suggesting that basic food metabolites could be sufficient to entrain peripheral oscillators (Hirota *et al.*, 2002). Another factor that can strongly influence the periphery without altering the SCN is fluctuating body temperature. Brown and colleagues (2002) have shown that body temperature rhythms in mammals can sustain oscillations in peripheral clocks.

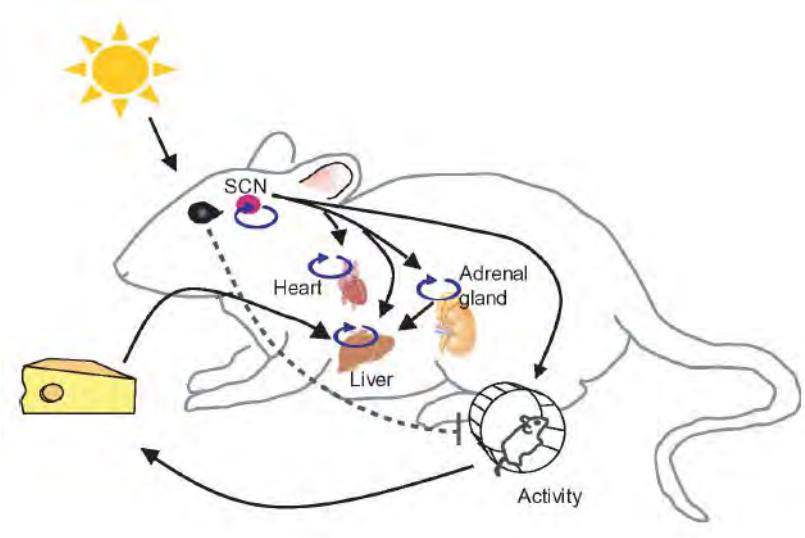

Fig. 2-12: Hierarchical organization of body clocks. Many tissues throughout the body continue to cycle for a few cycles when isolated in vitro, however, the oscillations eventually dampen. The SCN is generally considered to be the primary organizer of peripheral body oscillators, functioning to coordinate timing between various tissue oscillators and to synchronize oscillations among the cell-autonomous oscillators within a given tissue. Importantly, there is a food-entrainable oscillator that is maintained in SCN-lesioned animals exposed to a feeding schedule. Feedback likely involves glucocorticoid release from the adrenal gland into the bloodstream that is then sensed in brain regions outside the SCN (feedback not shown). In the intact system, the food-entrainable oscillator and the SCN oscillate in a coordinated manner due to SCN regulation of locomotor activity, the animal will only eat when it is awake, timed primarily by the SCN. Dashed line represents "masking". This figure and the figure legend are taken from the introductory workshop of the 72nd Cold Spring Harbor Laboratories Symposium (2007): Clocks & Rhythms.

The findings mentioned in this section can be summarized nicely citing the following metaphor of H. Oster (2006): "The SCN act like the conductor of an orchestra that gives the pace he reads from the score (e.g. the sun). The music, however, is played by the instruments, the peripheral oscillators controlling the physiological and the behavioural state of the organism."

Nevertheless, before the periphery can start to play music, the incoming information has to be integrated by the pacemaker located in the SCN. To achieve the accuracy and reliability needed within an organism, the clock needs a molecular set-up that is well-engineered. The cogwheels of the mammalian oscillator and how they are meshed will be further detailed in the following paragraph.

2.6.5 Molecular machinery of the circadian clock in mammals

2.6.5.1 How everything started: chronology of clock gene discovery

In mammals, the molecular set-up of the circadian clock is more complex and less understood although it shares many homologies with that of *Drosophila*. Deciphering of the mammalian clock components started in 1988 with the serendipitous discovery of the *tau* mutation in Syrian hamsters (Ralph & Menaker, 1988). This spontaneous mutation shortens the period of circadian locomotor rhythm dramatically: homozygous hamsters have rhythms with periods close to 20 hours. However, it was only in 2000 that mapping studies revealed that this mutation resides within casein kinase 1ε (*mCK1ε*) as a C to T transversion in position 178 (Lowrey *et al.,* 2000). This point mutation leads to a deficiency in the ability of CK1ε to phosphorylate its targets, including PER proteins (Dey *et al.*, 2005). Nevertheless, recent studies suggest that *tau* is a gain-of-function mutation on specific residues within the sequence targeting PER proteins (Gallego & Virshup, 2007; Meng *et al.,* 2008). After the discovery of the *tau* mutant, the field stagnated for several years. The unravelling of the circadian clock was continued in 1994 with the discovery of the first mammalian clock gene following a mutagenesis screen in mice. The gene has been named *mClock* (*circadian locomotor output cycles kaput*) because mice carrying a mutation in this gene lost their rhythmic wheel-running behaviour after two weeks in constant darkness (Vitaterna *et al.*, 1994). Between 1997 and 1998, scientists finally succeeded in isolating and characterizing the mammalian homologues of the *Drosophila period* genes, *mPer1* (initially named *Rigui*), *mPer2*, and *mPer3* (Sun *et al.,* 1997; Tei *et al.,* 1997; Zheng *et al*., 1999; Shearman *et al*., 2000; Zheng *et al*., 2001; Bae *et al.*, 2001). Several studies further attempted to identify the functional partner of CLOCK. In 1998, Hogenesch and colleagues discovered several binding partners *in vitro*. Due to the fact that they all carry a PAS domain, they were called “members of the PAS (MOP) superfamily”.

Within the following years, many circadian clock genes were identified in mammals and many of them were found to have orthologues in *Drosophila*: *mCry1* and *mCry2* (cryptochrome; van der Horst *et al.*, 1999; Vitaterna *et al.*, 1999), the *mClock* partner *mBmal1*

(brain and muscle ARNT-like 1; *mMop3*; orthologue to *cyc*; Bunger *et al.*, 2000), *mNpas2* (*mMop4*; analogue of *mClock*; Hogenesch *et al.*, 1998; Reick *et al.*, 2001). Later on, *mRev-Erbα* (*mNr1d1*; Preitner *et al.*, 2002), *mRorα* (*mNr1f1*; Sato e*t al.*, 2004), *mTim* (Barnes *et al.*, 2003), and the two basic helix-loop-helix (bHLH)-PAS proteins mDEC1 (SHARP2) and mDEC2 (SHARP1; Honma *et al.*, 2002; Rossner *et al.*, 2008) have been identified as well. A summary of current mammalian clock genes along with their properties and mutation phenotypes is listed in table 2-2.

Table 2-2: Mouse circadian clock and clock-related genes (adapted from: Ko & Takahashi, 2006)

	Average CT at peak expression				
Gene	**SCN**	**Periphery**	**Allele**	**Mutant phenotypes in DD**	**References**
Bmal1	15-21	22-02	*Bmal1*$^{-/-}$	Arrhythmic	Bunger *et al.*, 2000
Clock	Constitutive	21-03	*Clock*$^{\Delta 19/\Delta 19}$	4 h longer period/arrhythmic	Vitaterna *et al.*, 1994
			Clock$^{-/-}$	0.5 h shorter period	DeBruyne *et al.*, 2006
Per1	4-8	10-16	*Per1*^{Brdm1}	1 h shorter period	Zheng *et al.*, 2001
			Per1^{ldc}	0.5 h shorter period	Bae *et al.*, 2001
			Per1$^{-/-}$	0.5 h shorter pd /arrhythmic	Cermakian *et al.*, 2001
Per2	6-12	14-18	*Per2*^{Brdm1}	1.5 shorter pd /arrhythmic	Zheng *et al.*, 1999
			Per2^{ldc}	Arrhythmic	Bae *et al.*, 2001
Per3	4-9	10-14	*Per3*$^{-/-}$	0-0.5 h shorter period	Shearman *et al.*, 2000
Cry1	8-14	14-18	*Cry1*$^{-/-}$ [a]	1 h shorter period	van der Horst *et al.*, 1999 Vitaterna *et al.*, 1999
Cry2	8-14	8-12	*Cry2*$^{-/-}$ [a]	1 h longer period	van der Horst *et al.*, 1999 Thresher *et al.*, 1998
Rev-erbα	2-6	4-10	*Rev-Erbα*$^{-/-}$	0.5 h shorter period Disrupted photic entrainment	Preitner *et al.*, 2002
Rorα	6-10	arr. various[b]	*Staggerer*	0.5 h shorter period Disrupted photic entrainment	Sato *et al.*, 2004
Rorβ	4-8	18-22	*Rorβ*$^{-/-}$	0.5 h longer period	Andre *et al.*, 1998 Sumi *et al.*, 2002
Rorγ	N/A[c]	16-20 various[b]	*Rorγ*$^{-/-}$	Unknown	
NPAS2	N/A[c]	0-4	*NPAS2*$^{-/-}$	0.2 h shorter period	Dudley *et al.*, 2003
Bmal2	Constitutive			n/d[e]	Hogenesch *et al.*, 2000 Ikeda *et al.*, 2000 Okano *et al.*, 2001
CK1ε	Constitutive	Constitutive	*CK1ε*^{tau} [d]	0.4 h shorter period	Lowrey *et al.*, 2000
			CK1ε$^{-/-}$	0.3 h longer period	Meng *et al.*, 2008
CK1δ	Constitutive	Constitutive	*Csnk1δ*$^{-/+}$	0.5 h shorter period	Xu *et al.*, 2005
Dec1	2	14	*Dec1*$^{-/-}$	No difference in period	Grechez-Cassiau *et al.*, 2004
			Dec1$^{-/-}$	0.15 h longer period	Nakashima *et al.*, 2008
			Sharp2$^{-/-}$	No difference in period	Honma *et al.*, 2002 Rossner *et al.*, 2008
Dec2	6	14	*Sharp1*$^{-/-}$	No difference in period	Honma *et al.*, 2002 Rossner *et al.*, 2008
Tim	12[f]	various	n/d[e]	embryonically lethal	Barnes *et al.*, 2003 Li *et al.*, 2000
Fbxl3	n/d[e]	n/d[e]	*Fbxl3*$^{-/-}$	2-3 h longer period	Siepka *et al.*, 2007 Busino *et al.*, 2007 Godinho *et al.*, 2007

[a]Two independent groups generated *Cry1* and *Cry2* null mutants and the mice showed similar phenotypes.
[b]See: Akashi & Takumi, 2005; Guillaumond *et al.*, 2005 ; Ueda *et al.*, 2005
[c]N/A = not detected in the SCN
[d]Hamster mutation
[e]n/d = not determined
[f]The *Tim* full-length transcript is rhythmically expressed in the SCN but not the short form (Barnes *et al.*, 2003).

As further detailed below, the molecular clockwork in mammals is based on interlocked positive and negative transcriptional/translational feedback loops (TTLs) consisting partly of the genes mentioned above (fig. 2-13).

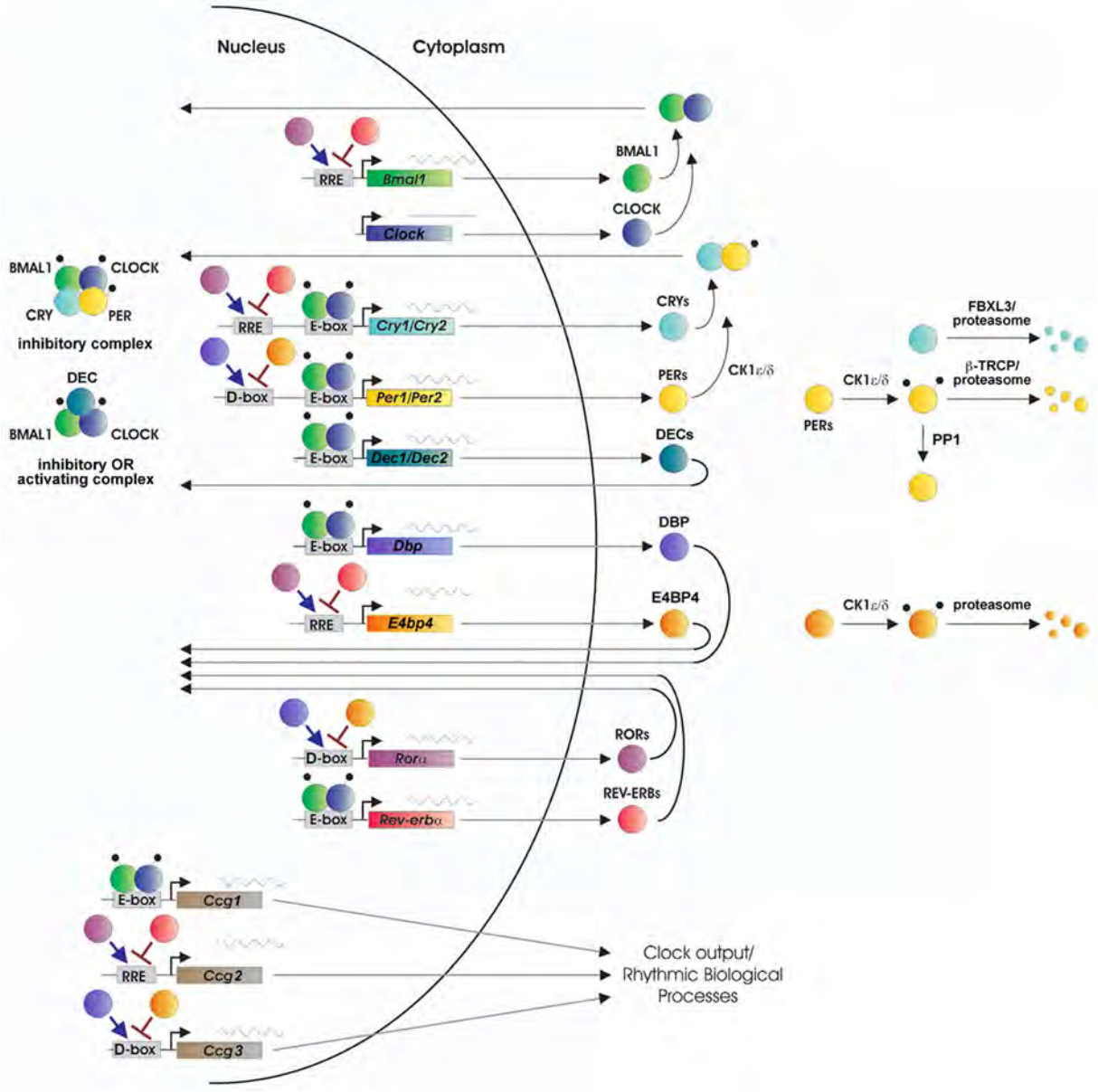

Fig. 2-13: A network of transcriptional-translational feedback loops constitutes the mammalian circadian clock. Clock gene and ccg transcription is regulated via three main enhancer motifs: E-box, RRE and D-box. Transcription from E-boxes is mediated by CLOCK/BMAL1 heterodimers. D-box dependent transcription is mediated by competitive binding of activators (mainly DBP, TEF and HLF) and its repressor (E4BP4). Similarly, RRE mediated transcription is activated by RORα and repressed by REV-ERBα. Black circles represent phosphorylation sites. ccg, clock-controlled gene; CK1, casein kinase 1; dbp, albumin D-element binding protein; D-box, DBP/E4BP4-binding element; E-box, CLOCK/BMAL1-binding element; E4bp4, E4 promoter binding-protein 4; RRE, retinoic acid related orphan receptor response element. The picture has been kindly provided by Sonja Langmesser who was inspired by Ko & Takahashi (2006) and the thesis of Gabriele Hampp (2007).

2.6.5.1 The core loop

The basis of the mammalian clockwork consists of the core loop composed by the following genes: *mClock, mBmal1, mPer1, mPer2, mPer3, mCry1* and *mCry2*.

The positive elements of the core loop are encoded by the two transcription factors CLOCK and BMAL1. Both of them harbour a bHLH-PAS domain, which allows DNA binding and heterodimerization. Once the complex has formed in the cytoplasm, the heterodimer translocates into the nucleus. This nuclear entry is mediated by BMAL1, which carries both nuclear localization signals and nuclear export signals that allow it to shuttle between the nucleus and the cytoplasm to promote nuclear translocation of CLOCK (Kwon *et al.*, 2006). CLOCK-BMAL1 heterodimers mediate transcriptional activation of target genes that present E-box (consensus sequence: CACGTG) *cis*-regulatory enhancer tandems in their promoter (Gekakis *et al.*, 1998; Hogenesch *et al.*, 1997; Hogenesch *et al.*, 1998; Travnickova-Bendova *et al.*, 2002; Yoo *et al.*, 2005; Nakahata *et al.*, 2008). These positively regulated genes include *Pers, Crys, Rev-Erbα, Rorα* and several other clock and clock-controlled genes. It is noteworthy, that their mRNA transcripts accumulate in antiphase to *Bmal1* mRNA (fig. 2-14). In the cytoplasm, PER proteins form complexes with CRYs, which then enter the nucleus. Once the complexes reach their destination, the CRYs inhibit the CLOCK/BMAL1 driven transcription, thereby establishing a negative feedback loop (Griffin *et al.*, 1999; Jin *et al.*, 1999; Kume *et al.*, 1999). The suppressed E-box driven transcription leads to a decline in

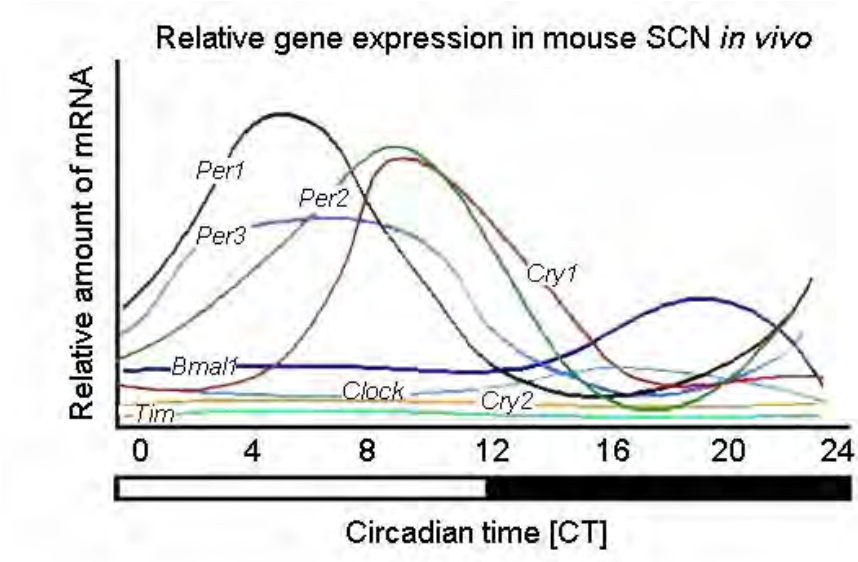

Fig. 2-14: Members of the negative limb oscillate in antiphase to *Bmal1*. In mammals, *Bmal1* mRNA peaks at around circadian time (CT) 18 and *Clock* is expressed constantly contrasting with the situation in *Drosophila*. *Per1* reaches its peak at midday whereas *Per2* and *Cry1* peak at the late day. *Per3* has a broader peak expression all over the day. *Cry2* and *Tim* seem not to cycle much. (Adapted from G.E. Duffield)

PER and CRY protein levels which finally leads to a re-activation of CLOCK-BMAL1 driven transcription. Hence the next circadian cycle is re-initiated.

This basic feed-back loop allows oscillations on a 24 hour basis. It is of note that the role of CLOCK in the circadian clock core loop has been challenged recently because a null mutation in *Clock* does not alter rhythmic locomotor behaviour of mice in DD. These results suggest that NPAS2 (a CLOCK paralog) could take over the role of CLOCK in its absence in knockout mice (DeBruyne *et al.,* 2006). Moreover, BMAL2 (MOP9; an analogue to BMAL1) has also been shown to form active heterodimers with either CLOCK or NPAS2 (Hogenesch *et al.*, 2000; Ikeda *et al.*, 2000). However, both the capacity to activate transcription and the extent of repression by the CRYs differ between the various heterodimers (i.e. CLOCK/BMAL1, CLOCK/BMAL2, NPAS2/BMAL1, NPAS2/BMAL2). This observation suggests that they fulfil slightly different roles within the molecular clock that may prove important *in vivo* (Dardente *et al.*, 2007).

2.6.5.2 The secondary loops

The oscillations generated by the core loop are further modulated (e.g. amplitude, precision, stability) by other interlocking feedback loops. These TTLs seem to be less important for normal rhythm generation as knock-out mice for those genes do not prevent self-sustained rhythmic behaviour. Nevertheless, they add to the precision of the clockwork and they reduce its sensitivity to external and internal "noise". The so-called stabilizing loop involving the orphan nuclear receptors REV-ERBα and RORα is probably the best characterized of these loops to date (fig. 2-13). Recently it has even been suggested that the nuclear receptor co-factor and master metabolic regulator PGC-1α (peroxisome proliferator-activated $PPAR_{\gamma}$ co-activator) potentiates RORα mediated activation of *Bmal1* transcription. Hence, PGC-1α could integrate the mammalian clock and the energy metabolism (Liu *et al.,* 2007).

2.6.5.2.1 The stabilizing loop

The REV-ERBα protein represses *Bmal1* transcription by binding to 2 RORE (ROR [retinoic acid related orphan receptor] response element) sequences in the *Bmal1* promoter (Preitner *et al.*, 2002; Ueda *et al.,* 2002). Besides REV-ERBα, RORα too binds the RORE sequences in the *Bmal1* promoter (Sato *et al.,* 2004). However, in contrast to REV-ERBα, RORα activates *Bmal1* transcription (Giguere, 1999; Akashi & Takumi, 2005). Hence the two proteins compete for the RORE sequences thus interconnecting the positive and negative limbs of the clock (Guillaumond *et al*., 2005). Their opposing effects on *Bmal1* expression is also reflected *in vivo*: *Rev-erbα* knock-out mice (Preitner *et al*., 2002) show constitutively high *Bmal1*

mRNA levels whereas *Staggerer* mice (loss-of-function mutation of *Rorα*; Sato *et al.*, 2004) show strongly reduced *Bmal1* levels. Expression of *Rev-Erbα* in the mouse SCN oscillates in a circadian fashion with a peak at midday and a trough at midnight (Onishi *et al.*, 2002; Panda *et al.*, 2002b; Preitner *et al.*, 2002; Ueda *et al*., 2002). Similarly, *Rorα* peaks at midday and has its minimum at midnight (Sato *et al.*, 2004). Additionally, it has been shown that members of ROR (α, β and γ) and REV-ERB (α and β) families are able to regulate *Bmal1* through ROREs in general (Guillaumond *et al*., 2005). Furthermore, tissue-specific molecular clock mechanisms could exist as *Rev-Erbs* appear to be rhythmically and ubiquitously expressed throughout the body (Guillaumond et al., 2005; Yamamoto *et al.*, 2004) whereas *Rors* are expressed in a tissue specific manner.

2.6.5.2.2 DEC1 & DEC2: an example of another interlocked loop

Both, *Dec1* and *Dec2* are bHLH transcription factors which are expressed rhythmically in the SCN with a peak at early day/midday and a trough at midnight/late night (Honma *et al.*, 2002). *In vitro* studies have suggested that their transcription is directly activated by CLOCK/BMAL1 heterodimers binding to E-boxes located in their promoter (Hamaguchi *et al.*, 2004; Kawamoto *et al*., 2004). In line with these observations it has been found that *Dec1* as well as *Dec2* levels are decreased in *Clock* mutant mice (Butler *et al.*, 2004). By competing with CLOCK/BMAL1 for binding to the E-box motifs, DEC1 and DEC2 inhibit their own transcription (Hamaguchi *et al.*, 2004; Kawamoto *et al*., 2004). However, it might also be possible that this inhibition is mediated through an interaction with BMAL1 because DEC1 and DEC2 can bind BMAL1 (Honma *et al.*, 2002). Furthermore, PERs and CRYs have also been shown to inhibit *Dec1* and *Dec2* transcription *in vitro* (Hamaguchi *et al.*, 2004; Kawamoto *et al*., 2004).

For the time being, DEC1 and DEC2 are thought to play an important role in inhibiting CLOCK/BMAL1 mediated transcription as it has been observed *in vitro* (Honma *et al.*, 2002; Hamaguchi *et al.*, 2004; Kawamoto *et al.*, 2004). Recently, two studies confirmed that DECs seem to play a role in fine tuning the regulation and robustness of the molecular clock (Rossner *et al.*, 2008; Nakashima *et al.*, 2008).

2.6.5.4 Timing of the loops via CK1

In addition to transcriptional regulation, posttranslational modifications of clock genes have been found to be critical in setting clock speed in mammals (Lee *et al.*, 2001; Gallego &

Virshup, 2007). Reversible phosphorylation for example provides a particularly functional tool for the regulated formation of protein complexes, their nuclear entry, and their subsequent degradation. Not surprisingly, phosphorylation of PER proteins by casein kinase 1ε or the highly homologous CK1δ has been shown to be crucial in determining the pace of the clock (Ralph & Menaker, 1988; Dey *et al.*, 2005; Meng *et al.*, 2008). CK1 activity can be inhibited through autophosphorylation of eight sites located in its C-terminus (Graves & Roach, 1995; Cegielska *et al.*, 1998; Gietzen & Virshup, 1999). Conversely, CK1 kinase activity can be restored by the action of PP1, PP2A, PP2B (calcineurin) and PP5 which are able to dephosphorylate these amino acids *in vitro* (Cegielska *et al.*, 1998; Lowrey *et al.*, 2000; Partch *et al.*, 2006).

Both, CK1ε and CK1δ are expressed constitutively in the mammalian SCN (Lowrey *et al.*, 2000; Takano *et al.*, 2000; Ishida *et al.*, 2001; Lee *et al.*, 2001). Furthermore, they have been shown to interact with and phosphorylate PER1 as well as PER2 in mice (Keesler *et al.*, 2000; Camacho *et al.*, 2001) and human (Vielhaber *et al.*, 2000; Akashi *et al.*, 2002; Eide *et al.*, 2002). On the contrary, PER3 does not show any stable interactions with CK1ε and is not translocated into the nucleus. This characteristic could explain why *Per1* (Cermakian *et al.*, 2001) and *Per2* (Zheng *et al.*, 1999) are able to sustain molecular circadian rhythms whereas *Per3* can't (Lee, Weaver & Reppert, 2004). However, CK1ε and CK1δ do not only interact with PERs but also complex with CRYs (Lee *et al.*, 2001) and CK1-mediated phosphorylation of BMAL1 increases its transcriptional activity (Eide *et al.*, 2002). Recent studies suggest that phosphorylation of PERs can be both destabilizing and stabilizing at once (Partch *et al.*, 2006; Vanselow *et al.*, 2006). This hypothesis has been further strengthened by the confirmation that $CK1\varepsilon^{tau}$ is a gain of function mutation which accelerates the clock (Meng *et al.*, 2008). PER (but not CRY) degradation seems to be enhanced at specific phases of the circadian cycle (i.e. early night) leading to asymmetric PER stability over time and subsequent altered phasing of physiology and behaviour. Similarly it has been shown that *CK1ε* knockouts display a slightly longer period under DD. However, hamsters heterozygous for $CK1\varepsilon^{tau}$ still have a shorter period under DD than the wild-type controls. From this, they conclude that CK1δ may phosphorylate PERs. Hence, wild-type CK1ε seems to be partially redundant with CK1δ in the circadian timing mechanism (Meng *et al.*, 2008). Nevertheless, this issue has to be clarified in the future using *CK1δ* knockouts. Altogether, CK1ε/δ is thought to ensure a tight regulation of the timing of transcriptional repression mediated by the members of the negative limb.

2.6.5.5 Multiple regulations of the molecular clock machinery

There exist two major prejudices about mRNA and protein abundance: mRNA oscillations are controlled by rhythmic transcription, and the amount of mRNA reflects the amount and activity of its corresponding protein. These assumptions may be true for many genes but in general, various mechanisms interfere with mRNA as well as protein levels and activity (Garbarino-Pico & Green, 2007). For instance, the amount of a particular mRNA can decrease although its transcription increases if the speed of its degradation increases even more. Not surprisingly, this assertion is also true for protein abundance. The final level and activity of a given protein is tightly regulated at several steps from the gene to the active protein. Although the TTL model is well established as being the basis of the circadian clockwork, many studies suggest that it does not sufficiently explain the accuracy of the clock machinery (see Hastings, 2001; Shu & Hong-Hui, 2004; Reddy *et al.*, 2004). Due to this, it is believed that additional levels of regulation must be present.

2.6.5.5.1 Transcriptional regulation

Besides the E-box and RORE motifs mentioned earlier, circadian transcription can be regulated via cyclic adenosine-3'-5'-monophosphate (cAMP) response elements (CRE) and structural modifications of chromatin. CRE motifs (TGACGTCA) have been found in *Per1* (Hida *et al.*, 2000) and *Per2* promoters (Travnickova-Bendova *et al.*, 2002). It has been shown that CRE motifs are important for the light-induced expression of *Per1* through CREB (CRE binding protein; Obrietan *et al.*, 1999; Travnickova-Bendova *et al.*, 2002). Upon light stimulation CREB is phosphorylated (pCREB) and hence activated by ERK1/2. The binding of pCREB to CRE requires the interplay of the two co-activators CBP and p300 (Kwok *et al.*, 1994; Lee *et al.*, 1996; De Cesare & Sassone-Corsi, 2000). Interestingly, it has been demonstrated that CRE-mediated transcription cycles rhythmically under DD conditions in the mouse SCN with a peak at CT2-6 and a nadir at CT18. Consistently pCREB abundance is cycling too in the SCN with highest expression at CT18-22 and a trough at CT10 (Obrietan *et al.*, 1999). It is worth mentioning that CRE-mediated transcription seems to be independent of CLOCK/BMAL1 regulation (Travnickova-Bendova *et al.*, 2002).

Additionally to the regulation via elements embedded in the promoter, transcription can be influenced by changes in chromatin structure. In the nucleus, DNA is tightly packed with histones. Eight of these proteins, together with about 200 bp of DNA, form a basic building unit called nucleosome (Kornberg, 1974). The conformation of chromatin can be altered by various histone modifications: acetylation, phosphorylation, methylation, ubiquitylation or

ADP-ribosylation (Strahl & Allis, 2000). These post-translational changes lead to either loosening or tightening of chromatin resulting in enhanced or reduced gene transcription respectively. Of course, like any other gene, clock gene expression is modulated by chromatin structure alterations. For instance, the acetylation of the histone H3 in *Per1* and *Per2* promoters displays a circadian rhythm (Etchegaray *et al.,* 2003). Increased acetylation of H3 and H4 has even been associated with *Per1* and *Per2* induction after a light pulse in the early subjective night (CT16; Naruse *et al.,* 2004). Furthermore, the histone acetyltransferases (HAT) CBP and p300 interact rhythmically with CLOCK and BMAL1 proteins (Takahata e*t al.,* 2000; Etchegaray *et al.*, 2003; Curtis *et al*., 2004). In 2006, CLOCK itself was identified to be a HAT (Doi *et al.,* 2006). In contrast to acetylation, histone deacetylation represses gene transcription. CRY1-mediated repression of *Per1* and *Per2* transcription is associated with the rhythmic recruitment of the co-regulator mSIN3 and the histone deacetylases (HDAC) 1 and 2 (Naruse *et al.,* 2004). Likewise, CRY2 inhibits transcription by disrupting the association of p300 with CLOCK (Curtis *et al.,* 2004). Moreover, REV-ERBα was found to recruit HDAC3 to the *Bmal1* promoter which decreases H3 and H4 acetylation (Yin & Lazar, 2005). Besides acetylation, also histone methylation changes rhythmically as demonstrated on the promoters of *Per1* (Brown *et al.,* 2005; Etchegaray *et al.,* 2006) and of the clock-controlled gene *Dbp* (*D-element binding protein*; Ripperger & Schibler, 2006).

2.6.5.5.2 Post-transcriptional regulation

Short oscillations of a few hours can be obtained by simple feedback loops (e.g., a two hour period for the auto-regulation of *Hes1*; Hirata *et al.*, 2002) whereas longer periods like circadian rhythms require numerous regulatory mechanisms. Contrary to transcription, post-transcriptional regulation of clock genes attracted relatively little attention so far. Nevertheless, the fate of mRNAs after transcription is crucial for proper timing of the clock (Harms *et al.*, 2004). The circadian system could modulate the mRNA during nuclear processing (e.g. capping, splicing, polyadenylation and messenger quality control), nuclear export, and sorting for storage of specific localization. It is a well-known fact that the 3'-UTR of mRNAs plays a crucial role in determining stability, localization and translational efficiency of its transcripts (Grzybowska *et al.*, 2001). Moreover, length regulation of the poly(A) tail, which is added to the 3'-end of mRNAs, is critical for their stability (Wilusz *et al.,* 2001). Shortening of the poly(A) tail triggers decapping of the 5'-end of RNA which in turn initiates degradation by exonucleases (Couttet *et al.,* 1997). To date, only few

mechanisms of post-transcriptional regulation have been discovered for the circadian clock and most of the ones that are known were unravelled only recently.

For example, the circadian regulation of *Per1* is influenced by the RNA binding protein LARK, which recognizes a *cis* element in the 3'-UTR of *Per1* mRNA. Alterations in *Lark* expression lead to significant changes in circadian period *in vitro* (Kojima *et al., 2*007). A recent report even shows that the abnormal circadian rhythms observed in patients suffering from fragile X could be due to altered regulation of the clock by LARK. They suggest that in flies, LARK and FMRP (fragile X mental retardation protein) cooperate to post-transcriptionally regulate target RNAs that are relevant for circadian and other biological functions (Sofola *et al.*, 2008). Furthermore, a circadian regulation of vasopressin (*Avp*) mRNA poly(A) tail length was observed in the SCN with lowest transcript levels during the night. Interestingly, mRNA species with short poly(A) tail length is detected at this time (Robinson *et al.*, 1988). In general, a long poly(A) tail stabilizes mRNA, suggesting that *Avp* mRNA decay rates are higher when the poly(A) tail is shorter. To date only one protein is known to alter the length of the poly(A) tail of clock gene mRNA. This deadenylase (an exoribonuclase specific for poly(A) tails of mRNAs) has been identified in *Xenopus* retina and was named NOCTURNIN (NOC) by virtue of its high nocturnal increase in transcript levels (Green & Besharse, 1996a/b). In 2003, it was shown in this frog that NOC is involved in circadian regulation of the stability and/or translation of mRNAs (Baggs & Green, 2003). As in *Xenopus*, the mammalian NOC is under circadian control (Wang *et al.*, 2001; Barbot *et al.*, 2002) and exhibits deadenylase activity (Garbarino-Pico *et al.*, 2007) indicating that it could influence a wide range of transcripts. Besides the post-transcriptional regulations already mentioned, circadian variations in splicing variants seem to be important as well in tuning the clock. In the mouse, *Presenilin2* expresses two forms that are rhythmic and a third one that is not (Belanger *et al.*, 2006). However, it is not clear whether this is due to circadian modulation of the spliceosome machinery or the stability of the splice variant itself. Moreover, the full-length mRNA of *Timeless* is rhythmically expressed in the SCN but not its short transcript variant (Barnes *et al.*, 2003).

2.6.5.5.3 Post-translational regulation

As already mentioned above, the clock's molecular machinery relies on tightly interlocked TTLs. This term indicates that proper timing of clock protein activity, dimerization, nuclear import and export, and finally degradation are indispensable for accurate functioning. In mammals, the first hint for the importance of post-translational regulation within the clock

came from the *tau* mutant hamster (Ralph & Menaker, 1988). As described previously, this mutation is located within the CK1ε gene (Lowrey *et al.*, 2000) and leads to changes in PER phosphorylation levels (Lowrey *et al.*, 2000; Takano *et al.*, 2000; Miyazaki *et al.*, 2004; Vanselow *et al.*, 2006). It turns out that phosphorylation is crucial in setting the pace of the clock. Several proteins of the core loop (e.g. PER1, PER2, CLOCK, BMAL1) were found to display rhythmic phosphorylation levels in the liver (Lee *et al.*, 2001 & 2004). In addition to the casein kinases, other kinases are involved in the clock. Glycogen synthase kinase 3 (GSK3) was found to phosphorylate CRY2 (Harada *et al.*, 2005), PER2 (Iitaka *et al.*, 2005), and REV-ERBα (Yin *et al.*, 2006). Phosphorylation of CRY2 and PER2 promotes their nuclear localization. Moreover, CRY2 is marked this way for proteasomal degradation (Harada *et al.*, 2005). By contrast, phosphorylated REV-ERBα is stabilised and protected form degradation by the proteasome pathway (Yin *et al.*, 2006). Furthermore, mitogen-activated protein kinases (MAPK; ERK) are implicated in BMAL1 phosphorylation (Sanada *et al.*, 2002) leading to a decrease in CLOCK-BMAL1-mediated transcription. More recently, CRY1 and CRY2 proteins were shown to be potential substrates for ERK too (Sanada *et al.*, 2004) resulting in a decreased ability to inhibit CLOCK-BMAL1-induced transcription. This could lead to a progressive release of the inhibition of transcription, which would allow initiating the next cycle. Hence, phosphorylation of CRY1 and CRY2 promotes gene transcription whereas phosphorylation of BMAL1 suppresses it. These opposite effects create a time-lag within the clock period.

Recent studies emphasize the importance of positive factors' phosphorylation in the core loop (i.e. CLOCK, BMAL1, NPAS2, BMAL2; Dardente *et al.*, 2007; Kondratov *et al.*, 2006). Dardente and co-workers found that dimerization through the PAS domain is required for phosphorylation and for subsequent transactivation to happen. Since phosphorylated forms of BMAL1 are predominantly found in the nucleus at the time of maximal transcriptional activity of CLOCK-BMAL1 it is thought that BMAL1 phosphorylation may enhance transactivation of E-box sites (Eide *et al.*, 2002; Akashi *et al.*, 2006; Cardone *et al.*, 2005, Kondratov *et al.*, 2003; Ripperger & Schibler, 2006). Altogether, it seems that phosphorylation of a given protein does not depend on a single, but on several kinases acting at different sites. Undoubtedly, phosphatases are crucial in the regulation of the clock as well to counteract the effects of the kinases. Protein phosphatase 1 (PP1) was found to regulate PER2 stability (Gallego *et al.*, 2006) and PP5 regulates the activity of CK1ε on clock proteins (Partch *et al.*, 2006).

Since the clock tightly controls transcriptional regulation, it is only logical that protein degradation is in command of the circadian system. Recently, a trio of papers demonstrated that CRYs are targeted for degradation by the F-box E3 ubiquitin ligase FBXL3 (fig. 2-15; Siepka *et al.*, 2007; Busino *et al.*, 2007; Godinho *et al.*, 2007). Following a mutagenesis screen in mice, a circadian mutant named Overtime (Ovtm) was found, which displays a long period of approximately 26 hours. The Ovtm mutation has been identified to cause an

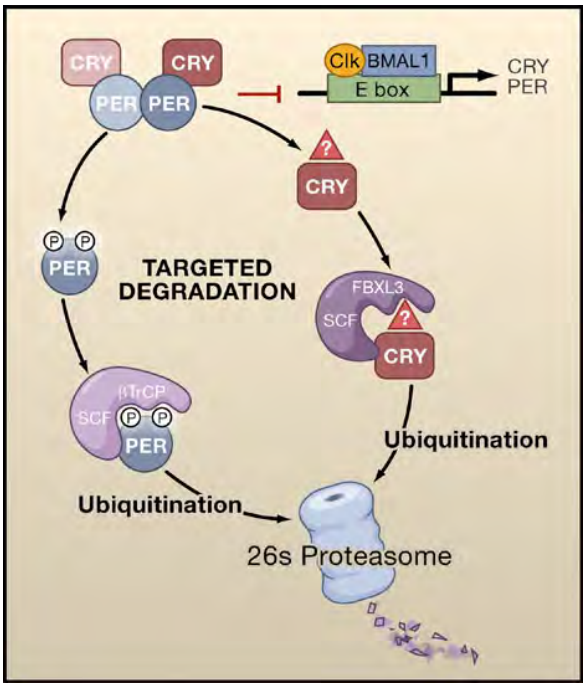

Fig. 2-15: Targeted degradation ends repression at night. PER and CRY proteins accumulate during the night and repress the CLOCK/BMAL1 heterodimeric transcriptional complex that controls PER and CRY transcription. Repression is relieved by degradation of PERs and CRYs; PER degradation requires phosphorylation by the casein kinase CK1ε, which mediates recruitment of the F-box ubiquitin ligase βTrCP. Degradation of CRYs requires their binding to the F-box protein FBXL3. Accelerated degradation of PERs shortens the circadian period, whereas delayed degradation of CRYs lengthens it. Whether CRYs are modified posttraslationally prior to FBXL3 binding is unknown (taken from Virshup & Forger, 2007).

isoleucine to threonine (I364T) substitution in the *Fbxl3* gene, which is a component of the SKP1-CUL1-F-box-protein (SCF) E3 ubiquitin ligase complex (Siepka *et al.*, 2007). Simultaneously, as it often happens in science, when screening mutagenized animals for alterations in rhythms of wheel-running activity, another group independently identified the same gene. Their mutated mouse displays free-running rhythms of about 27 hours in homozygotes. They named their mutation after hours (Afh) and found that it corresponds to a cystein to serine (C358S) substitution in the *Fbxl3* gene (Godinho *et al*, 2007). Although the two mutations are distinct from each other, both lie in the region of FBXL3 that binds to CRY. Hence the interaction of these two proteins is disrupted, preventing CRY degradation, thereby causing lengthening of the circadian period.

Note that another member of the F-box proteins, however, degrades PERs (Shirogane *et al.*, 2005). βTrCP recognizes phosphorylated but not unphosphorylated targets and mediates their degradation. Why the same F-box protein does not degrade both CRYs and PERs remains unknown. It is speculated that these proteins have to be degraded at different rates or times or

in different compartments (Virshup & Forger, 2007). The carefully controlled degradation of CRYs and PERs may influence the rate at which multimeric proteins accumulate in the cytoplasm as well as their disappearance from the nucleus.

Moreover, SUMOylation of BMAL1 has been discovered *in vitro* and *in vivo*. The small ubiquitin-related modifier protein (SUMO) is linked reversibly on a consensus sequence located between the two PAS domains involved in the interaction with CLOCK. It was shown that CLOCK-dependent SUMOylation of BMAL1 leads to its degradation (Cardone *et al.*, 2005).

2.6.6 Association of clock genes and photic entrainment of the SCN

The TTLs described above can be modulated by external signals. As mentioned previously, the strongest Zeitgeber for the clock is light. The RHT constituted of the pRGC of the retina directly innervates the core SCN and provide them with light information. In the laboratory, experimental animals can be completely isolated from the environment. To study the internal period of an animal it has to be placed under constant conditions. Nocturnal rodents are usually placed under constant darkness (DD) with food and water *ad libitum.* In rare cases they can be kept under constant light (LL). Endogenous rhythms are monitored by wheel-running activity, drinking behaviour, body temperature, etc. In the context of this thesis, wheel-running behaviour has been used exclusively. The wheel-revolutions the animal does are recorded by a computer and can be represented as so-called actograms (fig. 2-16).

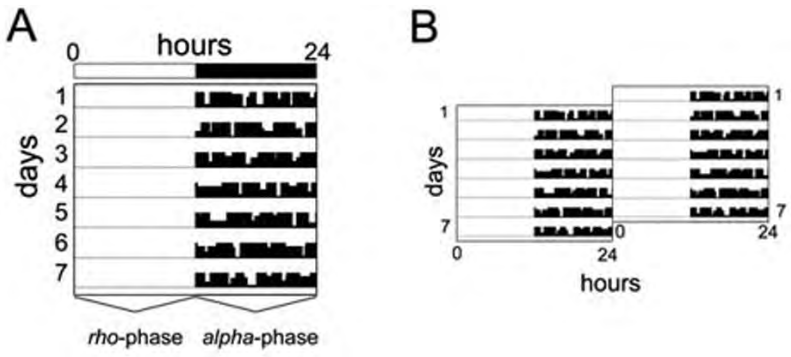

Fig. 2-16: Schematic single and double plotted actograms. (A) Wheel-running activity is plotted as an actogram with each horizontal line corresponding to one day. Black vertical bars plotted side-by-side represent the activity, i.e. number of wheel revolutions. The height of each vertical bar indicates the accumulated number of wheel revolutions for a given interval (e.g. 5 min). The rho- and alpha-phase marked at the bottom of the actogram refer to rest and activity, respectively. The white bar at the top of the scheme depicts light (12 h) and the black bar corresponds to darkness (12 h). **(B)** To better visualize behavioural rhythms, actograms are often double plotted by aligning two consecutive days horizontally (e.g. day 1 left and day 2 right; Jud *et al.*, 2005).

Under both DD and LL conditions, animals are found to "free-run" with a period slightly different from the 24-hour day. However, exposure to either DD or LL does not have

equivalent effects on the timing of rest and activity. LL conditions correspond to a constant exposure of the clock to a potent entraining agent whereas DD represents the absence of light input to the pacemaker. In LL, the period follows “Aschoff’s rule”: with increased light intensity the period of the locomotor cycle becomes longer and the length of time spent active decreases in nocturnal animals (Aschoff, 1960). For diurnal animals the opposite is true: increasing light intensity results in a decreased period and the time spent active expands.

2.6.6.1 Light pulses can provoke phase shifts in behaviour

To better study the impact of light on the circadian system animals kept under constant darkness are subjected to a brief light pulse at different time points. The effect of the stimulus can be studied by simply analyzing actograms or tissue samples. During the subjective day (corresponding to estimated day time for the animal) light has little or no effect on the resetting of the clock. By contrast, light exposure during the subjective night is capable of shifting the pacemaker (Aschoff, 1969; Daan & Pittendrigh, 1976). Furthermore, it depends whether the light is administered during the early or late night. While the former induces a phase delay (the locomotor activity of the animal will start later the next day) in nocturnal rodents, the latter leads to phase advances (activity will start earlier the next day; Daan & Pittendrigh, 1976). This phenomenon can be translated into a phase response curve (PRC; fig. 2-17), which plots the magnitude of the phase-shift as a function of the circadian phase when the light stimulus was applied. Another method to visualize this phenomenon is the phase transition curve (PTC) where the new phase of the animal is plotted versus the old phase. This graph does not distinguish between phase advances and delays.

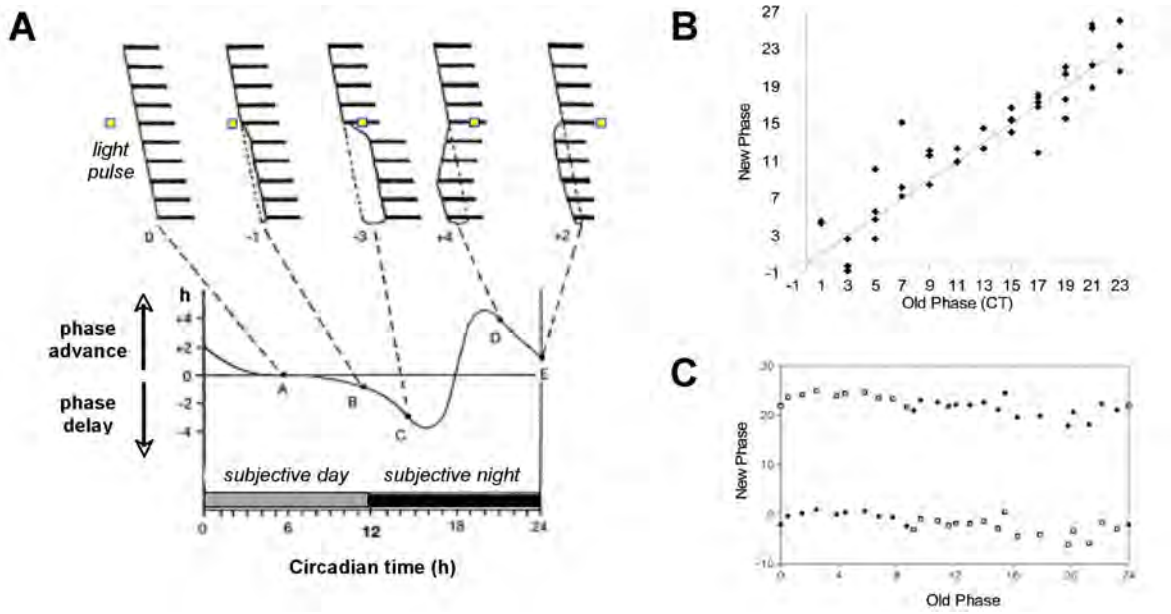

Fig. 2-17: PRC and PTC
(A) A light pulse (open yellow square) during the day (A) has no effect on the locomotor activity of a free-running nocturnal rodent. On the contrary, light at the beginning (B, C) and the end (D) of the night induces phase delays and phase advances in locomotor activity, respectively. Plotting the magnitude of the phase shifts as a function of the time of the light administration allows the drawing of a PRC (adapted from Serviere & Lavialle, 1996). **(B)** The phase transition curve (PTC) plots the old phase versus the new phase. If there is no phase shift observed after a light pulse, the dot lies on the diagonal (e.g. CT3). If the phase is shifted, the dot lies next to the diagonal (Carmona-Alcocer *et al.*, 2005: PTC of the freshwater crab). **(C)** Type 0 PTC of NIH3T3 cells. Dexamethasone can reset all clock gene phases in NIH3T3 cells. NIH3T3 cells transfected with *Bmal1*-luciferase were serum shocked at time 0. At the indicated circadian times (approximately every hour) parallel cultures were treated for 15 min with 100 nM dexamethasone. CT0 is defined as the time at which the minimal bioluminescence was observed. Black dots and opens squares can be considered as phase shifts measured on two consecutive days. For simplicity all points are plotted on both days. Note that all new phases are nearly identical irrespective of when cells were treated with dexamethasone. Hence the slope of the PTC is near zero, and the corresponding phase response curve is called type-zero PRC (taken from Nagoshi *et al.*, 2004).

However, Winfree defined two general types of PTC in phase resetting (Winfree, 1980). He termed the PTC for minor perturbations of the circadian system (e.g. shifts of up to six hours) Type 1 PTC due to the average slope of the diagonal that is close to 1. The other PTC (Type 0) is obtained for large magnitude perturbations with a zero average slope.

2.6.6.2 Phase shifts: the light-triggered signalling cascade

As described in section 6.2.3 the SCN clock receives light signals perceived by the pRGCs by two pathways: directly via the RHT or indirectly via the geniculohypothalamic tract (GHT). The pRGCs secrete glutamate (GLU) and pituitary adenylate cyclase activating peptide (PACAP) as the major neurotransmitters (Hannibal, 2002). The principal signalling molecules liberated by the GHT are gamma-aminobutyric acid (GABA) and neuopeptide Y (NPY; Harrington, 1997). By contrast, the RHT releases GLU and PACAP following nocturnal light pulses, which initiates a signalling cascade that results in a stable shift of the TTL. GLU is

released at both early and late night whereas PACAP secretion seems to be mainly important at late night (Kawaguchi *et al.*, 2003). The release of GLU recruits NMDA (N-methyl-D-aspartic acid; Abe *et al.*, 1992; Ding *et al.*, 1994) and AMPA (alpha-amino-3-hydroxy-5-methyl-4-isoxazolepropionic acid; Schurov *et al.*, 1999) receptors whose activation leads to an influx of calcium into the SCN cells. The increased calcium concentration activates the calcium/calmodulin-dependent kinase (CaMK), which phosphorylates the nitric oxide synthase (NOS; Agostino *et al.*, 2004; Ding *et al.*, 1994; Golombek *et al.*, 2004). The subsequent raise in NO provokes phase shifts at early and late night both *in vivo* and *in vitro* (Ding *et al.*, 1994). However, the mechanisms elicited by NO seem to depend on the time of the light pulse. In the late night (CT19), the inhibition of the cGMP-related protein kinase (PKG) suppresses the phase advancing effects of light and GLU *in vivo* (Weber *et al.*, 1995; Mathur *et al.*, 1996) and *in vitro* (Ding *et al.*, 1998), respectively. From this, it can be concluded that NO stimulates PKG via the activation of guanylyl cyclases (GC) which produce cGMP that activate PKG. By contrast, inhibition of PKG at early night does not abrogate GLU-induced phase delays. This suggests that the NO-GC-cGMP-PKG pathway is not implicated in phase shifts at this time (Weber *et al.*, 1995; Mathur *et al.*, 1996; Ding *et al.*, 1998). Instead of GC, NO activates the Ras-like G protein Dexras1 (Fang *et al.*, 2000), which in turn mediates the activation of the p42/44 mitogen activated protein kinase (MAPK) ERK (Cheng *et al.*, 2004; Cheng *et al.*, 2006). The up-regulation of MAPK (ERK1 & 2) phosphorylation leads to the activation of CREB (Obrietan *et al.*, 1998), which launches in its phosphorylated (Ser133 & Ser142) form the transcription of genes carrying a CRE motif in their promoter (Gau *et al.*, 2002; Ginty *et al.*, 1993; Obrietan *et al.*, 1999; Tischkau *et al.*, 1999; Travnickova-Bendova *et al.*, 2002). *In vivo*, the inhibition of ERK prevents the light-induced phase shifts, which suggests that ERK is important for coupling light signals to clock entrainment (Butcher *et al.*, 2002). Furthermore, it was shown that the inhibition of ERK abrogates the light-, GLU- and PACAP-induced phosphorylation of mitogen- and stress-activated protein kinase 1 (MSK1) in the SCN at both early and late night (Butcher *et al.*, 2005). This indicates that MSK1, which is a known regulator of CREB phosphorylation (Wiggin *et al.*, 2002), is implicated in the entrainment of the clock via light as well. In the late night, the light pulse-triggered release of PACAP recruits PAC1 receptors. Mice lacking these receptors show strongly attenuated phase-advances in response to light presented at late night (Kawaguchi *et al.*, 2003). Upon activation, G_S-coupled PAC1 receptors signal to the MAPK pathway via both $G_S\alpha$ and $G\beta\gamma$ mediated signalling cascade. The GTP-dependent dissociation

of these factors activates various downstream effectors of light signalling including ERK and adenylyl cyclases (AC).

In 2006, Cheng and colleagues have shown that Dexras1 seems to fulfil contrasting roles at early and late night respectively. While Dexras1 potentiates phase-delays in the early night, it reduces the magnitude of PACAP-mediated phase shifts at late night by inhibiting the activation of ERK via both the $G_S\alpha$- and the $G\beta\gamma$-mediated limb (Cheng *et al.*, 2006). Hence Dexras1 is thought to be a key signalling molecule which confers both phase specificity and sensitivity to the light stimulus (fig. 2-18).

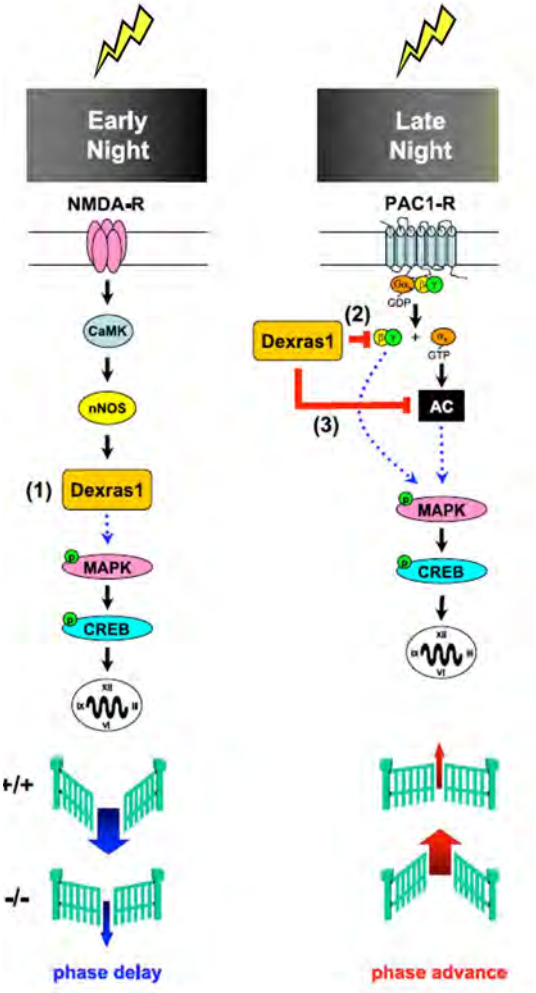

Fig. 2-18: Proposed model of Dexras1 in modulating photic responsiveness of the circadian clock. Photic effects are mediated in part by NMDA and PAC1 receptors expressed in the SCN. In the early night, light-induced activation of NMDA receptors via GLU leads to a nitrosylation-dependent enhancement of the guanine nucleotide exchange activity of Dexras1. (1) as a result, Dexras1 activates the MAPK pathway and promotes photic resetting in the early night. Light exposure in the late night leads to activation of G_S-coupled PAC1 receptors via PACAP, which signal via both the $G_S\alpha$ and $G\beta\gamma$ limbs to the MAPK cascade. Dexras1 inhibits PAC1-mediated MAPK pathway activation by suppressing $G\beta\gamma$ signalling events (2) as well as AC (3). Dexras1 may inhibit AC indirectly by a receptor-independent enhancement of tonic $G_{i/o}\alpha$ activity. In summary, light induces smaller phase delays in the early night and large phase advances in the night in *dexras1*$^{-/-}$ mice. AC, adenylyl cyclase (adapted from Cheng *et al.*, 2006)

Besides the factors mentioned above, ryaonodine receptors (RyR) are also likely to be involved in the photic entrainment of the clock - at least during the early night. RyR are integral membrane proteins associated with cellular organelles that sequester calcium (e.g. endoplasmatic reticulum; McPherson *et al.*, 1991). During early night, inhibition of RyR prevents GLU-induced phase delays both *in vivo* and *in vitro* whereas the activation of RyR by caffeine induces delays (Ding *et al.*, 1998).

Although a big progress can be observed in deciphering the molecules that are implicated in the light-mediated entrainment of the clock, many parameters remain unknown. Additional work will be required to further elucidate the signalling events that underlie light-induced phase shifts during both early and late night.

2.6.6.3 Phase shifts: perturbation of the transcription/translation feedback loop

It is known that a light pulse leads to an increase in H3 acetylation and phosphorylation (Crosio *et al.*, 2000) which facilitates transcription from a given DNA region. The finding of CRE-mediated transcription after light administration is in line with the fact that a light pulse is able to induce expression of a number of clock genes within the SCN. Besides *Per1* (Shigeyoshi *et al.*, 1997) mentioned earlier, *Per2* (Sherman *et al.*, 1997) and *Dec1* (Honma *et al.*, 2002) were found to be light inducible as well. However, they only respond to light during the subjective night but not during the subjective day. Moreover, not all of these clock genes are induced at the same time. Depending whether the light is administered during the beginning or the end of the subjective night, one sees different induction patterns. Whereas *Per2* expression is mainly triggered by a light pulse at the beginning of the night (Yan *et al.*, 1999; Field *et al.*, 2000; Yan & Okamura, 2002), *Per1* (Shigeyoshi *et al.*, 1997; Albrecht *et al.*, 1997; Field *et al.*, 2000; Yan & Silver, 2002) and *Dec1* (Honma *et al.*, 2002) are induced both at the beginning and the end of the night phase. This observation leads to the hypothesis that *Per1* may be implicated in mechanisms responsible for phase advances while *Per2* would be implicated in phase delays. This idea is supported by experiments in *Per1* and *Per2* mutant mice. It was found that *Per1* mutant mice fail to advance their clock at ZT22 (late night) whereas *Per2* mutants are unable to delay their clock upon a light pulse at ZT14 (early night; Albrecht *et al.*, 2001). However, later studies challenged these findings as *Per1* and *Per2* mutants were found to be still able to accomplish both phase advances and phase delays (Cermakian *et al.*, 2001; Bae & Weaver, 2003; Spoelstra *et al.*, 2004). Importantly, huge experimental differences exist between the studies. Albrecht and colleagues used an Aschoff type II protocol in which mice were subjected to a light pulse for 15 min under LD conditions (Aschoff, 1965). After the light pulse they were released into DD. Bae and Weaver used T cycle paradigms exposing mice to one hour of light per day at T = 24 hours for phase delays and T = 22 hours for phase advances. Under these conditions, both *Per1* and *Per2* mutant mice display phase advances as well as phase delays. Cermakian and co-workers applied an Aschoff type I protocol where animals were kept under DD for two to five days (Aschoff, 1965). Then mice were light-pulsed for 30 min at CT14 and CT20. Last but not least,

Spoelstra and collaborators managed to link the divergent findings of the different studies. They subjected their mice to 15 min light pulses under two different paradigms: first the animals were treated during the first cycle in DD and second under free-running conditions. The first experiment confirmed the findings obtained by Albrecht *et al.,* whereas the second corroborated the results of the other groups. This indicates that the outcome of the experiment depends strongly on the "light history" the mice went through. Nevertheless, *Per1* and *Per2* seem to accomplish different roles within the oscillator because they are induced in different SCN regions. In the early subjective night, *Per1* expression following a light stimulus is restricted to the GRP-expressing cells of the core SCN. *Per2* on the other hand is found to be induced in both GRP- and AVP-immunoreactive cells which are located in both core and shell (Dardente *et al.,* 2002; Yan & Silver, 2002). In the late subjective night, the induction pattern of *Per1* changes with an initial increase in the core and a subsequent raise in the shell (Yan & Silver, 2002). Besides the three clock genes mentioned already *Bmal1* seems to be implicated in the light-mediated resetting too. It was found that BMAL1 protein levels decrease after a light pulse at both early (CT15) and late subjective night (CT21; Tamaru *et al*., 2000). However, the attempt by another group to confirm this observation failed (von Gall *et al.*, 2003).

In addition to clock genes another group of genes – the so-called immediate early genes (e.g. *c-fos, junB, egr1*) – are induced after a light pulse. These genes respond even quicker to the light stimulus than clock genes do. The most prominent member of this gene family is *c-fos* whose mRNA and protein levels are increased upon light perception (Aronin *et al.*, 1990; Rusak *et al.*, 1990; Kornhauser *et al.,* 1992) through the binding of pCREB on the CRE motif found in its promoter (Ginty *et al.,* 1993). Mice mutant for *c-fos* are able to entrain to LD cycles and they show a PRC to light which is comparable to the one observed for wild-types (Honrado *et al.,* 1996).

Although the use of model organisms improves people's understanding of life and human diseases knowledge gained from studying them cannot be taken over one-to-one to humans. Hence data obtained in model organisms have to be verified in human subjects. That is why the next paragraph will be focused on circadian rhythms in humans.

2.7 Effects of the circadian clock on the human body

Our modern "24/7" society is a growing source of circadian stress, which leads to disruption in the normal programming of our behavioural and physiological rhythms. This provokes

reduced well-being and even illness, as observed in shift work, jet lag, psychiatric illness, ageing, or cardiovascular disease. Knowledge about the circadian clock in model organisms such as flies or mice is of use and interest for men because human beings are also subjected to circadian variations. Furthermore, the circadian system seems to be greatly conserved within organisms. Many physiological parameters in men fluctuate during the day in a circadian manner: melatonin levels rise during the night, body temperature raises in the morning before waking up and peaks in the evening before going to bed, immune system activity reaches its crest in the late evening and has its trough in the morning, blood pressure and heart rate are dropping during night, etc. The most obvious circadian rhythm in humans is the sleep-wake cycle. Recently, researchers have discovered that diseases also have predictable cyclic rhythms (e.g. asthma attacks peak at 4 AM; myocardial infarction at 9 AM; Muller, 1999) and that the timing of medication regimes can improve outcomes in some of them. All these circadian rhythms in humans even culminate in a death and accident peak in the early morning due to cardiovascular episodes and sleep-related accidents that take place in a "vulnerability window" between 1 and 6 a.m. (e.g. Chernobyl 1:23 a.m., Three-Mile Island 4:00 a.m.).

Dysfunctions of the circadian clock in humans are associated with physiological disorders of the sleep-wake cycle. For instance, there exist two inherited sleep phase disorders: familial advanced sleep phase syndrome (FASPS; Jones *et al.,* 1999) and delayed sleep phase syndrome (DSPS). Compared to the average population, patients suffering from one of these disorders display an advanced or delayed sleep-wake rhythm, respectively. In some patients suffering from DSPS, the symptoms are self-imposed due to social influences. Shift workers for example stay awake late into the morning hours or students study all night long. Nonetheless, a length polymorphism in *hPER3* within a region encoding a putative phosphorylation domain is linked to DSPS (Archer *et al*., 2003; Okawa & Uchiyama, 2007). Lately, it has been shown that a mis-sense mutation in *hPER2* is responsible for FASPS. People suffering from this hereditary disease have sleep schedules that move ahead by about 4 hours. The reason for this is that the mutated hPER2 cannot be phosphorylated by CSNKIε (human CKIε) and therefore stabilises hPER2, which in turn may phase advance the clock (Toh *et al.,* 2001). In addition, it has been shown that differential phosphorylation of hPER2 due to mutations in *hCK1ε* and *hCK1δ* leads to the same phenotype (Xu *et al.,* 2005; Xu *et al.,* 2007). Furthermore, *Per2* seems to be a tumour suppressor because mice lacking *Per2* are prone to cancer (Fu *et al.,* 2002). Besides the fact that clock genes are directly implicated in the development of cancer, disturbances of the circadian rhythms could lead to cancer.

Interestingly, grafted tumours develop more rapidly in mice which are subjected to chronic jet lag schedules (Filipski *et al*., 2004). These findings will hopefully lead to a circadian timing of chemotherapy (Hrushesky *et al.,* 1990; Kobayashi *et al*., 2002; Gholam *et al.*, 2006; Lévi *et al.,* 2008). However, a phase III clinical trial revealed that gender could largely affect the survival outcome of cancer patients on chronotherapeutic delivery (Giacchetti *et al.,* 2007; Lévi *et al*., 2007). These last two findings show the potential of circadian research in finding cures for many diseases and sleep disorders. Especially solving sleep problems may be very interesting objectives to further investigate possible changes in the molecular set-up of the circadian clock in humans because recent findings implicate an influence of the circadian clock on both homeostatic (*mCry*; Wisor *et al.*, 2002) and circadian regulation (*mPer1/2*; Kopp *et al.*, 2002) of sleep. Human clock gene polymorphisms might be involved in circadian rhythm sleep disorders (such as delayed sleep phase insomnia).

Another promising field for chronobiological treatment is depression: it has been demonstrated that sleep deprivation (increases sleep pressure), a phase shift, or an increase in Zeitgeber strength can improve or even cure mild depressive states (Boivin, 2000; McClung, 2007; Wirz-Justice, 2006; Wirz-Justice & Van den Hoofdakker, 1999). Seasonal affective disorder (SAD) is a seasonal depressive state due to an imbalance of serotonin and dopamine (Lam & Levitan, 2000; Levitan, 2007; Magnusson & Boivin, 2003). Moreover, it was found that SAD is associated with single-nucleotide polymorphisms (SNPs) in the three circadian clock genes *hPER2, hBMAL1* (*hARNTL*), and *hNPAS2* (Partonen *et al.,* 2007). SAD consists of two or more consecutive major depressive episodes in autumn or winter and a spontaneous remission in spring or summer. This sort of heritable depression can be improved by light therapy, where the patient is just exposed to light in order to strengthen his internal clock and increase dopamine and serotonin levels. To increase Zeitgeber strength is not only a useful treatment for SAD but also for blind patients: melatonin intake can alleviate their sleep problems by undertaking the task of light as a Zeitgeber (Sack *et al.,* 2000). Even Schizophrenia and Alzheimer's disease patients show improvement of their health state when they have to follow strict rhythms of bed, food, and nap times. Exposure to very bright light in the day and darkness at night can also consolidate the random patterns of rest and activity in Alzheimer's disease patients (Volicer *et al.,* 2001; Dowling *et al.,* 2008). As a general rule: the better the entrainment the less severe the symptoms of the illness.

Apart from the disorders described in this paragraph, numerous other disorders of the central nervous system (CNS) involve disrupted circadian parameters. To close this section, some of them are summarized in table 2-3.

Table 2-3: Rhythm/sleep endophenotypes in human CNS disease (taken from: Barnard & Nolan, 2008)

Human disease or condition	Disturbed rhythm/sleep endophenotype	Relevant phenotypes in mouse models
Familial advanced sleep phase syndrome (FASPS)	Early sleep and wake times, shortened circadian rhythms	Mice expressing human mis-sense mutations in *Per2* or *CK1δ* have advanced phase of activity in a light-dark schedule and a shortened activity rhythms
Delayed sleep phase syndrome (DSPS)	Extreme evening preference, delayed phase of activity, sleep, core body temperature, and melatonin	No model
Seasonal affective disorder (SAD)	Depressive symptoms occur during shorter winter days	No model
Mood disorders (unipolar depression) and psychoses (schizophrenia, bipolar)	Depression. Increased sleep latency, impaired sleep continuity, phase advance in endogenous circadian system relative to sleep schedule, phase advances in growth hormone, plasma melatonin, increased plasma cortisol at night, All major affective disorders include circadian phase disturbances in sleep, activity, temperature, and hormone levels	No accurate mouse model. Mutants in serotonergic and dopaminergic systems show disturbances in circadian phase and/or sleep parameters. *Clock* mutant has low anxiety, mania, and hyperactivity. Cognitive disturbances in *Npas2* mutant. Abnormal sensitization to drugs of abuse in *Clock* and *Per* mutants.
Autism spectrum disorders (ASD)	Longer sleep latency and greater sleep fragmentation. Abnormalities in circadian rhythm and mean concentration of plasma melatonin.	Mice expressing a conditional deletion of *Pten* have a significantly longer free-running period.
Down syndrome	Reduced sleep maintenance, sleep fragmentation, reduction in percent REM sleep, sleep apnea.	Ts65Dn mouse mutant shows increased activity in the light phase, a reduction in rhythm amplitude, and a 4-h advance in the phase activity.
Smith-Magenis syndrome	Inverted rhythm of melatonin secretion. Advanced sleep/wake phase. Nighttime wakening, daytime sleepiness. Reduced total and NREM sleep.	Heterozygous deletion mutant mice have a hypoactive phenotype and a significantly shorter circadian period.
Prader-Willi syndrome	Sleep apnea, sleep-related and behavioural disturbances including daytime napping and excessive daytime sleepiness.	Mice deficient for mage-like 2 gene (*Magel2*) have reduced circadian activity amplitude with increased daytime activity.
Parkinson disease (PD)	Sleep fragmentation, sleep apnea, REM sleep behaviour disorder, excessive daytime sleepiness.	No recorded circadian or sleep disturbances in genetic mouse models.
Huntington disease (HD)	Nocturnal awakening and progressive disintegration of daily activity rhythms.	R6/2 mouse transgenic line has increased daytime and reduced nocturnal activity. Progresses to a complete disintegration of diurnal and circadian activity rhythms.
Alzheimer disease (AD)	Fragmented sleep, increased nocturnal activity, and reduced daytime activity. Delayed phase in peak of daily activity.	Alterations in sleep regulation and timing in Tg2576 and PDAPP mice. Tg2576 mice also have a significantly longer circadian period. Both TgCRND8 and APP23 mice show changes in daily activity profiles potentially analogous to those seen in AD patients.
Aging	Sleep disturbances due to earlier wake time and reduced sleep consolidation. Partially attributed to age-related reduction in amplitude and advance in phase of circadian rhythms.	Aging lengthens the period and reduces the amplitude of circadian activity. The onset of daily activity is significantly delayed and the variability of onsets in increased.
Prion diseases	Severe sleep abnormalities, progressive loss of circadian rest-activity, and melatonin rhythms.	Increased sleep fragmentation and significantly longer circadian period in activity in prion protein null mutants.

2.7.1 Melatonin and human chronobiology

To date, the profiles of melatonin measured in blood and saliva, as well as its metabolite 6-sulphatoxymelatonin (aMT6s) found in urine, are by far the best indicators of clock timing in humans (Klerman *et al.*, 2002). Melatonin is synthesized rhythmically in the pineal gland (Latin, e*piphysis cerebri, glandula pinealis*) with a peak exclusively during the night (fig. 2-19; Laakso *et al*., 1990 & 1994). Due to its strong nocturnal expression pattern, melatonin got the colloquial sobriquet "hormone of the darkness". Since bright light suppresses the release of melatonin it is even called "Dracula of hormones".

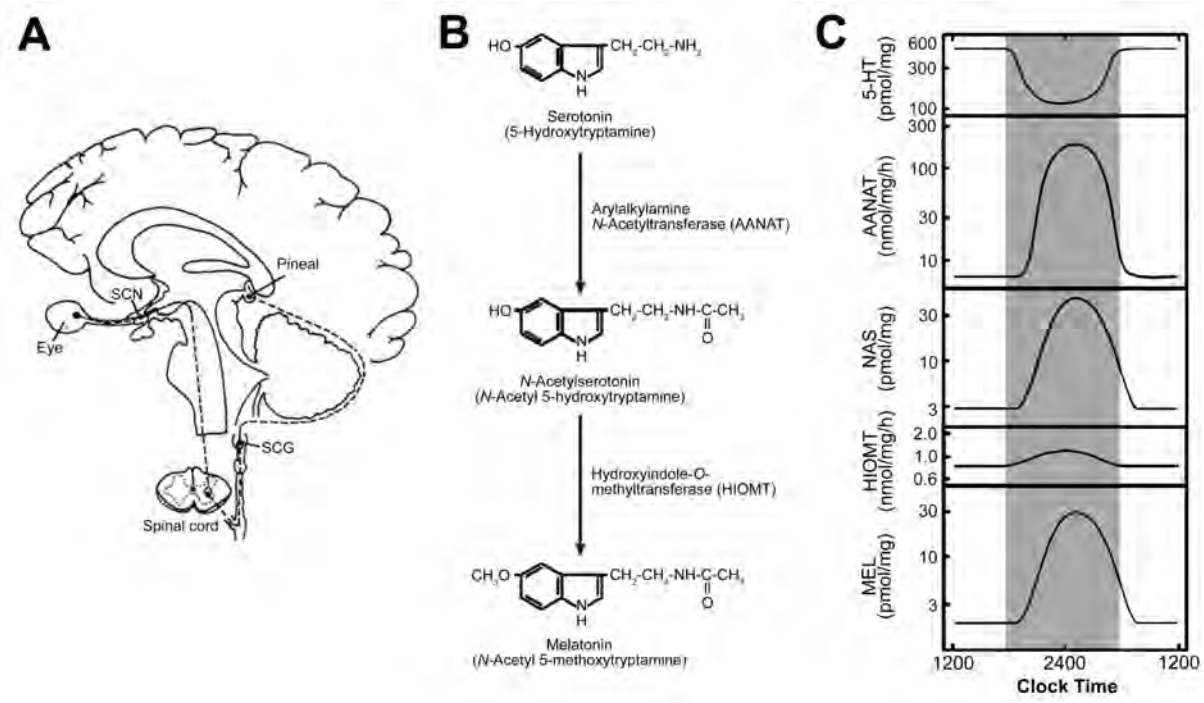

Fig. 2-19: Synthesis of melatonin within the pineal gland.
(A) Sagital view of a human brain showing the pineal gland and its innervations. The retinohypothalamic tract sends the light signals received by the eye to the SCN. The SCN project to the intermediolateral gray column in the spinal cord from where preganglionic neurons pass to the superior cervical ganglion (SCG). These neurones then project to the pineal in nervi conarii (modified from Ganong, 1997). **(B)** The neurotransmitter serotonin is the precursor of the small indoleamine melatonin. To yield the latter, serotonin is acetylated and then methylated within the pineal gland. The enzyme arylalkylamine N-acetyltransferase (AANAT) has been found to be rate limiting for melatonin synthesis. **(C)** All enzymes involved in melatonin synthesis and intermediate products are found to accumulate in a rhythmic fashion over time. Melatonin is found to peak between 2:00 and 6:00, irrespective of whether a person is asleep or awake in dim light. B and C are taken from Klein, 2007 (annual report of the division of intramural research, Eunice Kennedy Shriver national institute of child health and human development).

In addition to its huge role in the human circadian system, melatonin is evolutionarily well conserved and present in most organisms, from unicellular algae to humans (Pelham *et al.*, 1973; Smith *et al.*, 1976; Hardeland & Fuhrberg, 1996). In some amphibians and reptiles, melatonin is involved in changing skin colour. Indeed, the first indication that the pineal gland

contains a biologically active substance came from a work in *Xenopus laevis*. Application of bovine pineal extracts to tadpole skin provoked skin lightening mediated by the movement of melanosomes (melanin-containing pigment granules) with dermal melanophores (McCord & Allen, 1917). Many years later, the substance responsible for this skin lightening was identified as 5-methoxy *N*-acetyltryptamine and named "melatonin" (Greek, *melas* = black, *tosos* = labor; Lerner *et al.,* 1958 &1959). Furthermore, it was proved that melatonin could be synthesized within the pineal gland (Axelrod & Weissbach, 1960; Weissbach *et al.,* 1960 & 1961). This finding was confirmed by pinealectomy in rats which abolishes circadian rhythms of melatonin (Ozaki & Lynch, 1976; Lewy *et al.* 1980). Later on it was found that the pineal gland is the main source of melatonin in rhesus monkeys (Tetsuo *et al.,* 1982) and humans as well (Neuwelt & Lewy, 1983; Petterborg *et al.,* 1991). Last but not least, a role could be attributed to this small neuroendocrine organ (100 mg in humans), which was discovered over two millennia ago by Herophilos (325-280 B.C.) who was a famous anatomist at the University of Alexandria in Egypt.

In mammals, the primary role of melatonin is to convey daylength information to physiology. Since nighttime length differs between summer and winter, the variation in duration and quantity of melatonin production can be used as a seasonal marker. Hence, melatonin is involved in the regulation of photoperiodic functions such as reproduction, behaviour, coat growth or camouflage colouring in seasonal animals (Martinet & Allain, 1985; Zucker *et al*., 1991). Similarly, human melatonin regulation is suggested to be influenced by seasonal variation of natural lighting conditions (Illnerová *et al.*, 1985; Martikainen *et al*., 1985; Kauppila *et al.,* 1987; Kivelä *et al.,* 1988; Bojkowski & Arendt, 1988; Laakso *et al*., 1994; Stokkan & Reiter, 1994; Luboshitzky *et al.,* 1998). According to current knowledge, the physiological role of the human pineal is mainly related to the function of melatonin, which is regulated by the circadian system and light-dark cycles. In addition to its role in the circadian system, melatonin may have effects on reproduction (reviewed by Luboshitzky & Lavie, 1999) and immune system. Furthermore, it is known to be a potent antioxidant. This property could also explain why it is conserved between phylae. One hypothesis says that the living cells would have used melatonin to detoxify highly reactive oxygen radicals (Paietta, 1982; Poeggeler *et al.,* 1993; Reiter *et al.,* 1993; Tan *et al.,* 1993; Tan *et al.,* 2002).

Assessing circadian rhythms in humans requires highly controlled conditions (constant routine methodology), which will be discussed in the next section. In humans, the gold standard to determine circadian timing is the measurement of melatonin or its metabolite aMT6s. Unfortunately, there exist no established guidelines on when and how the various

methods for sampling and analyzing melatonin should be used. This absence of well-defined melatonin phase markers impedes on the comparison of results obtained from different studies. Recently these divergences between laboratories were tackled and led to a special article about measuring melatonin in humans (Benloucif *et al.*, 2008). Nonetheless, until now the most commonly used phase marker of the internal clock is the "dim-light melatonin onset" (DLMO), which indicates the start of its rise in the evening (fig. 2-20). Taking the DLMO as reference point has the advantage that it avoids overnight sampling (Lewy & Sack, 1989). Disadvantages of this practice are that it provides no information on the duration of secretion, peak levels, and total production. In addition, DLMO is only an approximation of the onset of synthesis and secretion and sometimes is even determined by visual estimate of a change in slope. Besides DLMO, "dim-light melatonin offset" (DLMOff) is used as a phase marker.

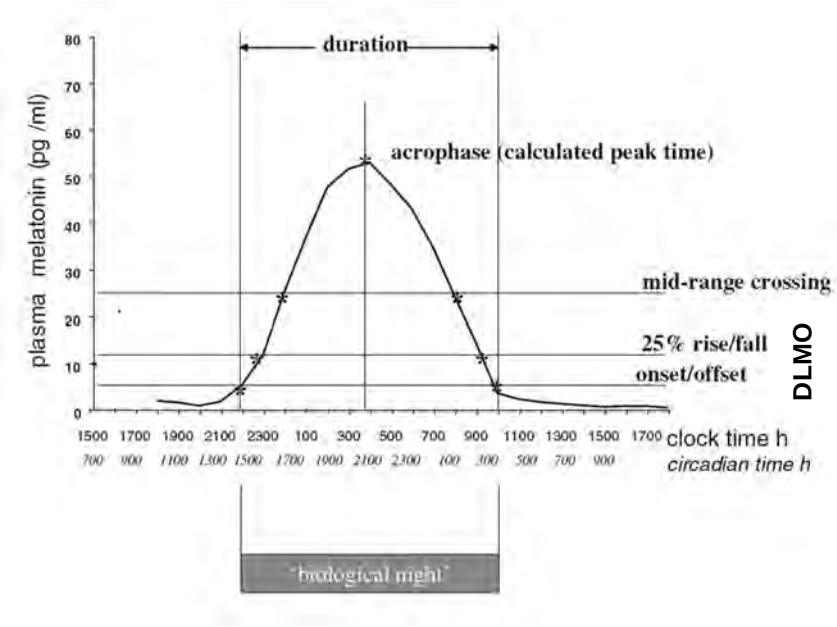

Fig. 2-20: Illustration of the phase markers for melatonin (plasma, saliva) and 6-sulphatoxymelatonin (aMT6s; urine). The markers used to characterize melatonin and aMT6s rhythms are illustrated diagrammatically. Area under the curve or total 24-h excretion is used to assess total secretion. At present, there is no standard definition of onset-offset (and hence duration). Hence, in this graph the DLMO can be defined as the sample named "onset/offset" or as 25 % rise in melatonin. Depending on which threshold is used, the duration of melatonin secretion varies significantly (adapted from: Arendt, 2005).

Melatonin can be measured either in saliva or in plasma while its primary metabolite aMT6s is determined in the urine. The advantage of using plasma melatonin is that samples can be taken during sleep, whereas sampling of saliva implies disruption of sleep. Frequent saliva collection can even completely deprive the subject from sleep which strongly limits its overnight use. Blood samples on the other hand can be sampled at frequent intervals through the use of intravenous catheters. Disadvantages are that plasma sampling is invasive and is restricted due to preservation of blood volume. Moreover, the use of catheters requires trained medical personnel. This fact renders it almost impossible to use plasma melatonin assessments for field studies. To compare plasma to saliva levels it is important to keep in

mind that melatonin levels are about three times greater in blood than in saliva. Urine collection on the other hand yields less resolution than blood or saliva (2 to 8 hour bins) and is limited by ability to void. Since the overnight aMT6s excretion levels can be calculated from the first morning void, this method does not require any waking up of the subject. Although intraindividual melatonin profiles are very stable, huge interindividual differences are observed frequently. It is thought that these large variations are due to the size of the pineal gland rather than due to changes in enzymatic activity (Gomez Brunet *et al.*, 2002). Surprisingly, there exist few apparently normal subjects who show no detectable melatonin levels in plasma at all times of day (Arendt, 2005).

2.7.2 Assessing circadian rhythms in humans

The first attempt to determine endogenous circadian rhythms in humans was undertaken 70 years ago. In 1938, two human subjects were studied on non-24-hour sleep/wake, light/dark, and meal schedules. They were isolated within Kentucky's Mammoth Cave (longest known cave on Earth) and hence completely shielded from any environmental time cues (Kleitman, 1963). A 28-hour rest/activity was imposed which freed their internal clocks from the sleep-wake cycle. Despite the forced six-days weeks, the body temperature rhythm of one subject persisted for one month with a near-24-hour period. The use of this so-called "forced desyonchrony protocol" distributed the influence of behavioural masking effects equally across the circadian cycle. Later on, Jürgen Aschoff and Rütger Wever questioned the results of this first underground cave study conducted on humans. They performed several month-long studies to determine the average period of human circadian rhythms. Their subjects were isolated from the environment in underground bunkers in Germany. To shield them completely from the outside world, the researchers even coiled copper wire around the rooms in which the subjects were accommodated. By this means, they aimed to counteract natural electromagnetic fields. However, the results they obtained showed that humans have a free-running activity rhythm of 25.2 hours with huge interindividual variations between subjects (13 to 65 hours). Moreover, they showed that the circadian period of body temperature was nearly 25 hours on average. Their results were confirmed later on by several studies conducted all over the planet (Siffre, 1964; Chouvet *et al.*, 1974; Jouvet *et al.*, 1974; Mills, 1964; Siffre, 1975; Findley, 1966; Webb & Agnew, 1974; Weitzmann *et al.*, 1981). All of these experimental setups allowed subjects to self-select their bedtimes and wake times and they could even turn on and off the lights as they wished. Hence subjects do not expose

themselves equally to light across the circadian cycle, as it is the case in a forced desynchrony protocol. It is of note that at that time it was incorrectly thought that the human circadian system was insensitive to light (Wever, 1970 & 1974; Aschoff, 1976). It was only in 1999 that it turned out that the first findings obtained in 1938 were correct. In this study a 28-hour day of activity and rest was imposed on the subjects and during wakening times only dim light was allowed. Recording body temperature and hormone rhythms in 24 subjects revealed that the human clock ticks with an internal period of 24.18 ± 0.26 hours (Czeisler *et al.,* 1999). The findings of this study revealed that the major pitfall of the former studies was the unrestricted access to light, which continuously delayed the circadian phase of the subjects. Hence Kleitman's results were finally confirmed.

Another technique to assess human circadian rhythms is the use of "constant routine protocols". Like forced desynchrony protocols, they allow to minimize the influence of behavioural and environmental factors which obscure ("mask") circadian rhythms. It is now generally accepted that the internal clock is subjected to exogenous influences. For instance, core body temperature is raised by physical activity and lowered by sleep (Minors & Waterhouse, 1989) or secretion of insulin is widely modulated by sleep and food intake from the gut (Van Cauter *et al.,* 1991). A way to reduce masking effects is to keep an individual's environment and lifestyle constant, which is the basis of the various constant routine protocols (Mills *et al.,* 1978; Czeisler *et al.,* 1986). This might include constant posture (e.g. semirecumbant), constant wakefulness, evenly distributed food intake (e.g. snacks every two hours), constant temperature, and continuous dim light (e.g. < 5 lux). To keep homeostatic sleep pressure low, nap protocols might be used instead of continuous wakefulness. Under such conditions, the phase and amplitude of various endogenous circadian rhythms can be studied in the absence of exogenous noise.

2.7.3 Entrainment of the human pacemaker to light

Once the incorrect conclusion that the human circadian system is insensitive to light was disproved, a whole bunch of studies showed that the human pacemaker is nicely entrainable to light. Moreover, it was found that not social interaction but light is the primary circadian synchronizer in humans (Czeisler, 1978 & 1995; Czeisler *et al.,* 1981; Shanahan *et al.,* 1997; Czeisler & Wright, 1999; Shanahan & Czeisler, 2000; Zeitzer *et al.,* 2000; Wright *et al.,* 2001; Gronfier *et al.,* 2004 & 2007; Lockley, 2007). The resetting of the human circadian system depends on the phase at which the light stimulus is administered. Light exposure in the morning leads to phase advances whereas light exposure in the evening and early night delays

the clock (Honma *et al.,* 1987; Czeisler *et al.,* 1989; Minors *et al.,* 1991; Khalsa *et al.,* 2003). In addition to the Type 1 PRC observed after single light pulses, it was reported that multiple light pulses lead to a strong Type 0 resetting in humans (Czeisler *et al.,* 1989; Shanahan *et al.,* 1999). Not surprisingly, the light PRC opposes the one obtained by melatonin (Lewy *et al.,* 1992; Zaidan *et al.,* 1994; Lewy *et al.,* 1998). In contrast to the PRC observed in other mammals, the human PRC does not exhibit a dead zone of sensitivity during the subjective daytime. This may indicate that the human circadian system reacts to light across all circadian phases (Jewett *et al.,* 1997; Khalsa *et al.,* 2003). Furthermore, it was shown that the response of the circadian pacemaker to light does not only depend on the timing but also on the intensity of the photic stimulus (Brainard *et al.,* 1988; Roenneberg & Foster, 1997, Czeisler & Wright, 1999). So-called dose-response curves of single light pulses during the early night were used to assess the effect of different polychromatic light intensities (i.e. lux) on humans (Boivin *et al.,* 1996; Zeitzer *et al.,* 2000). It was found that light even as weak as candlelight can induce small shifts of the human circadian system (Wright *et al.,* 2001). In addition to timing and intensity, the wavelength of the light plays a crucial role for its efficiency in resetting the clock. As detailed earlier (section 6.2.3.1) the mammalian circadian system receives light input via both the visual and the non-visual system. Like other mammals, humans are sensitive to short wavelength light (blue; Czeisler *et al.,* 1995; Zaidi *et al.,* 2007). Melatonin suppression and circadian phase resetting is achieved most efficiently after exposure to bright monochromatic blue light (Brainard *et al.,* 2001; Thapan *et al.,* 2001; Lockley *et al.,* 2003). Nonetheless, humans react to long-wavelength light, which confirms that cones may function as circadian photoreceptors in humans (Zeitzer *et al.,* 1997).

Chapter 3

Aim of this thesis

3 Aim of this thesis

Circadian rhythms have a huge impact on our daily life. Our mental and physical conditions alternate between states of high activity and recuperation with a 24-hour rhythm. Deregulation of the internal clock can lead to sleeping disorders, depression and various other health problems. Thus it is important to understand the mechanisms, which allow our clock to tick properly. Since circadian clocks are quite conserved between species, model organisms such as mice can be used for basic research on the molecular clock mechanisms and its impact on physiology.

For the last three decades, many studies have addressed the question how circadian rhythms emerge. Some results pointed to an important role for pre- and postnatal maternal entrainment (Davis *et al.*, 1985; Reppert & Schwartz, 1986; Weaver & Reppert, 1987; Duffield & Ebling, 1998; Viswanathan, 1999) whereas other strengthened the importance of genetic predisposition (Ohta *et al.*, 2002). One objective of this thesis was to find out, which of these two hypotheses is true. To elucidate this, wild-type male mice were bred with arrhythmic $Per1^{Brdm1}Per2^{Brdm1}$ or $Per2^{Brdm1}Cry1^{-/-}$ double mutant females. Offspring born to these mice were heterozygous for either *Per1 & Per2* or *Per2 & Cry1*. Hence they bore at least one functional copy of each gene and had the genetic constitution for a functional circadian clock. To exclude any influence of light on the females and the developing pups, matings were set-up in constant darkness. Moreover, all manipulations on cages and animals were done using night vision goggles. As soon as the first signs of pregnancy were detectable, females and males were kept in separate cages. At six weeks of age, pups and parents were placed in individual wheel-running cages and wheel-revolutions were recorded. Actograms were analyzed to find out whether maternal entrainment is mandatory for circadian rhythms to start or whether genetic predisposition is sufficient.

Apart from the question “what triggers the emergence of circadian rhythms in offspring”, it is important to understand how the different cogwheels cooperate to sustain circadian rhythms. The generation and subsequent analysis of animals missing one or several genes turned out to be a valuable tool for analyzing potential clock genes and their roles within the feedback loop. A second aim of this thesis was to shed some more light on the role of both *Per1* and *Rev-Erbα* in the circadian machinery. For this we crossed $Per1^{Brdm1}$ (Zheng *et al.*, 2001) and $Rev\text{-}Erb\alpha^{-/-}$ (Preitner *et al.*, 2002) animals to obtain double mutant mice. Subsequently, the

animals were tested for their basic wheel-running behavior, their response to light, the expression of core clock genes and other parameters.

Although, circadian clocks are especially well conserved between mammals, not all results obtained in mice can be extrapolated directly to humans. While mice are nocturnal animals, humans are active during the day. This difference already implies that there must be a difference between these two species. Better understanding of the human circadian system is not only of great interest for every individual but also for the industry. Apart from faulty equipment, weather conditions, or human error, fatigue caused by sleep deprivation contributes to a huge number of accidents. Every year, the costs of property damage and medical treatment could be diminished considerably if companies would think about the impact of circadian disruptions on the efficiency of their employees. Moreover a better insight in circadian physiological processes could decrease the amount of medicine needed and reduce its side effects. The same substance taken in the identical dose can provoke either a strong or no response depending on when it is administered (Scheving, 1976).

Still nowadays, only little is known about the human molecular clock. One reason for this is that human tissue is hard to access due to ethical considerations. So far, studying clock gene expression is only possible in blood samples or biopsies (Boivin *et al.*, 2003; Bjarnason *et al.*, 2001). Unfortunately, both cannot be taken endlessly from human subjects because they are rather invasive. Due to this limitation, the idea arose to develop a method allowing to chronotype human beings as minimally invasive as possible. Hence a third aim of this thesis was to standardize and to validate a method for measuring clock gene expression in oral mucosa samples. Subjects were asked to scratch the inside of their cheek using either a pipette tip or special brushes. In the laboratory, clock gene expression was measured within each sample using probe-based quantitative real-time PCR and normalized to the levels of the housekeeping gene *GAPDH*. The optimal primer and probe concentrations had to be determined for every gene to be analyzed (i.e. *PER2*, *PER1*, and *BMAL1*). Once the method was established, it was validated in two studies where the effect of green or blue monochromatic light on clock gene expression was tested. Ongoing experiments still take advantage of this method.

In addition to the aims mentioned above, three collaborations allowed to further understand the role of the circadian system within the body. One study investigated the role of the fragile

X mental retardation gene (*Fmr1*) and a fragile X related gene (*Fxr2*) in regulating circadian behavioral rhythms. The role of *Per2* in vascular endothelial function was investigated in a second study. A third one aimed at finding out more about the role of the circadian system in illness related fatigue. Infectious and autoimmune diseases typically lead to an increase in TNF-α and IL-1β. It was found that TNF-α inhibits CLOCK-BMAL1-mediated transcription, which suggest that its increase impairs clock gene functions and causes fatigue.

Chapter 4

Results

4.1 Development of circadian rhythms in murine pups

“Circadian rhythms in murine pups develop in absence of a functional maternal circadian clock.”

C. Jud and U. Albrecht

2006

Published in *Journal of Biological Rhythms* 21(2): 149-154

Circadian Rhythms in Murine Pups Develop in Absence of a Functional Maternal Circadian Clock

Corinne Jud and Urs Albrecht[1]
Department of Medicine, Division of Biochemistry, University of Fribourg, Fribourg, Switzerland

Abstract A genetic approach was used to investigate whether the emergence of circadian rhythms in murine pups is dependent on a functional maternal clock. Arrhythmic females bearing either the $mPer1^{Brdm1}/Per2^{Brdm1}$ or $mPer2^{Brdm1}/Cry1^{-/-}$ double-mutant genotype were crossed with wild-type males under constant darkness. The heterozygous offspring have the genetic constitution for a functional circadian clock. Individual pups born to arrhythmic $mPer1^{Brdm1}/Per2^{Brdm1}$ and $mPer2^{Brdm1}/Cry1^{-/-}$ mothers in constant darkness without external zeitgeber developed normal circadian rhythms, but their clocks were less synchronized to each other compared to wild-type animals. These findings indicate that development of circadian rhythms does not depend on a functional circadian clock in maternal tissue, extending previous findings obtained from pups born to SCN-lesioned mothers.

Key words circadian rhythm, development, synchronization, Per1, Per2, Cry1

In mammals, circadian clocks control the rhythmic expression of numerous physiological processes (reviewed in Hastings et al., 2003). A self-sustaining clock mechanism is present in every individual cell (Nagoshi et al., 2004). At the molecular level, a set of clock genes drives recurrent rhythms in mRNA and protein synthesis (reviewed in Reppert and Weaver, 2002; Albrecht and Eichele, 2003). The individual cellular rhythms may then be synchronized in a tissue via gap junctions (Long et al., 2005) and other means of cellular communication (Pennartz et al., 2002). The SCNs synchronize the different tissue clocks through neuronal and endocrine outputs (Buijs and Kalsbeek, 2001) and themselves are entrainable by the daily LD cycle through the retinohypothalamic tract, which connects the eye with the SCN.

How circadian rhythms emerge during development has been of interest for many years. One focus of research has been centered on the question of whether development of circadian rhythms in mammals is under the influence of maternal entrainment or whether it is genetically predisposed. Maternal entrainment of pups to the environmental LD cycle has been demonstrated by studying metabolism of C^{14}-labeled desoxyglucose in fetal rat SCN tissue (Reppert and Schwartz, 1983). Using the same technique, Reppert and Schwartz (1984) demonstrated that oscillating metabolic activity in the SCN is observed as early as the 19th day of rat gestation. In the mouse, *Per1* and *Per2* expression is observed in the developing SCN on day 17 of gestation (Shearman et al., 1997), but rhythmic expression of these genes is not detectable until after birth (Sládek et al., 2004; Li and Davis, 2005). Rat pups born and reared under constant darkness display a circadian rhythm of pineal N-acetyltransferase (NAT) that is in phase with the circadian time of the mother, which indicates maternal synchronization of the clock in pups

1. To whom all correspondence should be addressed: Chemin du Musée 5, 1700 Fribourg, Switzerland; e-mail: urs.albrecht@unifr.ch.

JOURNAL OF BIOLOGICAL RHYTHMS, Vol. 21 No. 2, April 2006 149-154
DOI: 10.1177/0748730406286264

(Reppert et al., 1984). Similarly, evidence for maternal entrainment of developing rhythms was found in hamsters (Davis and Gorski, 1985). The role of the maternal SCN in entrainment of the fetal clock was investigated by SCN-lesion experiments (Reppert and Schwartz, 1986; Davis and Gorski, 1988). These investigations showed that the fetal clock was unaffected by maternal SCN lesion, but synchrony between pups was altered. These experiments indicated a prominent role of the maternal SCN in litter synchronization. However, conclusions on the role of the maternal clock on the development of the fetal circadian system are difficult to make, for the following reasons. First, lesions in dams have been performed at gestation day 7, and hence, an impact of the SCN before surgery can not be excluded. Second, removal of the SCN leaves peripheral clocks functional while synchronization between organs is abolished (Yoo et al., 2004).

To study the fetal circadian system in the complete absence of a functional maternal circadian clock, we studied the appearance of circadian wheel-running activity in heterozygous pups derived from *mPer1*^{Brdm1}/*Per2*^{Brdm1} and *mPer2*^{Brdm1}/*Cry1*$^{-/-}$ double-mutant females crossed with wild-type males. We found that all offspring developed a circadian rest-activity rhythm, and within a litter, individual phases were less synchronous compared to the wild-type control litters. These findings indicate that development of the fetal circadian system is independent of a functional maternal clock.

MATERIALS AND METHODS

Animals

The *mPer2*^{Brdm1}/*Cry1*$^{-/-}$ (Oster et al., 2002) and *mPer1*^{Brdm1}/*Per2*^{Brdm1} (Zheng et al., 2001) double-mutant mice used in this study were generated by crossing *mPer2*^{Brdm1} mutant mice (Zheng et al., 1999) with *mCry1* knockout animals (van der Horst et al., 1999) or with *mPer1*^{Brdm1} (Zheng et al., 2001) knockout mice, respectively. Matching wild-type control animals were produced by intercrossing heterozygous animals.

Housing, Breeding, and Rearing Conditions

The *mPer2*^{Brdm1}/*Cry1*$^{-/-}$ and *mPer2*^{Brdm1}/*Per1*^{Brdm1} double-mutant females and the wild-type mice were reared under a normal 12:12-h LD cycle with food and water ad libitum. They were kept and mated in transparent plastic cages (267 mm long × 207 mm wide × 140 mm high; Techniplast Makrolon type 2 1264C001) with a stainless-steel wire lid (Techniplast 1264C116). To exclude any influence of time cues on the offspring, matings were set up under defined environmental conditions and constant darkness in isolated cabinets of our wheel-running facility (Jud et al., 2005). All manipulations were performed using night-vision goggles (Rigel 3200), and light sources that could be detected with the night-vision goggles were covered with aluminum foil prior to the experiment. The built-in infrared illuminator of the night-vision goggles was covered with dark paper to dampen it. Furthermore, the time of day of routine care was randomized. The *mPer2*^{Brdm1}/*Per1*^{Brdm1} heterozygous pups were produced in 3 matings. One wild-type male was bred with 1 double-mutant female and gave birth to 2 litters (P1 and P3, see below). Another wild-type male was bred with 2 double-mutant females (litters P4 and P5). The 3rd mating consisted of 1 wild-type male and 1 double-mutant female (litter P2). The *mPer2*^{Brdm1}/*Cry1* heterozygous pups were produced by 3 matings. One wild-type male and 1 double-mutant female produced litter C1. Another wild-type male and 1 double-mutant female produced litter C2. A 3rd wild-type male was mated with 2 double-mutant females, which resulted in litters C3 and C4. The wild-type control animals were produced by 3 matings, each with 1 wild-type male and 1 wild-type female (litters W1-W3). Nestlets (5 × 5 cm; EBECO) were placed into the cages to encourage nesting and improve breeding. Once double-mutant females became pregnant (determined by visual inspection) or at the latest after 2 weeks, the wild-type males were moved to a separate cage and isolation cabinet. Females received cotton nestlets and were left undisturbed for 2 to 3 d before and after delivery. A total of 18 wild-type mice, 40 *mPer2*^{Brdm1}/*Per1*^{Brdm1} heterozygous mice, and 25 *mPer2*^{Brdm1}/*Cry1*$^{-/-}$ heterozygous mice were obtained (see Table 1). Pups were weaned 3 weeks after birth and kept in small groups of maximum 5 animals up to the age of 6 weeks in constant darkness.

Locomotor Activity Monitoring

Starting from the 7th week of age, each of the heterozygous offspring was placed in an individual running-wheel cage (Jud et al., 2005). To put mice in running wheels directly after weaning is not recommended because heat loss is greater than heat generation at that age, and pups die when kept individually. The heterozygous pups, the mother,

and the father were placed into the same isolation cabinet. Activity was assessed and evaluated using the ClockLab software package (Actimetrics). Activity records were double plotted in threshold format for 6-min bins. Period length and rhythmicity were assessed by χ^2 periodogram analysis.

Determination of Within-Litter Synchrony

The activity onset on the 2nd day of wheel running was determined for each individual. A regression line was drawn through onsets using ClockLab software (Actimetrics). The activity onset closest to the point where the regression line hit time axis on day 2 of the wheel-running experiment was defined as onset of activity at day 2. We determined the length of the average vector *r* for each litter, which represents the scatter of phases within a litter (Rayleigh test and tables for significance; see Zar, 1999). Midnight corresponded to 0°.

RESULTS

To study the emergence of circadian rhythms in absence of a maternal clock, we crossed *mPer1*^{Brdm1}/*Per2*^{Brdm1} and *mPer2*^{Brdm1}/*Cry1*$^{-/-}$ double-mutant females with wild-type males in constant darkness. Because these double-mutant females display altered clock gene expression and no circadian rest-activity behavior (Zheng et al., 2001; Oster et al., 2002), it was reasonable to assume that the pups develop in the absence of a maternal clock. The pups were conceived, developed, and grew up in constant darkness and were tested at the age of 6 weeks for wheel-running activity.

We found that the wild-type control as well as the heterozygous offspring displayed a circadian rhythm (Fig. 1A, 1B, 1C) with a $\tau \pm$ SEM of 23.93 ± 0.05 h for wild-type offspring (N = 18) (Fig. 1M), 23.19 ± 0.05 h for *mPer1*^{Brdm1}/*Per2*^{Brdm1} heterozygous offspring (N = 40) (Fig. 1N), and 22.98 ± 0.1 h for *mPer2*^{Brdm1}/*Cry1* heterozygous offspring (N = 25) (Fig. 1O). The free-running period length of the heterozygous offspring was significantly different from that of their wild-type fathers (Fig. 1N, 1O) whereas this was not the case between the wild-type offspring and their parents (Fig. 1M). The difference in period of heterozygous animals to their fathers is probably caused by difference in genotype. The *mPer1*^{Brdm1}/*Per2*^{Brdm1} double-mutant female shown in Figure 1H and the inset in Figure 1K shows an initial ultradian rhythm of 15.2 h, which was subsequently lost. In the beginning, the *mPer2*^{Brdm1}/*Cry1*$^{-/-}$ double-mutant mother shows an ultradian rhythm of 11.2 h (Fig. 1I, upper inset in 1L), which was lost later on. It then developed another ultradian rhythm of 14.8 h before it became arrhythmic (Fig. 1I, lower inset in 1L). In general, we observed that all double-mutant females periodically displayed ultradian rhythms.

Table 1. Within-Litter Synchrony

Litter	n	r	p
W1	8	0.95	***
W2	4	0.85	n.a.
W3	6	0.78	*
P1	9	0.87	***
P2	6	0.9	**
P3	9	0.40	n.s.
P4	9	0.54	n.s.
P5	7	0.56	n.s.
C1	8	0.55	n.s.
C2	9	0.56	n.s.
C3	2	0.73	n.a.
C4	6	0.69	n.s.

NOTE: W = wild-type; P = *mPer1*^{Brdm}/*Per2*^{Brdm1} heterozygous; C = *mPer2*^{Brdm1}/*Cry1* heterozygous mice; n.a. = not applicable (n too small); n.s. = not significant.

*p < 0.05; **p < 0.01; ***p < 0.001 (Rayleigh test).

Because pups are synchronized by mothers, we determined within-litter synchrony. Results are shown in Table 1 for wild-type (W1, 2, 3), *mPer1*^{Brdm1}/*Per2*^{Brdm1} heterozygous (P1, 2, 3, 4, 5), and *mPer2*^{Brdm1}/*Cry1* heterozygous (C1, 2, 3, 4) offspring.

DISCUSSION

In mammals, mothers are in intimate contact with their offspring to ensure their survival starting from the day of conception. Maternally provided factors such as carbohydrates, lipids, amino acids, and hormones influence the development of the embryo. Because many metabolic pathways in the maternal organism are structured in a circadian fashion, the question arises of whether the maternal circadian clock is imposed on the embryos, leading to maternally mediated circadian rhythms in the offspring. In the 1980s, experiments investigating metabolism of C^{14}-labeled desoxyglucose and pineal N-acetyltransferase in mothers and their pups indicated an influence of the maternal circadian rhythm on their offspring (Reppert and Schwartz, 1983; Reppert et al., 1984; Davis and Gorski, 1985). However, the fetal clock developed normally when the maternal SCN was

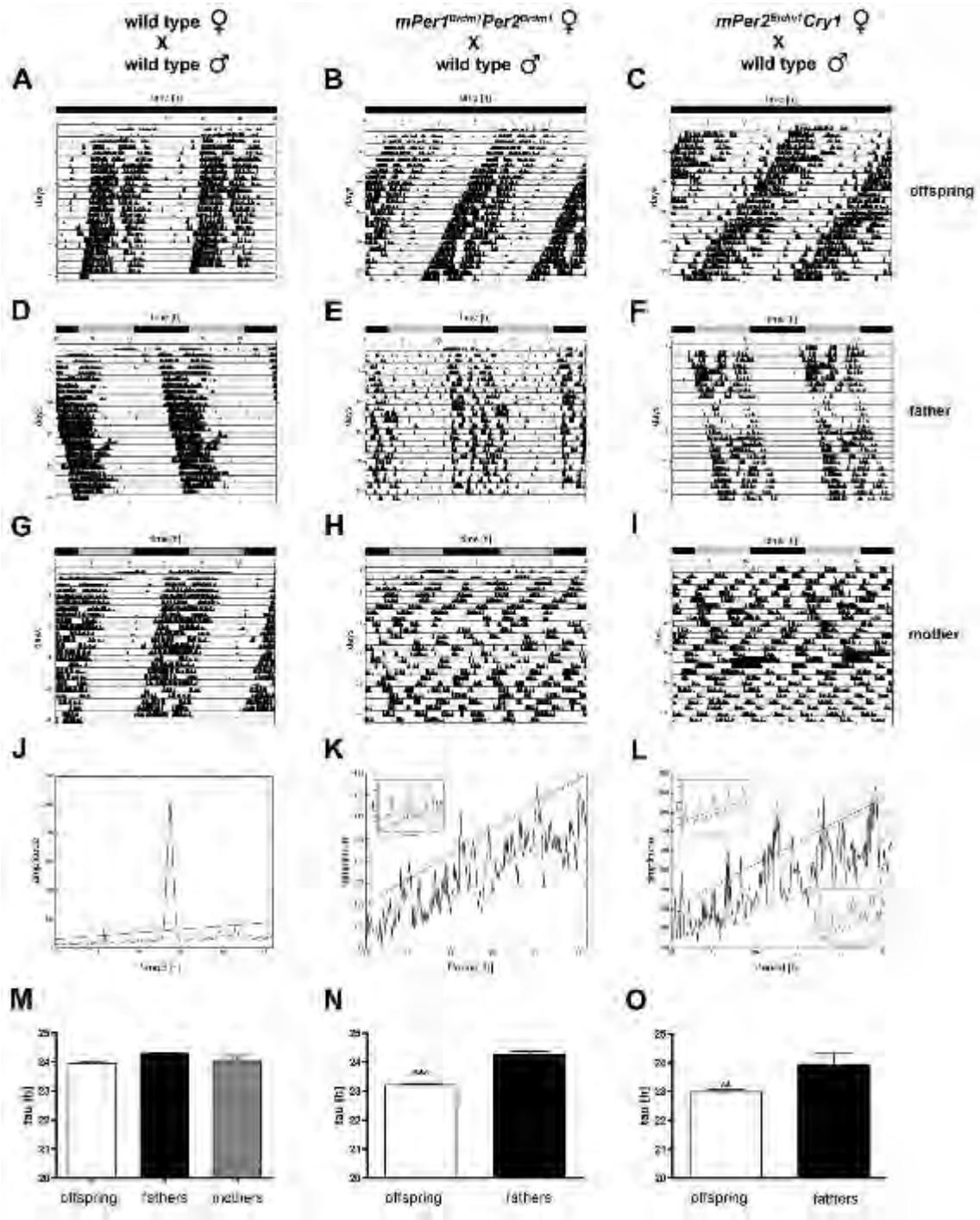

Figure 1. Representative locomotor activity records, χ^2 periodograms, and free-running period length. Locomotor activity records of wild-type (A), *mPer1*^{Brdm1}/*Per2*^{Brdm1} heterozygous (B), and *mPer2*^{Brdm1}/*Cry1* heterozygous (C) pups born and reared under DD conditions (black bar on the top of the graph), indicating that these animals never experienced an LD cycle. (D-F) Actograms of the corresponding wild-type fathers. Black bar, gray bar = subjective night and day, respectively. (G-I) Actograms of the corresponding mothers. (J-L) The χ^2 periodograms of the mothers; the straight line in the χ^2 periodogram represents a statistical significance of $p < 0.001$. Periodogram (J) corresponds to the activity plot of the wild-type mother shown in (G) ($\tau = 23.7$ h), (K) corresponds to the activity plot shown in (H), and (L) corresponds to the activity plot shown in (I). In (K), the big χ^2 periodogram = entire period of 26 days (arrhythmic), inset upper-left corner = days 1 to 8 ($\tau_1 = 15.2$ h, $\tau_2 = 22.8$ h, $\tau_3 = 30.3$ h). In (L), the big χ^2 periodogram = entire period of 26 days, inset upper-left corner = days 1 to 6 ($\tau_1 = 11.2$ h, $\tau_2 = 16.9$ h, $\tau_3 = 22.5$ h, $\tau_4 = 28.1$ h, $\tau_5 = 33.7$ h), inset lower-right corner = days 10 to 15 ($\tau_1 = 14.8$ h, $\tau_2 = 22.2$ h, $\tau_3 = 29.8$ h). (M-O) Average free-running period length of the offspring compared to their parents. White bar = pups; black bar = fathers; gray bar = mothers. Data are represented as mean ± SEM. Unpaired *t* test was performed to compare the free-running period length of the pups to their wild-type parents. **$p = 0.0056$; ***$p > 0.0001$.

surgically removed at gestation day 7 (Reppert and Schwartz, 1986; Davis and Gorski, 1988), indicating that a functional maternal SCN is not necessary for development of circadian rhythms in pups. Our observations using a genetic approach confirm these results. Female mice with mutations in *mPer1/Per2* and *mPer2/Cry1* genes do not display circadian wheel-running behavior (Zheng et al., 2001; Oster et al., 2002), and cultured fibroblasts of these double-mutant animals display no circadian rhythmicity in *Bmal1*-promoter–driven luciferase activity (Brown et al., 2005). Because in our experimental set-up, double-mutant females are arrhythmic before and after mating with a wild-type male, there is most likely no influence of the maternal clock on the fertilized egg and the developing embryos. Therefore, the observed circadian rhythms in the heterozygous offspring (Fig. 1) probably developed through an internal program starting the circadian cycling of the clock. However, we cannot exclude the possibility that the ultradian rhythms observed in double-mutant females might contribute to initiate circadian rhythmicity in their offspring.

Table 1 shows that significant within-litter synchrony is observed in wild-type pups, whereas this is not the case for most of the mutant heterozygous litters. If circadian rhythms in the heterozygous offspring were triggered by external factors, the animals within a heterozygous litter would show a good synchronization of clock phase. However, this is not observed (Table 1) except for litters P1 and P2, which were assessed during a period of construction at our university. It also appears that handling, occurring for all animals within a litter at the same time, is probably not the signal for onset of circadian clock activity. In this context, it is important to note that variations in τ are similar between wild-type (23.93 ± 0.05 h; Fig. 1M, white bar) and heterozygous (23.19 ± 0.05 h and 22.98 ± 0.1 h; Fig. 1N and 1O, white bars) animals, indicating that the differences of synchrony within a litter (Table 1) appear not to be caused by τ variation. However, we cannot exclude this possibility. A reciprocal cross with a mutant father and a wild-type mother might shed more light on litter synchronization.

Taken together, we show evidence for autonomous development of circadian rhythms in pups from mothers with a genetic defect of the circadian clock. Our findings are in agreement with previous observations made in SCN-lesioned animals and extend them, allowing to propose autonomous clock development in absence of central and peripheral maternal clocks.

ACKNOWLEDGMENTS

The authors thank Dr. Jürgen Ripperger for critically reading the manuscript. This work was supported by the Swiss National Science Foundation, the State of Fribourg, and EC grant Braintime QLG3-CT-2002-01829.

REFERENCES

Albrecht U and Eichele G (2003) The mammalian circadian clock. Curr Opin Genet Dev 13:271-277.

Brown SA, Fleury-Olela F, Nagoshi E, Hauser C, Juge C, Meier CA, Chicheportiche R, Dayer JM, Albrecht U, and Schibler U (2005) The period length of fibroblast circadian gene expression varies widely among human individuals. PLoS Biol 3:e338.

Buijs RM and Kalsbeek A (2001) Hypothalamic integration of central and peripheral clocks. Nat Rev Neurosci 2:521-526.

Davis FC and Gorski RA (1985) Development of hamster circadian rhythms, I. Within-litter synchrony of mother and pup activity rhythms at weaning. Biol Reprod 33:353-362.

Davis FC and Gorski RA (1988) Development of hamster circadian rhythms: role of the maternal suprachiasmatic nucleus. J Comp Physiol [A] 162:601-610.

Hastings MH, Reddy AB, and Maywood ES (2003) A clockwork web: circadian timing in brain and periphery, in health and disease. Nat Rev Neurosci 4:649-661.

Jud C, Schmutz I, Hampp G, Oster H, and Albrecht U (2005) A guideline for analyzing circadian wheel-running behavior in rodents under different lighting conditions. Biol Proceed Online 7:101-116.

Li X and Davis FC (2005) Developmental expression of clock genes in the Syrian hamster. Brain Res Dev Brain Res 158:31-40.

Long MA, Jutras MJ, Connors BW, and Burwell RD (2005) Electrical synapses coordinate activity in the suprachiasmatic nucleus. Nat Neurosci 8:61-66.

Nagoshi E, Saini C, Bauer C, Laroche T, Naef F, and Schibler U (2004) Circadian gene expression in individual fibroblasts: cell-autonomous and self-sustained oscillators pass time to daughter cells. Cell 119:693-705.

Oster H, Yasui A, van der Horst GTJ, and Albrecht U (2002) Disruption of *mCry2* restores circadian rhythmicity in *mPer2* mutant mice. Genes Dev 16:2633-2638.

Pennartz CM, de Jeu MT, Bos NP, Schaap J, and Geurtsen AM (2002) Diurnal modulation of pacemaker potentials and calcium current in the mammalian circadian clock. Nature 416:286-290.

Reppert SM, Coleman RJ, Heath HW, and Swedlow JR (1984) Pineal N-acetyltransferase activity in 10-day-old rats: a paradigm for studying the developing circadian system. Endocrinology 115:918-925.

Reppert SM and Schwartz WJ (1983) Maternal coordination of the fetal biological clock in utero. Science 220:969-971.

Reppert SM and Schwartz WJ (1984) The suprachiasmatic nuclei of the fetal rat: characterization of a functional

circadian clock using 14C-labeled deoxyglucose. J Neurosci 4:1677-1682.

Reppert SM and Schwartz WJ (1986) Maternal suprachiasmatic nuclei are necessary for maternal coordination of the developing circadian system. J Neurosci 6:2724-2729.

Reppert SM and Weaver DR (2002) Coordination of circadian timing in mammals. Nature 418:935-941.

Shearman LP, Zylka MJ, Weaver DR, Kolakowski LF Jr, and Reppert SM (1997) Two period homologs: circadian expression and photic regulation in the suprachiasmatic nuclei. Neuron 19:1261-1269.

Sládek M, Sumová A, Kováciková Z, Bendová Z, Laurinová K, and Illnerová H (2004) Insight into molecular core mechanism of embryonic and early postnatal rat suprachiasmatic nucleus. Proc Natl Acad Sci U S A 101:6231-6236.

van der Horst GT, Muijtjens M, Kobayashi K, Takano R, Kanno S, Takao M, de Wit J, Verkerk A, Eker APM, van Leenen D, et al. (1999) Mammalian Cry1 and Cry2 are essential for maintenance of circadian rhythms. Nature 398:627-630.

Yoo SH, Yamazaki S, Lowrey PL, Shimomura K, Ko CH, Buhr ED, Siepka SM, Hong HK, Oh WJ, Yoo OJ, et al. (2004) PERIOD2::LUCIFERASE real-time reporting of circadian dynamics reveals persistent circadian oscillations in mouse peripheral tissues. Proc Natl Acad Sci U S A 101:5339-5346.

Zar JH (1999) *Biostatistical Analysis*, 4th ed. Englewood Cliffs, NJ: Prentice-Hall Inc.

Zheng B, Albrecht U, Kaasik K, Sage M, Lu W, Vaishnav S, Li Q, Sun ZS, Eichele G, Bradley A, et al. (2001) Nonredundant roles of the *mPer1* and *mPer2* genes in the mammalian circadian clock. Cell 105:683-694.

Zheng B, Larkin DW, Albrecht U, Sun ZS, Sage M, Eichele G, Lee CC, and Bradley A (1999) The *mPer2* gene encodes a functional component of the mammalian circadian clock. Nature 400:169-173.

4.2 Light induced *Cry1* coincides with high amplitude phase resetting in *Rev-Erbα/Per1* double mutant mice

Corinne Jud and Urs Albrecht[1]

Department of Medicine, Unit of Biochemistry, University of Fribourg, Fribourg, Switzerland

[1] To whom all correspondence should be addressed: Chemin du Musée 5, 1700 Fribourg, Switzerland, e-mail: urs.albrecht@unifr.ch

Abstract

Over time, organisms developed various strategies to adapt to their environment. The continuous light-dark cycles caused by the rotation of the Earth around its own axis facilitated the evolution of circadian clocks. These generate rhythms that persist with a period of about 24 hours even in the absence of environmental cues. However, to tick in time, they have to continuously synchronize themselves to the prevailing photoperiod by appropriate phase shifts. In this study, we disrupted two cogwheels of the mammalian circadian oscillator, *Rev-Erbα* and *Period1* (*Per1)*. We found that these mice displayed robust circadian rhythms with significantly shorter periods under constant darkness conditions. Strikingly, they showed high amplitude resetting (Type 0) in response to a brief light pulse at the end of their subjective night phase, which is rare in mammals. *cFos* was induced to comparable levels as those in wild-type mice, which indicates that the photosensitivity is normal in the double mutant animals. Surprisingly, the otherwise not light responsive gene *Cry1* was also induced under these conditions. Hence, *Rev-Erbα* and *Per1* may be part of a mechanism that evolved to prevent drastic phase shifts in mammals.

Key words: circadian rhythm, *Per1*, *Rev-Erbα*, Type 0 PRC, *Cry1* induction

Introduction

In mammals many physiological and behavioural parameters are subjected to daily variations. For instance, blood pressure, heart rate, body temperature, or sleep-wake cycles change considerably during the course of a day. The central circadian (Latin: “around a day”) clock, which governs these rhythms, is located in the suprachiasmatic nuclei (SCN) of the ventral hypothalamus (Stephan and Zucker 1972; Ralph, Foster et al. 1990). Since this internal pacemaker can tell time only approximately, it has to be reset every day by environmental signals. The strongest synchronizer for the endogenous clock is light, which signals directly to the SCN via the retinohypothalamic tract (Moore and Lenn 1972). To reset peripheral oscillators, rhythms generated in the SCN are sent to the rest of the body via both neuronal and humoral signals.

Much of the understanding concerning the functioning of the circadian clock has come from extensive work done in model organisms mutant for one or several clock genes. In mammals, it was found that the molecular clockwork is based on cell-autonomous interlocked positive and negative transcriptional/translational feedback loops (TTLs; Takahashi, Hong et al. 2008). The positive limb of the core loop is formed by the transcription factors CLOCK and BMAL1. Heterodimers of these proteins bind to E-box motifs in the promoters of *Pers, Crys, Rev-Erbα* and other genes controlled by the clock. In the cytoplasm, the PER proteins form complexes with the CRYs, which then enter the nucleus. Once the complexes reach their destination, the CRYs inhibit the CLOCK/BMAL1 driven transcription, thereby establishing a negative feedback loop (Griffin, Staknis et al. 1999; Jin, Shearman et al. 1999; Kume, Zylka et al. 1999). The suppressed E-box driven transcription leads to a decline in PER, CRY and REV-ERBα protein levels, which finally re-activates CLOCK-BMAL1 driven transcription. Due to the fall in REV-ERBα, *Bmal1* transcription is no longer inhibited (Preitner, Damiola et al. 2002; Ueda, Chen et al. 2002). Hence RORα can activate *Bmal1* expression by binding to the now vacant retinoic acid related orphan receptor response elements (RORE) in its promoter (Giguere 1999; Sato, Panda et al. 2004; Akashi and Takumi 2005).

The TTLs described above can be modulated by external signals. As mentioned previously, the strongest Zeitgeber (literally, “time giver” in German) for the mammalian clock is light. To better study the impact of light on the circadian system animals kept under constant darkness (DD) are subjected to a brief light pulse at different time points. During the subjective day, light has little or no effect on the resetting of the clock. By contrast, light exposure during the subjective night is capable of shifting the pacemaker. Depending on

whether the light is administered during the early or late subjective night, the animal either delays or advances its clock, respectively (Pittendrigh 1960; Aschoff 1969; Daan and Pittendrigh 1976).

Several studies attempted to identify the molecular mechanisms underlying resetting in response to a light pulse. However, in mammals only little is understood compared to *Drosophila* and zebrafish (Lin, Song et al. 2001; Koh, Zheng et al. 2006; Tamai, Young et al. 2007). Both *Rev-Erbα*$^{-/-}$ and *Per1*^{Brdm1} single mutant mice are characterized by an aberrant light response during late night. Therefore we were interested in analyzing the resetting phenotype of double mutants. We monitored their wheel-running behaviour under constant conditions and established a PRC to brief light pulses. Here we show that *Rev-Erbα*$^{-/-}$ *Per1*^{Brdm1} double mutant mice maintain a functional circadian clock although they display a shorter period with reduced precision. Moreover, clock gene expression and their light inducibility are altered in mice deficient for both *Rev-Erbα* and *Per1*. Strikingly, they show high amplitude resetting (Type 0) and *Cry1* becomes light inducible in these mice after a light pulse delivered at the end of the subjective night. Hence we hypothesize that *Rev-Erbα* and *Per1* may participate in a mechanism that prevents drastic light responses in mammals.

Material & Methods

Animals

All animal work was performed in accordance with the guidelines of the Schweizer Tierschutzgesetz (TSchG, SR455, Abschnitt 2: Art. 5 + 7, Abschnitt 5: Art. 11 and Abschnitt 6: Art.12-19).

The *Rev-Erbα*$^{-/-}$*Per1*^{Brdm1} double mutant mice used in this study were generated by crossing *Rev-Erbα*$^{-/-}$ (Preitner, Damiola et al. 2002) and *Per1*^{Brdm1} (Zheng, Albrecht et al. 2001) single mutants. Intercrossing double heterozygous animals produced matching *Rev-Erbα*$^{-/-}$, *Per1*^{Brdm1}, *Rev-Erbα*$^{-/-}$*Per1*^{Brdm1} and wild-type animals. Homozygous breeding pairs were established using F2 offspring. To prevent genetic drift as much as possible, these matings were kept together as long as possible. The animals were regularly backcrossed to minimize epigenetic effects. The genotype of the offspring was determined by PCR. The PCR protocol for *Rev-Erbα* was kindly provided by U. Schibler (Geneva, Switzerland). The following primers were used:

*Per1*_1: 5'-ACA AAC TCA CAG AGC CCA TCC-3'

*Per1*_2: 5'-ATA TTC CTG GTT AGC TGT AGG-3'

*Per1*_3: 5'-CGC ATG CTC CAG ACT GCC TTG-3'

*Rev-Erbα*_1: 5'-CAC CTT ACA CAG TAG CAC CAT GCC ATT CA-3'

*Rev-Erbα*_2: 5'-AAA CCA GGC AAA GCG CCA TTC GCC ATT CA-3'

*Rev-Erbα*_3: 5'-CCA GGA AGT CTA CAA GTG GCC ATG GAA GA-3'

The final primer concentration was 0.5 µM, dNTP (Roche) concentration was 0.2 mM, and $MgCl_2$ concentration was 1.5 mM for *Per1* and 3.5 mM for *Rev-Erbα*, respectively. To improve annealing, 12 nM or 6 nM $(NH_4)_2SO_4$ was added to the reaction mix for *Per1* and *Rev-Erbα*, respectively. 2.5 U *Taq* DNA polymerase (Qiagen) were used per 50 µl reaction for *Per1* and 1.25 U per 25 µl reaction for *Rev-Erbα*. A final concentration of 0.2x Q-solution was used to increase PCR specificity of the *Per1* reaction. An initial denaturation was done at 94°C for 2 min. Subsequent denaturation was done at 94°C for 10 s followed by an annealing step of 30 s and an elongation at 72°C for 1 min. The annealing temperature was 56°C for *Per1* and 62°C for *Rev-Erbα*, respectively. After 34 (*Per1*) or 36 (*Rev-Erbα*) cycles, the PCR was ended with a final extension at 72°C for 10 min. From time to time, Southern blot analysis was used to confirm the PCR for *Per1* (Ramirez-Solis, Zheng et al. 1993; Zheng, Albrecht et al. 2001).

Locomotor activity monitoring and circadian phenotype analysis

Mice housing and handling were performed as described earlier (Jud, Schmutz et al. 2005). Animals were entrained in LD 12:12h for 7-15 days before they were released into DD. Activity was assessed and evaluated using the ClockLab software package (Actimetrics). Activity records were double plotted in threshold format for 6-min bins. Period length was assessed by χ^2 periodogram analysis for days 4-10 in constant darkness. To determine light induced phase shifts, an Aschoff Type I protocol was used (Aschoff 1965). Animals were allowed to stabilize their free-running rhythm for at least 2 months prior to the light pulse. The circadian time (CT) at the beginning of the light pulse was calculated for every mouse individually. The phase response curve was established administering 15 min light pulses at CT0 (N [wild-type/ *Rev-Erbα*$^{-/-}$*Per1*^{Brdm1}] = 8/11), CT2 (N = 11/4), CT10 (N = 8/8), CT14 (N = 15/8), CT18 (N = 14/15), CT20 (N = 8/10), and CT22 (N = 13/6).

Mice subjected to experimental jet lag were entrained to LD 12:12h (e.g. lights on 7:00 – 19:00) before the photoschedule was advanced by switching off the light 8 hours earlier than before (e.g. 11:00). Animals were allowed to re-entrain to the new LD cycle for about 1 month. Once stable entrainment was achieved, the photoschedule was delayed by keeping the light switched on 8 hours longer (e.g. until 19:00).

***In situ* hybridization**

To determine circadian gene expression, adult mice were first anesthetized with Attane^{TM} Isoflurane (Provet AG) and then sacrificed on day 6 in DD. For light induction experiments, animals were kept in DD for about 2 months before they were exposed to a 15 min light pulse (400 lux) at different CTs. 45 min after the end of the light pulse, the mice were sacrificed. Control animals were sacrificed without prior light exposure.

Specimen preparation and *in situ* hybridization were carried out as described previously (Albrecht, Sun et al. 1997). Briefly, the ^{35}S-UTP (1250 Ci/mmol, PerkinElmer) labelled riboprobes were synthesized using the RNAMaxx^{TM} High Yield transcription kit (Stratagene) according to manufacturer's protocol. The *Bmal1* probe was made from a cDNA corresponding to nucleotides (nt) 654-1290 (accession no. AF015953; (Oster, Yasui et al. 2002)), *Cry1* corresponds to nt 190-771 (AB000777; (Oster, Yasui et al. 2002)), *Cry2* to nt 231-945 (AF156987), *Per2* to nt 229-768 (AF036893; (Albrecht, Sun et al. 1997)), *cFos* to nt 237-332 (Albrecht, Sun et al. 1997). 7 µm thick paraffin sections were dewaxed, rehydrated and fixed in 4 % paraformaldehyde. Sections were then permeabilized using a proteinase K (Roche) digestion before they were fixed again and acetylated. After serial dehydration,

hybridization was performed over-night at 55°C in a humid chamber. Stringency washes were carried out at 63°C. Slides were subjected to a ribonuclease A (Sigma) digestion and then dehydrated in graded ethanol series. Quantification was performed by densitometric analysis (GS-700 or GS-800, BioRad) of autoradiography films (Amersham Hyperfilm) using the Quantity One software (BioRad). Data from the SCN were normalized subtracting the optical density measured in the lateral hypothalamus next to the SCN. For each experiment at least 3 animals per genotype were used and 4 to 9 adjacent SCN sections per animal were analyzed. Relative RNA abundance values were calculated by defining the highest wild-type mean value of each experiment as 100 %. For statistical analysis, all normalized values obtained for one brain were averaged to obtain one final value per animal.

Statistical analysis

Significant differences were determined using GraphPad Prism 4 software. Depending on the type of data, either unpaired t-test, one- or two-way ANOVA with Bonferroni post-test were performed. Values were considered significantly different with $p < 0.05$ (*), $p < 0.01$ (**), or $p < 0.001$ (***).

Results

Generation of *Rev-Erbα*$^{-/-}$*Per1*^{Brdm1} double mutant mice

To better understand the *in vivo* function of *Rev-Erbα* and *Per1*, mice double mutant for these two genes were generated. For this, *Rev-Erbα* (Preitner, Damiola et al. 2002) and *Per1* (Zheng, Albrecht et al. 2001) single mutants were crossed. Double mutant offspring were intercrossed to produce both wild-type and mutant animals. Genotyping (supl. fig. 1) of these mice revealed that all genotypes were obtained at the expected Mendelian ratios (supl. fig. 2A). Moreover, they were all morphologically indistinguishable from their wild-type littermates. In addition, *Rev-Erbα*$^{-/-}$*Per1*^{Brdm1} double mutants are fertile and give birth to normally sized litters at common intervals (supl. fig. 2B & C).

Rev-Erbα$^{-/-}$*Per1*^{Brdm1} double mutant mice display a shorter circadian period in DD

To study the effect of absent *Rev-Erbα* and *Per1* on locomotor activity, mice were housed individually and their wheel-running activity was monitored (Jud, Schmutz et al. 2005). Initially, animals were kept in a 12-h light:12-h dark cycle (LD 12:12h) for several days until they were stably entrained. Subsequently, they were released into constant darkness (DD). Under LD conditions, *Rev-Erbα*$^{-/-}$*Per1*^{Brdm1} double mutants displayed an activity pattern comparable to that of wild-type mice (supl. fig. 3). Upon release into DD, double mutants remained rhythmic and ran with a circadian period of 22.62 ± 0.1 h (mean ± SEM; N = 34) which is significantly shorter than that of the wild-type (23.86 ± 0.02 h; N = 38) and *Rev-Erbα*$^{-/-}$ (23.62 ± 0.05 h; N = 27) or *Per1*^{Brdm1} (23.35 ± 0.06 h; N = 22) single mutant mice (fig. 1). This might indicate that the absence of these two clock genes has a cumulative effect on circadian period in DD. Under constant light conditions, double mutant mice display a period, which is comparable to the one of wild-type animals (supl. table 1).

Clock gene expression levels of *Rev-Erbα*$^{-/-}$*Per1*^{Brdm1} double mutant mice are similar to those observed for *Rev-Erbα*$^{-/-}$ single mutants

In situ hybridization analysis was used to extend our investigations to the molecular level. Clock gene expression patterns in the SCN were determined on coronal brain sections of mice kept in DD for six days. *Bmal1* mRNA accumulation in *Rev-Erbα*$^{-/-}$*Per1*^{Brdm1} double mutant mice was constantly high (fig. 2A). However, levels were slightly lower than those reported for *Rev-Erbα*$^{-/-}$ single mutants (Preitner, Damiola et al. 2002). This in combination with the

observation that the increase in *Bmal1* mRNA was significantly truncated in *Per1*^{Brdm1} single mutant mice could indicate that PER1 may activate *Bmal1* expression.

The expression of *Cry1* was rhythmic with similar peak levels in all four genotypes (fig. 1B). By contrast, the amplitude in *Cry1* mRNA accumulation was dampened in *Rev-Erbα*$^{-/-}$ single and *Rev-Erbα*$^{-/-}$*Per1*^{Brdm1} double mutant mice due to an elevated trough at CT0. *Cry2* was expressed at slightly higher transcript levels in *Rev-Erbα*$^{-/-}$ single and *Rev-Erbα*$^{-/-}$*Per1*^{Brdm1} double mutant mice compared to *Per1*^{Brdm1} single mutant and wild-type animals (fig. 1C). However, these differences were only statistically significant at CT0 for the double mutant animals compared to the wild-type. Interestingly, disruption of *Per1*, *Rev-Erbα*, or both did not alter *Per2* expression patterns (fig. 1D). To sum up, our observations confirmed the previous findings that disrupting *Rev-Erbα* considerably affected the expression of *Bmal1* and *Cry1* but had only little or no consequences on *Cry2* and *Per2* transcript levels (Preitner, Damiola et al. 2002). While *Bmal1* expression seemed to be less changed in *Rev-Erbα*$^{-/-}$ *Per1*^{Brdm1} double mutant mice compared to *Rev-Erbα*$^{-/-}$ single mutants, *Cry1* expression was unchanged between these two mutants. Nevertheless, *Cry2* mRNA oscillations displayed bigger changes in the double than in the single mutant compared to wild-type animals.

Rev-Erbα$^{-/-}$*Per1*^{Brdm1} double mutant mice display a Type 0 PRC and adapt faster to a rescheduled light/dark cycle

The impact of the combined absence of *Rev-Erbα* and *Per1* on the photic response was studied by administering single 15 min light pulses to the animals according to an Aschoff Type I protocol (Aschoff 1965). While wild-type mice displayed the expected low amplitude (Type I) phase response curve (PRC), *Rev-Erbα*$^{-/-}$*Per1*^{Brdm1} double mutants showed high amplitude (Type 0) resetting (fig. 3A & B; Winfree 1970; Winfree 1980). For double mutant animals, the so-called "breakpoint" (transition from phase delays to phase advances) was observed between CT22 and CT24. At this time point it was not possible to distinguish whether the animals make huge phase advances or delays. Interestingly, some mice became transiently arrhythmic after a light pulse given at CT22 for some days (data not shown). The difference between weak and strong resetting can be visualized more clearly when data are plotted as a phase transition curve (PTC). Thus, the time the light pulse was given is compared to the time the phase is shifted to after the light pulse (i.e. "old" *versus* "new phase"). In wild-type mice, all data points were found to be close to the diagonal of the square, which has a slope of 1 (fig. 3C). Hence, the new phase was almost identical with the

old one and they displayed a so-called Type 1 resetting. By contrast, the average slope for *Rev-Erbα*$^{-/-}$*Per1*^{Brdm1} double mutants was close to 0 (fig. 3D).

Due to the strong resetting phenotype of the double mutant animals we were curious to find out, how fast they adapt to an experimental jet lag. Hence we entrained them to LD 12:12h before they were subjected to an 8 h advance of the lighting schedule. *Rev-Erbα*$^{-/-}$*Per1*^{Brdm1} double mutant mice achieved stable re-entrainment already after 4.00 ± 0.69 days (mean ± SEM; N= 7) while it took two times longer for wild-type animals (10.67 ± 1.26 days; N = 6; fig. 3E). Likewise, *Rev-Erbα*$^{-/-}$*Per1*^{Brdm1} (2.80 ± 0.20 days; N = 5) double mutants adapted faster to an 8 h delay in the photoschedule (fig. 3F) compared to wild-type mice (4.33 ± 0.21 days; N = 6).

Cry1 is light inducible in *Rev-Erbα*$^{-/-}$*Per1*^{Brdm1} double mutant mice

To find an explanation for the Type 0 resetting observed in mutants lacking both *Rev-Erbα* and *Per1*, we examined the light inducibility of some clock genes. Surprisingly, the otherwise not light inducible gene *Cry1* was increased after a light pulse at CT22 in double mutant animals relative to dark controls (fig. 4A). As expected, wild-type and single mutant mice did not show any *Cry1* induction neither at CT22 nor at CT14 (fig. 4B). In contrast to CT22, light did not induce *Cry1* expression in *Rev-Erbα*$^{-/-}$*Per1*^{Brdm1} double mutant mice at CT14. This observation was in line with the finding that double mutants showed relatively normal phase shifts at this time point. In addition, *Per2* was induced to a higher extent in double mutant mice compared to the three other genotypes at CT22 (fig. 4C) but not at CT14 (data not shown). Expression of *Dec1*, another known light inducible clock gene, was increased stronger in double mutants relative to the other genotypes at both CT14 and CT22 (data not shown). The signal intensity for *cFos* was similar between all genotypes after a light pulse at CT22 (fig. 4D) indicating that the light signalling pathway is not oversaturated. Hence the Type 0 PRC is rather elicited by changes in the circadian pacemaker (fig. 4A & C) then by a hypersensitivity to light (fig. 4D).

To sum up *Rev-Erbα*$^{-/-}$*Per1*^{Brdm1} double mutant mice were fertile and morphologically indistinguishable from wild-type animals. Although they displayed a shorter circadian period in DD, their molecular oscillator seemed to be still functional. However, their response to brief light pulses was altered and they displayed high amplitude resetting. Interestingly, *Cry1* became light inducible if the photic signal was presented at the end of the subjective night.

Discussion

Here we show that mice deficient for both *Rev-Erbα*$^{-/-}$ and *Per1*^{Brdm1} displayed a dramatically shorter circadian period in DD compared to single mutants and wild-types (fig. 1). As reported previously, *Rev-Erbα*$^{-/-}$ and *Per1*^{Brdm1} single mutant mice on their part exhibited significantly shorter circadian periods relative to wild-type animals (Zheng, Albrecht et al. 2001; Preitner, Damiola et al. 2002). Hence the shorter period observed in the double mutants might indicate that the concomitant absence of these two clock genes has an additive effect on circadian period in DD.

To avoid any influence of prior light exposure, we chose an Aschoff Type I protocol to study photic entrainment. Hence animals were kept in DD until stable entrainment was achieved (after about 2 month). Then they were subjected to brief light pulses at different CTs. In agreement with earlier studies, both, *Rev-Erbα*$^{-/-}$ and *Per1*^{Brdm1} deficient animals phase advanced their wheel-running behaviour after a light pulse administered at the end of the subjective night (data not shown; Preitner, Damiola et al. 2002; Spoelstra, Albrecht et al. 2004). In contrast to the other genotypes, *Rev-Erbα*$^{-/-}$*Per1*^{Brdm1} double mutants did show high amplitude resetting at the end of the night (fig. 3A-D). A similar phenotype has already been reported for heterozygous *Clock* mice, which exhibit a Type 0 PRC in response to 6-h light pulses (Vitaterna, Ko et al. 2006). Interestingly, light inducibility of both *Per1* and *Per2* was not affected by the *Clock*$^{+/-}$ mutation. However, basal expression levels of *Per* genes were significantly blunted in both *Clock* homo- and heterozygous mice. In contrast to their observations we could not detect any dampened *Per2* expression in our animals. *In situ* hybridization profiles for *Per2* were completely identical between *Rev-Erbα*$^{-/-}$*Per1*^{Brdm1} double mutant and wild-type animals (fig. 2D). Moreover, they could not detect any differences in light induction of either *Per1* or *Per2* between *Clock* heterozygous and wild-type mice (Vitaterna, Ko et al. 2006). By contrast, we found that *Per2* induction was stronger in *Rev-Erbα*$^{-/-}$*Per1*^{Brdm1} double mutants compared to wild-types (fig. 4C). These findings indicate that the mechanisms underlying the Type 0 PRC in *Rev-Erbα*$^{-/-}$*Per1*^{Brdm1} double mutant mice are different from those in *Clock* mutants.

Whether Type 0 or a Type 1 resetting is exhibited depends not only on species but also on the strength of the stimulus. Increasing the light dose can convert a Type 1 into a Type 0 PRC. Other factors like genetic mutations or background light quality and/or intensity can affect the sensitivity of the pacemaker to the light pulse. Hence perception of stimulus strength is changed (Johnson 1992). Concerning the *Rev-Erbα*$^{-/-}$*Per1*^{Brdm1} double mutant mice an

oversaturation of the circadian system can be excluded because *cFos* was induced comparably in all genotypes at CT22 (fig. 4D). Hence it is rather unlikely that the observed Type 0 PRC is caused by a hypersensitivity to light. It is more likely that it is elicited by changes in the core clock components (fig. 4A & C).

Surprisingly, we observed that *Cry1* became light inducible in *Rev-Erbα*$^{-/-}$*Per1*^{Brdm1} double mutant mice by a light pulse delivered at CT22 but not at CT14 (fig. 4A & B). So far, *Cry1* was thought not to respond to light pulses at all in mammals (Okamura, Miyake et al. 1999; Field, Maywood et al. 2000). However, a recent study has shown that *Cry1a* acts as a light-signalling molecule in the zebrafish (*Danio rerio*) clock (Tamai, Young et al. 2007) as its induction was found to be critical for light-induced phase shifts. Nonetheless, *Cry1a* seems not to be the only actor in the light input pathway to the zebrafish clock as light pulses also strongly induced *Per2*. Interestingly, we observed an induction of *Per2* in our double mutants too (fig. 4C). In the past few years, the zebrafish became one of the most valuable lower vertebrate models for studying circadian clock function. It is thought that the teleost (= "perfectly boned fish") circadian system might be the more ancestral vertebrate clock that became far more specialized in mammals due to selective pressure. Hence *Rev-Erbα* and *Per1* might have acquired additional features, which prevent strong resetting in mammals. Moreover, the circadian pacemakers in zebrafish cell lines showed high amplitude phase shifts in response to light pulses (Vallone, Gondi et al. 2004; Tamai, Young et al. 2007). Contrary to mammals, most, if not all, of the zebrafish tissues are directly light responsive (Whitmore, Foulkes et al. 1998; Whitmore, Foulkes et al. 2000; Yoo, Yamazaki et al. 2004) as it is the case for *Drosophila* (Vansteensel, Michel et al. 2008). It is speculated that a great degree of similarity exists between the observations made in cell culture and what happens in the whole fish (Carr, Katherine Tamai et al. 2006). This idea is strengthened by the fact that the heart taken from *Period3-luciferase* transgenic zebrafish showed a Type 0 PRC (Kaneko, Hernandez-Borsetti et al. 2006). However, the spleen (Kaneko, Hernandez-Borsetti et al. 2006) and the melatonin production rhythm from cultured pineal glands showed a Type 1 PRC (DeBruyne, Hurd et al. 2004).

Another remarkable fact is that *Cry1* has been reported to be a potentially rate-limiting factor in behavioural adjustments to time zone transitions in mammals (Reddy, Field et al. 2002). Usually, animals take longer to phase advance than to delay their clock in response to an acute shift in the complete lighting schedule (Takamure, Murakami et al. 1991; Yamazaki, Numano et al. 2000; Reddy, Field et al. 2002). Consistent with observations in rodents, subjective impressions of people travelling rapidly across time zones indicate that phase

delays are accomplished more rapidly and with fewer disturbances than phase advances. In contrast to phase delays, the clock cannot be advanced more than three hours per day. Hence the activity-rest cycle has to be advanced gradually whereas delays are completed rapidly. Reddy and colleagues saw that during both gradual advances and immediate delays, the shift of the *Cry1* loop matched that for the activity-rest rhythm. Since they observed concomitant changes in *Per2* they hypothesized that the regulation of *Cry1* could be a consequence of altered PER2 expression. However further details about the role of *Per1* and *Per2* in resetting need to be elucidated. Finally, they concluded that the *Cry1* response in the SCN might be sufficient to explain gradual resetting of locomotor behaviour. Moreover, they hypothesized that delay resetting is easier to achieve because it occurs when endogenous *Cry1* levels are high. Interestingly, they propose that PER2 may have an effect on *Cry1* expression independently of its proposed regulation of BMAL1 (Reddy, Field et al. 2002).

Since *Rev-Erbα*$^{-/-}$*Per1*^{Brdm1} double mutant mice displayed Type 0 resetting we thought that they might adapt faster to rescheduled light/dark cycles. Indeed they adjusted their wheel-running behaviour much faster to an advanced light/dark cycle relative to wild-types (fig. 3E). Furthermore, they accomplished phase delays faster than the other genotypes (fig. 3F). Surprisingly, unpaired t-test did not reveal a significant difference for double mutant mice between the two jet lag paradigms. Hence it took them about the same time to adapt to either advances or delays. As expected, wild-type mice took dramatically longer to adapt to a phase advance than to a delay (fig. 3E & F). Our findings suggest that the actual adaptation to a new time would be fast but is slowed down by components of the circadian clock. This is in line with previous findings where they demonstrate that rapid phase resetting in the liver is counteracted by active signalling pathways (Le Minh, Damiola et al. 2001).

As reported in previous studies, the orphan nuclear receptor REV-ERBα is able to repress *Cry1* expression by two different ways. First, REV-ERBα inhibits *Bmal1* transcription, which indirectly represses *Cry1* expression (Preitner, Damiola et al. 2002). Our *in situ* hybridization profiles for *Cry1* and *Bmal1* in *Rev-Erbα*$^{-/-}$ single and *Rev-Erbα*$^{-/-}$*Per1*^{Brdm1} double mutant mice confirmed the initial finding. In the absence of *Rev-Erbα, Bmal1* was constantly high (fig. 2A) and *Cry1* trough levels were less profound compared to wild-type animals (fig. 2B). Second REV-ERBα can directly suppress *Cry1* transcription by binding to RORE motifs located in the *Cry1* promoter (Etchegaray, Lee et al. 2003). Apart from REV-ERBα, CLOCK/BMAL1 heterodimers activate *Cry1* transcription by binding to E-box motifs. Recently, this model has been challenged by the hypothesis that CLOCK/BMAL1 activates

some promoters while repressing others (Kondratov, Shamanna et al. 2006). Indeed *Cry1* was up-regulated in *Bmal1*$^{-/-}$ mice while *Per1* was down-regulated (Kondratov, Shamanna et al. 2006; Hirayama, Sahar et al. 2007). In a cell-based transient transfection approach both *Cry1* and *Per1* promoters were activated by CLOCK/BMAL1 but to different extents. *Cry1* was induced by only 2-fold from its basal expression level whereas *Per1* was induced by more than 20-fold. However, basal levels differed quite drastically between the two genes with *Cry1* displaying more than 15-fold higher basal levels. Adding CRY1 inhibited the CLOCK/BMAL1- dependent transactivation of *Per1* to a level still higher than the basal activity. By contrast, *Cry1* expression was repressed to levels about 3-fold lower than basal. From this they concluded that *Cry1* expression is mostly regulated by transrepression and *Per1* by transactivation (Kondratov, Shamanna et al. 2006). In addition, PER1 seems to have an activating effect on *Bmal1* transcription because its peak level is lowered in *Per1*^{Brdm1} single mutant mice (fig. 2A). Hence *Cry1* transcription might be influenced by the disruption of both *Rev-Erbα* and *Per1* to a different degree. Moreover, the altered abundance of *Cry1* transcripts might influence its own transcription to a bigger extent in the absence of the two regulating genes *Rev-Erbα* and *Per1*. The missregulation of *Cry1* expression might then culminate in its light inducibility due to lacking repression. However, the mechanisms beneath *Cry1* regulation have to be further elucidated. Likewise, it is not yet clear whether *Cry1* induction alone leads to a Type 0 resetting in *Rev-Erbα*$^{-/-}$*Per1*^{Brdm1} double mutant mice. It seems that in the course of evolution complex mechanisms have been added to prevent light inducibility of *Cry1* in mammals as compared to zebrafish or *Drosophila*. In conclusion, our results suggest that *Rev-Erbα* and *Per1* exhibit a gain of function phenotype in mammals. Hence disrupting them seems to lead to a loss of function, which results in strong Type 0 resetting.

Acknowledgements

First of all the authors thank Prof. Russell Foster for his precious input. Moreover they thank the laboratory technicians A. Hayoz and S. Baeriswyl for their help and Dr. J.A. Ripperger and I. Schmutz for critically reading the manuscript. This work has been supported by the Swiss National Science Foundation, the EUCLOCK project and the state of Fribourg (Switzerland).

References

Akashi, M. and T. Takumi (2005). "The orphan nuclear receptor RORalpha regulates circadian transcription of the mammalian core-clock Bmal1." Nat Struct Mol Biol **12**(5): 441-8.

Albrecht, U., Z. S. Sun, et al. (1997). "A differential response of two putative mammalian circadian regulators, mper1 and mper2, to light." Cell **91**(7): 1055-64.

Aschoff, J. (1965). Response curves in circadian periodicity. Circadian clocks. J. Aschoff. Amsterdam, North-Holland Publishing Co.**:** 95-111.

Aschoff, J. (1969). "Desynchronization and resynchronization of human circadian rhythms." Aerosp Med **40**(8): 844-9.

Carr, A. J., T. Katherine Tamai, et al. (2006). "Light reaches the very heart of the zebrafish clock." Chronobiol Int **23**(1-2): 91-100.

Daan, S. and C. S. Pittendrigh (1976). "A functional analysis of circadian pacemakers in rodents. II. The variability of phase response curves." J Comp Physiol **106**: 253-66.

DeBruyne, J., M. W. Hurd, et al. (2004). "Isolation and phenogenetics of a novel circadian rhythm mutant in zebrafish." J Neurogenet **18**(2): 403-28.

Etchegaray, J. P., C. Lee, et al. (2003). "Rhythmic histone acetylation underlies transcription in the mammalian circadian clock." Nature **421**(6919): 177-82.

Field, M. D., E. S. Maywood, et al. (2000). "Analysis of clock proteins in mouse SCN demonstrates phylogenetic divergence of the circadian clockwork and resetting mechanisms." Neuron **25**(2): 437-47.

Giguere, V. (1999). "Orphan nuclear receptors: from gene to function." Endocr Rev **20**(5): 689-725.

Griffin, E. A., Jr., D. Staknis, et al. (1999). "Light-independent role of CRY1 and CRY2 in the mammalian circadian clock." Science **286**(5440): 768-71.

Hirayama, J., S. Sahar, et al. (2007). "CLOCK-mediated acetylation of BMAL1 controls circadian function." Nature **450**(7172): 1086-90.

Jin, X., L. P. Shearman, et al. (1999). "A molecular mechanism regulating rhythmic output from the suprachiasmatic circadian clock." Cell **96**(1): 57-68.

Johnson, C. H. (1992). Phase response curves: what can they tell us about circadian clocks? Circadian clocks from cell to human. T. Hiroshige and K. Honma. Sapporo, Hokkaido University Press**:** 209-249.

Jud, C., I. Schmutz, et al. (2005). "A guideline for analyzing circadian wheel-running behavior in rodents under different lighting conditions." Biol Proced Online **7**: 101-16.

Kaneko, M., N. Hernandez-Borsetti, et al. (2006). "Diversity of zebrafish peripheral oscillators revealed by luciferase reporting." Proc Natl Acad Sci U S A **103**(39): 14614-9.

Koh, K., X. Zheng, et al. (2006). "JETLAG resets the Drosophila circadian clock by promoting light-induced degradation of TIMELESS." Science **312**(5781): 1809-12.

Kondratov, R. V., R. K. Shamanna, et al. (2006). "Dual role of the CLOCK/BMAL1 circadian complex in transcriptional regulation." FASEB J **20**(3): 530-2.

Kume, K., M. J. Zylka, et al. (1999). "mCRY1 and mCRY2 are essential components of the negative limb of the circadian clock feedback loop." Cell **98**(2): 193-205.

Le Minh, N., F. Damiola, et al. (2001). "Glucocorticoid hormones inhibit food-induced phase-shifting of peripheral circadian oscillators." Embo J **20**(24): 7128-36.

Lin, F. J., W. Song, et al. (2001). "Photic signaling by cryptochrome in the Drosophila circadian system." Mol Cell Biol **21**(21): 7287-94.

Moore, R. Y. and N. J. Lenn (1972). "A retinohypothalamic projection in the rat." J Comp Neurol **146**(1): 1-14.

Okamura, H., S. Miyake, et al. (1999). "Photic induction of mPer1 and mPer2 in cry-deficient mice lacking a biological clock." Science **286**(5449): 2531-4.

Oster, H., A. Yasui, et al. (2002). "Disruption of mCry2 restores circadian rhythmicity in mPer2 mutant mice." Genes Dev **16**(20): 2633-8.

Pittendrigh, C. S. (1960). "Circadian rhythms and the circadian organization of living systems." Cold Spring Harb Symp Quant Biol **25**: 159-84.

Preitner, N., F. Damiola, et al. (2002). "The orphan nuclear receptor REV-ERBalpha controls circadian transcription within the positive limb of the mammalian circadian oscillator." Cell **110**(2): 251-60.

Ralph, M. R., R. G. Foster, et al. (1990). "Transplanted suprachiasmatic nucleus determines circadian period." Science **247**(4945): 975-8.

Ramirez-Solis, R., H. Zheng, et al. (1993). "Hoxb-4 (Hox-2.6) mutant mice show homeotic transformation of a cervical vertebra and defects in the closure of the sternal rudiments." Cell **73**(2): 279-94.

Reddy, A. B., M. D. Field, et al. (2002). "Differential resynchronisation of circadian clock gene expression within the suprachiasmatic nuclei of mice subjected to experimental jet lag." J Neurosci **22**(17): 7326-30.

Sato, T. K., S. Panda, et al. (2004). "A functional genomics strategy reveals Rora as a component of the mammalian circadian clock." Neuron **43**(4): 527-37.

Spoelstra, K., U. Albrecht, et al. (2004). "Phase responses to light pulses in mice lacking functional per or cry genes." J Biol Rhythms **19**(6): 518-29.

Stephan, F. K. and I. Zucker (1972). "Circadian rhythms in drinking behavior and locomotor activity of rats are eliminated by hypothalamic lesions." Proc Natl Acad Sci U S A **69**(6): 1583-6.

Takahashi, J. S., H. K. Hong, et al. (2008). "The genetics of mammalian circadian order and disorder: implications for physiology and disease." Nat Rev Genet **9**(10): 764-75.

Takamure, M., N. Murakami, et al. (1991). "Rapid reentrainment of the circadian clock itself, but not the measurable activity rhythms to a new light-dark cycle in the rat." Physiol Behav **50**(2): 443-9.

Tamai, T. K., L. C. Young, et al. (2007). "Light signaling to the zebrafish circadian clock by Cryptochrome 1a." Proc Natl Acad Sci U S A **104**(37): 14712-7.

Ueda, H. R., W. Chen, et al. (2002). "A transcription factor response element for gene expression during circadian night." Nature **418**(6897): 534-9.

Vallone, D., S. B. Gondi, et al. (2004). "E-box function in a period gene repressed by light." Proc Natl Acad Sci U S A **101**(12): 4106-11.

Vansteensel, M. J., S. Michel, et al. (2008). "Organization of cell and tissue circadian pacemakers: a comparison among species." Brain Res Rev **58**(1): 18-47.

Vitaterna, M. H., C. H. Ko, et al. (2006). "The mouse Clock mutation reduces circadian pacemaker amplitude and enhances efficacy of resetting stimuli and phase-response curve amplitude." Proc Natl Acad Sci U S A **103**(24): 9327-32.

Whitmore, D., N. S. Foulkes, et al. (2000). "Light acts directly on organs and cells in culture to set the vertebrate circadian clock." Nature **404**(6773): 87-91.

Whitmore, D., N. S. Foulkes, et al. (1998). "Zebrafish Clock rhythmic expression reveals independent peripheral circadian oscillators." Nat Neurosci **1**(8): 701-7.

Winfree, A. T. (1970). "Integrated view of resetting a circadian clock." J Theor Biol **28**(3): 327-74.

Winfree, A. T. (1980). The geometry of biological time. Biomathematics. New York, Springer Verlag. **8**.

Yamazaki, S., R. Numano, et al. (2000). "Resetting central and peripheral circadian oscillators in transgenic rats." Science **288**(5466): 682-5.

Yoo, S. H., S. Yamazaki, et al. (2004). "PERIOD2::LUCIFERASE real-time reporting of circadian dynamics reveals persistent circadian oscillations in mouse peripheral tissues." Proc Natl Acad Sci U S A **101**(15): 5339-46.

Zheng, B., U. Albrecht, et al. (2001). "Nonredundant roles of the mPer1 and mPer2 genes in the mammalian circadian clock." Cell **105**(5): 683-94.

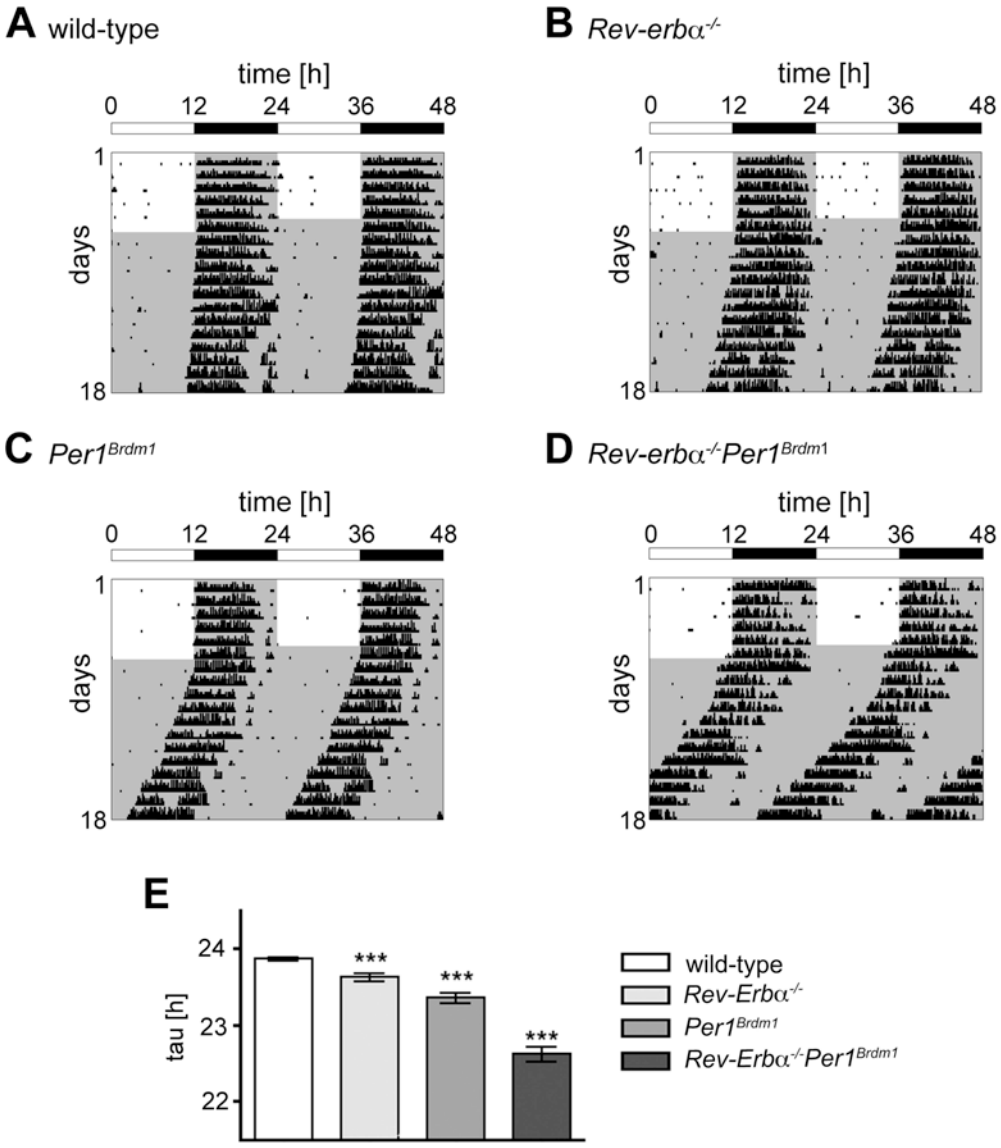

Figure 1: Representative wheel-running activity plots.
(A-D) Representative locomotor activity records of wild-type (A), *Rev-Erbα*$^{-/-}$ (B), *Per1*^{Brdm1} (C), and *Rev-Erbα*$^{-/-}$*Per1*^{Brdm1} double mutant mice (D) under both light/dark (white and grey shaded, respectively) and constant darkness (grey shaded) conditions. Black bars represent wheel-revolutions. The actograms are double-plotted with the activity of the following light/dark cycle plotted to the right and below the previous light/dark cycle. The white and black bar on the top of each actogram indicates light and darkness, respectively. **(E)** Average free-running period (tau) in constant darkness. Data are represented as mean ± SEM. Unpaired t-test was performed to compare the free-running period length of *Rev-Erbα*$^{-/-}$ (23.62 ± 0.05 h; N = 27), *Per1*^{Brdm1} (23.35 ± 0.06 h; N = 22), and *Rev-Erbα*$^{-/-}$*Per1*^{Brdm1} (22.62 ± 0.1 h; N = 34) mutant to wild-type (23.86 ± 0.02 h; N = 38) mice. *** $p < 0.0001$.

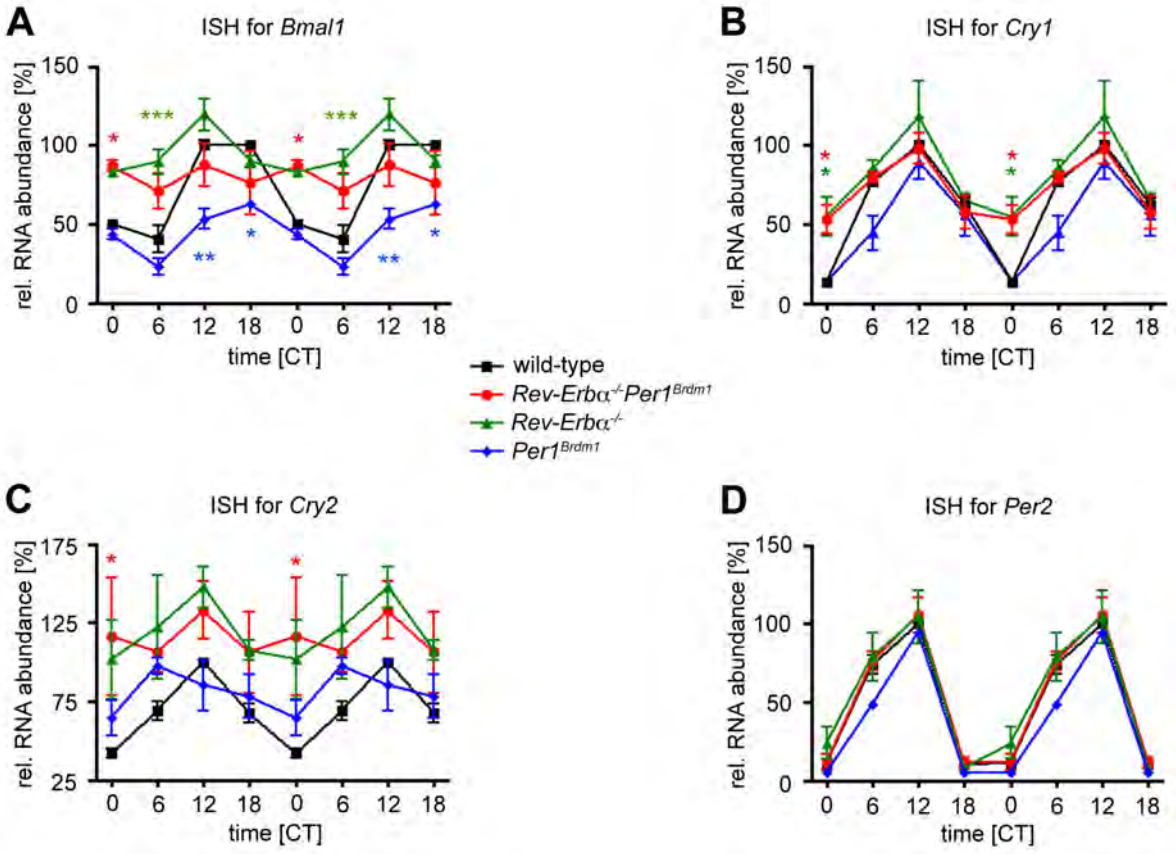

Figure 2: *In situ* hybridization (ISH) profiles of cycling clock gene expression in the SCN of wild-type (black line), *Rev-Erbα*$^{-/-}$*Per1*^{Brdm1} (red line), *Rev-Erbα*$^{-/-}$ (green line), and *Per1*^{Brdm1} (blue line) mice kept in DD for 6 days. Values are double plotted and represented as mean ± SEM (N = 3). **(A)** *Bmal1* expression; **(B)** *Cry1* expression; **(C)** *Cry2* expression; **(D)** *Per2* expression. Two-way ANOVA with Bonferroni post-test was performed to determine significant differences between genotypes. * $p < 0.05$; ** $p < 0.01$; *** $p < 0.001$.

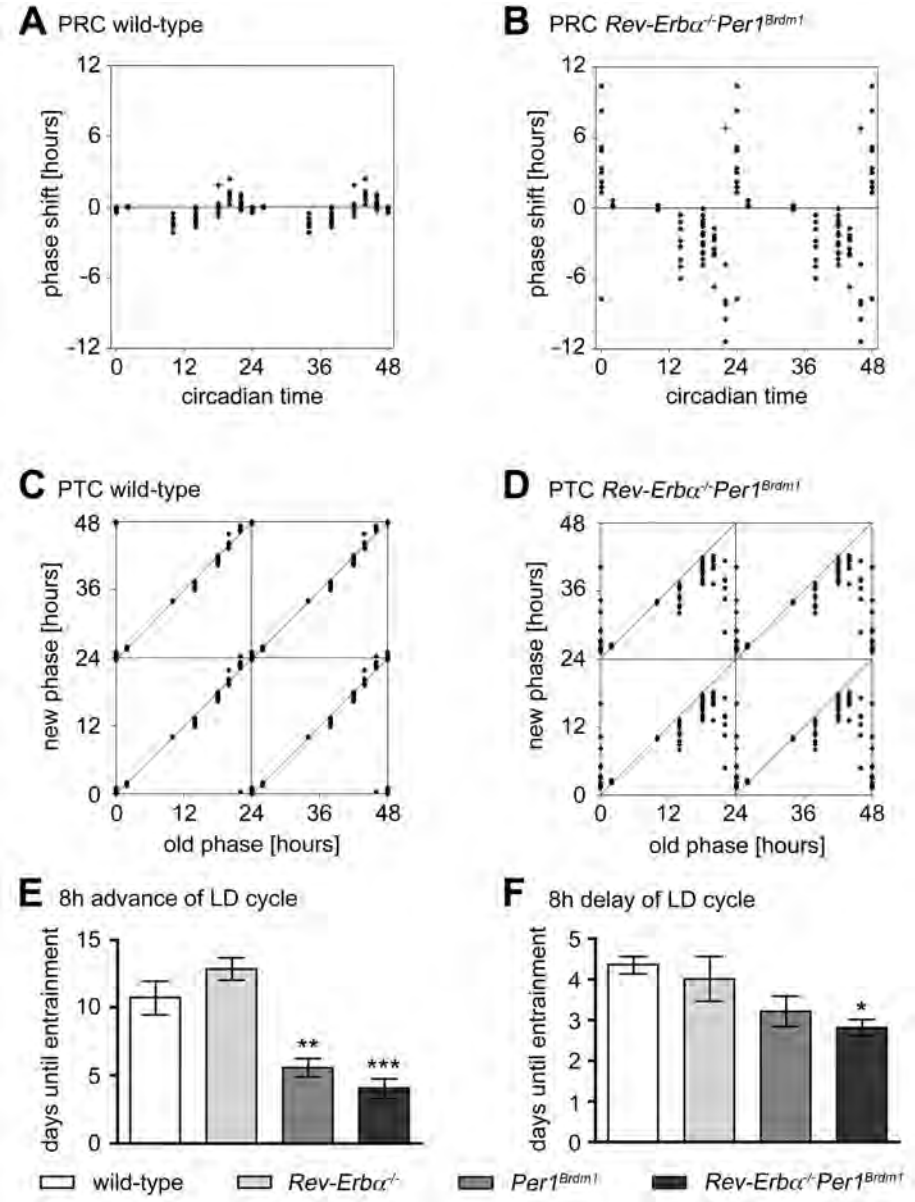

Figure 3: Phase shifting responses to light pulses and rescheduled light/dark cycles.
(A/B) Phase response curve (PRC) of wild-type (A; N = 4-15) and *Rev-Erb*$^{-/-}$*Per1*^{Brdm1} (B; N = 8-15) double mutant mice to 15 min light pulses. The x-axis indicates the circadian time the light pulse was administered and the y-axis represents the phase shift produced by the light pulse. Each dot represents the phase shift of one animal. **(C/D)** Phase transition curve (PTC) of wild-type (C) and *Rev-Erb*$^{-/-}$ *Per1*^{Brdm1} (D) double mutant mice to 15 min light pulses. Data of A and B are replotted to obtain C and D, respectively. The x-axis indicates the circadian time the light pulse was administered (old phase). The y-axis displays the circadian time to which locomotor activity was shifted after the light pulse (new phase). **(E)** Average time to adjust to an 8-hour advance of the light/dark (LD) cycle. Data are represented as mean ± SEM. Unpaired t-test was performed to compare the days until re-entrainment of *Rev-Erbα*$^{-/-}$ (12.80 ± 0.80 days; N = 5), *Per1*^{Brdm1} (5.50 ± 0.67 days; N = 6), and *Rev-Erbα*$^{-/-}$*Per1*^{Brdm1} (4.00 ± 0.69; N = 7) mutant to wild-type (10.67 ± 1.26 days; N = 6) mice. ** $p < 0.01$; *** $p < 0.001$. **(F)** Average time to adjust to an 8-hour delay of the light/dark (LD) cycle. Data are represented as mean ± SEM. Unpaired t-test was performed to compare the days until re-entrainment of *Rev-Erbα*$^{-/-}$ (4.00 ± 0.55 days; N = 5), *Per1*^{Brdm1} (3.20 ± 0.37 days; N = 5), and *Rev-Erbα*$^{-/-}$*Per1*^{Brdm1} (2.80 ± 0.20 days; N = 5) mutant to wild-type (4.33 ± 0.21 days; N = 6) mice. * $p < 0.05$.

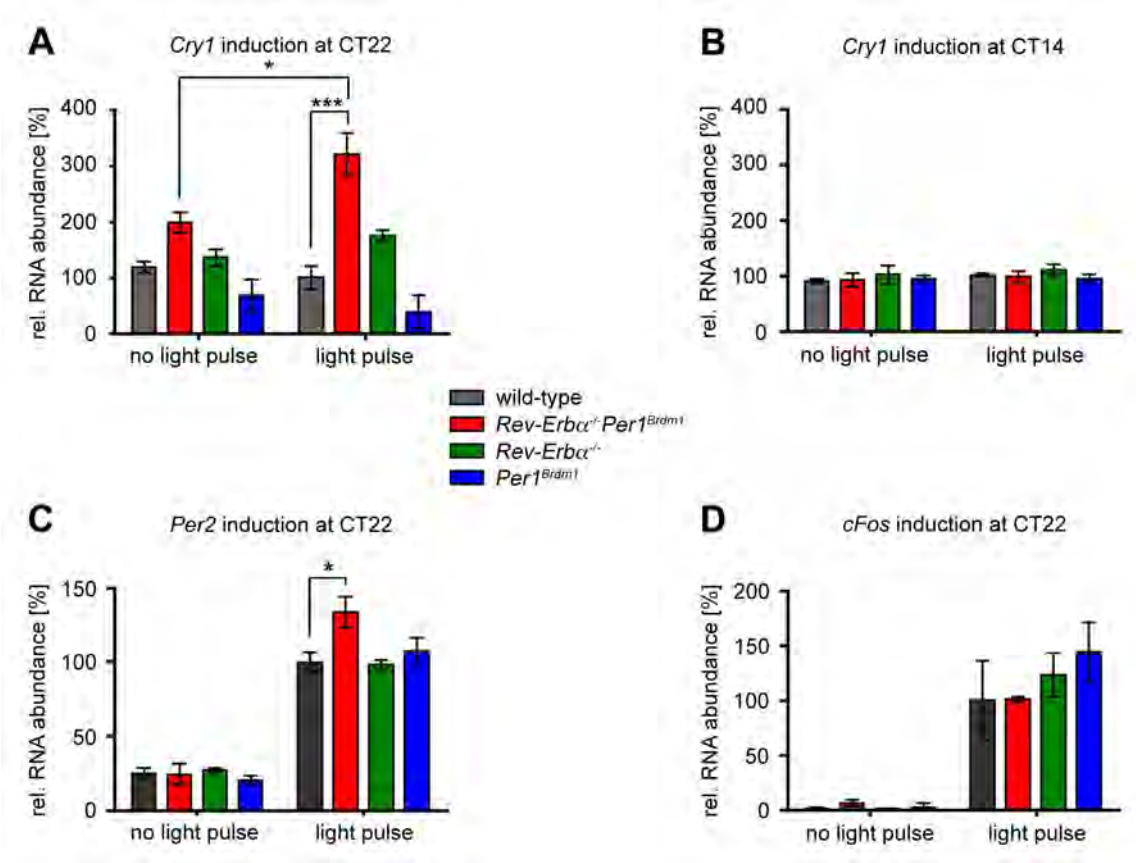

Figure 4: Light induced mRNA accumulation in the SCN of wild-type (black), *Rev-Erbα*$^{-/-}$ *Per1*^{Brdm1} (red), *Rev-Erbα*$^{-/-}$ (green), and *Per1*^{Brdm1} (blue) mice. Values are represented as mean ± SEM. **(A)** *Cry1* induction after a light pulse at CT22 (N = 3); **(B)** *Cry1* induction after a light pulse at CT14 (N = 3); **(C)** *Per2* induction after a light pulse at CT22 (N = 3-5); **(D)** *cFos* induction after a light pulse at CT22 (N = 3). Two-way ANOVA with Bonferroni post-test was performed to determine significant differences between genotypes. Unpaired to t-test was used to determine significant differences between light pulsed and dark control animals. * $p < 0.05$; *** $p < 0.001$.

Supplemental data

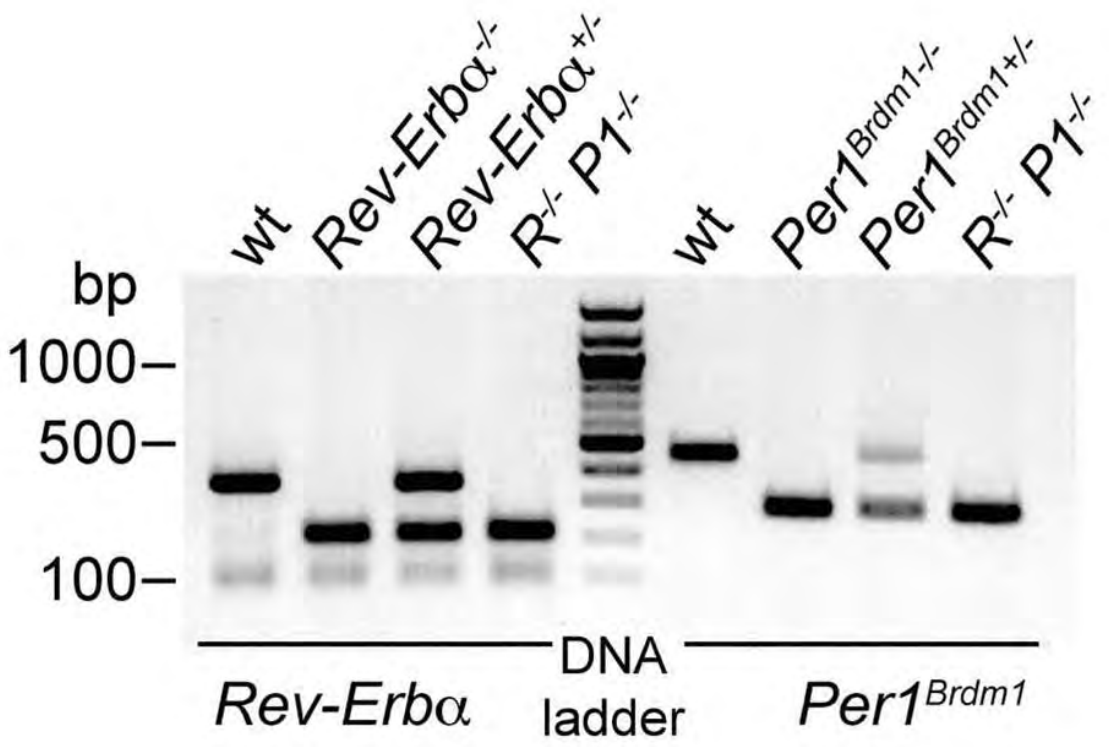

Supplemental figure 1: PCR analysis of mouse tail DNA for *Rev-Erbα* and *Per1*.
Primers for *Rev-Erbα* amplify a fragment of about 340 nt on the wild-type allele and of about 200 nt on the mutant allele. The PCR for *Per1* amplifies a fragment of about 290 nt on the mutant allele and of about 450 nt on the wild-type allele.

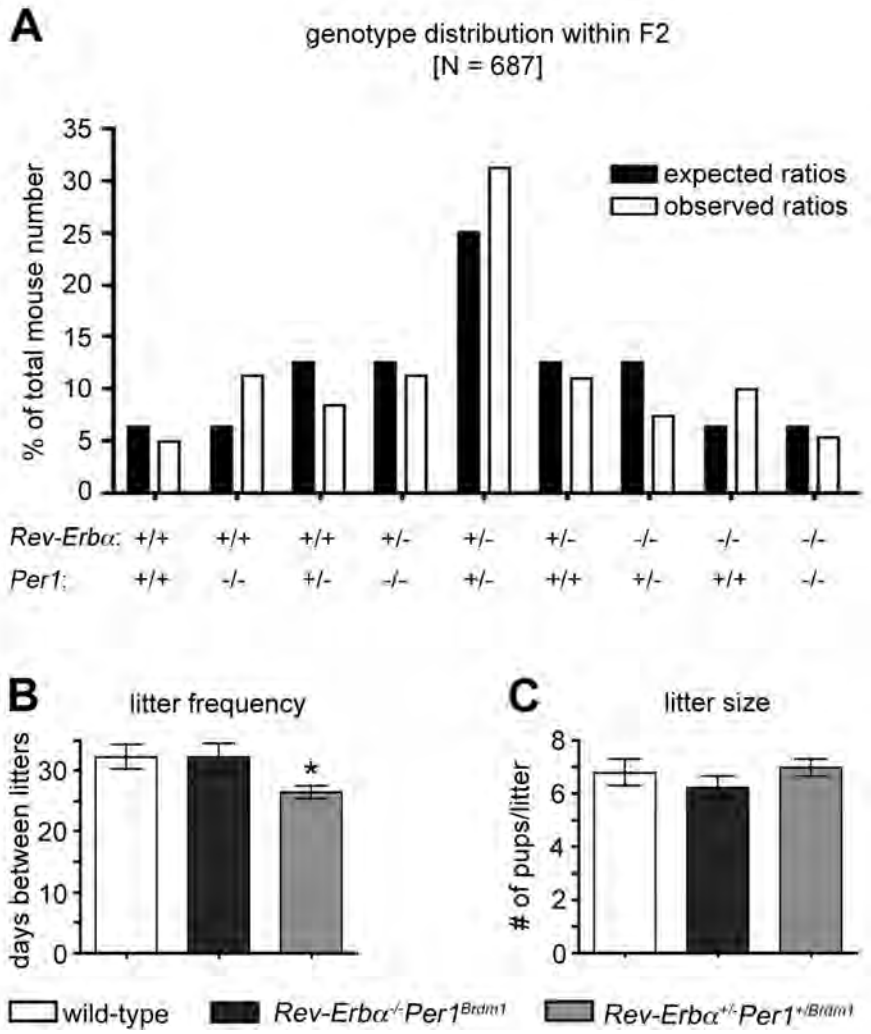

Supplemental figure 2: Breeding statistics.
(A) Distribution of genotypes in the F2 generation born to *Rev-Erbα*$^{+/-}$*Per1*$^{+/Brdm1}$ double heterozygous parents. Black bars represent the expected Mendelian distribution while white bars display the observed ratios. The x-axis indicates the genotype of the F2 offspring. The percent of the total mouse number displaying a certain genotype is plotted on the y-axis. **(B)** Litter frequency of wild-type (white), *Rev-Erbα*$^{-/-}$*Per1*^{Brdm1} double homozygous (dark grey), and *Rev-Erbα*$^{+/-}$*Per1*$^{+/Brdm1}$ double heterozygous (light grey) breeding pairs. Data are represented as mean ± SEM. On average, wild-type matings gave birth to a new litter every 32.22 ± 2.06 days (N = 41), *Rev-Erbα*$^{-/-}$*Per1*^{Brdm1} double homozygous breeding pairs every 32.12 ± 2.33 days (N = 33), and *Rev-Erbα/Per1* double heterozygous couples every 26.42 ± 1.04 days (N = 60). One-way ANOVA with Bonferroni's multiple comparison was performed to compare the litter frequency of the three genotypes. * $p < 0.05$. **(C)** Number of pups born to wild-type (white), *Rev-Erbα*$^{-/-}$*Per1*^{Brdm1} double homozygous (dark grey), and *Rev-Erbα*$^{+/-}$*Per1*$^{+/Brdm1}$ double heterozygous (light grey) breeding pairs. Data are represented as mean ± SEM. On average, wild-type couples gave birth to 6.76 ± 0.51 pups (N = 38), *Rev-Erbα*$^{-/-}$*Per1*^{Brdm1} double homozygous breeding pairs to 6.18 ± 0.43 pups (N = 33), and *Rev-Erbα/Per1* double heterozygous couples to 6.94 ± 0.31 pups (N = 69). One-way ANOVA with Bonferroni's multiple comparison did not reveal any significant differences in litter size between the three genotypes.

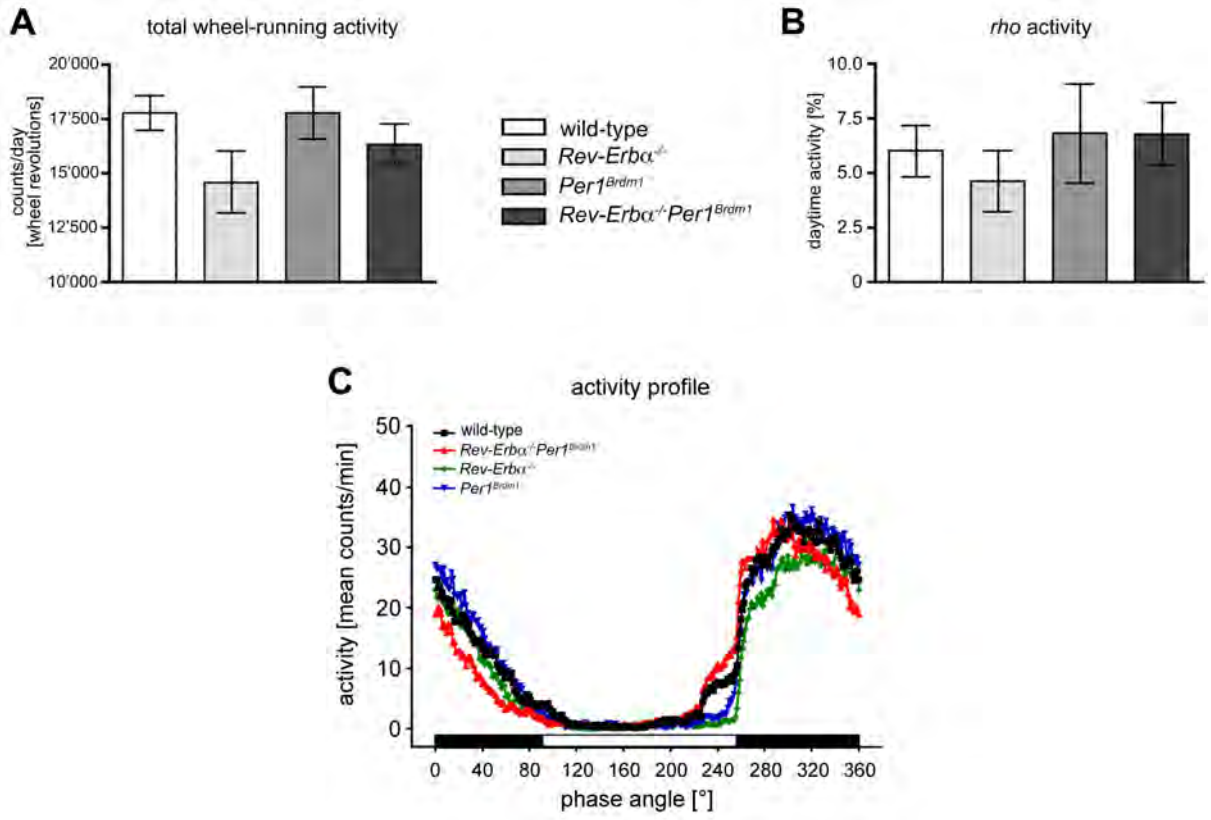

Supplemental figure 3: Total and daytime wheel-running activity.
(A) Total wheel-running activity of mice kept under LD 12:12 h. On average, wild-type mice make 17'738 ± 808 wheel-revolutions per day (N = 32), *Rev-Erbα*$^{-/-}$*Per1*^{Brdm1} double mutants 16'307 ± 929 (N = 29), *Rev-Erbα*$^{-/-}$ single mutants 14'551 ± 1420 (N = 17), and *Per1*^{Brdm1} single mutants 17'718 ± 1195 (N = 16). **(B)** Rest (*rho*) phase activity of mice kept under LD 12:12 h. Wild-type mice spend 5.98 ± 1.18 % (N = 32) of their total activity during the day, *Rev-Erbα*$^{-/-}$*Per1*^{Brdm1} double mutants 6.74 ± 1.4 % (N = 29), *Rev-Erbα*$^{-/-}$ single mutants 4.6 ± 1.4 % (N = 17), and *Per1*^{Brdm1} single mutants 6.76 ± 2.3 % (N = 16). Data are represented as mean ± SEM. One-way ANOVA with Bonferroni's multiple comparison did not reveal any significant difference between genotypes for both total and *rho* phase activity. **(C)** 24-h average distribution of activity for wild-type (black; N = 32), *Rev-Erbα*$^{-/-}$*Per1*^{Brdm1} double mutant (red; N = 29), *Rev-Erbα*$^{-/-}$ single mutant (green; N = 17), and *Per1*^{Brdm1} single mutant mice (blue; N = 15) kept in LD 12:12 h. The black and white bar on the bottom depicts the light and dark phase, respectively. Data are represented as mean only. The x-axis indicates the phase angle while the y-axis displays the activity as average counts/minute over a ten-minute interval. Statistical analysis did not reveal any difference between the genotypes.

Genotype	*tau* in LL	SEM	N	arrhythmic or inactive animals	total number of animals analyzed
wild-type	25.18	0.11	12	0	12
Rev-Erbα$^{-/-}$*Per1*^{Brdm1}	24.88	0.30	11	3	14
Rev-Erbα$^{-/-}$	24.78	0.14	8	0	8
Per1^{Brdm1}	27.70	0.19	7	5	12

Supplemental table 1: Average period (tau) of wild-type, *Rev-Erbα*$^{-/-}$*Per1*^{Brdm1}, *Rev-Erbα*$^{-/-}$, and *Per1*^{Brdm1} mutant mice kept under constant light (LL; 400 lux). The period was calculated using the onsets of days 4-10 in LL. N, number of mice analyzed.

4.2.1 Additional data

4.2.1.1 Light induction of *Dec1*, *Per2* and *cFos*

To further elucidate the role of altered clock gene induction in the strong Type 0 resetting we analyzed *Dec1* induction at both CT14 and CT22. In the literature, it has been reported that light induces *Dec1* both at the beginning and at the end of the night phase (Honma *et al.*, 2002). Our findings confirmed these former results as *Dec1* was induced at both CT14 and CT22 in wild-type mice (add. fig. 1A & B). Moreover, *Dec1* induction was even higher in *Rev-Erbα*$^{-/-}$*Per1*^{Brdm1} double mutants. However, *Dec1* induction may play only a minor role in the high amplitude resetting because it is increased to the same extent at both time points. *Per2* on the other hand was induced to the same level in both wild-type and *Rev-Erbα*$^{-/-}$ *Per1*^{Brdm1} double mutant mice at CT14 (add. fig. 1C). These findings are in line with the rather normal resetting observed at this time point. Moreover, *cFos* induction was unchanged between wild-type and double mutant animals at CT14 (add. fig. 1D) as well as CT22 (fig. 4D).

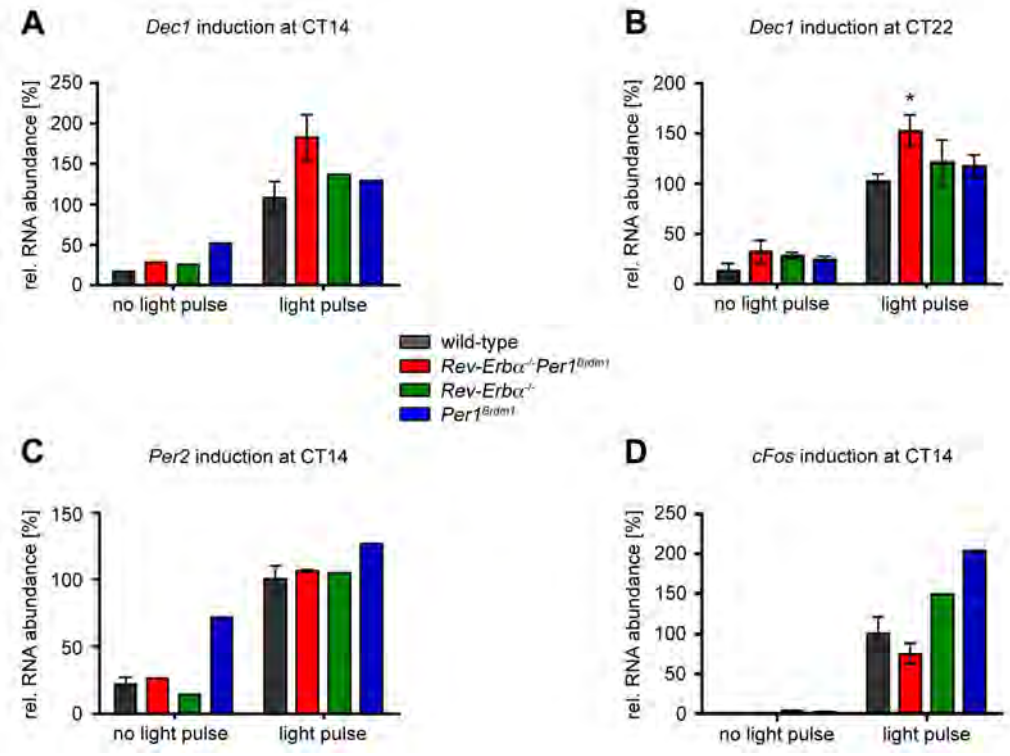

Additional figure 1: Light induced mRNA accumulation in the SCN of wild-type (black), *Rev-Erbα*$^{-/-}$*Per1*^{Brdm1} (red), *Rev-Erbα*$^{-/-}$ (green), and *Per1*^{Brdm1} (blue) mice. Values are represented as mean ± SEM. **(A)** *Dec1* induction after a light pulse at CT14 (N = 2 for wild-type and light pulsed *Rev-Erbα*$^{-/-}$*Per1*^{Brdm1}; N = 1 for the others). **(B)** *Dec1* induction after a light pulse at CT22 (N = 3). Two-way ANOVA with Bonferroni post-test was performed to determine significant differences between genotypes. * $p < 0.5$. **(C)** *Per2* induction after a light pulse at CT14 (N = 2 for wild-type and light pulsed *Rev-Erbα*$^{-/-}$*Per1*^{Brdm1}; N = 1 for the others). **(D)** *cFos* induction after a light pulse at CT14 (N = 2 for wild-type and light pulsed *Rev-Erbα*$^{-/-}$*Per1*^{Brdm1}; N = 1 for the others).

4.2.1.2 Might misregulated *Dexras1* cause the Type 0 PRC?

Dexamethasone-induced RAS protein 1 (*Dexras1*) encodes a Ras-related protein, which is stimulated by dexamethasone (Kemppainen & Behrend, 1998). Recently, it was reported to fulfil contrasting roles in the resetting at early and late night, respectively. While *Dexras1* potentiates phase-delays in the early night, it reduces the magnitude of PACAP-mediated phase shifts at late night by inhibiting the activation of ERK via both the $G_S\alpha$- and the $G\beta\gamma$-mediated limb (Cheng *et al.*, 2006). Hence *Dexras1* is thought to be a key signalling molecule, which confers both phase specificity and sensitivity to the light stimulus.

Since our double mutant mice showed a light response, which differed at early and late night, we decided to study *Dexras1* expression. In wild-type animals, *Dexras1* was expressed rhythmically with a peak at CT14 (add. fig. 2A) as it has already been published (Panda *et al.*, 2002; Ueda *et al.*, 2002; Takahashi *et al.*, 2003). Identical peak levels were observed in *Rev-Erbα*$^{-/-}$ single and *Rev-Erbα*$^{-/-}$*Per1*^{Brdm1} double mutant mice. By contrast, the amplitude in *Dexras1* mRNA accumulation was dampened in these animals due to an elevated trough at CT0. Interestingly, the difference in *Dexras1* expression was found at the end of the night, where the breakpoint of the Type 0 PRC was located in the double mutant mice.

Additional figure 2: *Dexras1* expression in the SCN of wild-type (black), *Rev-Erbα*$^{-/-}$*Per1*^{Brdm1} (red line), *Rev-Erbα*$^{-/-}$ (green), and *Per1*^{Brdm1} (blue) mice. (A) *In situ* hybridization (ISH) profile for basal *Dexras1* levels in wild-type (N = 2), *Rev-Erbα*$^{-/-}$*Per1*^{Brdm1} double (N = 2) and *Rev-Erbα*$^{-/-}$ single mutant mice (N = 1). Animals were kept in constant darkness for 6 days before they were sacrificed. Values are represented as mean ± SEM. Two-way ANOVA with Bonferroni post-test was performed for statistical analysis. * $p < 0.5$. **(B)** Light induced accumulation of *Dexras1* mRNA in the SCN of wild-type (N = 3), *Rev-Erbα*$^{-/-}$*Per1*^{Brdm1} double (N = 3-4), *Per1*^{Brdm1} single (N = 3), and *Rev-Erbα*$^{-/-}$ single mutant mice (N = 3). Two-way ANOVA with Bonferroni post-test did not reveal any significant differences between genotypes. However, unpaired t-test revealed significant differences between genotypes with and without light pulse (wild-type $p = 0.001$; *Rev-Erbα*$^{-/-}$*Per1*^{Brdm1} $p = 0.0478$).

Since these first results looked rather promising for *Dexras1* being involved in the strong resetting phenotype, we studied *Dexras1* induction before and after a light pulse administered

at CT22. Surprisingly, *Dexras1* seemed to be suppressed uniformly by light in all genotypes (add. fig. 2B). From this we concluded that *Dexras1* is probably not the cause for the Type 0 resetting observed in the *Rev-Erbα*$^{-/-}$*Per1*^{Brdm1} double mutant mice.

Nonetheless, we examined the regulation of the *Dexras1* promoter by *Rev-Erbα* and *Rorα* because it has been reported to contain a RORE motif 1.1 kbp upstream of the translation start site (Ueda *et al.*, 2002; Takahashi *et al.*, 2003). Hence we cloned a luciferase reporter construct containing a 1.7 kb *Dexras1* 5' promoter sequence. To find the optimal cell line to work with, we transfected several cell lines with 0.5 or 1.0 µg of either *pGL3-Dexras1::luc* or the positive control *pGL2-Bmal1::luc*. In parallel we added 0.0, 0.1, 0.5 or 1.0 µg of the *pSCT-Rev-Erbα* expression plasmid to test whether the luciferase activity decreases or not. Unexpectedly, the *Dexras1* promoter was activated by REV-ERBα in a dose dependant manner in all cell lines and at both promoter plasmid concentrations (e.g. add. fig. 3A & B). By contrast, the *Bmal1* promoter was repressed by REV-ERBα as expected in NIH-3T3 cells. However, it was activated at higher concentrations in COS-7 (add. fig. 3A), NG108-15, and HepG2 (data not shown) cells. This phenomenon is known as squelching and means that higher concentrations of inhibitor or activator interfere with normal cell function by the sequestration of endogenous proteins. Due to these results we decided to test lower *pSCT-Rev-Erbα* concentrations. Hence we transfected COS-7 and NIH3T3 cells with 0.5 µg of the reporter construct and with very small amounts of inhibitor. Indeed, squelching of the *Bmal1* promoter started only at 0.5 µg *pSCT-Rev-Erbα* in COS-7 cells (add. fig. 3C). At lower concentrations luciferase activity was inhibited, as one would expect. Nonetheless, the *Dexras1* promoter was still not repressed by REV-ERBα at these lower concentrations. In NIH3T3 cells, the *Bmal1* reporter construct was only inhibited starting at a concentration of 0.02 µg *pSCT-Rev-Erbα* (add. fig. 3D). Moreover, the *Dexras1* promoter seemed not to be regulated by REV-ERBα at any concentration in NIH3T3 cells. Last but not least, we tested whether *Dexras1* was activated or not by RORα in COS-7 cells. The *Bmal1* reporter construct responded to increasing *pSCT-Rorα4* concentrations as expected. However, at 1.0 µg squelching occurred again (add. fig. 3E). By contrast, the *Dexras1* promoter did not respond to RORα at all.

Although these transfection assays did not give any promising results, it is rather unlikely that *Dexras1* is not regulated by REV-ERBα and RORα. For instance, *Dexras1* peak expression is down-regulated in *Rorα* mutant mice (Sato *et al.*, 2004) and up-regulated in *Rev-Erbα* mutants (add. fig. 2A). Therefore the promoter fragment seems to be too short and a longer

one should be cloned because a second RORE motif is located 3.3 kbp upstream of the translation start site. However, we decided to abandon studying *Dexras1* because of its light response. Nonetheless it could be interesting to continue this work within another subject.

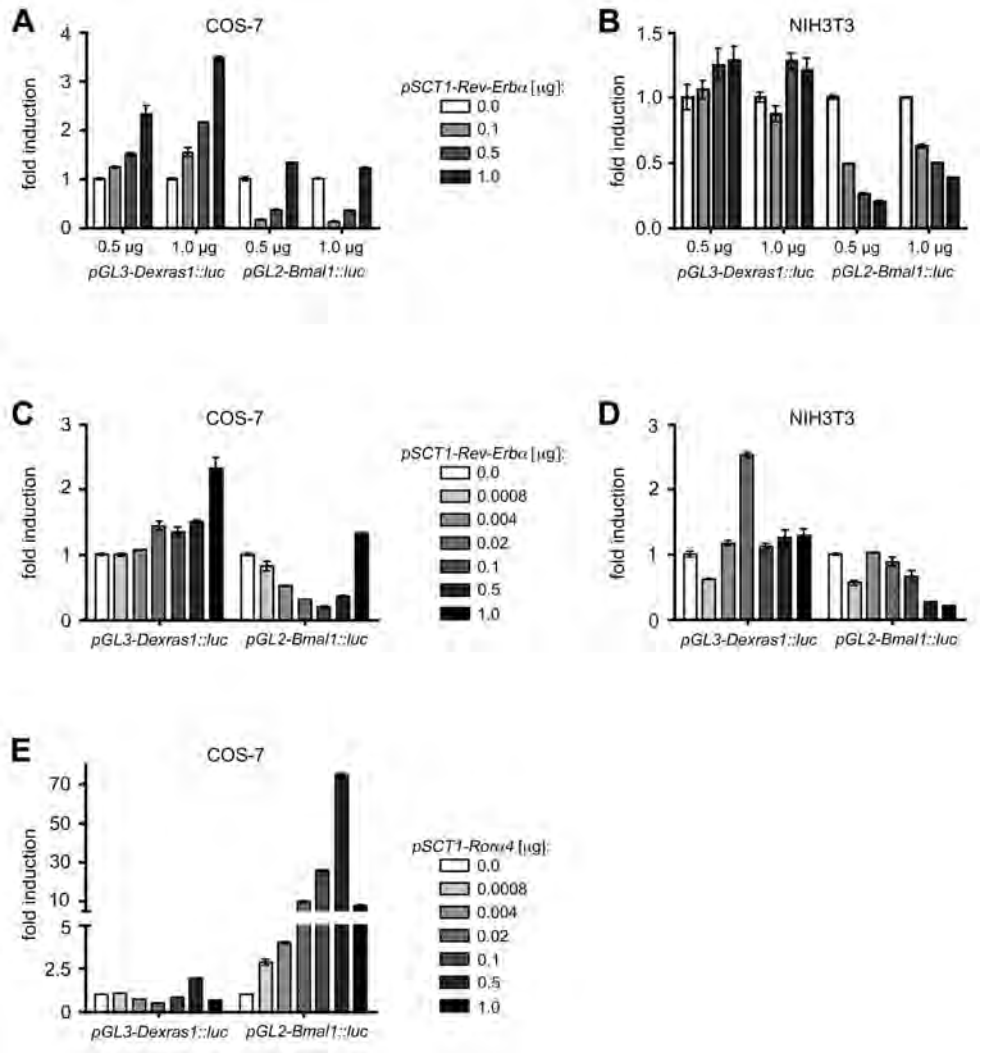

Additional figure 3: Opposing regulation of the *Dexras1* promoter by REV-ERBα and RORα4. Luciferase reporter constructs containing a 1.7 kb *Dexras1* 5' promoter sequence were used for transcriptional assays. The *pGL2-Bmal1::luciferase* construct was used as a positive control (provided by U. Schibler [Nagoshi et al., 2004]). All experiments have been done once. Duplicates are represented as mean ± SEM. **(A/B)** COS-7 (A) and NIH3T3 (B) cells were transfected with 0.5 or 1.0 μg of either *pGL3-Dexras1::luc* or *pGL2-Bmal1::luc*. Different concentrations (0.1, 0.5 and 1.0 μg) of the *pSCT1-Rev-Erbα* expression plasmid were added to see whether it represses transcription from the *Dexras1* promoter. **(C/D)** COS-7 (C) and NIH3T3 (D) cells were transfected with 0.5 μg of either *pGL3-Dexras1::luc* or *pGL2-Bmal1::luc*. Since higher concentrations of REV-ERBα showed squelching, lower concentrations (0.0008, 0.004 and 0.02 μg) were tested. The values where 0.0 and 0.1 μg *pSCT1-Rev-Erbα* expression plasmid were added are represented as mean ± SEM of 2 independent experiments (each done in duplicates). **(E)** COS-7 cells were transfected with 0.5 μg of either *pGL3-Dexras1::luc* or *pGL2-Bmal1::luc*. Different concentrations (0.1-1.0 μg) of the *pSCT1-Rorα4* expression plasmid were added to see whether or not it activates transcription from the *Dexras1* promoter.

4.2.3 Other attempts to explain the Type 0 PRC

To decipher the molecular cause of the strong resetting phenotype observed in the *Rev-Erbα*$^{-/-}$ *Per1*^{Brdm1} double mutant mice we tested the expression and light inducibility of additional genes. For instance, the MAP kinase phosphatase 1 (*Mkp1*) negatively regulates the mitogen-activated protein kinase (MAPK)-mediated signal transduction. The MAPK pathway is involved in the regulation of numerous transcription factors and plays a role in certain forms of neuronal plasticity. Moreover, MAPK signalling is induced rapidly by photic stimulation during the subjective night (Obrietan *et al.*, 1998; Butcher *et al.*, 2002). *Mkp1* expression is induced by stimuli that activate the MAPK pathway. Interestingly, *Mkp1* was reported to be a light-inducible and clock-controlled gene, which shows an expression profile that is similar to the one of *Per1*. In addition, *Mkp1* has a *Per1*-like promoter containing two cAMP responsive elements and an E-box (Doi *et al.*, 2007). Our results confirmed these findings. *Mkp1* expression was rhythmic and peaked during the subjective day in both wild-type and *Rev-Erbα*$^{-/-}$ *Per1*^{Brdm1} double mutant mice (add. fig. 4A). Likewise, a brief light pulse at CT22 induced *Mkp1* (add. fig. 4B). However, there was no difference between the two genotypes. Hence we concluded that *Mkp1* may not be involved in the observed Type 0 resetting.

Another approach was to study the circadian expression of the two neuropeptides vasoactive intestinal polypeptide (VIP) and gastrin-releasing peptide (GRP), which are expressed in the retinorecipient core region of the SCN. Former studies reported that VIP and GRP mRNA in the SCN are clock-controlled in mice and peak during the middle of the subjective night. The supposed role of VIP is to synchronize mammalian clock neurons and to maintain their rhythmicity (Aton *et al*., 2005). However, the acute induction of *Per1* by light is thought to be independent of VIP and its receptor VPAC2 (Maywood *et al.*, 2007). GRP on the other hand is thought to be an intra-SCN light signal that activates MAPK, CREB, and *Per* induction (Gamble *et al.*, 2007).

We found that VIP was expressed in a circadian fashion in wild-type and especially *Rev-Erbα*$^{-/-}$ *Per1*^{Brdm1} double mutant mice (add. fig. 4C). Interestingly, VIP seemed to be light inducible in the double mutant animals after a light pulse at CT22 (add. fig. 4D). However, these results should be interpreted with caution because only one animal was analyzed per time point. For instance, double mutants show higher basal VIP levels at CT22 (add. fig. 4C) and lower levels for the dark control taken at CT23 (add. fig. 4D). Nonetheless, VIP expression seems to differ between the two genotypes and could be an interesting target for further research. By contrast, GRP expression was rather similar between wild-type and double mutant animals (add. fig. 4E). But again, these findings need further confirmation.

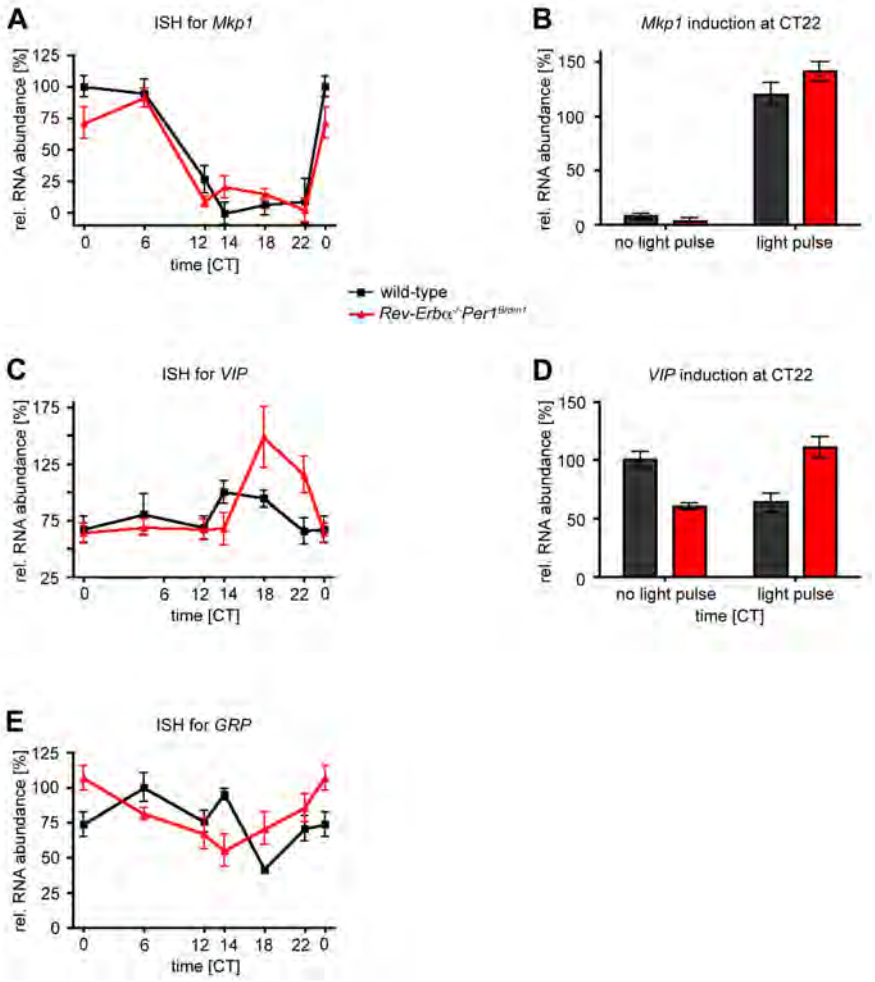

Additional figure 4: *In situ* hybridization (ISH) analysis for *Mkp1*, *VIP* and *GRP*. All experiments have been done once. Data are represented as mean ± SEM for all replicates (N ≈ 6). **(A/C/E)** ISH hybridization profiles for *Mkp1* (A), *VIP* (C) and *GRP* (E) expression. The x-axis indicates circadian time (CT) while the y-axis displays the relative RNA abundance. **(B/D)** Light induced mRNA accumulation in the SCN of wild-type (black) and *Rev-Erbα*$^{-/-}$*Per1*^{Brdm1} double mutant mice (red) for *Mkp1* (B) and *VIP* (D). The light pulse was administered at CT22.

4.3 The effect of blue light on the human circadian system in the evening

"Evening exposure to blue light stimulates the expression of the clock gene *PER2* in humans."

C. Cajochen, C. Jud, M. Münch, S. Kobialka, A. Wirz-Justice, U. Albrecht 2006

Published in *Journal of Neurosciences* 23(4): 1082-1086

European Journal of Neuroscience, Vol. 23, pp. 1082–1086, 2006 doi:10.1111/j.1460-9568.2006.04613.x

SHORT COMMUNICATION
Evening exposure to blue light stimulates the expression of the clock gene *PER2* in humans

Christian Cajochen,[1] Corinne Jud,[2] Mirjam Münch,[1] Szymon Kobialka,[1] Anna Wirz-Justice[1] and Urs Albrecht[2]
[1]Centre for Chronobiology, Psychiatric University Clinics, University of Basel, CH-4025 Basel, Switzerland
[2]Department of Medicine, Division of Biochemistry, University of Fribourg, CH-1700 Fribourg, Switzerland

Abstract

We developed a non-invasive method to measure and quantify human circadian *PER2* gene expression in oral mucosa samples and show that this gene oscillates in a circadian (= about a day) fashion. We also have the first evidence that induction of human *PER2* expression is stimulated by exposing subjects to 2 h of light in the evening. This increase in *PER2* expression was statistically significant in comparison to a non-light control condition only after light at 460 nm (blue) but not after light exposure at 550 nm (green). Our results indicate that the non-image-forming visual system is involved in human circadian gene expression. The demonstration of a functional circadian machinery in human buccal samples and its response to light opens the door for investigation of human circadian rhythms at the gene level and their associated disorders.

Introduction

Our light-sensing systems' familiar function is to collect and process light to generate an image of the world. Although light primarily serves vision, it is now known that it also exerts powerful non-visual effects on a number of physiological variables in humans, among them synchronization of circadian rhythms (the circa-24-h rhythms) (Lockley *et al*., 2003; Warman *et al*., 2003), suppression of the hormone melatonin (Brainard *et al*., 2001a,b; Thapan *et al*., 2001; Lockley *et al*., 2003; Cajochen *et al*., 2005), an increase in cortisol and heart rate (Scheer & Buijs, 1999; Scheer *et al*., 1999; Cajochen *et al*., 2005), and an acute alerting response (Badia *et al*., 1991; Cajochen *et al*., 2005). In mammals, light activates signalling pathways in a brain region where the central circadian pacemaker is located – the suprachiasmatic nuclei (SCN) (Klein *et al*., 1991) – that coordinates the daily temporal organization of physiology and behaviour. The molecular mechanisms underlying circadian rhythmicity involve self-sustaining transcriptional/translational feedback loops based on rhythmic expression of the mRNA and proteins of clock components. Synchronization of the SCN to light ultimately leads to expression of a set of clock genes, among them *Per1* and *Per2* (Albrecht *et al*., 1997). Thus, light exposure acutely activates expression of *Per1* and *Per2* in the SCN of mice (Albrecht *et al*., 1997; Zylka *et al*., 1998; Yan *et al*., 1999).

Reports about circadian regulation of clock genes in humans are rare. Two recent studies provide evidence that clock genes (*PER1*, *PER2*, *PER3* and *DEC1*) in human peripheral blood mononuclear cells (Boivin *et al*., 2003) and human oral mucosa (*PER1*, *CRY1* and *BMAL1*) are expressed in a circadian manner (Bjarnason *et al*., 2001). In the present study we aimed at developing a method to measure circadian expression of *PER2* expression in a non-invasive way via collection of oral mucosa samples. In a second step, we tested the hypothesis that evening light exposure induces an immediate increase in *PER2* expression in human mucosa. Furthermore, because part of light's non-visual effects are mediated by non-classical photoreceptors with melanopsin acting as photopigment with a maximum sensitivity in the 'blue' part of the visible electromagnetic spectrum (Lucas *et al*., 1999; Melyan *et al*., 2005; Panda *et al*., 2005; Qiu *et al*., 2005), we applied light in the 460 nm range and compared its effect to light at a different wavelength (550 nm) to test to what extend the novel photoreceptor system is involved in the regulation of *PER2*.

Correspondence: Dr C. Cajochen, as above.
E-mail: christian.cajochen@unibas.ch

Received 29 June 2005, revised 2 December 2005, accepted 8 December 2005

Materials and methods

Study participants

Twelve male volunteers were studied in the light study (mean age ± SD, 25.3 ± 3.6 years), and 12 female and male volunteers in the circadian study (28.4 ± 9.9 years). All study participants were free from medical, psychiatric and sleep disorders, as assessed by history, a physical examination and questionnaires. For the participants in the light study an ophthalmological examination was carried out prior to and after completion of the study in order to exclude volunteers with visual impairments as well as to be certain that our light application was not harmful. The volunteers were instructed to abstain from excessive caffeine and alcohol consumption for 1 week before the study. They were asked to keep a regular sleep–wake schedule (bedtimes and waketimes within ± 30 min of self-selected target time) during 1 week prior to their admission to the laboratory. Adherence to this regular schedule was verified with a wrist actigraph (Cambridge Neurotechnologies®, UK) and daily sleep diaries for the participants in the light study. All volunteers gave written informed consent. The protocol, screening questionnaires and consent form were approved by the Ethical Committee of Basel, Switzerland, and were in agreement with the Declaration of Helsinki.

Study protocol

Light study

The study consisted of three arms, performed in a balanced order, separated by a 1-week intervening period (Fig. 1). Based on the

volunteers' habitual bedtimes, a constant posture (CP) protocol started 10 h after usual waketime in the early evening (e.g. 18.00 h) and ended the next day, 2 h after usual waketime (e.g. 10.00 h). Under CP conditions, the volunteers experienced a controlled lying down episode of 1.5 h under 2 lux, followed by a 2-h dark adaptation episode under complete darkness (0 lux). After that, light exposure was initiated for the next 2 h. During this 2-h episode, the volunteers received monochromatic light at 460 nm, or monochromatic light at 550 nm, or no-light (0 lux). After this, the volunteers remained awake for another 1.5-h episode under 2 lux (polychromatic white light) before they were allowed to sleep for 7.75 h. One study participant developed a mild cold during one of the study arms and was therefore excluded from further analysis. To quantify *PER2* expression, oral mucosa samples were collected at 18.30 h before light exposure, at 24.00 h after light exposure and the next morning at 10.00 h. For two study participants not enough mucosa material was available for a reliable quantification of *PER2*, resulting in a total of nine subjects for statistical analysis.

Circadian study

The study comprised a 30-h episode, which the volunteers spent in one of our temperature-controlled chronobiology suites. The volunteers were allowed to read, work on a laptop and listen to music. Ambient light levels were kept low, <15 lux at the angle of gaze, and meals were provided by the clinic (lunch, dinner and breakfast). An 8-h sleep episode was scheduled according to the volunteers' habitual bedtime. The mucosa and the saliva samples for melatonin were taken in 3-hourly intervals, starting 3 h after habitual bedtime (on average at 9.00, 12.00, 15.00, 18.00, 21.00, 24.00, 3.00, 6.00, 9.00, 12.00 h). For double-plotting, the last two data points at 9.00 and 12.00 h were omitted. In order to take the 3.00 and 6.00 h samples, volunteers had to wake up, take the sample and go back to sleep. One subject discontinued the study after 12 h because of difficulties in taking mucosa samples, and two subjects had to be excluded because not enough mucosa material was available for a reliable quantification of *PER2*. The circadian study was conducted 3 months after the light study was completed. Because the experimental conditions of the subjects in the two studies were different it is not possible to compare the *PER2* data of the two studies in their absolute dimension, as the Q-PCR method used was based on relative measures in each experiment.

Light exposure

Monochromatic 2-h light exposure was scheduled at a circadian phase at which polychromatic white light exposure induces robust phase delays and alerting effects (Cajochen *et al*., 1992, 1998; Khalsa *et al*., 2003). The monochromatic light was generated by a 300 Watt arc-ozone-free Xenon lamp (Thermo Oriel, Spectra Physics, Statford, CT, USA), filtered by either 460 nm or 550 nm (Interference filter, ± 10 nm half-peak bandwidth, Spectra Physics, Statford, CT, USA) and transmitted via two glass fibre bundles (L.O.T. Oriel-Suisse, Romanel-sur-Morges, Switzerland) through the wall into the sound-proof and temperature-controlled chronobiology suite on to the goggles, which covered the volunteers' eyes. The custom-built goggles (K. Haug AG, Basel, Switzerland) consisted of two spheres (27.5 mm inner radius) coated with white reflectance paint (two component polyurethan-acryl anti-fading paint, Lachenmeier & Co. AG, Basel, Switzerland). Each sphere was illuminated via three branches of the main fibre optic cable in order to provide constant uniform illumination. Equal photon densities (2.8×10^{13} photons/cm^2/s) for the 460 nm and 550 nm wavelength light were administered. This irradiance level (12.1 μW/cm^2 for 460 nm and 10.05 μW/cm^2 for 550 nm) was chosen according to recently reported results on monochromatic light on the human circadian timing system (Lockley *et al*., 2003). Irradiances were measured with a laser power meter (Laser Check, Coherent, Auburn, CA, USA) before the beginning and at the end of each light exposure. During light exposure as well as during the non-light condition, volunteers were asked to keep their eyes open and to fix their gaze on the middle of the spheres. A technician checked the latter by on-line monitoring the polysomnographic recordings and also verifying that the subjects remained awake. The volunteer's pupils were not dilated in order to avoid possible repercussions of the dilation agent *per se* on thermoregulation, heart rate and alertness. However, we tested the effects of the light stimulus on pupil constriction by applying monocular light exposure (light via the goggle of the right eye) and concomitantly measuring the pupil size on the left eye via an infrared camera. The entire control protocol was conducted at the same time of day (evening) and with the same light intensity in six subjects. Results from the control experiment revealed a significantly smaller pupil size after the short wavelength light at 460 nm than after light at 550 nm in comparison to the dark condition ($P < 0.01$), Duncan's multiple range test performed after a one-way ANOVA for repeated measures with the factor 'light condition' ($P < 0.02$; dark, 460 nm and 550 nm).

Salivary melatonin

Saliva was collected at 30-min intervals during scheduled wakefulness. A direct double-antibody radioimmunoassay was used for the melatonin assay validated by gas-chromatography-mass spectroscopy (Bühlmann Laboratories, Allschwil, Switzerland). The minimum detectable dose of melatonin (analytical sensitivity) was determined to be 0.2 pg/mL. The functional least detectable dose using the $<20\%$ coefficient of interassay variation criterion was below 0.65 pg/mL, and individual serum and saliva melatonin profiles showed excellent parallelism ($r = 0.977$–0.999, slopes $= 0.21$–0.63).

Human oral mucosa collection and quantification of PER2

Human oral mucosa was collected using blue pipette tips (Treff AG, 2 mm of tissue into the tip) and then was dissolved in lysis buffer containing β-mercaptoethanol provided in the Absolutely RNA Nanoprep Kit (Stratagene). Subsequently, the samples were frozen at −80 °C. The RNA was isolated according to the manufacturer's instructions of the kit using 200 μL of lysis buffer followed by a DNase treatment of 30 min. The cDNA was generated using SuperScript™ II Reverse Transcriptase (Invitrogen) and poly(dT)$_{15}$ primers (Roche). Subsequently, TaqMan quantitative real-time RT-PCR was performed using iQ Supermix (Bio-Rad) to determine *GAPDH* and *PER2* levels for each sample. The following primers and probes were used:

PER2 TaqMan probe:
5′-[FAM]ATGCCTTCAGCGATGCCAAGTT[BHQ]-3′
PER2 sense primer:
5′-GCATCCATATTTCACTGTAAAAGA-3′
PER2 anti-sense primer:
5′-AGTAAAAGAATCTGCTCCACTG-3′
GAPDH TaqMan probe:
5′-[FAM]AGCCTCAAGATCATCAGCAATGCC [BHQ]-3′
GAPDH sense primer:
5′-TGTGAACCATGAGAAGTATGAC-3′
GAPDH anti-sense primer:
5′-ATGAGTCCTTCCACGATACC-3′.

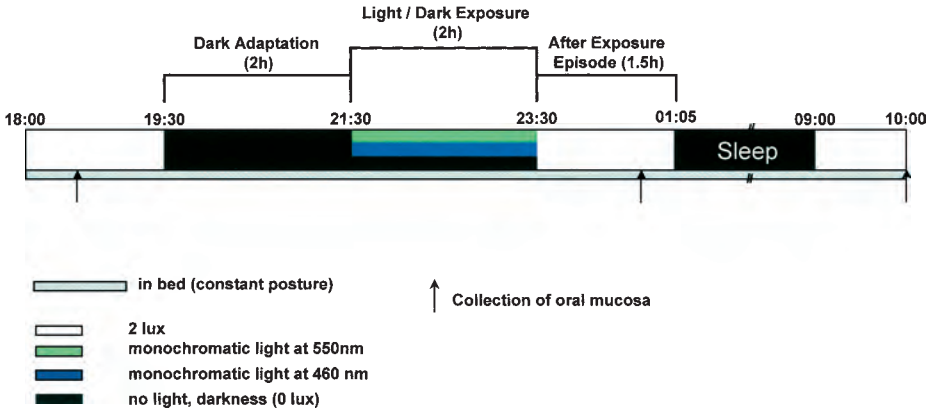

FIG. 1. Overview of the light study protocol design. After 1.5 h under 2 lux, subjects were dark adapted for 2 h, followed by another 2 h in darkness or light exposure at 460 nm or 550 nm (for details about the light exposures, see Materials and methods). Subsequently, subjects spent 1.5 h under 2 lux before they were allowed to sleep for 8 h. The entire protocol was carried out under constant recumbent posture conditions in bed.

The final primer concentration was 300 nM, fluorescent oligomeric probe concentration was 100 nM and $MgCl_2$ concentration was 5 mM. The amplification was carried out at 55 °C for 1 min followed by a denaturation at 94 °C for 15 s using the iCycler (Bio-Rad). After 55 cycles, ΔC_T was determined. The samples of one subject (all time points) in the reaction mix were applied with filter tips (Axigen) onto a 0.2 mL semiskirted thermo-fast 96-well plate (ABgene AB-0900), which was covered with an optically clear adhesive seal sheet (ABgene AB-1170). Additionally to the single *GAPDH* controls, a dilution curve for *GAPDH* was run on each plate for one time point to control for reaction efficiency.

GAPDH was used as standard because of its constant expression in mucosa tissue (Pan *et al*., 2002) and its validation as a standard gene for this tissue under injury and repair conditions (Warburton *et al*., 2005).

Data analysis

For both the circadian and the light study three reference *GAPDH* values and three or four *PER2* values were obtained for each mucosa sample (triplets or quadruplets a, b, c, d). A ΔC_T value per mucosa sample was calculated according to the comparative C_T ($2^{-\Delta\Delta CT}$) method, which could be applied because the efficiencies of the *GAPDH* and *PER2* assays were optimized to be comparable (Livak & Schmittgen, 2001). A validation assay was performed where serial dilutions were assayed for both genes. This method minimizes the variation in performance of the iCycler apparatus. Another advantage of this relative quantification compared with the absolute method is that it corrects for variance in the efficiency of cDNA synthesis.

The formula below was used to calculate the ΔC_T values:

$$\Delta C_T = (2^{GAPDHa-PER2a} + 2^{GAPDHa-PER2b} + 2^{GAPDHa-PER2c} + 2^{GAPDHb-PER2a} + 2^{GAPDHb-PER2b} + 2^{GAPDHb-PER2c} + 2^{GAPDHc-PER2a} + 2^{GAPDHc-PER2b} + 2^{GAPDHc-PER2c})/9$$

In the case of quadruplets, the formula was changed accordingly. This method allowed the use of parametric statistics repeated-measure ANOVA (RANOVA) with the factor 'light condition' and 'time of day'.

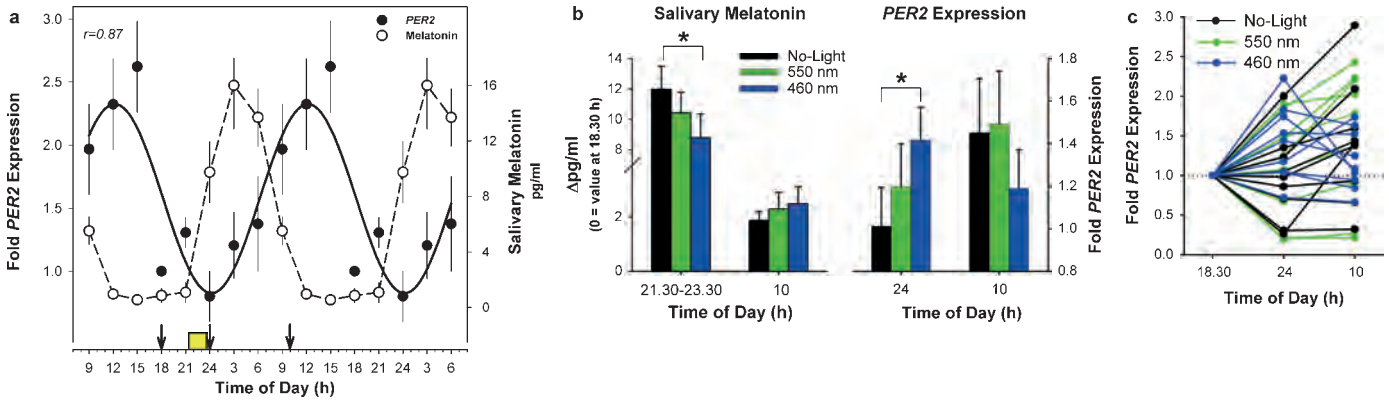

FIG. 2. (a) Twenty-four-hour profile of *PER2* expression in human oral mucosa (●) and of salivary melatonin levels (○). Samples were taken in 3-h intervals under dim light conditions (< 15 lux) throughout a 30-h period ($n = 9$, mean values ± SEM). For better visualization of the 24-h rhythms, all values were double-plotted and *PER2* values fitted with a sine function. The *r*-value, an estimate of the goodness of fit, was 0.87 with $P = 0.0001$ for *PER2*. Arrows on the abscissa indicate the timing of mucosa collection and the timing of the 2-h light exposure (yellow bar) in the experiment in (b). (b) Left-hand side: Salivary melatonin levels during 2-h light exposure at 460 nm and 550 nm and during the control no-light condition. Right hand side: *PER2* expression in oral mucosa after the 2-h light exposure (460 and 550 nm) and no-light exposure at 24.00 h and 10.00 h the next morning. Values were expressed as percentages to the value before light treatment at 18.30 h (0 = value at 18.30 h; $n = 9$, mean values + SEM; $^*P < 0.05$, Duncan's multiple range test). (c) Scatter plot of the individual normalized data. After blue light at 460 nm, for most of the subjects values > 1.0 can be observed at 24 h, but also for some subjects after green light at 550 nm and for two subjects in the dark condition. Only in the blue light condition did the values at 24.00 h differ significantly from the 18.30 h values (paired *t*-test, $P = 0.017$). For most of the subjects in the blue light condition, the values at 10.00 h the next morning decreased, statistical analyses revealed a trend for lower values after blue light, when compared with the green condition (paired *t*-test; $P = 0.09$).

For each subject, we expressed the transformed values relative to the value obtained at 18.00 h in the circadian study and to the value obtained at 18.30 h in the light study, as in the light study the sample taken at 18.30 h was the only sample taken under the same lighting conditions and was the closest in terms of time to the 18.00 h sample taken in the circadian study. All *P*-values derived from rANOVAs were based on Huynh–Feldt's (H–F) corrected degrees of freedom, but the original degrees of freedom are reported. For *post-hoc* comparisons the Duncan's multiple range test was used.

The time course of *PER2* expression in the circadian study was fitted with a sinusoidal function comprising the fundamental oscillation (24-h component):

$$f(t) = y_0 + A \ \sin[(2\pi t/\tau_{24}) + c].$$

Data were fit with a non-linear least-square fitting analysis based upon the Marquardt–Levenberg algorithm to find the coefficients (parameters) of the independent variable(s) that give the best fit between the equation and the data (SigmaPlot for Windows, Version 7.0, Richmond, CA, USA, Systat Software). The goodness-of-fit of each sine fit was assessed by calculating the adjusted correlation coefficient and the power, or the probability that the model correctly describes the relationship of the variables, if there is a relationship. The statistical package Statistica® (StatSoft 2004, Statistica for Windows, Tulsa, OK, USA, Version 6.0) was used.

Results

PER2 gene expression in the circadian study showed a clear diurnal rhythm (Fig. 2a). The sine fit to the data points yielded a good fit with a *r*-value of 0.87, and the power that the model correctly describes the relationship between the variables was 0.99. Maximal *PER2* gene expression in oral mucosa, sampled in 3-h intervals throughout a 30-h period under controlled dim lighting conditions, occurred between 12.00 and 15.00 h during the biological day, while minimal *PER2* expression was found between 21.00 and 03.00 h during the biological night, defined as the period of melatonin secretion. The circadian profile of the salivary melatonin exhibited the well-known time course (Fig. 2a), with maximal values during night-time hours and low values during daytime. The phase and amplitude of the melatonin curve was very similar to the one we have recently reported (Knoblauch *et al*., 2003).

Figure 2b illustrates changes in *PER2* expression and salivary melatonin in the light study. A rANOVA with the factor 'light condition' and 'time of day' yielded a significant effect of 'time of day' ($F_{1,8} = 8.4$, $P = 0.020$) and a significant interaction between 'light condition' and 'time of day' ($F_{2,16} = 4.6$, $P = 0.027$). *Post-hoc* comparisons revealed a significant increase in *PER2* expression after blue light at 460 nm at 24.00 h ($P = 0.032$), but not after green light at 550 nm ($P = 0.28$). The comparison between blue and green light at this time point (24.00 h) did not reach significance ($P = 0.18$). Melatonin was significantly suppressed after blue light at 460 nm (from 12.0 pg/mL to 8.8 pg/mL, $P = 0.021$), but not after green light at 550 nm. At this time point *PER2* levels are usually near minimal levels (Fig. 2a).

PER2 gene expression the next morning at 10.00 h no longer differed significantly, nor did melatonin levels. Nonetheless, a tendency for a lower *PER2* gene expression was found after blue light at 460 nm when compared with green light at 550 nm ($P = 0.098$).

In the scatter plot showing individual data (Fig. 2c), for most of the subjects values > 1.0 can be observed at 24 h after blue light, but also for some subjects after green light and for two subjects in the dark condition. However, only in the blue light condition did the values at 24.00 h differ significantly from the 18.30 h values (paired *t*-test $P = 0.017$). For most of the subjects in the blue light condition, the values at 10.00 h the next morning decreased and a trend for lower values after blue light when compared with the green light was found (see paragraph above).

Discussion

We were able to show rhythmic expression of a clock gene *PER2* in peripheral human tissue collected non-invasively from the oral mucosa. In addition, our findings provide the first evidence in humans that a circadian regulator gene, *PER2*, acutely responds to light. Importantly, this response to light was clearly wavelength-dependent, such that the increase in *PER2* after light is blue-shifted relative to the three-cone visual photopic system, supporting a role of the novel 'non-photic' photoreceptors at the level of human clock gene expression.

Circadian expression of *PER2* in our study peaked on average 12 h later, during the biological day at 15.00 h, with respect to maximal melatonin expression at 03.00 h. Although a bit later into the day, it is in accordance with Boivin *et al*. (2003), who reported peak *PER2* expression mostly during the habitual time of activity (around noon) in human peripheral blood mononuclear cells.

We have evidence that the induction of *PER2* is acutely stimulated by evening light exposure in the human mucosa. Studies in rats show that the clock of peripheral tissues, such as liver and kidney, takes more time to adjust its phase to a shifted light–dark cycle compared with the SCN (Yamazaki *et al*., 2000). In contrast, our study indicates that oral mucosa might be a tissue that responds rather quickly to such changes as shown by the rapid response of the *PER2* gene to light in this tissue. Whether this represents an acute stimulation of *PER2* in the central circadian clock in the SCN can not be conclusively proven in this study. However, the light-evoked reduction of melatonin and increase in core body temperature and heart rate published in the same subject sample (Cajochen *et al*., 2005) are clear indications for non-visual circadian effects of light, which are mediated by the SCN. Therefore, we assume that the light effects reported here on *PER2* were most likely mediated via the circadian system. Further support for this comes from the fact that only the short-wavelength light (i.e. blue light) evoked this effect. It is known that the human circadian system is particularly sensitive to non-visual effects of ocular light at short wavelengths via novel photoreceptors (Provencio *et al*., 2000; Hankins & Lucas, 2002; Hattar *et al*., 2002; Gooley *et al*., 2003).

The demonstration of a functional circadian machinery in human buccal samples and its response to the most important Zeitgeber light suggests that this method may be useful for the investigation of human circadian rhythms at the gene level and their associated disorders.

Acknowledgements

We thank Dr Corina Schnitzler and Professor Selim Orgül for medical screenings, Claudia Renz, Giovanni Balestrieri and Marie-France Dattler for their help in data acquisition, Dr Jürgen Ripperger for reading the manuscript and the volunteers for participating. This research was supported by the Velux Foundation, Switzerland, and in part by the Swiss National Foundation Grants START #3130-054991.98 and #3100-055385.98 to C.C., the State of Fribourg, the EC grant 'Braintime' QLG-CT-2002-01829 the Federal Office for Science and Education to U.A., and by the EU 6th Framework Project EUCLOCK (#018741).

Abbreviations

CP, constant posture; SCN, suprachiasmatic nuclei.

References

Albrecht, U., Sun, Z.S., Eichele, G. & Lee, C.C. (1997) A differential response of two putative mammalian circadian regulators, mper1 and mper2, to light. *Cell*, **91**, 1055–1064.

Badia, P., Myers, B., Boecker, M. & Culpepper, J. (1991) Bright light effects on body temperature, alertness, EEG and behavior. *Physiol. Behav.*, **50**, 583–588.

Bjarnason, G.A., Jordan, R.C.K., Wood, P.A., Li, Q., Lincoln, D.W., Sothern, R.B., Hrushesky, W.J.M. & Ben-David, Y. (2001) Circadian expression of clock genes in human oral mucosa and skin. *Am. J. Pathol.*, **158**, 1793–1801.

Boivin, D.B., James, F.O., Wu, A., Cho-Park, F., Xiong, H. & Sun, Z.S. (2003) Circadian clock genes oscillate in human peripheral blood mononuclear cells. *Blood*, **102**, 4143–4145.

Brainard, G.C., Hanifin, J.P., Greeson, J.M., Byrne, B., Glickman, G., Gerner, E. & Rollag, M.D. (2001b) Action spectrum for melatonin regulation in humans: evidence for a novel circadian photoreceptor. *J. Neurosci.*, **21**, 6405–6412.

Brainard, G., Hanifin, J.P., Rollag, M.D., Greeson, J., Byrne, B., Glickman, G., Gerner, E. & Sanford, B. (2001a) Human melatonin regulation is not mediated by the three cone photopic visual system. *J. Clin. Endocrinol. Metab.*, **86**, 433–436.

Cajochen, C., Dijk, D.J. & Borbély, A.A. (1992) Dynamics of EEG slow-wave activity and core body temperature in human sleep after exposure to bright light. *Sleep*, **15**, 337–343.

Cajochen, C., Kräuchi, K., Danilenko, K.V. & Wirz-Justice, A. (1998) Evening administration of melatonin and bright light: interactions on the EEG during sleep and wakefulness. *J. Sleep Res.*, **7**, 145–157.

Cajochen, C., Münch, M., Kobialka, S., Kräuchi, K., Steiner, R., Oelhafen, P., Orgül, S. & Wirz-Justice, A. (2005) High sensitivity of human melatonin, alertness, thermoregulation and heart rate to short wavelength light. *J. Clin. Endocrinol. Metab.*, **90**, 1311–1316.

Gooley, J.J., Lu, J., Fischer, D. & Saper, C.B. (2003) A broad role for melanopsin in nonvisual photoreception. *J. Neurosci.*, **23**, 7093–7106.

Hankins, M.W. & Lucas, R.J. (2002) The primary visual pathway in humans is regulated according to long-term light exposure through the action of a nonclassical photopigment. *Curr. Biol.*, **12**, 191–198.

Hattar, S., Liao, H.W., Takao, M., Berson, D.M. & Yau, K.W. (2002) Melanopsin-containing retinal ganglion cells: architecture, projections, an intrinsic photosensitivity. *Science*, **295**, 1065–1071.

Khalsa, S.B.S., Jewett, M.E., Cajochen, C. & Czeisler, C.A. (2003) A phase response curve to single bright light pulses in human subjects. *J. Physiol.*, **549**.**3**, 945–952.

Klein, D.C., Moore, R.Y. & Reppert, S.M. (1991) *Suprachiasmatic Nucleus: the Mind's Clock*. Oxford University Press, New York.

Knoblauch, V., Martens, W., Wirz-Justice, A., Kräuchi, K., Graw, P. & Cajochen, C. (2003) Regional differences in the circadian modulation of human sleep spindle characteristics. *Eur. J. Neurosci.*, **18**, 155–163.

Livak, K.J. & Schmittgen, T.D. (2001) Analysis of relative gene expression data using real-time quantitative PCR and the 2-[Delta][Delta]CT method. *Methods*, **25**, 402–408.

Lockley, S.W., Brainard, G.C. & Czeisler, C.A. (2003) High sensitivity of the human circadian melatonin rhythm to resetting by short wavelength light. *J. Clin. Endocrinol. Metab.*, **88**, 4502–4505.

Lucas, R.J., Freedman, M.S., Munoz, M., Garcia-Fernandez, J.M. & Foster, R.G. (1999) Regulation of the mammalian pineal by non-rod, non-cone, ocular photoreceptors. *Science*, **284**, 505–507.

Melyan, Z., Tarttelin, E.E., Bellingham, J., Lucas, R.J. & Hankins, M.W. (2005) Addition of human melanopsin renders mammalian cells photoresponsive. *Nature*, **433**, 741–745.

Pan, X., Terada, T., Irie, M., Saito, H. & Inui, K.-I. (2002) Diurnal rhythm of H+-peptide cotransporter in rat small intestine. *Am. J. Physiol. Gastrointest. Liver Physiol.*, **283**, G57–G64.

Panda, S., Nayak, S.K., Campo, B., Walker, J.R., Hogenesch, J.B. & Jegla, T. (2005) Illumination of the melanopsin signaling pathway. *Science*, **307**, 600–604.

Provencio, I., Rodriguez, I.R., Jiang, G., Hayes, W.P., Moreira, E.F. & Rollag, M.D. (2000) A novel human opsin in the inner retina. *J. Neurosci.*, **20**, 600–605.

Qiu, X., Kumbalasiri, T., Carlson, S.M., Wong, K.Y., Krishna, V., Provencio, I. & Berson, D.M. (2005) Induction of photosensitivity by heterologous expression of melanopsin. *Nature*, **433**, 745–749.

Scheer, F.A.J.L. & Buijs, R.M. (1999) Light affects morning salivary cortisol in humans. *J. Clin. Endocrinol. Metab.*, **84**, 3395–3398.

Scheer, F.A.J.L., Van Doornen, L.J.P. & Buijs, R.M. (1999) Light and diurnal cycle affect human heart rate: possible role for the circadian pacemaker. *J. Biol. Rhythms*, **14**, 202–212.

Thapan, K., Arendt, J. & Skene, D.J. (2001) An action spectrum for melatonin suppression: evidence for a novel non-rod, non-cone photoreceptor system in humans. *J. Physiol.*, **535**, 261–267.

Warburton, G., Nares, S., Angelov, N., Brahim, J.S., Dionne, R.A. & Wahl, S.M. (2005) Transcriptional events in a clinical model of oral mucosal tissue injury and repair. *Wound Repair Regeneration*, **13**, 19–26.

Warman, V.L., Dijk, D.-J., Warman, G.R., Arendt, J. & Skene, D.J. (2003) Phase advancing human circadian rhythms with short wavelength light. *Neurosci. Lett.*, **342**, 37–40.

Yamazaki, S., Numano, R., Abe, M., Hida, A., Takahashi, R., Ueda, M., Block, G.D., Sakaki, Y., Menaker, M. & Tei, H. (2000) Resetting central and peripheral circadian oscillators in transgenic rats. *Science*, **288**, 682–685.

Yan, L., Takekida, S., Shigeyoshi, Y. & Okamura, H. (1999) Per1 and Per2 gene expression in the rat suprachiasmatic nucleus: circadian profile and the compartment-specific response to light. *Neuroscience*, **94**, 141–150.

Zylka, M.J., Shearman, L.P., Weaver, D.R. & Reppert, S.M. (1998) Three period homologs in mammals: differential light responses in the suprachiasmatic circadian clock and oscillating transcripts outside of brain. *Neuron*, **20**, 1103–1110.

4.3.1 Additional data

PER1 and *BMAL1* expression was measured in the same samples that had been used for the circadian study (Cajochen *et al.*, 2006). Both *PER1* and *BMAL1* mRNA levels showed a clear diurnal rhythm as it had been reported for *PER2* in the same samples (add. fig. 1). *BMAL1* expression peaked in anti-phase to *PER1* and *PER2*. However, peak clock gene expression varied between subjects. *PER1* was high in the morning between 9:00 and 12:00 h. Variations in *PER2* expression were more prominent. In subjects 8 and 10 it peaked between 12:00 and 15:00 h while it reached its summit at 6:00 h in subject 9. *BMAL1* profiles of subject 8 and 10 were rather similar with peak expression at 3:00 and 24:00 h, respectively. In subject 9, *BMAL1* levels were highest at 18:00 h.

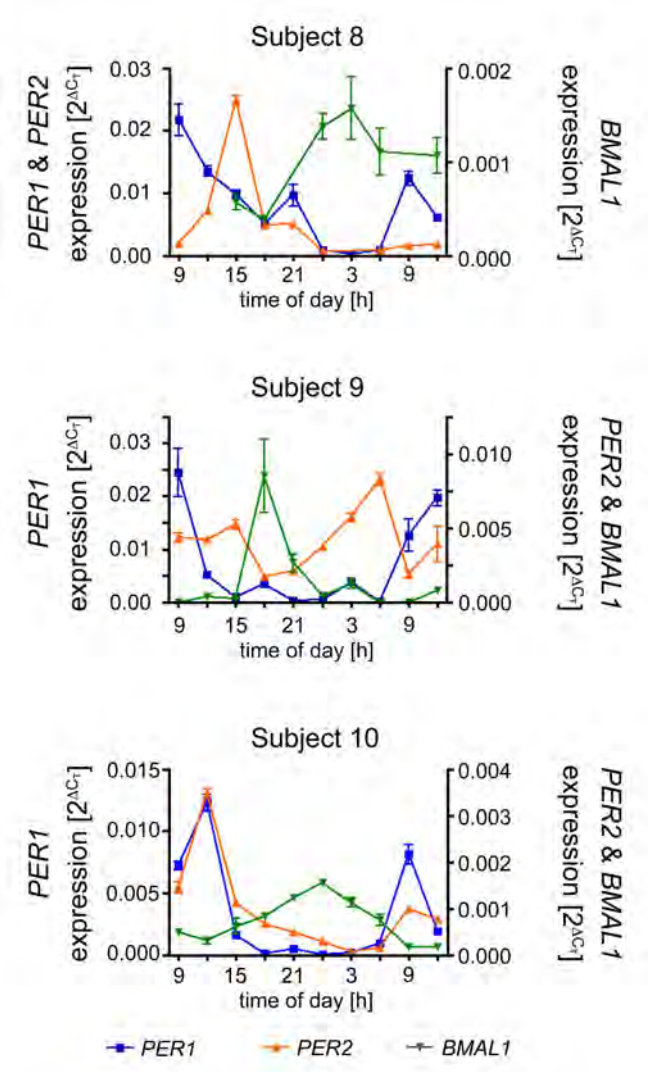

Additional figure 1: Twenty-four hour profile for *PER1*, *PER2*, and *BMAL1* expression in human oral mucosa of three subjects. Samples were taken in 3 h intervals under dim light conditions (< 15 lux) throughout a 30 h period. Values are represented as mean ± SEM for all replicates (N ≈ 9).

4.4 The effect of blue light on the human circadian system in the morning

"Age-dependent change in *PER2* levels after early morning blue light."

C. Jud, S. Chappuis, V.L. Revell, T.L. Sletten, D. Saaltink, D.J. Skene, U. Albrecht

2008

Submitted to *Journal of Biological Rhythms*

Age-dependent change in *PER2* levels after early morning blue light

Corinne Jud[1], Sylvie Chappuis[1], Victoria L. Revell[2], Tracey L. Sletten[2,3], Dirk-Jan Saaltink[1,4], Debra J. Skene[2] and Urs Albrecht[1,5]

[1] Department of Medicine, Unit of Biochemistry, University of Fribourg, Fribourg, Switzerland

[2] Centre for Chronobiology, Faculty of Health and Medical Sciences, University of Surrey, Guildford, Surrey, GU2 7XH, United Kingdom

[3]Current address: Sleep and Chronobiology Research Group, School of Psychology, Psychiatry and Psychological Medicine, Monash University, Victoria, Australia, 3800

[4] Current address: Medical Pharmacology, University of Leiden, The Netherlands

[5] To whom all correspondence should be addressed: Chemin du Musée 5, 1700 Fribourg, Switzerland, e-mail: urs.albrecht@unifr.ch

Number of pages: 8 excluding references; 12 including references

Number of illustrations: 2

Text

Humans and other mammals receive light information affecting the circadian system mainly via a subset of non-visual intrinsically photosensitive retinal ganglion cells (ipRGC) situated in the inner retina (Berson et al. 2002; Moore et al. 1995; Provencio et al. 2000; Sekaran et al. 2003). These cells express the blue-light sensitive photopigment melanopsin (Gooley et al. 2001; Hattar et al. 2002; Lucas et al. 2001; Provencio et al. 2000) and send photic information directly to the SCN via the RHT (Moore and Lenn 1972). Since exposure to short-wavelength light has a huge impact on mood and vitality, disturbances in the ipRGC photoreception can lead to physiological and psychological problems (Buijs et al. 2006; Klerman 2005). For instance, blue light exposure acutely increases core body temperature, heart rate (Cajochen et al. 2005), alertness (Cajochen et al. 2005; Lockley et al. 2006) and cognition (Vandewalle et al. 2007). With age, the crystalline lens absorbs more light (Pokorny et al. 1987; Turner and Mainster 2008; Weale 1985) and the pupil area decreases (Verriest 1971; Yang et al. 2002); thus, blue light transmission is reduced. This could result in impaired circadian photoreception (Herljevic et al. 2005) and be in part responsible for the changes observed in the sleep-wake cycle and circadian rhythmicity in the elderly (Bliwise 1993; Duffy et al. 1998).

The clock genes *Per1* and *Per2* are differentially inducible by a nocturnal light pulse in mice (Albrecht et al. 1997; Yan and Silver 2002). In humans evening blue light can induce expression of *PER2* in oral mucosa (Cajochen et al. 2006). The aim of the present study was to investigate whether early morning blue light exposure is also capable of influencing *PER2* levels in human oral mucosa and in addition, whether such a change would be age-dependent.

Eleven young (23.0 ± 2.9 years) and fifteen old (65.8 ± 5.0 years) healthy males participated in this study and were pupil dilated and subjected to a 2 h intermittent monochromatic light exposure 8.5 h after their individual dim light melatonin onset (DLMO); for protocol details

see Sletten et al. (in press). As the time of light administration, the portion of the light phase response curve was chosen where advances have been demonstrated to show the highest amplitude (Revell and Eastman 2005). Subjects received blue (λ_{max} 456 nm) or green (λ_{max} 548 nm) light matched for photon density (6 x 10^3 photons/cm^2/s) on separate occasions. Oral mucosa was sampled at clock times equivalent to 0.5, 5.0, and 10.0 hours after light exposure on a baseline day and 24 hours later on the day of light exposure (Fig. 1).

Some samples were lost from analysis as *PER2* levels could not be determined in every sample due to insufficient amounts of mRNA (young N = 6-11; old N = 7-13; for both green and blue light). We found that *PER2* expression levels were significantly increased in young subjects 10.0 h after blue, but not green, light (Fig. 2A, B). By contrast, neither blue nor green light had an effect on *PER2* expression in oral mucosa samples of older subjects (Fig. 2C, D). In addition, the overall baseline amplitude of *PER2* expression was lower by about 50 % in the elderly compared to the young – this amplitude phenomenon has been reported previously for circadian rhythms in temperature and sleep (Carrier et al. 1996; Monk et al. 1995).

The effect of early morning blue light on *PER2* expression is probably due to a shift of the baseline expression curve, because the 0.5 hour sample does not show acute *PER2* mRNA induction (Fig. 2A, C). By contrast, blue light applied in the evening results in an acute induction of *PER2* in human oral mucosa after 0.5 hours (Cajochen et al. 2006). This time dependent acute inducibility of human *PER2* is in line with previous observations in mice where *Per2* is acutely induced in the early dark phase but poorly in the late dark phase (Albrecht et al. 1997; Yan and Silver 2002).

Therefore the significant difference of *PER2* levels in young subjects 10 hours after the blue light pulse versus no light is likely due to a phase shift of the mRNA expression curve (Fig. 2A). However, our data do not provide information about the direction of the shift. Nevertheless, plasma melatonin profiles from the same subjects indicate a phase advance of

the clock caused by early morning blue light (Sletten et al. in press). Interestingly, evening blue light not only causes an acute induction of *PER2* in oral mucosa, but it also appears that *PER2* levels tend to be lower compared to controls 10 hours after light administration (Cajochen et al. 2006), Fig. 2b). This indicates a potential phase delay due to evening blue light. Taken together, it appears that light has comparable effects on human *PER2* mRNA levels as previously observed in mice. Furthermore, our results in humans indicate that ageing impairs light activated responses impinging on the circadian system (Fig. 2C) as previously observed in hamsters (Zhang et al. 1996) and humans (Herljevic et al. 2005; Sletten et al. in press).

In conclusion, the current results highlight similarities in the light response of the circadian system between rodents and humans. In addition, our report illustrates that buccal samples are a valuable tool for studying the response of clock genes to light in humans.

Acknowledgements

The authors thank the laboratory technician A. Hayoz for her help and S. Langmesser for critically reading the manuscript. We thank Phillips Lighting (Eindhoven, The Netherlands) for supplying the light sources. This work has been supported by the Swiss National Science Foundation, the EUCLOCK project (EC 6th framework), the EU Marie Curie RTN Grant, the Velux foundation and the state of Fribourg (Switzerland).

Appendix (Materials & Methods)

The study protocol was as described by Sletten et al. (in press). The collection of human oral mucosa and the subsequent RNA isolation, cDNA synthesis and quantitative real-time RT-PCR for *GAPDH* and *PER2* were performed as described previously (Cajochen et al. 2006). $2^{\Delta CT}$ value per mucosa sample was calculated according to the following formula (*X* = gene of interest and *a*, *b* and *c* correspond to replicate 1, 2 and 3):

$$2^{\Delta CT} = (2^{GAPDHa-Xa} + 2^{GAPDHa-Xb} + 2^{GAPDHa-Xc} + 2^{GAPDHb-Xa} + 2^{GAPDHb-Xb} + 2^{GAPDHb-Xc} + 2^{GAPDHc-Xa} + 2^{GAPDHc-Xb} + 2^{GAPDHc-Xc}) / 9$$

For statistical analysis, the mean $2^{\Delta CT}$ value was used for every subject.

References

Albrecht U, Sun ZS, Eichele G and Lee CC (1997) A differential response of two putative mammalian circadian regulators, mper1 and mper2, to light. *Cell* 91:1055-1064.

Berson DM, Dunn FA and Takao M (2002) Phototransduction by retinal ganglion cells that set the circadian clock. *Science* 295:1070-1073.

Bliwise DL (1993) Sleep in normal aging and dementia. *Sleep* 16:40-81.

Buijs RM, Scheer FA, Kreier F, Yi C, Bos N, Goncharuk VD and Kalsbeek A (2006) Organization of circadian functions: interaction with the body. *Prog Brain Res* 153:341-360.

Cajochen C, Jud C, Munch M, Kobialka S, Wirz-Justice A and Albrecht U (2006) Evening exposure to blue light stimulates the expression of the clock gene PER2 in humans. *Eur J Neurosci* 23:1082-1086.

Cajochen C, Munch M, Kobialka S, Krauchi K, Steiner R, Oelhafen P, Orgul S and Wirz-Justice A (2005) High sensitivity of human melatonin, alertness, thermoregulation, and heart rate to short wavelength light. *J Clin Endocrinol Metab* 90:1311-1316.

Carrier J, Monk TH, Buysse DJ and Kupfer DJ (1996) Amplitude reduction of the circadian temperature and sleep rhythms in the elderly. *Chronobiol Int* 13:373-386.

Duffy JF, Dijk DJ, Klerman EB and Czeisler CA (1998) Later endogenous circadian temperature nadir relative to an earlier wake time in older people. *Am J Physiol* 275:R1478-1487.

Gooley JJ, Lu J, Chou TC, Scammell TE and Saper CB (2001) Melanopsin in cells of origin of the retinohypothalamic tract. *Nat Neurosci* 4:1165.

Hattar S, Liao HW, Takao M, Berson DM and Yau KW (2002) Melanopsin-containing retinal ganglion cells: architecture, projections, and intrinsic photosensitivity. *Science* 295:1065-1070.

Herljevic M, Middleton B, Thapan K and Skene DJ (2005) Light-induced melatonin suppression: age-related reduction in response to short wavelength light. *Exp Gerontol* 40:237-242.

Klerman EB (2005) Clinical aspects of human circadian rhythms. *J Biol Rhythms* 20:375-386.

Lockley SW, Evans EE, Scheer FA, Brainard GC, Czeisler CA and Aeschbach D (2006) Short-wavelength sensitivity for the direct effects of light on alertness, vigilance, and the waking electroencephalogram in humans. *Sleep* 29:161-168.

Lucas RJ, Freedman MS, Lupi D, Munoz M, David-Gray ZK and Foster RG (2001) Identifying the photoreceptive inputs to the mammalian circadian system using transgenic and retinally degenerate mice. *Behav Brain Res* 125:97-102.

Monk TH, Buysse DJ, Reynolds CF, 3rd, Kupfer DJ and Houck PR (1995) Circadian temperature rhythms of older people. *Exp Gerontol* 30:455-474.

Moore RY and Lenn NJ (1972) A retinohypothalamic projection in the rat. *J Comp Neurol* 146:1-14.

Moore RY, Speh JC and Card JP (1995) The retinohypothalamic tract originates from a distinct subset of retinal ganglion cells. *J Comp Neurol* 352:351-366.

Pokorny J, Smith VC and Lutze M (1987) Aging of the human lens. *Applied Optics* 26:1437-1440.

Provencio I, Rodriguez IR, Jiang G, Hayes WP, Moreira EF and Rollag MD (2000) A novel human opsin in the inner retina. *J Neurosci* 20:600-605.

Revell VL and Eastman CI (2005) How to trick mother nature into letting you fly around or stay up all night. *J Biol Rhythms* 20:353-365.

Sekaran S, Foster RG, Lucas RJ and Hankins MW (2003) Calcium imaging reveals a network of intrinsically light-sensitive inner-retinal neurons. *Curr Biol* 13:1290-1298.

Sletten TL, Revell VL, Middleton B, Lederle KA and Skene DJ (in press) Age-related changes in acute and phase advancing responses to monochromatic light. *J Biol Rhythms*.

Turner PL and Mainster MA (2008) Circadian photoreception: ageing and the eye's important role in systemic health. *Br J Ophthalmol* 92:1439-1444.

Vandewalle G, Gais S, Schabus M, Balteau E, Carrier J, Darsaud A, Sterpenich V, Albouy G, Dijk DJ and Maquet P (2007) Wavelength-dependent modulation of brain responses to a working memory task by daytime light exposure. *Cereb Cortex* 17:2788-2795.

Verriest G (1971) [Influence of age on visual functions in humans]. *Bull Acad R Med Belg* 11:527-578.

Weale RA (1985) Human lenticular fluorescence and transmissivity, and their effects on vision. *Exp Eye Res* 41:457-473.

Yan L and Silver R (2002) Differential induction and localization of mPer1 and mPer2 during advancing and delaying phase shifts. *Eur J Neurosci* 16:1531-1540.

Yang Y, Thompson K and Burns SA (2002) Pupil location under mesopic, photopic, and pharmacologically dilated conditions. *Invest Ophthalmol Vis Sci* 43:2508-2512.

Zhang Y, Kornhauser JM, Zee PC, Mayo KE, Takahashi JS and Turek FW (1996) Effects of aging on light-induced phase-shifting of circadian behavioral rhythms, fos expression and CREB phosphorylation in the hamster suprachiasmatic nucleus. *Neuroscience* 70:951-961.

Figure Legends

Figure 1: Overview of the protocol design. The figure illustrates an example protocol for a participant maintaining a 2300-0700 h sleep schedule with light and buccal sampling timed according to a dim light melatonin onset (DLMO) at 2100 h. Subjects had to maintain a consistent, self-selected sleep schedule 7 days prior to and throughout the study. In the laboratory, the volunteers took part in a baseline phase assessment followed by an experimental light session where they were subjected to 2 h of either blue (single-hatched) or green (cross-hatched) light in the early morning. Oral mucosa was sampled at identical time points on the baseline day (between night 1 [N1] and N2) and 0.5, 5.0, and 10.0 h after the light administration (between N2 and N3). The entire protocol was carried out under controlled light levels, posture and meals.

Figure 2: Age- and wavelength-dependent changes in *PER2* expression in human oral mucosa. Young and old subjects were exposed to either 2 h of monochromatic blue (λ_{max} 456 nm) or green (λ_{max} 548 nm) light. *PER2* expression was measured using quantitative real-time PCR. Data are represented as mean ± SEM, N for each condition and time point is indicated at the bottom of the respective bars. Samples taken after the light pulse were compared to the matching baseline samples (taken between N1 and N2). * p = 0.0380 as determined by unpaired t-test.

Figure 1

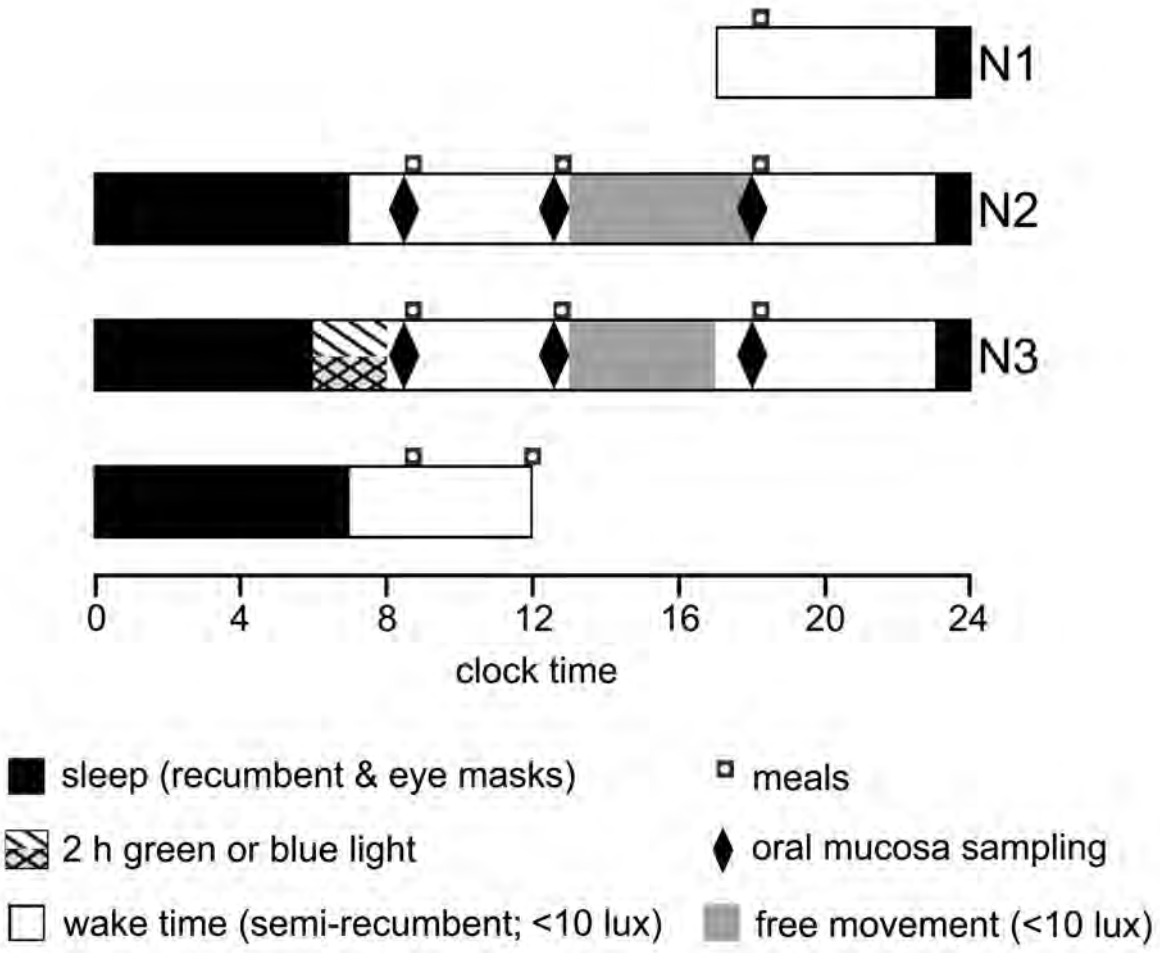
N1
N2
N3
0
4
8
12
16
20
24
clock time
sleep (recumbent & eye masks)
2 h green or blue light
wake time (semi-recumbent; <10 lux)
meals
oral mucosa sampling
free movement (<10 lux)

Figure 2

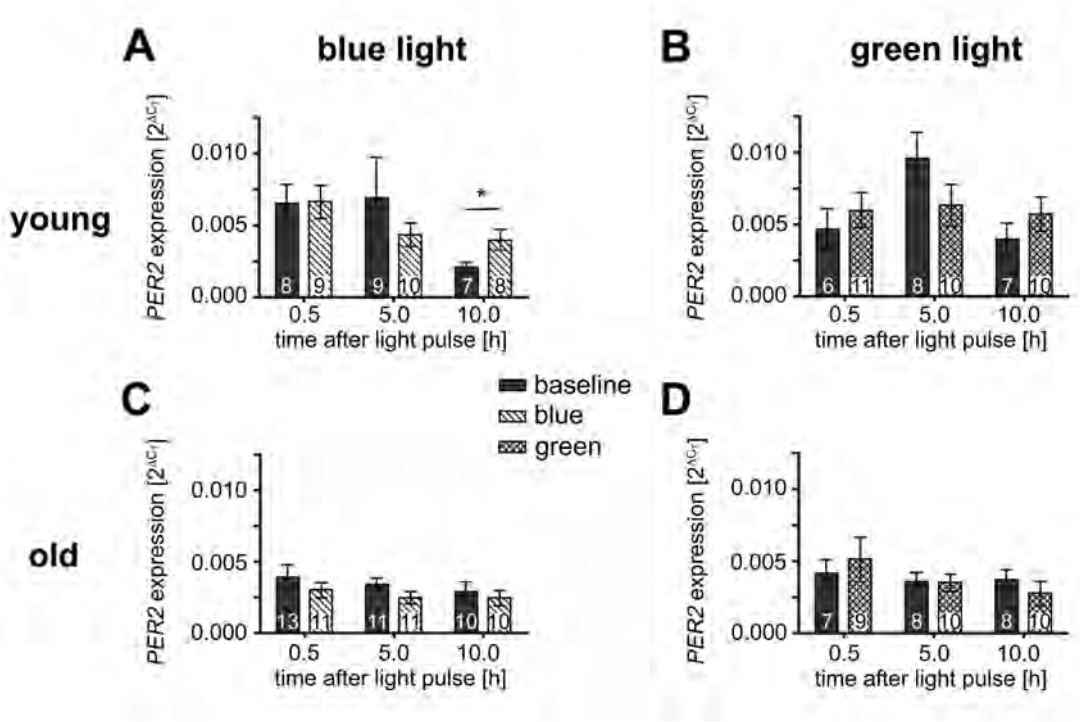
A
blue light
B
green light
young
C
D
old
baseline
blue
green
PER2 expression [2^ΔCt]
0.010
0.005
0.000
0.5
5.0
10.0
time after light pulse [h]
*
8
9
9
10
7
8
6
11
8
10
7
10
13
11
11
11
10
10
7
9
8
10
8
10

4.4.1 Additional data

PER1 (add. fig. 1) and *BMAL1* (add. fig. 2) expression was studied in the same samples but the sample numbers were too low to make any definite conclusions.

Pooling all the data irrespective of age did not reveal significant differences for all three genes measured (add. fig. 3).

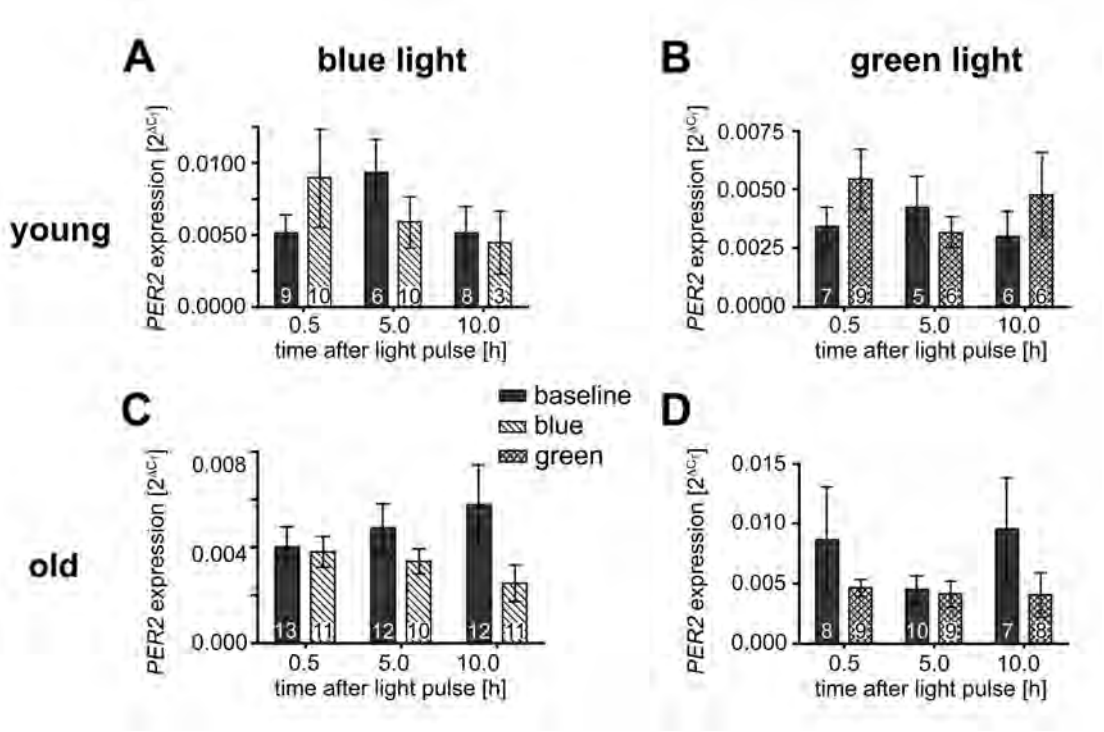

Additional figure 1: *PER1* expression in human oral mucosa. Young (A/B; N = 3-10) and old (C/D; N = 7-13) subjects were exposed to either 2 h of monochromatic blue (A/C; λ_{max} 456 nm) or green (B/D; λ_{max} 548 nm) light. *PER1* expression was measured using quantitative real-time PCR. Data are represented as mean ± SEM, N for each condition and time point is indicated at the bottom of the respective bars. Samples taken after the light pulse were compared to the matching baseline samples (taken between N1 and N2). Unpaired t-test did no reveal significant differences.

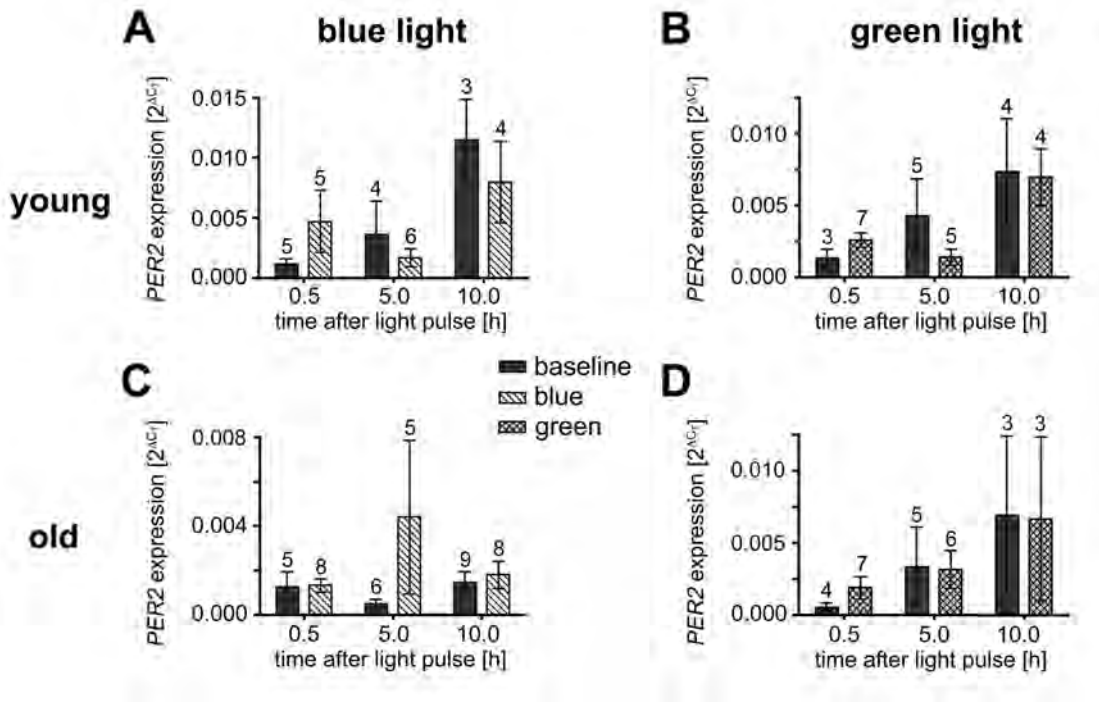

Supplemental figure 2: *BMAL1* expression in human oral mucosa. Young (A/B; N = 3-7) and old (C/D; N = 3-9) subjects were exposed to either 2 h of monochromatic blue (A/C; λ_{max} 456 nm) or green (B/D; λ_{max} 548 nm) light. *BMAL1* expression was measured using quantitative real-time PCR. Data are represented as mean ± SEM, N for each condition and time point is indicated at the top of the respective bars. Samples taken after the light pulse were compared to the matching baseline samples (taken between N1 and N2). Unpaired t-test did no reveal significant differences.

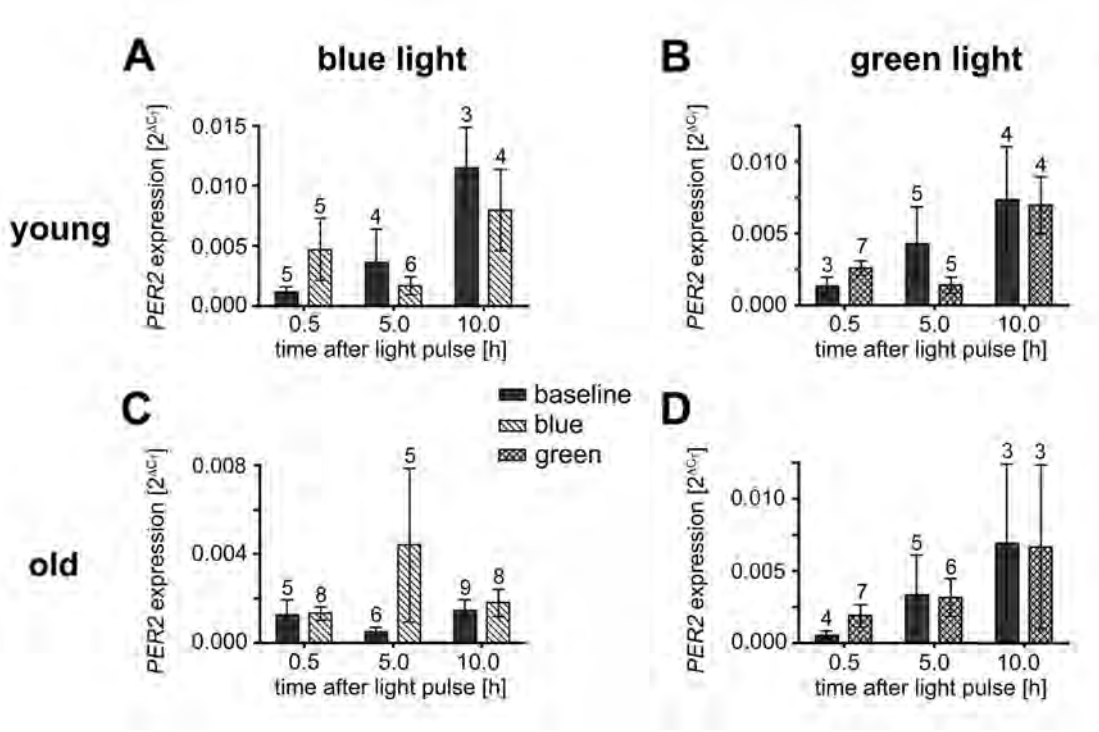

Supplemental figure 3: *PER2*, *PER1*, and *BMAL1* expression in human oral mucosa. Subjects were exposed to either 2 h of monochromatic blue (A/C/E; λ_{max} 456 nm) or green (B/D/F; λ_{max} 548 nm) light. *PER2* (A/B; N = 13-21), *PER1* (C/D; N = 13-22), and *BMAL1* (E/F; N = 6-13) expression was measured using quantitative real-time PCR. Data are represented as mean ± SEM, N for each condition and time point is indicated at the top of the respective bars. Samples taken after the light pulse were compared to the matching baseline samples (taken between N1 and N2). Unpaired t-test did no reveal significant differences.

Chapter 5

Discussion & Perspectives

5 Discussion and Perspectives

Most interpretations that arise from the work presented here have been elaborated in the discussion part of the included publications. Therefore this part will try to elucidate some additional aspects of our results.

5.1 Development of circadian rhythms in mammals

5.1.1 Discussion

The aim of this study was to investigate whether the emergence of circadian rhythms in mammals is dependent on a functional maternal clock - a question that has been of interest for many years. Maternal entrainment of the fetal clock has been documented in many studies (Reppert & Schwartz, 1983; Reppert *et al.*, 1984; Davis & Gorski, 1985; reviewed in: Reppert, 1995). However, maternal influence on the circadian system of the offspring differs tremendously between species. In precocial species (i.e. highly developed at birth; e.g. guinea pigs, spiny mice and sheep), maternal entrainment ends at birth and the prevailing light-dark cycle becomes the strongest Zeitgeber for them. By contrast, the maternal circadian system continues to coordinate the timing of altricial pups (i.e. less developed at birth; e.g. humans, mice, rats or hamsters). In addition, other experiments have shown that the clock was unaffected in pups born to SCN-lesioned dams. By contrast, synchrony between pups was altered (Reppert & Schwartz, 1986; Davis & Gorski, 1988).

The present study was the first one to investigate the emergence of circadian rhythms in offspring of genetically ablated females. It was found that heterozygous offspring born to $Per1^{Brdm1}Per2^{Brdm1}$ or $Per2^{Brdm1}Cry1^{-/-}$ double mutant arrhythmic females crossed with wild-type males under constant conditions developed normal circadian wheel-running behaviour. However, their clocks were less synchronized to each other as compared to wild-type controls. These results indicate that the development of circadian clocks is genetically predetermined and does not depend on a functional maternal clock or prenatal Zeitgebers. Interestingly, similar observations were reported for *Drosophila*. Flies raised under constant darkness and temperature developed robust circadian locomotor activity but at random phases (Sehgal *et al.*, 1992). Hence one can assume that circadian rhythms in humans may emerge in an analogous way. However, this hypothesis is difficult to prove because studies in humans are limited due to ethical considerations. Table 5-1 summarizes what is known about the fetal development of the circadian system in humans.

All of those who have had children can confirm that unfortunately babies do not follow circadian rhythms in sleep-wake cycles. This observation is rather surprising, knowing that circadian rhythms develop early *in utero* (Reppert & Schwartz, 1984; Reppert, 1992). In humans, the SCN become visible as early a time as 18 weeks of gestation (Reppert *et al.*, 1988). At about the same time (20-22 weeks), circadian rhythms in heart rate, respiration, and movements become apparent (De Vries *et al.*, 1987). However, these rhythms seem to be driven by maternal signals that are able to cross the placenta (Honnebier *et al.*, 1989). Nonetheless, strong external signals may set circadian phase in the fetal SCN as suggested by experiments performed in squirrel monkeys (Reppert & Schwartz, 1984). These observations are in line with results obtained during a construction period at our university. All of a sudden the otherwise not synchronized $Per1^{Brdm1}Per2^{Brdm1}$ heterozygous offspring showed marked within-litter synchrony for clock phase.

Table 5-1: Development of the human circadian system: prenatal to postnatal (adapted from: Allen, 2000).

Gestational age	Cycle characteristics	Significant features
3-6 weeks	Monkey SCN neurogenesis.	Squirrel monkey, also likely for humans.
18 weeks	Human SCN detected.	Melatonin labeling; likely present earlier, but not studied.
	Fetal circadian rhythms develop.	Heart rate, respiration, adrenal function linked to mother's cycle by melatonin, nutrients, etc. (circadian stimulation aids development for premature infants).
End of gestation	SCN show internal circadian metabolic cycle.	Confirmed by studies in monkeys; unknown but assumed for humans.
Birth	Labor onset most likely during early morning.	Linked mostly to maternal cycle; may be influenced by fetal cycles.
	Most infant circadian phases match maternal phases.	Some infants are out of phase with their mothers, uncertain significance of this lack of synchrony.
1-2 weeks	Loss of most fetal circadian rhythms. No melatonin rhythm. Some entrainment to low-level lights. Human SCN not fully matured. No clear circadian pattern of activity.	Fetal heart rate, respiration cycles lost. No clear temperature cycle. Demonstrated for baboons and humans.
		Vasopressinergic neurons 13 % of adult levels. Demonstrated for baboons and humans.
	Multiultradian sleep-wake cycles.	Near random alterations of sleep-wake times, mostly sleep.
1-2 months	Circadian activity rhythm develops. Sleep begins to occur more at night.	Temperature nadir in early morning by week 4.
3-4 months	Sleep mostly at night (70 % of children).	One solid sleep period at night for 70 % of children.
	Ultradian pattern stabilizes.	Midday naps begin to develop – usually 2-3 naps.
	Melatonin production clearly present.	Melatonin rhythm appears, gradually increases to month 6.

To sum up, this study demonstrates that circadian rhythms develop autonomously and do not need a functional circadian clock in maternal tissue. In addition, these results are similar to

what has been observed in other organisms suggesting that they can be extrapolated to humans. The more we understand about the development of circadian rhythms in the fetus and the neonate the better they will be shephered from a chronobiolgical point of view. Alarmingly, most preterm babies face the timeless environment of the Neonatal Intensive Care Nursery because perinatal chronomedicine is still in the fledgling stages.

5.1.1 Perspectives

To really test whether the results obtained in mice can be extrapolated to humans one would have to study the development of circadian rhythms in a fetus carried by a woman who has no functional SCN under constant conditions. In humans, two case reports show that tumors and congenital lesions in the SCN region result in the loss of temperature rhythms (Schwartz *et al.*, 1986) and disorganized sleep-wake patterns (Rivkees, 2001). These findings are similar to what has been reported in SCN-lesioned rodents (Moore & Eichler, 1972; Stephan & Zucker, 1972). However, it will be almost impossible to find such a woman who is willing to participate in such an experiment during pregnancy. Moreover, ethical constraints will further impede on the realization of such a study.

Alternatively, one could conduct the study in baboons or squirrel monkeys that are likely very close to humans. Nonetheless, experiments performed on apes are heavily contested nowadays too.

5.2 Analysis of *Rev-Erbα/Per1* double mutant mice

5.2.1 Discussion

To better understand the interplay between *Rev-Erbα* and *Per1* within the circadian clock machinery we generated mice deficient for these two genes. Subsequently, the double mutant animals were tested for their basic wheel-running behaviour, their response to light, the expression of core clock genes and other parameters. We found that mice mutated for *Rev-Erbα* and *Per1* displayed rather normal wheel-running behaviour. However, their circadian period in DD was dramatically shortened compared to single mutants and wild-types. Strikingly, administration of brief light pulses provoked high amplitude resetting in *Rev-Erbα*$^{-/-}$*Per1*^{Brdm1} double mutant mice. Moreover, *Cry1* became inducible after a light pulse delivered at CT22 but not CT14 in these mice. This observation is surprising because *Cry1* was thought not to respond to light pulses at all in mammals (Okamura *et al.*, 1999; Field *et al.*, 2000). By contrast, *Cry1a* has been identified to be a key player in light entrainment of

the zebrafish clock as part of a signaling pathway to the circadian pacemaker (Tamai *et al.*, 2007). In the past few years, *Danio rerio* became one of the most valuable lower vertebrate models for studying circadian clock function. It is thought that the teleost circadian system might be the more ancestral vertebrate clock that became far more specialized in mammals due to selective pressure. Hence *Rev-Erbα* and *Per1* might have acquired additional features, which prevent strong resetting in mammals. Contrary to mammals, most if not all, of the zebrafish tissues are directly light responsive (Whitmore *et al.*, 1998 & 2000; Yoo *et al.*, 2004), as it is the case for *Drosophila* (Vansteensel *et al.*, 2008). The fruit fly has one single cryptochrome gene that acts as a blue light photopigment by binding TIM and PER upon light activation. This interaction causes the subsequent degradation of the protein complexes (Ceriani *et al.*, 1999; Rosato *et al.*, 2001; Busza *et al.*, 2004). Mutants lacking *Cry* were unable to shift their clocks in response to light (Stanewsky *et al.*, 1998). Originally, cryptochromes were identified in *Arabidopsis thaliana* as a photoactive pigment with high homology to photolyases (Ahmad & Cashmore, 1993). In mammals, the role of the cryptochromes is less clear. Both homologs are expressed in the inner retina as well as the SCN (Miyamoto & Sancar; 1998; Thompson *et al.*, 2003). They accomplish light-independent negative regulatory functions in the transcriptional feedback loop to help to run the circadian clock (Kume *et al.*, 1999; Van der Horst *et al.*, 1999; Vitaterna *et al.*, 1999). Apart from this, there is a big controversy in the field whether cryptochromes act as photoreceptors in mammals too. Some state that cryptochromes are not required for photoentrainment mainly due to the results of one study. Okumara and co-workers (1999) showed that $Cry1^{-/-}Cry2^{-/-}$ double mutants were still able to reset their clock upon a light pulse. However, mice carrying a retinal degeneration mutation (*rd*; depleting rods and cones) and lacking both cryptochromes were no longer able to react to light. Induction of *cFos* was increased in *rd/rd* mutants compared to wild-types while it was drastically decreased in mice lacking *Cry1* and *Cry2*. In the triple mutants, *cFos* induction was virtually eliminated (Selby *et al.*, 2000; Van Gelder *et al.*, 2002). Interestingly, mice lacking all visual opsins (*rd/rd*) and melanopsin ($Opn4^{-/-}$) have lost all photoresponses. By contrast, mice deficient for melanopsin only showed a normal response to light (Hattar *et al.*, 2003; Panda *et al.*, 2002 & 2003; Ruby *et al.*, 2002). However, these findings are questioned by recent studies, which demonstrated that the ablation of melanopsin cells altered the effects of light on circadian rhythms (Göz *et al.*, 2008; Hatori *et al.*, 2008). To summarize, these data suggest that phototransduction to the SCN by cryptochromes requires melanopsin or the outer retina (Partch & Sancar, 2005). Moreover, mice mutant for retinol-binding protein (*rbp*) as well as *Cry1* and *Cry2* kept on a

vitamin A-free diet have no *cFos* induction compared to *rbp*$^{-/-}$ controls. This indicates that cryptochromes are required for photoreception in mice depleted of ocular retinal (Thompson *et al.*, 2004). Altogether, these data strongly suggest a role for mouse cryptochromes in photoreception.

Considering that we found a light inducibility of *Cry1* in *Rev-Erbα*$^{-/-}$ *Per1*^{Brdm1} double mutants, our data strengthen the idea that mammalian cryptochromes might be involved in light signaling. Moreover, our findings suggest that Rev-Erbα and Per1 suppress *Cry1* induction. However, the mechanisms beneath *Cry1* regulation have to be further elucidated. To better understand what is going on, it would be interesting to investigate *Cry2* induction by light in the double mutants. In humans, CRY2 has been reported to be highly abundant in the inner retina. From this, it has been concluded that CRY2 could be involved in photoreception (Thompson *et al.*, 2003). Another interesting attempt would be to study whether *Rev-Erbα*$^{-/-}$*Per1*^{Brdm1} fibroblasts become directly light sensitive, as it is the case for zebrafish cells. If this would be the case, *Rev-Erbα*$^{-/-}$*Per1*^{Brdm1} cells would be an attractive model system for studying light input to the circadian clock in mammals. These cells would offer an alternative to the synthetically produced photo-responsive melanopsin complemented NIH3T3 cells (Ukai *et al.*, 2007). Moreover, this would further strengthen the hypothesis that *Rev-Erbα* and *Per1* exhibit a gain of function phenotype in mammals. All of a sudden the famous but discredited “light behind the knee experiment” (Campbell & Murphy, 1998) would make again some sense – at least if it would have been performed in subjects carrying mutations in *Rev-Erbα* and *Per1*.

5.2.2 Perspectives

As already mentioned in the discussion part, it would be interesting to study the light responsiveness of *Rev-Erbα*$^{-/-}$*Per1*^{Brdm1} fibroblasts. However, before starting these experiments one should study the responsiveness of the cells to serum or dexamethasone. This experiment will tell, whether *Rev-Erbα*$^{-/-}$*Per1*^{Brdm1} fibroblasts are synchronized normally and whether clock genes are induced comparable to wild-type cells. Hence one can exclude that an eventual difference observed after light administration is just due to general differences in the cells. In a next step, the fibroblasts have to be exposed to light and it has to be tested whether clock genes are induced. If this were the case, one would have to repeat the experiment in the presence of a protein synthesis inhibitor (e.g. hexamide). Hence one can find out whether eventual RNA induction is based on *de novo* protein synthesis. Moreover, it

would be interesting to test the effect of different wavelengths (i.e. blue, green, red) on the cells. Last but not least, one could transfect the cells with a luciferase reporter construct and follow the expression of the reporter in real time in the lumicycler. Finally, one could apply light pulses at different phases and record the shifts.

Another interesting approach to clarify whether *Cry1* induction alone leads to the Type 0 PRC in animals deficient for *Rev-Erbα* and *Per1* would be to generate mice triple mutant for *Cry1, Rev-Erbα* and *Per1*. If these mice would show normal light resetting, the importance of *Cry1* in this high amplitude resetting would be underlined. However, it is generally rather difficult to obtain triple mutants due to fertility problems.

In addition, it would be important to analyze what happens within the SCN and with single neurons following a light pulse at CT22. It is known that only a subset of mostly ventrolateral SCN neurons receive retinal input and seem to shift their clocks immediately (Albus *et al.,* 2005). These neurons then send a synchronizing signal to the rest of the SCN neurons. In parallel, the SCN constantly receives feedback information from other brain areas (e.g. sleep centers, locomoter-associated areas). These signals can attenuate phase shifts (Vanstensel *et al.,* 2003). In this context it would be interesting to study VIP in the double mutants because VIP is supposed to synchronize mammalian clock neurons and to maintain their rhythmicity (Aton *et al.,* 2005). Indeed, preliminary results suggest that this is a good approach. We found that VIP was expressed in a circadian fashion in wild-type and especially *Rev-Erbα*$^{-/-}$ *Per1*^{Brdm1} double mutant mice. Interestingly, VIP seemed to be light inducible in the double mutant animals after a light pulse at CT22. However, these results should be interpreted with caution because only one animal was analyzed per time point. For instance, double mutants show higher basal VIP levels at CT22 and lower levels for the dark control taken at CT23. Nonetheless, VIP expression seems to differ between the two genotypes and could be an interesting target for further research.

5.3 The influence of light on clock gene expression in humans

In our modern society, investigation of human circadian rhythms and their associated disorders is a hot topic because they represent a huge risk for health and welfare. People suffering from sleeping disorders, jet-lag, shift work associated disorders, or mood disturbances are less performing at work. Due to such disturbances of the circadian system, industry loses tremendous amounts of money every year. Hence, analyzing human tissue for

clock gene expression may be a useful tool to better understand the mechanisms underlying these disorders.

For this purpose we developed a non-invasive method to measure and quantify clock gene expression in human oral mucosa. We demonstrated that *PER1, PER2,* and *BMAL1* were expressed rhythmically in buccal cells. Interestingly, *PER1* and *PER2* mRNA accumulation occurred in anti-phase to *BMAL1* expression as it has been described for rodents (Abe *et al.,* 1998; Albrech *et al.,* 1997). Moreover, our findings are in accordance with Bjarnason *et al.* (2001), who reported similar expression profiles for *PER1* and *BMAL1* in human oral mucosa and skin biopsies taken under local anesthesia. Hence our results confirm the existence of a functional circadian machinery in human buccal cells.

Once the accuracy of our method had been proven we tested the influence of blue light on *PER2* expression in human mucosa. Interestingly, the effect of blue light on *PER2* mRNA levels varied depending on the time it was perceived. Evening blue light exposure acutely induced *PER2* expression while early morning blue light had no immediate effect. These findings parallel observations for *Per2* in mice (Albrecht *et al.,* 1997; Yan & Silver, 2002). In contrast to evening blue light, early morning blue light significantly increased *PER2* mRNA levels 10.0 hours after the light pulse. This increase is probably due to a phase shift of the *PER2* expression curve. However, our data do not provide information about its direction.

The effectiveness of light administration was not only time-dependent but varied also with wavelength. All effects on *PER2* expression were only observed after blue, but not green, light. Our findings indicate that the changes in *PER2* mRNA levels are due to non-visual effects of the circadian system, which are mediated by the SCN. The spectral sensitivity of the response in young subjects is in accordance with multiple studies in humans assessing non-visual light responses (Brainard *et al.,* 2001; Thapan *et al.,* 2001; Cajochen *et al.,* 2005; Lockley *et al.,* 2003; Revell *et al.,* 2005 & 2006).

Moreover, early morning blue light had no effect on *PER2* expression in the elderly. These data support the diminished response to blue light observed in older people in both the subjective alerting response (Sletten *et al.,* in press) and melatonin suppression response (Herljevic *et al.,* 2005). This observation could be explained in part by the fact that, with age, the crystalline lens progressively transmits less light (Pokorny *et al.,* 1987; Turner & Mainster, 2008; Weale, 1985). Consequently, less light information reaches the SCN.

In conclusion, our findings demonstrate that human buccal samples are a valuable tool for studying the response of *PER2* to light and clock gene rhythms. Hence, this method could

help shed more light onto the molecular mechanisms underlying disorders associated with the internal clock. Moreover, this study proves that findings obtained in rodents or other model organisms are of great use for the understanding of the human circadian system. Ongoing experiments in healthy and ill subjects still take advantage of this method. Increasing knowledge will allow the development of better therapeutic approaches for human circadian disorders caused by ageing or diseases.

Chapter 6

Materials & Methods

6 Materials and Methods

6.1 Materials

6.1.1 Chemicals and solvents

Product	Manufacturer	Cat. Number
ABTS	SIGMA-ALDRICH	A 1888
Acetic acid (glacial) 100 %	MERCK	1.00063.1000
Acetic anhydride	SIGMA-ALDRICH	A 6404
Agarose (SeaKem®LE)	Cambrex (BioConcept)	50004E
Agarose Low Melting (SeaPlaque®)	Cambrex (BioConcept)	50101
Ammonium acetate (GR for analysis)	MERCK	1.01116.0500
Ammonium persulfate	BioRad	161-0700
Ammonium sulfate	Riedel de Haen	31119
Ampicillin	SIGMA-ALDRICH	A 9518
ATP disodium salt	SIGMA-ALDRICH	A 7699
ATP-α-S, Sp-Isomer	Roche	775 746
Beeswax, bleached, white	SIGMA-ALDRICH	243221
BisBenzimide (Hoechst No. 33258 trihydrochloride)	SIGMA-ALDRICH	B 2883
Bovine Serum Albumine, fract. V (BSA)	Uptima (Interchim)	UP283910
5-Bromo-4-chloro-3-indoxyl-α-D-galactopyranoside	Biosynth	B-7141
Bromphenol blue	SIGMA-ALDRICH	B 0126
Calciumchloride	MERCK	1.02382.0500
Calf thymus type I DNA	SIGMA-ALDRICH	D 1501
Canada Balsam	SIGMA-ALDRICH	C 1795
Chloroform	Fluka	25690
Coenzyme A	SIGMA-ALDRICH	C 3144
Colophony	Fluka	60895
Coomassie® Briliant Blue R250	Fluka	27816
Dextransulfate	SIGMA-ALDRICH	D 8906
Dimethyl sulfoxide (DMSO)	Fluka	41639
di-Potassium hydrogen phosphate trihydrate	MERCK	1.05099.1000
di-Sodium hydrogen phosphate dodecahydrate	MERCK	1.06573.1000
Dexamethasone	SIGMA-ALDRICH	D 4902
Dithiothreitol (DTT)	SIGMA-ALDRICH	D 9779
DL-Fluorocitric acid	SIGMA-ALDRICH	F 9634
Dimethylsulfoxid (DMSO)	Fluka	41639
DNA from Herring Sperm	Roche	223 646
EDTA	Fluka	03680
EGTA	Fluka	03779
Ethanol	Fluka	02860
Ethidiumbromide	Fluka	46067
Formaldehyde solution min. 37 %	MERCK	1.04003.1000
Formamide (for molecular biology)	Fluka	47671
Glycerol 87 %	Fluka	49782
Glycine	Fluka	50046
Goat serum	SIGMA-ALDRICH	G 9022
HEPES	Fluka	54461
Herring sperm DNA	SIGMA-ALDRICH	D 3159
Hydrochloric acid	MERCK	1.00317.1000
Isopropanol (anhydrous 99.8+ %)	Acros Organics	149320010
Kanamycin sulfate	Fluka	60615
Linear polyethyleneimine 25 kDa (LINPEI25)	Polysciences Europe	23966-5

Lithium chloride	Fluka	62480
Luciferin (D)	SIGMA-ALDRICH	L 6882
Magnesium chloride hexahydrate	MERCK	1.05833.0250
Magnesium sulphate anhydrous	Fluka	63135
Manganese chloride	SIGMA-ALDRICH	M 3634
2-Mercaptoethanol	Fluka	63690
Methanol	Fluka	65543
Methyl salicylate	Fluka	84330
MOPS (3-Morpholinopropanesulfonic acid)	Fluka	69947
MUG	SIGMA-ALDRICH	M 1633
$NADP^+$	SIGMA-ALDRICH	240-305
NADPH	SIGMA-ALDRICH	N-1630
Paraformaldehyde (granules)	Electron Microscopy Sciences	19280
Paraplast tissue embedding medium (Paraffin)	McCormick™(Medite)	81076100
Paraquat CL tetrahydrate	SIGMA-ALDRICH	PS366
Phenol	Acros Organics	327105000
PIPES	SIGMA-ALDRICH	P 1851
Potassium chloride	Fluka	60130
Potassium dihydrogen phosphate	MERCK	1.04873.1000
Potassium hydroxide	Fluka	60375
2-Propanol	Fluka	59300
Rabbit Serum	SIGMA-ALDRICH	R 9133
Rapilait (skim milk powder)	Migros	
Select Agar	GIBCO BRL	30391-023
Select Peptone 140	GIBCO BRL	30392-021
Select Yeast Extract	GIBCO BRL	30393-029
Sodium acetate	MERCK	1.06268.0250
Sodium azide	Fluka	71290
Sodium chloride	MERCK	1.06404.5000
Sodium cyanide	SIGMA-ALDRICH	S 3296
Sodium dihydrogen phosphate monohydrate GR	MERCK	1.06346.0500
Sodium dodecyl sulphate (SDS)	Carl Roth GmbH & Co.	2326.2
Sodium fluoride	SIGMA-ALDRICH	S 7920
Sodium hydrogen phosphate dodecahydrate	Fluka	71650
Sodium hydroxide	MERCK	1.06498.1000
Sodium hypochlorite 13-14 %	Schweizerhall	28804
Sodium orthovanadate (Na_3VO_4)	SIGMA-ALDRICH	S 6508
Spermidine	MERCK	7904.0001
Spermine tetrahydrochloride	SIGMA-ALDRICH	S 2876
Sucrose	Fluka	84105
TEA	SIGMA-ALDRICH	T 1377
TEMED	Fluka	87687
TRIS Ultra Qualität	Carl Roth GmbH & Co.	5429.3
tri-Sodium citrate dihydrate	MERCK	112005.0100
Triton-X 100	Fluka	93426
t-RNA (from baker's yeast)	Roche	109 495
Tween®-20	Fluka	95773
Uridine-5'-triphosphate [α-^{35}S]	PerkinElmer	NEG-039H
Xylene cyanole FF	SIGMA-ALDRICH	X 4126
Xylene	Fluka	95690

6.1.2 Kits and ready for use solutions

Kit	Manufacturer	Cat. Number
Absolutely RNA nanoprep Kit	Stratagene	400 753
Corticosterone ^{3}H RIA Kit (rat & mouse)	MP Biomedicals	07-120002
ECL™ Western Blotting Analysis System	GE Healthcare (Amersham)	RPN2109
FastLane Cell cDNA Kit	Qiagen	215011
iQ SYBR Green Supermix	BioRad	170-8880
iQ Supermix	BioRad	170-8862
Megaprime DNA Labelling System	GE Healthcare (Amersham)	RPN1606
Illustra™ ProbeQuant™ G-50 Micro Columns	GE Healthcare	28-9034-08
PureYield™ Plasmid Maxiprep System	Promega	A2393
QIAfilter™ Plasmid Maxi Kit (25)	Qiagen	12263
QIAprep Spin Miniprep Kit (250)	Qiagen	27106
QIAquick Gel Extraction Kit (50)	Qiagen	28704
RNAMaxx™ High Yield Transcription Kit	Stratagene	200339
S.N.A.P.™ Gel Purification Kit	Invitrogen	K1999-25
TOPO TA Cloning® Kit Dual Promoter (with PCR®II-TOPO® Vector)	Invitrogen	K4600-40
TOPO® XL PCR Cloning Kit (with PCR® XL-TOPO vector)	Invitrogen	K4750-20
Premix Ex Taq™ (Perfect Real Time)	TaKaRa	RR039
Vectastain® Elite® ABC Kit (rabbit IgG)	Vector Laboratories	PK-6101
Vectastain® Elite® ABC Kit (goat IgG)	Vector Laboratories	PK-6105
Wizard® SV Gel and PCR Clean-Up System	Promega	A 9281
Solution	**Manufacturer**	**Cat. Number**
Aquatex	Merck	1.08562.0050
Attane™ Isoflurane ad us. vet.	Provet AG	QN01AB06
BCA™ Protein Assay Kit	Thermo Scientific (Pierce)	23227
Bradford Protein Assay	Bio-Rad	500-0006
Developer D-19	Kodak (SIGMA)	P-5670
Denhardt's solution	SIGMA-ALDRICH	D 2532
Fast™ 3,3'-Diaminobenzidine (DAB) tablet set	SIGMA-ALDRICH	D 4168
Fixer	Kodak (SIGMA)	P 6557
Kodak liquid emulsion NTB-2	Mandel Scientific Co. Ltd.	165 4433
OptiPhase "HiSafe" 2 scintillation cocktail	Perkin Elmer (Wallac Scintillation products)	SC/9195/21 1200-436
pH 4.0 red buffer	Beckman Instruments, Inc.	582517
pH 7.0 green buffer	Beckman Instruments, Inc.	582521
pH 9.0 buffer solution (Borate)	Metrohm	6.2307.120
pH 10.0 blue buffer	Beckman Instruments, Inc.	582525
Phenol : Chloroform : Isoamyl Alcohol 25:24:1	SIGMA	P 2069
PCR Nucleotide Mix [10 mM]	Roche	11 814 362 001
Primer $p(dT)_{15}$ for cDNA Synthesis	Roche	10 814 270 001
Protease inhibitor cocktail (compl., EDTA free)	Roche	11 873 580 001
QuickHyb®	Stratagene	201220
RNA-Bee	TEL-TEST, INC. (ams)	CS-105B
RNA*later*®	Qiagen	1017980
Ultraclear	J. T. Backer	3905
X-ray Developer LX 24	Kodak	507 0933
X-ray Fixer AL 4	Kodak	507 1071

6.1.3 Radioactive chemicals

Nucleotide	Manufacturer	Cat. Number
Deoxycytidine 5'-Triphosphate [α-^{32}P]	Perkin Elmer	NEG513H
Uridine 5'-(α-Thio)Triphosphate [^{35}S]	Perkin Elmer	NEG 039H

6.1.4 Ladders and enzymes

Ladder	Manufacturer	Cat. Number
1 kb DNA Ladder	New England Biolabs	N3232L
100 bp DNA Ladder	New England Biolabs	N3231L
2-Log DNA Ladder	New England Biolabs	N3200G
Gene Ruler™ 50 bp DNA Ladder	Fermentas	SM0378
Gene Ruler™ 100 bp DNA Ladder Plus	Fermentas	SM0328
Precision Plus Protein Dual Color Standard	BioRad	161-0374
Spectra™ Multicolor Broad Range Protein Ladder	Fermentas	SM1841
Enzyme	**Manufacturer**	**Cat. Number**
Catalase [329.3 U/µl]	Fluka	60640
CIP (Calf Intestinal Phosphatase) [10 U/µl]	New England Biolabs	M0290L
Collagenase type I	SIGMA-ALDRICH	C 0130
DNase I, RNase-free [10 U/µl]	Roche	10 776 785 001
Isocitrate Dehydrogenase	SIGMA	I-2516
L-Lactic Dehydrogenase	SIGMA	L-2625
Lysozyme	Applichem	A3711,0010
M-MLV Reverse Transcriptase (Rnase H$^-$)	Promega	M 3681
Peroxidase	SIGMA-ALDRICH	P 1432
ProofStart™ DNA Polymerase	Qiagen	202203
Proteinase K	Roche	1 000 144
Restriction Enzymes	New England Biolabs	
RNase A	SIGMA	R 5503
RNasin	Promega	N211A
SP6 RNA Polymerase [15 U/µl]	Promega	P108B
SuperScript™ II RNase H$^-$ Reverse Transcriptase [200 U/µl]	Invitrogen	18064-014
T3 RNA Polymerase [50 U/µl]	Stratagene	600111-51
T4 DNA Quick Ligase	New England Biolabs	M2200S
T7 RNA Polymerase [200 U/µl]	Stratagene	200339-51
*Taq*DNA Polymerase	Qiagen	201205
TrypsinEDTA 10x (0.5 % with EDTA 4Na)	Gibco	15400-054

6.1.5 Cell lines

Name	Origin	Morphology
COS-7	Monkey African green kidney, SV40 transformed (Gluzman *et al*., 1981)	fibroblast
HEK293	Human embryonic kidney, Ad5 transformed (Graham *et al.*, 1977)	epithelial-like
HEPG2	Human Caucasian liver hepatocellular carcinoma (Aden *et al.*, 1979)	epithelial-like
HER911	Human embryonic retina, Ad5 transformed (Fallaux *et al*., 1996)	epithelial-like
NG108-15	Mouse neuroblastoma x rat glioma hybrid (Banker & Goslin, 1988)	neuronal
NIH3T3	Mouse NIH Swiss embryo (Jainchill *et al*., 1969)	fibroblasts

6.1.6 Cell culture products

Product	Manufacturer	Cat. Number
Amphotericine B	SIGMA-ALDRICH	A 2411
Collagenase type I	SIGMA-ALDRICH	C 0130
Dexamethasone	SIGMA-ALDRICH	D 4902
DMEM high Glucose [4.5 g/l]	Amimed (BioConcept)	1-26F01-I
DMEM high Glucose [4.5 g/l]	SIGMA-ALDRICH	D6429
DMEM high Glucose [4.5 g/l] w/o Phenol Red	Amimed (BioConcept)	1-26F22-I
FCS (Fetal Calf Serum)	Amimed (BioConcept)	2-01F10-I
Lab-Tek® Chamber slides™ (Permanox, 8 wells)	Fisher Scientific	B1008Y
L-Glutamine [200 mM]	Amimed (BioConcept)	5-10K00-H
Linear polyethyleneimine 25 kDa (LINPEI25)	Polysciences Europe	23966-5
Penicillin [10'000 IU/ml]/Streptomycin [10'000 µg/ml]	Amimed (BioConcept)	4-01F00-H
TrypsinEDTA 10x (0.5 % with EDTA 4Na)	Gibco	15400-054

6.1.7 Oligonucleotides

The oligonucleotides have been ordered desalted from Microsynth.

Name	Use	DNA sequence 5'→3'
mCatalaseF	ISH probe	CAC CTG AAG GAC GCT CAG C
mCatalaseR	ISH probe	GTA ATA GGA GAA TAC ACT ATT CTC G
mDexras1f	ISH probe	CCA AGA AGA ACA GCA GCT TG
mDexras1r	ISH probe	TGG CAA CAC CAA TCA CAG AC
mDexras1	oligo annealing (antisense)	CAT GGG GTA GAG GGG CC
mDexras1	oligo annealing (sense)	CCT CTA CCC
mDexras1Pf	reporter construct	CTA GAT CTA GCT GAT GAG TCC
mDexras1Pr	reporter construct	GGT GTA AGC ATC CTC GAA ACG
mFxr2f	ISH probe	GTC AAT TCC AGT TCC CTT GCA ACC
mFxr2r	ISH probe	GTC TCT TCA CCC AAC TCA ATG G
mMkp1f	ISH probe	CAA CGT CTC AGC CAA TTG TCC
mMkp1r	ISH probe	GAG CCT CTC CCA GAG TTA TTG C
*mPrkca*F	ISH probe	CCA TCA GTG GGA AGT GAT CC
*mPrkca*R	ISH probe	TGG TTG TGC TAT GAT GAC TG
mRorα1f	full length clone	AAA ACA TGG AGT CAG CT
mRorα1r	full length clone	TTT GTA CTC CAG ATG TTC TAG A
mRorα4f	full length clone	CGT AAA GGA TGT ATT TTG TGA T
mRorα4r	full length clone	CTC TTA CTT TCA TGT TGT ACT C

6.1.8 Antibodies

Antibody	Manufacturer	Cat. Number
Anti-Actin (rabbit)	SIGMA-ALDRICH	A5060
Anti-BMAL1 (rabbit)	U. Schibler, Geneva	
Anti-CLOCK (rabbit)	U. Schibler, Geneva	
Anti-CREB (48H2; rabbit)	Cell Signaling (Bioconcept)	9197
Anti-CRY1 (rabbit)	Alph Diagnostic	CRY1 1-A
Anti-CRY1 (rabbit)	U. Schibler, Geneva	
Anti-HSP90α/β (F-8; mouse)	Santa Cruz (Labforce)	SC-13119
Anti-Mouse IgG Peroxidase Conjugate	SIGMA-ALDRICH	A 9044
Anti-Phospho RNA Polymerase II (rabbit)	Bethyl	A300-654A
Anti-Rabbit IgG Peroxidase Conjugate	SIGMA-ALDRICH	A 9169

6.1.9 Bacteria and vectors used for cloning

The *E. coli* TOP10 strain (provided with the TOPO TA Cloning® Kit from Invitrogen) and HB101 strain (amplified and made competent in our laboratory) have been used for general cloning. Both strains were rendered competent by a chemical treatment. The genotype of the TOP10 strain is F^-, *mcr*A, Δ(*mrr-hsd*RMS-*mcr*BC), Φ80*lac*ZΔM15, Δ*lac*X74, *rec*A1, *ara*D139, Δ(*ara-leu*)7697, *gal*U, *gal*K, *rps*L, (Str^R), *end*A1, *nup*G whereas the genotype of the HB101 strain is *thi-1, hsdS20 (r_B-, m_B-), supE44, recA13, ara-14, leu B6, pro A2, lac Y1, rpsL20 (str^r), xyl-5, mtl-1*.

Probes for *in situ* hybridization have been cloned using the pCR®II-TOPO® vector (TOPO TA Cloning® Kit from Invitrogen) because this vector contains both, a T7 and an Sp6 RNA polymerase promoter allowing *in vitro* transcription of the insert to produce sense or anti-sense products. This vector is supplied linearized with single 3'-thymidine overhangs and covalently bound topoisomerase I. Some older *in situ* hybridization probes have been cloned into the pPCR-Script Amp SK(+) vector from Stratagene. This vector carries a T3 promoter on one side of the insert and a T7 promoter on the other side.

For rapid cloning of long PCR products (3 to 10 kb) the pCR® XL-TOPO vector (TOPO® XL PCR Cloning Kit from Invitrogen) has been used. Its function is based on the same principle than the one described for the pCR®II-TOPO® vector.

Luciferase reporter constructs have been cloned using the pGL3 basic vector from Promega. The pSCT1 vector (Dr. S. Rusconi) has been used as backbone for protein expression vectors.

6.1.10 Plasmids

Plasmids used for Southern blot					
#	**Name**	**Vector**	**Resistance**	**How to release probe**	
177	*mCry1*	pSP72	ampicillin	release with HindIII	
178	*mCry2*	pCRII-TOPO	ampicillin	release with EcoRI	
162	*mPer1*	pBSK+	ampicillin	release with SpeI	
161	*mPer2*	pBSK+	ampicillin	release with SalI	
Plasmids used for transfection					
#	**Name**	**Vector**	**Resistance**	**Purpose**	
444	*mBmal1*	pGL2	kanamycin	promoter-luciferase construct	
370	*mDexras1*	pGL3 basic	ampicillin	promoter-luciferase construct	
226	*pCMV-LacZ*	pSCT1	ampicillin	β-galactosidase expression plasmid	
332	*mRev-Erbα*	pSCT1	ampicillin	full-length expression plasmid	
335	*mRorα4*	pSCT1	ampicillin	full-length expression plasmid	
Plasmids used for *in situ* hybridization					
#	**Name**	**Vector**	**Resistance**	**How to get AS or S probe**	
157	*mAvp*	pBSK	ampicillin	T7 AS EcoRV	T3 S HindIII
153	*mBmal1*	pCR-Script SK	ampicillin	T7 AS NotI	T3 S EcoRI
418	*mCatalase*	pCRII-TOPO	ampicillin	T7 AS BamHI	Sp6 S XhoI
419	*mCatalase*	pCRII-TOPO	ampicillin	Sp6 AS XhoI	T7 S BamHI
105	*mcFos*	pB SK-	ampicillin	T3 AS EcoRI	T7 S SacI
101	*mClock*	pCR-Script SK	ampicillin	T7 AS XhoI	T3 S NotI
156	*mCry1*	pCRII-TOPO	ampicillin	T7 AS SpeI	Sp6 S EcoRV
196	*mCry2*	pCRII-TOPO	ampicillin	T7 AS SpeI	Sp6 S Eco RV
284	*mDec1*	pCRII-TOPO	ampicillin	T7 AS BamHI	Sp6 S XhoI
354	*mDexras1*	pCRII-TOPO	ampicillin	Sp6 AS XhoI	T7 S BamHI
355	*mDexras1*	pCRII-TOPO	ampicillin	T7 AS BamHI	Sp6 S XhoI
278	*mFxr2*	pCRII-TOPO	ampicillin	Sp6 AS EcoRV	T7 S SpeI
361	*mMkp1* (*dusp1*)	pCRII-TOPO	ampicillin	T7 AS BamHI	Sp6 S XhoI
98	*mPer1*	pB SK-	ampicillin	T3 AS XhoI	T7 S BamHI
104	*mPer2*	pCR-Script SK	ampicillin	T3 AS EcoRI	T7 S NotI
390	*mPrkca*	RII-TOPO	ampicillin	Sp6 AS XhoI	T7 S BamHI

6.1.11 Mouse strains

Clock gene mutant mice: The mutant and wild-type mice used were derived from intercrosses between heterozygous animals. The *mPer1*^{Brdm1} mutants were generated using embryonic stem cell technology replacing a 4.3 kb long genomic region in the mPer1 gene (encompassing 15 of the 23 exons) by an Hprt (hypoxanthine phosphoribosyltransferase) minigene (Zheng *et al.*, 2001; fig. 6.1-1A). The *mPer2* ^{Brdm1} mutant mice have been generated using a deletion mutation that removes a major part of the PAS domain of the mPer2^{Brdm1} gene (Zheng *et al.*, 1999; fig. 6.1-1B). The *mPer1*^{Brdm1}*/mPer2*^{Brdm1} double mutant mice have been generated by intercrossing *mPer1*^{Brdm1} and *mPer2*^{Brdm1} single mutant animals (Zheng *et al.*, 2001). Similarly, *mPer1*^{Brdm1}*/mCry1* and *mPer1*^{Brdm1}*/mRev-Erbα* double mutant mice have been derived from *mPer1*^{Brdm1} and *mCry1* (van der Horst *et al.*, 1999; fig. 6.1-1C) single

mutants and *mPer1*^{Brdm1} and *mRev-Erbα* (Preitner *et al.*, 2002; fig. 6.1-1D) single mutants respectively.

Fragile X mutant mice: The different fragile X mutants (*Fmr1*$^{-/-}$, *Fxr2*$^{-/-}$, *Fmr1*$^{-/-}$*Fxr2*$^{-/-}$) and corresponding wild-type mice were bred and housed in the Baylor College of Medicine in Houston. All of them were bred on a C57BL/6 background (Spencer *et al.*, 2006; Peier *et al.*, 2000; Bontekoe *et al.*, 2002; Zhang *et al.*, 2008).

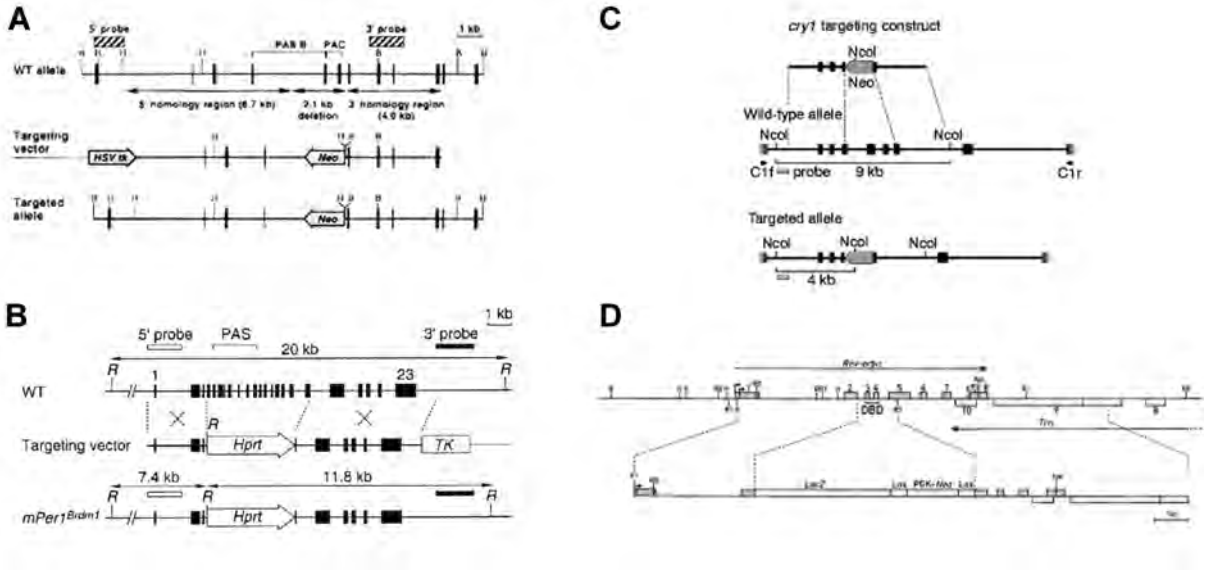

Fig. 6.1-1: Targeted disruption of the *Per1*, *Per2*, *Cry1* and *Rev-Erbα* genes.
A Genomic structure of the murine *mPer1* gene, the targeting vector, and the predicted structure of the targeted allele. Exons are indicated by vertical black bars with the first and last exons numbered. WT, wild-type; R, *Eco*RI; *Hprt*, hypoxanthine phosphoribosyltransferase gene; TK, *Herpes Simplex* Virus thymidine kinase gene (Zheng *et al*., 2001). **B** Genomic structure of a portion of the mouse *mPer2* gene, the targeting vector and the predicted structure of the targeted allele. H, *Hin*dIII; B, *Bam*HI; Neo, neomycin resistance gene; *HSV* tk, *Herpes simplex* virus thymidine kinase gene (Zheng *et al*., 1999). **C** Physical map of the wild-type *mCry1* locus, the targeting construct and the disrupted *mCry1* locus. Exons are indicated by black filled boxes. Note that the use of PCR-derived genomic DNA does not allow proper exon numbering. The probe used for screening homologous recombinants and genotyping mice, localized external to the construct, is represented by a grey box. Primers used for RNA analysis by RT-long-range PCR are depicted as black arrowheads (van der Horst *et al*., 1999). **D** Strategy used to delete the DNA binding domain (DBD) of the *Rev-erbα* allele. The cartoon displays a map of the eight *Rev-erbα* exons on the top strand and the 3′ terminal *Trα* (thyroid hormone receptor α) exons on the bottom strand. These two genes are oriented in opposite directions on chromosome 11 and are partially overlapping. The positions of the recognition sites for the following restriction endonucleases are given: BamH1 (B), KpnI (K), HindIII (H), EcoR1 (R1), EcoR5 (R5), and XhoI (X). Atg and tga indicate the positions of the initiation and termination codons, respectively. The structure of the targeting vector, in which part of exon 2, intron 2, exon 3, intron 3, exon 4, intron 4, and part of exon 5 have been replaced by a *LacZ* and a PGK-*neo* gene, is given below the *Rev-erbα/Trα* locus (Preitner *et al*., 2002).

6.1.12 Computer programs

Program	Use
Adobe Acrobat Reader	Reading of PDF files
Adobe Photoshop CS3	Figures
AxioVision 3.1	Picture taking on the Zeiss microscope
BeaconDesigner 2.1	Primer and probe design for quantitative real-time PCR
DNA Strider 1.4f8	DNA and protein sequence analysis
EndNote	Manage references
GraphPad Prism 4.0a	Statistical analysis
iCycler iQ™ Software 2002	qRT-PCR
Internet Explorer, Safari	Access the *World Wide Web*
KC4TM v.3.4. BIO-TEK software	Multidetection microplate reader (BIO-TEK)
Matlab/Clocklab	Wheel running analysis
Microsoft Excel 2004	Work sheets
Microsoft PowerPoint 2004	Figures / Presentations
Microsoft Word 2004	Text processing
Molecular Analyst	Densitometric analysis (GS-700)
Quantitiy One 1-D	Densitometric analysis (GS-800)
WinGlow	Luminometer (EG & G Berthold)

6.1.13 Consumer material

All disposable plastic ware was manufactured from Eppendorf, Nunc, Millian, Falcon, Corning Incorporated, Axygen, BD Plastipak™, TPP, Costar and Treff AG.

Product	Manufacturer	Cat. Number
Absolute QPCR Seal	Axon Lab	AB-1170
Amersham Hyperfilm™ MP	GE Healthcare	28-9068-46
Blotting Premium extra white (210 g/m^2)	sihl+eika	4500088517
Cleanroom suit	VWR	113-0165
Cytobrush plus GT	Medscand Medical	C0105
Filter unit 0.2 µm	Whatman	10 462 205
Genescreen plus® transfer membrane	Perkin Elmer	NEF988001PK
Glass slides (Histobond, Marienfeld)	Medite	85-0951-00
Glass coverslips (24 x 55 mm)	Medite	46-7155-00
Glass coverslips (24 x 60 mm)	Medite (Menzel-Glaser)	85-0191-00
Hybond™-ECL™ Nitrocellulose membrane	Amersham Biosciences	RPN303D
Mask	VWR	114-3438
Microvette® 100 Z	Sarstedt	20.1280
Mouse complete feed	Provimi Kliba AG	3432
Nestlests	Ebeco	3097055
PCR strip caps	Axygen	PCR-02CP-A
PCR strip tubes	Axygen	PCR-0208-A
Scintillation glass vials	Fisher Scientific (Wheaton)	0120 916
Shoe covers “Easy”	Milian	27-298
Stoppers with flanges (for glass test tubes)	Milian	AIL-123-07
Test tube (10x75 mm, Duran, glass)	GMB Glasmechanik	83613-103
96 well PCR plates	Axon Lab	AB-0900
96 MicroWell plates (white, polysorp)	Nunc	436111

6.1.14 Appliances

Appliance	Manufacturer	Model
Amersham Hypercassette™ (8 x 10 in)	GE Healthcare	RPN 11649
Balances	Mettler Toledo (SUI)	PBI501-S
	Mettler Toledo (SUI)	AB54-S
Centrifuges for Eppendorf tubes	Heraeus	Biofuge *pico*
	Hettich (GER)	MIKRO 20
Centrifuges for Falcon tubes	Hermle	Z383K
	Du Pont (Sorvall)	Econo Spin
Container for liquid nitrogen	CRYO Diffusion (FRA)	CT120R
Densitometer	Bio-Rad	GS-700 & GS-800
DNA Thermal Cyclers	Perkin Elmer (USA)	Cetus
	Biometra (GER)	TGradient
Enhancer screen	Amersham	
Freezer for –20°C	Liebherr	comfort
Freezer for –80°C	Froilabo (FRA)	CV 390 –85°C
Heating block	Eppendorf (GER)	Thermomixer compact
Heating plate with magnetic stirrer	Heidolph	MR-30001K
Homogenizer	Heidolph	RZR 2102 control
Homogenizer for test tubes	IKA®-Werke, GmbH & Co	Ultra-Turrax T8
Hood	SKAN AG	Telstar BIO-II-A
Horizontal Gel Electrophoresis system	GibcoBRL (Invitrogen)	Sunrise™, 21069
Hybridization ovens	SHEL LAB (USA)	1012
	SHEL LAB (USA)	1004
iCycler iQ™	BioRad	
Incubator for cells	Heraeus Instruments	BB 5060
Incubator with shaker for bacteria	HT Infors AG (SUI)	AT 258
Intensifying screen	Amersham	
Liquid scintillation analyzer	Packard	Tri carb 2200CA
Microplate Reader	Bio-Rad	3550
Microplate Luminometer	EG & G Berthold	LB 96V
Microscopes	Nikkon (JAP)	TMS-F
	Zeiss	Axioplan 2 imaging
Microwave	AEG	Micromat 21Mini Gel
Migration Trough	COSMO BIO CO., LTD.	Mupid-21
Multi detection microplate reader	BIO-TEK	Synergy HT
Night vision goggles	Rigel (USA)	3200
	Night Optics USA	D-2MV
pH-Meter	Knick	766 Calimatic
Pipettes (10, 20, 200 and 1000 µl)	Gilson	Pipetman Ultra
Pipetting assistance	IBS	Pipetboy acu
	Hirschmann Laborgeräte (GER)	Pipetus®-akku
Potter	THOMAS® (USA)	BB 935
Refrigerator	Liebherr	profi line
Rocking platform	Biometra (GER)	WT 16
IR-thermometer noncontact	TFA Dostmann	ScanTemp 440
Scintillation counter	Canberra Packard	
Spectrophotometer	WPA	lightwave II
Staining station	Miles	Tissue-Tek II
StrataCooler Cryo Preservation Module	Stratagene	400005
Ultracentrifuge	Sorvall	RC-5B & RC-5C
Ultrasonic homogenizer	BioLogics, Inc.	300 V/T
UV-lamp	Vilber Lourmat	TFX-20LM
Vortex	IKA® Works, Inc. (USA)	MS1 Minishaker

Water baths (for 65°C)	SHEL LAB (USA)	
(for 37°C)	GFL	
(for 42°C)	University of Fribourg (SUI)	
Western comb, spineless, 15 wells	Hoefer Scientific Instruments	SE 211A-15-1.5
Western comb, spineless, 10 wells	Hoefer Scientific Instruments	SE 211A-10-1.5
Western electrophoresis apparatus	Hoefer Scientific Instruments	SE 250 Mighty Small II
Western 4-gel caster (10 x 8 cm)	Hoefer Scientific Instruments	SE 275
Western notched alumina plate (10x8)	Hoefer Scientific Instruments	SE202N-10
Western rectangular glass plates (10x8)	Hoefer Scientific Instruments	SE202P-10
Western red clamps with springs	Hoefer Scientific Instruments	SE 252
Western spacers	Hoefer Scientific Instruments	SE2119T-.1.5
Western space saver plate	Hoefer Scientific Instruments	SE 217
Western wet transfer tank	BioRad	Mini Trans-Blot® Cell
Wheel running cages	Techniplast	1155M

6.2 Methods

6.2.1 Animals

6.2.1.1 Animal guidelines

All animal work is performed in accordance with the guidelines of the Schweizer Tierschutzgesetz (TSchG, SR455, Abschnitt 2: Art. 5 + 7, Abschnitt 5: Art. 11 and Abschnitt 6: Art.12-19).

6.2.1.2 Mouse breeding

Mice are kept under a 12 hours light and 12 hours dark cycle (12:12 h LD) with food and water *ad libitum* in cages covered with a filter top (Type 2 Polycarbonate Cage with top wiring, Tecniplast, Italy), which are stockpiled in custom made racks. Matings are set up as pairs of males and females according to Robertson (fig. 6.2-1). Offspring is weaned three weeks after birth and separated for its gender. A maximum of five mice are housed per cage. Genotypes are determined by PCR (*mRev-Erbα*) or Southern blot hybridization using genomic DNA extracted from tail tips as described below (6.2.1.4).

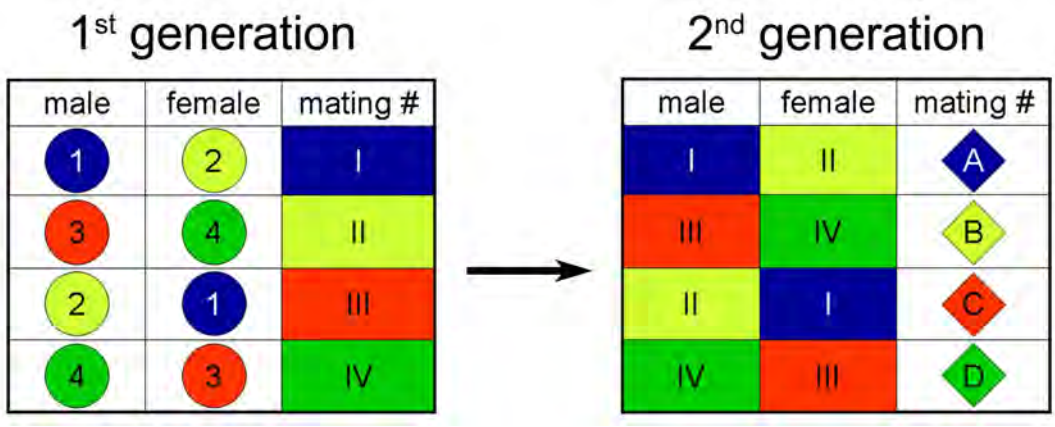

Fig. 6.2-1: Mating scheme according to Robertson
Using this mating setup reduces the probability that an observed phenotype is due to paternal imprinting because a male and a female of every line have been used.

6.2.1.3 Mouse activity recording

Jud C, Schmutz I, Hampp G, Oster H, Albrecht U (2005): A guideline for analyzing circadian wheel-running behavior in rodents under different lighting conditions. *Biological Procedures Online*, **7**:101-16

Biol. Proced. Online 2005; 7(1): 101-116.
doi:10.1251/bpo109
July 13, 2005

A guideline for analyzing circadian wheel-running behavior in rodents under different lighting conditions

Corinne Jud[1], Isabelle Schmutz[1], Gabriele Hampp[1], Henrik Oster[2] and Urs Albrecht[1]*

[1]Department of Medicine, Division of Biochemistry, University of Fribourg, 1700 Fribourg, Switzerland.

[2]Max-Planck-Institute for Experimental Endocrinology, 30625 Hannover, Germany.

*Corresponding Author: Urs Albrecht, Rue du Musée 5, 1700 Fribourg, Switzerland. Phone: +41 (0)26 300 86 36; Email: urs.albrecht@unifr.ch

Submitted: April 25, 2005; Revised: June 8, 2005; Accepted: June 20, 2005.

Indexing terms: Photoperiod, Chronobiology; Circadian Rhythm; Mice.

ABSTRACT

Most behavioral experiments within circadian research are based on the analysis of locomotor activity. This paper introduces scientists to chronobiology by explaining the basic terminology used within the field. Furthermore, it aims to assist in designing, carrying out, and evaluating wheel-running experiments with rodents, particularly mice. Since light is an easily applicable stimulus that provokes strong effects on clock phase, the paper focuses on the application of different lighting conditions.

INTRODUCTION

Life of almost all organisms is governed by various biological rhythms that are defined as physiological and behavioral oscillations. These rhythms are distinguished by their period length (τ) with circadian (*lat: circa diem*, around a day) rhythms displaying a τ of approximately 24 hours that evolved in adaptation to the daily rotation of the earth around its axis. They are found in many organisms from unicellular fungi and bacteria to higher organisms such as insects and mammals, including men. The bases of these oscillations are internal molecular clocks that maintain their rhythm even in the absence of external timing signals.

The circadian clockwork has evolved to improve an organism's adaptation to its environment and to ensure timed coordination of life-sustaining activities such as feeding, sleeping as well as the coordination of physiological and biochemical mechanisms.

With the availability of manipulative *in vivo* techniques and with the rise of forward and reverse genetic approaches in the field of chronobiology it became increasingly interesting to investigate circadian behavioral phenotypes of wild type and mutant animals under different conditions. Since light is the most potent timing signal of the circadian system – and lighting conditions are relatively easy to control – this paper aims to provide a general guidance for testing and evaluating circadian wheel-running behavior under different lighting conditions.

DEFINITIONS

Actogram

Circadian locomotor activity rhythms are frequently represented as a graph called *actogram* (Fig. 1A), where each horizontal line represents one day. Black vertical bars plotted side-by-side represent the activity, or number of wheel revolutions. The height of each vertical bar indicates the accumulated number of wheel

revolutions for a given interval (e.g. 5 min). Aligning the same actogram twice so that two consecutive days are plotted one after the other and the second day being re-plotted in the right half of the successive line results in a so-called *double plotted* actogram (Fig. 1B). This way of representation often facilitates the identification of existing rhythms. Once the presence of a – not necessarily circadian – rhythm has been established, the chronobiologist divides the cycle into an activity (*alpha*) and a rest (*rho*) phase. Sometimes, scattered activity can be observed in the *rho*-phase because the animal interrupts its sleep for a short time. One advantage of recording wheel-running revolutions as compared to using light beam interruptions is the *activity noise* during the rest phase. Obviously, under normal light/dark conditions *alpha*- and *rho*-phases are at opposite times in regard to the 24 hours solar cycle in diurnal and nocturnal organisms (1).

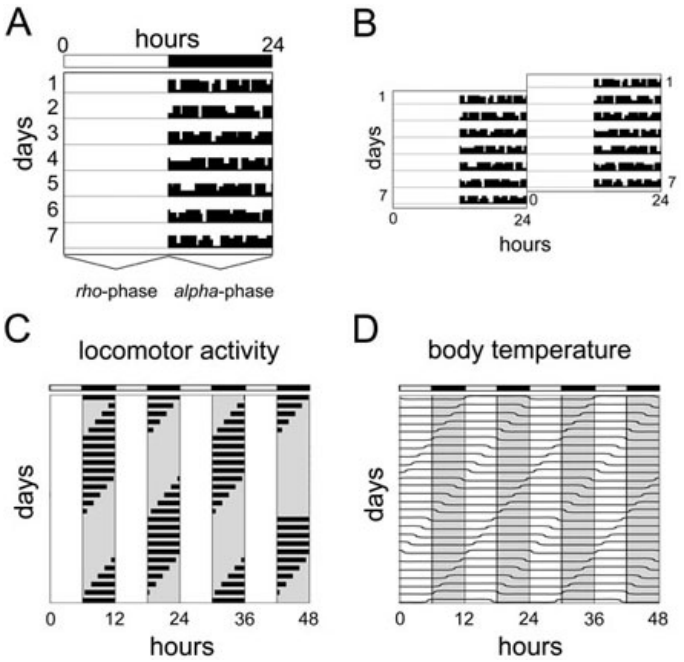

Fig. 1: Schematic single and double plotted actograms and masking. (A) Wheel-running activity is plotted as an actogram with each horizontal line corresponding to one day. Black vertical bars plotted side-by-side represent the activity, or number of wheel revolutions. The height of each vertical bar indicates the accumulated number of wheel revolutions for a given interval (e.g. 5 min). The *rho*- and *alpha*-phase marked at the bottom of the actogram refer to rest and activity, respectively. The white and black bar at the top of the scheme depicts light (12 h) and darkness (12 h), respectively. **(B)** To better visualize behavioral rhythms, actograms are often double plotted by aligning two consecutive days horizontally (e.g. day 1 left and day 2 right). **(C)** Schematic actogram of a nocturnal animal kept in very short photoperiods (LD 6:6). Since the animal is only showing activity during the dark phases it seems to entrain to the prevailing LD cycle. **(D)** Parallel monitoring of body temperature reveals that this apparent entrainment is only masking. Although the readout parameter "activity" seemingly adapts to the new schedule, body temperature continues to cycle with its free-running period length implicating that the circadian clock of the animal is not entrained. LD, light-dark cycle.

Entrainment and masking

Many environmental variables including light, temperature, humidity, food availability, and even social cues oscillate with a 24-hour period. Even though the endogenous circadian clock functions in the absence of external time cues, it periodically measures some of these environmental parameters to synchronize internal and external time under natural conditions to so-called *diurnal* rhythms. This mechanism of synchronization is called *entrainment* (2-6) and the environmental signal that can phase-set circadian clocks is called *Zeitgeber* (1, 5). All of the mentioned *Zeitgebers* may act as entraining agents although the daily 24 hour light-dark (LD) cycle is the most prominent one divided into a dark period or so-called *scotophase* and a light period or so-called *photophase*. Furthermore, organisms can only entrain to synchronizers cycling with a period close to 24 hours (7) (see T-cycles below). If the entraining period is too short or too long thereby exceeding the *range of entrainment* the circadian system cannot follow the *Zeitgeber* anymore and starts to *free-run* (see below). Since a strong Zeitgeber defines the rhythm of the clockwork, time is expressed as *Zeitgeber time* (ZT). Within a lighting schedule of 12 hours of light and 12 hours of darkness (LD 12:12), ZT0 is defined as "lights on," the beginning of the light phase, and ZT12 corresponds to "lights off," the end of the light phase.

The time difference [h] between the entraining external and the displayed internal rhythm, e.g. the onset of an animal's activity or the peak blood concentration of an endocrine factor, is called *phase angle difference* (Ψ). True entrainment is characterized by a stable phase angle difference between two synchronized rhythms. The value of this phase angle, however, may vary with the strength of the applied *Zeitgeber* stimulus (e.g. the light intensity or its wave length).

A certain rhythm may often only apparently be entrained to a *Zeitgeber* while the internal clock at the same time is not affected. This phenomenon is called *masking* (8). It can be observed when the *Zeitgeber* exerts - besides its influence on the clock - an additional dominant effect on the chosen readout parameter. One example is the suppressing influence of bright light on the activity of nocturnal rodents. In very short photoperiods (see below) mice seem to entrain to the dark phases, as shown

in the schematic drawing (Fig. 1C). The rest time during the light phases, however, is only a masking effect as revealed by parallel monitoring of the same animal's body temperature (Fig. 1D). Consequently, this masking problem can often be overcome by changing the readout parameter (e.g. here temperature).

Free-run

Organisms kept under constant conditions by shielding them from external time cues display so-called *free-running* or *circadian* rhythms that may persist indefinitely. The period length of these free-running rhythms is often no longer equal to 24 and differs from species to species. Therefore, time cannot be expressed in ZT but is expressed in *circadian time* (CT) units. One circadian cycle is divided into 24 equally sized circadian units (or *circadian hours*) with one unit being defined as the division of the internal period length (τ) by 24 hours. In nocturnal organisms and constant darkness conditions (DD), one circadian unit usually is less than 1 hour because the internal rhythm of these animals is typically shorter than 24 hours. Wild type mice (C57BL/6*Tyr*$^{c\text{-}Brd}$ × 129S7) for example have an internal period length of 23.7 ± 0.1 h (9) and thus 1 CT equals 59.25 min. CT0 designates the beginning of the subjective day (the rest phase in nocturnal rodents) and CT12 that of the subjective night (their activity phase). The same is true in diurnal animals only that they have their activity phase starting at CT0 and their rest phase at CT12, respectively. Since many experiments are carried out under constant conditions, CT calculations will be described later in the materials and methods section.

To monitor circadian rhythms some researchers use dim red light instead of complete darkness. The advantage of using dim red light is ease of animal handling. However, one should keep in mind that the range of wavelengths, to which the visual receptors of nocturnal animals respond, varies from species to species. Djungarian hamsters, for example, have a very high photosensitivity to red light (10). A recent publication suggests not using dim red light because it can increase the circadian period in mice compared to constant darkness (11). Therefore, it is recommended to use complete darkness protocols and to handle the animals using night vision goggles equipped with an infrared beam. However, in case one wants to use dim red light, it is better to constantly illuminate the chamber rather than switching on a red light while checking the animals.

Transients and aftereffects

During entrainment to a new external period or after release into constant conditions, transient cycles (12) can be observed before stable entrainment to the Zeitgeber or free-run occurs (blue bars in Fig. 2 panels A and B). Those transients reflect the disequilibrium or the altered phase angle between the overt rhythm and the Zeitgeber in response to a phase shift (1). A phase shift is a change in the phasing of the rhythm due to a distinct external stimulus (e.g. a light pulse). Transient cycles should be excluded from the determination of the displayed internal period or the phase-angle difference.

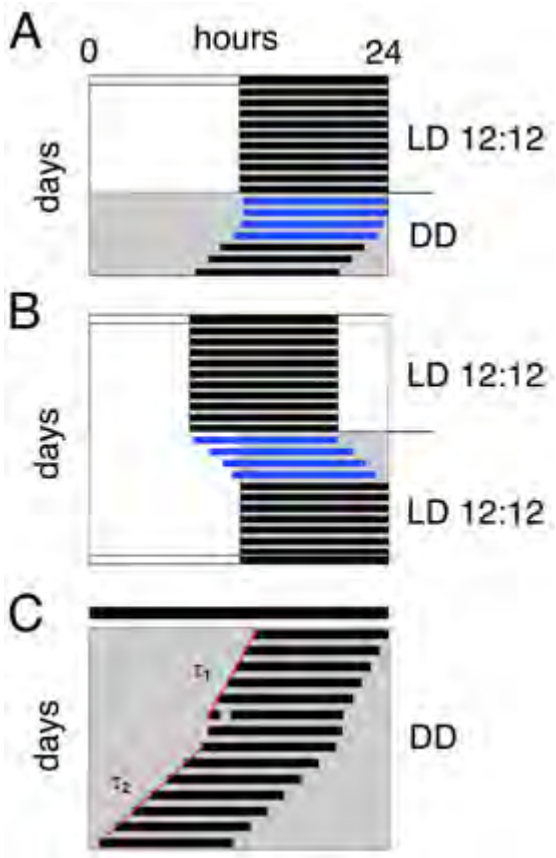

Fig. 2: Transients and Aftereffects. Transients (blue bars) can be caused by various treatments, such as the release of the animal into constant conditions (**A**) or a shift in the lighting regime (**B**). These transients usually persist for several days depending on the strength of the provoking signal. The white and black bar at the top of the scheme depicts light (12 h) and darkness (12 h), respectively. **(C)** An animal kept in constant darkness (DD) displays a stable free-running rhythm with a period length τ_1 before it is subjected to a light pulse. This pulse leads to a phase shift and often provokes τ_2, which is different from τ_1, as an aftereffect. If the animal is left in DD long enough after this treatment, it will again display its old period length τ_1. The red regression lines are drawn through the onsets before and after the light pulse to determine τ_1 and τ_2, respectively. The black bar at the top of the scheme represents constant darkness (24 h) conditions. DD, constant darkness; LD, light-dark cycle.

Even though the rhythm of a free-run can be remarkably precise, a certain plasticity of individual period length is a result of prior entrainment conditions. These so called *aftereffects* (12) can persist for several weeks and are also observed frequently after phase shifting stimuli (see below). Figure 2C shows the two different period lengths that can be observed before (τ_1) and after (τ_2) the stimulus.

T-cycles

To determine the stability range of entrainment, light cycles of different periods can be applied (4). Those *T-cycles* (with L + D = T) have periods deviating from the natural 24-hour period. For example, 22 hour or 26 hour T-cycles (LD 11:11 and LD 13:13, respectively), may be used to define the limits of stable entrainment. This limit differs from species to species and is depending on the nature of the applied *Zeitgeber*. In order to entrain to a 22 hour T-cycle (Fig. 3A), the organism has to constantly accelerate its internal rhythm whereas it decelerates its internal clock in response to a 26 hour T-cycle (Fig. 3E). This adaptation is only feasible within a close range. The mammalian circadian system has a plasticity of approximately 2 hours around its internal τ. Outside this critical range, entrainment is not possible anymore and the clock will start to free-run as indicated in Fig. 3A and E where the white and gray areas represent light and darkness, respectively. As long as the mice entrain to the T-cycle, they synchronize their activity onsets with lights-off (Fig. 3B and D). The phase-angle difference between lights-off and activity onset may increase with increasing deviation of T from the internal τ but will remain stable under given conditions as long as the animal still entrains.

Photoperiods and dim light ramps

Seasonal variations influencing circadian behavior can be simulated by applying different experimental *photoperiods*. A photoperiod is described by the ratio of light to darkness during a 24-hour cycle. Under laboratory conditions, summertime light conditions are typically represented by cycles of 18 hours light and 6 hours dark or of 14 hours light and 10 hours dark (LD 18:6 and LD 14:10, respectively), whereas winter light conditions are mimicked by an LD 6:18 cycle or an LD 10:14 cycle. In photoperiod experiments the external time of the Zeitgeber rhythm is specified as ExT (External Time) with ExT12 corresponding to the middle of the light-phase (Fig. 4) (13, 14).

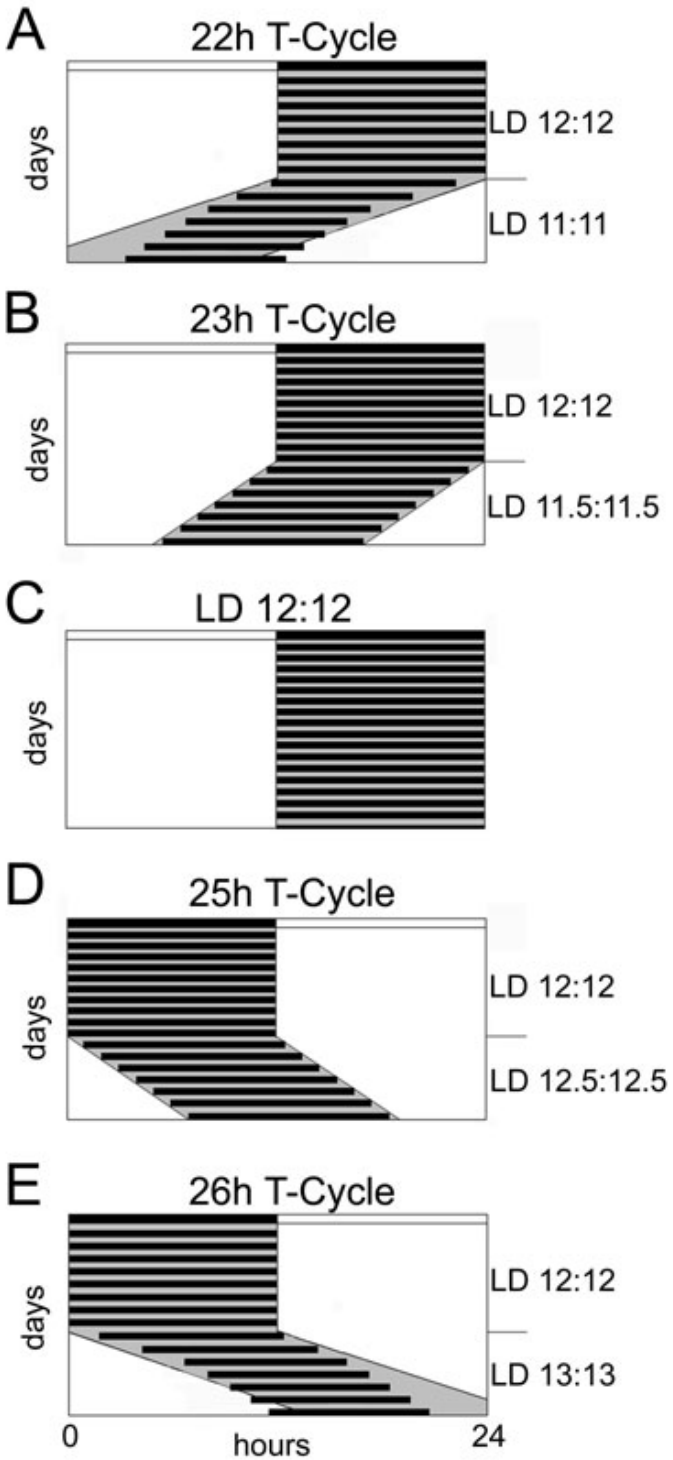

Fig. 3: T-cycles. T-cycles are LD cycles with a period length other than 24 hours (T = L + D). Mice are able to entrain to T-cycles of 23 (B) and 25 (D) hours but not to T-cycles of 22 (A) and of 26 (E) hours. Panel C represents a normal 24 hours LD 12:12 cycle. All schemes are plotted on 24 hours scale where the white area represents lights on and the gray area lights off, respectively. The white and black bar at the top of the scheme depicts light and darkness of the LD 12:12 cycle the animals were entrained to in the beginning of each panel. Each species has a distinct range of entrainment; the schemes here represent the range for mice. The black horizontal bars display the active time of the animals. LD, light–dark cycle; T, period or cycle time of a Zeitgeber; h, hours.

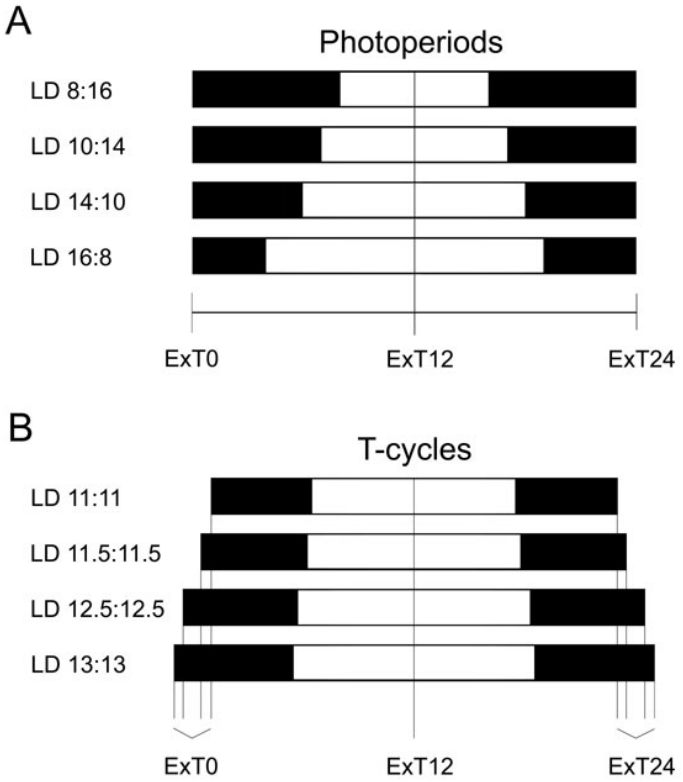

Fig. 4: Schematic representation of external time (ExT) in photoperiods and T-cycles. External time (ExT) subdivides any light-dark cycle into 24 units using the following formula: *number of hours*24/T* elapsed since the middle of the dark period. ExT0 (= ExT24) is determined as the middle of the dark period. ExT12 corresponds to the middle of the light phase. Vertical black lines indicate the corresponding external time. Black bars represent the dark period whereas the white bars correspond to lights on. **(A)** Schematic representation of ExT for photoperiods. **(B)** Schematic representation of ExT for T-cycles. ExT, external time; LD, light–dark cycle; T, period or cycle time of a Zeitgeber; h, hours.

Most laboratories use a rapid transition from light to dark and from dark to light and apply the same wavelength range and light intensity during the whole light period. However, this does not truly reflect natural lighting conditions. To more faithfully mimic the different sunlight conditions in a circadian context, one can use *dim light* ramps simulating dusk and dawn for light-dark transitions. Dim light conditions may allow a better understanding of daily events taking place in an organism in response to light. This procedure is still not commonly used – mainly due to technical and historical reasons. Moreover, the question of how much influence the dim light has on the establishment of circadian rhythmicity still remains to be answered.

Phase shift

A *phase shift* (ϕ) is defined as the resetting of the organism's internal rhythm in response to an external stimulus such as nocturnal light exposure (3). Such a phase shift can either result in a *phase advance* or a *phase delay*, where the former is the exact opposite of the latter. To specify, this means that a phase advance shifts the activity onset to an earlier position in the circadian cycle, whereas a phase delay shifts it to a later time. As an example, a shift of the activity phase by 2 circadian hours from CT12 to CT10 represents a 2 circadian hour phase advance. To analyze this resetting ability, animals displaying a stable free-running rhythm are kept in constant darkness and a light pulse is administered at a specific CT (Fig. 5A and B). Animals having an unstable free-running rhythm, receive the light at a certain ZT before they are released into DD (Fig. 5C). An overview of the daily variations in an animal's ability to shift its rhythm in response to a certain stimulus is given by the phase response curve (PRC) whose shape varies depending on species and stimulus (15). Figure 5D shows a typical light PRC of a nocturnal rodent. It can be divided into three parts, a phase delaying zone (CT12 to CT18 in Fig. 5D), a phase advancing zone (CT18 to CT2), and a dead zone (CT2 to CT12), where the stimulus has no or little effect on the activity phase. In a light PRC, this dead zone normally corresponds to the subjective day.

Jet lag

Traveling across several time zones and shift work schedules disturb the circadian clock and lead to fatigue, insomnia, irritability, etc. All these symptoms taken together are referred to as *jet lag* and are provoked by the transients generated during the resetting of the internal pacemaker to re-synchronize with external time. Since jet lag is generated artificially by our fast-living society, this problem is predominantly observed in humans. However, it can be mimicked in rodents by an abrupt shift in the lighting schedule (Fig. 5E). Depending on the amplitude of the shift, the animal needs several days to re-adjust to the new light regimen. In mice (and in human) back-shifting normally is accomplished considerably faster than forward-shifting of a similar time span, but activity read-outs are often overlaid by the masking influence of the new light phase (Fig. 5E, lower part of the actogram). For example, wild type mice need around 4 days to adapt to a 4 hours phase delay and around 6 days to adapt to a 4 hours phase advance.

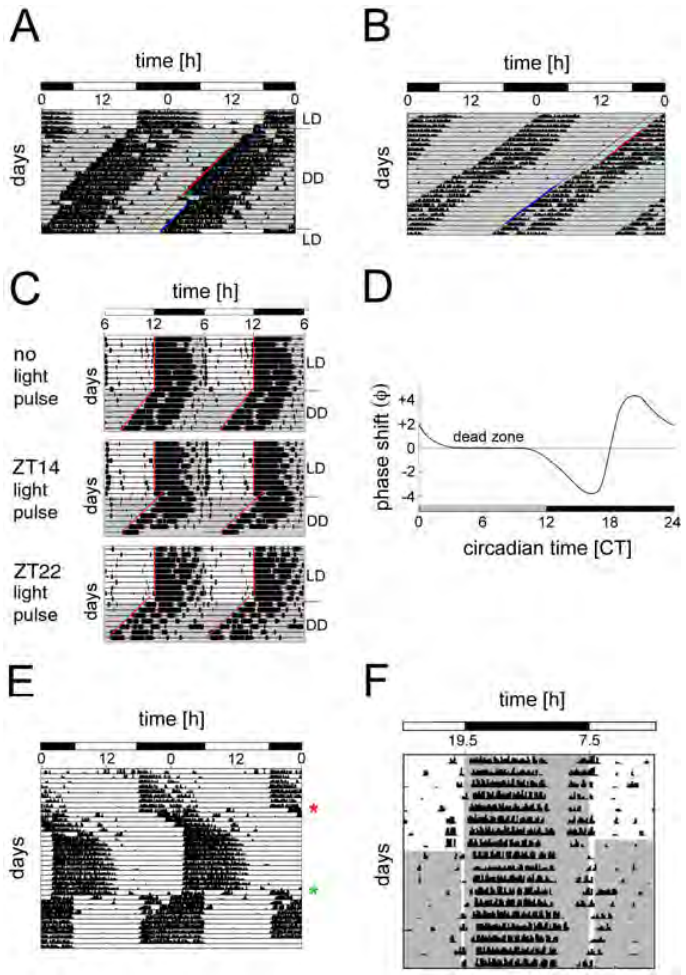

Fig. 5: Real actograms and phase response curve (PRC). (A) Plot of mouse locomotor activity before and after administering a light pulse (LP) at CT14 provoking a phase delay. The mouse was entrained to an LD 12:12 cycle before it was released into constant darkness (DD). The line above "DD" indicates the transition from LD to DD. When a stable free-running rhythm was established, a LP (green arrow) was administered at CT14 for 15 min. In order to quantify the phase shift, regression lines are drawn through 10 activity onsets before (red) and through 6 onsets after (blue) the LP. The horizontal distance between them corresponds to the phase shift triggered by the LP. **(B)** Plot of mouse locomotor activity before and after administering a LP at CT22 provoking a phase advance. The mouse was entrained to LD 12:12 (not shown) and then released into DD. As soon as a stable free-running rhythm was established, a LP (green arrow) was administered at CT22 for 15 min. In order to quantify the phase shift, regression lines are drawn through 6 activity onsets before (red) and through 7 onsets after (blue) the LP. The horizontal distance between them corresponds to the phase shift triggered by the LP. **(C)** Typical actograms of wild-type mice subjected to an Aschoff type II protocol. Mice were entrained to an LD 12:12 cycle (10 days) before releasing them into DD. The line above "DD" indicates the transition from LD to DD. The grey background represents darkness. Upon release into DD, no light pulse was administered to the mouse in the upper panel, whereas light pulses of 15 min were applied to the mouse at ZT14 (middle panel) and ZT 22 (lower panel). Regression lines (red) are drawn through the onsets of wheel-running activity in order to calculate the phase shift. Adapted from (26). **(D)** Typical light phase response curve (PRC) for nocturnal rodents. The grey and black bars below the PRC indicate subjective day and night, respectively. The X-axis shows the circadian time (CT) at which the light pulse was applied whereas the Y-axis displays the observed phase shift (ϕ) [h]. Light pulses administered between CT11 and CT18 provoke a phase delay (negative values). Light pulses between CT19 and CT3, on the other hand, generate phase advances (positive values). Between CT4 and CT10, no phase shift can be observed (dead zone). **(E)** Jet lag can be mimicked in the lab by subjecting entrained animals to a rapid shift in the lighting schedule. This actogram shows the locomotor behavior of a mouse that was first entrained to LD 12:12 with light from 6 am to 6 pm. After 10 days, the lighting schedule was still LD 12:12 but shifted to "lights on" at 2 pm and "lights off" at 2 am (red star). The mouse only entrains after around 7 days of transition to the new LD cycle. 17 days after the first shift, the lighting schedule was again shifted to the original schedule (LD 12:12 from 6 am to 6 pm; green star). **(F)** Panel F shows an actogram of a mouse subjected to a skeleton photoperiod. The mouse was first entrained to LD 12:12 with lights on from 7:30 am to 7:30 pm for 8 days. The grey background represents lights off, whereas the white area stands for lights on. After day 8, an asymmetrical skeleton photoperiod was applied with a shorter pulse in the evening (dusk) and a longer one in the morning (dawn). Due to the two light pulses, the mouse remains entrained and wheel-running activity does not differ tremendously compared to LD 12:12. Adapted from ref. 31. LD, light-dark cycle; h, hours; DD, constant darkness.

Skeleton photoperiods

In nature, nocturnal animals are only foraging during the night and hiding in their burrows during the day where they normally do not perceive any light. The standard LD cycles of the laboratory therefore do only weakly reflect natural conditions. To overcome this and mimic the periodic crepuscular light exposure *skeleton photoperiods* may be used (4).

Animals subjected to skeleton photoperiods are kept in constant darkness with two short light pulses per circadian cycle. In skeleton photoperiods, one distinguishes three parts: dawn (light), daytime (dark) and dusk (light). One pulse is applied at the beginning and one at the end of an otherwise complete photoperiod (e.g. one 15 min light pulse every 12 hours). The duration of the pulses is arbitrary (16). If the dawn- and the dusk-pulse have the same duration, the skeleton photoperiod is called symmetrical. In contrast, asymmetrical skeleton photoperiods are determined by pulses, where one is longer than the other. In general, the dawn pulse is longer than the dusk pulse (e.g. 3 hour dawn pulse and 30 min dusk pulse).

Skeleton photoperiods – like dim light – can also be used to overcome the masking effects of the LD cycle on the activity onset phase-angle and the alpha phase (Fig. 5F).

MATERIALS AND METHODS

Why wheel-running?

Monitoring wheel-running activity is only one of several possible ways to track circadian locomotor activity.

Compared to infrared beam or emitter-based measurements, wheel-running only registers voluntary movements. In contrast, the two other methods record all the movements including eating, drinking and grooming which increases noise levels. A mentionable advantage of the emitter-based measurement is that many modern systems allow you to easily record locomotor activity and certain physiological parameters such as body temperature or heart beat simultaneously.

Wheel-running facility

Circadian rhythms can be influenced by several environmental cues such as light, noise, vibrations, temperature, humidity, or pheromones. Due to this, it is important to perform any wheel-running experiment under defined environmental conditions. To achieve this, wheel-running experiments in our lab are carried out in an isolated, soundproof and air-conditioned room (17).

Isolation cabinets and cages

Animals are housed individually in plastic cages (280 mm long x 105 mm wide x 125 mm high, Tecniplast 1155M) equipped with a steel running wheel (115 mm in diameter, Trixie GmbH, Article No. 6083) (Fig. 6A). Diameter and type of the running wheel may influence the amount of wheel-running activity of mice (18, 19). The cages are provided with little bedding and one nestlet (5 x 5 cm; EBECO). One should take care not to use excessive amounts of bedding to avoid wheel blockage. Food and water are accessible *ad libitum*. Wheel revolutions are measured by a small magnet (Fehrenkemper Magnetsysteme, Article No. 34.601300702) embedded in a plastic disk that is fitted to the axis of the wheel (Fig. 6B). Upon rotation of the wheel, the magnet opens and closes a magnetic switch (Reed-Relais 60; Conrad Electronic AG, No. 503835-22), which is fixed outside the cage. Signals are registered on a computer using the ClockLab data aquisitition system (Actimetrics).

Maximally twelve of these wheel-running cages can be placed in a light-tight box. These isolation cabinets (Fig. 6 panels C and D) are ventilated and contain two fluorescent light bulbs (Mazdafluor Symphony AZURA 965, 18 W) mounted on the ceiling of the cabinet.

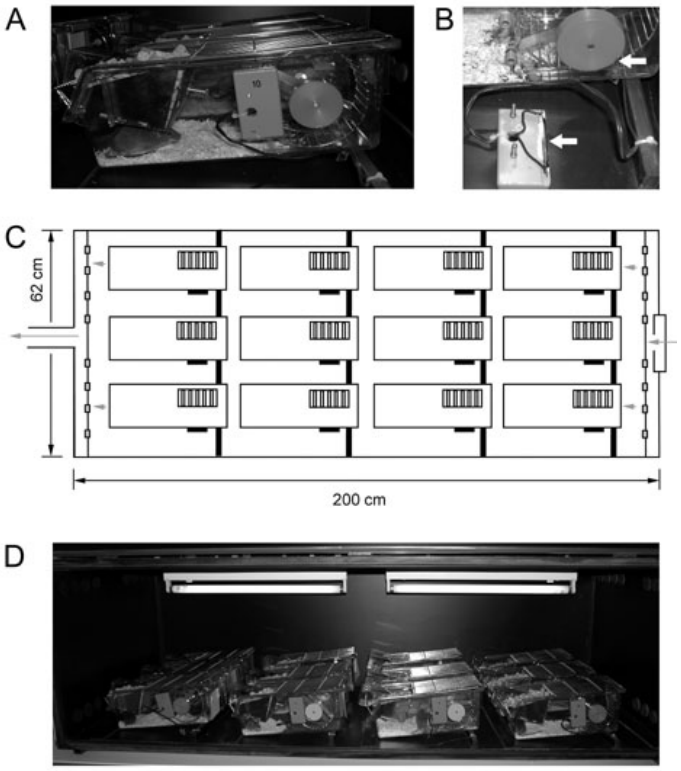

Fig. 6: Wheel-running cages and isolation cabinets. (A) Individually housed mouse in a wheel-running cage connected via a magnetic switch to the system recording wheel revolutions. On each rotation of the running wheel, the magnetic switch is once opened and closed. **(B)** Detailed view of the magnet (upper arrow) and the magnetic switch (lower arrow). **(C)** Schematic representation of a ventilated isolation cabinet (200 x 62 cm) offering space for 12 wheel-running cages. The arrows represent the airflow through the cabinet. **(D)** Picture of a fully occupied isolation cabinet with two light bulbs at the ceiling.

The lighting conditions can be adjusted *via* a timer without opening the box. In order to minimize reflection of light and guarantee comparable lighting conditions for each cage, the interior of the isolation chamber should be black and non-reflective. Although the isolation cabinets are well ventilated, the heat produced by the two light bulbs can't be eliminated completely by ventilation. Therefore there are diurnal temperature variations of 2-3.5°C (min. 23.5-24°C; max. 26-27°C) within the cabinets. However, light is a stronger and more immediate *Zeitgeber* compared to temperature and therefore the observed temperature variations under LD conditions can be neglected. Under constant lighting conditions temperature needs to be constant, because environmental temperature cycles can sustain peripheral circadian clocks (20). In our isolation cabinets this is the case and temperature remains constant after lights off (around 22.5°C).

Fluorescent light bulbs and lighting regimen

The choice of the correct fluorescent light bulb is a critical factor for wheel-running experiments. Usually, a light intensity of 300-400 lux at the level of the cage is chosen. Working with albino animals, one should keep in mind that they do not have any eye pigments. In this case, lower light intensities should be chosen in order not to damage their eyes.

Besides the mere intensity the color temperature of the bulb is also important. Color temperature is a measure of the visual "whiteness" of the light and its unit is degrees Kelvin (K). Light sources described as warm have a low color temperature and range from red to yellow. Cold ones on the other hand display a high color temperature and range towards the blue end of the spectrum. Natural daylight has a temperature between 6000 and 7000 K. The bulb described above has a luminous flux of 1000 lumen and a color temperature of 6500 K.

Entrainment to LD 12:12 and subsequent release into constant darkness

For standard wheel-running experiments mice should be between 2 and 6 months of age. Mice being younger than 2 months could freeze to death in the well ventilated cabinets while older mice often show low performance and other age related effects both of which can influence the analysis of running-wheel experiments (21, 22).

Additionally, it is normally preferable to use only male animals because in females the estrous cycle may influence general activity and wheel-running performance, which adds an additional rhythmic component that may complicate the evaluation.

Before any experiment can take place, it is essential that the mice are fully adapted to the isolation cabinets, to the cage and the wheel. For this, animals are entrained for 2 weeks to a standard LD cycle (e.g. LD 12:12 for mice, or LD 14:10 for hamsters) (Fig. 7A). After this time the experiments can be started.

In an entrained situation, the following parameters can be determined: Onset phase angle, onset variation, duration of the activity phase (α) and the rest phase (ϱ), the daily overall activity and the percentage of light phase activity. To determine τ, animals are transferred to constant darkness (DD) by switching off the lights in the isolation cabinets at ZT12 and not turning them on again the next day. In DD, animals begin to free-run with an internal period close to 24 hours. On the first 2-3 days, animals often display unstable period lengths. These transients should be excluded from the evaluation.

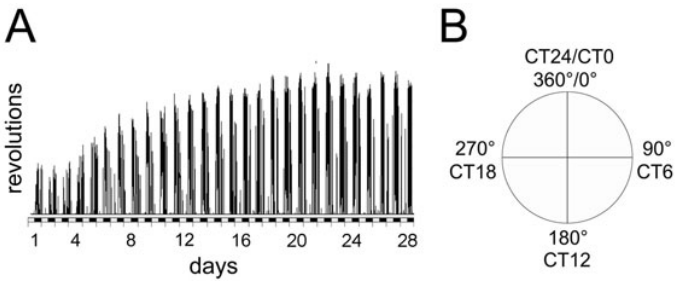

Fig. 7: Adaptation time and CT diagram. (A) Linear recording of wheel-running activity of a male wild type mouse (C57BL/6 x 129SV) under LD 12:12 conditions. Without prior wheel-running experience mice need two to three weeks to fully develop their wheel-running capacity. Only after this initial training (and entraining) phase experimental manipulations should be applied (X-axis: days of experiment; Y-axis wheel revolutions; black and white bars indicate dark and light phases, respectively; bin size for activity counts is 6 min). **(B)** Diagram comparing circadian time (CT) in degrees versus CT units.

Animals should be kept in constant darkness for at least 2 weeks. Once a stable free-running rhythm is established, one can determine the onset error, the length of the *alpha* and *rho* phases, the internal period length, and the overall activity (revolutions/day). The onset error is the average difference (in hours or minutes) of the true activity onsets compared to the theoretical onsets predicted by a least square fit regression line drawn through all onsets of the analyzed time span. *Alpha* and *rho* phase can be calculated after determination of onset and offset times. The batch analysis function of the ClockLab data analysis software (Actimetrics) allows the automatic determination of most of these values for a given set of animals.

Calculation of CTs

For many circadian experiments it is necessary to calculate the subjective phases (CT, or *circadian time*) of an animal's rhythm. A specific CT value is calculated upon the individual organism's free-running rhythm. For this, one needs to determine the internal period length (τ) and the onset of activity on the day prior to the day of the experiment (Day A).

It is important that the organism tested displays a stable rhythm during the time used to calculate the period

length. Activity onsets should be determined for at least 6 consecutive days and a least square fit should be used to calculate τ. The last onset before the day of the experiment is determined as CT12 (Day A). CT12 on the following day (Day B) is calculated as follows:

$$\text{CT12 } \textit{Day B} = \text{CT12 } \textit{Day A} + \tau - 24 \text{ hrs}$$

To calculate circadian hours (or *units*), one divides the internal period length by 24 (see definitions section):

$$1 \text{ circadian hour} = \tau / 24$$

To define a circadian time earlier than CT12 (CT0 to CT12), one has to subtract X times one circadian hour from the predicted CT12 $_{Day\ B}$.

$$\text{CTX}_{\text{earlier than CT12}} = \text{CT12}_{Day\ B} - X * 1 \text{ circadian hour}$$

For CTX values later than CT12 (CT13 to CT24), one has to add X times 1 circadian hour to CT12 $_{Day\ B}$.

$$\text{CTX}_{\text{later than CT12}} = \text{CT12}_{Day\ B} + X * 1 \text{ circadian hour}$$

Some scientists do not use circadian time but divide the subjective circadian day into 360 degrees. In this case 0° corresponds to CT0, 180°C to CT12 and 360° to CT24 (Fig. 7B).

Phase resetting by brief light pulses

Aschoff type I

Resetting experiments according to *Aschoff type I* protocol (23) are done with mice that display a stable free-running rhythm in constant darkness and do not lose circadian rhythmicity (24). To determine a full light phase response curve (PRC), pulses have to be applied subsequently at CTs throughout the circadian cycle. Because of the long dead zone of the rodent light PRC exposure times can normally be restricted to the subjective night. However, one or two time points during the subjective day should be considered to exclude unexpected light responsiveness during this time (for example in a transgenic mouse strain). To get a rough overview, light pulses are normally given only at cardinal wild-type PRC time points of the circadian cycle like CT10 (the end of the dead zone), CT14 (maximum phase delay), and CT22 (maximum phase advance).

In this setup the circadian time has to be determined individually for each mouse. When kept in the described 12 cage isolation chambers, individual animals have to be removed from the chamber in their cages and be placed under an illumination screen for the time of the light exposure.

It is crucial, that the mice are not unnecessarily disturbed by changing cages or by supplying food or water for at least four days before and after the light pulse. As a standard, pulse durations of 15 min are used. After a light pulse mice are returned to constant darkness for about ten days before the next light pulse can be administered.

For quantification of the phase shift, regression lines are drawn through six to ten activity onsets prior to the light pulse and a minimum of six onsets after the light pulse (Fig. 5A and B). The activity onsets of the two to three days following the stimulus are normally not included in the regression lines because the oscillator is still in transition. To determine the extent of the phase shift, the distance between the two lines is calculated on the first day after the light pulse. The period length of the free-running rhythm can change slightly after a light pulse (see aftereffects). In this case, the regression lines drawn through the onsets are not in parallel.

Phase advances are noted as positive values while phase delays result in negative phase shifts. The value of the phase shift depends on the species/strain and the experimental setup. For 129SvEvBrd/129 Ola mice one can expect phase delays of up to 90 min (CT14) and phase advances of up to 40 min (CT22) after 15 min light exposure (25). By pulsing all animals sitting in the same isolation cabinet at once, a PRC can be created (Fig. 5D). Retrospectively, the CT when the light pulse was administered is calculated for each animal. Doing so with many animals, one gets easily the phase shifts for each CT and thus can establish a PRC.

Aschoff type II

When working with animals that display unstable circadian rhythmicity in constant darkness, the

determination of circadian times may cause problems and testing phase shifts with an Aschoff type I protocol is not possible. In this case we suggest using the *Aschoff type II* protocol as follows (23, 26).

After 2 weeks of entrainment to LD 12:12 conditions, mice are released into a first period of constant darkness during 2-3 weeks. Thereafter, mice are re-entrained to a LD 12:12 cycle (15 days) before release into DD for at least ten days. In the first day of DD (with the nocturnal time points starting immediately after the last "lights off"), the light pulse is administered at the desired time points. Advantages of this protocol are that the light pulses can be administered simultaneously to all the mice without any disturbance like manipulating the cage (see Aschoff type I protocol).

For the determination of the phase shift in this protocol, regression lines are fitted through 6 consecutive activity onsets before (LD) and after the light pulse (DD). For the DD regressions the first day is disregarded because of possible transition effects. The phase shift is calculated as the difference between the two regression lines on the first day after the light pulse. Some species/strains show an apparent phase-shift after release into DD even without prior light administration. Therefore it is mandatory to monitor LD-DD transitions without light pulse and adjust the experimental data accordingly (Fig. 5C).

Jet lag

In the lab, delaying the LD cycle (simulating westward flights) or advancing it (simulating eastward flights) can simulate jet lag very easily. After 10 days in the same LD cycle (e.g. LD 12:12, lights on from 6 am to 6 pm) the LD cycle is delayed (e.g. by 8 hours; LD 12:12, lights on from 10 pm to 10 am) for 2 to 3 weeks. Since the animals cannot adjust their rhythm immediately to such a shift, some transients will be observed. After a stable entrainment is established, the LD cycle can again be advanced to the initial LD cycle (e.g. LD 12:12, lights on from 6 am to 6 pm), which simulates a transmeridian flight to the east. Sporadic jet lags have only minor impact on the general health state while regular jet lags have been shown to influence physiology, the immune system and may even promote cancer (27). Chronic jet lags can be observed in persons working predominantly at night, often changing their work shift, or frequently traveling by transmeridian flights.

To assess chronic jet lag in the laboratory, mice are entrained to LD 12:12 for around 10 days with lights on at 6 am and lights off at 6 pm (Fig. 5E). After full entrainment is accomplished, the animals are confronted to chronic jet lag by advancing the LD 12:12 cycle in series of 8 hours every 2 days for 10 days. This means that the first shift changes lights on from 6 am to 2 pm, the second from 2 pm to 10 pm, the third from 10 pm to 6 am, and so forth. After the 6^{th} shift, the animals are released into DD for 2 days before sacrificing them at the desired CTs (28). Alternatively, mice can also be subjected to alternating advance and delay shifts to study chronic jet lag. Such a protocol is a more realistic simulation, because usually one travels to another continent and back home.

Constant light conditions

A second type of free-run condition (as opposed to DD) is constant light (LL). In LL, behavior in response to different light intensities can be tested. After a standard training phase in LD, one normally starts with a period of DD before gradually increasing the light intensity. Standard paradigms use 14 to 20 days per lighting condition. It should, however, be ensured that the rhythm is stabilized in a particular condition before applying the next level of intensity. Like in DD, onset error, the length of the *alpha*- and *rho*-phases, the internal period length, and the overall activity (revolutions/day) can be determined for any given light intensity.

In wild type mice, the robustness of the activity rhythm is decreased with increasing light intensities. Besides the activity depressing effect of bright light exposure, the tonic light signaling to the SCN hampers the coupling of the single cell oscillators in this area and eventually renders the pacemaker output arrhythmic (29). In addition, constant light modulates the period length of

the circadian system with τ increasing roughly in proportion with the logarithm of the applied light intensity ("Aschoff's rule") (30).

APPENDIX

Does constant darkness have an impact on the health of mice?

To demonstrate that wheel-running in constant darkness is not harmful for mice, their state of health was daily monitored by gently checking them with night vision goggles (Rigel 3200) during their active phase as it is demanded and approved by the Swiss Federal Veterinay Office (FVO). Additionally, a small-scale study has been done by their request to further demonstrate this. For this, four females and four males with a mixed C75BL/6 x 129S5/SvEvBrd background together with four males carrying a 129SvEvBrd/129 Ola background were held in constant darkness in an isolation cabinet as described above. Body weight was determined every two to three days for three weeks with a balance (WEDO Digi 2000, 2000g/1g). Night vision goggles possessing an infrared beam were used for all manipulations because of the insensitivity of the rodent visual system to these longer wavelengths. Infrared light may act as a Zeitgeber in reptiles whereas it does not in rodents.

Our results show that constant darkness does not have any negative effects on the health of mice during wheel-running experiments. Both females and males (C75BL/6 x 129S5/SvEvBrd) did not lose any significant weight during monitoring. The same is true for males carrying a 129SvEvBrd/129 Ola background (Fig. 8A and B). A single male animal that lost weight within this group was overweight in the beginning of the experiment. It steadily lost weight during the first twelve days and stabilized it then on the same extent than his companions. Weighing mice is only one of many possible parameters to assess health status. In conclusion, this implicates that the exposure to constant darkness for a period of some weeks has no negative consequences on the health of mice.

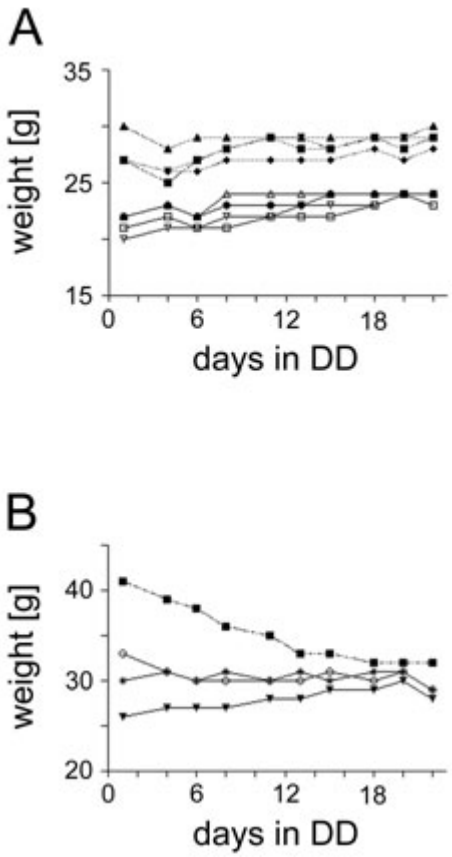

Fig. 8: Impact of constant darkness on weight and overall activity of wild-type mice. (A) Weight curves of 8 littermates (males: solid lines / females: hatched lines) with a mixed C75BL/6 x 129S5/SvEvBrd background. Mice were reared in a normal LD 12:12 cycle and then transferred to constant darkness (DD). They were housed individually in wheel-running cages where food and water were accessible *ad libitum*. During 22 days, they were weighed regularly using night vision goggles. The x-axis displays the days spent in constant darkness whereas the y-axis displays the weight [g]. **(B)** Weight curves of 4 male mice with a 129SvEvBrd/129Ola background. Only one mouse (■) that was overweight in the beginning looses weight during monitoring.

SUPPLEMENTAL INFORMATION

Web resources

1. http://circadiana.blogspot.com
2. www.actimetrics.com
3. www.amillar.org
4. www.circadianpubcrawler.org
5. www.cbt.virginia.edu
6. www.epbr-society.com
7. www.srbr.org

ACKNOWLEDGMENTS

We would like to thank April Bezdek and Gurudutt Pendyala for critically reading the manuscript. Financial

support from the Swiss National Science Foundation, the BrainTime project (EC 5th framework Grant QLRT-2001-01829) and the State of Fribourg is gratefully acknowledged.

REFERENCES

1. Dunlap JC, Loros JL, DeCoursey PJ. CHRONOBIOLOGY – biological timekeeping. *Sinauer Associates* 2004; 3(24):67-105.
2. Pittendrigh CS. On the mechanism of the entrainment of a circadian rhythm by light cycles. In: *Circadian clocks;* edited by: Aschoff J, Amsterdam: *Elsevier* (1965); 277-297.
3. Pittendrigh CS. Circadian systems: entrainment. In: *Handbook of behavioral neurobiology*, Vol. 4 Biological Rhythms, edited by Aschoff J, New York: *Plenum Press (*1981); 95-124.
4. Pittendrigh CS, Daan S. A functional analysis of circadian pacemakers in nocturnal rodents. IV. Entrainment: Pacemaker as clock. *J Comp Physiol A* 1976; 106:291-331.
5. Aschoff J, Daan S, Honma KI. Zeitgeber, entrainment, and masking: some unsettled questions. In: *Vertebrate Circadian System (Structure and Physiology)*, edited by Aschoff J, Daan S, Gross GA, Berlin: *Springer-Verlag* (1982); 13-24.
6. Takahashi JS, Turek FW, Moore RY. Circadian Clocks. *Handbook of Behavioral Neurobiology* 2001; 12:7-43.
7. Fuller CA, Fuller P. Circadian Rhythms. Encyclopedia of the human brain. (2002); 793-812.
8. Aschoff J. Exogenous and endogenous components in circadian rhythms. *Cold Spring Harbor Symp Quant Biol* 1960; 25:11-28.
9. Zheng B, Albrecht U, Kaasik K, Sage M, Lu W, Vaishnav S, Li Q, Sun ZS, Eichele G, Bradley A, Lee CC. Nonredundant roles of the *mPer1* and *mPer2* genes in the mammalian circadian clock. *Cell* 2001; 105(5):683-694.
10. Klante G, Steinlechner S. A short red light pulse during dark phase of LD-cycle perturbs the hamster's circadian clock. *J Comp Physiol* 1995; 177(6):775-780.
11. Hofstetter JR, Hofstetter AR, Hughes AM, Mayeda AR. Intermittent long-wavelength red light increases the period of daily locomotor activity in mice. *J Circadian Rhythms* 2005; 3(1):8.
12. Pittendrigh CS, Daan S. A functional analysis of circadian pacemakers in nocturnal rodents. I. The stability and liability of spontaneous frequency. *J Comp Physiol A* 1976; 106:223-252.
13. Daan S, Merrow M, Roenneberg T. External time – internal time. *J Biol Rhythms* 2002; 17(2):107-109.
14. Steinlechner S, Jacobmeier B, Scherbarth F, Dernbach H, Kruse F, Albrecht U. Robust circadian rhythmicity of Per1 and Per2 mutant mice in constant light, and dynamics of Per1 and Per2 gene expression under long and short photoperiods. *J Biol Rhythms* 2002; 17(3):202-209.
15. Daan S, Pittendrigh CS. A functional analysis of circadian pacemakers in nocturnal rodents. II. The variability of phase response curves. *J Comp Physiol A* 1976; 106:253-266.
16. Zivkovic B. Clock tutorial #6: To entrain or not to entrain, that is the question. (2005); http://circadiana.blogspot.com
17. Albrecht U, Foster RG. Placing ocular mutants into a functional context: a chronobiological approach. *Methods* 2002; 28:465-477.
18. Banjanin S, Mrosovsky N. Preferences of mice, Mus musculus, for different types of running wheel. *Lab Anim* 2000; 34(3):313-318.
19. Deboer T, Tobler I. Running wheel size influences circadian rhythm period and its phase shift in mice. *J Comp Phys* 2000; 186(10):969-973.
20. Brown SA, Zumbrunn G, Flwury-Olela F, Preitner N, Schibler U. Rhythms of mammalian body temperature can sustain peripheral circadian clocks. *Curr Biol* 2002; 12:1574-1583.
21. Ingram DK, London ED, Reynolds MA, Waller SB, Goodrick CL. Differential effects of age on motor performance in two mouse strains. *Neurobiol Aging* 1981; 2(3):221-227.
22. Valentinuzzi VS, Scarbrough K, Takahashi JS, Turek FW. Effects of aging on the circadian rhythm of wheel-running activity in C57BL/6 mice. *American Physiol Soc* 1997; R1957-R1964.
23. Aschoff J. Response curves in circadian periodicity. In: *Circadian Clocks*, edited by Aschoff J, North-Holland Amsterdam (1965); 95-111.
24. Albrecht U, Oster H. The circadian clock and behavior. *Behav Brain Res* 2001; 125(1-2):89-91.
25. Oster H, Baeriswyl S, Van Der Horst GT, Albrecht U. Loss of circadian rhythmicity in aging mPer1-/-

mCry2-/- mutant mice. *Genes Dev* 2003; 17(11):1366-1379.
26. Albrecht U, Zheng B, Larkin D, Sun ZS, Lee CC. mPer1 and mPer2 are essential for normal resetting of the circadian clock. *J Biol Rhythms* 2001; 16(2):100-104.
27. Knutsson A. Health disorders of shift workers. *Occup Med (London)* 2003, 53(2):103-108.
28. Filipski E, Delaunay F, King VM, Wu M, Claustrat B, Gréchez-Cassiau A, Guettier C, Hastings MH, Lévi F. Effects of chronic jet lag on tumor progression in mice. *Cancer Res* 2004; 64:7879-7885.
29. Ohta H, Yamazaki S, McMahon DG. Constant light desynchronizes mammalian clock neurons. *Nat Neurosci* 2005; 8(3):267-269.
30. Aschoff J. Changes of frequency of periods of activity of mice in constant light and lasting darkness. *Pflugers Arch* 1952; 255(3):197-203.
31. Kennaway DJ. Resetting the suprachiasmatic nucleus clock. *Front Biosci* 2004; 9:56-62.

PROTOCOLS

Equipment

- Wheel-running facility
- Isolation cabinets:
  - Light bulb: Mazdafluor, Symphony AZURA 965, 18 W
  - Light bulb mounting: Mazda, type: Mx204-118 (230V, 50Hz, 0.37A)
  - Fan: accessories by Monacor, Article No. 03.1670 (CF-1212, 12V=/500mA)
- Wheel-running cages:
  - Cage: Tecniplast 1155M (280 mm long x 105 mm wide x 125 mm high)
  - Stainless steel wire lid: Tecniplast 1155M115
  - Stainless running wheel: Trixie GmbH, Article No. 6083 (diameter 115 mm)
  - Magnet: Fehrenkemper Magnetsysteme, Article No. 34.601300702
  - Magnetic switch: Reed-Relais 60, Conrad Electronic AG, No. 503835-22
- Mouse housing:
  - Water bottles: Tecniplast ACBTO262 (260 ml, 55 x 128 mm, polycarbonate, with silicone ring)
  - Bottle caps: Tecniplast ACCP2521
  - Nestlets (5 x 5 cm): EBECO
  - Animal bedding: Schill AG Bedding type 3-4
  - Food (γ irradiated): Provimi Kliba, No. 3432
- Computer Hardware and software [4]:
  - Microsoft Windows PC (e.g. Dell, Intel Pentium III running Windows 2000 or better)
  - Data acquisition board: National Instruments AMUX 64-T (fitted with 10-kΩ resistors)
  - RJ45 socket
  - PCI 6503 card National Instruments
  - National Instruments NI-DAQ software
  - ClockLab software package, Actimetrics
  - All components listed above can be purchased in a ready to use package from Actimetrics

Methods

Abbreviations

LD	light dark cycle (usually LD 12:12 cycles)
DD	constant darkness
LL	constant light
ZT	Zeitgeber time (ZT0 corresponds to lights on)
CT	circadian time

Experimental set-up

- 6 mutant mice and 6 wild-type controls (2-6 months old)
- Mutant and wild-type mice need to have the same genetic background and should be of similar age (most suitable are littermates)

Table 1: Aschoff type I

Lighting condition	Duration	Measurements
LD 12:12	10-15 days	
DD	10-15 days	Period length of free-running rhythm (τ), onset error, length of activity period (*alpha*-period)
Light pulse at CT14	15 min	Phase shift
DD	10-15 days	
Light pulse at CT22	15 min	Phase shift
DD	10-15 days	
Light pulse at CT10	15 min	Phase shift
DD	10-15 days	
LD 12:12	10-15 days	Onset phase angle, onset error, rel. light phase activity, length of activity period

Table 2: Aschoff type II

Lighting condition	Duration	Measurements
LD 12:12	10-15 days	
DD	10-15 days	Period length, onset error, length of activity period
LD 12:12	10-15 days	Onset phase angle, onset error, rel. light phase activity, length of activity period
Light pulse at ZT14	15 min	Phase shift (compare to LD → DD without light pulse)
DD	10-15 days	
LD 12:12	10-15 days	Onset phase angle, onset error, rel. light phase activity, length of activity period → compare to previous LD 12:12
Light pulse at ZT22	15 min	Phase shift (compare to LD → DD without light pulse)
DD	10-15 days	

Table 3: Optional for Aschoff type I and Aschoff type II

Lighting condition	Duration	Measurements
LL (~5 lux)	10-15 days	Period length, onset error, length of activity period
LL (~50 lux)	10-15 days	Period length, onset error, length of activity period
LL (~500 lux)	10-15 days	Period length, onset error, length of activity period

Overall activity (revolutions/day) has to be monitored for every lighting condition. Above experiments should be done with at least 10 to 12 mice before performing statistical analysis.

Formulas for CT calculations

1CT = internal period length / 24

$CTX_{\text{earlier than CT12}} = CT12_{Day\ B} - X * 1CT$

$CTY_{\text{earlier than CT12}} = CTX + 24$

$CTX_{\text{later than CT12}} = CT12_{Day\ B} + X * 1CT$

$CTY_{\text{later than CT12}} = CTX - 24$

Relative time = absolute time / 60

Jet lag: An example of a typical experimental setup

Table 4 : Simulating a westward transmeridian flight

Lighting condition	Duration	Measurements
LD 12:12 (L 6 am to 6 pm)	10-15 days	Onset phase angle, onset error, rel. light phase activity, length of activity period
LD 12:12 (L 10 pm to 10 am)	2-3 weeks	Onset phase angle, onset error, rel. light phase activity, length of activity period, time in transience
LD 12:12 (L 6 am to 6 pm)	10-15 days	Onset phase angle, onset error, rel. light phase activity, length of activity period

Table 5 : Simulating an eastward transmeridian flight

Lighting condition	Duration	Measurements
LD 12:12 (L 6 am to 6 pm)	10-15 days	Onset phase angle, onset error, rel. light phase activity, length of activity period
LD 12:12 (L 10 pm to 10 am)	2-3 weeks	Onset phase angle, onset error, rel. light phase activity, length of activity period, time in transience
LD 12:12 (L 6 am to 6 pm)	10-15 days	Onset phase angle, onset error, rel. light phase activity, length of activity period

Table 6: Chronic jet lag: An example of a typical experimental setup (Ref: 28)

Lighting condition	Duration	Measurements
LD 12:12 (L 6 am to 6 pm)	10 days	Onset phase angle, onset error, rel. light phase activity, length of activity period
LD 12:12 (L 2 pm to 2 am)	2 days	
LD 12:12 (L 10 pm to 10 am)	2 days	
LD 12:12 (L 6 am to 6 pm)	2 days	
LD 12:12 (L 2 pm to 2 am)	2 days	
LD 12:12 (L 10 pm to 10 am)	2 days	
LD 12:12 (L 6 am to 6 pm)	2 days	
DD	2 days	

One should always keep in mind that jet lag can be caused by both shifting time backwards and forwards.

Definitions

Overall activity - Average activity bouts (revolutions/day) over the specified period (*alpha*- and *rho*-phase).

Period length - Length of displayed overt rhythm. In DD, it represents the endogenous internal rhythm (τ).

Onset error - Difference [h] between the onsets of activity and the constructed regression line. To achieve this, a least square fit regression line is plotted through the onsets of activity for the specified period.

Onset phase angle - Difference [h] between an external (entraining) and an internal period of an entrained organism e.g. anticipated or delayed activity onset.

Rel. light phase activity - Activity [%] during light phase (*rho*-phase in mice) relative to the overall activity.

Length of activity period - Duration [h] of the *alpha*-phase (often given as relative value compared to the period length).

6.2.1.4 Genotyping of mice

6.2.1.4.1 Solutions

- **Lysis buffer (pH 8.0):**

20 mM	Tris-HCl
5 mM	EDTA
400 mM	NaCl
1 % (w/v)	SDS

- **6 x Loading dye:**

80 %	Glycerol 100 %
20 %	0.5 M EDTA pH 8
2 mg	Bromophenol Blue
2 mg	Xylene Cyanole

- **1x TE (pH 8):**

10 mM	Tris-HCl
1 mM	EDTA

- **Proteinase K [20 mg/ml]:**

20 mg	Proteinase K
1 ml	ddH_2O

- **50 x TAE:**

242 g	Tris
57.1 ml	glacial acetic acid
100 ml	EDTA 0.5 M pH 8.0

  The volume is completed to 1000 ml with ddH_2O.

- **EtBr [10 mg/ml]:**
  1 g of EtBr is dissolved in 100 ml ddH_2O and stored in a reaction tube wrapped with aluminium foil and stored in a dark place.

- **20 x SSC (pH 7.0):**

175.3 g	NaCl
88.2 g	tri-Na-Citrate x 2 H_2O (AW: 294.1)
800 ml	dH_2O

  The pH is adjusted to 7.0 and the volume is completed to 1 l with dH_2O.

- **10 % SDS:**

100 g	SDS

  The powder is dissolved in a total of 1000 ml dH_2O under shaking at 37°C. The solution is stored at RT without autoclaving.

- **2x SSC, 0.1 % SDS:**

100 ml	20x SSC
10 ml	10 % SDS
890 ml	dH_2O

- **0.1x SSC, 0.1 % SDS:**

5 ml	20x SSC
10 ml	10 % SDS
985 ml	dH_2O

- **Herring sperm DNA:**
  10 mg/ml herring sperm DNA is dissolved o/n and under continuous shaking in ddH_2O. Then NaCl is added to yield a final concentration of 0.1 M. The mixture is extracted with the same volume of phenol:chloroform. The aqueous phase is portioned into 1 ml aliquots. The DNA is sheared by forcing it 12 times through a 0.5 mm needle before it is sonicated. The DNA is precipitated by adding double the amount of cold 100 % EtOH and pelleted by centrifugation at 4°C and 13000 rpm for 20 min.

6.2.1.4.2 Digestion of mouse tails

On the day of weaning, the tail tip of mice is cut using scissors and they receive an ear mark for later identification. The tail tip is put into a safe lock reaction tube and then digested under continuous rotation over-night (o/n) at 60°C in a mixture of 500 µl lysis buffer pH 8.0 and 20 µl proteinase K [20 mg/ml].

6.2.1.4.3 Extraction of genomic DNA

The next morning, the tube is centrifuged at RT and 13'000 rpm for 3 min to pellet the cell debris. The supernatant (around 450 µl) is transferred to a new tube with wide bore tips. Using these tips reduces shearing of the DNA. To precipitate DNA, 800 µl of 100 % EtOH is mixed with the supernatant. The white DNA thread is then transferred to a new tube containing 500 µl of 70 % EtOH to wash away salts. After discarding as much 70 % EtOH as possible, 500 µl of 100 % EtOH is added to remove the remaining water. Then the 100 % EtOH is taken out completely and the DNA is air dried at RT for 5 min, before it is dissolved in 50-100 µl 1x TE. If the DNA pellet can not be dissolved after a while, the tube can be left at RT o/n or it can be incubated on a shaker at 37°C for about 2 h.

6.2.1.4.4 Genotyping by polymerase chain reaction (PCR)

Since the PCR is a very sensitive method, small changes in the reaction mixture or in the PCR cycle protocol can lead to dramatic changes in PCR efficiency. This is why every gene to be analyzed needs a specific setup which is listed below. Once the PCR is finished, 10 µl of the product is analyzed on a 1.5 % agarose gel. To be able to determine the length of the fragments, 1.5 µl of 100 bp DNA ladder are loaded as well.

PCR-program:

	mCry1	***mPer1***	***mPer2***	***mRev-Erbα***
Step 1	2 min at 94°C	2 min at 94°C	2 min at 94°C	2 min at 94°C
Step 2: Denaturation	30 s at 94 °C	30 s at 94 °C	30 s at 94 °C	30 s at 94 °C
Step 3: Annealing	30 s at 62°C	30 s at 56°C	30 s at 56°C	30 s at 62°C
Step 4: Elongation	7 min at 68°C	1 min at 72°C	1 min at 72°C	1 min at 72°C
Step 5	7 min at 68°C	10 min at 72°C	10 min at 72°C	10 min at 72°C
Step 6	∞ at 20°C	∞ at 20°C	∞ at 20°C	∞ at 20°C
Repeat step 2 to 4	35 cycles	34 cycles	33 cycles	36 cycles

PCR-mix:

	mCry1	***mPer1***	***mPer2***	***mRev-Erbα***
DNA	0.3 µg	0.3 µg	0.3 µg	0.3 µg
10x Buffer	2.5 µl	5.0 µl	2.5 µl	2.5 µl
$(NH_4)_2SO_4$ [60 nM]	2.5 µl	10.0 µl	2.5 µl	2.5 µl
$MgCl_2$	1.5 µl	-	-	2.0 µl
5x Q-Solution	1.25 µl	2.0 µl	-	-
Primer 1	1.0 µl [25 mM]	5.0 µl [5 µM]	3.5 µl [5 µM]	2.5 µl [5 µM]
Primer 2	1.0 µl [25 mM]	5.0 µl [5 µM]	3.5 µl [5 µM]	2.5 µl [5 µM]
Primer 3	1.0 µl [25 mM]	5.0 µl [5 µM]	3.5 µl [5 µM]	2.5 µl [5 µM]
Taq-polymerase [5 U/µl]	0.25 µl	0.5 µl	0.25 µl	0.25 µl
dNTP [10 mM]	1.0 µl	1.0 µl	0.5 µl	0.5 µl
ddH_2O	x µl	x µl	x µl	x µl
Total	25 µl	50.0 µl	25 µl	25 µl

Primers:

mCry1 primer 1 (mCry1 new fwd): 5'-GCA TGA CCC CTC TGT CTG AT-3'
mCry1 primer 2 (mCry1 new KO rev): 5'-TGA ATG AAC TGC AGG ACG AG-3'
mCry1 primer 3 (mCry1 new WT rev2): 5'-AAC ACG CAG ATG CAG TCG-3'

mPer1 primer 1 (gPer1f): 5'-ACA AAC TCA CAG AGC CCA TCC-3'
mPer1 primer 2 (gPer1r2): 5'-ATA TTC CTG GTT AGC TGT AGG-3'
mPer1 primer 3 (PKG hprt rev): 5'-CGC ATG CTC CAG ACT GCC TTG-3'

mPer2 primer 1 (gP2f2): 5'-GCT GGT CCA GCT TCA TCA ACC-3'
mPer2 primer 2 (gP2r2): 5'-GAA CAC ATC CTC ATT CAA AGG-3'
mPer2 primer 3 (PKG hprt rev): 5'-CGC ATG CTC CAG ACT GCC TTG-3'

mRev-Erbα primer 1 (WT29rev): 5'-CAC CTT ACA CAG TAG CAC CAT GCC ATT CA-3'
mRev-Erbα primer 2 (LacZ29rev): 5'-AAA CCA GGC AAA GCG CCA TTC GCC ATT CA-3'
mRev-Erbα primer 3 (comm29rev): 5'-CCA GGA AGT CTA CAA GTG GCC ATG GAA GA-3'

6.2.1.4.5 Genotyping by Southern blot

The method is named after the British biologist Edwin Southern who invented it in 1975 (Southern, 1975). This method allows checking for the presence of a specific DNA sequence in a sample via combination of agarose gel electrophoresis for size separation and subsequent

transfer of the DNA to a filter membrane. A labelled probe is then incubated with the membrane and the signal is detected by autoradiography or other methods.

Electrophoresis and neutral transfer

Before the DNA can be loaded on a 0.8 % agarose gel, 10 µg of tail tip DNA have to be digested o/n at 37°C, in a total volume of 50 µl, with a restriction enzyme that is specific for each gene.

- *mCry1*: NcoI
- *mCry2* and *mPer1*: EcoRI
- *mPer2*: BamHI

The DNA fragments are then loaded onto the gel to separate them by size o/n at 20 V or at 65 V during 6 to 7 hours in an electrophoresis chamber (Sunrise™, GibcoBRL). Once the migration is finished, the gel is coloured for 10 min in EtBr (20 µl EtBr in 1000 ml 1x TAE) to check whether the DNA bands migrated well or not. If the gel is fine, it is rinsed in dH_2O and then incubated twice in 0.25 M HCl for 5 min. It is important to respect the incubation time because HCl depurinates DNA, breaking it into small pieces, which improves their transfer from the gel to the membrane later on. The gel is rinsed once more in dH_2O, before it is incubated for 30 min in a mixture of 0.4 M NaOH and 0.6 M NaCl. In a next step the gel is incubated for 30 min in 1.5 M NaCl and 0.5 M Tris-HCl pH 7.5. After washing the gel shortly in dH_2O it is ready for neutral transfer in a glass chamber containing 10x SSC.

A big sheet of plotting paper is wetted in 10x SSC and the Gene Screen Plus transfer membrane (Perkin Elmer) is incubated for 10-15 min in 10x SSC. The big blotting paper is put on a platform located inside the glass chamber with its sides dipping into 10x SSC. Then the gel is placed upside down on a big wet plotting paper and the humidified membrane is laid over it. Eventually, bubbles have to be removed gently by rolling them out, before some sheets of dry plotting paper and several sheets of tissue paper are put on top of the stack. Parafilm is laid around the gel to prevent overlapping tissue paper that may touch the liquid from disturbing the capillary force which moves the DNA from the gel to the membrane. The DNA is bound to the membrane due to ion exchange interactions as the negatively charged DNA sticks to the positively charged membrane. The transfer is left o/n and the next morning the membrane is washed in 0.4 M NaOH for 1 min to denature the DNA. Before the DNA can be UV-cross linked to the membrane, the latter is neutralized in 0.2 M Tris-HCl pH 7.5 / 1x SSC for 1 min. After cross linking, the membrane is washed several times in dH_2O to remove ions, which could form crystals with the hybridization buffer.

Probe labelling and hybridization

The Southern blot probe templates for *mCry1*$^{-/-}$ (van der Horst *et al*., 1999), *mPer1*^{Brdm1} (Zheng *et al*., 2001) and *mPer2*^{Brdm1} (Zheng *et al*., 1999) are as described previously.

The probes are labelled with ^{32}P-dCTP using the Megaprime DNA Labelling System kit (Amersham, RPN1606). 50 ng of template DNA are mixed carefully with 5 µl primer, before the mixture is boiled for 3 min in a water bath. Then the mixture is allowed to cool down on ice for 2 min. The tube is then centrifuged shortly and the following components of the kit are added:

10.0 µl labelling buffer
5.0 µl ^{32}P-dCTP
2.0 µl Klenow enzyme

The mixture is incubated for 1 h at 37°C. Then the tube is centrifuged quickly and boiled for 3 min before it is put on ice for 2 min. In order to avoid contamination with radioactive aerosols the contents are spun down before unincorporated nucleotides are removed with ProbeQuant G-50 Micro Columns (Amersham) according to the manufacturer's instructions. 2 µl of the labelled probe are added to 2 ml of scintillation cocktail and counted in a scintillation counter. If at least 2 Mio cpm/µl are obtained, 50 µl of herring sperm DNA is added to the probe and the mixture is boiled for 2 min. Then the tube is cooled down on ice for 2 min.

Hybridization and posthybridization

The cross linked membrane is put into a hybridization bottle together with an appropriate volume (usually 10 ml) of hybridization buffer (QuickHyb, Stratagene) and incubated under rotation at 68°C for 20 min. Once the pre-hybridization is finished, the denatured probe is added directly into the hybridization bottle where it is hybridized for 1 to 1.5 hours at 68°C.

The excess buffer is decanted and the membrane is washed three times inside the bottle with 2x SSC containing 0.1 % SDS and then twice with 2x SSC/0.1 % SDS at RT for 20 min. Subsequently, the membrane is taken out of the bottle and washed twice with 0.1x SSC/0.1 % SDS at 62°C for 20 min in a shaking water bath. The membrane is wrapped with Saran paper and exposed to a film with an intensifying screen at -80°C for one to two days. Upon direct exposure of the film, only around 5 % of the X-ray photons will be absorbed by the film. The intensifying screen is a sheet of inorganic salt crystals, which emit fluorescent light when excited by X-ray radiation. This leads to an increase in detected photons of up to 40 %. Prior to development, the cassette has to be equilibrated at RT for 30 min.

6.2.2 Molecular biology applications

6.2.2.1 Solutions

- **10 x TAE:**

48.4 g	Tris
11.4 ml	glacial acetic acid
20.0 ml	EDTA 0.5 M pH 8.0

- **EtBr [10 mg/ml]:**
  1 g of EtBr is dissolved in 100 ml ddH_2O and stored in a reaction tube wrapped with aluminium foil and stored in a dark place.
- **6 x Loading buffer for DNA:**

25 mg	Bromophenol Blue
25 mg	Xylene Cyanol
7.0 ml	Glycerol
3.0 ml	ddH_2O

- **TE (pH 7.5):**

1 ml	Tris-HCl 1 M RNase free
0.2 ml	EDTA 0.5 M RNase free

  The volume is completed to 100 ml with ddH_2O and pH is adjusted to 7.5.
- **Amp 100 x stock [10 mg/ml]:**

500 mg	Ampicillin in 50 ml 70 % EtOH

  The solution is conserved at –20°C.
- **Kanamycin 1000 x stock [25 mg/ml]:**
  The powder is dissolved in ddH_2O and 1 ml aliquots are conserved at –20°C.
- **LB medium:**

1 %	NaCl
1 %	Select Peptone 140
0.5 %	Select Yeast extract

  For 1 l, 10 g Peptone, 10 g NaCl and 5 g yeast extract are dissolved in 950 ml dH_2O, adjusted to 1 l and autoclaved prior to use. It is stored at 4°C. Before use, 10 ml of antibiotic has to be added.
- **LB-Amp plates:**

1 %	NaCl
1%	Select Peptone 140
0.5 %	Select Yeast extract
1.5 %	Agar

  For 1 l, 10 g NaCl, 10 g Peptone, 5 g yeast extract and 15 g agar is dissolved in 1 l dH_2O and autoclaved prior to use. When the temperature cools down to around 50°C, 10 ml of 100 x Amp are added before the plates are poured (25 ml/plate) next to a Bunsen burner or under a hood. When they have solidified, they are inverted and stored at 4°C in the dark.
- **Lysozyme stock:**

10 mg/ml	Lysozme in dH_2O

  The solution is stored at –20°C.
- **TE/RNase:**

20 µg/ml	RNase A (DNase free) in TE buffer

  The solution is stored at –20°C.

- **TELT solution:**

5 ml	1 M Tris-HCl, pH 7.5
12.5 ml	0.5 M EDTA, pH 8.0
10.6 g	$LiCl_2$
4 ml	Triton-X100

  The volume is adjusted to 100 ml with dH_2O.

- **ATP [100 mM]:**
  30 mg of ATP disodium salt are dissolved in 800 µl ddH_2O. The pH is adjusted to 7.0 with 0.1 M NaOH (pH paper) and the volume is filled up to 1 ml. Small aliquots are stored at -20°C.
- **DTT [1 M]:**
  1.55 g DTT are dissolved in 10 ml ddH_2O and 1 ml aliquots are stored at -20°C. NEVER autoclave DTT!
- **10x Ligation buffer A:**

10 mM	ATP
100 mM	DTT

  500 µl aliquots are stored at -20°C
- **10x Ligation buffer B:**

500 mM	Tris-HCl pH 7.5
100 mM	$MgCl_2$
2 mg/ml	BSA solution

  500 µl aliquots are stored at -20°C
- **BSA [10 mg/ml]:**
  100 mg BSA are dissolved in 10 ml ddH2O and 10 µl 1 M DTT is added to the solution. 1 ml aliquots are stored at -20°C.
- **10x Annealing buffer:**

500 mM	Tris-HCl pH 7.5
500 mM	NaCl
100 mM	$MgCl_2$

6.2.2.2 Isolation of RNA

Many methods, such as *in situ* hybridization, require a plasmid containing a labelled probe sequence. The raw material for this insert is the mRNA extracted from mouse tissue.

RNA isolation is carried out using RNA-Bee, which promotes the formation of complexes of RNA with guanidine and water molecules, and prevents hydrophilic interactions between DNA and proteins. Consequently, DNA and proteins do not reach the aqueous phase and can be removed with phenol, leaving only the RNA remaining in the aqueous phase, from which it can be precipitated using isopropanol.

Mouse tissue (half a brain, piece of liver or one kidney) and 1 ml RNA-Bee are homogenised with a polytron in a 2 ml Eppendorf tube and put on ice. 100 µl of chloroform is added and the tube is vigorously shaken (not vortexed) until a milky solution forms. It is kept on ice for 5 min. After the incubation, the suspension is centrifuged at 13'000 rpm at 4°C for 15 min.

The homogenate now forms two phases: the lower blue phenol-chloroform phase and the colourless upper aqueous phase. DNA and proteins are located in the milky interphase and organic phase. The aqueous layer is transferred into a fresh tube and an equal volume of isopropanol is added to precipitate RNA. The tube is carefully inverted several times and stored at 4°C for 15 min. Finally, it is centrifuged at 13'000 rpm for 15 min at 4°C. A white pellet should form at the bottom of the tube. After this step, the procedure can be interrupted and the tube kept with the pellet and isopropanol at –80°C until further use.

If the RNA extraction was interrupted, the tube must be thawed on ice before removing the isopropanol. The pellet is washed once with 1 ml of 100 % ethanol by turning the tube in your hands. The ethanol is discarded and the pellet is briefly air-dried. The pellet is dissolved in a starting volume of 20 µl ddH_2O.

6.2.2.3 Spectrophotometric determination of nucleic acid concentration

The determination of RNA and DNA concentrations is achieved with a spectrophotometer by measuring the absorbance (A) at 260 nm and 280 nm. The purity of the sample is estimated by the ratio of A_{260}/A_{280}. The ratio values for a good DNA preparation should be around 1.8: values that are < 1.75 indicate protein contamination and values > 1.9 indicate RNA contamination. A good RNA preparation optimally shows ratios of around 2.

The following conversion values are used to calculate the nucleic acid concentrations:

1 A_{260} unit double stranded (ds) DNA	≅ 50 µg/ml
1 A_{260} unit single stranded (ss) DNA or RNA	≅ 40 µg/ml
1 A_{260} unit oligonucleotide	≅ 20 µg/ml

The following formula is used to calculate the concentration:

$$c\,[\mu g/\mu l] = \frac{d_f \cdot cf \cdot N_{A_{260}}}{1000}$$

df represents the dilution factor, cf the conversion factor, c the concentration and N_{A260} the measured number of absorbance units at 260 nm.

6.2.2.4 Agarose gel electrophoresis

Electrophoresis is used to separate biological molecules such as nucleic acids or proteins according to their size and charge in an electrical field. Length and purity of nucleic acid molecules can be accurately determined by agarose (a polysaccharide isolated from seaweed) gel electrophoresis as each nucleotide in a nucleic acid molecule carries a negative charge on its phosphate group. That is why this procedure is simpler than for proteins, since there is no need to add the negatively charged detergent SDS that is required to make protein molecules move uniformly toward the positive electrode. However, agarose gel electrophoresis only works for large nucleic acid molecules. According to the size of the fragment, agarose is prepared as follows: the longer the fragment the less concentrated the gel. 1 - 2 % (w/v) agarose gels are used to separate DNA or RNA fragments of 200 to 20'000 bp. For molecules smaller than 500 bp, less porous gels are needed, such as those made from polyacrylamide. These nucleic acid separation methods are widely used for both analytical and preparative purpose. Unfortunately, nucleic acid bands on agarose or polyacrylamide gels are invisible unless they are stained. One method for staining them is to add ethidium bromide (EtBr) to the gel, which fluoresces under UV light (312 nm) when intercalated between two neighbouring bases in a nucleic acid helix.

Agarose powder is dissolved in the appropriate volume of 0.5x TAE by heating it in a microwave until it reaches its boiling point. As soon as the solution is cooled down to approximately 50°C, ~0.2 µl EtBr (10 mg/ml) per 100 ml is added. After swirling the Erlenmeyer, the solution is poured into a horizontal electrophoretic chamber. When the gel is solidified, it is ready for use in a gel migration chamber. 0.5 x TAE is used as a migration buffer. The electrophoresis is carried out at either 50 V for around 40 min or at 100 V for ca. 20 min. To follow the migration of the nucleic acids across the gel, the samples are mixed with 6 x loading dye before filling the wells. This allows the observer to stop the electrophoresis at the point when the bromphenol blue (and with it DNA molecules) has migrated the desired distance. To be able to determine the length of the fragments, at least one well of the gel is filled with either a 1 kb or a 100 bp DNA Ladder.

At the end, a picture of the gel is taken with a photo documentation system and printed on thermal paper (MITSUBISHI, KP65HM-CE).

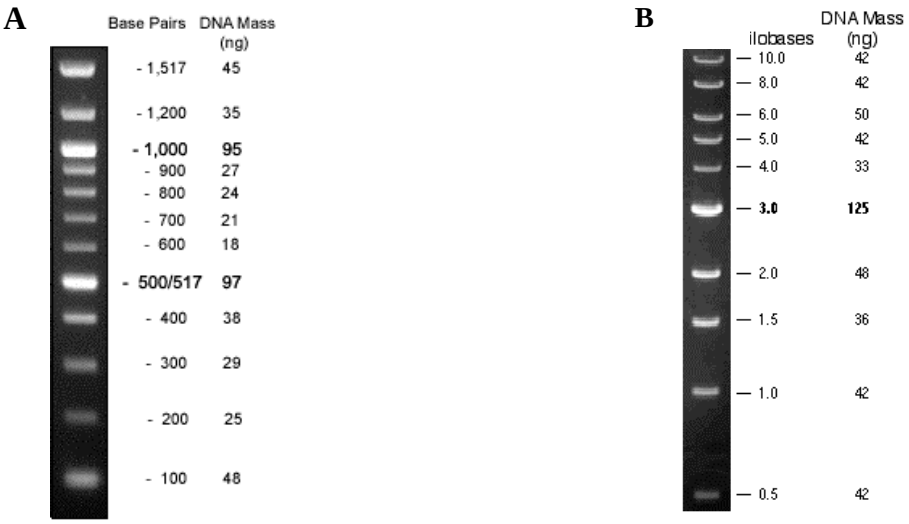

Fig. 6.2-2: A 0.5 µg of 100 bp DNA Ladder (NEB, N3231L) visualized with ethidium bromide staining on a 1.3% TAE agarose gel. **B** 0.5 µg of 1 kb DNA Ladder (NEB, N3232L) visualized with ethidium bromide staining on a 0.8% TAE agarose gel.

6.2.2.5 RT-PCR and cloning

The extracted mRNA (see 6.2.2.2 for extraction) must be transcribed into complementary DNA (cDNA) by reverse transcriptase before it can be amplified. The enzyme "reverse transcriptase" originates from retroviruses, such as the Moloney Murine Leukemia Virus (MMLV), and synthesizes a DNA chain from a RNA template. Single stranded (ss) cDNA molecules are then converted into double stranded (ds) DNA molecules by DNA polymerase. These molecules are then inserted into a plasmid or a virus vector and cloned.

Fig. 6.2-3: Classical cDNA synthesis via reverse transcription – short RT-PCR.

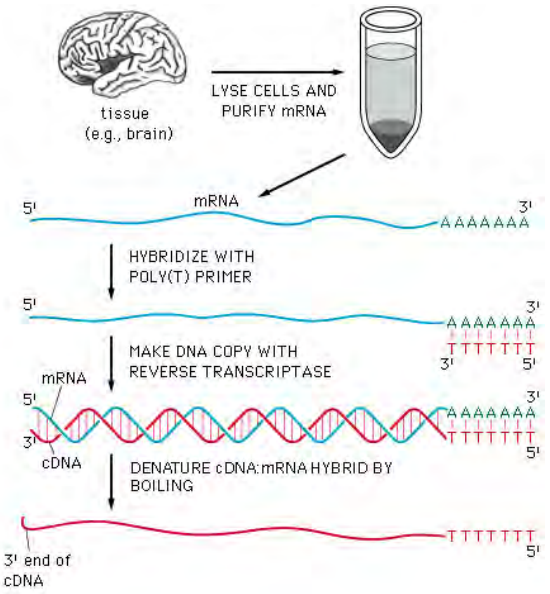

Between 1 ng – 5 µg of total RNA are used as a template for RT-PCR. First, 17 µl ddH_2O, 2 µl RNA and 4 µl oligo dT_{18} primer (1 µg/µl) are mixed in a nuclease-free microcentrifuge tube and annealed for 10 min at 70°C.

The tube is chilled for 2 min on ice and then the following substances are added:

4.0 µl	DTT (0.1 M)
8.0 µl	5 x First-Strand Buffer
2.0 µl	dNTPs (10 mM)
1.0 µl	RNasin (40 U/µl)
2.0 µl	SuperScript^{TM} II RNase H$^-$ Reverse Transcriptase (200 U/µl)
40.0 µl	total volume

The contents are gently mixed and incubated at 37°C for 1.5 h in a water bath. Then the mixture is heated to 95°C to inactivate the reaction and to denature the cDNA:mRNA hybrids. If the cDNA is not used directly for the PCR the tubes are frozen at –20°C, otherwise they are kept on ice. The PCR reaction is typically set up as follows:

2.0 µl	cDNA
4.0 µl	$MgCl_2$ (25 mM)
5.0 µl	$(NH_4)_2SO_4$ (60 nM)
5.0 µl	10 x QIAGEN PCR Buffer
5.0 µl	5' primer (5 µM)
5.0 µl	3' primer (5 µM)
0.5 µl	*Taq* DNA Polymerase (5 U/µl)
1.0 µl	dNTPs (10 mM)
22.5 µl	ddH_2O
50.0 µl	total volume

Ammonium sulphate is added to improve annealing of the primers. The volumes of cDNA or primer can vary for each set up, depending on their concentration. Final volume of 50 µl is obtained by completing the volume with water.

The components are gently mixed and the PCR started with an initial heating step at 94°C for 2 min followed by other 30 s at 94°C to separate the complementary strands (denaturation step). These strands are then annealed with an excess of two DNA oligonucleotides (each around 20 nucleotides long) that have been chemically synthesised to match sequences separated by several nucleotides (generally 150 to 2000). The annealed mixture is then incubated with DNA polymerase and the four nucleotides so that the regions of DNA downstream each of the two primers are selectively synthesised. The procedure of denaturing, annealing and extension is repeated several times. In turn, the newly synthesised fragments serve as templates and within a few cycles the predominant product is a single species of DNA fragment whose length corresponds to the distance between the two original primers. Annealing and extension (always at 72°C) conditions are primer and template dependent and have to be determined empirically for each reaction. Typically, 15 to 40 cycles are performed.

At the end of the PCR the quality of the amplified DNA is checked on an agarose gel as described in the 6.2.2.3 section. If the PCR was successful and DNA fragments of the right size have been amplified, then the product can be cloned into a vector for further use (e.g. ISH) either directly or after purification. Generally, a gel elution is required if several fragments are amplified by the PCR. For this the DNA fragment of interest is cut out of the gel using a sharp scalpel blade and transferred to a reaction tube. The DNA is then eluted from the gel according to the manufacturer's instructions of the kit used for purification (QIAquick gel extraction kit from Qiagen; Wizard®SV Gel and PCR Clean-Up System from Promega; S.N.A.P.™ Gel Purification Kit from Invitrogen).

For cloning, either the TOPO TA Cloning® Kit Dual Promoter containing the pCR®II-TOPO® vector or the TOPO® XL PCR cloning kit containing the PCR® XL-TOPO vector have been used (both kits are from Invitrogen). These kits take advantage of the single 3'-deoxyadenine overhangs that the PCR product has, by ligating them with the single 3'-deoxythymidine overhangs of the linearized vector using a covalently bound topoisomerase I (prevents DNA tangling during replication causing single-strand breaks). This enzyme from *Vaccinia* virus binds to duplex DNA at specific sites and cleaves the phosphodiester backbone after 5'-CCCTT in one strand. The energy from the broken strand is conserved by formation of a covalent bond between the 3' phosphate of the cleaved strand and a tyrosyl residue (Tyr-274) of topoisomerase I. The phospho-tyrosyl bond between DNA and enzyme can subsequently be attacked by the 5'hydroxyl of the original cleaved strand, reversing the reaction and releasing topoisomerase I (Shuman, 1994). The kit takes advantage of the fact that the topoisomerase I (covalently bound to the linearized vector) reseals the break between the ligated vector and the PCR product.

The cloning reaction is set up as follows:

1.0 µl	fresh PCR product
3.0 µl	sterile ddH_2O
1.0 µl	TOPO® vector
5.0 µl	total volume

The reaction is gently mixed and incubated for not more than 5 min at RT (22 – 23°C) and then placed on ice. 2 µl of the TOPO® Cloning product are added into a vial of One Shot® Chemically Competent *E. coli* that have been thawn on ice just prior to use. The bacteria and the cloning product are mixed very carefully, without pipetting up and down, before the tube is incubated on ice for 5 to 30 min. The cells are heat-shocked for 30 s at 42°C without shaking and immediately transferred to ice where 500 µl of room temperature SOC medium

are added. SOC Medium is a complex cell-growth medium that ensures maximum transformation efficiency when used in the final step of transformation. The tube is then put at 37°C in a water bath for 1 h. 100 µl of the transformation product is spread on a prewarmed LB selective plate and incubated overnight at 37°C.

6.2.2.6 Isolation and purification of recombinant DNA

Colonies obtained from the cloning procedure must first be checked to make sure that the desired insert is present, because bacteria that incorporate only the vector or the vector with a wrong insert are also resistant to ampicillin. Usually a minimum of 10 different colonies is tested for the insert by conducting a Miniprep.

The day before the Miniprep is done, 5 ml of LB medium with 50 µl 100 x Amp is placed in a 15 ml Falcon tube. For each colony to be tested, one tube has to be prepared next to a Bunsen burner. Each colony is picked with a pipette tip, which is then put in the Falcon tube and incubated o/n at 37°C with vigorous shaking (~250 rpm). Growth for more than 16 h should be avoided since cells may become too dense and begin to lyse causing reduced plasmid yields. The next day, the Miniprep is carried out with 1.5 ml of culture according to the protocol of the QIAprep Spin Miniprep Kit Protocol (QIAprep Miniprep Handbook 07/99, pp. 18-19) or according to the TELT method.

For the TELT method, 1.5 ml of cultured bacteria is centrifuged for one minute at 13000 rpm. The supernatant is discarded and the tube is centrifuged again to remove all residual liquid. The bacterial pellet is resuspended in 150 µl TELT-solution and 15 µl lysozyme solution by vortexing. The mixture is incubated for five minutes at room temperature before it is heated for two minutes at 100°C. Then the tube is chilled on ice for five minutes and centrifuged for 30 min at 13’000 rpm at 4°C. The lysate is transferred to a new Eppendorf tube and adding of 150 µl isopropanol precipitates the DNA. After a 5 min incubation at room temperature the tube is centrifuged for 10 min at 13’000 rpm at 4°C. The DNA pellet is washed once with 750 µl 70 % EtOH and then air dried before it is dissolved in about 50 µl TE buffer. Alternatively, the pellet can also be dissolved in TE/RNase but has then to be incubated for 30 min at 37°C on a shaker at 800 rpm.

8 µl of eluate or TELT-preparation is used for a test digestion with EcoRI, because the insert is flanked on both sides with this restriction site. The digestion is set up as follows:

8.0 µl	eluted plasmid
2.0 µl	10 x EcoRI buffer
1.0 µl	EcoRI (20 U/µl)
9.0 µl	ddH_2O
20.0 µl	total volume

The reaction is mixed carefully and incubated for 1 to 2 h at 37°C in a water bath. All digestions are then run on an agarose gel as described in the 6.2.2.3 section. Only clones containing an insert of the right length are kept.

The harvesting of probes from positive clones is done using a Maxiprep and starts with the inoculation of 250 ml LB medium with 2.5 ml 100x Amp in a 500 ml Erlenmeyer with 250 µl of a Miniprep culture one day before the experiment starts. They are incubated o/n at 37°C with vigorous shaking (~180 rpm), and incubation times should not exceed 16 h. The following day the cells are harvested by centrifugation at 6'000 rpm for 15 min at 4°C. The isolation of the plasmid is completed as described in the QIAGEN® Plasmid Purification Handbook (07/99, pp. 21-24) or in the Promega PureYield™ Plasmid Maxiprep System Handbook. The eluted DNA is also tested in an EcoRI digestion (as described for the Miniprep) and its purity and concentration is tested using the spectrophotometer (see 4.2.1.2). After its completion, a portion of each plasmid is sent to Microsynth for sequencing to determine both the direction and contents of the insert.

As a backup, bacteria that have been determined to carry the correct clone after sequencing may be stored at –80°C in a mixture of 800 µl culture medium and 200 µl 87 % glycerol.

6.2.2.7 Ligation in low-melting agarose

This method is based on the fact that the low-melting agarose can be melted at 65°C and stays in a liquid state at 37°C. This property allows the *in agarose* ligation of DNA fragments separated on a preparative low-melting agarose gel without further purification steps. A big advantage of this is that the method is less time consuming than conventional methods in which the DNA has to be processed before ligation (e.g. gel elution, glass bead purification, etc.). However, it has to be emphasized that this procedure is more risky due to the heating steps and the presence of ethidium bromide during the transformation.

Digested DNA fragments are separated according to their size on a low-melting agarose gel of convenient percentage that has been poured on a glass plate with 1x TAE buffer containing

0.5 µg/ml EtBr. The reason why the gels are poured on glass plates is that it is important to have gel slices that are as small as possible. Approximately 0.5 pmol of digested DNA are loaded per well. Once the bands migrated far enough, the gel is put on saran paper to avoid contamination with foreign DNA, a picture is taken and the bands of interest are cut out with a clean scalpel blade on a UV transilluminator. It is recommended to use the long UV wavelength of 365 nm and to minimize the exposure time because UV destroys the DNA. The gel slices are transferred to a clean reaction tube and around 50 µl of ddH_2O is added to improve melting. The tubes can be kept on ice for a while.

Meanwhile, a heating block is set to 65°C and a second one to 37°C. Furthermore, 500 µl ddH_2O are pre-heated to 65°C. A master ligation mix is prepared containing 7.5 µl 10x ligation buffer A + 7.5 µl ligation buffer B + 35 µl ddH_2O per planned reaction and all necessary positive and negative controls. It is assumed that 10 µl of each needed DNA fragment in form of melted agarose and 1 µl T4 DNA ligase will be added to each reaction later, leading to a final DNA fragment concentration of around 0.5 fmol/µl.

The gel slices containing the excised DNA fragments are melted in the 65°C warm heating block for 10 to 20 min, vortexed thoroughly, quickly spun down and kept in the heating block. The tubes containing the pre-pipetted ligation mix are put in the 37°C warm heating block and 10 µl of each DNA fragment are added where required. Since the low-melting agarose solidifies at ambient temperature, each pipette tip used has to be pre-warmed in the water-containing reaction tube at 65°C aspirating up and down before the DNA fragments can be pipetted. Optionally, 6 µl of solutions C_0-C_2 are added to the tube if oligonucleotides are used for the ligation (see 6.2.2.8). While keeping the tubes at 37°C, 1 µl of T4 DNA ligase is added to each tube at a concentration of 1 U/µl. The reaction mixtures are mixed well, quickly spun down and incubated at 4°C overnight. For ligations between blunt end fragments, the tubes are put on a floater on ice o/n, so that in the morning the tubes are floating on water.

6.2.2.8 Ligation using oligonucleotide linkers

Sometimes it is of great use to connect plasmids and DNA fragments using oligonucleotides of sizes up to 100 bp. For this it is important to design a sense and an antisense oligonucleotide that are annealed later on. The lyophilized oligonucleotides, ordered from Microsynth as genomic scale, are reconstituted in 1x TE in order to have a concentration of about 100 µM. The dilution is verified spectrophotometrically for its concentration,

measuring a mixture of 10 µl oligonucleotides and 490 µl 1x TE. The concentration is determined according to the following formula:

$$\mathbf{c\ [\mu M = pmol/\mu l] = df \times 100 \times A_{260} / N}$$

(with N = oligonucleotide length and df = dilution factor)

100 pmol of each oligonucleotide are annealed (sense + antisense) to a final annealed oligo concentration of 5 pmol/µl as follows:

100 pmol	sense oligo
100 pmol	antisense oligo
x µl	ddH_2O (x = amount of water to complete to 20 µl)
2.0 µl	10x annealing buffer
20.0 µl	total volume

To achieve the annealing, the mixture is boiled for 1 min and cooled down to RT by leaving the tubes float in the water allowing a gradual temperature decrease. Eventually, the tubes can be left like this o/n. To obtain optimal ligation conditions, three different molar amounts (C_0-C_2) of the oligonucleotide are prepared by sequential dilutions in 1x ligation mix (= 1 µl ligation buffer A + 1 µl ligation buffer B + 8 µl ddH_2O) on ice:

C_0: 5 µl of annealed oligo [5 pmol/µl] are added to 45 µl 1x ligation mix → 500 fmol/µl

C_1: 10 µl C_0 + 90 µl 1x ligation mix → 50 fmol/µl

C_2: 10 µl C_1 + 90 µl 1x ligation mix → 5 fmol/µl

6.2.3 Processing of human buccal cells

Relative RNA expression of the three clock genes *hPER1, hPER2 hBMAL1* and the housekeeping gene *GAPDH* (glyceraldehyde-3-phosphate dehydrogenase) was measured in human oral mucosa of healthy volunteers.

6.2.3.1 SOP – Sampling human oral mucosa

Prepared by: Corinne Jud	**SOP – sampling human oral mucosa** **April 26, 2006**
Revised by: Corinne Jud	 January 30, 2009

PURPOSE:

To establish a standard operating procedure for sampling oral mucosa

EQUIPMENT:

1 ml blue tips (Treff AG), 0.5 ml Eppendorf tubes, β-mercaptoethanol (included in Nanoprep Kit), Absolutely RNA™ Nanoprep Kit (Stratagene), powder free gloves

PROCEDURE:

Always wear clean gloves, change them frequently and use RNase free tips (1 ml) and tubes (500 μl). Tips and tubes should be autoclaved and only be touched with gloves (before and after autoclaving!).

1. Prepare a mixture of 0.7 μl β-mercaptoethanol and 100 μl lysis buffer (both provided in the Absolutely RNA™ Nanoprep Kit, Stratagene) for each sample you want to collect.
   Attention: The lysis buffer contains the irritant guanidine thiocyanate! The mixture always has to be prepared freshly and under the hood!!!
2. The subject should neither have eaten nor drunk anything (except water) before sampling because otherwise the samples will be contaminated. It improves the quality of the sample to rinse the mouth with water and rub the inside of the cheek gently with a very soft toothbrush (e.g. Meridol) prior to tissue collection.
3. The subject should wear gloves while he is collecting his mucosa samples. Pay attention that he never touches the tip without gloves. He should use 1 ml pipette tips (Treff AG) and scratch inside the cheek until a white pellet is visible.

4. The subject gives the tip to the technician (gloves!!!) who makes sure that the pellet is at least 2 mm big. Put the tip onto a pipette. Pipette up and down in the lysis buffer until the pellet floats in the lysis buffer.

   Attention: Watch out not to loose the tissue while you put the tip onto the pipette. Either put the piston down before putting the tip onto the pipette or dip the tip into the liquid before putting it onto the pipette!
5. In case you don't get enough material from one cheek, the subject can scratch the other cheek (use a new tip!). Put this sample in the same tube.
6. Vortex the tube until the sample is completely dissolved.
7. Centrifuge it shortly (not at high speed) to spin the solution down
8. Store it at -80°C or continue to isolate the RNA

The samples can be transported at this stag on dry ice.

6.2.3.2 SOP – Processing of human oral mucosa

Prepared by: Corinne Jud	**SOP – Processing human oral mucosa** **April 26, 2006**
Revised by: Corinne Jud	 November 22, 2007

PURPOSE:

To establish a standard operating procedure for processing human oral mucosa.

EQUIPMENT:

Absolutely RNA^{TM} Nanoprep Kit (Stratagene; #400753), reaction tubes, RNAse free filter pipette tips, Superscript^{TM} II RNAse H^{-} Reverse Transcriptase (Invitrogen; #18064-014), RNAsin (Promega; #N2111), oligo dT_{15} (Roche; #1 081 427 000 1), primer random $p(dN)_6$ (Roche; #1 034 731), dNTPs (Roche; #1 181 436 200 1), iQ^{TM} Supermix (BioRad; #170-8862), $MgCl_2$ [25 mM] (Qiagen, component of the Taq-polymerase kit), double distilled water, specific primers and probes (Microsynth), 96 well plate (AxonLab; #AB-0900), absolute QPCR seal (AxonLab; #AB-1170), iCycler (BioRad)

PROCEDURE:

RNA isolation

The RNA is isolated using the Absolutely RNA^{TM} Nanoprep Kit following the instructions in the manual provided by the manufacturer:

- The tubes containing lysis buffer, β-mercaptoethanol (β-ME), and oral mucosa are thawed on ice.
- 100 µl lysis buffer and 0.7 µl β-ME are mixed for each sample and added to the mix.
- 200 µl of 70 % ethanol are added to the cell lysate and mixed thoroughly until the lysate and the ethanol are mixed well (at least for 5 s).
- 1 min at 13'000 rpm
- The mixture is transferred to an RNA-binding nano-spin cup that has been seated within a 2 ml collection tube and is closed with a cap.
- 1 min at 13'000 rpm
- The filtrate is discarded and the spin cup reseated in the same 2 ml collection tube.
- DNase Treatment:
  - 300 µl of 1x Low-Salt Wash Buffer is added to the spin cup, which is then capped.
  - 1 min at 13'000 rpm
  - The filtrate is discarded, the tube reseated in the collection tube, capped, and centrifuged for 2 min at 13'000 rpm to dry the fiber matrix.
  - For each sample 12.5 µl of DNase Digestion Buffer is mixed with 2.5 µl of reconstituted DNaseI → mix gently because the DNase I is very sensitive to denaturation
  - 15 µl of DNase solution is directly added onto the fiber matrix inside the spin cup, which then is capped.
  - Incubation for 30 min at 37°C
- The Elution Buffer is pre-heated to 60°C.
- 300 µl of 1 x High-Salt Wash Buffer is added to the spin cup
- 1 min at 13'000 rpm
- The filtrate is discarded.
- 300 µl of 1 x Low-Salt Wash Buffer is added
- 1 min at 13'000 rpm
- The filtrate is discarded.
- A second Low-Salt wash is performed using again 300 µl.
- 1 min at 13'000 rpm

- The filtrate is discarded.
- 3 min at 13'000 rpm to dry the fiber matrix
- The spin cup is transferred to a 1.5 ml safe lock Eppendorf tube.
- 10 µl of 60°C warm Elution Buffer is directly added onto the fiber matrix inside the spin cup.
- Incubation for 2 min at RT
- 13000 rpm for 5 min
- 5 µl of 60°C warm Elution Buffer is directly added onto the fiber matrix inside the spin cup.
- 13'000 rpm for 5 min
- The eluate is transferred to a 0.5 ml Eppendorf tube and stored at –80°C.

cDNA Synthesis (SuperScript™ II RNase H⁻ Reverse Transcriptase)

- Reconstitute the oligo dT_{15} in 58 µl ddH_2O
- The following substances are added to a 0.5 ml reaction tube:
  - Oligo dT_{15} [1µg/µl] 8 µl
  - RNA eluate 10 µl
  - dNTPs [10 mM each] 4 µl
  - ddH_2O 26 µl
- Mix well and incubate the tube for 5 min at 65°C
- Chill the tube on ice
- Collect the contents of the tube by brief centrifugation
- Add the following substances:
  - 5 x First-Strand Buffer 16 µl
  - 0.1 M DTT 8 µl
  - RNasin [40 U/µl] 4 µl
- Incubate the tube for 2 min at 42°C
- Centrifuge briefly and then add:
  - SuperScript™ II RT 4 µl
    total volume 80 µl
- Incubate the sample for 1 h 45 at 42°C
- Inactivate the reaction for 10 min at 95°C
- Store the cDNA at –20°C until further use

Instead of the oligo dT_{15} one can also use random hexamer primers at a concentration of 0.1 µg/µl. If one is using random primers, the reaction has to be started with a 10 min incubation

at 25°C because they have a lower melting point compared to the oligo dT_{15}. Of course also the 2 min incubation before adding the transcriptase has to be done at 25°C instead of 42°C.

Quantitative Real-time PCR

- Things to always remember when preparing the samples:
  - Always wear powder free gloves
  - Change gloves frequently
  - Use autoclaved plastic ware only
  - Use filter tips only
  - Clean the pipettes before use (95 % alcohol or 10 % bleach; exposure to UV-light)
  - Make at least duplicates, better triplicates
  - Vortex all the samples before use
  - Vortex the master mixes before puting into the wells
- Prepare a master mix for the primers:
  - For 8 ml *GAPDH*, *PER2* or *BMAL1* master mix:

$MgCl_2$ [25 mM]	1600 µl
ddH_2O	6368 µl
TaqMan probe [100 µM]	20 µl
Forward primer [1 mM]	6 µl
Reverse primer [1 mM]	6 µl

    Adding 8 µl of this primer master mix to a final reaction volume of 20 µl yields a final concentration of 5 mM for $MgCl_2$, 300 nM for primers and 100 nM for TaqMan probe.
  - For 8 ml *PER1* master mix:

$MgCl_2$ [25 mM]	1600 µl
ddH_2O	6386 µl
TaqMan probe [100 µM]	10 µl
Forward primer [1 mM]	2 µl
Reverse primer [1 mM]	2 µl

    Adding 8 µl of this primer master mix to a final reaction volume of 20 µl yields a final concentration of 5 mM for $MgCl_2$, 100 nM for primers and 50 nM for TaqMan probe.
- The following ingredients are mixed for each sample:

iQ Supermix	10.0 µl
Primer master mix	8.0 µl
cDNA template	2.0 µl
total volume	20.0 µl

- Each reaction should be done in triplicates. A positive control is done using HER911 cDNA and *GAPDH* primers. A negative control without cDNA has to be done for each primer pair.
- Put all the samples on a 96 well Plate (Axon Lab, #AB-0900) and seal the plate with an ABsolute QPCR Seal (Axon Lab, #AB-1170).

The PCR-Protocol is as follows (iCycler, BioRad)**:**

Cycle 1:	(1X)	*Denature*	
	Step 1:	95.0ºC	for 03:00
Cycle 2:	(55X)	*Amplification*	
	Step 1:	95.0ºC	for 00:15
	Step 2:	55.0ºC	for 01:00
	📷 Data collection and real-time analysis enabled.		
Cycle 3:	(1X)		
	Step 1:	20.0ºC	HOLD

Primers [final concentration in reaction mix]**:**

PER2 TaqMan Probe [100 nM]: 5'-[FAM]ATG CCT TCA GCG ATG CCA AGT T[BHQ]-3'

PER2 sense primer [300 nM]: 5'-GCA TCC ATA TTT CAC TGT AAA AGA-3'

PER2 anti-sense primer [300 nM]: 5'-AGT AAA AGA ATC TGC TCC ACT G-3'

GAPDH TaqMan Probe [100 nM]: 5'-[FAM]AGC CTC AAG ATC ATC AGC AAT GCC[BHQ]-3'

GAPDH sense primer [300 nM]: 5'-TGT GAA CCA TGA GAA GTA TGAC-3'

GAPDH anti-sense primer [300 nM]: 5'-ATG AGT CCT TCC ACG ATA CC-3'

PER1 TaqMan Probe [50 nM]: 5'-[FAM]TTC GGG TTA CGA AGC TCC CCG GAT AC[BHQ]-3'

PER1 sense primer [100 nM]: 5'-CGC CTA ACC CCG TAT GTG A-3'

PER1 anti-sense primer [100 nM]: 5'- CGC GTA GTG AAA ATC CTC TTG TC-3'

BMAL1 TaqMan Probe [100 nM]: 5'-[FAM]AAT CCT GGG CCT TCA TTG GTT CCG[BHQ]-3'

BMAL1 sense primer [300 nM]: 5'-CGT TTG GAC CCA AGC TTA AC-3'

BMAL1 anti-sense primer [300 nM]: 5'-CAC ACA GGA AGC CCT CTA GC-3'

6.2.3.4 Sampling human oral mucosa using the cytobrush

As described under 6.2.3.1, the subject should not have eaten or drunk anything prior to sampling. If, however, the subject ate something, he should rinse his mouth with water and eventually rub the cheek with a soft toothbrush (e.g. Meridol). The oral mucosa is then

collected by rotating the cytobrush at the same place inside the cheek for at least 30 seconds. It is important to apply a certain pressure while rotating the brush because otherwise not enough tissue will be taken. A slight sensation of burning is a good sign for the correct pressure. However, bleeding due to too much pressure should be avoided.
After sampling, the brush is dipped into a 1.5 ml safe-lock Eppendorf tube containing 1 ml of RNA*later*®. The stem of the brush is cut just above the brush using scissors, before it is stored at -80°C until further use.

6.2.3.5 Processing of human oral mucosa sampled with the cytobrush

The tube containing the cytobrush is thawn on ice and then centrifuged in a horizontally fixed angle rotor at 7'000 rpm for 5 min. The cytobrush is removed using small forceps and carefully wiped along the side of the reaction tube to collect a maximum of tissue. After a second centrifugation, the RNA*later*® is discarded paying attention not to disturb the pellet. The latter is washed thoroughly in 1 ml of RNAse free 1x PBS by flicking the tube. Then the tube is centrifuged at 13'000 rpm in a normal Eppendorf tube centrifuge for 5 min and the supernatant is removed. The pellet is washed twice with 50 µl 1x PBS and centrifuged at 13'000 rpm for 3 min. The remaining PBS is discarded completely, before the pellet is dissolved in 300 µl lysis buffer containing 2.1 µl β-mercaptoethanol (Absolutely RNA Nanoprep kit, Stratagene). The suspension is mixed vigorously by vortexing until the pellet is completely homogenized. Lysis is allowed to take place during 10 min at RT before 300 µl of 70 % EtOH are added to the lysate. The tube is vortexed again before it is centrifuged at 13'000 rpm for 1.5 min. The supernatant is transferred to an RNA-binding nano-spin cup that has been seated within a 2 ml collection tube and it is closed with a cap. Then tube is centrifuged at 13'000 rpm for 1 min and the filtrate is transferred again onto the RNA-binding nano-spin cup. This step is repeated 3 times to improve the yield of RNA bound to the matrix. The following steps are as described in the 6.2.3.2 section.

6.2.4 *In Situ* Hybridization

6.2.4.1 Solutions

All solutions – except the SSC and NTE – have to be prepared RNase free! To do this, all glass bottles are flamed before filling and only ddH_2O is used. Gloves have to be worn at all times and should be changed frequently. Chemicals are directly weighed inside the bottle or on a piece of aluminium foil.

- **EDTA 0.5 M (pH 8.0):**
  93.1 g EDTA x 2 H_2O (AW: 372.24)
  400 ml ddH_2O
  The pH is adjusted to 8.0 with NaOH (around 10 g NaOH pellets). The volume is made up to 500 ml at the end.
- **RNase A [10 mg/ml]:**
  500 mg RNase A are dissolved in 50 ml ddH_2O and stored at –20°C in 200 µl aliquots
- **4 % PFA in 1 x PBS:**
  850 ml ddH_2O
  2 ml NaOH 1 M
  40 g PFA
  100 ml 10 x PBS RNase free
  The solution is stirred and heated to about 50°C. 30 drops of NaOH 10 M are added to dissolve the PFA. The pH is then adjusted to 7.4 and filled to 1 l. Finally, the solution is filtered.
- **10x PBS (pH 7.4):**
  80.0 g NaCl
  2.0 g KCl
  28.5 g Na_2HPO_4 x 12 H_2O (AW: 358.14)
  2.0 g KH_2PO_4 (AW: 136.09)
  800 ml ddH_2O
  The pH is adjusted to 7.4 then the volume is filled up to 1 l.
- **TEA 1 M (pH 8.0):**
  66.3 ml TEA
  The pH is adjusted to 8.0 and the volume is filled up to 1 l with ddH_2O.
- **10x Proteinase K buffer (pH 7.6):**
  250 ml Tris-HCl 1 M pH 8.0 RNase free
  50 ml EDTA 0.5 M pH 8.0 RNase free
  200 ml ddH_2O
  The pH is adjusted to 7.6 with concentrated HCl.
- **Yeast tRNA [10 mg/ml]:**
  100 mg tRNA are dissolved in 10 ml ddH_2O. Once the tRNA is completely dissolved, 1 ml aliquots are prepared in 2 ml tubes. Each aliquot is extracted twice with 1 ml of premixed phenol-chloroform-isoamylalcohol (SIGMA; 25:4:1 saturated with buffer). The aqueous phase of all tubes is transferred into a 15 ml Falcon tube and from this, 500 µl aliquots are prepared in 2 ml tubes. Adding 1 ml 100 % EtOH and 50 µl of 4 M NH_4Ac to every aliquot precipitates the tRNA. The pellets are dissolved in 150 µl ddH_2O each. The final concentration is adjusted to 10 µg/µl and aliquots are stored at -80°C.

- **Proteinase K [4 mg/ml]:**
  40 mg of Proteinase K is dissolved in 10 ml 50 mM Tris pH 7.6 and stored at –20°C as 1 ml aliquots.
- **Hyb-Mix (for ^{35}S-ISH):**

50 %	Formamide
0.3 M	NaCl
20 mM	Tris-HCl, pH 8.0
5 mM	EDTA
10 %	Dextransulfate
2x	Denhardt's solution
0.5 mg/ml	RNA from yeast

  The Hyb-Mix has to be prepared overnight on a shaker because it doesn't mix well otherwise. The 50 % dextransulfate solution should be prepared one day in advance since it takes a while to dissolve in ddH_2O. 10 ml of 50 % dextransulfate are mixed in a 50 ml Falcon tube with 3 ml 5 M NaCl, 1 ml 1 M Tris-HCl pH 8.0, 0.5 ml 0.5 M EDTA pH 8.0, 6 ml ddH_2O, and 25 ml formamide on a shaker overnight. On the next day, 2.5 ml yeast tRNA [10 mg/ml] and 2.0 ml of 50x Denhardt's solution are added and mixed on the shaker until everything is dissolved completely (± 30 min). 1 ml aliquots are prepared and kept at –80°C. Before using them, 10 µl of 10 M DTT (SIGMA; in ddH_2O) and 10 µl of 25 mM α-S-ATP (Roche; 146 µl of ddH_2O are used to dissolve 2 mg of powder) are added. The tube is vortexed at maximum speed for at least 15 s.
- **20 x SSC (pH 7.0):**

175.3 g	NaCl
88.2 g	tri-Na-Citrate x 2 H_2O (AW: 294.1)
800 ml	dH_2O

  The pH is adjusted to 7.0 and the volume is filled up to 1 l with dH_2O.
- **10 x NTE (pH 8.0):**

292.2 g	NaCl
100 ml	Tris-HCl 1 M pH 8.0 RNase free
100 ml	EDTA 0.5 M pH 8.0 RNase free

  The pH is adjusted to 8.0 and the volume is filled up to 1 l with dH_2O.

6.2.4.2 Tissue Fixation, Embedding and Sectioning

After dissection, the tissue is placed in a glass scintillation vial (20 ml) containing 4 % PFA in ice-cold PBS o/n at 4°C with gentle shaking. The water is subsequently removed from the tissue so that it can be embedded in paraffin, which is accomplished using the following dehydration steps: 30 % EtOH for 2 h, 50 % EtOH for 2 h, 70 % EtOH o/n, 100 % EtOH for 2 h, 100 % EtOH o/n. All dehydration steps are carried out at 4°C with gentle shaking.

This is followed by infiltrating the tissue with xylene. The 100 % EtOH is discarded and xylene is added while under the hood. The vial is gently shaken at RT for 1 h. The xylene is then replaced and the vial gently shaken for another 30 min at RT. Finally, the tissue is embedded in paraffin: xylene/paraffin (1:1) at 63°C for 2 h and twice paraffin at 63°C for 2 h. The paraffin (paraplast) wax is melted before use by placing a PET container covered with

aluminium foil in a warming oven at 63°C overnight. If melted paraffin is needed immediately, wax can be melted in a microwave for approximately 10 min. Some unmelted paraffin should be left in the liquid to avoid overheating. A small amount of wax is placed in a separate PET beaker. Around 10 min before use, an equal volume of xylene is added.

After the final wax step, new paraffin is added, the vial gently swirled to suspend the tissue in the melted wax, and then quickly poured into a plastic mold. The tissue is oriented in the mold and any bubbles are removed with autoclaved toothpicks. If the tissue fails to pour from the vial, more wax can be added to the vial and the tissue repoured. The blocks are left o/n at RT without disruption and, once solidified, can be stored indefinitely at RT.

To cut the paraffin blocks, excess wax is first cut from around the embedded tissue. The paraffin block is then mounted in the proper orientation on a wooden block by gently melting the surface of the wax with a lighter. In order to get wrinkle-free section ribbons, the sides of the wax block are cut at 90° angles. The sections are cut on a microtome under cold H_2O vapor at a thickness of 7 μm. The angle and position of the blade has to be determined experimentally for each block. The section ribbons are laid on clean black paper with the dull side up. After several ribbons have been cut, small segments (typically three brain sections) from three to four different ribbons are mounted on one slide in a 45-50 °C warm water bath containing ddH_2O. The mounted slides are kept in a slide warmer overnight at 42°C. The next day they are arranged in clean boxes where they can be stored indefinitely at RT.

6.2.4.3 Linearization of plasmids

To get *sense* or *anitsense* probes, the plasmid must be cut with a restriction enzyme. Usually, plasmids are cut either with XhoI or BamHI. The enzyme XhoI destroys the T7-promoter, BamHI the Sp6-promoter. If the insert contains a restriction site for one of these two enzymes, another restriction enzyme must be chosen (see pCR®II-TOPO-vector map).

For each preparation, 40 μg of plasmid DNA, 6 μl enzyme buffer and 4 μl restriction enzyme are used. The total volume is filled to 60 μl with ddH_2O and then incubated o/n at 37°C. To check whether the digestion is complete, a small aliquot of the reaction is run on a 1 % agarose gel. If the digestion is finished, the DNA is recovered from the digestion mix using a phenol/chloroform extraction and precipitated with ethanol. For this, 340 μl of ddH_2O and 400 μl of phenol/chloroform are added to the entire digestion mix. The tube is shaken vigorously and then centrifuged at 13'000 rpm for 1 min at 4°C to separate the phases. The aqueous upper phase is removed and placed in a new Eppendorf tube and again extracted with

400 µl of phenol/chloroform. To precipitate the DNA from the aqueous phase, 40 µl of 4 M NH_4Ac and 1 ml of 100 % ethanol are added. The tube is then inverted several times and kept at –80°C for 15 min. Afterwards, it is centrifuged at 13'000 rpm for 20 min at 4°C, the supernatant removed, the pellet air-dried and then resuspended in 20 µl of DEPC water. The concentration of the DNA is determined using the spectrophotometer (see 4.2.1.2) and then diluted to a concentration of 1 µg/µl.

6.2.4.4 *In vitro* Transcription

The following reagents of the "RNAMaxx^{TM} High Yield Transcription Kit" are put on ice and mixed carefully to avoid contamination with RNases (gloves, autoclaved tubes and tips):

x µl	DEPC water
6.0 µl	5 x transcription buffer
1.0 µl	DTT [0.75 M]
1.0 µl	rATP [100 mM]
1.0 µl	rCTP [100 mM]
1.0 µl	rGTP [100 mM]
1.0 µl	RNAse block
0.5 µl	yeast inorganic pyrophosphatase [0.75 U/µl]
1.0 µg	linearized DNA template
10.0 µl	^{35}S-rUTP [12.5 mCi/ml]
1.0 µl	RNA polymerase (dependent on the promoter: T7, T3 or SP6)
30.0 µl	total volume

The contents are mixed well and incubated for 3 h at 37°C in a water bath. If the Sp6 RNAse polymerase has been used, additional 1.5 µl are added to the reaction mix after 1.5 h. After incubation, 2 µl of DNase I [10 U/µl] are added to the tube and incubated for 15 min in a 37°C water bath to digest the linearized plasmids composed of DNA. To precipitate the RNA, the following substances are added:

190 µl	ddH_2O
10 µl	tRNA (10 mg/ml)
250 µl	NH_4Ac (4 M)
1000 µl	100 % EtOH

The tube is carefully inverted, put on ice for 7 min and centrifuged at 13'000 rpm for 7 min at 4°C.

The supernatant is discarded and the pellet is washed with:

200 µl NH_4Ac (4 M)

200 µl ddH_2O

1000 µl 100 % EtOH

The tube is carefully inverted and centrifuged at 13'000 rpm for 7 min at 4°C. During this time, a complete hyb-mix is prepared by adding 10 µl of 10 M DTT and 10 µl of 25 mM ATP-α-S to a 1 ml aliquot of hyb-mix. Now, the supernatant of the centrifuged tube is discarded and the pellet dissolved in 100 µl complete hyb-mix. 2 µl of the complete hyb-mix containing the probe is added to 2 ml of scintillation cocktail in a plastic scintillation vial and the incorporated radioactivity is then measured in a scintillation counter.

6.2.4.5 Dewaxing, postfixation and hybridization of sections

All solutions used for the prehybridization must be RNase-free. This is achieved by flaming all glass bottles for 10 x stock solutions and weighing salts in aluminium foils using a flamed spatula. The volumes are filled up approximately (standard on the bottle) with ddH_2O, and the solutions are then autoclaved.

Most prehybridization solutions can be reused several times if kept RNase free. The PFA solution can be used only twice and should be stored at 4°C. Approximately 30 min before starting the experiment the PFA should be removed from the refrigerator so that it can warm up to RT, which is important for the pH. The proteinase K and acetylation solutions must be made fresh each time. Care should be taken not to introduce water into the acetic anhydride stock because it hydrolyses to acetic acid in the presence of water.

The slides are placed in a rack and then transferred into each solutions in the following order:

1. 2 x ultraclear to remove paraffin for 10 min
2. 2 x 100 % EtOH for 2 min
3. Rehydration series in EtOH/water, starting at 95 and progressing to 80, 70, 50, and 30 %. The slides are agitated in each solution for 20 s
4. 0.9 % NaCl for 5 min
5. 1 x PBS for 5 min
6. 4 % PFA for 20 min (this solution is re-used in step 9)
7. Proteinase K for 5 min (20 µg/ml proteinase K in 50 mM Tris-HCl, pH 7.6, 5 mM EDTA) → After this step, the tissue is particularly susceptible to RNases and should be handled from here on with extreme caution!
8. 1 x PBS for 5 min

9. 4 % PFA for 20 min
10. Acetylation in 0.1 M TEA/HCl pH 8: 600 µl of acetic anhydride is added to the solution as it is being stirred in a hood; after 3 min, an additional 600 µl of acetic anhydride is added. Total time = 10 min
11. 1 x PBS for 5 min
12. 0.9 % NaCl for 5 min
13. Dehydration series of EtOH, starting at 30 and progressing to 50, 70, 80, 95, 100 and 100 % for 20 s each.

The slides are air-dried in a dust-free RNase-free place at RT. After drying, 2 to 6 Mio cpm/slide of the radioactive probe are added to the hybridization mix and thoroughly mixed. 50 µl of this hybridization mix containing the probe are put onto each slide and spread with a yellow tip. The slides are carefully overlaid with a coverslip, placed in a humidified, sealed chamber and incubated o/n at 55°C.

The chamber is humidified by soaking strips of Whatmann paper in 50 % formamide/5 x SSC and sealed with parafilm and tape.

6.2.4.6 Posthybridization washes and autoradiography

Post-hybridization washes do not need to be carried out under RNase-free conditions. The removal, formamide and NTE solutions are prepared the day before and put in the corresponding water baths so that they are equilibrated to the right temperature when used. The formamide solution can be used twice and is then thrown out with the removal solution into the radioactive liquid waste.

The slides are placed in a rack and then transferred into each solutions in following order:

1. Coverslip removal wash: 200 ml 5 x SSC + 350 µl ME for 30 min at 63°C
2. 50 % formamide, 2 x SSC and 700 µlME for 30 min at 63°C
3. 3 washes with 1 x NTE for 10 min at 37°C
4. Ribonuclease A in 1 x NTE for 30 min at 37°C
5. 1 x NTE for 15 min at 37°C
6. 50 % formamide, 2 x SSC and 700 µl ME for 30 min at 63°C (solution from step 2 re-used) → 700 µl ME is added again
7. 2 x SSC for 15 min at RT
8. 0.1 x SSC for 15 min
9. Dehydration series starting at 30 and progressing to 50, 60, 80 % EtOH/0.3 M NH_4Ac, 95 % and 2 x 100 % EtOH for 30 s each

After these washes, the slides are air-dried in a dust-free place and then fixed with tape onto a plexi-glass sheet, which is then placed inside a film cassette and exposed to a Hyperfilm^{TM} MP from Amersham pharmacia biotech for 1 to 3 days. During the exposure time, the film cassettes are kept in a drawer at room temperature.

The film is developed in complete darkness as follows:

1. Developer for 5 min
2. Tap water for 30 s
3. Fixer for 1 min
4. Tap water for around 30 s

The film is dried and can be analyzed with a densitometer. To do this, the film is put right-side up into the densitometer and scanned. Using the program *Molecular Analyst alias* a square is drawn over the region of interest (e. g. SCN) and a measurement is taken. A square of the same size is made in an adjacent region to record the background. Three sections per slide are chosen, each from a different line. The values are finally integrated and visualized on a graph.

6.2.4.7 Emulsion coating

The emulsion is prepared by adding 118 ml Kodak NTB-2 emulsion to 200 ml deionized water in darkness using night vision goggles. Before mixing, the solutions must be warmed to 42°C for approximately 30 min. The emulsion is aliquoted into glass scintillation vials, wrapped twice in aluminium foil, and put in a light-tight box at 4°C away from β-radiation.

Before coating the slides, the emulsion has to be melted in a 42°C water bath for 10 min in darkness. The emulsion is transferred to a slide mailer, which is also kept in the water bath. The slides are dipped for 4 s and then drained for 3 s using night vision goggles. The back of the slide is thoroughly wiped with a soft tissue in order to remove remaining emulsion, placed on a slide dryer rack, and then dried o/n (at least for 6 hours) in a ventilated chamber. The next day, the slides are placed in a black box and wrapped in aluminium foil twice. Finally, they are stored at 4°C for three times as long as the cronex film was exposed to them.

6.2.4.8 Development and Hoechst staining

The fixer and developer (Kodak D-19) are delivered as a powder in bags and are prepared in advance. For the fixer, the contents of one bag are first dissolved in 2.8 l of distilled water and then filled up to a final volume of 3.8 l. The developer powder is slowly added to 3.8 l of

52°C distilled water and stirred until dissolved. The developer is kept in a brown glass bottle because it is light sensitive.

The slides are removed from the fridge and equilibrated at RT for 30 min in the darkroom keeping them in the sealed box. Then the slides are placed in a rack while wearing night vision goggles and developed as follows:

1. Kodak D-19 developer for 2 min (not longer!) at RT
2. Rinse in water for 30 s
3. Kodak fixer for 5 min at RT
4. Rinse up to 10 min in deionized (DI) water
5. Stain with Hoechst dye 2 μg/ml in water for 2 min
   (add 20 μl of stock 20 mg/ml in DMSO to 200 ml of DI water)
6. Rinse in DI water for 2 min

The slides are air-dried face up at RT for at least 1 hour in a dust free place. The place where they are dried should be dark because the Hoechst stain is light sensitive. Once dry, the slides are covered with 50 μl of a solution of 5 g Canada balsam in 10 ml methyl salicylate and then overlaid with a coverslip. The slides are kept horizontal for at least 1 week in a dark place so that the mounting medium dries. The residual emulsion on the back of the dry slides can be removed with glacial acetic acid on a Q-tip followed by ethanol to remove the acid.

6.2.4.9 Viewing and Photography

Hoechst staining dyes cell nuclei (DNA) and thus allows determination of cell density and tissue morphology. It can be detected using the DAPI channel of an epifluorescence microscope. Silver grains deposited after exposure to the radiactive probe are detected using darkfield microscopy. By viewing Hoechst staining and silver grains at the same time, one can determine which structure is expressing the gene of interest. Since Hoechst dye may bleach under fluorescent light, care should be taken in order to minimize its exposure.

Images are taken with a videocamera linked to a computer. The pictures of Hoechst staining and darkfield are acquired using the same settings in black and white format. It is very important not to change the position of the image because otherwise the images cannot be superimposed later. Pictures are saved as TIFF images and edited in Adobe Photoshop 5.0.

6.2.5 Cell culture

6.2.5.1 Solutions

- **10x TBS (pH 7.6):**

60.5 g	Tris
87.6 g	NaCl
4.0 ml	HCl 1 M

  The pH is adjusted to 7.6 and the volume completed to 1 l with ddH_2O. The solution is autoclaved before use.

- **Na_2HPO_4 0.5 M:**

179 g	Na_2HPO_4 x 12 H_2O

  The solution is filled up to 1 l with ddH_2O and then autoclaved.

- **0.25 % Trypsin /1 mM EDTA:**

5 ml	20 x TBS
85 ml	ddH_2O
10 ml	trypsine 2.5 % in PBS
120 µl	Na_2HPO_4 0.5 M
200 µl	EDTA 0.5 M

  All components except trypsine and EDTA are mixed and autoclaved, before 10 ml trypsin 2.5 % are added. To obtain a trypsin (0.25 %) / EDTA (2 mM) solution, 200 µl EDTA 0.5 M are added.

- **DMEM-Medium:**

1 bottle	DMEM High Glucose (4.5 g/l) from Amimed
5 ml	penicillin/streptomycin solution
5 ml	L-glutamine 200 mM
50 ml	HIFCS

  Final concentrations: 1 % PEST, 1 % L-Gln, 10 % HIFCS. The medium has to be stored at 4°C.

- **10x PBS (pH 7.4):**

80 g	NaCl
2.0 g	KCl
2.4 g	KH_2PO_4
14.4 g	Na_2HPO_4

  The powder is dissolved in 900 ml dH_2O and the pH is adjusted to 7.4. The volume is then filled to 1 l and the solution is autoclaved before use.

- **Trypan blue 0.2 % (w/v):**
  0.1 g Trypan blue is dissolved in 1 x PBS and stored at 4°C.

- **HIFCS:**
  The FCS is defrozen at room temperature before it is heat-inactivated (HI) at 56°C for 30 min. 50 ml aliquots are stored at -20°C until further use. In order to avoid any problems with remaining soap traces, the FCS is always aliquoted into the same glass bottles that are only rinsed with ddH_2O and autoclaved again before use.

- **Trypan blue 0.2 % (w/v):**
  0.1 g Trypan blue is dissolved in 50 ml 1 x PBS and stored at 4°C.

- **Collagenase type I [100 mg/ml]:**
  Dissolve in PBS and store 100-500 µl aliquots at -20°C.

- **Amphotericine B [250 µg/ml]:**
  Dissolve in sterile water and store 0.5-1 ml aliquots at -20°C.
- **Dexamthasone [10 mM]:**
  The powder is dissolved in 100 % EtOH and stored at -20°C.
- **Digestion medium:**

50 µl	collagenase
100 µl	amphotericine B
200 µl	PEST 1000 U
5 ml	DMEM supplemented with 10 % FCS, 1 % PEST, 1 % glutamine

  Since collagenase is not sterile, the digestion medium has to be passed through a sterile 0.2 µm Whatman filter. Final concentrations: collagenase 1 mg/ml, amphotericine B 5 µg/ml, pen/strep 500 U. The unusally high concentrations are necessary in the beginning to avoid contamination problems; however, they should not be maintained in normal culture.
- **LINPEI25 stock solution [100 µM]:**
  0.5 g LINPEI25 is dissolved in 150 ml ddH_2O. After adjusting the pH to 6.5, the volume is filled up to 200 ml with ddH_2O. Then the solution is filtered through a sterile filter (0.2 µm) and 20-25 ml aliquots are stored at -80°C.
- **LINPEI25 working solution [10 µM]:**
  The 100 µM stock solution is diluted 1:10 in sterile ddH_2O. One aliquot is stored at 4°C for transfections, whereas the rest is kept at -80°C.
- **1x HBS buffer:**

20 mM	HEPES pH 7.4
150 mM	NaCl

  The solution is sterile filtered and stored at 4°C.
- **Calf thymus DNA (CT):**
  100 mg CT-DNA is dissolved in 10 ml TE at 37°C. The suspension is sonicated for around 40 seconds until the solution is nicely liquid and well homogenized. Sometimes it may help to increase the volume to 20 ml. The fragment sizes are checked on an agarose gel. 20 ml of phenol are added and the tube is centrifuged at 4500 rpm and RT for 15 min. The aqueous phase is transferred to a new tube and extracted once more with 20 ml chlorophorm-phenol. Again the aqueous phase is taken and 2 ml of 3 M NaCl and 25 ml of 100 % EtOH are added to the tube. The DNA is precipitated o/n at -20°C. The next morning the DNA is pelleted at 9000 rpm at RT for 15 min. The supernatant is decanted and the pellet is washed once with 80 % EtOH and once with 100 % EtOH. The pellet is then air-dried and dissolved in 50 ml TE. The amount of DNA is determined using the photospectrometer and adjusted to 0.5 µg/µl. Aliquots of 500 µl are stored at -20°C.
- **Lysis buffer:**

50 mM	Tris-HCl pH 8.0
10 %	Glycerol
10 mM	MgAc
0.2 %	10 % Triton X-100

- **10x reaction buffer for luciferase assay:**

250 mM	Tris-HCl pH 7.5
10 mM	ATP
100 mM	MgAc
1 mg/ml	BSA

  5 ml aliquots are stored at -20°C.

- **Coenzyme A stock solution [20 mg/ml]:**
  100 mg coenzyme A
  5 ml PIPES 25 mM
  100 µl aliquots are stored at -20°C.
- **Luciferine stock solution:**
  10 mg luciferine
  20 ml NaOH 5 mM
  Adjust the pH to 6.5 with HCl and fill up the volume to 35 ml with ddH_2O. 1 ml aliquots are stored at -20°C. Since the luciferine is light sensitive, it is important to wrap the tubes in aluminium foil.
- **MUG stock solution [10 mg/ml]:**
  0.5 g MUG
  50 ml DMSO
  The solution is stored at -20°C wrapped in aluminium foil.
- **Luciferine injection buffer:**
  100 µl coenzyme A stock
  1 ml luciferine stock
  250 µl PIPES 0.5 M
  The volume is filled up to 10 ml with ddH_2O and stored at -20°C wrapped in aluminium foil.
- **Reaction buffer for MUG assay:**
  100 mM Na_3PO_4
  2 mM $MgCl_2$
  The pH is adjusted to 8.0 with HCl.
- **Stop solution for MUG assay:**
  300 mM glycine
  15 mM EDTA
  The pH is adjusted to 11.5 with NaOH.

6.2.5.2 Maintenance of cells

Since mammalian cells are very sensitive to contaminations with bacteria, fungi or other micro-organisms, all manipulations have to be done under a hood with laminar flow. All cells are cultured in high glucose (4.5 g/l) Dulbecco's modified Eagle's medium (DMEM) supplemented with 5 mM L-glutamine, 1 % penicillin/streptomycin and heat inactivated fetal calf serum (HIFCS) in an incubator that is set to 37°C and 5% CO_2. Once the cells are confluent, most cell lines are detached from the plate using trypsin. For this, the cells are washed twice with 1x PBS before a small amount of trypsin is added. The plate is gently rotated and the excess trypsin is aspirated. After a short incubation of around 30 seconds to maximum five minutes in the incubator, the cells are detached from the plate adding DMEM. The cell suspension is then diluted in a final volume of 10 ml DMEM for a ∅10 cm plate and incubated again until confluent.

Since NIH108-15 cells do not adhere firmly to the plate they can be simply detached from the plate by vigorously pipetting up and down 1x PBS. The suspension is then centrifuged at RT and 1000 g for 5 min. Once the supernatant is discarded, the pellet is completely resuspended in DMEM and diluted for further culturing.

6.2.5.3 Counting of cells using a Neubauer hemacytometer

For some cell culture experiments it is very important to work with an exact number of cells. For this, the cells are counted using an improved Neubauer hemacytometer, an instrument for estimating the number of cells in a measured volume under the microscope. Developed originally for counting blood cells, these chambers are widely used in cell culture to determine the concentration of cells in a suspension. The improved Neubauer hemacytometer is a thick glass slide with two counting chambers, each 0.1 mm deep. Each chamber is divided into nine large squares delineated by triple white lines. The center square is further subdivided into 25 squares. These 25 squares are again subdivided into 16 squares. Hemacytometer cover slips must be used to ensure even surfaces and coverage of both counting chambers. The grid surface is 0.1 mm below the cover slip. Therefore the volume of fluid over one of the 1 mm^2 areas of the grid (they are nine in total) is 0.1 mm^3 or 0.0001 ml. Facultatively, trypan blue which is the most common stain used to distinguish viable cells from non-viable cells can be added. Only non-viable cells absorb the dye and appear blue and asymmetrical. Conversely, viable cells appear clear in a bluish background.

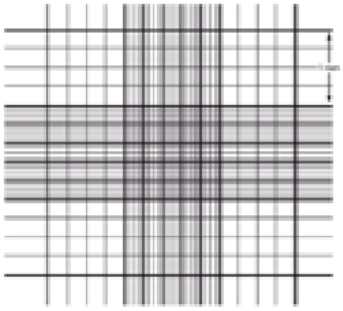

Fig. 6.2-4:
Improved Neubauer hemacytometer counting grid

The procedure is as follows:

1. 100 µl of cell suspension is mixed with 100 µl trypan blue 0.2 %. The dilution has to be done just prior to use since viable cells absorb trypan blue over time. This can affect counting and viability results.
2. A cover glass is centered over the hemacytometer chambers.
3. One chamber is filled with 10 µl of the cell dilution. The solution will pass under the cover glass by capillary action. If the solution spreads into the two lateral grooves adjoining the grid table, the hemacytometer has to be cleaned and the application has to be repeated. The same has to be done if there are any bubbles in the solution covering the grid table.

4. The hemacytometer is placed on the stage of an inverted microscope (Nikkon, TMS-F) and the focus is adjusted.
5. The white cells are counted in at least 3 squares using a hand-held counter. All the cells that touch the boundary of the area are counted on two sides, but not on the other two sides.
6. The number of cells per ml and the total number of cells is determined using the following calculations:

$$\text{cells/ml} = \frac{\#\text{ of cells counted}}{\#\text{ squares counted}} \bullet 10^4 \bullet \text{dilution factor}$$

$$\text{total cells} = \text{cells/ml} \bullet \text{vol. of original cell suspension}$$

The dilution factor is 2, the # of counted squares 3, and the volume of original cell suspension 5 ml.

7. The total cell suspension is diluted to 10'000 cells / 50 µl.
8. 50 µl of this dilution are applied to each well of a 96 well culture plate. For each genotype three plates are prepared (6 in total).
9. 100 µl of DMEM are added to each well to get a total volume of 150 µl per well.

The cells are incubated 1-2 days at 37°C and 5 % CO_2 to become confluent.

6.2.5.4 Preparation of mouse embryonic fibroblasts (MEFs)

6.2.5.4.1 Isolation of embryos and preparation of fibroblasts

Approximately two weeks before the embryos of a mouse can be harvested, the mating needs to be set up and must be checked to see if the female is pregnant. The morning of a successful copulation, one may see a white plaque at the back of the female and from this morning on, it will take about twelve days for the embryos to be ready. However, the form of the belly should also be checked to see whether it changes shape or not. If the belly becomes rounder on the sides, it is a good indication of pregnancy.

Before the female is killed, two Petri dishes, each with 1 x TBS are prepared under the hood. One of the dishes is left in the hood and the other is placed next to where the mouse will be sacrificed. The pregnant female is killed by cervical dislocation, the belly opened with scissors, and the womb transferred to the Petri dish. The dish is transported under the hood because the next steps must be carried out in a sterile environment.

First, the embryos are taken out of the womb. Their anatomy is compared to that in pictures from the book, "The Atlas of Mouse Development" (M. H. Kaufman) to determine at which embryonic stage they were. They are then dissected by cutting off the head and by removing the liver in TBS. After this, they are moved to a fresh Petri dish containing 1 x TBS, where they are cut into small pieces and then placed in a 2 ml syringe (without a needle). Four embryos are pressed through the syringe into a small cell culture bottle, given 5 ml of trypsin-EDTA (2 mM), and the bottle is then incubated at 37°C for 30 min to disintegrate the tissue structure. When the embryos become viscous, 20 ml of medium (DMEM high glucose: 10 % FCS, 1 % PEST, 1 % L-Gln) are added to stop the reaction. After the embryos have been resuspended in the medium, the mixture is transferred to a 50 ml Falcon tube and centrifuged for 5 min at 3'000 rpm to precipitate the fibroblasts. The supernatant is discarded and the cells are resuspended in 20 ml of medium and plated in two ∅10 cm plates. The fibroblasts are incubated o/n at 37°C and 5 % CO_2.

6.2.5.4.2 Splitting of fibroblasts 1 day after isolation (100 % confluent)

The Petri dishes are removed from the incubator, the old medium transferred to a 50 ml Falcon tube using a 25 ml sterile pipette, and then centrifuged for 5 min at 3'000 rpm. The supernatant is collected into a new 50 ml Falcon tube. During the centrifugation, the fibroblasts are split as follows:

1. 2 washes with 5 ml 1 x PBS
2. 1 ml of trypsin-EDTA (1 mM) for 1 min at 37°C
3. addition of 10 ml medium with a 10 ml pipette
   → the cells are loosened from the bottom of the dish by pipetting them up and down vigorously
4. 10 new Petri dishes are prepared out of one by moving 1 ml of the new medium containing the fibroblasts to each one of them
5. 8 ml of new medium is added to each one of the new plates
6. 1 ml of the old medium is added to each one of the new plates

It is very important to add some of the old medium to each new Petri dish because it contains factors that accelerate the growth of the fibroblasts. The plates are incubated until they are confluent (usually 2-3 days) at 37°C and 5 % CO_2.

6.2.5.4.3 Freezing of fibroblasts

Fibroblasts can be frozen as soon as they are confluent. To do this, 1 ml FCS/DMSO (10 %) is prepared in advance for each plate. For 10 ml of solution, 1 ml DMSO is mixed with 9 ml of FCS and chilled on ice. It is very important that this solution is ice cold because the DMSO will otherwise form crystals that will destroy the cells. To slowly cool down the fibroblasts, a freezing box (StrataCooler® Cryo Preservation Module, Stratagene, catalog #400005) is put at –20°C.

The plates are taken out of the incubator, washed twice with 5 ml 1 x PBS, and treated with 1 ml trypsin-EDTA (2 mM) for 1 min at 37°C. The reaction is stopped by adding 5 ml of medium. The fibroblasts are resuspended and moved to a 50 ml Falcon tube. Unfortunately, it is not possible to trypsinate all of the dishes simultaneously because the fibroblasts quickly readhere to the bottom of the dish after medium is added. Typically only four plates are treated at the same time. The entire medium containing the fibroblasts from these four dishes is collected in the same Falcon tube and centrifuged at 3'000 rpm for 5 min. The supernatant is discarded and the cells resuspended in 4 ml ice cold FCS-DMSO (10 %) and aliquoted into cryovials (1 ml each). The tubes are put into the pre-cooled freezing box and kept at –80°C overnight. The next day the fibroblasts are transferred into liquid nitrogen for long-term storage.

6.2.5.4.4 Thawing of fibroblasts

The cryovials are taken out of the liquid nitrogen, thawed at RT, and then 1 ml of warm medium (37°C) is added to each vial. After this, the cells are transferred to a 50 ml falcon tube containing 10 ml of warm medium and are then centrifuged at RT for 5 min at 3000 rpm. The supernatant is discarded, the cells resuspended in 10 ml medium and again centrifuged at RT for 5 min at 3000 rpm. The supernatant is again discarded and the cells are plated in 10 ml medium per plate. The Petri dishes are incubated o/n at 37°C and 5 % CO_2. If they are confluent the next day, they can be used for experiments, if not, the medium containing the dead cells is removed and they are washed twice with 1 x TBS. Then 10 ml new medium is added and they are incubated again until they are confluent.

6.2.5.5 Preparation of mouse dermal fibroblasts (MDFs)

Before the mouse is sacrificed, scissors and forceps have to be sterilized (70 % EtOH and flaming) and a falcon containing 10 ml of normal medium has to be put on ice (it is important to use the Amimed medium). The mouse is anesthetized with isoflurane and sacrificed by

cervical dislocation. The head of the mouse is sprayed with 70 % ethanol before the top parts of the ears are cut and put into the ice-cold medium. Alternatively, one can also use skin from the back. For this, the hairs have to be pulled out and the skin has to be sterilized by spraying 70 % EtOH. Then pieces of about 1 cm^2 are cut taking as little connective tissue and subcutaneous fat as possible. Under the hood, for each piece of tissue, a Petri dish containing 5 ml of digestion medium is prepared. In this medium, the tissue is cut into as small pieces as possible using a scalpel blade and left o/n in an incubator. The next day, the cell suspension is passed through a narrowed sterile glass Pasteur pipette (not more than 10 times) before it is centrifuged at 4000 rpm and RT for 10 min. The supernatant is discarded and the pellet is resuspended in 3 ml of DMEM supplemented with 20 % HIFCS, 1 % PEST, 1 % L-Gln before it is transferred to one well of a six-well plate. Once they are confluent, the cells are split and diluted in 20 % HIFCS / DMEM after trypsinization during three passages. It should be avoided to split them higher than 1:4 because they need to be in close contact to each other. One six-well split onto a 5 cm dish corresponds to a dilution of about 1:1.5 and a 5 cm dish split onto a 10 cm dish corresponds to about 1:3. After three passages, the cells can be transferred to a 10 cm dish and the HIFCS can be reduced to 10 %. Cells enter in crisis after about 6 to 7 passages but will continue to grow and eventually immortalize. MDFs can be frozen the same way as MEFs.

If bacterial contaminations are found in the cultures while the cells are still in six-well plates in spite of the antibiotics, immediately aspire the medium and fill the well with 70 % EtOH or Sekusept solution. Leave a few minutes at RT and aspire. Put the plate back into the incubator. If fungi are found, add 5 µg/ml amphotericine B to the medium until the cells are split, and keep them in medium supplemented with 2.5 µg/ml amphotericine B for the next passage.

6.2.5.5.1 Thawing of MDFs

The MDFs are thawed in a 37°C water bath until only a small piece of ice is left. Then the tube is sprayed with 70 % EtOH and wiped. The cells are transferred carefully into a 15 ml Falcon tube and 9 ml of normal medium is added slowly drop by drop before the tube is centrifuged at 4000 rpm for 5 min. The pellet is resuspended in 2 ml of DMEM and put into one well of a six-well plate. After one day, the medium has to be changed and the cells are split as soon as they are confluent.

6.2.5.5.2 Immortalizing of MDFs

Since primary cells reach their senescence after a limited number of population doublings one has to either re-establish fresh cultures from explanted tissue or to immortalize the cells. The MDFs immortalize spontaneously at low frequencies by passing through replicative senescence after around 20 passages. However, it is important to note that these spontaneously immortalized cells have unstable genotypes and are host to numerous genetic mutations compared to cells that are immortalized via viral transformation or through the expression of the telomerase reverse transcriptase protein. Although the process of viral transformation is relatively simple and reliable, these cells may also become genetically unstable and might lose the properties of primary cells.

The primary MDFs are defrozen as described above and then immortalized by successive transfer (Todaro and Green, 1963). Briefly, they are cultured in tissue culture flasks (75 cm^2) to decrease the contamination risk and split as soon as they are confluent. After six to seven passages they start to enter crisis and divide very slowly. During this time the medium has to be changed twice a week and the cells have to be detached from time to time with trypsine and put back 1:1 into a new flask. As soon as the cells look better again and divide faster they have to be split very carefully and should only be diluted 1:2 or 1:3. After around 20 passages they are immortalized and aliquots can be frozen and stored in liquid nitrogen as described above.

6.2.5.6 Synchronization of cells via dexamethasone shock

Since the master clock is missing in mammalian cell culture, all the cells in a culture dish are ticking according to their own internal rhythm. However, for some experiments it is important that their clocks all tick synchronously. This synchronization can be achieved by various methods such as a serum or a dexamethasone shock.

For the dexamethasone shock, the old medium has to be removed from the plate and replaced by new medium containing 100 nM dexamethasone (t = 0). For this, 0.1 µl of the 10 mM stock solution are added to 10 ml of fresh medium. The plate is put back into the incubator for 20 min. Then the cells are washed twice with serum-free medium before normal medium is added. The cells are now synchronized and can be put back into the incubator for some time depending on the phase of the gene or protein of interest. At its peak expression time or at regular intervals the cells are harvested and processed for either RNA or protein extraction.

One should always keep one control sample in which no dexamethasone has been administered.

6.2.5.7 Transfection of cells using linear polyethylenimine (LINPEI25)

Contrary to branched polyethylenimines, linear polyethylenimines contain only secondary amines. However, the characteristic of all polyethylenimines is that they have a high cationic-charge density, which makes them an excellent condensing agent with the negatively charged DNA. The linear polyethylenimine with a molecular weight of 25 kDa (LINPEI25) is an effective “proton sponge”. Once the DNA/LINPEI25 complex enters the cell, the DNA is protected from lysosomal degradation due to its interaction with LINPEI25. Many cell lines can be transfected at high efficiencies with LINPEI25 because of its low toxicity for the cells. Another advantage of LINPEI25 is that the presence of serum does not interfere with transfection efficiency.

6.2.5.7.1 Preparation of cells for co-transfection

About one day prior to transfection, cells were transferred from a ∅10 cm plate to a 6-well plate with 2 ml medium per well. Each cell line needs a different dilution:

- Cos-7 & NIH/3T3 cells → 1:4
- HEK293 cells → 1:3
- NG108-15 & HEPG2 cells → 1:2.5

NG108-15 cells were transfected at a confluence of 60-80 % whereas the other cell lines were transfected at 80 % confluence.

6.2.5.7.2 Preparation of the LINPEI25/DNA complex

Since the number of negative charges of the DNA phosphate groups and the number of positive charges of the LINPEI25 nitrogens depends on the pH of the solution it is easier to take into account the nitrogen molarity (N) on the phosphate molarity (P) ratio (N/P). In order to get optimal results, the amount of LINPEI25 used has to be calculated according to the following formula:

No. of equivalents = 15.44 x amount of DNA [μg]

One equivalent corresponds to the quantity of 10 μM LINPEI25 [μl] required to match the nitrogen content to phosphate contained in the DNA. The LINPEI25/DNA complex is prepared in 1x HBS buffer to a total volume of 200 μl. Each transfection mix contains 0.05

μg of CMV-*lacZ* DNA as transfection efficiency control, different amounts of promoter-luciferase construct DNA, and different amounts of protein expression plasmid DNA. Besides, calf thymus DNA and empty expression vector (pSCT1) is added to each mix to equilibrate for the maximal amount of DNA or expression plasmid used within the experiment. Furthermore, a negative control consisting of only calf thymus DNA has to be included in every experiment. Finally, the appropriate amount of LINPEI25 is pipetted to each tube. The mixture has to be vortexed immediately after the addition of the LINPEI25 for a few seconds before it is incubated at RT for 20 to 30 min. The incubation time influences the size of the complex and thus is important for transfection efficiency. After the incubation, the mixture is added gently drop by drop to the cells and the 6-well plate is gently rocked to evenly distribute the complexes within the medium. The cells are kept in the incubator for 6 hours. Then the medium is aspirated and replaced with 2 ml fresh medium. The cells are incubated again for 18-30 hours before they are harvested as described below. Alternatively, one can use 13 or less equivalents of 10 μM LINPEI25 and incubated the cells for 24-36 hours without changing the medium after the transfection.

6.2.5.7.1 Cell harvesting

24-36 hours after transfection, the medium is aspirated from the culture dish and adherent cells are rinsed twice with 1 ml 1x PBS. Then they are harvested in 1 ml 1x TBS/5 mM EDTA, transferred into a reaction tube and pelleted via a 1 min centrifugation at 9000 rpm and 4°C. Since NG108-15 cells are not really adherent to the plate, they can be harvested simply by detaching them from the plate with 1 ml 1x PBS without prior washing. Then they are centrifuged directly at 9000 rpm for 1 min and the pellet is washed once in 1x PBS. The supernatant is discarded and the pellet is resuspended by pipetting up and down in around 50-80 μl of lysis buffer depending on the pellet size. The tube is immediately put on ice for at least 5 min and then centrifuged at 9000 rpm and 4°C for 5 min. The lysate is transferred into a 96-well plate kept on ice and either assessed directly or stored at -20°C for up to one week.

6.2.5.7.2 Luciferase assay

The luciferase assay is carried out according to the manufacturer's instructions described in the manual "Luciferase Assay System" from Promega (Technical Bulletin 281). 10 μl of cell lysate are assayed in duplicates on a 96-well plate (NUNC^{TM} Brand Product) for the activity of the translated luciferase promoter construct. 100 μl of 1x reaction buffer is added to each

well and 100 µl of luciferine injection buffer is directly injected into each well by the luminometer, which measures the generated bioluminescence of each well for 10 seconds.

6.2.5.7.3 MUG assay

The measured luciferase activity of the promoter construct has to be normalized to the transfection efficiency of the experiment by determining the β-galactosidase activity of the co-transfected lacZ expression plasmid. MUG (4-methylumbelliferone b-D-galactopyranoside) is used as a substrate for β-galactosidase because it fluoresces upon hydrolysis by the enzyme. The hydrolysis product of MUG, 4-methylumbelliferone (MUB), has an excitation peak at 372 nm with a fluorescence emission peak at 445 nm.

For the assay, a mixture of 1.45 ml MUG stock solution and 13 ml MUG reaction buffer has to be pre-warmed to 37°C (MUG solution). Depending on the cell line used, the protein extracts have to be more or less diluted in lysis buffer. 10 µl duplicates of the diluted extract are pipetted onto a NUNC™ Brand Product 96-well plate that is placed on ice. 140 µl of the pre-warmed MUG solution are added to each well, before the plate is wrapped in aluminium foil and incubated at 37°C for 20 to 60 min depending on the cell line. Once the incubation time is over, 100 µl of MUG stop solution are added to each well and the fluorescence is read using the flurimeter (Multidetection microplate reader, BIO-TEK). The following endpoint protocol parameters are used:

- Excitation: 360/40
- Emission:460/40
- Optic position: Top
- Sensitivity: 30
- Plate type: 96 well
- Reading direction: horizontal
- Shaking: NO
- Temperature control: NO

The luciferase activity is then normalized dividing it by its corresponding β-galactosidase activity. Furthermore, the data can be expressed as fold induction normalizing it relative to the empty reporter plasmid.

6.2.5.8 RNA isolation from cells

The medium is aspirtated from the plate and the cells are washed twice with cold 1x PBS before they are lysed in RNAbee (2 ml RNAbee are added to a ∅10 cm plate and 1 ml to a ∅5 cm plate). Once the cells are completely detached, the plates can be either stored at -80°C or the lysate can be transferred to a reaction tube. 100 µl of chloroform are added to 1 ml of RNAbee before the tube is incubated on ice for at least 5 min. After the incubation, the

suspension is centrifuged at 13'000 rpm and 4°C for 15 min. The homogenate now forms two phases: the lower blue phenol-chloroform phase and the colourless upper aqueous phase. DNA and proteins are located in the interphase and organic phase. The aqueous layer is transferred into a fresh tube and an equal volume of isopropanol is added to this to precipitate the RNA. The tube is carefully inverted several times and stored at -20°C for 15 min. Then the DNA is pelleted at 13'000 rpm and 4°C for 20 min. The pellet is washed once with 75 % ethanol by turning the tube in your hands. The ethanol is discarded and the pellet is dissolved in DEPC-H_2O. The same volume of 0.4 M sodiumacetate/0.2 % SDS is added at room temperature. Then the mixture is extracted with one volume of chlorophorm-phenol. The aqueous layer is transferred to a new reaction tube and two volumes of 100 % ethanol are added. DNA precipitation is enhanced by an incubation of 20 min at -20°C. The tube is then centrifuged at 13’000 rpm and 4°C for 20 min. The pellet is washed once in 75 % and once in 100 % ethanol before it is air-dried and dissolved in DEPC-H_2O.

6.2.6 Protein methods

4.2.6.1 Cell fractionation for cytoplasmic and nuclear protein extracts

4.2.6.1.1 Solutions

- **Buffer A (hypotone):**

			for 50 ml:
10 mM	Hepes-KOH, pH 7.9		10.00 ml of a 0.05 M stock
1.5 mM	$MgCl_2$		75.00 µl of 1 M stock
10 mM	KCl		166.70 µl of a 3 M stock
	ddH_2O		fill up to 50 ml
0.5 mM	DTT	*add before use only*	1.00 µl/ml
	protease inhibitors		10.00 µl/ml*
0.5 M	NaF		10.00 µl/ml
200 mM	Na_3VO_4		1.00 µl/ml

- **Buffer B (hypertone):**

			for 10 ml:
20 mM	Hepes-KOH, pH 7.9		4.00 ml of a 0.05 M stock
25 %	Glycerol		2.94 ml of 87 % glycerol
0.42 M	NaCl		0.84 ml of a 5 M stock
1.5 mM	$MgCl_2$		15.00 µl of a 1 M stock
0.2 mM	EDTA		4.00 µl of a 0.5 M stock
	ddH_2O		fill up to 10 ml
0.5 mM	DTT	*add before use only*	1.00 µl/ml
	protease inhibitors		10.00 µl/ml*
0.5 M	NaF		10.00 µl/ml
200 mM	Na_3VO_4		1.00 µl/ml

*: of a solution of one complete EDTA-free protease inhibitor tablet (Roche) dissolved in 500 µl ddH_2O

- **Sucrose solution:**

2.4 M Sucrose
10 mM Hepes-KOH, pH 7.6
15 mM KCl
0.5 mM spermidine
0.15 mM spermine
} *dilute 1:4*

6.2.6.1.2 SCN fractionation

The animals are anesthetized using isoflurane and then sacrificed at the desired time point. The SCN region (fig. 6.2-5A) is extracted using two tweezers with ultra fine precision tips (e.g. Dumont tweezers #5) and frozen immediately in liquid nitrogen. Before homogenization, four samples are pooled in one tube and 280 µl (70 µl / animal) of buffer A containing protease inhibitors are added. The tissues are then homogenized thoroughly using an Eppendorf fitting pestle-homogenizer (fig. 6.2-5B) keeping tubes on ice at all times. The homogenate is then incubated on ice for 30 min, flicking the tubes from time to time. After adding NP40 substitute to 0.3% (diluted from a 10 % v/v stock), the mixture is forced 10

times through a 25 G needle on ice and incubated again on ice for another 30 min. Once the hypotonic lysis is finished, the tubes are vortexed for 10 s and then centrifuged at 1200 g (3600 rpm in an Eppendorf centrifuge) for 5 min at 4°C. The supernatant is transferred carefully to a fresh tube in order not to disturb the pellet because otherwise the cytosolic fraction could be contaminated with nuclei. The pellet is resuspended in 140 µl of buffer A containing 0.3 % NP40 substitute and the mixture is overlaid onto 800 µl of 0.6 M sucrose buffer. The tube is centrifuged for 2 min at 10'000 rpm and 4°C. The supernatant is discarded and the pellet is suspended again in 140 µl of buffer A containing 0.3 % NP40 substitute. After another centrifugation of 10'000 rpm for 6 min at 4°C, the pellet is suspended in 200 µl of buffer A (without NP40 substitute). The nuclei are pelleted in a microfuge at 3600 rpm and 4°C for 3 min. After having discarded the supernatant, 200 µl of buffer A (without NP40 substitute) are added to the pellet and the mixture is incubated on ice for 5 min before it is centrifuged at 3600 rpm and 4°C for 5 min. The purified nuclei are then lysed hypertonically in 55 µl of buffer B (13.75 µl / animal) at 4°C in rotating wheel during 30 min. The tube is then centrifuged at 13'000 rpm and 4°C for 15 min and the supernatant is taken as the nuclear fraction. The protein concentration is measured using the Bradford assay from BioRad. Two distinct standard curves have to be done for the cytoplasmic and the nuclear fraction, each containing the same volume of buffer A or B that has been used to extract samples.

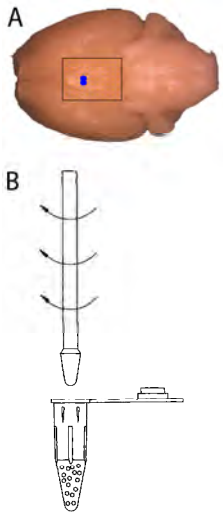

Fig. 6.2-5: **A** Ventral view of a mouse brain and marked SCN region
B Eppendorf fitting pestle-homogenizer

6.2.6.2 Determination of protein concentrations according to Bradford

Although protein assays don't tell us anything about the kind of proteins present in a sample, they are important to determine the total amount of proteins in a sample. A good protein assay should be specific, sensitive, and fast. Unfortunately, the perfect protein assay does not exist. Due to this, one test has to be chosen over another for ease of use or specific scientific limitations (e.g. interferences). Nowadays, the most commonly used protein assays are the Bradford and bicinchoninic acid (BCA) assays.

An advantage of the Bradford assay is that it is fast and easy to do and the variability between proteins is small. Furthermore, ready to use Bradford reagents can be bought from many companies (e.g. BioRad). Its principle is based on the observation that the maximum absorbance for an acidic solution of Coomassie Brilliant Blue G-250 shifts from 465 to 595 nm when binding to proteins occurs. Disadvantages of this assay are that Coomassie Blue

does not bind some specific proteins (e.g. trypsin) and that the Bradford reagent is acidic, which precipitates some proteins. Additionally, some detergents like Triton X-100, SDS or Chap interfere with the assay.

In parallel to each protein determination a standard curve has to be prepared. A concentration range should be used that produces an A_{595} that does not exceed 1.0 A units in the assay. The standard curve is prepared using 1, 2, 5, 7, 10 and 12 µg BSA. All samples have to be mixed well and incubated at room temperature for 10 to 20 min before measuring the absorption at 595 nm. For more details see the manufacturer's manual (BioRad). The reaction mixtures are pipetted as follows:

BSA standard curve	**samples**
x µl of BSA [1 µg/µl]	y µl of fraction
1200-x µl dH_2O	1200-y µl dH_2O
300 µl Bradford reagent	300 µl Bradford reagent

It is important to add the Bradford reagent to all tubes in parallel at the end.

6.2.6.3 Western blot

6.2.6.3.1 Solutions

- **10 % Ammoniumpersulfate (APS):**
  1 g APS
  10 ml ddH2O
  The solution can be stored for several months at 4°C. If the gels do not solidify anymore as they should, a fresh APS solution should be prepared.
- **20 % SDS:**
  100 g SDS
  350 ml ddH_2O
  Once the SDS is dissolved, the solution is filled up to 500 ml with ddH_2O and stored at RT.
- **4x Upper solution:**
  15.14 g Tris [final concentration (f.c.) ≡ 0.5 M]
  5 ml 20 % SDS stock
  The pH is adjusted to 6.8 and the volume completed to 250 ml. The solution is stored at RT.
- **4x Lower solution:**
  45.42 g Tris [f.c. ≡ 1.5 M]
  5 ml 20 % SDS stock
  The pH is adjusted to 8.8 and the volume completed to 250 ml. The solution is stored at RT.
- **10x Running buffer:**
  30 g Tris [f.c. ≡ 0.248 M]
  144 g Glycin [f.c. ≡ 1.918 M]
  800 ml ddH_2O
  The volume is adjusted to 1 l and the solution is stored at RT.

- **1x Running buffer:**

100 ml	10x running buffer
5 ml	20 % SDS stock
800 ml	ddH_2O

  The volume is adjusted to 1 l and the solution is stored at RT.

- **4x Loading buffer:**

2 ml	20 % SDS stock [f.c. ≡ 4 %]
3.6 ml	water-free glycerol [f.c. ≡ 36 %]
400 µl	β-mercaptoethanol [f.c. ≡ 4 %]
4 ml	4x upper solution, pH 6.8 [f.c. Tris ≡ 0.2 M]

  The solution is stored at RT.

- **10x PBS pH 7.4:**

2 g	KH_2PO_4 [f.c. ≡ 14.7 mM]
2 g	KCl [f.c. ≡ 26.8 mM]
80 g	NaCl [f.c. ≡ 1.37 mM]
14.2 g	Na_2HPO_4 x $2H_2O$ [f.c. ≡ 79.7 mM]
800 ml	ddH_2O

  The pH is adjusted to 7.4 and the volume completed to 1000 ml with ddH_2O.

- **Transfer buffer for wet transfer:**

1 vol	10x running buffer
2 vol	methanol (technical grade)
7 vol	dH_2O

  For a better transfer, 5 ml of the 20 % SDS stock can be added to 1000 ml of transfer buffer. The solution has to be stored at 4°C.

- **10x TBS pH 7.5:**

121.14 g	Tris
87.66 g	NaCl
800 ml	ddH_2O

  The pH is adjusted to 7.5 and the volume completed to 1000 ml with ddH_2O.

- **1x TBS-Tween®-20:**

100 ml	10x TBS pH 7.5
1 ml	Tween®-20
900 ml	ddH_2O

  Store at 4°C.

- **5 % (w/v) milk-TBS -Tween®-20:**

25 ml	10x TBS pH 7.5
0.25 ml	Tween®-20
12.5 g	Rapilait milk powder
200 ml	ddH_2O

  The volume is adjusted to 250 ml with ddH_2O and the solution is stored at 4°C.

6.2.6.4.1 Sodium dodecyl sulfate polyacrylamide gel electrophoresis (SDS-PAGE)

SDS-PAGE is a technique that is widely used to separate proteins according to their electrophoretic mobility, which depends on the length of the polypeptide chain, posttranslational modifications, protein folding, charge and other factors. The polyacrylamide gel can be prepared with a wide range of average pore sizes, which are determined by both the

total amount of acrylamide present and the amount of cross-linker present in the gel. Pore size increases with decreasing amount of polyacrylamide. The gel is composed of two layers: a stacking gel on the top, which concentrates the proteins at a thin starting zone (Kohlrausch reaction), and a resolving gel at the bottom, which separates the proteins according to their size and charge. The former is a large pore gel containing usually around 4-5 % polyacrylamide, whereas the latter is a small pore gel containing 4-30 % polyacrylamide.

The polyacrylamide gel is usually casted in a multiple gel caster as described in the manufacturers manual (SE 275, Hoefer Scientific Instuments). For each gel being prepared, one glass plate, one aluminium plate, two spacers and 1 comb have to be cleaned with 70 % EtOH before the gel sandwich is assembled within the gel caster. Then, the resolving gel is mixed according to table 6.2-1, poured into the gel caster to 2.5 cm below the top of the rectangular glass plate and overlayed with isopropanol. Once the gel solidified, the isopropanol is decanted and the gels are washed with dH_2O before the stacking gel mixture is poured on top of the resolving gel. The comb is inserted and the gel allowed to polymerize.

Once the gel has solidified, the comb is removed and the gel is cleaned with dH_2O. The gel is then put into the electrophoresis apparatus (SE 250 Mighty Small II, complete, Hoefer Scientific Instruments). The chambers are filled with 1x running buffer and then the denatured proteins are loaded into the wells. At least one lane of the gel is loaded with a molecular weight marker. An electric current of 100 V and about 30 mA is applied for the first 2 cm of the gel until the proteins leave the stacking gel. The voltage is then increased to 180 V until the bromphenol blue band of the loading buffer has run out of the gel.

Table 6.2-1:

Resolving gel composition for 10 ml (amounts indicated in ml):

Protein size in kDa				**25-200**	**15-100**	**10-70**	**12-45**	**4-40**
Gel in %	**5**	**6**	**7.5**	**8**	**10**	**12.5**	**15**	**20**
Lower Sol. (4x)	2.50	2.50	2.50	2.50	2.50	2.50	2.50	2.50
Acrylamide Stock 40 %	1.25	1.50	1.88	2.00	2.50	3.13	3.75	5.00
ddH_2O	6.10	5.90	5.50	5.40	4.90	4.30	3.60	2.40
10 % APS	0.1	0.1	0.1	0.1	0.1	0.1	0.1	0.1
TEMED	0.008	0.008	0.008	0.008	0.008	0.008	0.008	0.008

Stacking gel composition for 4 ml:

Gel in %	**4**	**5**
Upper Sol. (4x)	1.0 ml	1.0 ml
Acrylamide Stock 40 %	0.4 ml	0.5 ml
ddH_2O	2.6 ml	2.5 ml
10 % APS	30.0 µl	30.0 µl
TEMED	5.0 µl	5.0 µl

6.2.6.4.2 Wet transfer

Once the electrophoresis is finished, the gel sandwich is disassembled and the stacking gel is cut off before the resolving gel is equilibrated in ice-cold transfer buffer (containing 0.1 % SDS) for 15 min. Besides the gel, a nitrocellulose membrane (6 x 8 cm), 4 Whatman papers (7 x 9 cm) and two fibre pads have to be soaked in ice-cold transfer buffer for 15 min. The gel holder cassette is placed on a clean surface with the black side down and the sandwich is assembled on the black side of the gel holder cassette as shown in fig. 6.2-6. It is important to gently roll out any air bubbles from the sandwich using a glass tube or a small Falcon tube. The cassette is firmly closed, locked with the white latch and placed in the module, which is then placed inside the tank. After adding a small magnetic stirrer (helps to maintain even buffer temperature and ion distribution in the tank) and the frozen Bio-Ice cooling unit, the tank is filled complete with ice-cold transfer buffer and an electric current of 300 mA and 120 V is applied for 2 h 30 min. Upon completion of the run, the blotting sandwich is disassembled and the membrane is either put into TBS-Tween o/n at 4°C or blocked in 5 % (w/v) milk-TBS-Tween for 1 h at RT.

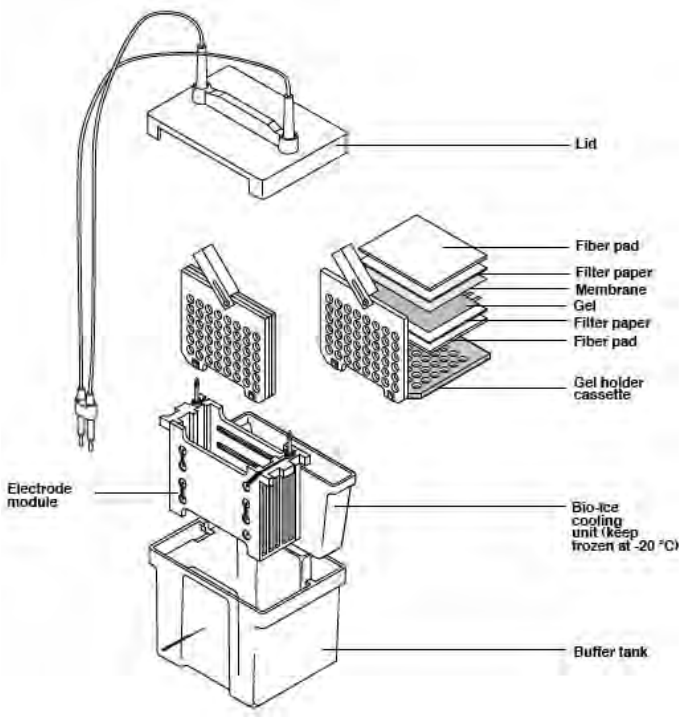

Fig. 6.2-6: Mini Trans-Blot® Cell description and assembly of parts (BioRad manual, catalog numbers 170-3930 or 170-3935).

6.2.6.4.3 Blocking of the membrane and labeling of the target protein

Before the 1st antibody can be applied to the membrane, the latter has to be blocked for non-specific binding, which is achieved by placing the membrane in a solution of diluted protein (either BSA or non-fat milk). These proteins attach to the membrane in vacant place (i.e. without target protein) leaving no space for the antibody to bind elsewhere. Hence the “noise” of the Western blot can be reduced and this leads to clearer results and may even eliminate false positives.

Usually, the membrane is blocked with 5 % (w/v) milk-TBS-Tween under gentle agitation for 1 h at RT before the 1st antibody is added. The optimal antibody concentration has to be determined by titration. The blocked membranes have been incubated with the following 1st antibody working dilutions in 5 % (w/v) milk-TBS-Tween at RT for 2 h or o/n at 4°C:

- ACTIN 1:2500 produced in rabbit
- BMAL1 1:1000 produced in rabbit
- CLOCK 1:1000 produced in rabbit
- CRY1 1:1000 produced in rabbit
- HSP90 1:2000 produced in mouse
- POLII 1:1000 produced in rabbit

Once the incubation is finished the membrane has to be rinsed twice quickly with 5 % (w/v) milk-TBS-Tween and has then to be washed two times with 5 % (w/v) milk-TBS-Tween for 5 min at RT on a shaker to remove unbound antibody. After rinsing, the membrane is exposed to the secondary antibody diluted in TBS-Tween at RT for one to two hours at the following concentrations:

- Anti-mouse 1:5000
- Anti-rabbit 1:7500

The secondary antibody is linked to horseradish peroxidase, which allows detection of the target protein as described in the next paragraph. Then the membrane is rinsed twice quickly with TBS-Tween and shaken twice in TBS-Tween at RT for 10 min.

6.2.6.4.4 Chemiluminescent detection of the target protein

The chemoluminescent detection of the target protein depends on incubation of the Western blot with luminol as a substrate, which will glow when exposed to horseradish peroxidase bound to the secondary antibody (fig. 6.2-7). The generated light is then detected by exposing the membrane to a film and the image is analysed by densitometry.

After the unbound secondary antibody is washed away, the excess wash buffer is drained from the membrane. A transparent plastic pocket is cut open on one side and taped into a film cassette. The membrane is then placed protein side up on the open plastic pocket. An equal volume of detection solution 1 is mixed with detection solution 2 (ECL™ Western blotting analysis system, GE Healthcare) and applied onto the membrane, which is incubated for 2 min or less at RT before the excess detection reagent is drained by puting the edge of the membrane in contact with a tissue. The sheet protector is then closed and eventually air-bubbles are smoothed out before an X-ray film sheet (Amersham Hyperfilm™ MP, GE Healthcare) is placed on top of the membrane and exposed for about 30 seconds. The film is

removed and replaced by a new one while the first piece is immediately developed. Based on the appearance of the first film the duration of the second exposure is estimated.

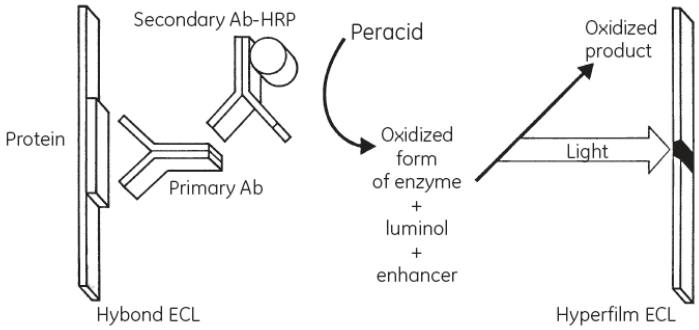

Fig. 6.2-7: Principles of ECL Western blotting. The membrane is soaked briefly in the detection reagent. This elicits a peroxidase-catalyzed oxidation of luminol and subsequently enhanced chemiluminescence (ECL), where the HRP labeled protein is bound to the antigen on the membrane. The resulting light is detcted on a film in minutes, or often seconds. [Product Booklet RPN 2109, GE Healthcare]

6.2.6.4 Corticosterone RIA

6.2.6.4.1 Blood sampling from the tail tip

Some cotton wool is put in a tight box (e.g. empty pipette box) and 1 ½ Pasteur pipettes of isoflurane (Attane^{TM} Isoflurane, Provet, ATC vet code: QN01AB06) are put on the cotton wool. The mouse is carefully put into the box, paying attention that is doesn't get wet with isoflurane. The mouse is left in the box until it loses consciousness. Monitoring the speed of breathing validates the deepness of anesthesia.

In order to assure that the mouse remains anesthetized during blood sampling a special container is fabricated out of a plastic beaker (fig. 6.2-8). Some air holes are drilled into the bottom of the beaker and a double bottom (plastic of disposable pipette rack) is inserted and fixed with some wire. Cotton is put between the two bottoms. The beaker is fixed on a surface (lower part of a pipettip box). Some isoflurane can now be added on the cotton using a Pasteur pipette.

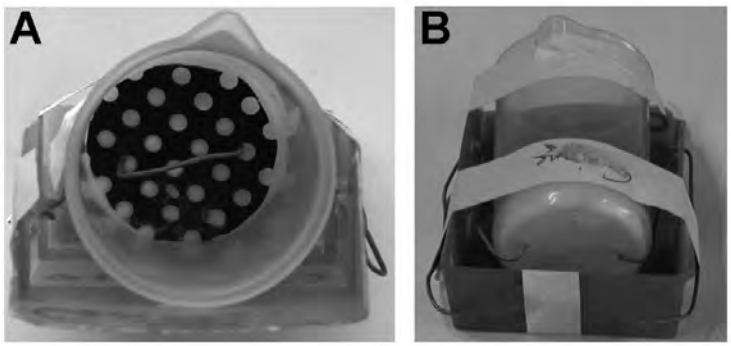

Fig. 6.2-8: Container to keep mouse anesthetized
A Front view of the container.
B Back view of the container.

As soon as the mouse is anesthetized deeply enough, it is taken out of the box and laid with its back on a table with the head inside the beaker. Inserting the mouse deeper into the beaker or taking it out of it can control the deepness of anesthesia. A small horizontal incision is made on the ventral part of the tail over the vessels 0.5 to 2 cm from the tail base using a scalpel blade. The blood is collected using a Microvette® 100 (Sarstedt, cat. #: 20.1280) for serum preparation. The tubes are kept on ice until they are centrifuged at 6000 rpm and 4°C for 10 min. The supernatant (serum) is kept at -20°C until further use.

6.2.6.4.2 Tube restraint

To check for the influence of stress on the mouse, corticosterone is determined before and after a 10 min tube restraint. Mice were individually housed for at least 1 day before blood sample collection.

50 ml Falcon tubes are used as restraining tubes. 3 air holes are drilled on the conical part distributed at equal distances. One additional hole is made on the head of the tube.

Blood is collected once prior to the tube restraint and once 30 min after the end of the 10 min restraint.

6.2.6.4.3 Corticosterone determination

Corticosterone levels are determined using the "Corticosterone ^{3}H RIA Kit (rats & mice)" of MP Biomedicals (cat #: 07-120002) and according to the manufacturers instructions with a few exceptions:

- 3 µl of serum are diluted in 1.5 ml of steroid diluent
- Incubation for around 3 h at 4°C
- 4 ml of scintillation cocktail are used

6.2.6.5 Immuncytochemistry

Immuncytochemistry allows the *in situ* detection of specific proteins in fixed cells. It is important to always include a negative control without the primary antibody to avoid any false positive interpretation of the results. Furthermore, one should include a positive control (e.g. actin) to assure that the assay is functional.

For the assay, 10'000 cells are cultured in 400 µl medium per well of an 8-well LabTek chamber slide o/n in an incubator. The next day, the medium is aspirated and the cells are fixed in 4% PFA for 15 min. Then the cell membranes are permeabilized incubating them in

0.1 % triton X-100/1x PBS for 2 min. The cells are washed once shortly and twice for 5 min with 1x PBS before the endogenous peroxidases are blocked with 0.06 % H_2O_2/MeOH for 30 min at RT. After washing the cells twice shortly with PBS, the cells are blocked for unspecific antibody binding incubating them with 5 % serum for 30 min at RT. It is important to use the serum from the animal in which the second antibody was produced. Then the cells are washed once shortly and twice for 5 min in 1x PBS. The first antibody is added together with 2 % serum in 1x PBS and incubated o/n at 4°C. The appropriate amount of the first antibody has to be determined for each antibody by preparing a dilution series (e.g. 1:100, 1:250 and 1:500).

The next morning, the cells are washed again once shortly and twice for 5 min in 1x PBS before the secondary antibody is added in a dilution of 1:200 in 1x PBS for 45 min at RT. During this incubation time, the AB-complex of the Vectastain® ABC kit has to be prepared diluting equal amounts of solution A and B (1:50) in 1x PBS (e.g. 80 µl A + 80 µl B + 3840 µl PBS). The principle of this kit is that the unlabeled primary antibody is recognized by a biotinylated secondary antibody. The biotin of the latter is then bound by a preformed **A**vidin and **B**iotinylated horseradish peroxidase macromolecular **C**omplex which remains stable for several hours after formation. Since avidin has an extraordinarily high binding affinity for biotin their binding is essentially irreversible.

The cells are washed once more as described above with PBS and then the AB-complex is added for 45 min at RT. In the mean time the DAB (3,3'-diaminobenzidine) reagent has to be prepared dissolving one urea and one DAB tablet in 1 ml of ddH_2O. DAB is widely used in immunhistology because it is a precipitating substrate for peroxidase. The intense brown-black stain that is produced is resistant to alcohol and can be coverslipped in the traditional manner and thus be stored for future reference. Once the incubation is finished, the cells are washed once shortly and twice for 5 min in 1x PBS. The DAB is added for some seconds to a few minutes and the reaction is stopped by adding ddH_2O as soon as a nice color development can be observed. Then the cells are washed three times with ddH_2O before the gasket is removed from the chamber slide by smoothly lifting it away. Excess water is gently removed using tissue paper and a glass coverslip is mounted on the slide using two drops of Aquatex.

Chapter 7

Abbreviations

A	absorbance unit
Amp	ampicillin
arnt	aryl hydrocarbon receptor nuclear translocator protein
ATP	adenosintriphosphate
av	average
AW	atomic weight
Bmal1	brain-muscle Arnt-like protein 1
bp	base pair
BSA	bovine serum albumin
CaMK	Ca^{2+}–calmodulin-dependent kinase
cAMP	cyclic adenosinmonophosphate
ccg	clock controlled gene
cDNA	complementary DNA
cGKII	cGMP-dependent protein kinase II (also known as PKGII)
cGMP	cyclic guanosinmonophosphate
Ci	curie
CKIε	casein kinase Iε
clk	clock
CNS	central nervous system
cpm	counts per minute
CRE	cAMP-responsive element
CREB	cAMP-responsive element binding protein
cry	cryptochrome
CT	circadian time
C_T	threshold cycle
cyc	cycle
dbt	doubletime
ddH_2O	bi-distilled water
DEPC	diethyl pyrocarbonate
dH_2O	distilled water
DI	deionized
DMEM	Dulbecco's modified Eagle's medium
DMSO	dimethyl sulfoxide
DNA	desoxyribonucleic acid
DNase	desoxyribonuclease
dNTP	2'-desoxynucleotide-5'-triphosphate
ds	double stranded
DTT	dithiothreitol
E. coli	*Escherichia coli*
EDTA	ethylen-diamine-tetra-acetic acid
e.g.	*exempli gratia* (Latin: “for example”)
et al.	*et alteri* (Latin: “and others”)
EtBr	ethidium bromide
EtOH	ethanol
FAM	carboxyfluorescein (phosphoramidite)
FASPS	familial advanced sleep phase syndrome
FCS	fetal calf serum
Fmr1	fragile X mental retardation 1 gene
Fxr1	fragile X mental retardation, autosomal homologue 1
Fxr2	fragile X mental retardation, autosomal homologue 2

g	gram
GAPDH	glycerol-3-phosphate dehydrogenase
h	hour
Hprt	hypoxanthine phosphribosyltransferase
Hyb-mix	hybridization mix
i.e.	*id est* (Latin: “that is”)
ISH	*in situ* hybridization
kb	kilo bases
KO	knockout
LB	Luria-Bertani
L-Glu	L-glutamine
m	milli: prefix denoting 10^{-3}
M	molar (mol/l)
MAPK	mitogen-activated peptide kinase
ME	2-mercaptoethanol
MEFs	mouse embryonic fibroblasts
MDFs	mouse dermal fibroblasts
mg	milligram
min	minute
Mio	million
mM	millimolar
MMLV	Moloney murine leukemia virus
MOPS	3-morpholinopropanesulfonic acid
mRNA	messenger RNA
mRNP	messenger ribonucleoprotein
mU	milliunit (mU = nmol/min)
n	nano: prefix denoting 10^{-9}
NBT	nitro blue tetrazolium
NEB	NEW ENGLAND *BioLabs* inc.
neg.	negative
ng	nanogram
NH_4Ac	ammonium acetate
Npas2	neuronal PAS domain protein 2 (also known as *Mop4*)
NTE	sodium chloride TRIS EDTA
OD	optic density
O/N	overnight
PAC	pas-associated c-terminal domain
PAS	per-arnt-sim dimerization domain
PB	phosphate buffer
PBS	phosphate buffered saline
PCR	polymerase chain reaction
Per1	period circadian protein 1
Per2	period circadian protein 2
PET	polyethylene
PFA	paraformaldehyde
pH	Neg. logarithm of the hydrogen ion concentration in moles per liter. *p* refers to power of 10 and *H* to hydrogen.
PKA	cAMP-activated protein kinase
PKC	protein kinase C
PEST	penicillin / streptomycin

PRC	phase response curve
PTC	phase transition curve
qRT	quantitative real-time
Ref.	reference
RHT	retinohypothalamic tract
RIA	radio immune assay
RNA	ribonucleic acid
RNase	ribonuclease
ROR	retinoid acid related orphan receptor
RORE	ROR response element
rpm	rotations per minute
RT	room temperature
RT	reverse transcription
s	second
SAD	seasonal affective disorder
SCN	suprachiasmatic nucleus
SD	standard deviation
SDS	sodium dodecyl sulfate
SEM	standard error of the mean
Sgg	shaggy
sim	single-minded protein
SOP	standard operating procedure
ss	single stranded
SSC	sodium saline citrate
TAE	TRIS - acetic acid - EDTA
Taq	*Thermophilus aquaticus*
TBS	TRIS buffered saline
TE	TRIS-EDTA
TEA	triethanolamine
tim	timeless
TP	time point
TRIS	tris-(hydroxymethyl)-aminomethane
U	Unit (U = μmol/min)
UTP	uridinetriphosphate
UV	ultraviolet
V	volt
VIP	vasointestinal active peptide
VIS	visible light
vri	vrille
v/v	volume per volume
WT	wild-type
w/v	weight per volume
ZT	Zeitgeber (German: “time giver”) time
μ	micro: prefix denoting 10^{-6}
μg	microgram
μl	microliter
μmole	micromole
°C	Celsius degree centigrades

Chapter 8

References

1. Abe H, Honma S, Namihira M, Tanahashi Y, Ikeda M and Honma K (1998) Circadian rhythm and light responsiveness of BMAL1 expression, a partner of mammalian clock gene Clock, in the suprachiasmatic nucleus of rats. *Neurosci Lett* 258:93-96.
2. Abe H, Rusak B and Robertson HA (1992) NMDA and non-NMDA receptor antagonists inhibit photic induction of Fos protein in the hamster suprachiasmatic nucleus. *Brain Res Bull* 28:831-835.
3. Abrahamson EE and Moore RY (2001) Suprachiasmatic nucleus in the mouse: retinal innervation, intrinsic organization and efferent projections. *Brain Res* 916:172-191.
4. Aden DP, Fogel A, Plotkin S, Damjanov I and Knowles BB (1979) Controlled synthesis of HBsAg in a differentiated human liver carcinoma-derived cell line. *Nature* 282:615-616.
5. Agostino PV, Ferreyra GA, Murad AD, Watanabe Y and Golombek DA (2004) Diurnal, circadian and photic regulation of calcium/calmodulin-dependent kinase II and neuronal nitric oxide synthase in the hamster suprachiasmatic nuclei. *Neurochem Int* 44:617-625.
6. Ahmad M and Cashmore AR (1993) HY4 gene of A. thaliana encodes a protein with characteristics of a blue-light photoreceptor. *Nature* 366:162-166.
7. Akashi M, Ichise T, Mamine T and Takumi T (2006) Molecular mechanism of cell-autonomous circadian gene expression of Period2, a crucial regulator of the mammalian circadian clock. *Mol Biol Cell* 17:555-565.
8. Akashi M and Takumi T (2005) The orphan nuclear receptor RORalpha regulates circadian transcription of the mammalian core-clock Bmal1. *Nat Struct Mol Biol* 12:441-448.
9. Akashi M, Tsuchiya Y, Yoshino T and Nishida E (2002) Control of intracellular dynamics of mammalian period proteins by casein kinase I epsilon (CKIepsilon) and CKIdelta in cultured cells. *Mol Cell Biol* 22:1693-1703.
10. Albrecht U, Sun ZS, Eichele G and Lee CC (1997) A differential response of two putative mammalian circadian regulators, mper1 and mper2, to light. *Cell* 91:1055-1064.
11. Albrecht U, Zheng B, Larkin D, Sun ZS and Lee CC (2001) MPer1 and mper2 are essential for normal resetting of the circadian clock. *J Biol Rhythms* 16:100-104.
12. Albus H, Vansteensel MJ, Michel S, Block GD and Meijer JH (2005) A GABAergic mechanism is necessary for coupling dissociable ventral and dorsal regional oscillators within the circadian clock. *Curr Biol* 15:886-893.
13. Allada R and Meissner RA (2005) Casein kinase 2, circadian clocks, and the flight from mutagenic light. *Mol Cell Biochem* 274:141-149.
14. Allen RP (2000) Development of the Human Circadian Cycle. In *Sleep and Breathing in Children: A Developmental Approach*, Informa Health Care.
15. Andre E, Conquet F, Steinmayr M, Stratton SC, Porciatti V and Becker-Andre M (1998) Disruption of retinoid-related orphan receptor beta changes circadian behavior, causes retinal degeneration and leads to vacillans phenotype in mice. *Embo J* 17:3867-3877.
16. Archer SN, Robilliard DL, Skene DJ, Smits M, Williams A, Arendt J and von Schantz M (2003) A length polymorphism in the circadian clock gene Per3 is linked to delayed sleep phase syndrome and extreme diurnal preference. *Sleep* 26:413-415.
17. Arendt J (2005) Melatonin: characteristics, concerns, and prospects. *J Biol Rhythms* 20:291-303.
18. Aronin N, Sagar SM, Sharp FR and Schwartz WJ (1990) Light regulates expression of a Fos-related protein in rat suprachiasmatic nuclei. *Proc Natl Acad Sci U S A* 87:5959-5962.
19. Aschoff J (1960) Exogenous and endogenous components in circadian rhythms. *Cold Spring Harb Symp Quant Biol* 25:11-28.
20. Aschoff J (1965) Response curves in circadian periodicity. In *Circadian clocks*, J Aschoff, ed, pp 95-111, North-Holland Publishing Co., Amsterdam.
21. Aschoff J (1969) Desynchronization and resynchronization of human circadian rhythms. *Aerosp Med* 40:844-849.
22. Aschoff J (1976) Circadian systems in man and their implications. *Hosp Pract* 11:51-97.
23. Ashmore LJ and Sehgal A (2003) A fly's eye view of circadian entrainment. *J Biol Rhythms* 18:206-216.
24. Aston-Jones G, Chen S, Zhu Y and Oshinsky ML (2001) A neural circuit for circadian regulation of arousal. *Nat Neurosci* 4:732-738.
25. Aton SJ, Colwell CS, Harmar AJ, Waschek J and Herzog ED (2005) Vasoactive intestinal polypeptide mediates circadian rhythmicity and synchrony in mammalian clock neurons. *Nat Neurosci* 8:476-483.
26. Axelrod J and Weissbach H (1960) Enzymatic O-methylation of N-acetylserotonin to melatonin. *Science* 131:1312.
27. Bae K, Jin X, Maywood ES, Hastings MH, Reppert SM and Weaver DR (2001) Differential functions of mPer1, mPer2, and mPer3 in the SCN circadian clock. *Neuron* 30:525-536.
28. Bae K and Weaver DR (2003) Light-induced phase shifts in mice lacking mPER1 or mPER2. *J Biol Rhythms* 18:123-133.

29. Baggs JE and Green CB (2003) Nocturnin, a deadenylase in Xenopus laevis retina: a mechanism for posttranscriptional control of circadian-related mRNA. *Curr Biol* 13:189-198.
30. Banker G and Goslin K (1988) Developments in neuronal cell culture. *Nature* 336:185-186.
31. Barbot W, Wasowicz M, Dupressoir A, Versaux-Botteri C and Heidmann T (2002) A murine gene with circadian expression revealed by transposon insertion: self-sustained rhythmicity in the liver and the photoreceptors. *Biochim Biophys Acta* 1576:81-91.
32. Bargiello TA, Jackson FR and Young MW (1984) Restoration of circadian behavioural rhythms by gene transfer in Drosophila. *Nature* 312:752-754.
33. Barnard AR and Nolan PM (2008) When clocks go bad: neurobehavioural consequences of disrupted circadian timing. *PLoS Genet* 4:e1000040.
34. Barnes JW, Tischkau SA, Barnes JA, Mitchell JW, Burgoon PW, Hickok JR and Gillette MU (2003) Requirement of mammalian Timeless for circadian rhythmicity. *Science* 302:439-442.
35. Belanger V, Picard N and Cermakian N (2006) The circadian regulation of Presenilin-2 gene expression. *Chronobiol Int* 23:747-766.
36. Bell-Pedersen D, Cassone VM, Earnest DJ, Golden SS, Hardin PE, Thomas TL and Zoran MJ (2005) Circadian rhythms from multiple oscillators: lessons from diverse organisms. *Nat Rev Genet* 6:544-556.
37. Benloucif S, Burgess HJ, Klerman EB, Lewy AJ, Middleton B, Murphy PJ, Parry BL and Revell VL (2008) Measuring melatonin in humans. *J Clin Sleep Med* 4:66-69.
38. Berson DM, Dunn FA and Takao M (2002) Phototransduction by retinal ganglion cells that set the circadian clock. *Science* 295:1070-1073.
39. Bjarnason GA, Jordan RC, Wood PA, Li Q, Lincoln DW, Sothern RB, Hrushesky WJ and Ben-David Y (2001) Circadian expression of clock genes in human oral mucosa and skin: association with specific cell-cycle phases. *Am J Pathol* 158:1793-1801.
40. Blau J and Young MW (1999) Cycling vrille expression is required for a functional Drosophila clock. *Cell* 99:661-671.
41. Boivin DB (2000) Influence of sleep-wake and circadian rhythm disturbances in psychiatric disorders. *J Psychiatry Neurosci* 25:446-458.
42. Boivin DB, Duffy JF, Kronauer RE and Czeisler CA (1996) Dose-response relationships for resetting of human circadian clock by light. *Nature* 379:540-542.
43. Boivin DB, James FO, Wu A, Cho-Park PF, Xiong H and Sun ZS (2003) Circadian clock genes oscillate in human peripheral blood mononuclear cells. *Blood* 102:4143-4145.
44. Bojkowski CJ and Arendt J (1988) Annual changes in 6-sulphatoxymelatonin excretion in man. *Acta Endocrinol (Copenh)* 117:470-476.
45. Bontekoe CJ, McIlwain KL, Nieuwenhuizen IM, Yuva-Paylor LA, Nellis A, Willemsen R, Fang Z, Kirkpatrick L, Bakker CE, McAninch R, Cheng NC, Merriweather M, Hoogeveen AT, Nelson D, Paylor R and Oostra BA (2002) Knockout mouse model for Fxr2: a model for mental retardation. *Hum Mol Genet* 11:487-498.
46. Bosler O and Beaudet A (1985) VIP neurons as prime synaptic targets for serotonin afferents in rat suprachiasmatic nucleus: a combined radioautographic and immunocytochemical study. *J Neurocytol* 14:749-763.
47. Brainard GC, Hanifin JP, Greeson JM, Byrne B, Glickman G, Gerner E and Rollag MD (2001) Action spectrum for melatonin regulation in humans: evidence for a novel circadian photoreceptor. *J Neurosci* 21:6405-6412.
48. Brainard GC, Lewy AJ, Menaker M, Fredrickson RH, Miller LS, Weleber RG, Cassone V and Hudson D (1988) Dose-response relationship between light irradiance and the suppression of plasma melatonin in human volunteers. *Brain Res* 454:212-218.
49. Brown SA, Ripperger J, Kadener S, Fleury-Olela F, Vilbois F, Rosbash M and Schibler U (2005) PERIOD1-associated proteins modulate the negative limb of the mammalian circadian oscillator. *Science* 308:693-696.
50. Brown SA, Zumbrunn G, Fleury-Olela F, Preitner N and Schibler U (2002) Rhythms of mammalian body temperature can sustain peripheral circadian clocks. *Curr Biol* 12:1574-1583.
51. Buijs RM, Chun SJ, Niijima A, Romijn HJ and Nagai K (2001) Parasympathetic and sympathetic control of the pancreas: a role for the suprachiasmatic nucleus and other hypothalamic centers that are involved in the regulation of food intake. *J Comp Neurol* 431:405-423.
52. Buijs RM, Hermes MH and Kalsbeek A (1998) The suprachiasmatic nucleus-paraventricular nucleus interactions: a bridge to the neuroendocrine and autonomic nervous system. *Prog Brain Res* 119:365-382.
53. Bunger MK, Wilsbacher LD, Moran SM, Clendenin C, Radcliffe LA, Hogenesch JB, Simon MC, Takahashi JS and Bradfield CA (2000) Mop3 is an essential component of the master circadian pacemaker in mammals. *Cell* 103:1009-1017.

54. Busino L, Bassermann F, Maiolica A, Lee C, Nolan PM, Godinho SI, Draetta GF and Pagano M (2007) SCFFbxl3 controls the oscillation of the circadian clock by directing the degradation of cryptochrome proteins. *Science* 316:900-904.
55. Busza A, Emery-Le M, Rosbash M and Emery P (2004) Roles of the two Drosophila CRYPTOCHROME structural domains in circadian photoreception. *Science* 304:1503-1506.
56. Butcher GQ, Doner J, Dziema H, Collamore M, Burgoon PW and Obrietan K (2002) The p42/44 mitogen-activated protein kinase pathway couples photic input to circadian clock entrainment. *J Biol Chem* 277:29519-29525.
57. Butcher GQ, Lee B, Cheng HY and Obrietan K (2005) Light stimulates MSK1 activation in the suprachiasmatic nucleus via a PACAP-ERK/MAP kinase-dependent mechanism. *J Neurosci* 25:5305-5313.
58. Butler MP, Honma S, Fukumoto T, Kawamoto T, Fujimoto K, Noshiro M, Kato Y and Honma K (2004) Dec1 and Dec2 expression is disrupted in the suprachiasmatic nuclei of Clock mutant mice. *J Biol Rhythms* 19:126-134.
59. Cahill GM (1996) Circadian regulation of melatonin production in cultured zebrafish pineal and retina. *Brain Res* 708:177-181.
60. Cahill GM (2002) Clock mechanisms in zebrafish. *Cell Tissue Res* 309:27-34.
61. Cahill GM, Hurd MW and Batchelor MM (1998) Circadian rhythmicity in the locomotor activity of larval zebrafish. *Neuroreport* 9:3445-3449.
62. Cajochen C, Munch M, Kobialka S, Krauchi K, Steiner R, Oelhafen P, Orgul S and Wirz-Justice A (2005) High sensitivity of human melatonin, alertness, thermoregulation, and heart rate to short wavelength light. *J Clin Endocrinol Metab* 90:1311-1316.
63. Camacho F, Cilio M, Guo Y, Virshup DM, Patel K, Khorkova O, Styren S, Morse B, Yao Z and Keesler GA (2001) Human casein kinase Idelta phosphorylation of human circadian clock proteins period 1 and 2. *FEBS Lett* 489:159-165.
64. Campbell SS and Murphy PJ (1998) Extraocular circadian phototransduction in humans. *Science* 279:396-399.
65. Card JP and Moore RY (1989) Organization of lateral geniculate-hypothalamic connections in the rat. *J Comp Neurol* 284:135-147.
66. Cardone L, Hirayama J, Giordano F, Tamaru T, Palvimo JJ and Sassone-Corsi P (2005) Circadian clock control by SUMOylation of BMAL1. *Science* 309:1390-1394.
67. Carmona-Alcocer V, Miranda-Anaya M and Barrera-Mera B (2005) Shifting phase of circadian locomotor activity by light in the freshwater crab pseudothelphusa americana. *Biological Rhythm Research* 36:123-129.
68. Castel M, Belenky M, Cohen S, Ottersen OP and Storm-Mathisen J (1993) Glutamate-like immunoreactivity in retinal terminals of the mouse suprachiasmatic nucleus. *Eur J Neurosci* 5:368-381.
69. Cegielska A, Gietzen KF, Rivers A and Virshup DM (1998) Autoinhibition of casein kinase I epsilon (CKI epsilon) is relieved by protein phosphatases and limited proteolysis. *J Biol Chem* 273:1357-1364.
70. Ceriani MF, Darlington TK, Staknis D, Mas P, Petti AA, Weitz CJ and Kay SA (1999) Light-dependent sequestration of TIMELESS by CRYPTOCHROME. *Science* 285:553-556.
71. Cermakian N, Monaco L, Pando MP, Dierich A and Sassone-Corsi P (2001) Altered behavioral rhythms and clock gene expression in mice with a targeted mutation in the Period1 gene. *Embo J* 20:3967-3974.
72. Cermakian N, Pando MP, Thompson CL, Pinchak AB, Selby CP, Gutierrez L, Wells DE, Cahill GM, Sancar A and Sassone-Corsi P (2002) Light induction of a vertebrate clock gene involves signaling through blue-light receptors and MAP kinases. *Curr Biol* 12:844-848.
73. Cermakian N and Sassone-Corsi P (2000) Multilevel regulation of the circadian clock. *Nat Rev Mol Cell Biol* 1:59-67.
74. Cheng HY, Dziema H, Papp J, Mathur DP, Koletar M, Ralph MR, Penninger JM and Obrietan K (2006) The molecular gatekeeper Dexras1 sculpts the photic responsiveness of the mammalian circadian clock. *J Neurosci* 26:12984-12995.
75. Cheng HY, Obrietan K, Cain SW, Lee BY, Agostino PV, Joza NA, Harrington ME, Ralph MR and Penninger JM (2004) Dexras1 potentiates photic and suppresses nonphotic responses of the circadian clock. *Neuron* 43:715-728.
76. Cheng MY, Bittman EL, Hattar S and Zhou QY (2005) Regulation of prokineticin 2 expression by light and the circadian clock. *BMC Neurosci* 6:17.
77. Cheng MY, Bullock CM, Li C, Lee AG, Bermak JC, Belluzzi J, Weaver DR, Leslie FM and Zhou QY (2002) Prokineticin 2 transmits the behavioural circadian rhythm of the suprachiasmatic nucleus. *Nature* 417:405-410.
78. Chou TC, Bjorkum AA, Gaus SE, Lu J, Scammell TE and Saper CB (2002) Afferents to the ventrolateral preoptic nucleus. *J Neurosci* 22:977-990.

79. Chou TC, Scammell TE, Gooley JJ, Gaus SE, Saper CB and Lu J (2003) Critical role of dorsomedial hypothalamic nucleus in a wide range of behavioral circadian rhythms. *J Neurosci* 23:10691-10702.
80. Chouvet G, Mouret J, Coindet J, Siffre M and Jouvet M (1974) Periodicite bicircadienne du cycle veille-sommeil dans des conditions hors du temps. *Electroencephalogr Clin Neurophysiol* 37:367-380.
81. Couttet P, Fromont-Racine M, Steel D, Pictet R and Grange T (1997) Messenger RNA deadenylylation precedes decapping in mammalian cells. *Proc Natl Acad Sci U S A* 94:5628-5633.
82. Crosio C, Cermakian N, Allis CD and Sassone-Corsi P (2000) Light induces chromatin modification in cells of the mammalian circadian clock. *Nat Neurosci* 3:1241-1247.
83. Csaki A, Kocsis K, Halasz B and Kiss J (2000) Localization of glutamatergic/aspartatergic neurons projecting to the hypothalamic paraventricular nucleus studied by retrograde transport of [3H]D-aspartate autoradiography. *Neuroscience* 101:637-655.
84. Curtis AM, Seo SB, Westgate EJ, Rudic RD, Smyth EM, Chakravarti D, FitzGerald GA and McNamara P (2004) Histone acetyltransferase-dependent chromatin remodeling and the vascular clock. *J Biol Chem* 279:7091-7097.
85. Cyran SA, Buchsbaum AM, Reddy KL, Lin MC, Glossop NR, Hardin PE, Young MW, Storti RV and Blau J (2003) vrille, Pdp1, and dClock form a second feedback loop in the Drosophila circadian clock. *Cell* 112:329-341.
86. Czeisler CA (1978) Human circadian physiology: Internal organization of temperature, sleep-wake, and neuroendocrine rhythms monitored in an environment free of time cues., Stanford University, Stanford, California.
87. Czeisler CA (1995) The effect of light on the human circadian pacemaker. *Ciba Found Symp* 183:254-290; discussion 290-302.
88. Czeisler CA, Allan JS, Strogatz SH, Ronda JM, Sanchez R, Rios CD, Freitag WO, Richardson GS and Kronauer RE (1986) Bright light resets the human circadian pacemaker independent of the timing of the sleep-wake cycle. *Science* 233:667-671.
89. Czeisler CA, Duffy JF, Shanahan TL, Brown EN, Mitchell JF, Rimmer DW, Ronda JM, Silva EJ, Allan JS, Emens JS, Dijk DJ and Kronauer RE (1999) Stability, precision, and near-24-hour period of the human circadian pacemaker. *Science* 284:2177-2181.
90. Czeisler CA, Kronauer RE, Allan JS, Duffy JF, Jewett ME, Brown EN and Ronda JM (1989) Bright light induction of strong (type 0) resetting of the human circadian pacemaker. *Science* 244:1328-1333.
91. Czeisler CA, Richardson GS, Zimmerman JC, Moore-Ede MC and Weitzman ED (1981) Entrainment of human circadian rhythms by light-dark cycles: a reassessment. *Photochem Photobiol* 34:239-247.
92. Czeisler CA, Shanahan TL, Klerman EB, Martens H, Brotman DJ, Emens JS, Klein T and Rizzo JF, 3rd (1995) Suppression of melatonin secretion in some blind patients by exposure to bright light. *N Engl J Med* 332:6-11.
93. Czeisler CA and Wright KP, Jr. (1999) Influence of light on circadian rhythmicity in humans. In *Neurobiology of sleep and circadian rhythms*, FW Turek and PC Zee, eds, p 149, Marcel Dekker, New York.
94. Daan S and Pittendrigh CS (1976) A functional analysis of circadian pacemakers in rodents. II. The variability of phase response curves. *J Comp Physiol* 106:253-266.
95. Dacey DM, Liao HW, Peterson BB, Robinson FR, Smith VC, Pokorny J, Yau KW and Gamlin PD (2005) Melanopsin-expressing ganglion cells in primate retina signal colour and irradiance and project to the LGN. *Nature* 433:749-754.
96. Damiola F, Le Minh N, Preitner N, Kornmann B, Fleury-Olela F and Schibler U (2000) Restricted feeding uncouples circadian oscillators in peripheral tissues from the central pacemaker in the suprachiasmatic nucleus. *Genes Dev* 14:2950-2961.
97. Dardente H, Fortier EE, Martineau V and Cermakian N (2007) Cryptochromes impair phosphorylation of transcriptional activators in the clock: a general mechanism for circadian repression. *Biochem J* 402:525-536.
98. Dardente H, Poirel VJ, Klosen P, Pevet P and Masson-Pevet M (2002) Per and neuropeptide expression in the rat suprachiasmatic nuclei: compartmentalization and differential cellular induction by light. *Brain Res* 958:261-271.
99. Davis FC and Gorski RA (1985) Development of hamster circadian rhythms. I. Within-litter synchrony of mother and pup activity rhythms at weaning. *Biol Reprod* 33:353-362.
100. Davis FC and Gorski RA (1988) Development of hamster circadian rhythms: role of the maternal suprachiasmatic nucleus. *J Comp Physiol [A]* 162:601-610.
101. De Cesare D and Sassone-Corsi P (2000) Transcriptional regulation by cyclic AMP-responsive factors. *Prog Nucleic Acid Res Mol Biol* 64:343-369.
102. de Vries JI, Visser GH, Mulder EJ and Prechtl HF (1987) Diurnal and other variations in fetal movement and heart rate patterns at 20-22 weeks. *Early Hum Dev* 15:333-348.

103. Debruyne JP, Noton E, Lambert CM, Maywood ES, Weaver DR and Reppert SM (2006) A clock shock: mouse CLOCK is not required for circadian oscillator function. *Neuron* 50:465-477.
104. Deurveilher S and Semba K (2005) Indirect projections from the suprachiasmatic nucleus to major arousal-promoting cell groups in rat: implications for the circadian control of behavioural state. *Neuroscience* 130:165-183.
105. Dey J, Carr AJ, Cagampang FR, Semikhodskii AS, Loudon AS, Hastings MH and Maywood ES (2005) The tau mutation in the Syrian hamster differentially reprograms the circadian clock in the SCN and peripheral tissues. *J Biol Rhythms* 20:99-110.
106. Ding JM, Buchanan GF, Tischkau SA, Chen D, Kuriashkina L, Faiman LE, Alster JM, McPherson PS, Campbell KP and Gillette MU (1998) A neuronal ryanodine receptor mediates light-induced phase delays of the circadian clock. *Nature* 394:381-384.
107. Ding JM, Chen D, Weber ET, Faiman LE, Rea MA and Gillette MU (1994) Resetting the biological clock: mediation of nocturnal circadian shifts by glutamate and NO. *Science* 266:1713-1717.
108. Doi M, Cho S, Yujnovsky I, Hirayama J, Cermakian N, Cato AC and Sassone-Corsi P (2007) Light-inducible and clock-controlled expression of MAP kinase phosphatase 1 in mouse central pacemaker neurons. *J Biol Rhythms* 22:127-139.
109. Dowling GA, Burr RL, Van Someren EJ, Hubbard EM, Luxenberg JS, Mastick J and Cooper BA (2008) Melatonin and bright-light treatment for rest-activity disruption in institutionalized patients with Alzheimer's disease. *J Am Geriatr Soc* 56:239-246.
110. Dudley CA, Erbel-Sieler C, Estill SJ, Reick M, Franken P, Pitts S and McKnight SL (2003) Altered patterns of sleep and behavioral adaptability in NPAS2-deficient mice. *Science* 301:379-383.
111. Duffield GE and Ebling FJ (1998) Maternal entrainment of the developing circadian system in the Siberian hamster (Phodopus sungorus). *J Biol Rhythms* 13:315-329.
112. Eide EJ, Vielhaber EL, Hinz WA and Virshup DM (2002) The circadian regulatory proteins BMAL1 and cryptochromes are substrates of casein kinase Iepsilon. *J Biol Chem* 277:17248-17254.
113. Emery P, Stanewsky R, Hall JC and Rosbash M (2000) A unique circadian-rhythm photoreceptor. *Nature* 404:456-457.
114. Etchegaray JP, Lee C, Wade PA and Reppert SM (2003) Rhythmic histone acetylation underlies transcription in the mammalian circadian clock. *Nature* 421:177-182.
115. Etchegaray JP, Yang X, DeBruyne JP, Peters AH, Weaver DR, Jenuwein T and Reppert SM (2006) The polycomb group protein EZH2 is required for mammalian circadian clock function. *J Biol Chem* 281:21209-21215.
116. Fallaux FJ, Kranenburg O, Cramer SJ, Houweling A, Van Ormondt H, Hoeben RC and Van Der Eb AJ (1996) Characterization of 911: a new helper cell line for the titration and propagation of early region 1-deleted adenoviral vectors. *Hum Gene Ther* 7:215-222.
117. Fang M, Jaffrey SR, Sawa A, Ye K, Luo X and Snyder SH (2000) Dexras1: a G protein specifically coupled to neuronal nitric oxide synthase via CAPON. *Neuron* 28:183-193.
118. Field MD, Maywood ES, O'Brien JA, Weaver DR, Reppert SM and Hastings MH (2000) Analysis of clock proteins in mouse SCN demonstrates phylogenetic divergence of the circadian clockwork and resetting mechanisms. *Neuron* 25:437-447.
119. Filipski E, Delaunay F, King VM, Wu MW, Claustrat B, Grechez-Cassiau A, Guettier C, Hastings MH and Francis L (2004) Effects of chronic jet lag on tumor progression in mice. *Cancer Res* 64:7879-7885.
120. Findley JD (1966) Programmed environments for the experimental analysis of human behavior. In *Operant behavior: Areas of research and application*, WK Hong, ed, p 827, Appleton-Century-Crofts, New York.
121. Foster RG, Hankins MW and Peirson SN (2007) Light, photoreceptors, and circadian clocks. *Methods Mol Biol* 362:3-28.
122. Francois-Bellan AM and Bosler O (1992) Convergent serotonin and GABA innervation of VIP neurons in the suprachiasmatic nucleus demonstrated by triple labeling in the rat. *Brain Res* 595:149-153.
123. Fu L, Pelicano H, Liu J, Huang P and Lee C (2002) The circadian gene Period2 plays an important role in tumor suppression and DNA damage response in vivo. *Cell* 111:41-50.
124. Gallego M, Kang H and Virshup DM (2006) Protein phosphatase 1 regulates the stability of the circadian protein PER2. *Biochem J* 399:169-175.
125. Gallego M and Virshup DM (2007) Post-translational modifications regulate the ticking of the circadian clock. *Nat Rev Mol Cell Biol* 8:139-148.
126. Gamble KL, Allen GC, Zhou T and McMahon DG (2007) Gastrin-releasing peptide mediates light-like resetting of the suprachiasmatic nucleus circadian pacemaker through cAMP response element-binding protein and Per1 activation. *J Neurosci* 27:12078-12087.
127. Ganong WF (1997) *Review of Medical Physilogy*., Appleton & Lange, Stanford, Conneticut.
128. Garbarino-Pico E and Green CB (2007) Posttranscriptional regulation of mammalian circadian clock output. *Cold Spring Harb Symp Quant Biol* 72:145-156.

129. Garbarino-Pico E, Niu S, Rollag MD, Strayer CA, Besharse JC and Green CB (2007) Immediate early response of the circadian polyA ribonuclease nocturnin to two extracellular stimuli. *Rna* 13:745-755.
130. Gardner MJ, Hubbard KE, Hotta CT, Dodd AN and Webb AA (2006) How plants tell the time. *Biochem J* 397:15-24.
131. Gau D, Lemberger T, von Gall C, Kretz O, Le Minh N, Gass P, Schmid W, Schibler U, Korf HW and Schutz G (2002) Phosphorylation of CREB Ser142 regulates light-induced phase shifts of the circadian clock. *Neuron* 34:245-253.
132. Gaus SE, Strecker RE, Tate BA, Parker RA and Saper CB (2002) Ventrolateral preoptic nucleus contains sleep-active, galaninergic neurons in multiple mammalian species. *Neuroscience* 115:285-294.
133. Gekakis N, Staknis D, Nguyen HB, Davis FC, Wilsbacher LD, King DP, Takahashi JS and Weitz CJ (1998) Role of the CLOCK protein in the mammalian circadian mechanism. *Science* 280:1564-1569.
134. Gholam D, Giacchetti S, Brezault-Bonnet C, Bouchahda M, Hauteville D, Adam R, Ducot B, Ghemard O, Kustlinger F, Jasmin C and Levi F (2006) Chronomodulated irinotecan, oxaliplatin, and leucovorin-modulated 5-Fluorouracil as ambulatory salvage therapy in patients with irinotecan- and oxaliplatin-resistant metastatic colorectal cancer. *Oncologist* 11:1072-1080.
135. Giacchetti S, Bjarnason G, Garufi C, Genet D, Iacobelli S, Tampellini M, Smaaland R, Focan C, Coudert B, Humblet Y, Canon JL, Adenis A, Lo Re G, Carvalho C, Schueller J, Anciaux N, Lentz MA, Baron B, Gorlia T and Levi F (2006) Phase III trial comparing 4-day chronomodulated therapy versus 2-day conventional delivery of fluorouracil, leucovorin, and oxaliplatin as first-line chemotherapy of metastatic colorectal cancer: the European Organisation for Research and Treatment of Cancer Chronotherapy Group. *J Clin Oncol* 24:3562-3569.
136. Gietzen KF and Virshup DM (1999) Identification of inhibitory autophosphorylation sites in casein kinase I epsilon. *J Biol Chem* 274:32063-32070.
137. Giguere V (1999) Orphan nuclear receptors: from gene to function. *Endocr Rev* 20:689-725.
138. Gillette MU and Reppert SM (1987) The hypothalamic suprachiasmatic nuclei: circadian patterns of vasopressin secretion and neuronal activity in vitro. *Brain Res Bull* 19:135-139.
139. Ginty DD, Kornhauser JM, Thompson MA, Bading H, Mayo KE, Takahashi JS and Greenberg ME (1993) Regulation of CREB phosphorylation in the suprachiasmatic nucleus by light and a circadian clock. *Science* 260:238-241.
140. Gluzman Y (1981) SV40-transformed simian cells support the replication of early SV40 mutants. *Cell* 23:175-182.
141. Godinho SI, Maywood ES, Shaw L, Tucci V, Barnard AR, Busino L, Pagano M, Kendall R, Quwailid MM, Romero MR, O'Neill J, Chesham JE, Brooker D, Lalanne Z, Hastings MH and Nolan PM (2007) The after-hours mutant reveals a role for Fbxl3 in determining mammalian circadian period. *Science* 316:897-900.
142. Golden SS and Canales SR (2003) Cyanobacterial circadian clocks--timing is everything. *Nat Rev Microbiol* 1:191-199.
143. Golombek DA, Agostino PV, Plano SA and Ferreyra GA (2004) Signaling in the mammalian circadian clock: the NO/cGMP pathway. *Neurochem Int* 45:929-936.
144. Gomez Brunet A, Malpaux B, Daveau A, Taragnat C and Chemineau P (2002) Genetic variability in melatonin secretion originates in the number of pinealocytes in sheep. *J Endocrinol* 172:397-404.
145. Gooley JJ, Lu J, Chou TC, Scammell TE and Saper CB (2001) Melanopsin in cells of origin of the retinohypothalamic tract. *Nat Neurosci* 4:1165.
146. Goz D, Studholme K, Lappi DA, Rollag MD, Provencio I and Morin LP (2008) Targeted destruction of photosensitive retinal ganglion cells with a saporin conjugate alters the effects of light on mouse circadian rhythms. *PLoS ONE* 3:e3153.
147. Graham FL, Smiley J, Russell WC and Nairn R (1977) Characteristics of a human cell line transformed by DNA from human adenovirus type 5. *J Gen Virol* 36:59-74.
148. Graves PR and Roach PJ (1995) Role of COOH-terminal phosphorylation in the regulation of casein kinase I delta. *J Biol Chem* 270:21689-21694.
149. Grechez-Cassiau A, Panda S, Lacoche S, Teboul M, Azmi S, Laudet V, Hogenesch JB, Taneja R and Delaunay F (2004) The transcriptional repressor STRA13 regulates a subset of peripheral circadian outputs. *J Biol Chem* 279:1141-1150.
150. Green CB and Besharse JC (1996a) Identification of a novel vertebrate circadian clock-regulated gene encoding the protein nocturnin. *Proc Natl Acad Sci U S A* 93:14884-14888.
151. Green CB and Besharse JC (1996b) Use of a high stringency differential display screen for identification of retinal mRNAs that are regulated by a circadian clock. *Brain Res Mol Brain Res* 37:157-165.
152. Griffin EA, Jr., Staknis D and Weitz CJ (1999) Light-independent role of CRY1 and CRY2 in the mammalian circadian clock. *Science* 286:768-771.
153. Grima B, Chelot E, Xia R and Rouyer F (2004) Morning and evening peaks of activity rely on different clock neurons of the Drosophila brain. *Nature* 431:869-873.

154. Gronfier C, Wright KP, Jr., Kronauer RE and Czeisler CA (2007) Entrainment of the human circadian pacemaker to longer-than-24-h days. *Proc Natl Acad Sci U S A* 104:9081-9086.
155. Gronfier C, Wright KP, Jr., Kronauer RE, Jewett ME and Czeisler CA (2004) Efficacy of a single sequence of intermittent bright light pulses for delaying circadian phase in humans. *Am J Physiol Endocrinol Metab* 287:E174-181.
156. Grzybowska EA, Wilczynska A and Siedlecki JA (2001) Regulatory functions of 3'UTRs. *Biochem Biophys Res Commun* 288:291-295.
157. Guillaumond F, Dardente H, Giguere V and Cermakian N (2005) Differential control of Bmal1 circadian transcription by REV-ERB and ROR nuclear receptors. *J Biol Rhythms* 20:391-403.
158. Guo H, Brewer JM, Lehman MN and Bittman EL (2006) Suprachiasmatic regulation of circadian rhythms of gene expression in hamster peripheral organs: effects of transplanting the pacemaker. *J Neurosci* 26:6406-6412.
159. Hakim H, DeBernardo AP and Silver R (1991) Circadian locomotor rhythms, but not photoperiodic responses, survive surgical isolation of the SCN in hamsters. *J Biol Rhythms* 6:97-113.
160. Hall JC (2003) Genetics and molecular biology of rhythms in Drosophila and other insects. *Adv Genet* 48:1-280.
161. Hamaguchi H, Fujimoto K, Kawamoto T, Noshiro M, Maemura K, Takeda N, Nagai R, Furukawa M, Honma S, Honma K, Kurihara H and Kato Y (2004) Expression of the gene for Dec2, a basic helix-loop-helix transcription factor, is regulated by a molecular clock system. *Biochem J* 382:43-50.
162. Hampp G (2007) The relationship between the circadian clock and the mesolimbic dopaminergic signaling system. In *Unit of biochemistry*, University of Fribourg, Fribourg.
163. Hannibal J (2002) Neurotransmitters of the retino-hypothalamic tract. *Cell Tissue Res* 309:73-88.
164. Hannibal J, Ding JM, Chen D, Fahrenkrug J, Larsen PJ, Gillette MU and Mikkelsen JD (1997) Pituitary adenylate cyclase-activating peptide (PACAP) in the retinohypothalamic tract: a potential daytime regulator of the biological clock. *J Neurosci* 17:2637-2644.
165. Harada Y, Sakai M, Kurabayashi N, Hirota T and Fukada Y (2005) Ser-557-phosphorylated mCRY2 is degraded upon synergistic phosphorylation by glycogen synthase kinase-3 beta. *J Biol Chem* 280:31714-31721.
166. Hardeland R, Fuhrberg B, Uria H, Behrmann G, Meyer TJ, Burkhardt S and Poeggeler B (1996) Chronobiology of indoleamines in the dinoflagellate Gonyaulax polyedra: metabolism and effects related to circadian rhythmicity and photoperiodism. *Braz J Med Biol Res* 29:119-123.
167. Hardin PE (2005) The circadian timekeeping system of Drosophila. *Curr Biol* 15:R714-722.
168. Hardin PE, Hall JC and Rosbash M (1990) Feedback of the Drosophila period gene product on circadian cycling of its messenger RNA levels. *Nature* 343:536-540.
169. Harms E, Kivimae S, Young MW and Saez L (2004) Posttranscriptional and posttranslational regulation of clock genes. *J Biol Rhythms* 19:361-373.
170. Harrington ME (1997) The ventral lateral geniculate nucleus and the intergeniculate leaflet: interrelated structures in the visual and circadian systems. *Neurosci Biobehav Rev* 21:705-727.
171. Harrington ME, Nance DM and Rusak B (1985) Neuropeptide Y immunoreactivity in the hamster geniculo-suprachiasmatic tract. *Brain Res Bull* 15:465-472.
172. Hatori M, Le H, Vollmers C, Keding SR, Tanaka N, Schmedt C, Jegla T and Panda S (2008) Inducible ablation of melanopsin-expressing retinal ganglion cells reveals their central role in non-image forming visual responses. *PLoS ONE* 3:e2451.
173. Hattar S, Liao HW, Takao M, Berson DM and Yau KW (2002) Melanopsin-containing retinal ganglion cells: architecture, projections, and intrinsic photosensitivity. *Science* 295:1065-1070.
174. Hattar S, Lucas RJ, Mrosovsky N, Thompson S, Douglas RH, Hankins MW, Lem J, Biel M, Hofmann F, Foster RG and Yau KW (2003) Melanopsin and rod-cone photoreceptive systems account for all major accessory visual functions in mice. *Nature* 424:76-81.
175. Herljevic M, Middleton B, Thapan K and Skene DJ (2005) Light-induced melatonin suppression: age-related reduction in response to short wavelength light. *Exp Gerontol* 40:237-242.
176. Hickey TL and Spear PD (1976) Retinogeniculate projections in hooded and albino rats: an autoradiographic study. *Exp Brain Res* 24:523-529.
177. Hida A, Koike N, Hirose M, Hattori M, Sakaki Y and Tei H (2000) The human and mouse Period1 genes: five well-conserved E-boxes additively contribute to the enhancement of mPer1 transcription. *Genomics* 65:224-233.
178. Hirata H, Yoshiura S, Ohtsuka T, Bessho Y, Harada T, Yoshikawa K and Kageyama R (2002) Oscillatory expression of the bHLH factor Hes1 regulated by a negative feedback loop. *Science* 298:840-843.
179. Hirayama J, Cardone L, Doi M and Sassone-Corsi P (2005) Common pathways in circadian and cell cycle clocks: light-dependent activation of Fos/AP-1 in zebrafish controls CRY-1a and WEE-1. *Proc Natl Acad Sci U S A* 102:10194-10199.

180. Hirayama J, Fukuda I, Ishikawa T, Kobayashi Y and Todo T (2003a) New role of zCRY and zPER2 as regulators of sub-cellular distributions of zCLOCK and zBMAL proteins. *Nucleic Acids Res* 31:935-943.
181. Hirayama J, Nakamura H, Ishikawa T, Kobayashi Y and Todo T (2003b) Functional and structural analyses of cryptochrome. Vertebrate CRY regions responsible for interaction with the CLOCK:BMAL1 heterodimer and its nuclear localization. *J Biol Chem* 278:35620-35628.
182. Hirota T, Okano T, Kokame K, Shirotani-Ikejima H, Miyata T and Fukada Y (2002) Glucose down-regulates Per1 and Per2 mRNA levels and induces circadian gene expression in cultured Rat-1 fibroblasts. *J Biol Chem* 277:44244-44251.
183. Hogenesch JB, Chan WK, Jackiw VH, Brown RC, Gu YZ, Pray-Grant M, Perdew GH and Bradfield CA (1997) Characterization of a subset of the basic-helix-loop-helix-PAS superfamily that interacts with components of the dioxin signaling pathway. *J Biol Chem* 272:8581-8593.
184. Hogenesch JB, Gu YZ, Jain S and Bradfield CA (1998) The basic-helix-loop-helix-PAS orphan MOP3 forms transcriptionally active complexes with circadian and hypoxia factors. *Proc Natl Acad Sci U S A* 95:5474-5479.
185. Hogenesch JB, Gu YZ, Moran SM, Shimomura K, Radcliffe LA, Takahashi JS and Bradfield CA (2000) The basic helix-loop-helix-PAS protein MOP9 is a brain-specific heterodimeric partner of circadian and hypoxia factors. *J Neurosci* 20:RC83.
186. Honma K, Honma S and Wada T (1987) Phase-dependent shift of free-running human circadian rhythms in response to a single bright light pulse. *Experientia* 43:1205-1207.
187. Honma S, Kawamoto T, Takagi Y, Fujimoto K, Sato F, Noshiro M, Kato Y and Honma K (2002) Dec1 and Dec2 are regulators of the mammalian molecular clock. *Nature* 419:841-844.
188. Honnebier MBOM, Swaab DF and Mirmiran M (1989) Diurnal rhythmicity during early human development. In *Development of Circadian Rhythmicity and Photoperiods in Mammals*, SM Reppert, ed, pp 221-244, Perinatology, Ithaca, NY.
189. Honrado GI, Johnson RS, Golombek DA, Spiegelman BM, Papaioannou VE and Ralph MR (1996) The circadian system of c-fos deficient mice. *J Comp Physiol [A]* 178:563-570.
190. Hrushesky WJ, von Roemeling R, Lanning RM and Rabatin JT (1990) Circadian-shaped infusions of floxuridine for progressive metastatic renal cell carcinoma. *J Clin Oncol* 8:1504-1513.
191. Hurd MW, Debruyne J, Straume M and Cahill GM (1998) Circadian rhythms of locomotor activity in zebrafish. *Physiol Behav* 65:465-472.
192. Ibata Y, Takahashi Y, Okamura H, Kawakami F, Terubayashi H, Kubo T and Yanaihara N (1989) Vasoactive intestinal peptide (VIP)-like immunoreactive neurons located in the rat suprachiasmatic nucleus receive a direct retinal projection. *Neurosci Lett* 97:1-5.
193. Iitaka C, Miyazaki K, Akaike T and Ishida N (2005) A role for glycogen synthase kinase-3beta in the mammalian circadian clock. *J Biol Chem* 280:29397-29402.
194. Illnerova H, Zvolsky P and Vanecek J (1985) The circadian rhythm in plasma melatonin concentration of the urbanized man: the effect of summer and winter time. *Brain Res* 328:186-189.
195. Ishida Y, Yagita K, Fukuyama T, Nishimura M, Nagano M, Shigeyoshi Y, Yamaguchi S, Komori T and Okamura H (2001) Constitutive expression and delayed light response of casein kinase Iepsilon and Idelta mRNAs in the mouse suprachiasmatic nucleus. *J Neurosci Res* 64:612-616.
196. Ishikawa T, Hirayama J, Kobayashi Y and Todo T (2002) Zebrafish CRY represses transcription mediated by CLOCK-BMAL heterodimer without inhibiting its binding to DNA. *Genes Cells* 7:1073-1086.
197. Jainchill JL, Aaronson SA and Todaro GJ (1969) Murine sarcoma and leukemia viruses: assay using clonal lines of contact-inhibited mouse cells. *J Virol* 4:549-553.
198. Jewett ME, Rimmer DW, Duffy JF, Klerman EB, Kronauer RE and Czeisler CA (1997) Human circadian pacemaker is sensitive to light throughout subjective day without evidence of transients. *Am J Physiol* 273:R1800-1809.
199. Jin X, Shearman LP, Weaver DR, Zylka MJ, de Vries GJ and Reppert SM (1999) A molecular mechanism regulating rhythmic output from the suprachiasmatic circadian clock. *Cell* 96:57-68.
200. Johnson RF, Moore RY and Morin LP (1988) Running wheel activity in hamsters with hypothalamic damage. *Physiol Behav* 43:755-763.
201. Jones CR, Campbell SS, Zone SE, Cooper F, DeSano A, Murphy PJ, Jones B, Czajkowski L and Ptacek LJ (1999) Familial advanced sleep-phase syndrome: A short-period circadian rhythm variant in humans. *Nat Med* 5:1062-1065.
202. Kaneko M and Cahill GM (2005) Light-dependent development of circadian gene expression in transgenic zebrafish. *PLoS Biol* 3:e34.
203. Kauppila A, Kivela A, Pakarinen A and Vakkuri O (1987) Inverse seasonal relationship between melatonin and ovarian activity in humans in a region with a strong seasonal contrast in luminosity. *J Clin Endocrinol Metab* 65:823-828.

204. Kawaguchi C, Tanaka K, Isojima Y, Shintani N, Hashimoto H, Baba A and Nagai K (2003) Changes in light-induced phase shift of circadian rhythm in mice lacking PACAP. *Biochem Biophys Res Commun* 310:169-175.
205. Kawamoto T, Noshiro M, Sato F, Maemura K, Takeda N, Nagai R, Iwata T, Fujimoto K, Furukawa M, Miyazaki K, Honma S, Honma K and Kato Y (2004) A novel autofeedback loop of Dec1 transcription involved in circadian rhythm regulation. *Biochem Biophys Res Commun* 313:117-124.
206. Keesler GA, Camacho F, Guo Y, Virshup D, Mondadori C and Yao Z (2000) Phosphorylation and destabilization of human period I clock protein by human casein kinase I epsilon. *Neuroreport* 11:951-955.
207. Kemppainen RJ and Behrend EN (1998) Dexamethasone rapidly induces a novel ras superfamily member-related gene in AtT-20 cells. *J Biol Chem* 273:3129-3131.
208. Khalsa SB, Jewett ME, Cajochen C and Czeisler CA (2003) A phase response curve to single bright light pulses in human subjects. *J Physiol* 549:945-952.
209. Kiss J, Leranth C and Halasz B (1984) Serotoninergic endings on VIP-neurons in the suprachiasmatic nucleus and on ACTH-neurons in the arcuate nucleus of the rat hypothalamus. A combination of high resolution autoradiography and electron microscopic immunocytochemistry. *Neurosci Lett* 44:119-124.
210. Kivela A, Kauppila A, Ylostalo P, Vakkuri O and Leppaluoto J (1988) Seasonal, menstrual and circadian secretions of melatonin, gonadotropins and prolactin in women. *Acta Physiol Scand* 132:321-327.
211. Kleitman N (1963) Sleep and wakefulness. In *University of Chicago Press*, Chicago, Illinois.
212. Klerman EB, Gershengorn HB, Duffy JF and Kronauer RE (2002) Comparisons of the variability of three markers of the human circadian pacemaker. *J Biol Rhythms* 17:181-193.
213. Kobayashi M, Wood PA and Hrushesky WJ (2002) Circadian chemotherapy for gynecological and genitourinary cancers. *Chronobiol Int* 19:237-251.
214. Kobayashi Y, Ishikawa T, Hirayama J, Daiyasu H, Kanai S, Toh H, Fukuda I, Tsujimura T, Terada N, Kamei Y, Yuba S, Iwai S and Todo T (2000) Molecular analysis of zebrafish photolyase/cryptochrome family: two types of cryptochromes present in zebrafish. *Genes Cells* 5:725-738.
215. Koh K, Zheng X and Sehgal A (2006) JETLAG resets the Drosophila circadian clock by promoting light-induced degradation of TIMELESS. *Science* 312:1809-1812.
216. Kojima S, Matsumoto K, Hirose M, Shimada M, Nagano M, Shigeyoshi Y, Hoshino S, Ui-Tei K, Saigo K, Green CB, Sakaki Y and Tei H (2007) LARK activates posttranscriptional expression of an essential mammalian clock protein, PERIOD1. *Proc Natl Acad Sci U S A* 104:1859-1864.
217. Kondratov RV, Chernov MV, Kondratova AA, Gorbacheva VY, Gudkov AV and Antoch MP (2003) BMAL1-dependent circadian oscillation of nuclear CLOCK: posttranslational events induced by dimerization of transcriptional activators of the mammalian clock system. *Genes Dev* 17:1921-1932.
218. Kondratov RV, Kondratova AA, Lee C, Gorbacheva VY, Chernov MV and Antoch MP (2006) Post-translational regulation of circadian transcriptional CLOCK(NPAS2)/BMAL1 complex by CRYPTOCHROMES. *Cell Cycle* 5:890-895.
219. Konopka RJ and Benzer S (1971) Clock mutants of Drosophila melanogaster. *Proc Natl Acad Sci U S A* 68:2112-2116.
220. Kopp C, Albrecht U, Zheng B and Tobler I (2002) Homeostatic sleep regulation is preserved in mPer1 and mPer2 mutant mice. *Eur J Neurosci* 16:1099-1106.
221. Kornberg RD (1974) Chromatin structure: a repeating unit of histones and DNA. *Science* 184:868-871.
222. Kornhauser JM, Nelson DE, Mayo KE and Takahashi JS (1992) Regulation of jun-B messenger RNA and AP-1 activity by light and a circadian clock. *Science* 255:1581-1584.
223. Kramer A, Yang FC, Snodgrass P, Li X, Scammell TE, Davis FC and Weitz CJ (2001) Regulation of daily locomotor activity and sleep by hypothalamic EGF receptor signaling. *Science* 294:2511-2515.
224. Kraves S and Weitz CJ (2006) A role for cardiotrophin-like cytokine in the circadian control of mammalian locomotor activity. *Nat Neurosci* 9:212-219.
225. Kume K, Zylka MJ, Sriram S, Shearman LP, Weaver DR, Jin X, Maywood ES, Hastings MH and Reppert SM (1999) mCRY1 and mCRY2 are essential components of the negative limb of the circadian clock feedback loop. *Cell* 98:193-205.
226. Kwok RP, Lundblad JR, Chrivia JC, Richards JP, Bachinger HP, Brennan RG, Roberts SG, Green MR and Goodman RH (1994) Nuclear protein CBP is a coactivator for the transcription factor CREB. *Nature* 370:223-226.
227. Kwon I, Lee J, Chang SH, Jung NC, Lee BJ, Son GH, Kim K and Lee KH (2006) BMAL1 shuttling controls transactivation and degradation of the CLOCK/BMAL1 heterodimer. *Mol Cell Biol* 26:7318-7330.
228. Laakso ML, Porkka-Heiskanen T, Alila A, Stenberg D and Johansson G (1990) Correlation between salivary and serum melatonin: dependence on serum melatonin levels. *J Pineal Res* 9:39-50.
229. Laakso ML, Porkka-Heiskanen T, Alila A, Stenberg D and Johansson G (1994) Twenty-four-hour rhythms in relation to the natural photoperiod: a field study in humans. *J Biol Rhythms* 9:283-293.

230. Lahiri K, Vallone D, Gondi SB, Santoriello C, Dickmeis T and Foulkes NS (2005) Temperature regulates transcription in the zebrafish circadian clock. *PLoS Biol* 3:e351.
231. Lakin-Thomas PL (2006) Transcriptional feedback oscillators: maybe, maybe not. *J Biol Rhythms* 21:83-92.
232. Lam RW and Levitan RD (2000) Pathophysiology of seasonal affective disorder: a review. *J Psychiatry Neurosci* 25:469-480.
233. Lambert CM, Machida KK, Smale L, Nunez AA and Weaver DR (2005) Analysis of the prokineticin 2 system in a diurnal rodent, the unstriped Nile grass rat (Arvicanthis niloticus). *J Biol Rhythms* 20:206-218.
234. Le Minh N, Damiola F, Tronche F, Schutz G and Schibler U (2001) Glucocorticoid hormones inhibit food-induced phase-shifting of peripheral circadian oscillators. *Embo J* 20:7128-7136.
235. Leak RK and Moore RY (2001) Topographic organization of suprachiasmatic nucleus projection neurons. *J Comp Neurol* 433:312-334.
236. Leander P, Vrang N and Moller M (1998) Neuronal projections from the mesencephalic raphe nuclear complex to the suprachiasmatic nucleus and the deep pineal gland of the golden hamster (Mesocricetus auratus). *J Comp Neurol* 399:73-93.
237. Lee C, Etchegaray JP, Cagampang FR, Loudon AS and Reppert SM (2001) Posttranslational mechanisms regulate the mammalian circadian clock. *Cell* 107:855-867.
238. Lee C, Weaver DR and Reppert SM (2004) Direct association between mouse PERIOD and CKIepsilon is critical for a functioning circadian clock. *Mol Cell Biol* 24:584-594.
239. Lee JS, Zhang X and Shi Y (1996) Differential interactions of the CREB/ATF family of transcription factors with p300 and adenovirus E1A. *J Biol Chem* 271:17666-17674.
240. Lehman MN, Silver R, Gladstone WR, Kahn RM, Gibson M and Bittman EL (1987) Circadian rhythmicity restored by neural transplant. Immunocytochemical characterization of the graft and its integration with the host brain. *J Neurosci* 7:1626-1638.
241. Lerner AB, Case JD and Heinzelman RV (1959) Structure of melatonin. *J Am Chem Soc* 81:6084-6085.
242. Lerner AB, Case JD, Takahashi Y, Lee TH and Mori W (1958) Isolation of melatonin, the pineal gland factor that lightens melanocytes. *J Am Chem Soc* 80:2587.
243. Levi F, Altinok A, Clairambault J and Goldbeter A (2008) Implications of circadian clocks for the rhythmic delivery of cancer therapeutics. *Philos Transact A Math Phys Eng Sci* 366:3575-3598.
244. Levi F, Focan C, Karaboue A, de la Valette V, Focan-Henrard D, Baron B, Kreutz F and Giacchetti S (2007) Implications of circadian clocks for the rhythmic delivery of cancer therapeutics. *Adv Drug Deliv Rev* 59:1015-1035.
245. Levitan RD (2007) The chronobiology and neurobiology of winter seasonal affective disorder. *Dialogues Clin Neurosci* 9:315-324.
246. Lewy AJ, Ahmed S, Jackson JM and Sack RL (1992) Melatonin shifts human circadian rhythms according to a phase-response curve. *Chronobiol Int* 9:380-392.
247. Lewy AJ, Bauer VK, Ahmed S, Thomas KH, Cutler NL, Singer CM, Moffit MT and Sack RL (1998) The human phase response curve (PRC) to melatonin is about 12 hours out of phase with the PRC to light. *Chronobiol Int* 15:71-83.
248. Lewy AJ and Sack RL (1989) The dim light melatonin onset as a marker for circadian phase position. *Chronobiol Int* 6:93-102.
249. Lewy AJ, Tetsuo M, Markey SP, Goodwin FK and Kopin IJ (1980) Pinealectomy abolishes plasma melatonin in the rat. *J Clin Endocrinol Metab* 50:204-205.
250. Li Z, Stuart RO, Qiao J, Pavlova A, Bush KT, Pohl M, Sakurai H and Nigam SK (2000) A role for Timeless in epithelial morphogenesis during kidney development. *Proc Natl Acad Sci U S A* 97:10038-10043.
251. Liu C, Li S, Liu T, Borjigin J and Lin JD (2007) Transcriptional coactivator PGC-1alpha integrates the mammalian clock and energy metabolism. *Nature* 447:477-481.
252. Lockley SW, Barger LK, Ayas NT, Rothschild JM, Czeisler CA and Landrigan CP (2007) Effects of health care provider work hours and sleep deprivation on safety and performance. *Jt Comm J Qual Patient Saf* 33:7-18.
253. Lockley SW, Brainard GC and Czeisler CA (2003) High sensitivity of the human circadian melatonin rhythm to resetting by short wavelength light. *J Clin Endocrinol Metab* 88:4502-4505.
254. Lowrey PL, Shimomura K, Antoch MP, Yamazaki S, Zemenides PD, Ralph MR, Menaker M and Takahashi JS (2000) Positional syntenic cloning and functional characterization of the mammalian circadian mutation tau. *Science* 288:483-492.
255. Lu J, Zhang YH, Chou TC, Gaus SE, Elmquist JK, Shiromani P and Saper CB (2001) Contrasting effects of ibotenate lesions of the paraventricular nucleus and subparaventricular zone on sleep-wake cycle and temperature regulation. *J Neurosci* 21:4864-4874.

256. Luboshitzky R and Lavie P (1999) Melatonin and sex hormone interrelationships--a review. *J Pediatr Endocrinol Metab* 12:355-362.
257. Luboshitzky R, Yanai D, Shen-Orr Z, Israeli E, Herer P and Lavie P (1998) Daily and seasonal variations in the concentration of melatonin in the human pineal gland. *Brain Res Bull* 47:271-276.
258. Lucas RJ, Freedman MS, Lupi D, Munoz M, David-Gray ZK and Foster RG (2001) Identifying the photoreceptive inputs to the mammalian circadian system using transgenic and retinally degenerate mice. *Behav Brain Res* 125:97-102.
259. Magnusson A and Boivin D (2003) Seasonal affective disorder: an overview. *Chronobiol Int* 20:189-207.
260. Martikainen H, Tapanainen J, Vakkuri O, Leppaluoto J and Huhtaniemi I (1985) Circannual concentrations of melatonin, gonadotrophins, prolactin and gonadal steroids in males in a geographical area with a large annual variation in daylight. *Acta Endocrinol (Copenh)* 109:446-450.
261. Martinek S, Inonog S, Manoukian AS and Young MW (2001) A role for the segment polarity gene shaggy/GSK-3 in the Drosophila circadian clock. *Cell* 105:769-779.
262. Martinet L and Allain D (1985) Role of the pineal gland in the photoperiodic control of reproductive and non-reproductive functions in mink (Mustela vison). *Ciba Found Symp* 117:170-187.
263. Mathur A, Golombek DA and Ralph MR (1996) cGMP-dependent protein kinase inhibitors block light-induced phase advances of circadian rhythms in vivo. *Am J Physiol* 270:R1031-1036.
264. Maywood ES, O'Neill JS, Chesham JE and Hastings MH (2007) Minireview: The circadian clockwork of the suprachiasmatic nuclei--analysis of a cellular oscillator that drives endocrine rhythms. *Endocrinology* 148:5624-5634.
265. McClung CA (2007) Circadian genes, rhythms and the biology of mood disorders. *Pharmacol Ther* 114:222-232.
266. McCord CP and Allen FP (1917) Evidences associating pineal gland function with alterations in pigmentation. *J Exp Zool* 23:207-224.
267. McPherson PS, Kim YK, Valdivia H, Knudson CM, Takekura H, Franzini-Armstrong C, Coronado R and Campbell KP (1991) The brain ryanodine receptor: a caffeine-sensitive calcium release channel. *Neuron* 7:17-25.
268. Meng QJ, Logunova L, Maywood ES, Gallego M, Lebiecki J, Brown TM, Sladek M, Semikhodskii AS, Glossop NR, Piggins HD, Chesham JE, Bechtold DA, Yoo SH, Takahashi JS, Virshup DM, Boot-Handford RP, Hastings MH and Loudon AS (2008) Setting clock speed in mammals: the CK1 epsilon tau mutation in mice accelerates circadian pacemakers by selectively destabilizing PERIOD proteins. *Neuron* 58:78-88.
269. Meyer-Bernstein EL, Jetton AE, Matsumoto SI, Markuns JF, Lehman MN and Bittman EL (1999) Effects of suprachiasmatic transplants on circadian rhythms of neuroendocrine function in golden hamsters. *Endocrinology* 140:207-218.
270. Meyer-Bernstein EL and Morin LP (1996) Differential serotonergic innervation of the suprachiasmatic nucleus and the intergeniculate leaflet and its role in circadian rhythm modulation. *J Neurosci* 16:2097-2111.
271. Mikkelsen JD, Larsen PJ, O'Hare MM and Wiegand SJ (1991) Gastrin releasing peptide in the rat suprachiasmatic nucleus: an immunohistochemical, chromatographic and radioimmunological study. *Neuroscience* 40:55-66.
272. Mills JN (1964) Circadian Rhythms during and after Three Months in Solitude Underground. *J Physiol* 174:217-231.
273. Mills JN, Minors DS and Waterhouse JM (1978) Adaptation to abrupt time shifts of the oscillator(s) controlling human circadian rhythms. *J Physiol* 285:455-470.
274. Minors DS and Waterhouse JM (1989) Masking in humans: the problem and some attempts to solve it. *Chronobiol Int* 6:29-53.
275. Minors DS, Waterhouse JM and Wirz-Justice A (1991) A human phase-response curve to light. *Neurosci Lett* 133:36-40.
276. Miyamoto Y and Sancar A (1998) Vitamin B2-based blue-light photoreceptors in the retinohypothalamic tract as the photoactive pigments for setting the circadian clock in mammals. *Proc Natl Acad Sci U S A* 95:6097-6102.
277. Moga MM and Moore RY (1997) Organization of neural inputs to the suprachiasmatic nucleus in the rat. *J Comp Neurol* 389:508-534.
278. Moore RY and Card JP (1994) Intergeniculate leaflet: an anatomically and functionally distinct subdivision of the lateral geniculate complex. *J Comp Neurol* 344:403-430.
279. Moore RY and Eichler VB (1972) Loss of a circadian adrenal corticosterone rhythm following suprachiasmatic lesions in the rat. *Brain Res* 42:201-206.
280. Moore RY and Lenn NJ (1972) A retinohypothalamic projection in the rat. *J Comp Neurol* 146:1-14.
281. Moore RY and Speh JC (1993) GABA is the principal neurotransmitter of the circadian system. *Neurosci Lett* 150:112-116.

282. Moore RY, Speh JC and Card JP (1995) The retinohypothalamic tract originates from a distinct subset of retinal ganglion cells. *J Comp Neurol* 352:351-366.
283. Morin LP, Blanchard J and Moore RY (1992) Intergeniculate leaflet and suprachiasmatic nucleus organization and connections in the golden hamster. *Vis Neurosci* 8:219-230.
284. Muller JE (1999) Circadian variation in cardiovascular events. *Am J Hypertens* 12:35S-42S.
285. Nagoshi E, Saini C, Bauer C, Laroche T, Naef F and Schibler U (2004) Circadian gene expression in individual fibroblasts: cell-autonomous and self-sustained oscillators pass time to daughter cells. *Cell* 119:693-705.
286. Nakahata Y, Yoshida M, Takano A, Soma H, Yamamoto T, Yasuda A, Nakatsu T and Takumi T (2008) A direct repeat of E-box-like elements is required for cell-autonomous circadian rhythm of clock genes. *BMC Mol Biol* 9:1.
287. Nakajima M, Imai K, Ito H, Nishiwaki T, Murayama Y, Iwasaki H, Oyama T and Kondo T (2005) Reconstitution of circadian oscillation of cyanobacterial KaiC phosphorylation in vitro. *Science* 308:414-415.
288. Nakashima A, Kawamoto T, Honda KK, Ueshima T, Noshiro M, Iwata T, Fujimoto K, Kubo H, Honma S, Yorioka N, Kohno N and Kato Y (2008) DEC1 modulates the circadian phase of clock gene expression. *Mol Cell Biol* 28:4080-4092.
289. Naruse Y, Oh-hashi K, Iijima N, Naruse M, Yoshioka H and Tanaka M (2004) Circadian and light-induced transcription of clock gene Per1 depends on histone acetylation and deacetylation. *Mol Cell Biol* 24:6278-6287.
290. Neuwelt EA and Lewy AJ (1983) Disappearance of plasma melatonin after removal of a neoplastic pineal gland. *N Engl J Med* 308:1132-1135.
291. Obrietan K, Impey S, Smith D, Athos J and Storm DR (1999) Circadian regulation of cAMP response element-mediated gene expression in the suprachiasmatic nuclei. *J Biol Chem* 274:17748-17756.
292. Obrietan K, Impey S and Storm DR (1998) Light and circadian rhythmicity regulate MAP kinase activation in the suprachiasmatic nuclei. *Nat Neurosci* 1:693-700.
293. Ohta H, Honma S, Abe H and Honma K (2002) Effects of nursing mothers on rPer1 and rPer2 circadian expressions in the neonatal rat suprachiasmatic nuclei vary with developmental stage. *Eur J Neurosci* 15:1953-1960.
294. Oishi K, Sakamoto K, Okada T, Nagase T and Ishida N (1998) Antiphase circadian expression between BMAL1 and period homologue mRNA in the suprachiasmatic nucleus and peripheral tissues of rats. *Biochem Biophys Res Commun* 253:199-203.
295. Okamura H, Miyake S, Sumi Y, Yamaguchi S, Yasui A, Muijtjens M, Hoeijmakers JH and van der Horst GT (1999) Photic induction of mPer1 and mPer2 in cry-deficient mice lacking a biological clock. *Science* 286:2531-2534.
296. Okano T, Sasaki M and Fukada Y (2001) Cloning of mouse BMAL2 and its daily expression profile in the suprachiasmatic nucleus: a remarkable acceleration of Bmal2 sequence divergence after Bmal gene duplication. *Neurosci Lett* 300:111-114.
297. Okawa M and Uchiyama M (2007) Circadian rhythm sleep disorders: characteristics and entrainment pathology in delayed sleep phase and non-24-h sleep-wake syndrome. *Sleep Med Rev* 11:485-496.
298. Onishi H, Yamaguchi S, Yagita K, Ishida Y, Dong X, Kimura H, Jing Z, Ohara H and Okamura H (2002) Rev-erbalpha gene expression in the mouse brain with special emphasis on its circadian profiles in the suprachiasmatic nucleus. *J Neurosci Res* 68:551-557.
299. Ozaki Y and Lynch HJ (1976) Presence of melatonin in plasma and urine or pinealectomized rats. *Endocrinology* 99:641-644.
300. Paietta J (1982) Photooxidation and the evolution of circadian rhythmicity. *J Theor Biol* 97:77-82.
301. Panda S, Antoch MP, Miller BH, Su AI, Schook AB, Straume M, Schultz PG, Kay SA, Takahashi JS and Hogenesch JB (2002a) Coordinated transcription of key pathways in the mouse by the circadian clock. *Cell* 109:307-320.
302. Panda S, Provencio I, Tu DC, Pires SS, Rollag MD, Castrucci AM, Pletcher MT, Sato TK, Wiltshire T, Andahazy M, Kay SA, Van Gelder RN and Hogenesch JB (2003) Melanopsin is required for non-image-forming photic responses in blind mice. *Science* 301:525-527.
303. Panda S, Sato TK, Castrucci AM, Rollag MD, DeGrip WJ, Hogenesch JB, Provencio I and Kay SA (2002b) Melanopsin (Opn4) requirement for normal light-induced circadian phase shifting. *Science* 298:2213-2216.
304. Pando MP, Pinchak AB, Cermakian N and Sassone-Corsi P (2001) A cell-based system that recapitulates the dynamic light-dependent regulation of the vertebrate clock. *Proc Natl Acad Sci U S A* 98:10178-10183.
305. Pando MP and Sassone-Corsi P (2002) Unraveling the mechanisms of the vertebrate circadian clock: zebrafish may light the way. *Bioessays* 24:419-426.

306. Partch CL and Sancar A (2005) Cryptochromes and circadian photoreception in animals. *Methods Enzymol* 393:726-745.
307. Partch CL, Shields KF, Thompson CL, Selby CP and Sancar A (2006) Posttranslational regulation of the mammalian circadian clock by cryptochrome and protein phosphatase 5. *Proc Natl Acad Sci U S A* 103:10467-10472.
308. Partonen T, Treutlein J, Alpman A, Frank J, Johansson C, Depner M, Aron L, Rietschel M, Wellek S, Soronen P, Paunio T, Koch A, Chen P, Lathrop M, Adolfsson R, Persson ML, Kasper S, Schalling M, Peltonen L and Schumann G (2007) Three circadian clock genes Per2, Arntl, and Npas2 contribute to winter depression. *Ann Med* 39:229-238.
309. Paxinos G and Franklin KBJ (2001) The mouse brain stereotaxic coordinates - Second Edition. *New York - Academic Press*.
310. Peier AM, McIlwain KL, Kenneson A, Warren ST, Paylor R and Nelson DL (2000) (Over)correction of FMR1 deficiency with YAC transgenics: behavioral and physical features. *Hum Mol Genet* 9:1145-1159.
311. Pelham RW, Vaughan GM, Sandlock KL and Vaughan MK (1973) Twenty-four-hour cycle of a melatonin-like substance in the plasma of human males. *J Clin Endocrinol Metab* 37:341-344.
312. Peng Y, Stoleru D, Levine JD, Hall JC and Rosbash M (2003) Drosophila free-running rhythms require intercellular communication. *PLoS Biol* 1:E13.
313. Petterborg LJ, Thalen BE, Kjellman BF and Wetterberg L (1991) Effect of melatonin replacement on serum hormone rhythms in a patient lacking endogenous melatonin. *Brain Res Bull* 27:181-185.
314. Pickard GE (1985) Bifurcating axons of retinal ganglion cells terminate in the hypothalamic suprachiasmatic nucleus and the intergeniculate leaflet of the thalamus. *Neurosci Lett* 55:211-217.
315. Pittendrigh CS (1993) Temporal organization: reflections of a Darwinian clock-watcher. *Annu Rev Physiol* 55:16-54.
316. Plautz JD, Kaneko M, Hall JC and Kay SA (1997) Independent photoreceptive circadian clocks throughout Drosophila. *Science* 278:1632-1635.
317. Poeggeler B, Reiter RJ, Tan DX, Chen LD and Manchester LC (1993) Melatonin, hydroxyl radical-mediated oxidative damage, and aging: a hypothesis. *J Pineal Res* 14:151-168.
318. Pokorny J, Smith VC and Lutze M (1987) Aging of the human lens. *Applied Optics* 26:1437-1440.
319. Postlethwait JH, Yan YL, Gates MA, Horne S, Amores A, Brownlie A, Donovan A, Egan ES, Force A, Gong Z, Goutel C, Fritz A, Kelsh R, Knapik E, Liao E, Paw B, Ransom D, Singer A, Thomson M, Abduljabbar TS, Yelick P, Beier D, Joly JS, Larhammar D, Rosa F, Westerfield M, Zon LI, Johnson SL and Talbot WS (1998) Vertebrate genome evolution and the zebrafish gene map. *Nat Genet* 18:345-349.
320. Preitner N, Damiola F, Lopez-Molina L, Zakany J, Duboule D, Albrecht U and Schibler U (2002) The orphan nuclear receptor REV-ERBalpha controls circadian transcription within the positive limb of the mammalian circadian oscillator. *Cell* 110:251-260.
321. Price JL, Blau J, Rothenfluh A, Abodeely M, Kloss B and Young MW (1998) double-time is a novel Drosophila clock gene that regulates PERIOD protein accumulation. *Cell* 94:83-95.
322. Provencio I, Cooper HM and Foster RG (1998) Retinal projections in mice with inherited retinal degeneration: implications for circadian photoentrainment. *J Comp Neurol* 395:417-439.
323. Provencio I, Rodriguez IR, Jiang G, Hayes WP, Moreira EF and Rollag MD (2000) A novel human opsin in the inner retina. *J Neurosci* 20:600-605.
324. Ralph MR, Foster RG, Davis FC and Menaker M (1990) Transplanted suprachiasmatic nucleus determines circadian period. *Science* 247:975-978.
325. Ralph MR and Menaker M (1988) A mutation of the circadian system in golden hamsters. *Science* 241:1225-1227.
326. Reddy P, Zehring WA, Wheeler DA, Pirrotta V, Hadfield C, Hall JC and Rosbash M (1984) Molecular analysis of the period locus in Drosophila melanogaster and identification of a transcript involved in biological rhythms. *Cell* 38:701-710.
327. Reick M, Garcia JA, Dudley C and McKnight SL (2001) NPAS2: an analog of clock operative in the mammalian forebrain. *Science* 293:506-509.
328. Reiter RJ (1993) Interactions of the pineal hormone melatonin with oxygen-centered free radicals: a brief review. *Braz J Med Biol Res* 26:1141-1155.
329. Reppert SM (1992) Pre-natal development of a hypothalamic biological clock. *Prog Brain Res* 93:119-131; discussion 132.
330. Reppert SM (1995) Interaction between the circadian clocks of mother and fetus. *Ciba Found Symp* 183:198-207; discussion 207-111.
331. Reppert SM, Coleman RJ, Heath HW and Swedlow JR (1984) Pineal N-acetyltransferase activity in 10-day-old rats: a paradigm for studying the developing circadian system. *Endocrinology* 115:918-925.
332. Reppert SM and Schwartz WJ (1983) Maternal coordination of the fetal biological clock in utero. *Science* 220:969-971.

333. Reppert SM and Schwartz WJ (1984) Functional activity of the suprachiasmatic nuclei in the fetal primate. *Neurosci Lett* 46:145-149.
334. Reppert SM and Schwartz WJ (1986) Maternal suprachiasmatic nuclei are necessary for maternal coordination of the developing circadian system. *J Neurosci* 6:2724-2729.
335. Reppert SM and Weaver DR (2002) Coordination of circadian timing in mammals. *Nature* 418:935-941.
336. Reppert SM, Weaver DR, Rivkees SA and Stopa EG (1988) Putative melatonin receptors in a human biological clock. *Science* 242:78-81.
337. Revell VL, Arendt J, Fogg LF and Skene DJ (2006) Alerting effects of light are sensitive to very short wavelengths. *Neurosci Lett* 399:96-100.
338. Revell VL, Arendt J, Terman M and Skene DJ (2005) Short-wavelength sensitivity of the human circadian system to phase-advancing light. *J Biol Rhythms* 20:270-272.
339. Ripperger JA and Schibler U (2006) Rhythmic CLOCK-BMAL1 binding to multiple E-box motifs drives circadian Dbp transcription and chromatin transitions. *Nat Genet* 38:369-374.
340. Rivkees SA (2001) Arrhythmicity in a child with septo-optic dysplasia and establishment of sleep-wake cyclicity with melatonin. *J Pediatr* 139:463-465.
341. Robinson BG, Frim DM, Schwartz WJ and Majzoub JA (1988) Vasopressin mRNA in the suprachiasmatic nuclei: daily regulation of polyadenylate tail length. *Science* 241:342-344.
342. Roenneberg T and Foster RG (1997) Twilight times: light and the circadian system. *Photochem Photobiol* 66:549-561.
343. Rosato E, Codd V, Mazzotta G, Piccin A, Zordan M, Costa R and Kyriacou CP (2001) Light-dependent interaction between Drosophila CRY and the clock protein PER mediated by the carboxy terminus of CRY. *Curr Biol* 11:909-917.
344. Rossner MJ, Oster H, Wichert SP, Reinecke L, Wehr MC, Reinecke J, Eichele G, Taneja R and Nave KA (2008) Disturbed clockwork resetting in Sharp-1 and Sharp-2 single and double mutant mice. *PLoS ONE* 3:e2762.
345. Ruby NF, Brennan TJ, Xie X, Cao V, Franken P, Heller HC and O'Hara BF (2002) Role of melanopsin in circadian responses to light. *Science* 298:2211-2213.
346. Rusak B, Robertson HA, Wisden W and Hunt SP (1990) Light pulses that shift rhythms induce gene expression in the suprachiasmatic nucleus. *Science* 248:1237-1240.
347. Sack RL, Brandes RW, Kendall AR and Lewy AJ (2000) Entrainment of free-running circadian rhythms by melatonin in blind people. *N Engl J Med* 343:1070-1077.
348. Sakurai T, Nagata R, Yamanaka A, Kawamura H, Tsujino N, Muraki Y, Kageyama H, Kunita S, Takahashi S, Goto K, Koyama Y, Shioda S and Yanagisawa M (2005) Input of orexin/hypocretin neurons revealed by a genetically encoded tracer in mice. *Neuron* 46:297-308.
349. Sanada K, Harada Y, Sakai M, Todo T and Fukada Y (2004) Serine phosphorylation of mCRY1 and mCRY2 by mitogen-activated protein kinase. *Genes Cells* 9:697-708.
350. Saper CB, Lu J, Chou TC and Gooley J (2005a) The hypothalamic integrator for circadian rhythms. *Trends Neurosci* 28:152-157.
351. Saper CB, Scammell TE and Lu J (2005b) Hypothalamic regulation of sleep and circadian rhythms. *Nature* 437:1257-1263.
352. Sato TK, Panda S, Miraglia LJ, Reyes TM, Rudic RD, McNamara P, Naik KA, FitzGerald GA, Kay SA and Hogenesch JB (2004) A functional genomics strategy reveals Rora as a component of the mammalian circadian clock. *Neuron* 43:527-537.
353. Schaap J, Albus H, VanderLeest HT, Eilers PH, Detari L and Meijer JH (2003) Heterogeneity of rhythmic suprachiasmatic nucleus neurons: Implications for circadian waveform and photoperiodic encoding. *Proc Natl Acad Sci U S A* 100:15994-15999.
354. Scheving LE (1976) The dimension of time in biology and medicine: chronobiology. *Endeavour* 35:66-72.
355. Schurov IL, McNulty S, Best JD, Sloper PJ and Hastings MH (1999) Glutamatergic induction of CREB phosphorylation and Fos expression in primary cultures of the suprachiasmatic hypothalamus in vitro is mediated by co-ordinate activity of NMDA and non-NMDA receptors. *J Neuroendocrinol* 11:43-51.
356. Schwartz WJ, Busis NA and Hedley-Whyte ET (1986) A discrete lesion of ventral hypothalamus and optic chiasm that disturbed the daily temperature rhythm. *J Neurol* 233:1-4.
357. Sehgal A, Price J and Young MW (1992) Ontogeny of a biological clock in Drosophila melanogaster. *Proc Natl Acad Sci U S A* 89:1423-1427.
358. Sehgal A, Price JL, Man B and Young MW (1994) Loss of circadian behavioral rhythms and per RNA oscillations in the Drosophila mutant timeless. *Science* 263:1603-1606.
359. Sekaran S, Foster RG, Lucas RJ and Hankins MW (2003) Calcium imaging reveals a network of intrinsically light-sensitive inner-retinal neurons. *Curr Biol* 13:1290-1298.

360. Selby CP, Thompson C, Schmitz TM, Van Gelder RN and Sancar A (2000) Functional redundancy of cryptochromes and classical photoreceptors for nonvisual ocular photoreception in mice. *Proc Natl Acad Sci U S A* 97:14697-14702.
361. Serviere J and Lavialle M (1996) [The suprachiasmatic nucleus: cellular approach to clock functioning]. *Pathol Biol (Paris)* 44:497-508.
362. Shanahan TL and Czeisler CA (2000) Physiological effects of light on the human circadian pacemaker. *Semin Perinatol* 24:299-320.
363. Shanahan TL, Kronauer RE, Duffy JF, Williams GH and Czeisler CA (1999) Melatonin rhythm observed throughout a three-cycle bright-light stimulus designed to reset the human circadian pacemaker. *J Biol Rhythms* 14:237-253.
364. Shanahan TL, Zeitzer JM and Czeisler CA (1997) Resetting the melatonin rhythm with light in humans. *J Biol Rhythms* 12:556-567.
365. Shearman LP, Jin X, Lee C, Reppert SM and Weaver DR (2000) Targeted disruption of the mPer3 gene: subtle effects on circadian clock function. *Mol Cell Biol* 20:6269-6275.
366. Shearman LP, Zylka MJ, Weaver DR, Kolakowski LF, Jr. and Reppert SM (1997) Two period homologs: circadian expression and photic regulation in the suprachiasmatic nuclei. *Neuron* 19:1261-1269.
367. Sherin JE, Shiromani PJ, McCarley RW and Saper CB (1996) Activation of ventrolateral preoptic neurons during sleep. *Science* 271:216-219.
368. Shigeyoshi Y, Taguchi K, Yamamoto S, Takekida S, Yan L, Tei H, Moriya T, Shibata S, Loros JJ, Dunlap JC and Okamura H (1997) Light-induced resetting of a mammalian circadian clock is associated with rapid induction of the mPer1 transcript. *Cell* 91:1043-1053.
369. Shirogane T, Jin J, Ang XL and Harper JW (2005) SCFbeta-TRCP controls clock-dependent transcription via casein kinase 1-dependent degradation of the mammalian period-1 (Per1) protein. *J Biol Chem* 280:26863-26872.
370. Siepka SM, Yoo SH, Park J, Song W, Kumar V, Hu Y, Lee C and Takahashi JS (2007) Circadian mutant Overtime reveals F-box protein FBXL3 regulation of cryptochrome and period gene expression. *Cell* 129:1011-1023.
371. Siffre M (1964) *Beyond time.*, McGraw Hill, New York.
372. Siffre M (1975) Six months alone in a cave. In *Natl Geogr Mag*, p 426.
373. Silver R, LeSauter J, Tresco PA and Lehman MN (1996) A diffusible coupling signal from the transplanted suprachiasmatic nucleus controlling circadian locomotor rhythms. *Nature* 382:810-813.
374. Simonneaux V and Ribelayga C (2003) Generation of the melatonin endocrine message in mammals: a review of the complex regulation of melatonin synthesis by norepinephrine, peptides, and other pineal transmitters. *Pharmacol Rev* 55:325-395.
375. Siwicki KK, Eastman C, Petersen G, Rosbash M and Hall JC (1988) Antibodies to the period gene product of Drosophila reveal diverse tissue distribution and rhythmic changes in the visual system. *Neuron* 1:141-150.
376. Sletten TL, Revell VL, Middleton B, Lederle KA and Skene DJ (in press) Age-related changes in acute and phase advancing responses to monochromatic light. *J Biol Rhythms*.
377. Smith I, Mullen PE, Silman RE, Snedden W and Wilson BW (1976) Absolute identification of melatonin in human plasma and cerebrospinal fluid. *Nature* 260:716-718.
378. Sofola O, Sundram V, Ng F, Kleyner Y, Morales J, Botas J, Jackson FR and Nelson DL (2008) The Drosophila FMRP and LARK RNA-binding proteins function together to regulate eye development and circadian behavior. *J Neurosci* 28:10200-10205.
379. Southern EM (1975) Detection of specific sequences among DNA fragments separated by gel electrophoresis. *J Mol Biol* 98:503-517.
380. Spencer CM, Serysheva E, Yuva-Paylor LA, Oostra BA, Nelson DL and Paylor R (2006) Exaggerated behavioral phenotypes in Fmr1/Fxr2 double knockout mice reveal a functional genetic interaction between Fragile X-related proteins. *Hum Mol Genet* 15:1984-1994.
381. Spoelstra K, Albrecht U, van der Horst GT, Brauer V and Daan S (2004) Phase responses to light pulses in mice lacking functional per or cry genes. *J Biol Rhythms* 19:518-529.
382. Stanewsky R, Kaneko M, Emery P, Beretta B, Wager-Smith K, Kay SA, Rosbash M and Hall JC (1998) The cryb mutation identifies cryptochrome as a circadian photoreceptor in Drosophila. *Cell* 95:681-692.
383. Stephan FK and Zucker I (1972) Circadian rhythms in drinking behavior and locomotor activity of rats are eliminated by hypothalamic lesions. *Proc Natl Acad Sci U S A* 69:1583-1586.
384. Stokkan KA and Reiter RJ (1994) Melatonin rhythms in Arctic urban residents. *J Pineal Res* 16:33-36.
385. Stokkan KA, Yamazaki S, Tei H, Sakaki Y and Menaker M (2001) Entrainment of the circadian clock in the liver by feeding. *Science* 291:490-493.
386. Stoleru D, Peng Y, Agosto J and Rosbash M (2004) Coupled oscillators control morning and evening locomotor behaviour of Drosophila. *Nature* 431:862-868.

387. Strahl BD and Allis CD (2000) The language of covalent histone modifications. *Nature* 403:41-45.
388. Stratmann M and Schibler U (2006) Properties, entrainment, and physiological functions of mammalian peripheral oscillators. *J Biol Rhythms* 21:494-506.
389. Sujino M, Masumoto KH, Yamaguchi S, van der Horst GT, Okamura H and Inouye ST (2003) Suprachiasmatic nucleus grafts restore circadian behavioral rhythms of genetically arrhythmic mice. *Curr Biol* 13:664-668.
390. Sumi Y, Yagita K, Yamaguchi S, Ishida Y, Kuroda Y and Okamura H (2002) Rhythmic expression of ROR beta mRNA in the mice suprachiasmatic nucleus. *Neurosci Lett* 320:13-16.
391. Sun ZS, Albrecht U, Zhuchenko O, Bailey J, Eichele G and Lee CC (1997) RIGUI, a putative mammalian ortholog of the Drosophila period gene. *Cell* 90:1003-1011.
392. Takahashi H, Umeda N, Tsutsumi Y, Fukumura R, Ohkaze H, Sujino M, van der Horst G, Yasui A, Inouye ST, Fujimori A, Ohhata T, Araki R and Abe M (2003) Mouse dexamethasone-induced RAS protein 1 gene is expressed in a circadian rhythmic manner in the suprachiasmatic nucleus. *Brain Res Mol Brain Res* 110:1-6.
393. Takahata S, Ozaki T, Mimura J, Kikuchi Y, Sogawa K and Fujii-Kuriyama Y (2000) Transactivation mechanisms of mouse clock transcription factors, mClock and mArnt3. *Genes Cells* 5:739-747.
394. Takano A, Shimizu K, Kani S, Buijs RM, Okada M and Nagai K (2000) Cloning and characterization of rat casein kinase 1epsilon. *FEBS Lett* 477:106-112.
395. Tamai TK, Young LC and Whitmore D (2007) Light signaling to the zebrafish circadian clock by Cryptochrome 1a. *Proc Natl Acad Sci U S A* 104:14712-14717.
396. Tamaru T, Isojima Y, Yamada T, Okada M, Nagai K and Takamatsu K (2000) Light and glutamate-induced degradation of the circadian oscillating protein BMAL1 during the mammalian clock resetting. *J Neurosci* 20:7525-7530.
397. Tan DX, Poeggeler B, Reiter RJ, Chen LD, Chen S, Manchester LC and Barlow-Walden LR (1993) The pineal hormone melatonin inhibits DNA-adduct formation induced by the chemical carcinogen safrole in vivo. *Cancer Lett* 70:65-71.
398. Tan DX, Reiter RJ, Manchester LC, Yan MT, El-Sawi M, Sainz RM, Mayo JC, Kohen R, Allegra M and Hardeland R (2002) Chemical and physical properties and potential mechanisms: melatonin as a broad spectrum antioxidant and free radical scavenger. *Curr Top Med Chem* 2:181-197.
399. Tanaka M, Ichitani Y, Okamura H, Tanaka Y and Ibata Y (1993) The direct retinal projection to VIP neuronal elements in the rat SCN. *Brain Res Bull* 31:637-640.
400. Tei H, Okamura H, Shigeyoshi Y, Fukuhara C, Ozawa R, Hirose M and Sakaki Y (1997) Circadian oscillation of a mammalian homologue of the Drosophila period gene. *Nature* 389:512-516.
401. Tetsuo M, Perlow MJ, Mishkin M and Markey SP (1982) Light exposure reduces and pinealectomy virtually stops urinary excretion of 6-hydroxymelatonin by rhesus monkeys. *Endocrinology* 110:997-1003.
402. Thapan K, Arendt J and Skene DJ (2001) An action spectrum for melatonin suppression: evidence for a novel non-rod, non-cone photoreceptor system in humans. *J Physiol* 535:261-267.
403. Thompson CL, Bowes Rickman C, Shaw SJ, Ebright JN, Kelly U, Sancar A and Rickman DW (2003) Expression of the blue-light receptor cryptochrome in the human retina. *Invest Ophthalmol Vis Sci* 44:4515-4521.
404. Thompson CL, Selby CP, Partch CL, Plante DT, Thresher RJ, Araujo F and Sancar A (2004) Further evidence for the role of cryptochromes in retinohypothalamic photoreception/phototransduction. *Brain Res Mol Brain Res* 122:158-166.
405. Thompson RH, Canteras NS and Swanson LW (1996) Organization of projections from the dorsomedial nucleus of the hypothalamus: a PHA-L study in the rat. *J Comp Neurol* 376:143-173.
406. Thresher RJ, Vitaterna MH, Miyamoto Y, Kazantsev A, Hsu DS, Petit C, Selby CP, Dawut L, Smithies O, Takahashi JS and Sancar A (1998) Role of mouse cryptochrome blue-light photoreceptor in circadian photoresponses. *Science* 282:1490-1494.
407. Tischkau SA, Barnes JA, Lin FJ, Myers EM, Barnes JW, Meyer-Bernstein EL, Hurst WJ, Burgoon PW, Chen D, Sehgal A and Gillette MU (1999) Oscillation and light induction of timeless mRNA in the mammalian circadian clock. *J Neurosci* 19:RC15.
408. Todaro GJ and Green H (1963) Quantitative studies of the growth of mouse embryo cells in culture and their development into established lines. *J Cell Biol* 17:299-313.
409. Toh KL, Jones CR, He Y, Eide EJ, Hinz WA, Virshup DM, Ptacek LJ and Fu YH (2001) An hPer2 phosphorylation site mutation in familial advanced sleep phase syndrome. *Science* 291:1040-1043.
410. Travnickova-Bendova Z, Cermakian N, Reppert SM and Sassone-Corsi P (2002) Bimodal regulation of mPeriod promoters by CREB-dependent signaling and CLOCK/BMAL1 activity. *Proc Natl Acad Sci U S A* 99:7728-7733.
411. Turner PL and Mainster MA (2008) Circadian photoreception: ageing and the eye's important role in systemic health. *Br J Ophthalmol* 92:1439-1444.

412. Ueda HR, Chen W, Adachi A, Wakamatsu H, Hayashi S, Takasugi T, Nagano M, Nakahama K, Suzuki Y, Sugano S, Iino M, Shigeyoshi Y and Hashimoto S (2002) A transcription factor response element for gene expression during circadian night. *Nature* 418:534-539.
413. Ukai H, Kobayashi TJ, Nagano M, Masumoto KH, Sujino M, Kondo T, Yagita K, Shigeyoshi Y and Ueda HR (2007) Melanopsin-dependent photo-perturbation reveals desynchronization underlying the singularity of mammalian circadian clocks. *Nat Cell Biol* 9:1327-1334.
414. Vallone D, Lahiri K, Dickmeis T and Foulkes NS (2005) Zebrafish cell clocks feel the heat and see the light! *Zebrafish* 2:171-187.
415. Van Cauter E, Blackman JD, Roland D, Spire JP, Refetoff S and Polonsky KS (1991) Modulation of glucose regulation and insulin secretion by circadian rhythmicity and sleep. *J Clin Invest* 88:934-942.
416. van den Pol AN and Tsujimoto KL (1985) Neurotransmitters of the hypothalamic suprachiasmatic nucleus: immunocytochemical analysis of 25 neuronal antigens. *Neuroscience* 15:1049-1086.
417. van der Horst GT, Muijtjens M, Kobayashi K, Takano R, Kanno S, Takao M, de Wit J, Verkerk A, Eker AP, van Leenen D, Buijs R, Bootsma D, Hoeijmakers JH and Yasui A (1999) Mammalian Cry1 and Cry2 are essential for maintenance of circadian rhythms. *Nature* 398:627-630.
418. van Esseveldt KE, Lehman MN and Boer GJ (2000) The suprachiasmatic nucleus and the circadian time-keeping system revisited. *Brain Res Brain Res Rev* 33:34-77.
419. Van Gelder RN, Gibler TM, Tu D, Embry K, Selby CP, Thompson CL and Sancar A (2002) Pleiotropic effects of cryptochromes 1 and 2 on free-running and light-entrained murine circadian rhythms. *J Neurogenet* 16:181-203.
420. Vansteensel MJ, Yamazaki S, Albus H, Deboer T, Block GD and Meijer JH (2003) Dissociation between circadian Per1 and neuronal and behavioral rhythms following a shifted environmental cycle. *Curr Biol* 13:1538-1542.
421. Vielhaber E, Eide E, Rivers A, Gao ZH and Virshup DM (2000) Nuclear entry of the circadian regulator mPER1 is controlled by mammalian casein kinase I epsilon. *Mol Cell Biol* 20:4888-4899.
422. Virshup DM and Forger DB (2007) After hours keeps clock researchers CRYing Overtime. *Cell* 129:857-859.
423. Viswanathan N (1999) Maternal entrainment in the circadian activity rhythm of laboratory mouse (C57BL/6J). *Physiol Behav* 68:157-162.
424. Vitaterna MH, King DP, Chang AM, Kornhauser JM, Lowrey PL, McDonald JD, Dove WF, Pinto LH, Turek FW and Takahashi JS (1994) Mutagenesis and mapping of a mouse gene, Clock, essential for circadian behavior. *Science* 264:719-725.
425. Vitaterna MH, Selby CP, Todo T, Niwa H, Thompson C, Fruechte EM, Hitomi K, Thresher RJ, Ishikawa T, Miyazaki J, Takahashi JS and Sancar A (1999) Differential regulation of mammalian period genes and circadian rhythmicity by cryptochromes 1 and 2. *Proc Natl Acad Sci U S A* 96:12114-12119.
426. Volicer L, Harper DG, Manning BC, Goldstein R and Satlin A (2001) Sundowning and circadian rhythms in Alzheimer's disease. *Am J Psychiatry* 158:704-711.
427. von Gall C, Noton E, Lee C and Weaver DR (2003) Light does not degrade the constitutively expressed BMAL1 protein in the mouse suprachiasmatic nucleus. *Eur J Neurosci* 18:125-133.
428. Wang Y, Osterbur DL, Megaw PL, Tosini G, Fukuhara C, Green CB and Besharse JC (2001) Rhythmic expression of Nocturnin mRNA in multiple tissues of the mouse. *BMC Dev Biol* 1:9.
429. Watts AG and Swanson LW (1987) Efferent projections of the suprachiasmatic nucleus: II. Studies using retrograde transport of fluorescent dyes and simultaneous peptide immunohistochemistry in the rat. *J Comp Neurol* 258:230-252.
430. Watts AG, Swanson LW and Sanchez-Watts G (1987) Efferent projections of the suprachiasmatic nucleus: I. Studies using anterograde transport of Phaseolus vulgaris leucoagglutinin in the rat. *J Comp Neurol* 258:204-229.
431. Weale RA (1985) Human lenticular fluorescence and transmissivity, and their effects on vision. *Exp Eye Res* 41:457-473.
432. Weaver DR and Reppert SM (1987) Maternal-fetal communication of circadian phase in a precocious rodent, the spiny mouse. *Am J Physiol* 253:E401-409.
433. Webb WB and Agnew HW, Jr. (1974) Sleep and waking in a time-free environment. *Aerosp Med* 45:617.
434. Weber ET, Gannon RL and Rea MA (1995) cGMP-dependent protein kinase inhibitor blocks light-induced phase advances of circadian rhythms in vivo. *Neurosci Lett* 197:227-230.
435. Weissbach H, Redfield BG and Axelrod J (1960) Biosynthesis of melatonin: enzymic conversion of serotonin to N-acetylserotonin. *Biochim Biophys Acta* 43:352-353.
436. Weissbach H, Redfield BG and Axelrod J (1961) The exzymic acetylation of serotonin and other naturally occurring amines. *Biochim Biophys Acta* 54:190-192.
437. Weitzman ED, Czeisler CA and Moore-Ede MC (1981) Sleep-wake, endocrine and temperature rhythms in man during temporal isolation. In *The twenty-four hour workday: Proceedings of a NIOSH Symposium of*

Variations in Work-Sleep Schedules, LC Johnson and e al., eds, p 105, U.S. Department of Health and Human Services, Cincinnati, Washington, D.C.

438. Welsh DK, Logothetis DE, Meister M and Reppert SM (1995) Individual neurons dissociated from rat suprachiasmatic nucleus express independently phased circadian firing rhythms. *Neuron* 14:697-706.
439. Wever R (1970) [Strength of a light-dark cycle as a time determiner for circadian rhythm in man]. *Pflugers Arch* 321:133-142.
440. Wever R (1974) The influence of light on human circadian rhythms. *Nord Council Arct Med Res Rep* 10:33.
441. Whitmore D, Foulkes NS and Sassone-Corsi P (2000) Light acts directly on organs and cells in culture to set the vertebrate circadian clock. *Nature* 404:87-91.
442. Whitmore D, Foulkes NS, Strahle U and Sassone-Corsi P (1998) Zebrafish Clock rhythmic expression reveals independent peripheral circadian oscillators. *Nat Neurosci* 1:701-707.
443. Wiggin GR, Soloaga A, Foster JM, Murray-Tait V, Cohen P and Arthur JS (2002) MSK1 and MSK2 are required for the mitogen- and stress-induced phosphorylation of CREB and ATF1 in fibroblasts. *Mol Cell Biol* 22:2871-2881.
444. Wilusz CJ, Wormington M and Peltz SW (2001) The cap-to-tail guide to mRNA turnover. *Nat Rev Mol Cell Biol* 2:237-246.
445. Winfree AT (1980) The geometry of biological time. In *Biomathematics*, Springer Verlag, New York.
446. Wirz-Justice A (2006) Biological rhythm disturbances in mood disorders. *Int Clin Psychopharmacol* 21 Suppl 1:S11-15.
447. Wirz-Justice A and Van den Hoofdakker RH (1999) Sleep deprivation in depression: what do we know, where do we go? *Biol Psychiatry* 46:445-453.
448. Wisor JP, O'Hara BF, Terao A, Selby CP, Kilduff TS, Sancar A, Edgar DM and Franken P (2002) A role for cryptochromes in sleep regulation. *BMC Neurosci* 3:20.
449. Wright KP, Jr., Hughes RJ, Kronauer RE, Dijk DJ and Czeisler CA (2001) Intrinsic near-24-h pacemaker period determines limits of circadian entrainment to a weak synchronizer in humans. *Proc Natl Acad Sci U S A* 98:14027-14032.
450. Xu Y, Padiath QS, Shapiro RE, Jones CR, Wu SC, Saigoh N, Saigoh K, Ptacek LJ and Fu YH (2005) Functional consequences of a CKIdelta mutation causing familial advanced sleep phase syndrome. *Nature* 434:640-644.
451. Xu Y, Toh KL, Jones CR, Shin JY, Fu YH and Ptacek LJ (2007) Modeling of a human circadian mutation yields insights into clock regulation by PER2. *Cell* 128:59-70.
452. Yamaguchi S, Isejima H, Matsuo T, Okura R, Yagita K, Kobayashi M and Okamura H (2003) Synchronization of cellular clocks in the suprachiasmatic nucleus. *Science* 302:1408-1412.
453. Yamamoto T, Nakahata Y, Soma H, Akashi M, Mamine T and Takumi T (2004) Transcriptional oscillation of canonical clock genes in mouse peripheral tissues. *BMC Mol Biol* 5:18.
454. Yamazaki S, Numano R, Abe M, Hida A, Takahashi R, Ueda M, Block GD, Sakaki Y, Menaker M and Tei H (2000) Resetting central and peripheral circadian oscillators in transgenic rats. *Science* 288:682-685.
455. Yan L and Okamura H (2002) Gradients in the circadian expression of Per1 and Per2 genes in the rat suprachiasmatic nucleus. *Eur J Neurosci* 15:1153-1162.
456. Yan L and Silver R (2002) Differential induction and localization of mPer1 and mPer2 during advancing and delaying phase shifts. *Eur J Neurosci* 16:1531-1540.
457. Yan L, Takekida S, Shigeyoshi Y and Okamura H (1999) Per1 and Per2 gene expression in the rat suprachiasmatic nucleus: circadian profile and the compartment-specific response to light. *Neuroscience* 94:141-150.
458. Yin L and Lazar MA (2005) The orphan nuclear receptor Rev-erbalpha recruits the N-CoR/histone deacetylase 3 corepressor to regulate the circadian Bmal1 gene. *Mol Endocrinol* 19:1452-1459.
459. Yin L, Wang J, Klein PS and Lazar MA (2006) Nuclear receptor Rev-erbalpha is a critical lithium-sensitive component of the circadian clock. *Science* 311:1002-1005.
460. Yoo SH, Ko CH, Lowrey PL, Buhr ED, Song EJ, Chang S, Yoo OJ, Yamazaki S, Lee C and Takahashi JS (2005) A noncanonical E-box enhancer drives mouse Period2 circadian oscillations in vivo. *Proc Natl Acad Sci U S A* 102:2608-2613.
461. Yoo SH, Yamazaki S, Lowrey PL, Shimomura K, Ko CH, Buhr ED, Siepka SM, Hong HK, Oh WJ, Yoo OJ, Menaker M and Takahashi JS (2004) PERIOD2::LUCIFERASE real-time reporting of circadian dynamics reveals persistent circadian oscillations in mouse peripheral tissues. *Proc Natl Acad Sci U S A* 101:5339-5346.
462. Yoshida K, McCormack S, Espana RA, Crocker A and Scammell TE (2006) Afferents to the orexin neurons of the rat brain. *J Comp Neurol* 494:845-861.
463. Zaidan R, Geoffriau M, Brun J, Taillard J, Bureau C, Chazot G and Claustrat B (1994) Melatonin is able to influence its secretion in humans: description of a phase-response curve. *Neuroendocrinology* 60:105-112.

464. Zaidi FH, Hull JT, Peirson SN, Wulff K, Aeschbach D, Gooley JJ, Brainard GC, Gregory-Evans K, Rizzo JF, 3rd, Czeisler CA, Foster RG, Moseley MJ and Lockley SW (2007) Short-wavelength light sensitivity of circadian, pupillary, and visual awareness in humans lacking an outer retina. *Curr Biol* 17:2122-2128.
465. Zeitzer JM, Dijk DJ, Kronauer R, Brown E and Czeisler C (2000) Sensitivity of the human circadian pacemaker to nocturnal light: melatonin phase resetting and suppression. *J Physiol* 526 Pt 3:695-702.
466. Zeitzer JM, Kronauer RE and Czeisler CA (1997) Photopic transduction implicated in human circadian entrainment. *Neurosci Lett* 232:135-138.
467. Zerr DM, Hall JC, Rosbash M and Siwicki KK (1990) Circadian fluctuations of period protein immunoreactivity in the CNS and the visual system of Drosophila. *J Neurosci* 10:2749-2762.
468. Zhang J, Fang Z, Jud C, Vansteensel MJ, Kaasik K, Lee CC, Albrecht U, Tamanini F, Meijer JH, Oostra BA and Nelson DL (2008) Fragile X-related proteins regulate mammalian circadian behavioral rhythms. *Am J Hum Genet* 83:43-52.
469. Zheng B, Albrecht U, Kaasik K, Sage M, Lu W, Vaishnav S, Li Q, Sun ZS, Eichele G, Bradley A and Lee CC (2001) Nonredundant roles of the mPer1 and mPer2 genes in the mammalian circadian clock. *Cell* 105:683-694.
470. Zheng B, Larkin DW, Albrecht U, Sun ZS, Sage M, Eichele G, Lee CC and Bradley A (1999) The mPer2 gene encodes a functional component of the mammalian circadian clock. *Nature* 400:169-173.
471. Zhuang M, Wang Y, Steenhard BM and Besharse JC (2000) Differential regulation of two period genes in the Xenopus eye. *Brain Res Mol Brain Res* 82:52-64.
472. Ziv L, Levkovitz S, Toyama R, Falcon J and Gothilf Y (2005) Functional development of the zebrafish pineal gland: light-induced expression of period2 is required for onset of the circadian clock. *J Neuroendocrinol* 17:314-320.
473. Zucker I, Lee TM and Dark J (1991) The suprachiasmatic nucleus and annual rhythms of mammals. In *Suprachiasmatic Nucleus: the Mind's Clock*, DC Klein, RY Moore and SM Reppert, eds, pp 246-259, Oxford University Press, New York.

Chapter 9

Curriculum Vitae

Corinne JUD

Route d'Ependes 21
CH-1732 Arconciel
Mobile: +41 (0)79 646 08 89
e-Mail: corinne.jud@unifr.ch

Swiss
Single
29 years
18.12.1979

EDUCATION

2004-2009	**PhD thesis in Biochemistry** (Advisor: Prof. Dr. Urs E. Albrecht) Subject: "The influence of light on the circadian clock of mice and men" Department of Medicine, Unit of Biochemistry, University of Fribourg (CH)
1999-2003	**Diploma in Biochemistry** (Advisor: Prof. Dr. Urs E. Albrecht) Title of the thesis: "The Circadian Clock: From Mice to Men" Department of Medicine, Unit of Biochemistry, University of Fribourg (CH)
1994-1998	**Swiss high school type B** (Latin), Wattwil (canton St.Gallen, CH)

COMPLEMENTARY COURSES

2006 (2 months)	**Attendance of the workshop "What a young entrepreneur has to know"** Elaboration as well as presentation of a business plan, **won 2nd price** of 2000 CHF Title: "Kinderhof/AniCrèche" (Institute for value based enterprise, Fribourg, CH)
2004-2005 (10 months)	**Post graduate diploma in academic didactics** (Advisor: Prof. Dr. B. Charlier) Title of the thesis: "Rédaction d'un protocole moderne pour le travail pratique *Cellular Fractionation*" (Centre for University Didactics Fribourg, CH)
2003-present	Attendance of several courses about various subjects: • "The sexual cycle" (2008, 4 days, Villars-sur-Ollon, CH) • "Genes, Genomes and Evolution" (2007, 4 days, Villars-sur-Ollon, CH) • "Drug Development: From Bench to Bedside" (2007, 1 day, Fribourg, CH) • "Understanding epidemics and pandemics" (2006, 4 days, Villars-sur-Ollon, CH) • "IVth International Course on Chronopharmacology" (2003, 9 days, Heidelberg, D)

TEACHING EXPERIENCE

2004-present	Supervision of master, bachelor and guest students
2004-present	Teaching assistant for the practical course "Cellular Fractionation" for ~10 bachelor students in biochemistry (block course of 3 weeks)
2005-present	Independent organization of an annual two-day WINS (*Women in Science and Technology*) training for high school students with the title "Genotyping via PCR"
2002-2004	Teaching assistant for practical courses for medical students

KEY SKILLS

Scientific:	Elaborate protocols and documentations, analyze data, give scientific and vulgarized talks, elaborate projects
Technical:	Molecular biology, cell culture, mouse breeding, mouse behavioral tests, histology
Personal:	Open-minded, motivating, level-headed, accurate, well organized Besides, the LEONARDO 345® questionnaire has determined my 3 strengths within a team that are: *development*, *organization*, and *promotion* of a project.

COMPUTER SKILLS

MS Office (Word, Excel, PowerPoint), Photoshop, efficient use of web browsers, Prism (statistics), DNA Strider (sequence manipulation), ClockLab (data analysis and collection for circadian biology)

LANGUAGES (According to the Common European Framework of Reference for Languages)

German: mother tongue
English: C2 (fluently written and spoken)
French: C2 (fluently written and spoken)
Spanish: A1 (basics)

PERSONAL INTERESTS

First aid trainings, Egyptology, sports (badminton, judo, jiu-jitsu, fitness), handcraft

WORK EXPERIENCE

1999	Serono S.A. (Geneva, CH)	Data typist for clinical trials (9 months)
1996-2002	Several summerjobs, e.g.:	
	• Pramol-Chemie AG (Bazenheid, CH)	Quality controller of detergents
	• Treff AG (Degersheim, CH)	Operator of injection molding machines for laboratory consumables, shift work

PEER REVIEWED PUBLICATIONS

1. J Zhang, Z Fang, **C Jud**, MJ Vansteensel, K Kaasik, CC Lee, U Albrecht, F Tamanini, JH Meijer, BA Oostra, DL Nelson (2008): "Fragile X and Related Proteins Regulate Mammalian Circadian Behavioral Rhythms". *Am J Hum Genet*, 83(1):43-52
2. G Cavadini, S Petrzilka, P Kohler, **C Jud**, I Tobler, T Birchler, A Fontana (2007): "TNFα suppresses the expression of clock genes by interfering with E-box-mediated transcription". *Proc Natl Acad Sci USA*, 104(31):12843-8
3. H Viswambharan, JM Carvas, V Antic, A Marecic, **C Jud**, CE Zaugg, XF Ming, JP Montani, U Albrecht, Z Yang (2007): "Mutation of the circadian clock gene *Per2* alters vascular endothelial function". *Circulation*, 115:2188-2195
4. **C Jud**, U Albrecht (2006): "Circadian rhythms in murine pups develop in absence of a functional maternal circadian clock". *J Biol Rhythms*, 21(2):149-54
5. C Cajochen, **C Jud**, M Münch, S Kobialka, A Wirz-Justice, U Albrecht (2006): "Evening exposure to blue light stimulates the expression of the clock gene *PER2* in humans". *Eur J Neurosci*, 23(4):1082-6
6. **C Jud**, I Schmutz, G Hampp, H Oster, U Albrecht (Epup 2005): "A guideline for analyzing circadian wheel-running behavior in rodents under different lighting conditions". *Biol Proced Online*, 7:101-16

INVITED SEMINARS

16.12.08	Title: "*Rev-Erbα/Per1* double mutant mice display a Type 0 phase response curve" Psychiatric University Clinics Basel (CH), Centre for Chronobiology
24.03.05	Title: "Emergence of Circadian Rhythms: Genetics versus Maternal Conditioning" Psychiatric University Clinics Basel (CH), Centre for Chronobiology

ATTENDED MEETINGS

25.-29.01.09	EUCLOCK Annual Meeting (Frauenchiemsee, D) Presentation of a **talk** and a **poster**
11.7.08	FENS Satellite Symposium on Sleep function (Lausanne, CH)
21.-25.1.08	EUCLOCK Annual Meeting (Frauenchiemsee, D) Presentation of a **talk**
30.5.-4.6.07	72nd Cold Spring Harbor Laboratory Symposium: Clocks and Rhythms (USA) **Poster** presentation, **funding raised** on my own
21.-24.1.07	EUCLOCK Annual Meeting (Frauenchiemsee, D) Presentation of a **talk**
23.-24.2.06	USGEB Annual Meeting (Geneva, CH) **Poster** presentation
8.-9.9.05	Annual BrainTime Meeting (Rotterdam, NL) Presentation of a **talk**
1.-2.12.04	Annual Meeting Swiss Society for Sleep Research, Sleep Medicine and Chronobiology and Eltem-Neurex Trinational Workshop (Basel, CH)
7.-8.10.04	Genomic Days (Lausanne, CH)
8.-10.9.04	Annual BrainTime Meeting (Frauenchiemsee, D) Presentation of a **talk**
11.-13.3.04	Annual BrainTime Meeting (Fribourg, CH) Presentation of a **talk**
4.-5.7.03	Annual BrainTime Meeting (Hannover, D) Presentation of a **talk**
30.6.-4.7.03	53th Meeting of Nobel Laureates (Lindau, D)

Chapter 10

Appendix

Preface to the Appendix

During my thesis I have not only worked on my main projects but I also was implicated in several collaborations. Since I did a small part of the work comprised in the following publications, I decided to attach them in the form of an appendix. Although I was not in the core team of these projects, my work has further enriched them.

Appendix I

"Fragile X-related proteins regulate mammalian circadian behavioral rhythms."

J. Zhang, Z. Fang, C. Jud, M.J. Vansteensel, K. Kaasik, C.C. Lee, U. Albrecht, F. Tamanini, J.H. Meijer, B.A. Ostra, D.L. Nelson

2008

Published in *American Journal of Human Genetics*, 83(1): 43-52

Please cite this article in press as: Zhang et al., Fragile X-Related Proteins Regulate Mammalian Circadian Behavioral Rhythms, The American Journal of Human Genetics (2008), doi:10.1016/j.ajhg.2008.06.003

ARTICLE

Fragile X-Related Proteins Regulate Mammalian Circadian Behavioral Rhythms

Jing Zhang,[1] Zhe Fang,[1] Corinne Jud,[2] Mariska J. Vansteensel,[3] Krista Kaasik,[4] Cheng Chi Lee,[4] Urs Albrecht,[2] Filippo Tamanini,[5] Johanna H. Meijer,[3] Ben A. Oostra,[6] and David L. Nelson[1,*]

Fragile X syndrome results from the absence of the fragile X mental retardation 1 (*FMR1*) gene product (FMRP). *FMR1* has two paralogs in vertebrates: *fragile X related gene 1* and *2* (*FXR1* and *FXR2*). Here we show that *Fmr1/Fxr2* double knockout (KO) and *Fmr1* KO/*Fxr2* heterozygous animals exhibit a loss of rhythmic activity in a light:dark (LD) cycle, and that *Fmr1* or *Fxr2* KO mice display a shorter free-running period of locomotor activity in total darkness (DD). Molecular analysis and in vitro electrophysiological studies suggest essentially normal function of cells in the suprachiasmatic nucleus (SCN) in *Fmr1/Fxr2* double KO mice. However, the cyclical patterns of abundance of several core clock component messenger (m) RNAs are altered in the livers of double KO mice. Furthermore, FXR2P alone or FMRP and FXR2P together can increase PER1- or PER2-mediated BMAL1-Neuronal PAS2 (NPAS2) transcriptional activity in a dose-dependent manner. These data collectively demonstrate that *FMR1* and *FXR2* are required for the presence of rhythmic circadian behavior in mammals and suggest that this role may be relevant to sleep and other behavioral alterations observed in fragile X patients.

Introduction

Fragile X syndrome (FXS [MIM #300624]) is the most common form of inherited mental retardation, with an estimated prevalence of 1 in 4000 males and 1 in 8000 females.[1] Typical fragile X patients display physical and behavioral abnormalities, such as a long, narrow face, large ears, macroorchidism, cognitive impairment, hyperactivity, and autistic behaviors.[2] The common form of this syndrome is caused by an expansion mutation of a CGG triplet repeat in the 5′ UTR of the *FMR1* gene, which transcriptionally silences the gene and leads to loss of FMRP.[3] FMRP is an RNA-binding protein that associates with translating polyribosomes.[4–6] *Fmr1* mRNA and FMRP are expressed ubiquitously, particularly the brain and testes.[7]

FMRP (MIM *309550), FXR1P (MIM *600819), and FXR2P (MIM *605339) compose a small family of RNA-binding proteins (fragile X-related protein family; *FXR* family).[8,9] These three proteins share >60% amino acid identity and are able to form homo- and heterotypic interactions with each other.[9,10] It has been postulated that the presence of FXR1P and FXR2P could partially compensate for the loss of FMRP in the fragile X syndrome. *Drosophila* has a single gene, *Drosophila* FMR1 (*dfmr1*) or *Drosophila* Fmr1-related gene (*dfxr*), whose product shares sequence identity and biochemical properties with the fragile X-related protein family.[11] To unravel the molecular and cellular bases of fragile X syndrome and to explore therapeutic strategies, both *Drosophila* and mouse models have been produced. We and others tested *dfmr* loss-of-function flies and found altered circadian behavior without detectable alteration in central clock components.[12,13] The disturbed activity-rest cycle of the fly, together with the observed sleep disorders in fragile X patients,[2,14] led us to investigate circadian behavior in mice with viable mutations in members of the *FXR* family.[15,16]

In this study, we demonstrate that mice lacking FMRP or FXR2P display a shorter free-running period of locomotor activity in total darkness. In the absence of both proteins, completely arrhythmic activity was observed in animals maintained in a light:dark cycle. This arrhythmic phenotype is unique among circadian defects described in mouse models to date. Interestingly, in the absence of FMRP/FXR2P, the cyclical patterns of abundance of several core clock component mRNAs are altered in the liver, which contains a major peripheral clock. By using an in vitro luciferase transfection assay, we observed that FXR2P alone or FMRP and FXR2P together can increase PER1- or PER2-mediated BMAL1-NPAS2 transcriptional activity in a dose-dependent manner. These data collectively demonstrate that *FMR1* and *FXR2* are required for the presence of behavioral circadian rhythms and indicate that this role may be relevant to the behavioral alterations observed in fragile X patients.

Material and Methods

Locomotor Assays

All experiments were performed with male C57BLl/6J mice of the following genotypes: *Fmr1* KO, *Fxr2* KO, *Fmr1/Fxr*2 double KO, *Fmr1* KO/*Fxr2* heterozygous, and their nonmutant littermates as controls (6- to 10-month-old). Animals were individually housed in standard cages equipped with running wheels within ventilated, light-tight chambers with time-controlled lighting.

[1]Department of Molecular and Human Genetics, Baylor College of Medicine, One Baylor Plaza, Houston, TX 77030, USA; [2]Department of Medicine, Division of Biochemistry, University of Fribourg, 1700 Fribourg, Switzerland; [3]Department of Molecular Cell Biology, Leiden University Medical Center, Postal Zone S5-P, P.O. Box 9600, 2300 RC Leiden, The Netherlands; [4]Department of Biochemistry and Molecular Biology, University of Texas Health Science Center, Houston, TX 77030, USA; [5]MGC, Department of Genetics, [6]Department of Clinical Genetics, Erasmus University Medical Center, 3000 CA Rotterdam, The Netherlands

*Correspondence: nelson@bcm.tmc.edu

DOI 10.1016/j.ajhg.2008.06.003.

Please cite this article in press as: Zhang et al., Fragile X-Related Proteins Regulate Mammalian Circadian Behavioral Rhythms, The American Journal of Human Genetics (2008), doi:10.1016/j.ajhg.2008.06.003

Experimental animals were continuously provided with food and water. Wheel-running activity was recorded by a computer data-acquisition system (Chronobiology kit, Stanford Software Systems). Animals were maintained on a 12:12 light/dark cycle for 2 weeks and then were transferred to constant darkness for at least 2 weeks. The raw activity data can be visualized and analyzed with a χ^2 periodogram (Chronobiology kit). The data were plotted in double plot activity histograms. The free-running period, τ, and total activity were analyzed with the Chronobiology kit.

In Situ Hybridization

Adult wild-type (6- to 10-month-old), *Fmr1* mutant, *Fxr2* mutant, and *Fmr1/Fxr2* double mutant mice were maintained in 12:12 LD cycle for 2 weeks and then released into DD. At 36th, 42nd, 48th, and 54th hour in the constant darkness, the mice were sacrificed for the experiments. Specimen preparation and in situ hybridization were carried out as described previously.[17] In brief, the [^{35}S]UTP (1250 Ci/mmol, PerkinElmer)-labeled riboprobes were synthesized with the RNAMaxx High Yield transcription kit (Stratagene) according to manufacturer's protocol. The *mBmal1* probe was made from a cDNA corresponding to nucleotides (nt) 654–1290 (accession number AF015953), *mCry1* corresponds to nt 190–771 (AB000777), *mPer1* to nt 620–1164 (AF022992), and *mPer2* to nt 229–768 (AF036893). 7 μm thick paraffin sections were dewaxed, rehydrated, and fixed in 4% paraformaldehyde. Sections were then permeabilized with a proteinase K (Roche) digestion before they were fixed again and acetylated. After serial dehydration, hybridization was performed overnight at 55°C in a humid chamber. Stringency washes were carried out at 63°C. Slides were subjected to a ribonuclease A (Sigma) digestion and then dehydrated in graded ethanol series. Quantification was performed by densitometric analysis (GS-700 or GS-800, BioRad) of autoradiography films (Amersham Hyperfilm) with the Quantity One software (BioRad). Data from the SCN were normalized by subtracting the optical density measured in the lateral hypothalamus next to the SCN. For each experiment, 2 animals per genotype were used and 4 to 9 adjacent SCN sections per animal were analyzed. Relative RNA abundance values were calculated by defining the highest wild-type mean value of each experiment as 100%. For statistical analysis, two-way ANOVA with Bonferroni post-test (GraphPad Prism software) was performed.

In Vitro Electrophysiology

The multiunit electrical activity rhythms of SCN neurons were recorded as described previously.[18] In short, brains of WT, *Fmr1* KO, and *Fmr1/Fxr*2 double KO mice were rapidly dissected from the skull at the same Zeitgeber times (1.7 hr to 2.4 hr after lights on). Coronal hypothalamic slices that contained the SCN were sectioned and transferred to an interface chamber. Slices were oxygenated with humidified 95% O_2/5% CO_2 and perfused with artificial cerebrospinal fluid (ACSF) at 35°C. We used one slice per animal and attempted simultaneous recordings of multiunit neuronal activity from the dorsal and ventral SCN with two stationary electrodes.

Northern Blot Analysis

Liver total RNA was isolated by guanidinium isothiocyanate extraction and CsCl centrifugation[19] from adult wild-type (6- to 10-month-old), *Fmr1* mutant, *Fxr2* mutant, and *Fmr1/Fxr2* double mutant mice. These animals were maintained in 12:12 LD cycle for 2 weeks and then released into DD for at least 24 hr. For all northern blot analyses, 25 μg of total RNA was separated on 1.2% agarose-formaldehyde gels and transferred to nylon membranes. The UV crosslinked membranes were hybridized with ^{32}P-labeled cDNA probes for *Bmal1, Clock, Per1, Per2*, *Cry1, Npas2*, and *Actin* according to the instructions of the manufacturer (BD Biosciences). To calculate relative RNA abundance, optical densities of *Bmal1, Clock, Per1, Per2, Cry1*, and *Npas2* hybridization were divided by densities from *Actin* hybridization to the same blot. Normalized values were then averaged for the blots prepared from different sets of RNA samples.

Real-Time PCR

The same RNA isolated for northern blot analysis was also used for real-time PCR analysis. To prepare cDNA, 1–3 μg total RNA was reverse-transcribed with random primers at a final concentration of 3 mM $MgCl_2$, 75 mM KCl, and 50 mM Tris-HCl (pH 8.3), 1 mM each of dNTPs, 10 units of RNase inhibitor, and 100 units of Superscript II Rnase H$^-$reverse transcriptase (Invitrogen). The reaction mixture was incubated at 37°C for 60 min. Real-time PCR was performed with the ABI PRISM 7000 Sequence Detector System (SDS) (Applied Biosystems) and MicroAmp optical 96-well plates (Applied Biosystems). Gene expression assays were performed with commercially available Pre-made TaqMan Gene Expression assays for eight genes. The specific Pre-made TaqMan Gene Expression assays used in this study were: *Bmal1* (Applied Biosystems, Assay ID: Mm00500226_m1), *Clock* (Mm00455950_m1), *Per1* (Mm00501813_m1), *Per2* (Mm00478113_m1), *Cry1* (Mm00514392_m1), and *Npas2* (Mm00500848_m1). Eukaryotic 18S rRNA (Applied Biosystems 4333760T) was used as endogenous control. The thermocycling profile for all PCR reactions began with 1 cycle of 2 min at 50°C and 10 min at 95°C and was followed by 40 cycles of 15 s at 95°C and 1 min at 60°C. All samples were run in triplicate.

Dual Luciferase Reporter Assays

Transient transfection was carried out with the Lipofectamine^{2000} reagent (Invitrogen) according to the manufacturer's instructions. In brief, 1×10^5 HeLa cells were seeded in each well of a 24-well tissue culture plate. The cells were incubated until 85%–90% confluence. Cells in each well were transfected with 10 ng of the *mPer1-luc* or 40 ng *mPer2-luc* reporter construct. Expression vectors for BMAL1, CLOCK, NPAS2, PER1, PER2, CRY1, FMR1, and FXR2 were cotransfected respectively. The renilla luciferase reporter pRL-TK plasmid (Promega) was cotransfected as an internal control. The pcDNA3.1 (Invitrogen) vector was used to bring the total amount of plasmid DNA to 0.8 μg/well. Transfection was done with Lipofectamine^{2000} reagent. After transfection for 18 hr, cells were collected and lysed and the firefly and renilla luciferase activity were measured with Dual-Luciferase Reporter Assay System (Promega) according to the manufacturer's instructions with a TD-20e luminometer (Turner designs).

Results

Fmr1 or *Fxr2* KO Mice Display a Shorter Free-Running Period of Locomotor Activity in DD

To determine whether mutations in the fragile X-related protein family alter circadian behavior, we measured the circadian wheel-running activity of *Fmr1* knockout (*Fmr1* KO) mice, *Fxr2* knockout (*Fxr2* KO) mice, and of their

Please cite this article in press as: Zhang et al., Fragile X-Related Proteins Regulate Mammalian Circadian Behavioral Rhythms, The American Journal of Human Genetics (2008), doi:10.1016/j.ajhg.2008.06.003

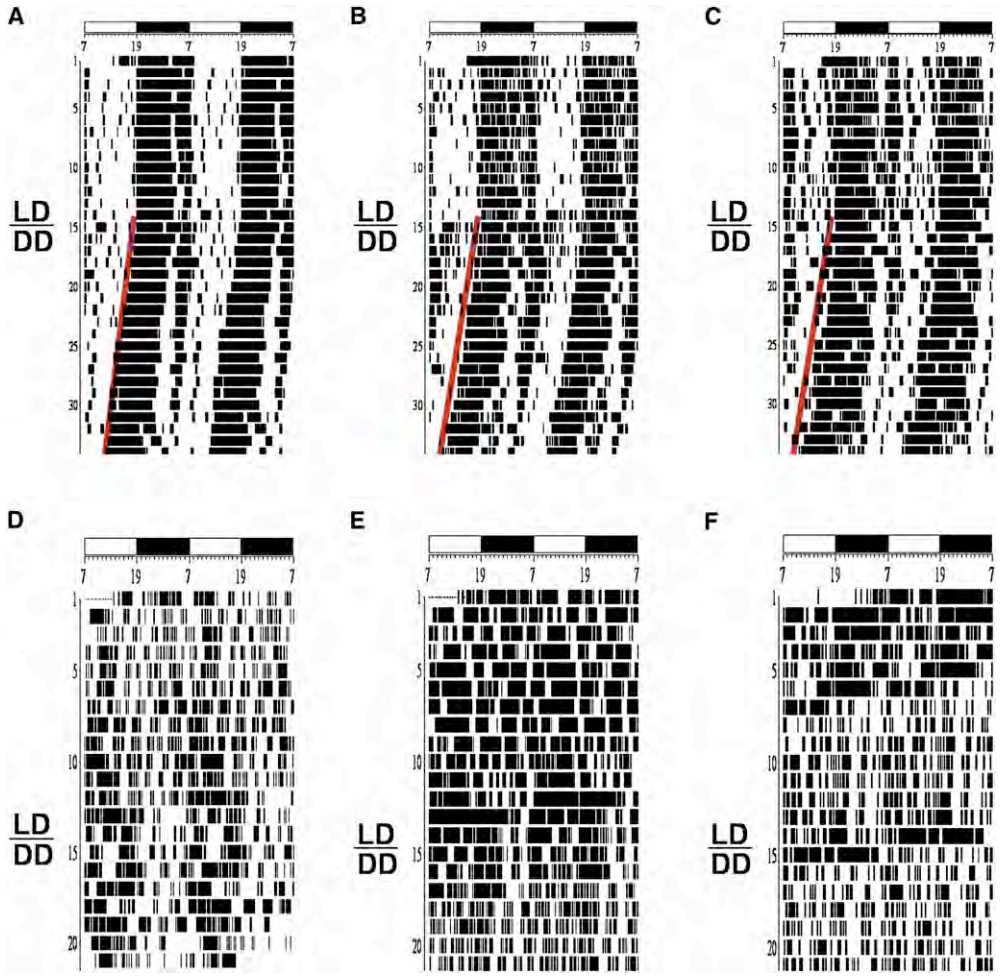

Figure 1. Representative Locomotor Activity Records of Wild-Type, ***Fmr1*** KO, ***Fxr2*** KO, and ***Fmr1***/***Fxr2*** Double KO Mice
(A) Representative locomotor activity records of WT mice.
(B) Representative locomotor activity records of *Fmr1* KO mice.
(C) Representative locomotor activity records of *Fxr2* KO mice.
(D–F) Representative locomotor activity records of *Fmr1/Fxr2* double KO mice. Activity records are double-plotted, so that 48 hr is shown on each horizontal trace with a 24 hr day presented both beneath and to the right of the preceding day. Times of activity are indicated by black vertical marks. All records show activity in wheel running activity during exposure to a 12:12 light/dark cycle and after release into constant darkness (as indicated by the LD/DD in the margin). The slope of the line (in red) aligned with the points of onset of activity on a 24 hr scale plot reflects the period length in DD. The open and dark rectangles at the top of the figure indicate the LD cycle during entrainment.

wild-type (WT) littermates individually in circadian activity-monitoring chambers. Mice were initially maintained in a 12 hr light:12 hr dark (12:12 LD) cycle for 2 weeks to establish entrainment. After release in constant darkness (DD), the WT animals showed a free-running period (tau or τ) of slightly less than 24 hr ($\tau = 23.88 \pm 0.05$; $n = 12$) (Figure 1A). *Fmr1* and *Fxr2* knockout mice displayed significantly shorter circadian periods than their WT littermates in DD ($\tau = 23.71 \pm 0.06$, $p < 0.01$; $n = 18$; and $\tau = 23.56 \pm 0.05$, $p < 0.01$; $n = 28$; respectively) (Figures 1B and 1C; for all tau values, see Figure S1A available online). These findings suggest that FMRP and FXR2P affect the period length of the circadian system. Under LD conditions, *Fmr1* and *Fxr2* knockout mice were entrained by light (Figures 1B and 1C), suggesting that a deficiency in either gene alone does not produce a detectable loss of entrainment of locomotor activity.

Fmr1/Fxr2 Double KO and *Fmr1* KO/*Fxr2* Heterozygous Mice Exhibit a Loss of Rhythmic Activity in Both LD and DD

Because *Fmr1* knockout mice express FXR2P at normal levels (and vice versa), functional redundancy may blur phenotypic outcomes in single KO animals. It was of interest, therefore, to examine *Fmr1*/*Fxr2* double knockout mice, which are viable and do not exhibit major physical defects.[20] Unexpectedly, the locomotor activity patterns of these double mutant animals not only exhibited a striking and complete loss of circadian rhythm in constant darkness but were also arrhythmic under LD cycles (Figures

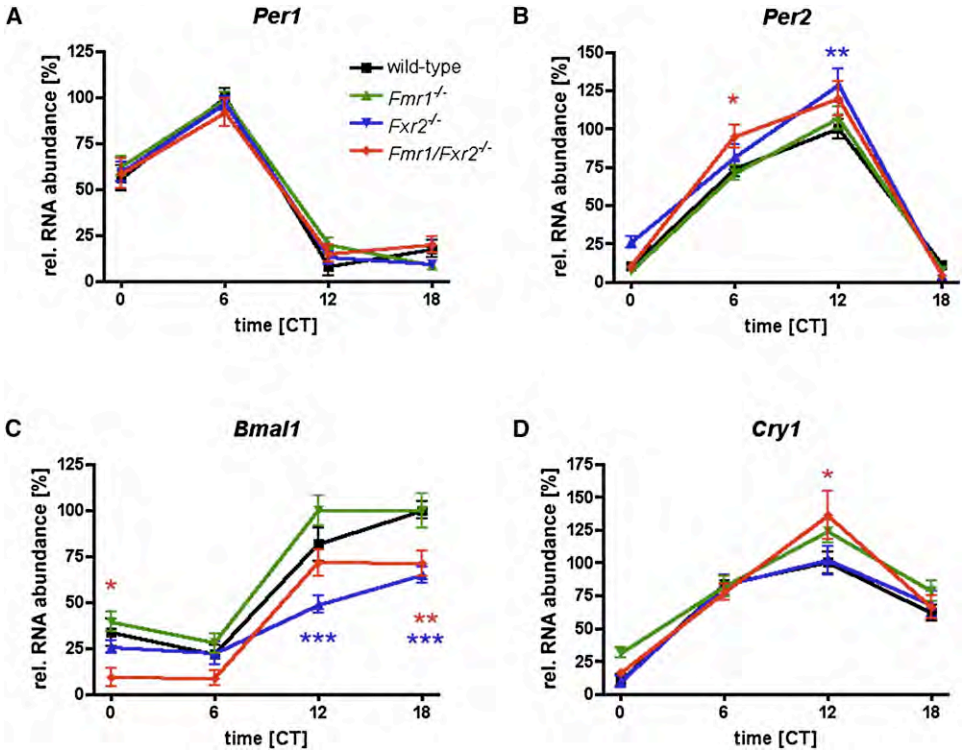

Figure 2. Expression Analysis of Wild-Type, ***Fmr1*** KO, ***Fxr2*** KO, and ***Fmr1/Fxr***2 Double KO under DD Conditions in SCN
In situ hybridization results for brains isolated from WT and the three knockout genotypes sacrificed at four different time points for *Per1* (A), *Per2* (B), *Bmal1* (C), and *Cry1* (D) mRNA levels of *Per1, Per2, Bmal1*, and *Cry1* were quantified and normalized. Graphs illustrate the relative transcript level of these four genes. The largest value of WT is normalized to 100%. Error bars indicate the SEM. *p < 0.05, **p < 0.01, ***p < 0.001. CT, circadian time.

1D–1F, n = 12; for more samples from double KO mice under LD conditions, see Figures S2A–S2D). Chi-square periodogram analysis in LD for double knockout mice showed no measurable circadian rhythm (Figures S2E–S2H). Interestingly, *Fmr1* knockout mice that were heterozygous for the *Fxr2* mutation (n = 8) also demonstrated wheel-running patterns that were largely comparable to double-knockout mice (Figures S2I–S2P), with weakly cyclical activity in LD that does not appear to be synchronized to the 24 hr period. Apparently, in the absence of FMR1, half normal levels of FXR2 are inadequate to establish entrainment in the LD cycle. Because the average levels of wheel-running activity did not differ significantly ($p > 0.05$ by one-way ANOVA) among the four genotypes in DD (wheel rotations per day for WT, *Fmr1*, *Fxr2*, and double knockout mice are 26,512 ± 2,898; 27,924 ± 2,378; 26,735 ± 1,836; and 23,980 ± 2,798, respectively), the absence of a circadian rhythm cannot be explained by a change in total activity.

Our behavioral experiments demonstrate that disruption of either of the two fragile X mental retardation genes results in alterations of circadian period, and combined disruption of both results in arrhythmicity in behavior. Light and visual perception in double KO mice are normal[20] and no abnormalities could be detected in the eyes of these animals by histology (data not shown). These results indicate that FXRPs function in the mammalian circadian clock or act downstream in the control of activity.

Molecular Analysis and In Vitro Electrophysiological Studies Suggest Normal SCN Function in the *Fmr1/Fxr2* Double KO Mice

To investigate whether the behavioral differences between the three knockout strains and their WT littermates might be due to a defect in the central circadian pacemaker, we examined clock gene expression in the suprachiasmatic nucleus (SCN) of the brain. Figure 2 illustrates expression of clock gene mRNAs (*Per1, Per2, Bmal1*, and *Cry1*) in the mouse SCN by in situ hybridization. The expression of *Per1, Per2, Bmal1*, and *Cry1* was rhythmic in the SCN over 24 hr in constant darkness (Figure 2). Significant quantitative differences were observed between genotypes. For example, *Fmr1/Fxr2* double knockout animals showed an increased level of *Cry1* expression at CT12, which coincides with the predicted time of light off (Figure 2D). Nonetheless, the overall pattern of clock gene expression in the SCN appears unchanged between animals of different genotypes. We also investigated the electrical activity of the SCN pacemaker of WT, *Fmr1* KO (n = 6), and *Fmr1/Fxr2* double KO (n = 7) mice. Electrical activity is controlled by the core clock and serves as a major output signal of the SCN. We found that the SCN electrical activity shows high amplitude circadian rhythmicity in WT (data not

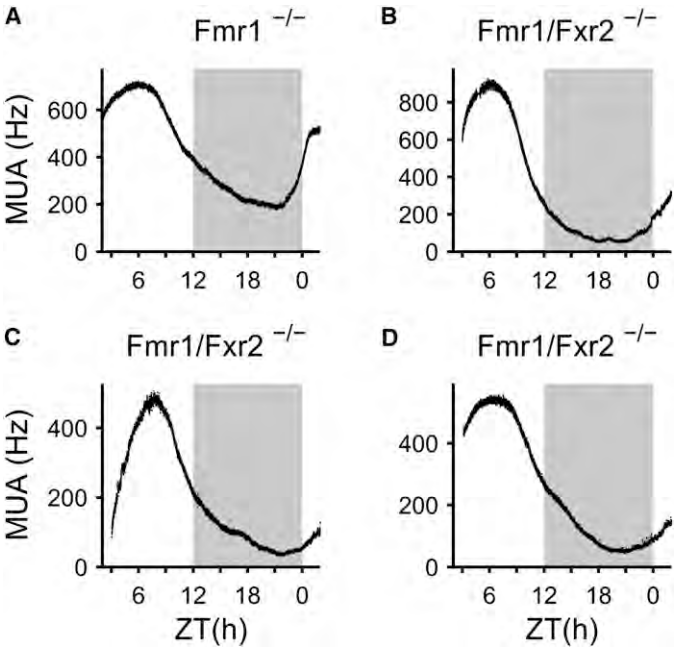

Figure 3. Representative Recordings of SCN Electrical Activity in ***Fmr1*** KO and ***Fmr1/Fxr***2 Double KO Mice

(A) Representative recordings of SCN electrical activity in *Fmr1* KO mice.

(B–D) Representative recordings of SCN electrical activity in *Fmr1/Fxr2* double KO mice. The electrical activity traces are individual examples of neuronal ensemble recordings. The open and dark rectangles at the top of the figure indicate the LD cycle to which the animals were entrained before slice preparation, and time is indicated on the *x* axis. The electrical activity is counted per 10 s and presented on the *y* axis. MUA, multiunit electrical activity.

shown), *Fmr1* KO (Figure 3A), and *Fmr1/Fxr2* double KO (Figures 3B–3D) mice, with no significant differences in peak time ($p > 0.2$). Preparation of slices 12 hr out of phase from *Fmr1/Fxr2* double KO animals results in similar peak time (data not shown). Our molecular and in vitro electrophysiological data suggest that the SCN pacemaker is intact in knockout animals and that behavioral differences observed between wild-type and *Fmr1* KO, *Fxr2* KO, and *Fmr1/Fxr2* double KO animals are unlikely to result from a deficiency in the SCN but could be caused by a deficiency downstream of the SCN pacemaker.

The Cyclical Patterns of Abundance of Several Core Clock Component mRNAs Are Altered in the Liver of Double KO Mice

When we examined the mRNA levels in the liver, which is probably the best described peripheral clock in mammals, we observed a substantial change in clock gene expression in knockout animals. Expression of *Bmal1* in the livers of double knockout mice is decreased at CT0 (Figures 4A, 4B, and 5A; Figures S3A and S3G). Compared to WT mice, *mPer1* expression in the liver of *Fxr2* and *Fmr1/Fxr2* double mutants is significantly increased at CT6 ($p < 0.01$ for both genotypes, Figures 4A, 4B, and 5C; Figures S3C and S3G). It is also notable that the distributions of levels of *mPer1* expression are much wider at CT6 and CT12 in the liver of *Fxr2* and *Fmr1/Fxr2* double knockout mice (Figure 5C; Figure S3C). *mPer2* expression in the liver peaks approximately 6 hr earlier in *Fmr1/Fxr2* double mutants compared to *Fmr1* knockout or WT animals (Figures 4A, 4B, and 5D; Figures S3D and S3G). Similar to *mPer1*, the variations of *mPer2* expression levels at CT6 in the liver of *Fxr2* and *Fmr1/Fxr2* double knockout mice are much more broad than those in WT animals (Figure 5D; Figure S3D). The expression of *Cry1* is significantly increased at CT12 in the livers of both double and either of the single KO mice (Figures 4A, 4B, and 5E; Figures S3E and S3G). *Clock*, which does not cycle in WT animals, was not significantly altered in the livers of the mutants (Figures 4A, 4B, and 5B; Figures S3B and S3G).

Npas2, a transcription factor that is highly similar to *Clock*, heterodimerizes with *Bmal1* and activates *Per* transcription.[21,22] Because *Clock* expression was indistinguishable between WT and mutants, we tested the expression of *Npas2* transcript in the liver (*Npas2* expression cannot be detected by in situ hybridization in the SCN). *Npas2* expression in *Fmr1* mutants is similar to that in WT. However, *Npas2* expression in *Fxr2* mutants is slightly increased at CT18 and significantly decreased at CT0. In double mutants, *Npas2* expression peaks at CT18, whereas it peaks at CT0 in WT controls (Figures 4A, 4B, and 5F; Figures S3F and S3G). This indicates that in the absence of *Fxr2, Npas2* expression is altered and that *Fmr1* has an additive effect on *Npas2* cycling. These data suggest that the loss of FMRP, FXR2P, or both affects peripheral circadian clock function.

FXR2P Alone or FMRP and FXR2P Together Can Increase PER1- or PER2-Mediated BMAL1-NPAS2 Transcriptional Activity in a Dose-Dependent Manner

To determine whether FMRP and FXR2P can directly regulate clock gene expression, we performed a luciferase reporter assay in HeLa cell transfection assays. Initial studies showed that addition of mPER2 enhanced BMAL1-NPAS2-dependent transcription from either *mPer1* or *mPer2* promoter as previously described.[23] Coexpression of FXR2P or the combination of FMRP and FXR2P together significantly enhanced the mPER2-induced BMAL1-NPAS2 transcriptional activity from both promoters (Figures 6A and 6B). Similarly, mPER1-induced BMAL1-NPAS2 transcription from the *mPer1* promoter is further activated by FXR2P or FMRP and FXR2P together (Figure 6C). Furthermore, this effect on transcriptional stimulation was dependent on the dose of FXRPs (Figures S5A and S5B), which agrees with the observations that FMRP functions in a dose-dependent manner in flies, mice, and human patients.[13,24,25] However, coexpression of FMRP or FXR2P or both together was not found to influence CRY1 repression of BMAL1-NPAS2 stimulation (Figures S4A and S4B). Interestingly, similar transfection studies with

Please cite this article in press as: Zhang et al., Fragile X-Related Proteins Regulate Mammalian Circadian Behavioral Rhythms, The American Journal of Human Genetics (2008), doi:10.1016/j.ajhg.2008.06.003

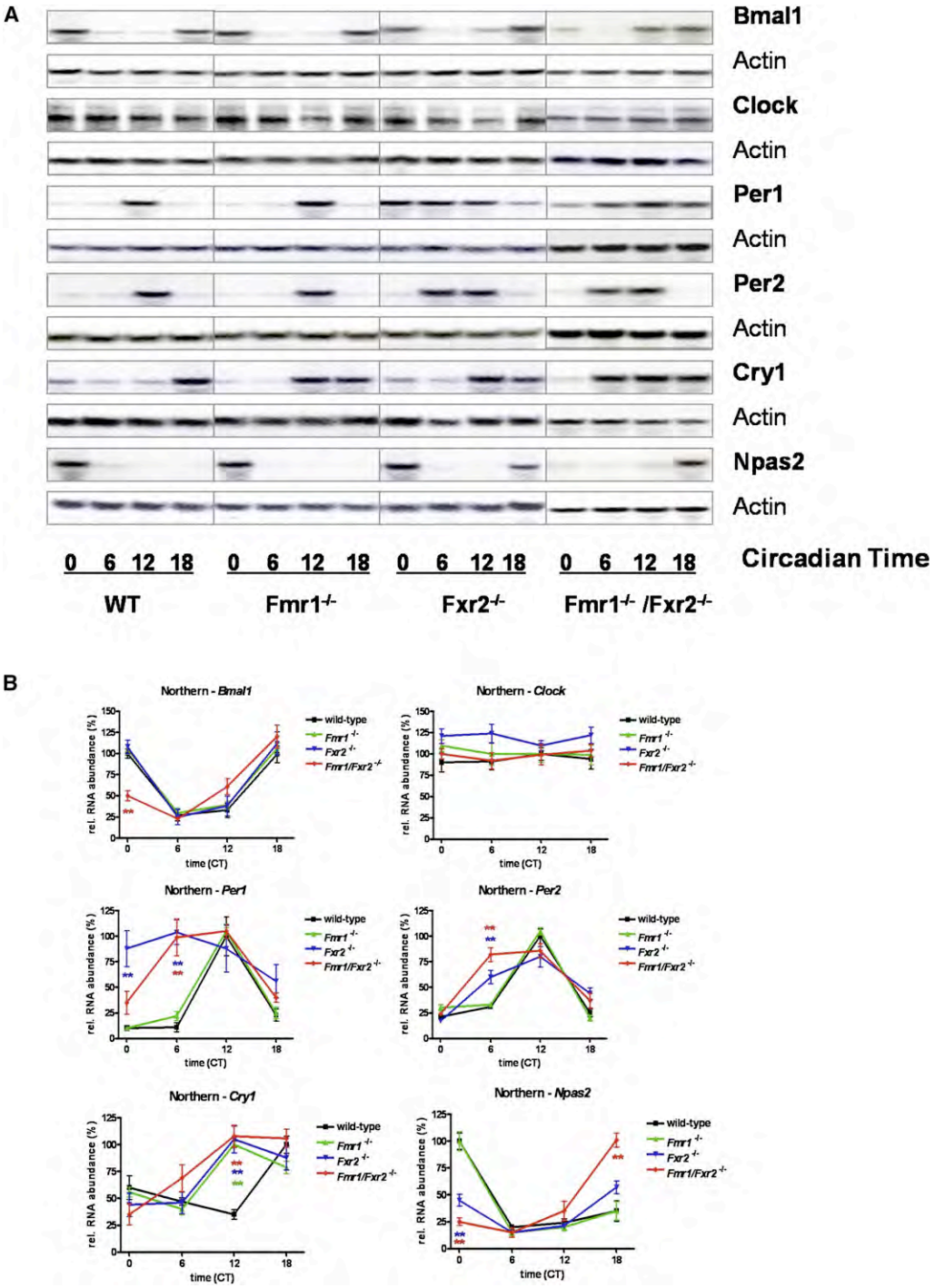

Figure 4. Expression Analysis of Wild-Type, ***Fmr1*** KO, ***Fxr2*** KO, and ***Fmr1***/***Fxr2*** Double KO Mice under DD Conditions in Liver

(A) Northern blotting results on liver tissues of WT and three different knockout mouse genotypes sacrificed at four different time points. The probes are indicated on the right. Rehybridization of the same filter with an actin probe was used to control for loading and RNA integrity. Representative results are shown from one out of four sets of WT, three sets of *Fmr1* KO, four sets of *Fxr2* KO, and five sets of *Fmr1/Fxr2* double KO mice. Each set of animals represents an independent experiment.

(B) RNA levels of *Bmal1, Clock, Per1, Per2, Cry1*, and *Npas2* were quantified and normalized in reference to actin mRNA levels. The largest value of WT is normalized to 100%. Graphs illustrate the relative transcript level of these six genes. Error bars indicate the SEM. *$p < 0.05$, **$p < 0.01$.

BMAL1-CLOCK showed no stimulation by either FMRP or FXR2P or by both together (data not shown). Our data indicate that FMRP and FXR2P have direct influence on the molecular clock feedback loop and that these effects are mediated by the BMAL1-NPAS2 rather than the BMAL1-CLOCK complex. Based on these findings and on our observations

Please cite this article in press as: Zhang et al., Fragile X-Related Proteins Regulate Mammalian Circadian Behavioral Rhythms, The American Journal of Human Genetics (2008), doi:10.1016/j.ajhg.2008.06.003

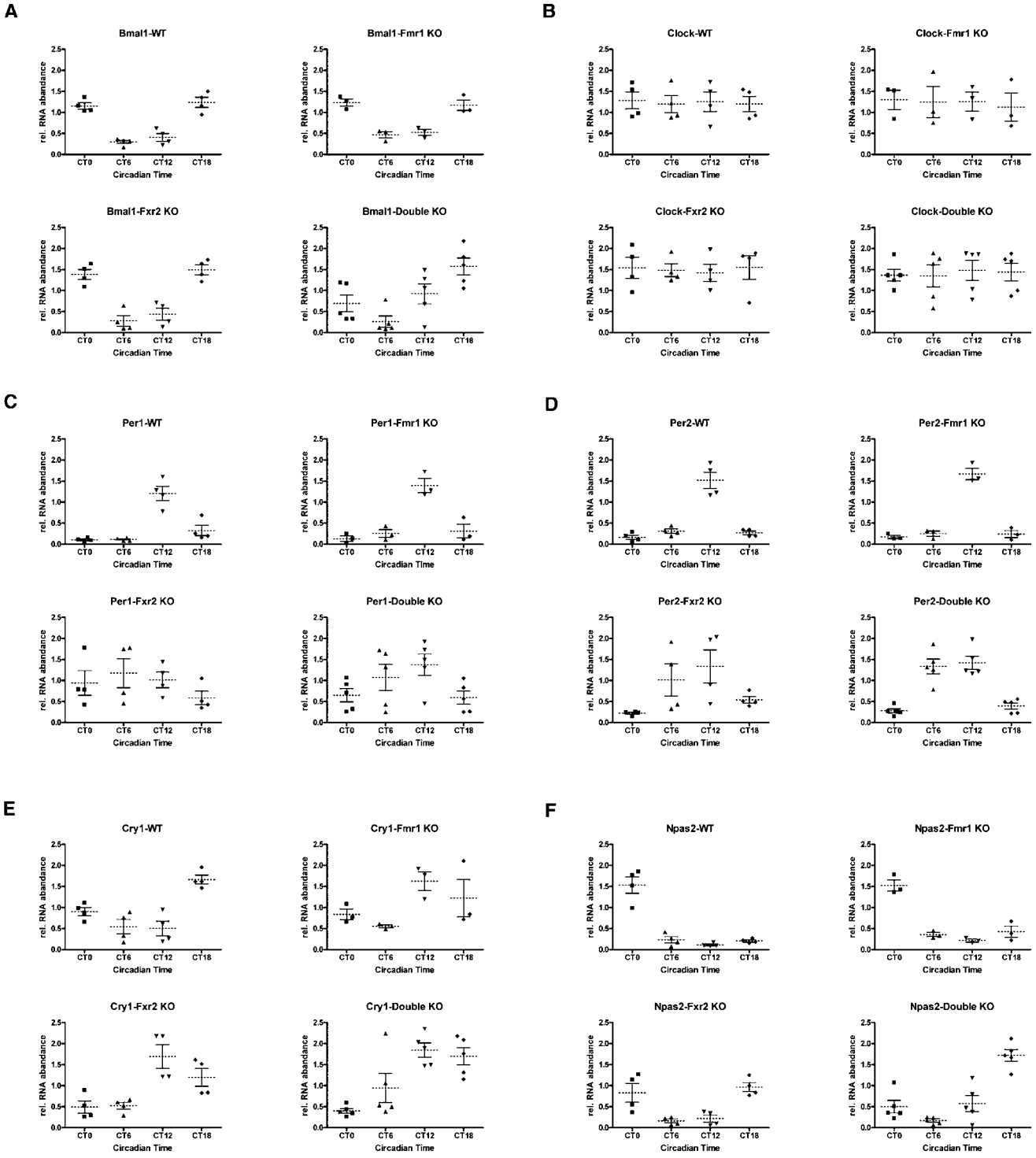

Figure 5. Expression Analysis of Four Sets of Wild-Type, Three Sets of ***Fmr1*** KO, Four Sets of ***Fxr2*** KO, and Five Sets of ***Fmr1***/***Fxr2*** Double KO Mice under DD Conditions in Liver

RNA levels of *Bmal1* (A), *Clock* (B), *Per1* (C), *Per2* (D), *Cry1* (E), and *Npas2* (F) were quantified and normalized in reference to actin mRNA levels. The data on relative mRNA abundance were averaged across different time points. Error bars indicate the SEM.

that *Npas2* expression is altered significantly in the livers of *Fxr* mutant animals, we propose that *NPAS2* plays an important role in the effects of the fragile X gene family on peripheral circadian oscillators and behavioral activity patterns.

Discussion

Circadian rhythmicity is a fundamental biological phenomenon in living organisms. Among animals, the fruit

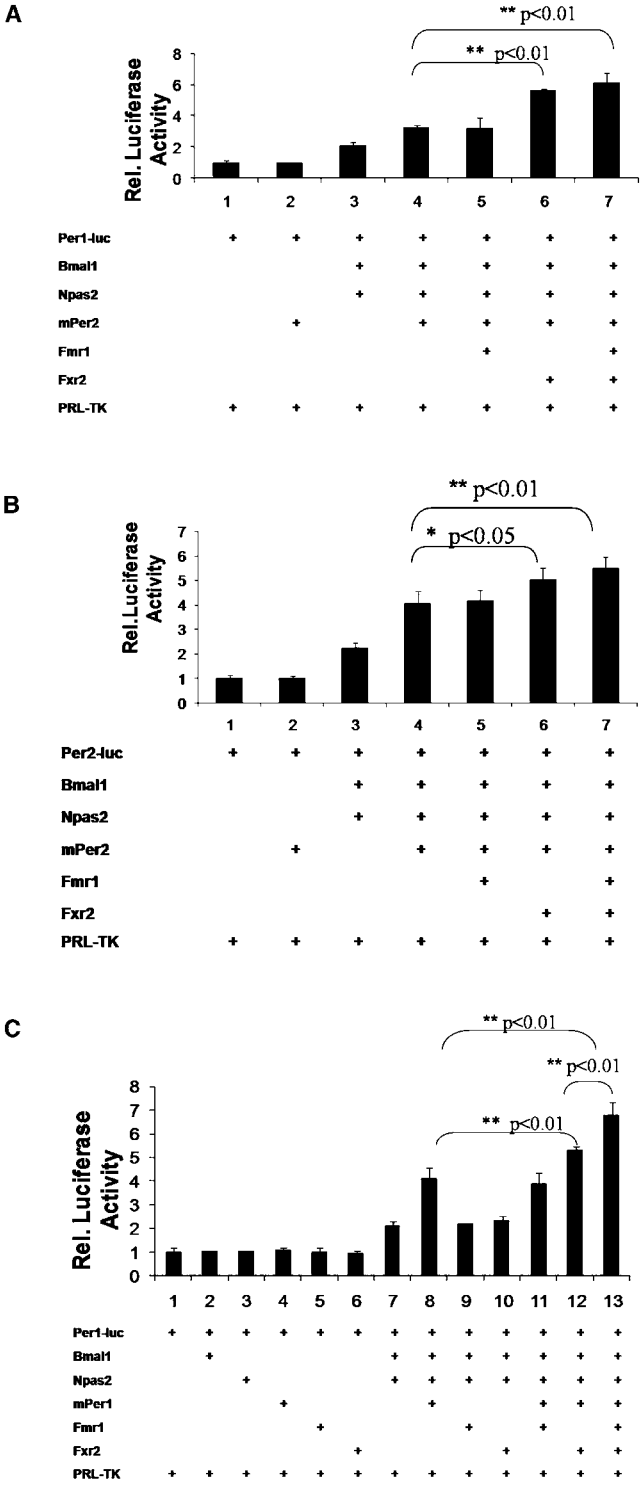

Figure 6. Upregulation of BMAL1-NPAS2-Mediated Transcription by FMR1 and FXR2 in the Presence of mPER1 or mPER2

(A) Upregulation of BMAL1-NPAS2-mediated transcription on *mPer1* promoter by FMR1 and FXR2 in the presence of mPER2.

(B) Upregulation of BMAL1-NPAS2-mediated transcription on *mPer2* promoter by FMR1 and FXR2 in the presence of mPER2.

(C) Upregulation of BMAL1-NPAS2-mediated transcription on *mPer1* promoter by FMR1 and FXR2 in the presence of mPER1. HeLa cells were cotransfected with the reporter construct *mPer1-luc* or *mPer2-luc* and control reporter construct Renilla luciferase encoding plasmids PRL-TK and various combinations of expression construct (Material and Methods). Luciferase activity in samples transfected with reporter constructs only is adjusted as 1.0. Error bars indicate the SD (n = 4).

fly and the mouse have provided the most information on the mechanism of central circadian pacemakers. These species' clocks share conserved gene products, although there are significant differences between the explanatory models for maintenance of rhythmicity.[26] In the fly, loss-of-function mutations of the *dfmr* gene have been shown to alter circadian behavior without detectably affecting the function of the central pacemaker, suggesting a role for *dfmr* in circadian output.[12,13] In the mouse, CLOCK, BMAL1, PER, and CRY are core components of the circadian oscillatory mechanisms. The active CLOCK-BMAL1 complex drives expression of numerous genes including PER and CRY, whereas PER and CRY repress CLOCK-BMAL1 transcriptional activities and therefore form a feedback regulation loop.[27,28] Regulation of CLOCK-BMAL1 activity is central to the mammalian clock. The appropriate delay between the activation and repression of transcription maintains the daily oscillations of clock proteins and gives the clock a ~24 hr period.[29] Here, we report a function for the *Fmr1* and *Fxr2* genes in circadian behavior and clock gene expression in the liver of mice. The dramatic circadian activity phenotype found in *Fmr1/Fxr2* double KO mice is unprecedented, demonstrating a significant role of those genes in clock function or output. The alterations to clock gene mRNAs in the liver, but not in the master clock, suggest that FMRP and FXR2P are acting downstream of the circadian pacemaker in mammals. CLOCK and NPAS2 have been shown to have partially redundant functions in the SCN, with CLOCK having a dominant role.[30] Our transfection data would suggest that the FXR proteins exert effects on NPAS2/BMAL1 complex rather than CLOCK/BMAL1. Thus, it is not surprising that the SCN is less affected than the liver in *Fxr* mutant animals. The differences between the SCN and liver of *Fxr* mutant mice suggest examination of the roles of FMRP and FXR2P in mice with mutations in *Clock* and/or *Npas2*. Intriguingly, animals lacking both *Clock* and *Npas2* show rhythmic activity in LD,[30] whereas *Fmr1/Fxr2* double knockouts are arrhythmic.

It is worth while to note that in addition to FMRP and FXR2P, FXR1P, another member of *FMR1* gene family, may play a compensatory role in the absence of *Fmr1*, *Fxr2*, or in *Fmr1/Fxr2* double knockout mice. Because of the early postnatal death of *Fxr1* knockout mice, a conditional *Fxr1* knockout model was produced.[31] These mice exhibit muscle defects, but the generation of *Fmr1/Fxr1/Fxr2* triple mutant mice should provide more information on potential functional interactions in circadian clock regulation and may offer a more direct comparison to the *Drosophila* loss-of-function model, where a single *FMR1*-like protein may perform many of the functions distributed among the three mammalian genes.

The neural connections between the SCN and other parts of the nervous system are important for the control of

circadian rhythms in the central nervous system.[32] Interestingly, it has been shown that the absence of FMRP causes abnormal neurotransmitter signaling, which could be responsible for neurological deficiencies in fragile X syndrome.[33,34] It is possible, therefore, that the loss of FMRP and FXR2P results in arrhythmicity resulting from inappropriate neuronal communication within the central nervous system.

A link between abnormal sleep patterns and mental retardation has been suggested from several other mental retardation disorders,[35] including Smith-Magenis syndrome,[36] where the RAI1 transcriptional activator appears to be a major contributor to phenotype. To our knowledge, our data provide the first molecular evidence to connect a protein involved in cognitive ability with the circadian system. Although sleep abnormalities are a frequent feature in males with fragile X syndrome, the level of severity varies significantly in different patients.[2,14] Our data that in the absence of *Fmr1*, losing half normal levels of *Fxr2* can result in loss of light-dark entrainment suggest that genetic variation in *Fxr2* could be responsible for the variability of sleep problems in fragile X population. Sleep abnormality could add to the phenotype; several lines of evidence suggest a role for normal sleep in learning and memory.[37] The close association between the circadian system and the timing of sleep and wakefulness together with the typical disturbances of circadian behavior and sleep in fragile X syndrome opens up a new perspective for the investigation and treatment of patients suffering from this disorder.

Supplemental Data

Five figures are available at http://www.ajhg.org/.

Acknowledgments

This work was supported in part by grant HD38038 from the US National Institute of Child Health and Human Development to D.L.N. and B.A.O., grant HD24064 from the BCM Intellectual and Developmental Disabilities Research Center, the FRAXA Research Foundation, and by Swiss National Science Foundation and EUCLOCK to U.A. The authors wish to thank Richard Paylor, Yanghong Gu, and Jianfa Zhang for their input and discussion.

Received: March 13, 2008
Revised: May 21, 2008
Accepted: June 3, 2008
Published online: June 26, 2008

Web Resources

The URL for data presented herein is as follows:

Online Mendelian Inheritance in Man (OMIM), http://www.ncbi.nlm.nih.gov/Omim/

References

1. Warren, S.T., and Nelson, D.L. (1994). Advances in molecular analysis of fragile X syndrome. JAMA *271*, 536–542.
2. Hagerman, R.J. (1996). Fragile X Syndrome: Diagnosis, Treatment, and Research, Second Edition (Baltimore: John Hopkins University Press), pp. 3–87.
3. Verkerk, A.J., Pieretti, M., Sutcliffe, J.S., Fu, Y.H., Kuhl, D.P., Pizzuti, A., Reiner, O., Richards, S., Victoria, M.F., Zhang, F.P., et al. (1991). Identification of a gene (*FMR-1*) containing a CGG repeat coincident with a breakpoint cluster region exhibiting length variation in fragile X syndrome. Cell *65*, 905–914.
4. Eberhart, D.E., Malter, H.E., Feng, Y., and Warren, S.T. (1996). The fragile X mental retardation protein is a ribonucleoprotein containing both nuclear localization and nuclear export signals. Hum. Mol. Genet. *5*, 1083–1091.
5. Corbin, F., Bouillon, M., Fortin, A., Morin, S., Rousseau, F., and Khandjian, E.W. (1997). The fragile X mental retardation protein is associated with poly(A)+ mRNA in actively translating polyribosomes. Hum. Mol. Genet. *6*, 1465–1472.
6. Feng, Y., Absher, D., Eberhart, D.E., Brown, V., Malter, H.E., and Warren, S.T. (1997). FMRP associates with polyribosomes as an mRNP, and the I304N mutation of severe fragile X syndrome abolishes this association. Mol. Cell *1*, 109–118.
7. Devys, D., Lutz, Y., Rouyer, N., Bellocq, J.P., and Mandel, J.L. (1993). The FMR-1 protein is cytoplasmic, most abundant in neurons and appears normal in carriers of a fragile X premutation. Nat. Genet. *4*, 335–340.
8. Siomi, M.C., Siomi, H., Sauer, W.H., Srinivasan, S., Nussbaum, R.L., and Dreyfuss, G. (1995). FXR1, an autosomal homolog of the fragile X mental retardation gene. EMBO J. *14*, 2401–2408.
9. Zhang, Y., O'Connor, J.P., Siomi, M.C., Srinivasan, S., Dutra, A., Nussbaum, R.L., and Dreyfuss, G. (1995). The fragile X mental retardation syndrome protein interacts with novel homologs FXR1 and FXR2. EMBO J. *14*, 5358–5366.
10. Kirkpatrick, L.L., McIlwain, K.A., and Nelson, D.L. (2001). Comparative genomic sequence analysis of the FXR gene family: *FMR1*, *FXR1*, and *FXR2*. Genomics *78*, 169–177.
11. Wan, L., Dockendorff, T.C., Jongens, T.A., and Dreyfuss, G. (2000). Characterization of dFMR1, a *Drosophila melanogaster* homolog of the fragile X mental retardation protein. Mol. Cell. Biol. *20*, 8536–8547.
12. Dockendorff, T.C., Su, H.S., McBride, S.M., Yang, Z., Choi, C.H., Siwicki, K.K., Sehgal, A., and Jongens, T.A. (2002). *Drosophila* lacking *dfmr1* activity show defects in circadian output and fail to maintain courtship interest. Neuron *34*, 973–984.
13. Morales, J., Hiesinger, P.R., Schroeder, A.J., Kume, K., Verstreken, P., Jackson, F.R., Nelson, D.L., and Hassan, B.A. (2002). *Drosophila* fragile X protein, DFXR, regulates neuronal morphology and function in the brain. Neuron *34*, 961–972.
14. Gould, E.L., Loesch, D.Z., Martin, M.J., Hagerman, R.J., Armstrong, S.M., and Huggins, R.M. (2000). Melatonin profiles and sleep characteristics in boys with fragile X syndrome: a preliminary study. Am. J. Med. Genet. *95*, 307–315.
15. The Dutch-Belgian Fragile X Consortium, Bakker, C.E., Verheij, C., Willemsen, R., Vanderhelm, R., Oerlemans, F., Vermey, M., Bygrave, A., Hoogeveen, A.T., Oostra, B.A., et al. (1994). *Fmr1* knockout mice: a model to study fragile X mental retardation. Cell *78*, 23–33.
16. Bontekoe, C.J., McIlwain, K.L., Nieuwenhuizen, I.M., Yuva-Paylor, L.A., Nellis, A., Willemsen, R., Fang, Z., Kirkpatrick, L., Bakker, C.E., McAninch, R., et al. (2002). Knockout mouse model for *Fxr2*: a model for mental retardation. Hum. Mol. Genet. *11*, 487–498.

17. Albrecht, U., Sun, Z.S., Eichele, G., and Lee, C.C. (1997). A differential response of two putative mammalian circadian regulators, *mper1* and *mper2*, to light. Cell *91*, 1055–1064.
18. Meijer, J.H., Schaap, J., Watanabe, K., and Albus, H. (1997). Multiunit activity recordings in the suprachiasmatic nuclei: in vivo versus in vitro models. Brain Res. *753*, 322–327.
19. Chirgwin, J.M., Przybyla, A.E., MacDonald, R.J., and Rutter, W.J. (1979). Isolation of biologically active ribonucleic acid from sources enriched in ribonuclease. Biochemistry *18*, 5294–5299.
20. Spencer, C.M., Serysheva, E., Yuva-Paylor, L.A., Oostra, B.A., Nelson, D.L., and Paylor, R. (2006). Exaggerated behavioral phenotypes in *Fmr1/Fxr2* double knockout mice reveal a functional genetic interaction between Fragile X-related proteins. Hum. Mol. Genet. *15*, 1984–1994.
21. Hogenesch, J.B., Gu, Y.Z., Jain, S., and Bradfield, C.A. (1998). The basic-helix-loop-helix-PAS orphan MOP3 forms transcriptionally active complexes with circadian and hypoxia factors. Proc. Natl. Acad. Sci. USA *95*, 5474–5479.
22. Reick, M., Garcia, J.A., Dudley, C., and McKnight, S.L. (2001). NPAS2: an analog of clock operative in the mammalian forebrain. Science *293*, 506–509.
23. Kaasik, K., and Lee, C.C. (2004). Reciprocal regulation of haem biosynthesis and the circadian clock in mammals. Nature *430*, 467–471.
24. Peier, A.M., McIlwain, K.L., Kenneson, A., Warren, S.T., Paylor, R., and Nelson, D.L. (2000). (Over)correction of FMR1 deficiency with YAC transgenics: behavioral and physical features. Hum. Mol. Genet. *9*, 1145–1159.
25. Menon, V., Leroux, J., White, C.D., and Reiss, A.L. (2004). Frontostriatal deficits in fragile X syndrome: relation to *FMR1* gene expression. Proc. Natl. Acad. Sci. USA *101*, 3615–3620.
26. Allada, R., Emery, P., Takahashi, J.S., and Rosbash, M. (2001). Stopping time: the genetics of fly and mouse circadian clocks. Annu. Rev. Neurosci. *24*, 1091–1119.
27. Reppert, S.M., and Weaver, D.R. (2002). Coordination of circadian timing in mammals. Nature *418*, 935–941.
28. Lowrey, P.L., and Takahashi, J.S. (2004). Mammalian circadian biology: elucidating genome-wide levels of temporal organization. Annu. Rev. Genomics Hum. Genet. *5*, 407–441.
29. Gallego, M., and Virshup, D.M. (2007). Post-translational modifications regulate the ticking of the circadian clock. Nat. Rev. Mol. Cell Biol. *8*, 139–148.
30. DeBruyne, J.P., Weaver, D.R., and Reppert, S.M. (2007). CLOCK and NPAS2 have overlapping roles in the suprachiasmatic circadian clock. Nat. Neurosci. *10*, 543–545.
31. Mientjes, E.J., Willemsen, R., Kirkpatrick, L.L., Nieuwenhuizen, I.M., Hoogeveen-Westerveld, M., Verweij, M., Reis, S., Bardoni, B., Hoogeveen, A.T., Oostra, B.A., and Nelson, D.L. (2004). Fxr1 knockout mice show a striated muscle phenotype: implications for Fxr1p function in vivo. Hum. Mol. Genet. *13*, 1291–1302.
32. Schwartz, W.J., Gross, R.A., and Morton, M.T. (1987). The suprachiasmatic nuclei contain a tetrodotoxin-resistant circadian pacemaker. Proc. Natl. Acad. Sci. USA *84*, 1694–1698.
33. Bear, M.F., Huber, K.M., and Warren, S.T. (2004). The mGluR theory of fragile X mental retardation. Trends Neurosci. *27*, 370–377.
34. D'Hulst, C., De Geest, N., Reeve, S.P., Van Dam, D., De Deyn, P.P., Hassan, B.A., and Kooy, R.F. (2006). Decreased expression of the GABAA receptor in fragile X syndrome. Brain Res. *1121*, 238–245.
35. Lamont, E.W., Legault-Coutu, D., Cermakian, N., and Boivin, D.B. (2007). The role of circadian clock genes in mental disorders. Dialogues Clin. Neurosci. *9*, 333–342.
36. De Leersnyder, H., Claustrat, B., Munnich, A., and Verloes, A. (2006). Circadian rhythm disorder in a rare disease: Smith-Magenis syndrome. Mol. Cell. Endocrinol. *252*, 88–91.
37. Ji, D., and Wilson, M.A. (2007). Coordinated memory replay in the visual cortex and hippocampus during sleep. Nat. Neurosci. *10*, 100–107.

Supplemental Data

Fragile X-Related Proteins Regulate

Mammalian Circadian Behavioral Rhythms

Jing Zhang, Zhe Fang, Corinne Jud, Mariska J. Vansteensel, Krista Kaasik, Cheng Chi Lee, Urs Albrecht, Filippo Tamanini, Johanna H. Meijer, Ben A. Oostra, and David L. Nelson

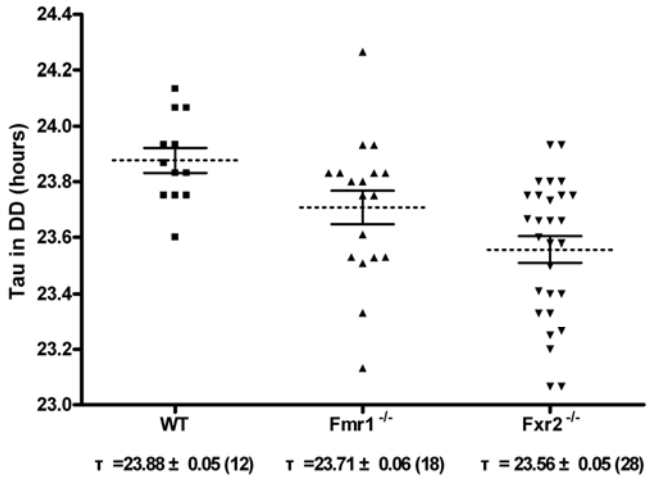

Figure S1. Distribution of Free-Running Period of Locomotor Activity Rhythm in DD of Wild-Type, *Fmr1* KO, and *Fxr2* KO Mice

The data on free-running period (tau) were averaged across different genotypes. Error bars indicate the standard error of the mean (SEM)

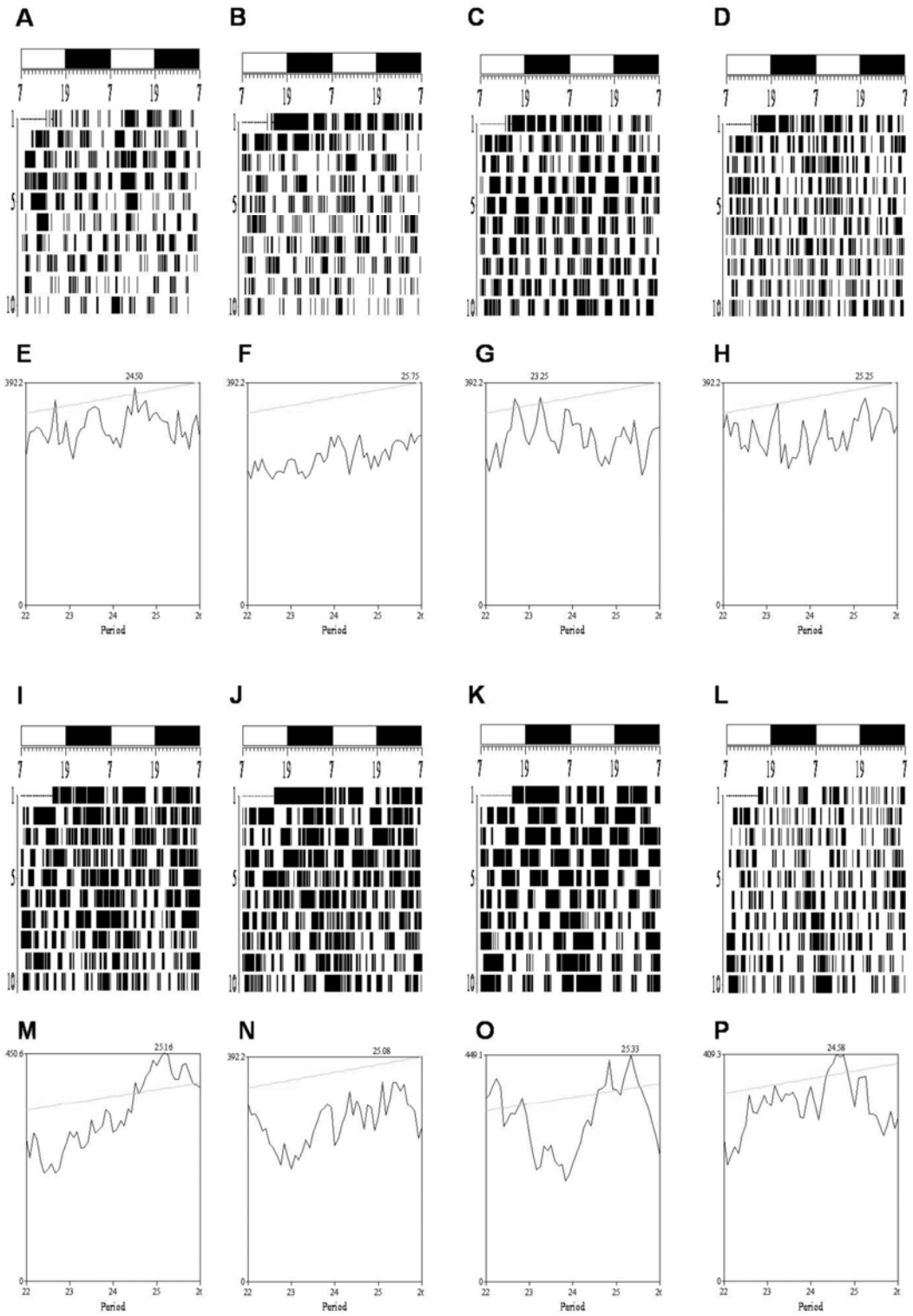

Figure S2. Representative Locomotor Activity Records of *Fmr1*/*Fxr2* Double KO and *Fmr1* KO/*Fxr2* Heterozygous Mice

(A–D) Representative locomotor activity records of *Fmr1*/*Fxr2* double KO mice. Activity records are double-plotted, so that 48 hr is shown on each horizontal trace with a 24 hr day presented both beneath and

to the right of the preceding day. Times of activity are indicated by black vertical marks. All records show activity in wheel running activity during exposure to a 12:12 light/dark cycle. The open and dark rectangles at the top of the figure indicate the LD cycle during entrainment.

(E–H) Chi-square periodogram analysis over LD cycle shown in actograms, corresponding to the activity recording in (A)–(D), respectively.

(I–L) Representative locomotor activity records of *Fmr1* KO/*Fxr2* heterozygous mice.

(M–P) Chi-square periodogram analysis over LD cycle shown in actograms, corresponding to the activity recording in (I)–(L), respectively.

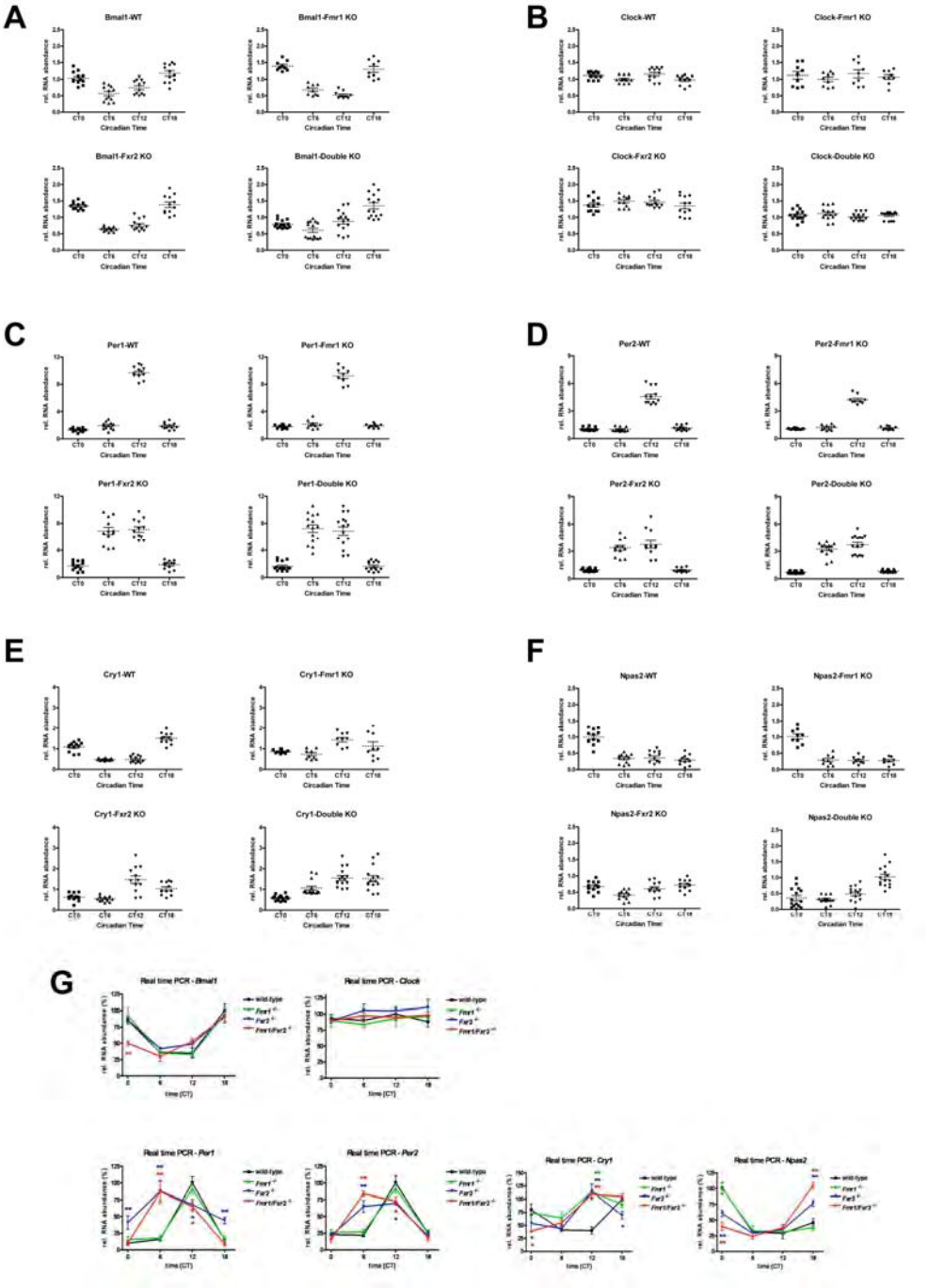

Figure S3. Expression Analysis of Wild-Type, *Fmr1* KO, *Fxr2* KO, and *Fmr1*/*Fxr2* Double KO Mice under DD Conditions in Liver

Amount of *Bmal1* (A), *Clock* (B), *Per1* (C), *Per2* (D), *Cry1* (E), and *Npas2* (F) mRNA expression was quantified by real-time PCR and calibrated in reference to *18S* RNA levels. The data on relative mRNA abundance were averaged across different time points. Error bars indicate the SEM. Graphs of (G) illustrate the relative transcript levels of these six genes. The largest value of wt is normalized to as 100%. *$p < 0.05$, **$p < 0.01$.

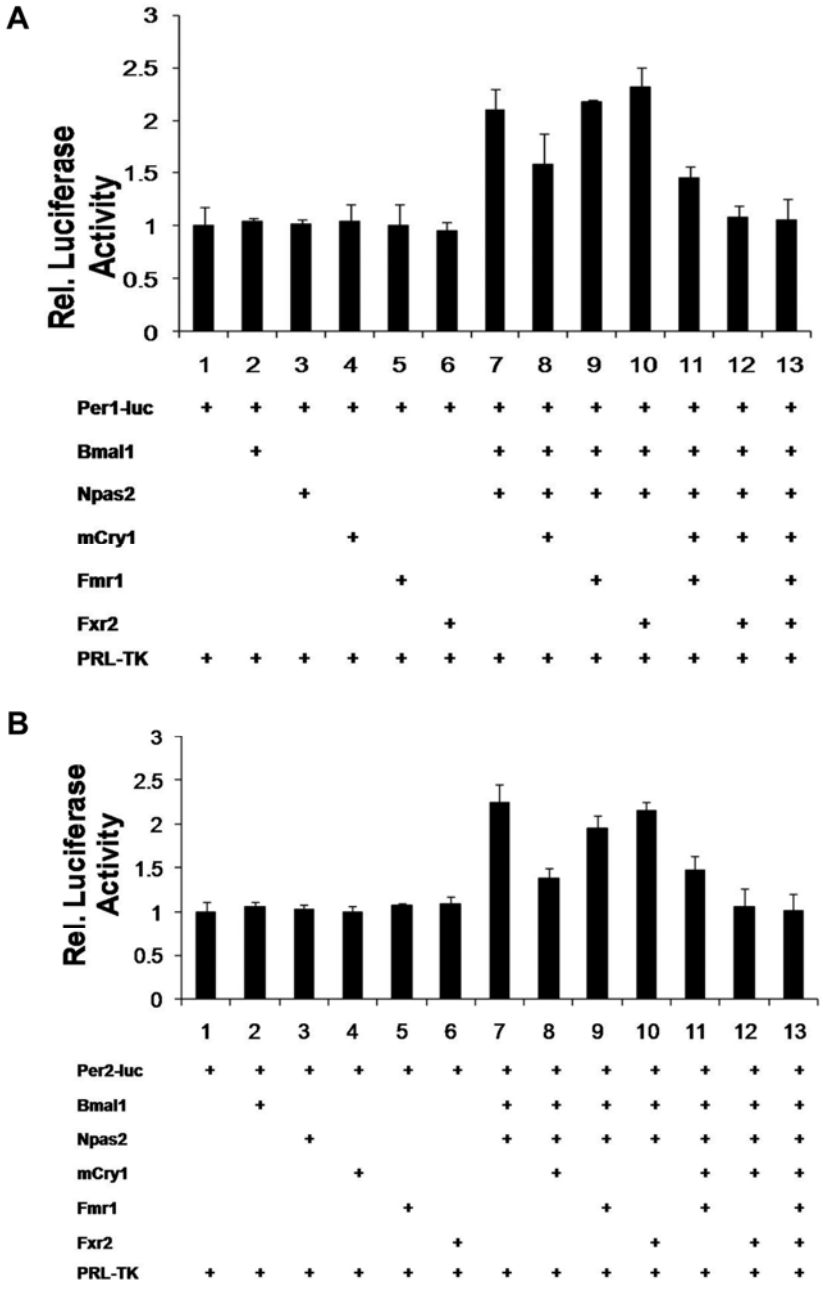

Figure S4. Regulation of BMAL1-NPAS2-Mediated Transcription by FMR1 and FXR2 in the Presence of CRY1

Reporter assay studies used *mPer1* promoter (A) or *mPer2* promoter (B). HeLa cells were cotransfected with the reporter construct *mPer1-luc* (A) or *mPer2-luc* (B), and control reporter construct Renilla luciferase encoding plasmids PRL-TK and various combination of expression construct (Material and Methods). Luciferase activity in samples transfected with reporter constructs only is adjusted as 1.0. Error bars indicate the SD (n = 4).

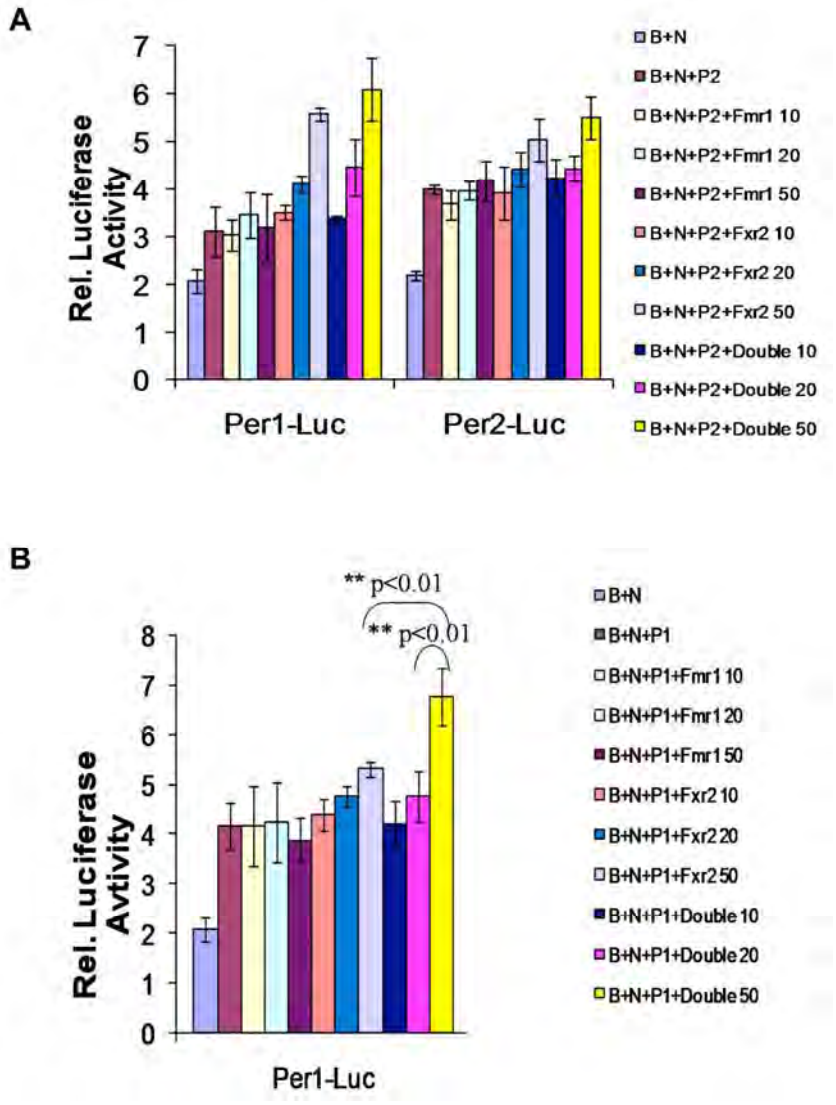

Figure S5. Regulation of mPER1- or mPER2-Induced BMAL1-NPAS2-Mediated Transcription by Different Dose of FMR1 and FXR2 Based on *mPer1* Promoter or *mPer2* Promoter

HeLa cells were cotransfected with the reporter construct *mPer1-luc* or *mPer2-luc*, control reporter construct PRL-TK and mPER2 (A) or mPER1 (B) and various combination of expression construct (Material and Methods). Luciferase activity in samples transfected with reporter constructs only is adjusted as 1.0. Error bars indicate the SD (n = 4). **p < 0.01. B, BMAL1; N, NPAS2; P1, mPER1; P2, mPER2.

Appendix II

"TNF-alpha suppresses the expression of clock genes by interfering with E-box-mediated transcription."

G. Cavadini, S. Petrzilka, P. Kohler, C. Jud, I. Tobler, T. Birchler, A. Fontana

2007

Published in *Proceedings of the National Academy of Sciences of the United States of America*, 104(31): 12843-12848

TNF-α suppresses the expression of clock genes by interfering with E-box-mediated transcription

Gionata Cavadini*, Saskia Petrzilka*, Philipp Kohler*, Corinne Jud†, Irene Tobler‡, Thomas Birchler*§, and Adriano Fontana*§

*Division of Clinical Immunology, University Hospital Zurich, Haeldeliweg 4, CH-8044 Zurich, Switzerland; †Institute of Biochemistry, University of Fribourg, Rue du Musée 5, CH-1700 Fribourg, Switzerland; and ‡Institute of Pharmacology and Toxicology, University of Zurich, Winterthurerstrasse 190, CH-8057 Zurich, Switzerland

Edited by Charles A. Dinarello, University of Colorado Health Sciences Center, Denver, CO, and approved June 15, 2007 (received for review February 22, 2007)

Production of TNF-α and IL-1 in infectious and autoimmune diseases is associated with fever, fatigue, and sleep disturbances, which are collectively referred to as sickness behavior syndrome. In mice TNF-α and IL-1 increase nonrapid eye movement sleep. Because clock genes regulate the circadian rhythm and thereby locomotor activity and may alter sleep architecture we assessed the influence of TNF-α on the circadian timing system. TNF-α is shown here to suppress the expression of the PAR bZip clock-controlled genes *Dbp*, *Tef*, and *Hlf* and of the period genes *Per1*, *Per2*, and *Per3* in fibroblasts *in vitro* and *in vivo* in the liver of mice infused with the cytokine. The effect of TNF-α on clock genes is shared by IL-1β, but not by IFN-α, and IL-6. Furthermore, TNF-α interferes with the expression of *Dbp* in the suprachiasmatic nucleus and causes prolonged rest periods in the dark when mice show spontaneous locomotor activity. Using clock reporter genes TNF-α is found here to inhibit CLOCK-BMAL1-induced activation of E-box regulatory elements-dependent clock gene promoters. We suggest that the increase of TNF-α and IL-1β, as seen in infectious and autoimmune diseases, impairs clock gene functions and causes fatigue.

behavior | circadian rhythms | cytokines | innate immunity

In microbial infections, host defense mechanisms activate the innate and adaptive arms of the immune response. Microbial recognition by Toll-like receptors (TLR) expressed by macrophages and dendritic cells leads to the activation of signal transduction pathways with induction of various genes including IL-1, TNF-α, IL-6, and IFN-α/β (1–3). These cytokines mediate the acute-phase response, which is a systemic generalized reaction characterized by fever, fatigue, and weight loss, an increase in the number of neutrophils, and the induction of synthesis of acute-phase proteins in the liver with increased haptoglobin, antiproteases, complement components, fibrinogen, ceruloplasmin, and ferritin in the blood (4). An acute phase response with a dose-dependent state of lethargy and severe fatigue has been described in cancer patients treated with TNF-α (5). A link between production of TNF-α and daytime fatigue has also been suggested in rheumatoid arthritis (RA) and in the obstruction sleep apnea syndrome (OSAS). Inhibition of TNF-α by soluble TNF-receptor p75 improves disabling fatigue in patients with RA (6). A TNF-α-308 (A-G) single-nucleotide polymorphism and elevated TNF-α serum levels have been described in OSAS (7, 8). Moreover, neutralization of TNF-α reduces daytime sleepiness in sleep apneics (9). Direct effects of TNF-α on spontaneous sleep are also shown in animal studies. i.v., i.p., or intracerebroventricular injections of TNF-α or IL-1 enhance nonrapid eye-movement (NREM) sleep (for reviews, see refs. 10 and 11). This increase in NREM sleep is independent of the fever-inducing capacity of these cytokines (12). Although there is good evidence for TNF-α and IL-1 as mediators of altered sleep–wake behavior, the underlying mechanisms remain elusive.

The regulation of sleep depends on a circadian control and a homeostatic drive (13, 14). The circadian influence is provided by the suprachiasmatic nuclei (SCN) of the hypothalamus being entrained by light stimuli to the environment. This self-sustaining circadian pacemaker uses a molecular mechanism similar to the one used in subsidiary oscillators present in any type of cell in the organism. The molecular clockwork involves the transcriptional repressor genes *Per1*, *Per2*, *Cry1*, and *Cry2*, as well as the transcriptional activators *Bmal1* and *Clock*. The heterodimerized transcription factor BMAL1:CLOCK activates *Per* and *Cry* gene transcription by binding to E-box motives in their promoters. PER and CRY proteins inhibit BMAL1:CLOCK complexes, thereby inhibiting their own gene expression. This feedback-loop mechanism generates circadian oscillations of *Per* and *Cry* expression. The same positive and negative regulatory components also govern the rhythmic expression of the nuclear orphan receptor *Rev-Erb*α, which in turn represses the transcription of *Bmal1* through direct binding to a REV-ERBα response element in the *Bmal1* promoter. Thereby, REV-ERBα interconnects the cyclic expression of positive- and negative-loop members (for reviews, see refs. 15 and 16). The targeted inactivation of *Bmal1* showed that this gene is indispensable for the maintenance of circadian functions (17). *Clock*-deficient mice show robust circadian patterns of locomotor activity with period lengths shortened by only 20 min; *Dbp* mRNA rhythm, however, was severely blunted in both the SCN and the liver (18). The deletion of the clock-controlled genes (CCG) PAR bZip transcription factors *Dbp*, *Tef*, and *Hlf* only moderately affects the circadian clock but leads to pronounced disturbances of locomotor activity. In the present study, our objective was to examine (*i*) whether and how TNF-α influences the circadian timing system and modulates the expression of clock genes and CCGs, and (*ii*) whether TNF-α affects locomotor activity, rest time, and periodicity in mice.

Results

Suppressed Expression of Clock Genes in TNF-α-Treated Synchronized Fibroblasts. To determine whether TNF-α interferes with circadian gene expression, we used NIH 3T3 fibroblast cultures synchronized by a 2-h serum shock; this system elicits a well described circadian expression of central clock genes and CCGs for at least three cycles (19). We analyzed serum shocked

Author contributions: G.C. and S.P. contributed equally to this work; T.B. and A.F. contributed equally to this work; G.C., S.P., I.T., T.B., and A.F. designed research; G.C., S.P., P.K., C.J., T.B., and A.F. performed research; C.J. and I.T. contributed new reagents/analytic tools; G.C., S.P., I.T., T.B., and A.F. analyzed data; and T.B. and A.F. wrote the paper.

This article is a PNAS Direct Submission.

Abbreviations: TLR, Toll-like receptor; RA, rheumatoid arthritis; NREM, nonrapid eye movement; SCN, suprachiasmatic nuclei; CCG, clock-controlled gene; ZT, Zeitgeber time; LD, 12-h light/12-h dark.

§To whom correspondence may be addressed. E-mail: thomas.birchler@usz.ch or adriano.fontana@usz.ch.

This article contains supporting information online at www.pnas.org/cgi/content/full/0701466104/DC1.

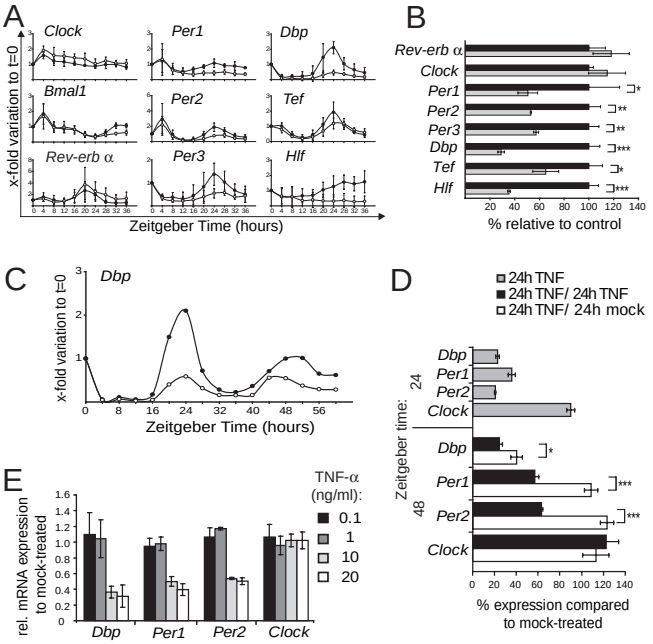

Fig. 1. TNF-α impairs expression of clock genes in synchronized NIH 3T3 fibroblasts. (*A*) TNF-α attenuates circadian *Per1/2/3* and PAR bZIP family (*Dbp*, *Tef*, and *Hlf*) gene expression. After serum shock (ZT 0–2), cells were kept in serum-free medium with TNF-α (10 ng/ml; open circles) or without the cytokine (filled circles) and analyzed every 4 h with quantitative real-time RT-PCR. Results are shown as *x*-fold variations to nonsynchronized fibroblast cultures at ZT 0; three independent experiments; mean values ± SD. (*B*) *Per* and PAR bZIP family genes are significantly down-regulated at the 24-h peak (TNF-α: gray bars; controls: black bars), whereas *Clock* and *RevErb*α are not affected. Expression of *Rev-Erb*α was assessed at its peak at ZT 20. Data show one representative experiment done in triplicate (mean ± SD) of four experiments. (*C*) The amplitude of *Dbp* expression in serum-shocked NIH 3T3 fibroblasts was attenuated during 60 h in the presence of TNF-α (open circles) compared with controls (filled circles). (*D*) Withdrawal of TNF-α after the first peak at ZT 24 shows that the suppression of *Dbp*, *Per1*, and *Per2* at the second peak at ZT 48 is reversible. After serum shock, cells were treated with TNF-α for 24 h (gray bars), or for 48 h with or without a withdrawal of TNF-α after 24 h (white and black bars, respectively). Gene expression was compared with mock-treated cells at the respective ZT (100% expression). Data show one representative experiment done in triplicates (mean ± SD) of three experiments. (*E*) The suppression of the expression of *Dbp*, *Per1*, and *Per2* in synchronized fibroblasts at ZT 24 is dose-dependent being significant ($P < 0.005$) at doses higher than 1 ng/ml TNF-α. Data show the mean ± SD of three independent experiments performed in triplicates. For BDE, we used the independent-sample *t* test; *, $P \leq 0{,}05$; **, $P \leq 0{,}005$; ***, $P \leq 0.0005$.

fibroblasts challenged over time with or without TNF-α (10 ng/ml). RNA was extracted every 4 h thereafter up to Zeitgeber time (ZT) 36 and analyzed by using quantitative real-time RT-PCR methods. Within the first 12 h, the course of the examined clock gene expression was not altered by TNF-α treatment. However, around the peak (ZT 20–28), TNF-α strikingly suppressed the expression of the central clock genes *Per1*, *Per2*, and *Per3* and of the CCGs *Dbp*, *Tef*, and *Hlf*. Peak expression of *Rev-erb*α mRNA at ZT 20 was slightly increased, whereas *Bmal1* expression was not affected by TNF-α. *Clock* expression was slightly increased. For all genes, TNF-α did not affect the phases but rather attenuated the amplitude of expression (Fig. 1*A*). Therefore, we assessed the extent of clock gene expression at their main peak at ZT 24. TNF-α induced a significant reduction of gene expression for *Per1*, *Per2*, *Per3*, *Dbp*, *Tef*, and *Hlf* genes. *Rev-Erb*α expression, as assessed at its peak of expression at ZT 20, remained unchanged by TNF-α, as did *Clock* (Fig. 1*B*). We extended the time of observation over a

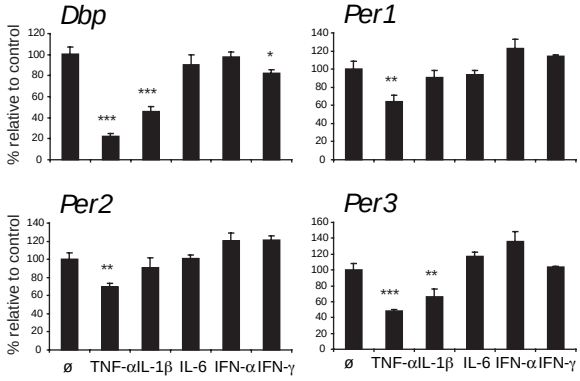

Fig. 2. Cytokine effects on *Dbp*, *Per1*, *Per2*, and *Per3* in NIH 3T3 fibroblasts. Confluent cells were synchronized with 50% horse serum for 2 h (ZT 0–2). After serum shock, cells were kept in serum-free medium with TNF-α (10 ng/ml), IL-1β (10 ng/ml), IL-6 (10 ng/ml), IFN-α (10 ng/ml), IFN-γ (20 ng/ml) or without cytokines and analyzed at ZT 24 with quantitative real-time RT-PCR. Results are shown as percent of expression to noncytokine-treated fibroblast cultures; one representative experiment of three; mean values of triplicates ± SD; independent sample *t* test; *, $P \leq 0{,}05$; **, $P \leq 0{,}005$; ***, $P \leq 0.0005$.

second circadian cycle and analyzed rhythmic expression up to 60 h. In this, emphasis was placed on *Dbp* expression, because its amplitude was the most affected by TNF-α. Rhythmicity and period length of *Dbp* expression were not changed by TNF-α, but its amplitude was severely suppressed at both peaks (Fig. 1*C*). To determine whether the TNF-α-mediated suppression is reversible, we washed out TNF-α after the first cycle (at ZT 24) and analyzed the second peak at ZT 48. By washing out TNF-α, the second peak of expression of *Per1* and *Per2* was restored, and *Dbp* expression increased compared with the control where TNF-α still led to reduced peak expression. The expression of *Clock* was not affected when extending the time of TNF-α treatment to 48 h (Fig. 1*D*). Moreover, the suppression of *Dbp*, *Per1*, and *Per2* gene expression in synchronized NIH 3T3 fibroblasts is clearly dose-dependent, being most significantly affected with concentrations >1 ng/ml TNF-α. The expression of *Clock* remained unchanged irrespective of the dose of TNF-α (Fig. 1*E*).

IL-1β, but Neither IFN Nor IL-6, Shares with TNF-α the Effect to Down-Regulate Clock Genes. Besides TNF-α, other cytokines are produced by TLR-activated macrophages and dendritic cells that have been implicated in the sickness behavior syndrome, namely the proinflammatory cytokines IL-1, IL-6, and IFN-γ and type I IFN cytokines IFN-α and -β (20). Therefore, we examined whether the effect of TNF-α on clock genes is a unique property of TNF-α or is shared by other cytokines. Besides TNF-α, also IL-1β suppressed the expression of both, *Dbp* and *Per3* (Fig. 2). The expression of *Dbp*, *Per1*, *Per2*, and *Per3* was not inhibited by treatment of synchronized fibroblasts with IL-6 and IFN-α. IFN-γ induced a significant, albeit minor, suppression of *Dbp* expression.

TNF-α Interferes with E-Box-Dependent Transcription of Clock Genes. Circadian transcriptional activation of Per genes and of the PAR bZip transcription factor genes *Dbp*, *Tef*, and *Hlf* is thought to depend on the binding of the heterodimer BMAL1:CLOCK to the canonical or noncanonical E-box, a basic helix–loop–helix transcription factor-binding site ideally harboring the sequence CACGTG (21). In our study, TNF-α affected suppression only of the transcription of those clock genes harboring an E-box upstream of the transcription initiation site (*Per* genes and *Dbp*, *Tef*, and *Hlf*). No suppression was observed on *Bmal1* and *Clock*

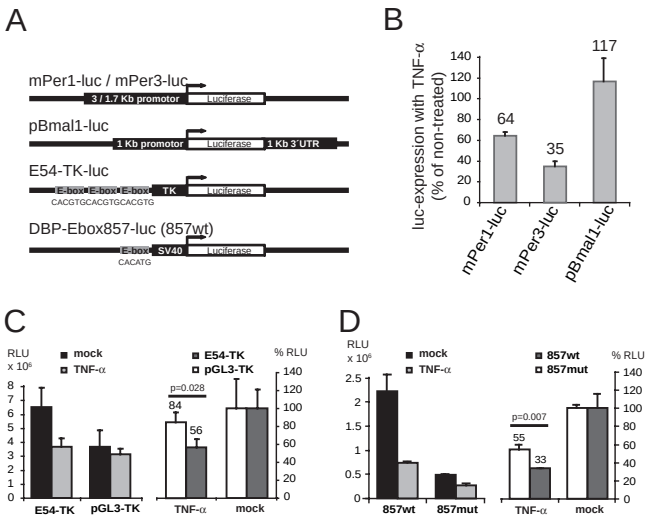

Fig. 3. TNF-α suppresses E-box-mediated transcription of clock genes. (*A*) Schematic representation of the luciferase reporter genes used. mPer1-luc (3-kb promoter fragment) and mPer3-luc (1.7-kb promoter fragment) contain promoter sequences upstream of their genes in the pGL3basic vector. pBmal1-luc is regulated by a 1-kb promoter fragment and a 1-kb sequence of the 3′UTR from *mBmal1* gene. E54-TK consists of the three E-boxes of the mouse *Per1* gene and their immediate flanking sequences in front of a TK promoter. DBP-Ebox857-luc contains one of four E-boxes of the *Dbp* promoter regulating the activity of a SV40 promoter. (*B*) Native clock gene promoters bearing an E-box are affected by TNF-α. Percent luciferase expression of mPer1-luc, mPer3-luc, and pBmal1-luc transfected NIH 3T3 cells after treatment with 10 ng/ml TNF-α overnight compared with untreated controls (100% luciferase expression) is shown. (*C*) E-boxes of *mPer1* are affected by TNF-α treatment. TNF-α significantly reduces E54-TK-dependent luciferase expression but not pGL3-TK lacking E-boxes and flanking sequences as shown by raw data (RLU, relative light units; *Left*) and percent inhibition (*Right*). (*D*) The E-box of *Dbp* gene at position +857 is repressed by TNF-α even when CLOCK and BMAL1 are overexpressed. Cotransfection with CLOCK and BMAL1 leads to four to five times higher relative luciferase activity of 857wt compared with the mutated E-box vector (857mut) indicating that the interaction of CLOCK:BMAL1 with the E-box is functional. Luciferase activity is efficiently suppressed by overnight treatment with TNF-α as shown by raw data (*Left*) and percent inhibition (*Right*). TNF-α leads to a higher repression in 857wt than in 857mut. For all assays, mean ± SD of triplicates from one representative experiment of three; independent sample *t* test.

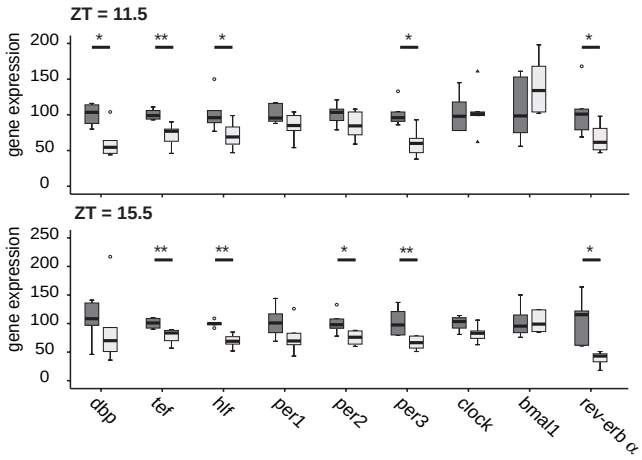

Fig. 4. Impaired expression of clock genes in livers of TNF-α-infused mice. Animals were entrained to a LD cycle during 2 weeks, and their locomotor activity was constantly monitored via a passive infrared sensor and a running wheel. Mice were then implanted with osmotic minipumps delivering TNF-α (light gray bars) or saline as control (dark gray bars). On the third day after the operation, mice were killed at ZT = 11.5 or = 15.5 (ZT = 0, light on; ZT = 12, light off). Livers were extracted and gene expression assessed by real-time PCR. (*A*) *Per1/2/3*, *RevErbα*, and PAR bZip family genes, *Dbp*, *Hlf*, and *Tef*, are down-regulated at both time points, the suppression of PAR bZip family genes is highly significant. In contrast to fibroblast data, *RevErbα* is strongly down-regulated. Results are shown as percentages relative to the mean of the control group. One representative experiment of three is shown ($n = 6$ per group; Mann–Whitney test. *, $P \leq 0{,}05$; **, $P \leq 0{,}005$.)

expression, their transcription not being E-box-dependent. Thus, TNF-α may interfere with E-box-mediated transcriptional activation. To test this hypothesis, we performed transient transfections of NIH 3T3 cells with luciferase reporter genes under the control of the native 3- or 1.7-kB promoter sequences of mouse *Per1* and *Per3*, respectively, and of the 1-kB promoter of *Bmal1* (Fig. 3*A*). Consistent with the gene expression studies, *Per1* and *Per3* promoter activity was suppressed after TNF-α administration but not that of the *Bmal1* promoter, which is devoid of E-box elements (Fig. 3*B*). To specify the possible effect on E-boxes, we performed assays using NIH 3T3 cells stably transfected with a luciferase reporter plasmid consisting of three E-boxes within 2.0 kb of the 5′ flanking region of the mouse *Per1* gene with their immediate flanking sequence linked together and joined to the thymidine kinase promoter (22) (Fig. 3*A*). Again, treatment with TNF-α reduced luciferase activity by 45%, corresponding to the basal activity of the basic pGL3-TK vector without E-boxes (Fig. 3*C*). An E-box reporter construct of the *Dbp* gene (Dbp-E-box857; Fig. 3*A*) that was cotransfected with plasmids expressing CLOCK and BMAL1 proteins showed expression reduced by 67%, indicating that overexpressed CLOCK and BMAL1 are still efficiently blocked. In contrast, with the mutated E-box (ACCAGT instead of CACATG) reporter construct (Dbp-857 mut), the activity was significantly derepressed (Fig. 3*D*). We suggest therefore that TNF-α suppresses E-box-mediated transcription of clock genes. Thus, selective down-regulation of clock genes or CCGs is likely to depend on the presence of E-box elements in the respective genes.

Reduction of Clock Genes and CCGs in TNF-α-Treated Mice. To assess the effect of TNF-α on the expression of clock genes *in vivo*, C57BL/6 mice were constantly infused with TNF-α (1.5 μg/day or 0.075 mg/kg per day) via an osmotic minipump inserted s.c. on the back of the mice over a period of 7 days (see *Materials and Methods*). The dose chosen is ≈10-fold lower than the dose used to induce a septic shock-like disease in rats (0.7 mg/kg, administered intravenously) (23). Histopathology revealed no evidence for TNF-α-induced vascular damage, hemorrhages, or inflammation in the liver, lung, and kidney based on morphological criteria and on the expression of heme oxygenase (HO-1), a marker for oxidative stress. Macrophages of mice infused with TNF-α showed signs of being activated in the liver and kidney [supporting information (SI) Fig. 6]. We found TNF-α serum concentrations at 43 (±10.9) pg/ml at day three in TNF-α-treated mice compared with 10 (±0.8) pg/ml in controls (SI Fig. 7). In mice with experimental septic shock the respective value for TNF-α exceeds 10 ng/ml (24). In controls, osmotic pumps were filled with diluent (PBS, 0.1% BSA). Total RNA was extracted from the liver of mice treated with TNF-α or control; expression of clock genes was tested at day three at ZT 11.5 and ZT 15.5 (ZT 0 = 6 a.m. lights on, ZT 12 = 6 p.m. lights off), when we encountered maximal inhibition of locomotion (Fig. 5*A*). As shown for fibroblasts *in vitro*, TNF-α also suppressed the expression of *Dbp*, *Tef* and *Hlf*, and *Per3*, but not of *Bmal1* and *Clock* (Fig. 4). Although *Per1 and Per2* were down-regulated, this was not significant. However, at a later time point (ZT 15.5), when *Per2* normally reaches its peak of expression, significant suppression of *Per2* was observed (Fig. 4 *Lower*). In contrast to the fibroblast data, we found that TNF-α suppressed the expres-

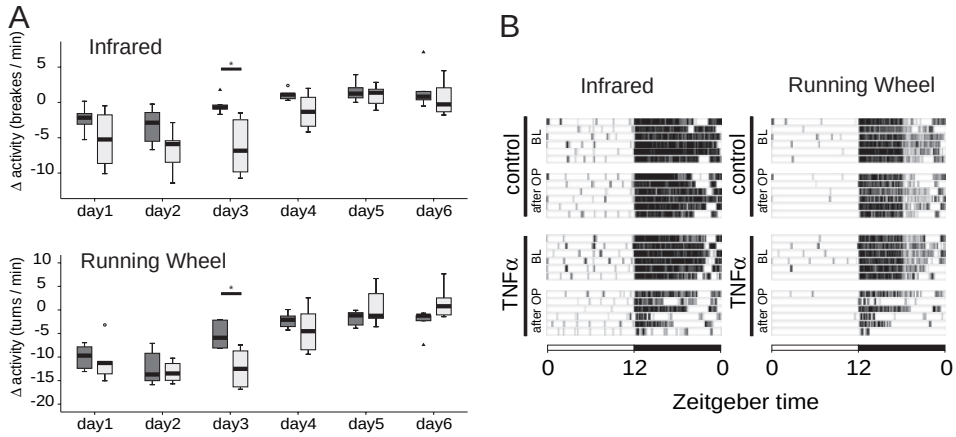

Fig. 5. TNF-α reduces locomotor activity of mice but does not alter their circadian rest-activity cycles in free running conditions. (*A*) Reduced locomotor activities in mice with constant TNF-α infusions are detected from days 1–4. Boxplot showing the changes of locomotor activity for each day after minipump implantation (TNF-α, 1.5 μg/day, for 6 days) or saline as control, compared with the baseline (mean of 3 days immediately before the operation). The TNF-α-treated group is shown as light gray bars and the control group as dark gray bars; circles are outliers, and triangles are extreme values. Six mice per group were analyzed. Data show one experiment (ANOVA for repeated measures, followed by independent-sample *t* tests; *, $P \leq 0.05$). The effect of TNF-α to impair locomotor activity was confirmed at day 3 in two independent experiments. (*B*) TNF-α reduces locomotor activity in the second half of the dark phase. Actograms (as measured by infrared and running wheel) show data from six individual mice before and after the minipump insertion. Each line represents one individual mouse per treatment, 1 day before the implantation of minipumps (baseline, BL) and 3 days after the operation (OP).

sion of *Rev-Erb*α. TNF-α induced reduction of expression of the *Per* genes and of PAR bZip transcription factor genes is likely to influence the expression of clock output genes. Among the genes that are positively regulated by DBP is the liver-specific albumin gene (25). The capacity of TNF-α to interfere with *Dbp* mRNA expression is congruent with the observation of a decrease in albumin serum concentration by 41% in TNF-α-treated mice compared with controls (SI Fig. 8). TNF-α has already been described as inhibiting albumin synthesis in liver cells, but the mechanisms remain elusive (26). Taken collectively, these data provide evidence that the suppressive role of TNF-α on *Dbp* is associated with impaired activation of their target gene. TNF-α-treated mice also show higher endogenous expressions of IL-1β and TNF-α in the liver [both genes are well known to be induced by TNF-α (28)]; the level of expression of these cytokines correlates with each other (SI Fig. 9). Furthermore, the increased expression of the cytokines in the liver is associated with a decrease of the CCG *Dbp*, *Hlf*, and *Tef*; the extent of the decrease of these PAR bZip transcription factors fits to the TNF-α expression in individual mice (SI Fig. 9).

TNF-α Reduces Dbp Expression in the SCN in the Hypothalamic Region. To verify whether the effect of TNF-α is sustained across the blood–brain barrier and reaches the SCN, the expression of *Dbp* was quantified. As described above, mice were implanted with minipumps releasing TNF-α or diluent; mice were killed after 3 days at ZT 6, when peak expression of *Dbp* was expected. A slight (-15%) but statistically significant reduction of *Dbp* expression ($P = 0.003$) can be seen by *in situ* hybridization in the SCN of TNF-α-treated mice (SI Fig. 10). To verify the time point of the rhythm, we used *Bmal1*, which, at peak expression of *Dbp*, is not detectable. Indeed, unlike *Dbp* mRNA-positive cells, *Bmal1* transcripts were not identified by *in situ* hybridization at ZT 6.

TNF-α Reduces Locomotor Activity and Promotes Increased Rest Time in Mice. The function of TNF-α to interfere with the transcription of distinct clock genes or CCGs prompted us to evaluate whether TNF-α alters the circadian rhythm and/or the amount of locomotor activity *in vivo*. The timing and extent of locomotor activity were assessed with infrared sensors as well as by monitoring running-wheel activity in mice recorded under a 12-h light/12-h dark (LD) schedule. The surgical procedure led to a decrease in locomotor activity that lasted for 48 h (infrared; Fig. 5*A Upper*). However, beside the more pronounced impairment of locomotor activity on days 1 and 2, TNF-α led also to a severe suppression of locomotor activity on day 3; on this day, control mice had attained baseline levels of activity. When running-wheel activity was assessed, an analogous picture emerged with maximum inhibition at day 3 (Fig. 5 *A Lower* and *B*). At later time points, especially on days 5 and 6, TNF-α no longer exerted any effect on locomotor activity. This is most likely due to a failed release of TNF-α from the pump, because starting at day 4, hemorrhagic necrosis developed at the site of the pump. This local side effect was noticed when pumps were filled with TNF-α but not with control solution and has been described in areas of s.c. injection of TNF-α in mice (3 μg for 5 days) (29). Our results show that TNF-α leads to a decrease in the total amount of locomotor activity as measured by a running-wheel and infrared sensors until day 4 (Fig. 5*A*). The activity in both groups was still restricted to the dark period, and highest loss of activity in TNF-α treated animals can be observed during the second half of the active period (Fig. 5*B*). Further, based on these observations, we chose day 3 to investigate the frequency and duration of rest episodes during the LD period (SI Fig. 11*A*). During the light period, no change was observed. But in the dark period, when mice are usually active, a significant increase in rest episodes lasting 6–60 min was detected. As a readout of the endogenous circadian clock, we assessed locomotor activity in constant darkness ("free-running condition") after implantation of the minipumps and calculated the period length (τ). We observed no changes in the periodicity of τ (SI Fig. 11*B*). Taken together, mice treated continuously with TNF-α show reduced motor activity and more consolidated rest time but no change in period length under free-running conditions. These findings are consistent with experiments with fibroblasts showing that the amplitude of the expression of clock genes and CCGs are attenuated by TNF-α, rather than their circadian rhythm itself.

Discussion

Whereas the molecular mechanisms provided by clock genes to maintain the circadian rhythm are becoming increasingly clear, the potential influences of the immune system on the molecular

clockwork remain to be explored. Here, we provide evidence that TNF-α interferes with the expression of clock genes, namely the *Per* genes and the PAR bZip genes *Dbp*, *Tef*, and *Hlf*. TNF-α suppresses the expression of these genes in fibroblasts (and attenuates their amplitudes) *in vitro* and *in vivo* in the liver of mice infused with this cytokine. That the same genes (with the exception of *RevErb*α) are prone to TNF-α stimulation *in vitro* compared with *in vivo* speaks for a rather direct effect of TNF-α, although we cannot exclude other intermediates involved leading to the same response. *In situ* hybridization shows that the s.c. administration of TNF-α also leads to reduction of *Dbp* expression in the central circadian pacemaker, the SCN. Thus, it is tempting to speculate that TNF-α is likely to reach the SCN via the blood and to bind to TNF receptor (TNF-R) on neurons. At least in the hippocampus, both TNF-RI and -RII are expressed (30). In the present study E-box regulatory elements of clock genes are found here to play a pivotal role in the effect of TNF-α to inhibit clock gene expression. First, only clock genes with E-boxes in their promoter, the PAR bZip genes *Dbp*, *Tef*, and *Hlf* and the *Per* genes, are affected by TNF-α, whereas clock genes devoid of E-boxes such as *Clock* and *Bmal1* are not affected by TNF-α. Second, mutated E-boxes provide protection of TNF-α-induced suppression of clock reporter genes. E-boxes are functionally important components of DNA promoters that guide the expression of clock genes and thereby influence the circadian rhythm, including the sleep–wake cycle. Rhythmic binding of CLOCK and BMAL1 depends on E-boxes and is a prerequisite for robust waves of gene expression characteristic of circadian transcription (31, 32).

The effects of TNF-α on clock gene expression also become apparent when studying clock-dependent genes. *Dbp* has been described to mediate transcription of the albumin gene in hepatocytes (25). Albumin serum concentrations are found here to be lowered by 41% in TNF-α-treated mice compared with controls.

Recording of locomotor activity of TNF-α-treated mice shows more rest episodes during spontaneous activity. In line with the finding that TNF-α does not alter circadian rhythm in cultured fibroblasts but rather lowers the extent of expression of distinct clock genes, TNF-α did not influence period length of the circadian rhythm under "free running" conditions. Of interest for the findings presented here are data showing that the deletion of the *Dbp* gene in mice results in only a slight reduction of period length but in a striking impairment of spontaneous locomotor activity and running-wheel activity (33, 34). Whereas *Tef* and *Hlf* single-knockout mice show an increased period length, the inactivation of all three genes, *Dbp*, *Tef*, and *Hlf*, resulted in an unchanged circadian period length (27). Thus, a normal period length may be due to opposite effects leading to mutual neutralization of indirect clock gene dysfunction. Besides lowering the expression of PAR bZip transcription factors, TNF-α impaired *Per1*, *Per2*, and *Per3* mRNA. Target disruption of these genes results in slightly ($Per3^{-/-}$ mice) or more dramatically ($Per1^{-/-}$ mice) shortened period lengths or eventually gives rise to arrhythmic behavior ($Per2^{-/-}$ mice). Taken collectively, TNF-α interferes with the expression of E-box-dependent clock genes and leads to prolonged rest episodes during spontaneous activity of mice.

Sleep architecture in humans is affected by the endogenous circadian pacemaker, which regulates the timing of the sleep–wake cycle, presumably by circadian expression of clock genes (13, 35). Enhanced NREM sleep has been shown in mice treated with muramyl dipeptides, which activate TLR2 and TLR4 on macrophages (36, 37). TNF-α, as well as IL-1, is produced by TLR2- and TLR4-activated macrophages and is well described to enhance NREM sleep (11, 38, 39). In light of the overlapping properties of TNF-α and IL-1 on NREM sleep, it is interesting that our studies show IL-1 to share with TNF-α the inhibitory effect on expression of the *Dbp* and *Per3* genes in fibroblasts. As recently outlined, the effects of IL-6 on sleep differs from IL-1 and TNF-α, in that it may also act on systems involved in NREM sleep but not in REM sleep, which is suppressed by TNF-α and IL-1 but not by IL-6 (40). In this context, it may be of relevance that the expression of *Dbp* is found here not to be affected by IL-6. Although the expression of *Dbp* and *Per1* is also not inhibited by IFN-α, IFN-γ only slightly interfered with Dbp expression. This is remarkable, because in mice, the daily injection of IFN-α or -γ has been reported to lower *Per1*, *Per2*, *Per3*, and *Clock* after 6 days of treatment (41). The absence of effects of IFN-α and -γ on expression of the *Per* genes by synchronized fibroblasts *in vitro* indicates that IFNs down-regulate the *Per* and *Clock* genes by E-box-independent mechanisms or induce production of other clock gene-regulating factors when mice are treated over a long time period with the cytokines.

In infectious diseases, TNF-α serves to successfully eliminate the infectious agent. The function of TNF-α to interfere with the expression of clock genes, to impair locomotor activity, and to enhance rest may provide the link between the activation of the innate immunity and fatigue associated with infectious and autoimmune diseases, such as multiple sclerosis, RA, or Crohn's disease. In these disorders, both fatigue and elevated TNF-α concentrations have been described (6, 42, 43). It is still debated whether sleep changes in infections are beneficial to the host defense. Rabbits infected with *E. coli*, *Staphylococcus aureus*, or *Candida albicans* showed an improved prognosis when their sleep duration was prolonged (44). In this context, it is to be noted that $Per2^{-/-}$ mice are partially protected from LPS-induced shock (45). During the TNF-α-induced "inflammatory clock gene response," the expression of *Per1*, *Per2*, and *Per3* genes and of the PAR bZip transcription factors *Dbp*, *Tef*, and *Hlf* is down-regulated, the locomotor activity reduced, and rest episodes prolonged. Although this pathway may induce an adaptive state in infectious diseases, the "inflammatory clock gene response" may, by inducing fatigue, diminish the quality of life in autoimmune diseases. Our study will serve to lay an important foundation for further exploration of the connection between the TNF-α-induced "inflammatory clock gene response" and the TNF-α-triggered reduction of locomotor activity.

Materials and Methods

Cytokines. Recombinant murine (rm) TNF-α, rm IL-1β, and rm IL-6 were purchased either from Sigma (St. Louis, MO) (*in vitro* time course assays) or from Peprotech (London, U.K.) (*in vivo* assays); rm IFN-α from Immunotools (Friesoythe, Germany), and rm IFN-γ from Roche (Rotkreuz, Switzerland).

Synchronization of Fibroblasts by Serum Shock. NIH 3T3 fibroblasts were grown in DMEM (Gibco, Basel, Switzerland) supplemented with 10% FBS (PAA Laboratories, Pasching, Austria) and Glutamax (Gibco). For serum shock, cells were grown to confluency in 6-cm tissue culture dishes. At time $t = 0$, the medium was exchanged by 50% horse serum (Gibco) in DMEM/Glutamax; after 2 h, the medium was replaced with serum-free DMEM/Glutamax, with or without TNF-α. At the indicated time points, tissue culture dishes were washed once with Hanks; solution, frozen on a layer of liquid nitrogen, and kept at -70°C until the extraction of whole-cell RNA.

Transfection and Luciferase Assays. Unsynchronized NIH 3T3 cells were transfected with the following constructs by using Lipofectamine Plus (Life Technologies, Basel, Switzerland) or TransFectin (Bio-Rad, Hercules, CA) according to the manufacturer's protocol: mPer1-luc (46), kindly provided by David Earnest [Texas A&M, College Station, TX; E54-TK (22)], kindly provided by Sato Honma (Hokkaido University, Sapporo, Japan); Bmal1-luc (19), DBP-Ebox-luc and mut Ebox, pCDNA3.1-Clock

and pCDNA3.1-Bmal1 (47), kindly provided by U. Schibler (University of Geneva, Geneva, Switzerland); mPer3-luc (48), kindly provided by P. Sassone-Corsi (IGBMC, Illkirch, France). As an internal control for transfection efficiency, a GFP construct (pMax-GFP; Amaxa, Cologne, Germany) was cotransfected 1:10.

Twenty-four hours after transfection, the medium was replaced with serum-free DMEM/glutamax with or without TNF-α (10 ng/ml). After ≈15 h, cells were lysed by using Passive Lysis Buffer (Promega, Wallisellen, Switzerland) and enzyme activity was measured by the Luciferase Assay System (Promega). Bioluminescence was measured with a Luminometer (Berthold Technologies, Regensdorf, Switzerland) and normalized to transfection efficiency or protein concentration.

Animal Groups and Locomotor Activity Recording. Seven-week-old C57BL/6 male mice (Harlan Breeding Laboratory, AD Horst, The Netherlands) were housed in individual cages, equipped with a running-wheel and a passive infrared sensor in a temperature-controlled sound-proof light-tight room. Food and water were available ad libitum. We allowed mice 10–15 days of acclimatization to a LD cycle (light on at 0600, i.e., ZT 0; light off at 1800, i.e., ZT 12). Mice were operated under deep isoflurane anesthesia, and 30 μg of Temgesic anesthetic (buprenorphine; Essex Chemie, Lucerne, Switzerland) was applied. TNF-α (1.5 μg/day, diluted in 0.1% BSA/PBS) or 0.1% BSA/PBS as a control was administered s.c. by using osmotic minipumps (Model 1007D; Alzet, Cupertino, CA) implanted on the back, for 6 days. Locomotor activity was continuously measured via running-wheel and infrared sensors based on 1-min episodes by using the Chronobiology Kit software (Stanford Software Systems, Santa Cruz, CA), as described (49, 50). Rest episodes were defined as 1-min units with activity = zero. The free-running period of locomotion was calculated by periodogram analysis for days 2–6 after minipump implantation, when the mice were kept in constant darkness. In gene expression studies, livers were extracted 3 days after minipump insertion at two different ZTs known to approximately represent the peak of expression of *Dbp* (ZT = 11.5) or *Per2* (ZT = 15.5). Livers were frozen in TRIzol (Invitrogen, Basel, Switzerland) for subsequent RNA extraction. All experimental procedures were approved by the local committee of the veterinary office and in strict accordance with Swiss regulations on animal welfare.

RNA Isolation and Gene Expression Analysis. The method for RNA extraction, RT-PCR, and quantification of gene expression is described in *SI Text*.

***In Situ* Hybridization.** The method for *in situ* hybridization was published (51) and is described in *SI Text*.

We thank Dr. U. Schibler (University of Geneva) for helpful discussions and critical feedback on this manuscript and Dr. Michael Kurrer (Department of Pathology, University Hospital Zurich) for analysis of histopathological findings in TNF-α-treated mice. This study was supported by the Swiss National Science Foundation (Project no. 310000-109469/1 and NCCR Neural Plasticity and Repair, project 6), the Swiss Multiple Sclerosis Society, and the Gianni Rubatto Foundation.

1. Akira S, Uematsu S, Takeuchi O (2006) *Cell* 124:783–801.
2. Kishimoto T (2005) *Annu Rev Immunol* 23:1–21.
3. Beutler B, Cerami A (1987) *N Engl J Med* 316:379–385.
4. Dinarello CA (2004) *J Endotoxin Res* 10:201–222.
5. Spriggs DR, Sherman ML, Michie H, Arthur KA, Imamura K, Wilmore D, Frei E, 3rd, Kufe DW (1988) *J Natl Cancer Inst* 80:1039–1044.
6. Pollard LC, Choy EH, Gonzalez J, Khoshaba B, Scott DL (2006) *Rheumatology (Oxford)* 45:885–889.
7. Vgontzas AN, Papanicolaou DA, Bixler EO, Kales A, Tyson K, Chrousos GP (1997) *J Clin Endocrinol Metab* 82:1313–1316.
8. Riha RL, Brander P, Vennelle M, McArdle N, Kerr SM, Anderson NH, Douglas NJ (2005) *Eur Respir J* 26:673–678.
9. Vgontzas AN, Zoumakis E, Lin HM, Bixler EO, Trakada G, Chrousos GP (2004) *J Clin Endocrinol Metab* 89:4409–4413.
10. Opp MR (2005) *Sleep Med Rev* 9:355–364.
11. Krueger JM, Majde JA (2003) *Ann NY Acad Sci* 992:9–20.
12. Takahashi S, Kapas L, Fang J, Krueger JM (1999) *Am J Physiol* 276:R1132–R1140.
13. Daan S, Beersma DG, Borbely AA (1984) *Am J Physiol* 246:R161–R183.
14. Dijk DJ, Czeisler CA (1995) *J Neurosci* 15:3526–3538.
15. Schibler U, Sassone-Corsi P (2002) *Cell* 111:919–922.
16. Reppert SM, Weaver DR (2002) *Nature* 418:935–941.
17. Bunger MK, Wilsbacher LD, Moran SM, Clendenin C, Radcliffe LA, Hogenesch JB, Simon MC, Takahashi JS, Bradfield CA (2000) *Cell* 103:1009–1017.
18. Debruyne JP, Noton E, Lambert CM, Maywood ES, Weaver DR, Reppert SM (2006) *Neuron* 50:465–477.
19. Nagoshi E, Saini C, Bauer C, Laroche T, Naef F, Schibler U (2004) *Cell* 119:693–705.
20. Iwasaki A, Medzhitov R (2004) *Nat Immunol* 5:987–995.
21. Cermakian N, Sassone-Corsi P (2000) *Nat Rev Mol Cell Biol* 1:59–67.
22. Honma S, Kawamoto T, Takagi Y, Fujimoto K, Sato F, Noshiro M, Kato Y, Honma K (2002) *Nature* 419:841–844.
23. Tracey KJ, Beutler B, Lowry SF, Merryweather J, Wolpe S, Milsark IW, Hariri RJ, Fahey TJ, 3rd, Zentella A, Albert JD, *et al.* (1986) *Science* 234:470–474.
24. Evans TJ, Moyes D, Carpenter A, Martin R, Loetscher H, Lesslauer W, Cohen J (1994) *J Exp Med* 180:2173–2179.
25. Cereghini S (1996) *FASEB J* 10:267–282.
26. Perlmutter DH, Dinarello CA, Punsal PI, Colten HR (1986) *J Clin Invest* 78:1349–1354.
27. Gachon F, Fonjallaz P, Damiola F, Gos P, Kodama T, Zakany J, Duboule D, Petit B, Tafti M, Schibler U (2004) *Genes Dev* 18:1397–1412.
28. Tian B, Nowak DE, Brasier AR (2005) *BMC Genomics* 6:137.
29. Erickson SL, de Sauvage FJ, Kikly K, Carver-Moore K, Pitts-Meek S, Gillett N, Sheehan KC, Schreiber RD, Goeddel DV, Moore MW (1994) *Nature* 372:560–563.
30. Neumann H, Schweigreiter R, Yamashita T, Rosenkranz K, Wekerle H, Barde YA (2002) *J Neurosci* 22:854–862.
31. Munoz E, Brewer M, Baler R (2002) *J Biol Chem* 277:36009–36017.
32. Ripperger JA, Schibler U (2006) *Nat Genet* 38:369–374.
33. Lopez-Molina L, Conquet F, Dubois-Dauphin M, Schibler U (1997) *EMBO J* 16:6762–6771.
34. Franken P, Lopez-Molina L, Marcacci L, Schibler U, Tafti M (2000) *J Neurosci* 20:617–625.
35. Borbely AA, Achermann P (2005) in *Principles and Practice of Sleep Medicine*, eds Kryger MH, Roth T, Dement WC (Elsevier Saunders, Philadelphia), pp 405–417.
36. Krueger JM, Pappenheimer JR, Karnovsky ML (1982) *Proc Natl Acad Sci USA* 79:6102–6106.
37. Uehori J, Fukase K, Akazawa T, Uematsu S, Akira S, Funami K, Shingai M, Matsumoto M, Azuma I, Toyoshima K, Kusumoto S, Seya T (2005) *J Immunol* 174:7096–7103.
38. Krueger JM, Walter J, Dinarello CA, Wolff SM, Chedid L (1984) *Am J Physiol* 246:R994–R999.
39. Shoham S, Davenne D, Cady AB, Dinarello CA, Krueger JM (1987) *Am J Physiol* 253:R142–R149.
40. Hogan D, Morrow JD, Smith EM, Opp MR (2003) *J Neuroimmunol* 137:59–66.
41. Ohdo S, Koyanagi S, Suyama H, Higuchi S, Aramaki H (2001) *Nat Med* 7:356–360.
42. Heesen C, Nawrath L, Reich C, Bauer N, Schulz KH, Gold SM (2006) *J Neurol Neurosurg Psychiatry* 77:34–39.
43. Pimentel M, Chang M, Chow EJ, Tabibzadeh S, Kirit-Kiriak V, Targan SR, Lin HC (2000) *Am J Gastroenterol* 95:3458–3462.
44. Toth LA, Tolley EA, Broady R, Blakely B, Krueger JM (1994) *Proc Soc Exp Biol Med* 205:174–181.
45. Liu J, Mankani G, Shi X, Meyer M, Cunningham-Runddles S, Ma X, Sun ZS (2006) *Infect Immun* 74:4750–4756.
46. Allen G, Rappe J, Earnest DJ, Cassone VM (2001) *J Neurosci* 21:7937–7943.
47. Ripperger JA, Shearman LP, Reppert SM, Schibler U (2000) *Genes Dev* 14:679–689.
48. Doi M, Hirayama J, Sassone-Corsi P (2006) *Cell* 125:497–508.
49. Deboer T, Tobler I (2000) *J Comp Physiol [A]* 186:969–973.
50. Tobler I, Gaus SE, Deboer T, Achermann P, Fischer M, Rulicke T, Moser M, Oesch B, McBride PA, Manson JC (1996) *Nature* 380:639–642.
51. Albrecht U, Lu HC, Revelli JP, Xu XC, Lotan RGE (1998) in *Human Genome Methods*, ed Adolph KW (CRC, New York), pp 93–119.

SI Figure 6

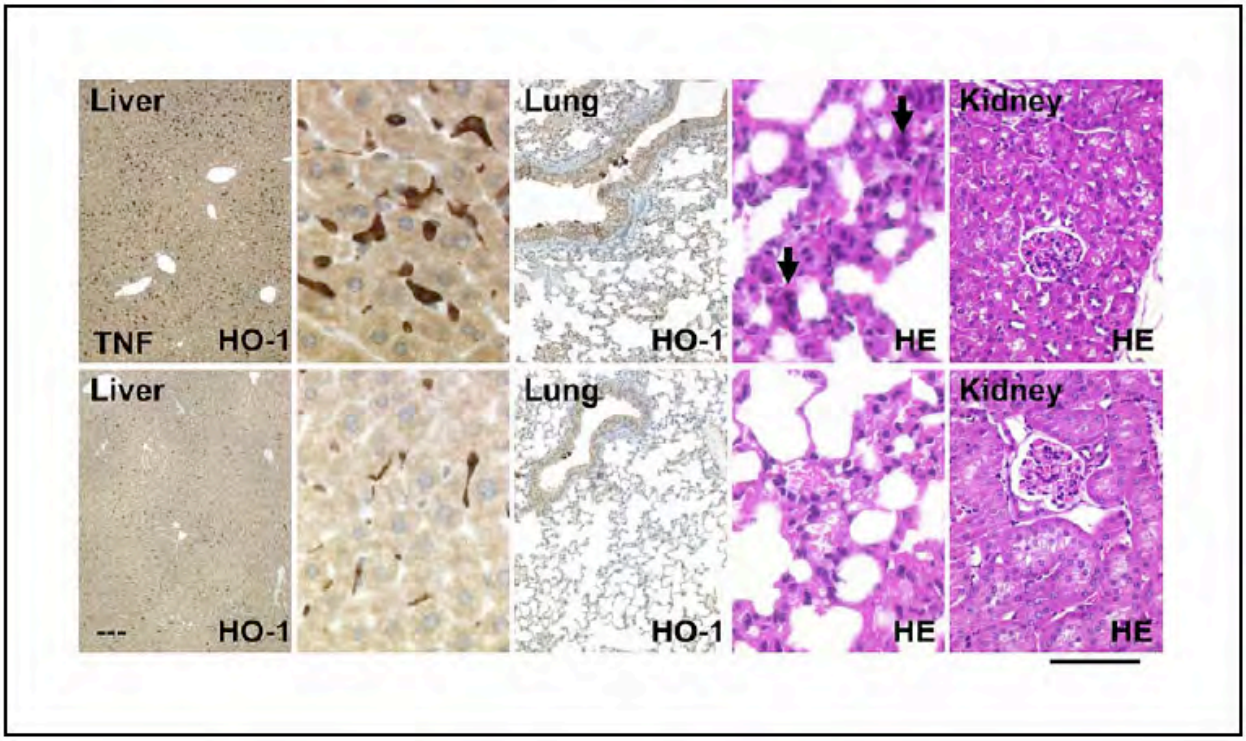
Liver
TNF
HO-1
Lung
HO-1
HE
Kidney
HE
Liver

HO-1
Lung
HO-1
HE
Kidney
HE

SI Figure 7

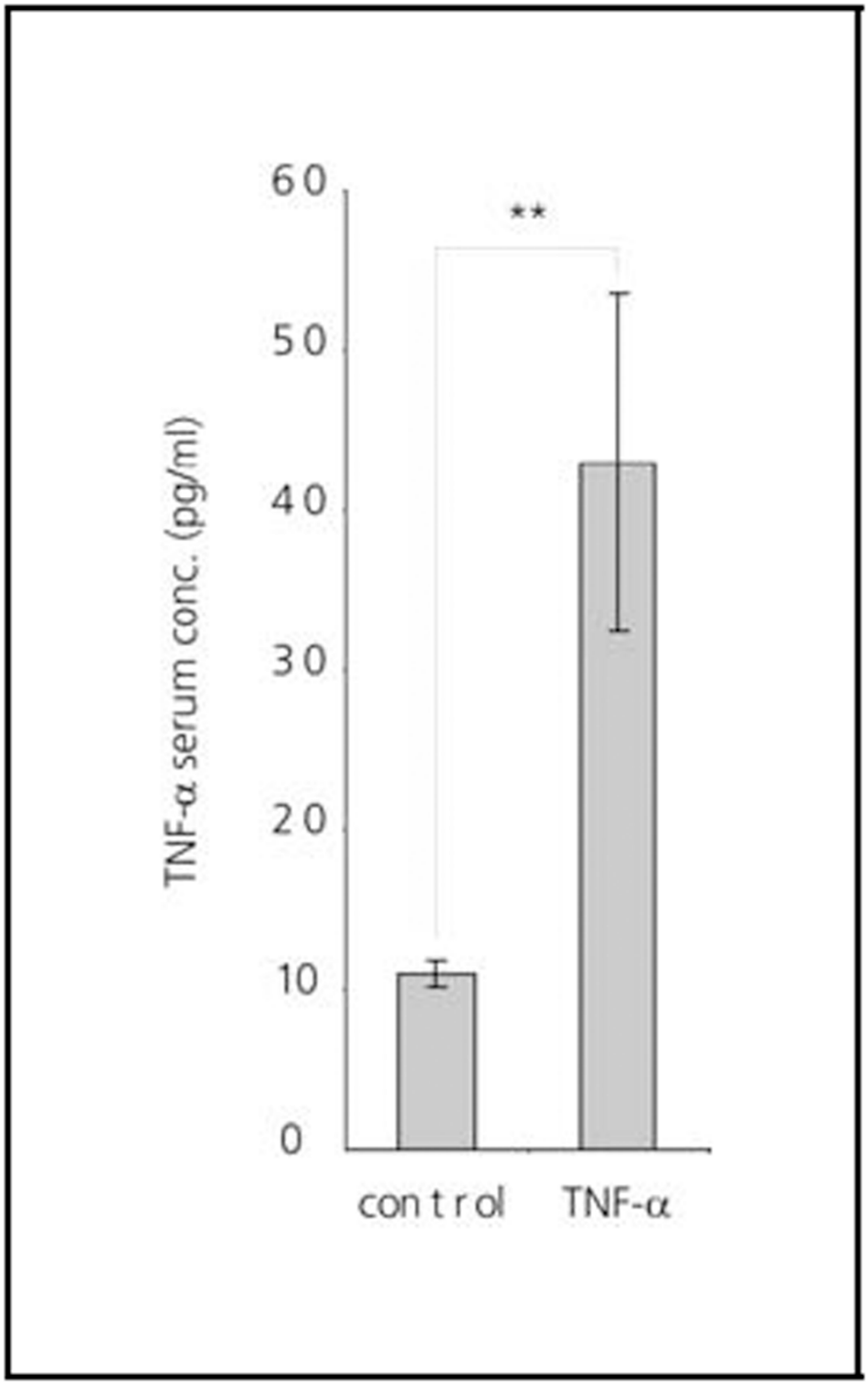

SI Figure 8

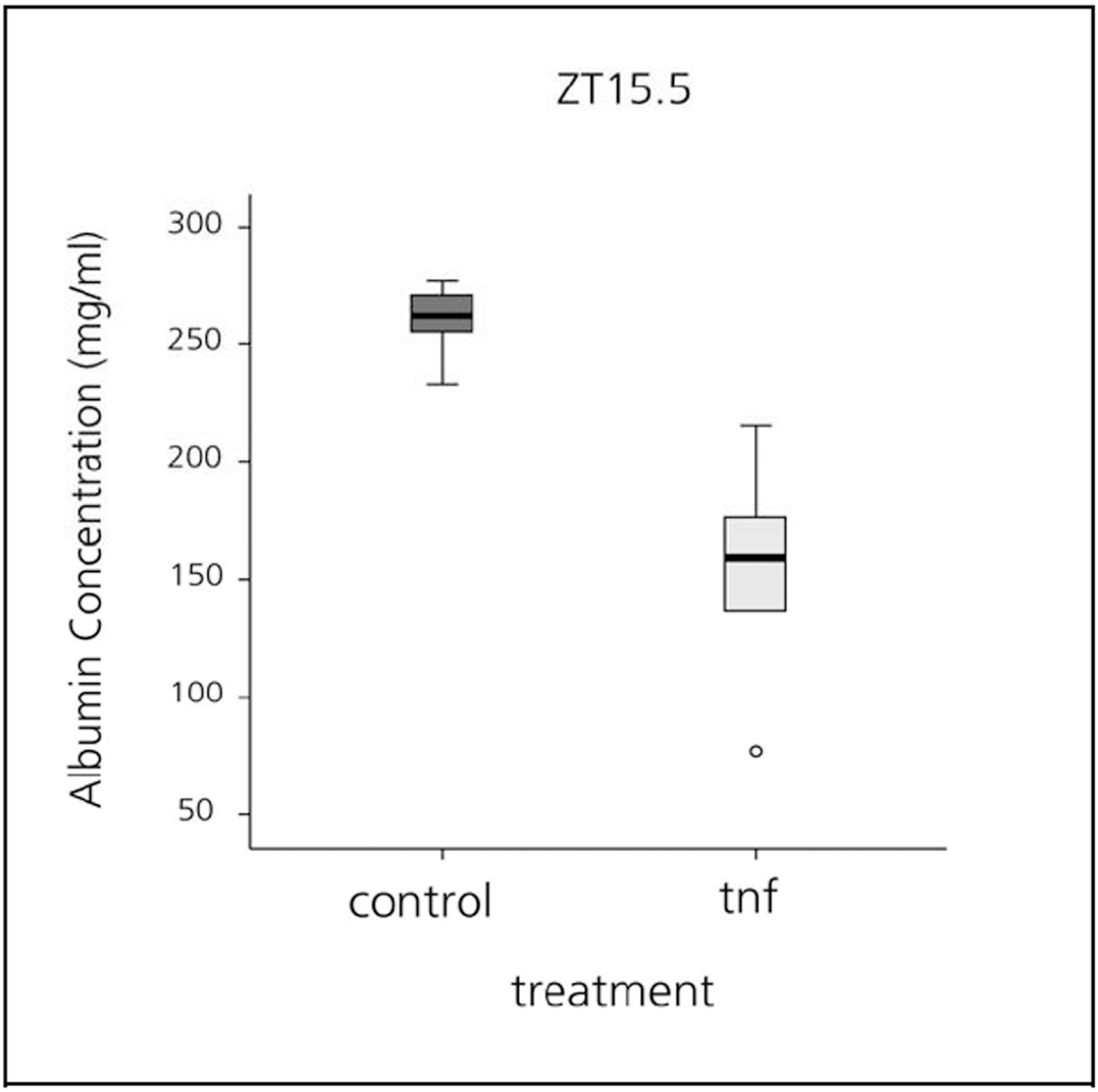
ZT15.5
Albumin Concentration (mg/ml)
300
250
200
150
100
50
control
tnf
treatment

SI Figure 9

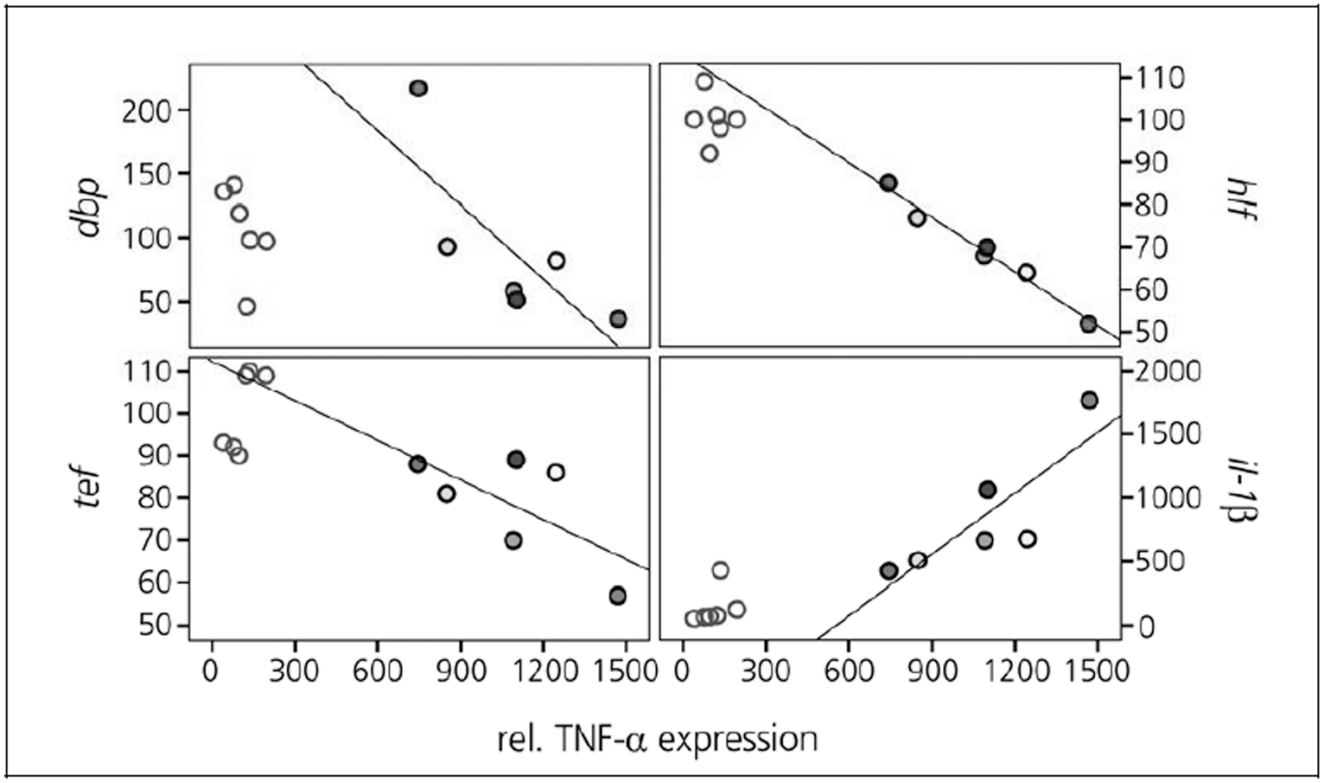

SI Figure 10

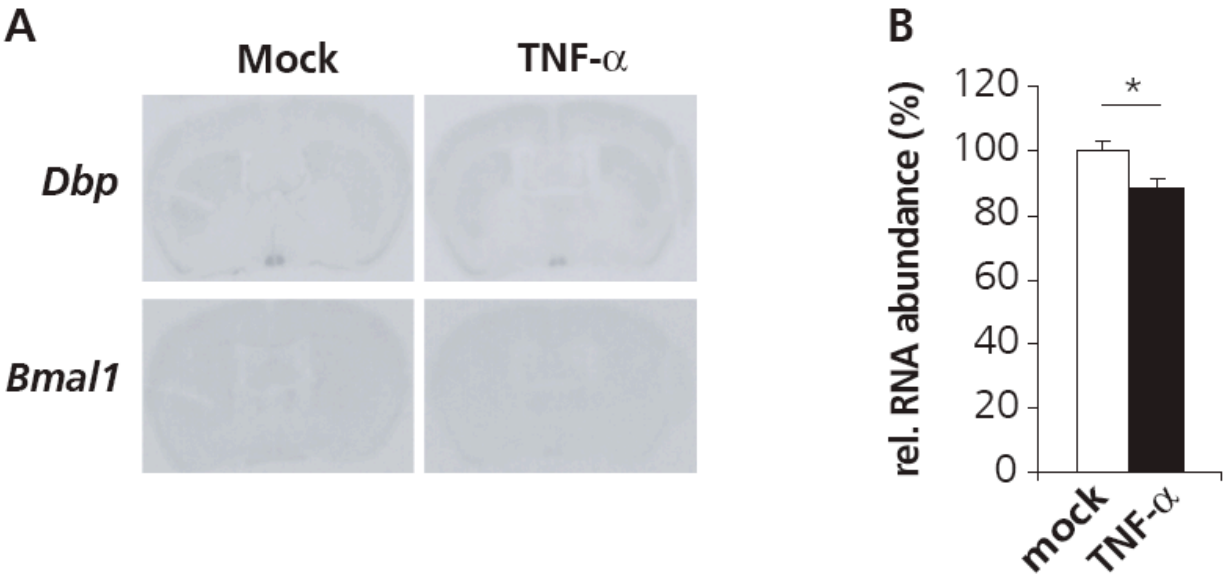

SI Figure 11

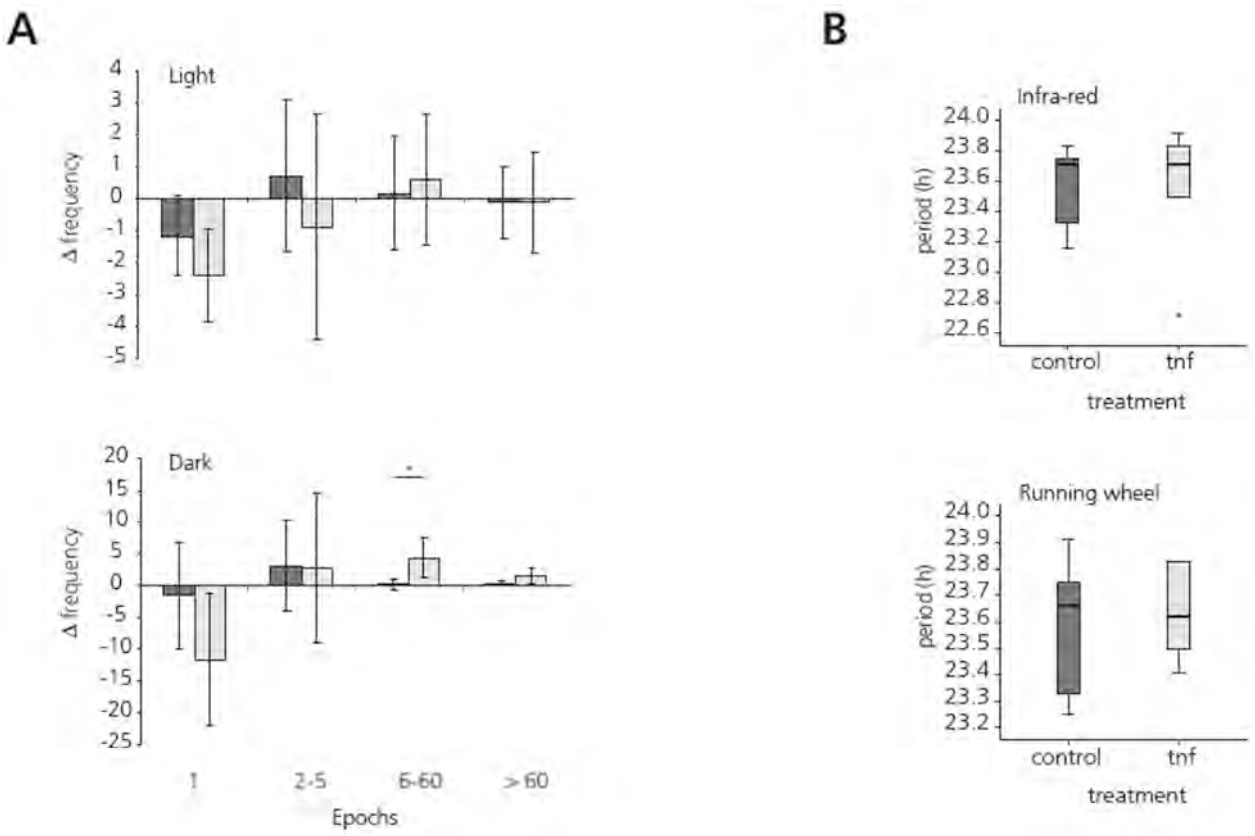

SI Table 1

Table 1. Sequences for primers and probes, normal concentrations used were 250 nM for probes and 400 nM for the primers

Gene name	forward primer 5' - 3'	probe 5'-FAM - 3' -TAMRA	reverse primer 5' - 3'
dbp	GCGAGAAGTGCAAAATTGGC	CGCGCGCCTGTGTCCCTTG	CGGGAGGCTCCTATAGTCTGG
hlf	CGCCAGGAGGTGGCTG	TTTAAGGAAGGAGCTGGGCAAATGCAA	GCCTCGTACTTGGCAAGTATGTT
rev-erb a	ACAGCAGCCGAGTGTCCC	CAGCAAGGGCACAAGCAACATTACCAAG	ACACAGTAGCACCATGCCATTC
bmal1	CCAAGAAAGTATGGACACAGACAAA	TGACCCTCATGGAAGGTTAGAATATGCAGAA	GCATTCTTGATCCTTCCTTGGT
clock	TTGCTCCACGGGAATCCTT	ACACAGCTCATCCTCTCTGCTGCCTTTC	GGAGGGAAAGTGCTCTGTTGTAG

	pre-developed taqman assays (Applied Biosystems)
18s rRNA	4310893E
Per1	Mm00501813_m1
Per2	Mm00478113_m1
Per3	Mm00478120_m1
Tef	Mm00457513_m1

TNF-α suppresses the expression of clock genes by interfering with E-box-mediated transcription

Cavadini et al. 10.1073/pnas.0701466104.

Supporting Information

Files in this Data Supplement:

SI Figure 6
SI Figure 7
SI Figure 8
SI Figure 9
SI Figure 10
SI Figure 11
SI Table 1
SI Text

SI Figure 6

Fig. 6. Photomicrographs of histological sections of liver, lung and kidney with (top row) and without (bottom row) TNF-a treatment: The liver shows an increase in HO-1 positive Kupffer cells. At high power magnification the cells appear also larger. No morphologically apparent liver cell damage is however detected. The lung shows unremarkable numbers of HO-1 positive macrophages in the bronchial mucus layer. No increase in HO-1 positive alveolar macrophages is seen. At high power magnification (hematoxylin eosin staining) increased numbers of megakaryocytes (indicated by arrows) are seen trapped within the alveolar vascular bed. There is, however, no evidence of pulmonary edema or acute pulmonary damage. Sections of the kidney (hematoxylin eosin staining) are unremarkable. The scale bar represents from left to right 400 mm, 50 mm, 200 mm, 50 mm, and 100 mm, respectively.

SI Figure 7

Fig. 7. At day 3 (ZT 15.5) after minipump insertion, serum was collected and TNF-a was measured by ELISA. Data are given as the mean ± SD of TNF-a serum concentrations measured in six animals per group. Independent samples t test, P = 0.001.

SI Figure 8

Fig. 8. Decreased concentrations of albumin in serum of TNF-a-treated mice. Serum was collected at day three after minipump implantation at ZT 15.5 and albumin concentrations were measured as described in materials and methods. Data show the mean ±SD of serum albumin concentrations in mice (six mice per group).

SI Figure 9

Fig. 9. IL1b expression correlates to TNF-a expression, both being increased in TNF-a treated animals (circles with different colors, each individual mouse representing one color) compared to animals infused with PBS (blue open circles) (day 3, at ZT 15.5; 6 mice per group). In contrary, Dbp, Hlf, and Tef are negatively correlated to the relative TNF-a expression.

SI Figure 10

Fig. 10. TNF-a impairs expression of the clock output genes, Dbp in the SCN. (A and B) Dbp and Bmal1 expression in the SCN at ZT 6 as determined by radioactive in situ hybridization. At the time point of peak expression of Dbp, when Bmal1 expression is lowest, TNF-a leads to a significant reduction by 15% of the Dbp mRNA. (means ± SEM of six consecutive sections per mouse SCN; four mice; paired t test; * P = 0.003).

SI Figure 11

Fig. 11. (A) Mice treated with TNF-a show increased long rest epochs in the dark phase. Analysis of rest epochs was performed at day 3 of TNF-a and control infused mice; the analysis being performed separately for the light and dark period. The data show the differences in numbers of 1-min episodes with activity = 0 compared to baseline (mean of the three days before minipump insertion). The occurrence of rest was arbitrarily subdivided in episodes for durations with rest = 0 activity counts: up to 1 min rest, between 2 and 5 min, 6 and 60 min, and more than 60 min. (ANOVA for repeated measures, followed by independent-samples t test; * P £0,05). (B) TNF-a does not affect the period length measured in constant darkness. On day 1 after minipump insertion the lights were turned off and the mice were kept in constant darkness. The circadian period of locomotion and running-wheel activity was determined by periodogram analysis over the 5 days in constant

darkness. Independent-sample t-tests were performed. TNF-a (1.5 mg/day; light gray bars) or saline as control (dark gray bars).

SI Text

RNA Isolation and Gene Expression Analysis

Whole-cell RNA from cultured cells was extracted using the NucleoSpin-RNA II kit (Macherey-Nagel, Switzerland). RNA from mouse tissues was extracted by homogenization of the organ in TRIzol (Invitrogen) according to the manufacturer's instructions. Subsequently, RNA was reverse-transcribed using random hexamers (Promega, for the in vitro assays; Roche, for the in vivo assays) and AMV reverse transcriptase (Promega, for the in vitro assays) or M-MuLV reverse transcriptase (Roche, for the in vivo assays). The cDNA equivalent to 50 ng of total RNA was PCR-amplified in an ABI PRISM 7700 detection system (PE-Applied Biosystems) using the TaqMan Universal PCR Master Mix (Applied Biosystems) and quantified as follows. Primers and probes for Taqman analysis were either purchased from Applied Biosystems or purchased from Microsynth, Balgach, Switzerland, as described in detail in SI Table 1. The relative levels of each RNA were calculated by the $2^{-}DD^{CT}$ method (CT standing for the cycle number at which the signal reaches the threshold of detection); 18s rRNA was used as a housekeeping gene. Each CT value used for these calculations is the mean of two duplicates of the same reaction. Relative RNA levels are expressed as x-fold variations compared to ZT = 0 (time course experiments) or as percentages of the average control groups (in the in vitro one-time-point experiments and in the in vivo experiments).

In situ hybridization

After infusion of mice with saline or TNF-a mice were killed at day three at ZT 6. Brains were embedded in paraffin and sectioned at 7-mm-thickness and hybridized with 35S-rUTP labeled riboprobes as described (1). The Bmal1 probe corresponded to nucleotides 654-1290 (accession no. AF015953) and the Dbp probe to nucleotides 2-951 (accession no. NM016974). Quantification was performed by densitometric analysis of autoradiograph films using the Molecular analyst program (Bio-Rad). Data from the SCN were normalized to the lateral hypothalamus next to the SCN. For each treatment

three animals were used and six sections per SCN were analyzed. We assessed the relative mRNA abundance values by defining the highest value of each experiment in mock treated animals as 100%.

ELISA

The concentration of albumin and TNF-a in the serum of mice implanted with osmotic minipumps was determined by ELISA (Mouse Albumin ELISA Quantitation Kit, Bethyl Laboratories, TX, and mouse TNF-a ELISA kit, KMC3012, Biosource).

1. Deboer T, Tobler I (2000) J Comp Physiol A 186:969-973.

Appendix III

"Mutation of the circadian clock gene Per2 alters vascular endothelial function."

H. Viswambharan, J.M. Carvas, V. Antic, A. Marecic, C. Jud, C.E. Zaugg, X.F. Ming, J.P. Montani, U. Albrecht, Z. Yang
2007

Published in *Circulation*, 115(16): 2188-2195

Mutation of the Circadian Clock Gene Per2 Alters Vascular Endothelial Function

Hema Viswambharan, João M. Carvas, Vladan Antic, Ana Marecic, Corinne Jud, Christian E. Zaugg, Xiu-Fen Ming, Jean-Pierre Montani, Urs Albrecht and Zhihong Yang

Circulation 2007;115;2188-2195; originally published online Apr 2, 2007;
DOI: 10.1161/CIRCULATIONAHA.106.653303
Circulation is published by the American Heart Association. 7272 Greenville Avenue, Dallas, TX 72514
 Print ISSN: 0009-7322. Online ISSN: 1524-4539

Mutation of the Circadian Clock Gene *Per2* Alters Vascular Endothelial Function

Hema Viswambharan, PhD*; João M. Carvas, MSc*; Vladan Antic, MD, PhD; Ana Marecic, MSc; Corinne Jud, MSc; Christian E. Zaugg, PhD; Xiu-Fen Ming, MD, PhD; Jean-Pierre Montani, MD; Urs Albrecht, PhD; Zhihong Yang, MD

Background—The circadian clock regulates biological processes including cardiovascular function and metabolism. In the present study, we investigated the role of the circadian clock gene *Period2* (*Per2*) in endothelial function in a mouse model.

Methods and Results—Compared with the wild-type littermates, mice with *Per2* mutation exhibited impaired endothelium-dependent relaxations to acetylcholine in aortic rings suspended in organ chambers. During transition from the inactive to active phase, this response was further increased in the wild-type mice but further decreased in the *Per2* mutants. The endothelial dysfunction in the *Per2* mutants was also observed with ionomycin, which was improved by the cyclooxygenase inhibitor indomethacin. No changes in the expression of endothelial acetylcholine-M_3 receptor or endothelial nitric oxide synthase protein but increased cyclooxygenase-1 (not cyclooxygenase-2) protein levels were observed in the aortas of the *Per2* mutants. Compared with *Per2* mutants, a greater endothelium-dependent relaxation to ATP was observed in the wild-type mice, which was reduced by indomethacin. In quiescent aortic rings, ATP caused greater endothelium-dependent contractions in the *Per2* mutants than in the wild-type mice, contractions that were abolished by indomethacin. The endothelial dysfunction in the *Per2* mutant mice is not associated with hypertension or dyslipidemia.

Conclusions—Mutation in the *Per2* gene in mice is associated with aortic endothelial dysfunction involving decreased production of NO and vasodilatory prostaglandin(s) and increased release of cyclooxygenase-1–derived vasoconstrictor(s). The results suggest an important role of the *Per2* gene in maintenance of normal cardiovascular functions. **(*Circulation*. 2007;115:2188-2195.)**

Key Words: acetylcholine ■ circadian rhythm ■ cyclooxygenase 1 ■ endothelium ■ nitric oxide ■ vasodilation

The master circadian clock in mammals, located in the suprachiasmatic nuclei of the hypothalamus, regulates many biochemical, physiological, and behavioral processes and allows an organism to anticipate diurnal changes.[1] In mammals, a set of clock genes constitutes the molecular machinery of the circadian clock.[2] The 2 transcription factors CLOCK and BMAL1 form heterodimers and induce expression of several genes by binding to E-box enhancer elements in the promoters of target genes.[2] Among these genes are the *Period* genes (*Per1/2/3*) and *Cryptochrome* genes (*Cry1/2*), whose protein products PER and CRY then negatively regulate the activation of their own expression by inhibiting the activity of the CLOCK/BMAL1 complex, thereby constituting a negative feedback loop.[2] Genetic studies revealed important roles of the circadian genes not only in the regulation of behavior but also in metabolism. For example, an autosomal dominant mutation in the human *Per2* gene results in familial advanced sleep phase syndrome,[3] and *Per2* mutant mice display impaired clock resetting and loss of circadian rhythmicity in constant darkness.[4] Recent studies suggest an important role of CLOCK and BMAL1 in glucose homeostasis.[5] Homozygous *Clock* mutant mice reveal not only behavioral changes but also phenotypes resembling metabolic syndrome, a cluster of cardiovascular risk factors including obesity, dyslipidemia, hypertension, insulin resistance, and hyperglycemia.[6] These risk factors can cause vascular injury, and in particular they promote endothelial dysfunction leading to cardiovascular diseases.[7]

Clinical Perspective p 2195

The endothelium regulates vascular function by releasing vasoactive factors including relaxing and contracting factors. An imbalance between the relaxing factors and contracting

Received July 20, 2006; accepted February 23, 2007.

From the Department of Medicine, Divisions of Physiology (H.V., J.M.C., V.A., A.M., X.M., J.M., Z.Y.) and Biochemistry (C.J., U.A.), University of Fribourg, Fribourg; and Department of Research, University Hospital Basel, Basel (C.E.Z.), Switzerland.

*The first 2 authors contributed equally to this article.

The online-only Data Supplement, consisting of Methods and figures, is available with this article at http://circ.ahajournals.org/cgi/content/full/CIRCULATIONAHA.106.653303/DC1.

Correspondence to Dr Zhihong Yang, Department of Medicine, Division of Physiology, University of Fribourg, Rue du Musée 5, CH-1700 Fribourg, Switzerland. E-mail Zhihong.Yang@unifr.ch

Circulation **is available at http://www.circulationaha.org** **DOI: 10.1161/CIRCULATIONAHA.106.653303**

factors participates in pathogenesis of cardiovascular diseases.[8] Research from the past decades has provided firm evidence for the vasoprotective role of endothelium-derived nitric oxide (NO), which is produced from L-arginine via endothelial NO synthase (eNOS). NO causes vasodilation and inhibits smooth muscle cell proliferation, platelet aggregation, and inflammatory responses.[9] Therefore, endothelial dysfunction, reflected by impaired endothelium-dependent relaxations in response to various agonists such as acetylcholine, ATP, histamine, and ionomycin, plays an essential role in pathogenesis of cardiovascular diseases.[10,11] The mechanisms underlying endothelial dysfunction are attributable to (1) a defect in eNOS gene expression; (2) eNOS enzymatic activation; or (3) an increase in oxidative stress.[12,13] Besides these mechanisms, increased production of endothelium-derived contracting factors from cyclooxygenase (COX) has also been implicated in endothelial dysfunction under various disease conditions by counteracting the vascular relaxing effect of NO.[14–16]

Clinical studies have well documented the circadian pattern of physiological cardiovascular functions and pathological cardiovascular events. The onset of unstable angina, myocardial infarction, sudden cardiac death, and stroke occurs usually at specific moments of the day.[17–21] It has been suggested that it is attributed primarily to the diurnal variations of cardiovascular parameters, such as sympathetic nerve activity, blood pressure, and heart rate, in addition to variations in plasma lipid, platelets, coagulation factors, or endothelial dysfunction.[22–29] However, it is unknown whether the diurnal variation of cardiovascular parameters is controlled primarily by circadian clock genes or influenced secondarily by external factors. The aim of the present study is to investigate whether there are alterations in endothelial functions in a mouse model with *Per2* mutation and whether the endothelial functional changes are associated with the metabolic cardiovascular risk factors, the phenotype observed in the *CLOCK* and *BMAL1* mutant mice.

Methods

Materials

See the online-only Data Supplement.

Animals

The *Per2* mutant mice were from Zheng et al[30] and propagated in our own facility. Adult 3-month-old male wild-type (WT) (C57Bl/6J) and *Per2* mutant littermates produced from heterozygote-heterozygote crosses were fed ad libitum and euthanized by decapitation. Artificial light was provided daily from 6 AM (Zeitgeber time [ZT0]) to 6 PM (ZT12) (12 hours of light/12 hours of darkness) with room temperature and humidity kept constant (temperature, 22±1°C; humidity, 55±5%). Mice were euthanized at ZT3, ZT6, ZT9, or ZT15. All the animal experimental protocols were approved by the Ethical Committee of Veterinary Office of Fribourg, Switzerland.

Vasomotor Responses

The descending thoracic aortas with intact endothelium were isolated and dissected free from perivascular tissues and cut into rings (3 mm in length). The rings were suspended in a Multi-Myograph System (model 610M, Danish Myo Technology A/S, Denmark) filled with Krebs-Ringer bicarbonate buffer (in mmol/L: 118 NaCl, 4.7 KCl, 2.5 $CaCl_2$, 1.2 $MgSO_4$, 1.2 KH_2PO_4, 25 $NaHCO_3$, 0.026 EDTA, and 11.1 glucose) at 37°C, aerated with 95% O_2 and 5% CO_2. Changes in isometric tension were recorded with MyoData software as previously described.[31]

Aortic rings were allowed to equilibrate for 45 minutes and were progressively stretched to a passive tension of 5.0 mN that gives the optimal length-tension relationship. To study the effects of *Per2* on endothelium-dependent or -independent relaxations, aortic rings from WT and *Per2* mutant mice were precontracted with norepinephrine (0.1 to 0.3 μmol/L) to match the precontraction. Acetylcholine, ATP, or ionomycin, which release NO from endothelial cells, or the NO donor sodium nitroprusside (0.1 nmol/L to 10 μmol/L) was added to the precontracted aortic rings. To study whether arginase and free radical formation are involved in the regulation of endothelial function, the arterial rings were treated with the arginase inhibitor L-norvaline (0.2 mmol/L, 60 minutes) in the presence of L-arginine (10 mmol/L) or with superoxide dismutase (150 U/mL) plus catalase (1000 U/mL; 15 minutes), respectively, followed by the response to acetylcholine (1 nmol/L to 10 μmol/L). To study the role of cyclooxygenase in regulation of vascular functions, the vascular rings were incubated with indomethacin (1 μmol/L) for 30 minutes. The endothelium-dependent responses to acetylcholine, ionomycin, or ATP were then performed.

Protein Expression of eNOS, COX, and Acetylcholine-M_3 Receptor in Mouse Aortas

Aortic segments with intact endothelium were snap-frozen and kept at −80°C until use. Crude protein extracts were obtained by homogenizing the aortic tissues in protein extraction buffer as described previously.[32] Protein concentrations were measured by the Lowry method; 30 μg of the extract was resolved by SDS-PAGE. The separated proteins were transferred to polyvinylidene fluoride membrane (Millipore). The proteins of interest were detected by immunoblotting with the use of antibodies against eNOS (1:2500), COX-1 (1:500), COX-2 (1:500), or acetylcholine-M_3 receptor (1:500) as primary antibodies followed by incubation with a corresponding secondary fluorophore-conjugated goat (polyclonal) anti-mouse or anti-rabbit antibody. The signals were visualized with the use of the Odyssey Infrared Imaging System (LI-COR Biosciences). Quantification of the signals was performed with the use of Odyssey Application Software 1.2. Protein levels were expressed as the ratio against tubulin.

In Vitro ECG

See the online-only Data Supplement.

Blood Pressure Measurement by Telemetry

All mice were instrumented with an arterial catheter connected to an implantable transducer (model TA11PA-C20, Data Sciences International) to monitor arterial pressure by telemetry. Through a paratracheal incision with the use of stereomicroscopy, the left carotid artery was exposed, briefly clamped, and punctured with a 26-gauge needle. The cannula was then inserted into the aortic arch against the flow and secured in place with tissue adhesive. The body of the implant was placed subcutaneously on the right flank. After completion of the surgery, the mice were housed in individual standard mouse cages (23×17×14 cm high, Indulab AG, Switzerland) for blood pressure measurement.[33] At least 12 days were given to animals to recover from surgery and for blood pressure and heart rate to stabilize.

Continuous arterial pressure monitoring was performed in unrestrained conscious mice. Each animal cage was equipped with 1 RPC-1 plastic receiver (Data Sciences International) fixed on the bottom of the cage and connected to an analog output device (R11-CPA), allowing for the continuous recording of the analog pulsatile arterial pressure signal. The analog pressure signal was then fed to a 12-bit analog-to-digital converter (Dash-16, Metrabyte Corp), sampled at 1 kHz, and processed with customized algorithms[34] for beat-to-beat analysis. To analyze only data from the undisturbed periods, the 2-hour period of animal maintenance and cage cleaning (8 to 10 AM) was excluded from the analysis.

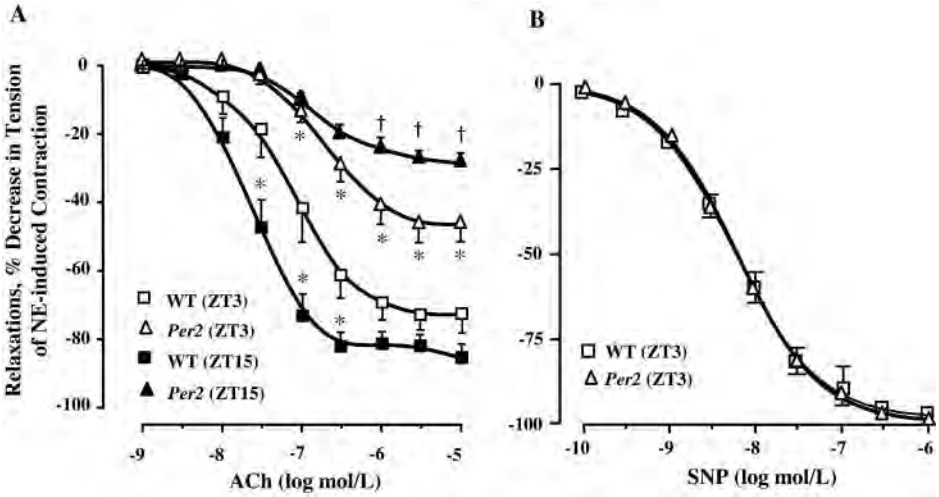

Figure 1. Endothelium-dependent relaxations to acetylcholine in *Per2* mutant mice. Endothelium-dependent relaxations to acetylcholine (ACh) (A) and endothelium-independent relaxations to the NO donor sodium nitroprusside (B) in the aortas of WT and *Per2* mutant mice at ZT3 (open symbol) and ZT15 (solid symbol) are shown. **P*<0.05 for WT (ZT15) or *Per2* (ZT3) vs WT (ZT3); †*P*<0.05 for *Per2* (ZT15) vs *Per2* (ZT3) at the indicated corresponding concentration between the compared groups. n=7 to 9; ANOVA with Bonferroni adjustment for ACh responses and Student unpaired *t* test for sodium nitroprusside responses. NE indicates norepinephrine; SNP, sodium nitroprusside.

Statistical Analysis

Relaxations were expressed as percentage of decrease in tension of the contraction to norepinephrine. Data are given as mean±SEM. In all experiments, n equals the number of animals from which the blood vessels were dissected. Area under the curve or responses to agents at each corresponding concentrations among the different groups of animals were compared either by the Student *t* test for unpaired observations or by ANOVA for multiple comparisons followed by Bonferroni adjustment. A 2-tailed value of $P \leq 0.05$ is considered to indicate a statistical difference.

The authors had full access to and take full responsibility for the integrity of the data. All authors have read and agree to the manuscript as written.

Results

Endothelium-Dependent Relaxations to Acetylcholine in *Per2* Mutant Mice

In aortic rings with intact endothelium precontracted with norepinephrine (0.1 or 0.3 μmol/L), acetylcholine (1 nmol/L to 10 μmol/L), which stimulates NO release from the endothelium via activation of endothelial acetylcholine-M_3 receptor,[35] evoked potent concentration-dependent relaxations in WT mice at ZT3, the beginning of the inactive phase for the rodents (Figure 1A; n=9). The response was significantly decreased in the *Per2* mutant mice (Figure 1A; n=9; $P<0.05$ versus WT). The smooth muscle sensitivity to NO as demonstrated by endothelium-independent relaxations to the NO donor sodium nitroprusside (0.1 nmol/L to 1 μmol/L) was comparable between the 2 groups of animals (Figure 1B; n=9; *P*=NS).

Western blots showed no difference in protein levels of endothelial acetylcholine-M_3 receptor or eNOS in the aortas of the WT and *Per2* mutant mice (Figure 2; n=5 to 6). Neither inhibition of oxidative stress by incubating aortic rings with superoxide dismutase (150 U/mL) plus catalase (1000 U/mL) nor inhibition of arginase by L-norvaline (20 mmol/L, 1 hour, to increase L-arginine substrate availability for eNOS) improved endothelium-dependent relaxations to acetylcholine in *Per2* mutant mice (Figure IA and IB in the online-only Data Supplement; n=6).

Furthermore, we showed that the decreased endothelium-dependent relaxations in response to acetylcholine in *Per2* mutant mice were consistently present during the inactive phase as demonstrated in animals at ZT6 and ZT9 (Figure II in the online-only Data Supplement). Interestingly, the endothelium-dependent relaxations induced by acetylcholine were further enhanced in the WT mice at ZT15, the beginning of the active phase (Figure 1A; n=7 to 9; $P<0.05$ versus WT

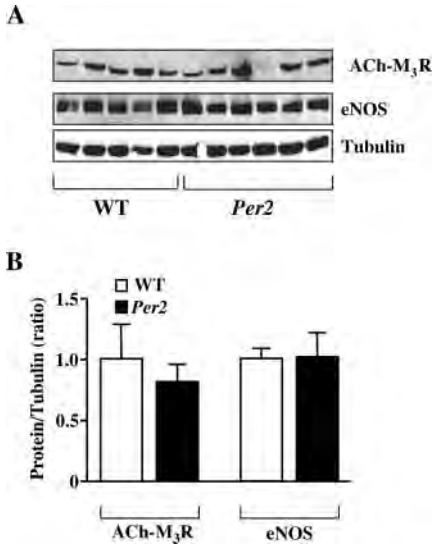

Figure 2. Acetylcholine-M_3 receptor and eNOS expression in *Per2* mutant mice. A, Western blot demonstrates comparable acetylcholine-M_3 receptor (ACh-M_3R) or eNOS protein levels in the aortas of WT and *Per2* mutant mice; B, Quantification of the acetylcholine-M_3 receptor or eNOS protein levels of the aforementioned experiments. n=5 to 6; Student unpaired *t* test for comparison of the expression of acetylcholine-M_3 receptor or eNOS between WT and *Per2* mutants.

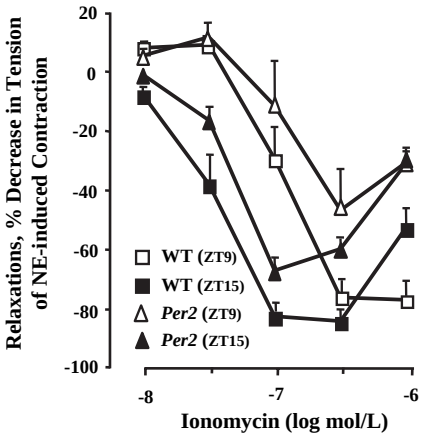

Figure 3. Endothelium-dependent relaxations to ionomycin in *Per2* mutant mice. Relaxation to ionomycin (10 nmol/L to 1 μmol/L) in the aortas of WT and *Per2* mutant mice during the inactive phase (open symbol) and the active phase (solid symbol) is shown. n=7 to 9; ANOVA with Bonferroni adjustment for the area under the curve among the 4 groups. NE indicates norepinephrine.

mice at ZT3), but decreased in the *Per2* mutants (Figure 1A; n=7 to 9; $P<0.05$ versus *Per2* mutants at ZT3).

Endothelium-Dependent Relaxations to Ionomycin in *Per2* Mutant Mice

Moreover, the endothelium-dependent relaxations to ionomycin (10 nmol/L to 1 μmol/L), which stimulates eNOS enzymatic activity via non–receptor-mediated increase in intracellular Ca^{2+} concentration, were also reduced significantly in the *Per2* mutant mice during the inactive phase (maximum effect: 46.7±12.1%) compared with the WT animals (maximum effect: 75.1±6.5%; $P<0.05$; Figure 3; n=7). During transition of the animals from the inactive to the active phase, the endothelium-dependent relaxations to ionomycin were significantly enhanced in both groups of animals ($P<0.05$ between ZT9 and ZT15 in the WT or *Per2* mutants). However, the relaxations remained weaker in the *Per2* mutants than the WT animals (Figure 3; n=7 to 9; $P<0.05$) also in the presence of indomethacin (Figure III in the online-only Data Supplement; n=7; $P<0.05$).

Role of COX in Endothelium-Dependent Responses in *Per2* Mutant Mice

We further analyzed whether COX-derived vasoactive prostanoids play a role in the functional changes in endothelium-dependent responses. Interestingly, a significantly higher protein level of COX-1 in aortas was found in the *Per2* mutant mice than in the WT animals by immunoblotting (1.8±0.3-fold increase; Figure 4A; n=9; $P<0.05$). No COX-2 signal could be detected in the aortas of the animals. Inhibition of COX by indomethacin (1 μmol/L, 30 minutes) did not affect the endothelium-dependent relaxations to acetylcholine in both WT and *Per2* mutant mice (Figure 4B; n=5 to 6; ZT3), whereas it significantly enhanced the relaxations to ionomycin in the *Per2* mutants (Figure 4C).

The enhanced production of COX-derived vasoconstrictor(s) in the *Per2* mutants was further demonstrated in the quiescent aortic rings stimulated by ATP in the presence of N^G-nitro-L-arginine methyl ester (L-NAME) (to eliminate the vasorelaxing effect of NO) (Figure 5A and 5B). ATP (0.1 to 10 μmol/L) evoked a transient but more pronounced vasoconstriction in the *Per2* mutant (14.5±1.8% of KCl 100 mmol/L) than the WT mice (5.0±1.3%; n=4; $P<0.05$). The contraction was abolished by the COX inhibitor indomethacin (Figure 5B; 1 μmol/L, 30 minutes).

Further experiments in the precontracted aortic rings demonstrated that ATP at 0.1 μmol/L did not cause vascular relaxation in both WT and *Per2* mutant mice (Figure 5C), whereas it caused an endothelium-dependent relaxation at 1 μmol/L, which was more pronounced in the WT (57.1±6.0%) than in the *Per2* mutant mice (21.3±7.7%; n=6; $P<0.05$) (Figure 5C). Incubation of the aortas with the

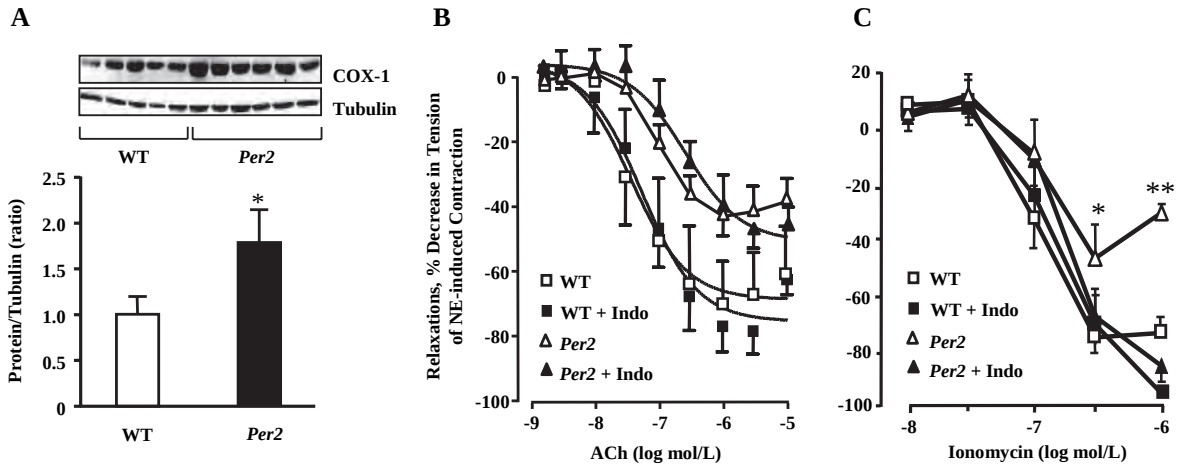

Figure 4. COX and endothelium-dependent relaxations in the *Per2* mutant mice. A, A representative immunoblotting shows increased COX-1 expression in the aortas of *Per2* mutant mice. B, Effects of the COX inhibitor indomethacin (Indo) (1 μmol/L, 30 minutes) on endothelium-dependent relaxations to acetylcholine (ACh) and ionomycin (C). No COX-2 signal could be detected in the aortas of the animals. NE indicates norepinephrine. n=7 to 9; *$P<0.05$ and **$P<0.01$ vs WT or *Per2*+Indo, Student unpaired *t* test for COX-1 expression between WT and *Per2* mutants and for the responses to acetylcholine or ionomycin in the presence or absence of indomethacin in WT or *Per2* mutant mice.

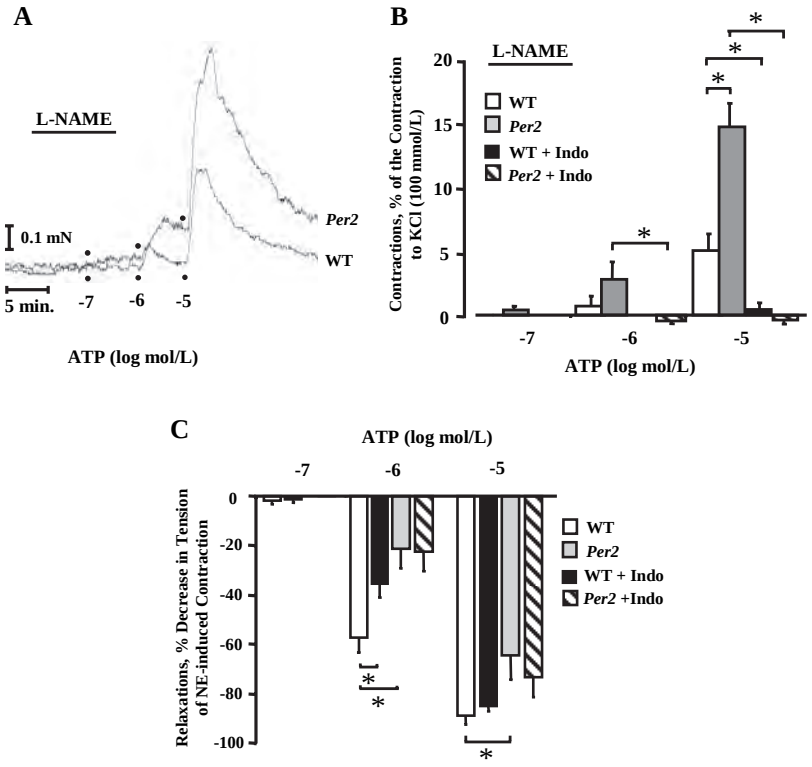

Figure 5. COX inhibition and endothelium-dependent responses to ATP. A, Original recording showing increased endothelium-dependent contractions induced by ATP in the quiescent aortas of the *Per2* mutant mice in the presence of eNOS inhibitor L-NAME (0.1 mmol/L). B, Increased contractions induced by ATP (0.1 to 10 μmol/L) in the aortas of the *Per2* mutant mice are abolished by the COX inhibitor indomethacin (Indo) (1 μmol/L); n=4. C, Inhibition of COX by indomethacin on endothelium-dependent relaxations to ATP in WT and *Per2* mutant mice; n=6 to 7. NE indicates norepinephrine. *$P<0.05$, ANOVA with Bonferroni adjustment for the ATP responses among the 4 groups at each concentration.

COX inhibitor indomethacin (1 μmol/L, 30 minutes) significantly reduced the relaxation to ATP at 1 μmol/L in the WT mice (Figure 5C; 35.4±5.6%; n=7; $P<0.05$) but was unable to affect the response in the *Per2* mutants. These relaxations in both WT and *Per2* mutant mice were fully inhibited by incubation of the aortas with the eNOS inhibitor L-NAME (0.1 mmol/L, 15 minutes; data not shown). Furthermore, the endothelium-dependent relaxation induced by the highest concentration of ATP (10 μmol/L) was also significantly reduced in the *Per2* mutant mice, and indomethacin was unable to significantly modulate the response in both groups (Figure 5C). Approximately 30% of relaxations were still present in the aortas incubated with indomethacin plus L-NAME, which can be fully blocked by KCl 100 mmol/L (data not shown), indicating the involvement of the endothelium-derived hyperpolarizing factor in endothelium-dependent relaxation to ATP at the highest concentration.

Metabolic and Hemodynamic Parameters

Mean arterial pressure for the whole-day period (22 hours) in *Per2* mutant animals (105.9±1.9 mm Hg; n=10) was significantly lower than that in their WT counterparts (116.5±2.1 mm Hg; n=9; $P<0.05$). Whole-day values for heart rate were not different between *Per2* mutant mice (530.9±5.7 bpm; n=10) and WT animals (535.7±11.3 bpm; n=9; P=NS). In vitro ECG showed no difference in changes of PP interval or PQ interval in response to increasing concentrations of acetylcholine (1 nmol/L to 0.1 mmol/L) between the 2 groups (Figure IV in the online-only Data Supplement; n=8).

There was no difference in plasma concentrations of total cholesterol and triglyceride between the 2 groups of animals (Figure V in the online-only Data Supplement; n=4). Notably, a previous study showed no difference in plasma glucose concentration between the WT and *Per2* mutant mice and an increased insulin sensitivity in the latter.[36]

Discussion

In the present study, we provided the first evidence for a role of the circadian clock gene *Per2* in the regulation of endothelium-mediated vascular responses in a mouse model, which is not associated with phenotypes resembling cardiovascular metabolic risk factors.

Endothelial Dysfunction in *Per2* Mutant Mice

The endothelium controls vascular functions by releasing NO from eNOS in response to various hormonal factors.[37] In the present study, we showed decreased endothelium-dependent relaxations in the *Per2* mutant mice on stimulation with acetylcholine but endothelium-independent relaxations to the NO donor sodium nitroprusside comparable to those in the WT animals. Notably, the decreased endothelium-dependent relaxation to acetylcholine persists throughout the daytime, the inactive phase of the rodents (Figure I in the online-only Data Supplement). This is not attributable to a differential eNOS gene expression or acetylcholine receptor expression between the 2 groups because the protein levels of eNOS and acetylcholine-M_3 receptor that mediate NO release from the endothelial cells[35] are comparable between the *Per2* mutants and WT littermates. Furthermore, impaired endothelium-dependent relaxations in the *Per2* mutants are also demonstrated with ATP as well as ionomycin, which activates eNOS by non–receptor-mediated increase in intracellular Ca^{2+} con-

centration, demonstrating endothelial dysfunction in the mutants.

Studies in the past demonstrate that besides alterations in eNOS gene expression, defective eNOS enzymatic activity and increased oxidative stress are potential mechanisms for the impairment of endothelial NO-mediated vascular relaxations.[9] It is unlikely that increased oxidative stress is responsible for the endothelial dysfunction in the *Per2* mutant mice because the decreased endothelium-dependent relaxations could not be reversed by scavenging reactive oxygen species with superoxide dismutase and catalase. Furthermore, inhibition of arginase to enhance L-arginine availability for eNOS or supplementation of the eNOS cofactor BH_4 had no effects on endothelium-dependent relaxations to acetylcholine in the *Per2* mutant mice (data not shown). It is noteworthy that *Per2* mutant mice have decreased calmodulin expression in the liver, as demonstrated in a previous study.[38] Because calmodulin is essential for the Ca^{2+}-dependent activation of eNOS by various agonists, it is conceivable that the decrease in calmodulin expression could also occur in the endothelial cells, which might be responsible for the impaired endothelium-dependent relaxations in the *Per2* mutant mice in response to the various agonists. This hypothesis warrants further investigation.

Diurnal Changes of Endothelial Function in *Per2* Mutant Mice

Interestingly, during the transition from the inactive to the active phase, the endothelium-dependent relaxation to acetylcholine is increased in the WT but decreased in the *Per2* mutant mice. In contrast to acetylcholine, the endothelium-dependent relaxation to ionomycin is enhanced in both groups of the animals during the transition from the inactive to the active phase, whereby the response still remains weaker in the *Per2* mutant mice. These results further demonstrate endothelial dysfunction in the mutant mice in the inactive as well as in the active phase. The increased response to ionomycin in both groups of animals in the active phase may be explained by the hemodynamic adaptation during this time period, ie, the increase in blood flow in the circulation, that increases NO release from the endothelium.[39] The possibility of different physical activity between WT and *Per2* mutant mice can be ruled out because a previous study showed normal behavioral activity of the *Per2* mutant mice under normal light/dark cycles.[30] The observation that the endothelium-dependent relaxations in response to acetylcholine are further decreased in the *Per2* mutant mice in the active phase might be due to opposite changes in the signal transduction pathways mediated by acetylcholine receptor, which leads to a further decrease in eNOS activation in the active phase of the *Per2* mutant mice. This conclusion is supported by the following evidence: First, ionomycin-induced endothelium-dependent relaxation is increased instead of decreased in the active phase, as shown in the present study; second, a study from another group showed that mouse aortic eNOS activity does not display 24-hour rhythmicity under a normal light/dark cycle.[40] Increased endothelium-dependent relaxation in healthy subjects in the morning hours has been reported in humans,[41] which is in agreement with the results from the WT mice, although the results are controversial in clinical studies.[28,29] The inconsistent results among the clinical studies are not clear but might be related to the different vascular beds investigated, ie, resistance vessels and conduit blood vessels, or might be due to changes in sympathetic nerve activity in vivo.[22] Whether our results can explain the increased incidence of cardiac events in the morning hours in certain patient populations[42] remains speculative.

Notably, the heart seems not to be affected by the defective acetylcholine response in the *Per2* mutant mice because the responses to acetylcholine in the heart, ie, increases in PP interval or PQ interval, that are mediated by acetylcholine-M_2 receptor[43] remain unchanged, as demonstrated by in vitro ECG. In addition, the blood pressure is significantly lower and heart rate is the same during 24 hours in the *Per2* mice compared with the WT animals, suggesting that the parasympathetic nerve or acetylcholine-mediated signaling in the heart of the *Per2* mutant mice remains intact.

COX-1 Expression and COX-Derived Vasoactive Prostanoids in *Per2* Mutant Mice

Another important finding of our present study is the increased expression of COX-1 (no signal of COX-2 detectable) in the aortas of the *Per2* mutant mice. The mechanism of the increased COX-1 expression in the *Per2* mutants is unknown. Whether COX-1 is a target gene of *Per2*, ie, regulated directly by *Per2*, or regulated secondarily remains to be investigated. Accordingly, the endothelium-dependent relaxations induced by ionomycin (but not acetylcholine) are enhanced by the COX inhibitor indomethacin in the *Per2* mutant mice, demonstrating that COX-1–derived vasoconstrictor(s) is stimulated by ionomycin but not by acetylcholine, which partly contributes to the endothelial dysfunction in the *Per2* mutant mice. The lack of the effect of indomethacin on acetylcholine-induced response in *Per2* mutants further indicates a defective acetylcholine receptor–mediated signaling in the aortic endothelial cells of these animals. It is possible that enhanced COX-1 expression could influence endothelial function in the *Per2* mutant mice if the defect in endothelial acetylcholine signaling could be corrected.

The increased production of COX-1–derived vasoconstrictor(s) is also demonstrated in the quiescent rings incubated with L-NAME (to inhibit eNOS and to unmask the contracting effect of COX-derived vasoconstrictors). Under this condition, ATP causes a more pronounced vasoconstriction in the *Per2* mutants than in WT mice, which is inhibited by indomethacin. However, indomethacin cannot improve endothelium-dependent relaxations to ATP (in contrast to ionomycin) in the *Per2* mutants, but it reduces the relaxation response to ATP (1 μmol/L) in the WT mice. These results suggest that ATP releases a vasodilator(s) produced from the COX pathway, most likely prostaglandin I_2, another well-known endothelial vascular protective factor, in the WT mice but not in the *Per2* mutants. Notably, the increased production of COX-1–derived vasoconstrictor(s) that was observed in the quiescent aortic rings of *Per2* mutant mice is apparently not sufficient to counteract the effect of NO induced by ATP (1 μmol/L). Only 3% of the maximum contraction to KCl 100 mmol/L was observed under this condition. Notably,

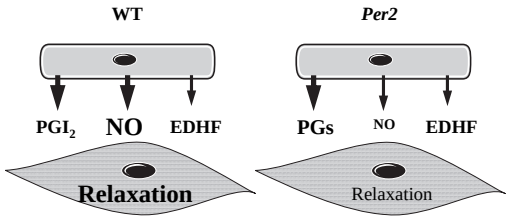

Figure 6. Alterations in endothelial function in the *Per2* mutant mice. *Per2* mutation is associated with decreased endothelial NO release and deficiency in vasodilatory prostaglandins, most likely prostacyclin (PGI_2), but increased vasoconstrictive prostaglandins (PGs). EDHF indicates endothelium-derived hyperpolarizing factor.

ATP at a higher concentration of 10 μmol/L also releases the endothelium-derived hyperpolarizing factor, which in part compensates the vasodilatory response to the agonist. Although 15% contraction occurs in response to the higher concentration of ATP of 10 μmol/L, the relaxation effect exerted by both NO and endothelium-derived hyperpolarizing factor is dominant in the *Per2* mutants. Nonetheless, the results in the quiescent rings demonstrate an increased production of COX-1–derived vasoconstrictor(s) in the aortas of the *Per2* mutant mice.

Vascular functions, including endothelial functions, can be impaired by various risk factors that are clustered in the metabolic syndrome.[7] Recent studies demonstrate that mice with disruption of the *Clock* gene are prone to develop a phenotype resembling metabolic syndrome.[6] In contrast to the *Clock* mutant mice, our *Per2* mutants have lower blood pressure and do not develop dyslipidemia. It has been shown recently that the *Per2* mutant mice have faster glucose clearance than the WT animals.[36] These results imply that the endothelial dysfunction in the *Per2* mutant mice is not associated with metabolic risk factors but rather is linked directly to the *Per2* gene. Whether the endothelial function is regulated directly by the peripheral circadian clock[44] or indirectly by the master clock in suprachiasmatic nuclei remains to be investigated.

In conclusion, mutation of circadian clock genes is not necessarily associated with metabolic syndrome. Functional loss of the *Per2* gene impairs endothelial function in mouse aortas involving decreased production of NO and a vasodilatory prostaglandin(s) as well as increased release of COX-1–derived vasoconstrictor(s) (Figure 6). The results suggest an important role of the *Per2* gene in maintenance of normal cardiovascular functions.

Sources of Funding

This work was supported by the Swiss National Science Foundation (grants 3100A0-105917/1 to Dr Yang, 3100A0-104222 to Dr Albrecht, and 3200BO-105900 to Dr Antic), the Swiss Heart Foundation, the Swiss Cardiovascular Research and Training Network Program, and the European Union Research Program EUCLOCK.

Disclosures

None.

References

1. Hastings MH, Reddy AB, Maywood ES. A clockwork web: circadian timing in brain and periphery, in health and disease. *Nat Rev Neurosci*. 2003;4:649–661.
2. Albrecht U, Eichele G. The mammalian circadian clock. *Curr Opin Genet Dev*. 2003;13:271–277.
3. Toh KL, Jones CR, He Y, Eide EJ, Hinz WA, Virshup DM, Ptacek LJ, Fu YH. An hPer2 phosphorylation site mutation in familial advanced sleep phase syndrome. *Science*. 2001;291:1040–1043.
4. Albrecht U, Zheng B, Larkin D, Sun ZS, Lee CC. MPer1 and mper2 are essential for normal resetting of the circadian clock. *J Biol Rhythms*. 2001;16:100–104.
5. Rudic RD, McNamara P, Curtis AM, Boston RC, Panda S, Hogenesch JB, Fitzgerald GA. BMAL1 and CLOCK, two essential components of the circadian clock, are involved in glucose homeostasis. *PLoS Biol*. 2004;2:e377.
6. Turek FW, Joshu C, Kohsaka A, Lin E, Ivanova G, McDearmon E, Laposky A, Losee-Olson S, Easton A, Jensen DR, Eckel RH, Takahashi JS, Bass J. Obesity and metabolic syndrome in circadian clock mutant mice. *Science*. 2005;308:1043–1045.
7. Kim JA, Montagnani M, Koh KK, Quon MJ. Reciprocal relationships between insulin resistance and endothelial dysfunction: molecular and pathophysiological mechanisms. *Circulation*. 2006;113:1888–1904.
8. Yang Z, Oemar B, Luscher TF. Mechanism of coronary bypass graft disease [in German]. *Schweiz Med Wochenschr*. 1993;123:422–427.
9. Yang Z, Ming XF. Recent advances in understanding endothelial dysfunction in atherosclerosis. *Clin Med Res*. 2006;4:53–65.
10. Schachinger V, Britten MB, Zeiher AM. Prognostic impact of coronary vasodilator dysfunction on adverse long-term outcome of coronary heart disease. *Circulation*. 2000;101:1899–1906.
11. Bugiardini R, Manfrini O, Pizzi C, Fontana F, Morgagni G. Endothelial function predicts future development of coronary artery disease: a study of women with chest pain and normal coronary angiograms. *Circulation*. 2004;109:2518–2523.
12. Yang Z, Ming XF. Endothelial arginase: a new target in atherosclerosis. *Curr Hypertens Rep*. 2006;8:54–59.
13. Forstermann U, Munzel T. Endothelial nitric oxide synthase in vascular disease: from marvel to menace. *Circulation*. 2006;113:1708–1714.
14. Yang ZH, von SL, Bauer E, Stulz P, Turina M, Luscher TF. Different activation of the endothelial L-arginine and cyclooxygenase pathway in the human internal mammary artery and saphenous vein. *Circ Res*. 1991;68:52–60.
15. Kobayashi T, Tahara Y, Matsumoto M, Iguchi M, Sano H, Murayama T, Arai H, Oida H, Yurugi-Kobayashi T, Yamashita JK, Katagiri H, Majima M, Yokode M, Kita T, Narumiya S. Roles of thromboxane A(2) and prostacyclin in the development of atherosclerosis in apoE-deficient mice. *J Clin Invest*. 2004;114:784–794.
16. Zou MH, Shi C, Cohen RA. High glucose via peroxynitrite causes tyrosine nitration and inactivation of prostacyclin synthase that is associated with thromboxane/prostaglandin H(2) receptor-mediated apoptosis and adhesion molecule expression in cultured human aortic endothelial cells. *Diabetes*. 2002;51:198–203.
17. Muller JE, Stone PH, Turi ZG, Rutherford JD, Czeisler CA, Parker C, Poole WK, Passamani E, Roberts R, Robertson T. Circadian variation in the frequency of onset of acute myocardial infarction. *N Engl J Med*. 1985;313:1315–1322.
18. Peckova M, Fahrenbruch CE, Cobb LA, Hallstrom AP. Circadian variations in the occurrence of cardiac arrests: initial and repeat episodes. *Circulation*. 1998;98:31–39.
19. D'Negri CE, Nicola-Siri L, Vigo DE, Girotti LA, Cardinali DP. Circadian analysis of myocardial infarction incidence in an Argentine and Uruguayan population. *BMC Cardiovasc Disord*. 2006;6:1.
20. Stergiou GS, Vemmos KN, Pliarchopoulou KM, Synetos AG, Roussias LG, Mountokalakis TD. Parallel morning and evening surge in stroke onset, blood pressure, and physical activity. *Stroke*. 2002;33:1480–1486.
21. Willich SN, Goldberg RJ, Maclure M, Perriello L, Muller JE. Increased onset of sudden cardiac death in the first three hours after awakening. *Am J Cardiol*. 1992;70:65–68.
22. Panza JA, Epstein SE, Quyyumi AA. Circadian variation in vascular tone and its relation to alpha-sympathetic vasoconstrictor activity. *N Engl J Med*. 1991;325:986–990.
23. Cohen MC, Rohtla KM, Lavery CE, Muller JE, Mittleman MA. Meta-analysis of the morning excess of acute myocardial infarction and sudden cardiac death. *Am J Cardiol*. 1997;79:1512–1516.
24. Singh RB, Cornelissen G, Weydahl A, Schwartzkopff O, Katinas G, Otsuka K, Watanabe Y, Yano S, Mori H, Ichimaru Y, Mitsutake G, Pella D, Fanghong L, Zhao Z, Rao RS, Gvozdjakova A, Halberg F. Circadian heart rate and blood pressure variability considered for research and patient care. *Int J Cardiol*. 2003;87:9–28.

25. Bremner WF, Sothern RB, Kanabrocki EL, Ryan M, McCormick JB, Dawson S, Connors ES, Rothschild R, Third JL, Vahed S, Nemchausky BM, Shirazi P, Olwin JH. Relation between circadian patterns in levels of circulating lipoprotein(a), fibrinogen, platelets, and related lipid variables in men. *Am Heart J*. 2000;139:164–173.
26. Walters J, Skene D, Hampton SM, Ferns GA. Biological rhythms, endothelial health and cardiovascular disease. *Med Sci Monit*. 2003;9: RA1–RA8.
27. Elherik K, Khan F, McLaren M, Kennedy G, Belch JJ. Circadian variation in vascular tone and endothelial cell function in normal males. *Clin Sci (Lond)*. 2002;102:547–552.
28. Otto ME, Svatikova A, Barretto RB, Santos S, Hoffmann M, Khandheria B, Somers V. Early morning attenuation of endothelial function in healthy humans. *Circulation*. 2004;109:2507–2510.
29. Kawano H, Motoyama T, Yasue H, Hirai N, Waly HM, Kugiyama K, Ogawa H. Endothelial function fluctuates with diurnal variation in the frequency of ischemic episodes in patients with variant angina. *J Am Coll Cardiol*. 2002;40:266–270.
30. Zheng B, Larkin DW, Albrecht U, Sun ZS, Sage M, Eichele G, Lee CC, Bradley A. The mPer2 gene encodes a functional component of the mammalian circadian clock. *Nature*. 1999;400:169–173.
31. Viswambharan H, Seebeck T, Yang Z. Enhanced endothelial nitric oxide-synthase activity in mice infected with *Trypanosoma brucei*. *Int J Parasitol*. 2003;33:1099–1104.
32. Ming XF, Viswambharan H, Barandier C, Ruffieux J, Kaibuchi K, Rusconi S, Yang Z. Rho GTPase/Rho kinase negatively regulates endothelial nitric oxide synthase phosphorylation through the inhibition of protein kinase B/Akt in human endothelial cells. *Mol Cell Biol*. 2002;22: 8467–8477.
33. Van Vliet BN, Chafe LL, Montani JP. Characteristics of 24 h telemetered blood pressure in eNOS-knockout and C57Bl/6J control mice. *J Physiol*. 2003;549:313–325.
34. Montani JP, Mizelle HL, Van Vliet BN, Adair TH. Advantages of continuous measurement of cardiac output 24 h a day. *Am J Physiol*. 1995;269:H696–H703.
35. Khurana S, Yamada M, Wess J, Kennedy RH, Raufman JP. Deoxycholyltaurine-induced vasodilation of rodent aorta is nitric oxide- and muscarinic M(3) receptor-dependent. *Eur J Pharmacol*. 2005;517:103–110.
36. Dallmann R, Touma C, Palme R, Albrecht U, Steinlechner S. Impaired daily glucocorticoid rhythm in Per1 (Brd) mice. *J Comp Physiol A Neuroethol Sens Neural Behav Physiol*. 2006;192:769–775.
37. Luscher TF, Richard V, Tschudi M, Yang ZH, Boulanger C. Endothelial control of vascular tone in large and small coronary arteries. *J Am Coll Cardiol*. 1990;15:519–527.
38. Holzberg D, Albrecht U. The circadian clock: a manager of biochemical processes within the organism. *J Neuroendocrinol*. 2003;15:339–343.
39. Joannides R, Haefeli WE, Linder L, Richard V, Bakkali EH, Thuillez C, Luscher TF. Nitric oxide is responsible for flow-dependent dilatation of human peripheral conduit arteries in vivo. *Circulation*. 1995;91: 1314–1319.
40. Tunctan B, Weigl Y, Dotan A, Peleg L, Zengil H, Ashkenazi I, Abacioglu N. Circadian variation of nitric oxide synthase activity in mouse tissue. *Chronobiol Int*. 2002;19:393–404.
41. Shaw JA, Chin-Dusting JP, Kingwell BA, Dart AM. Diurnal variation in endothelium-dependent vasodilatation is not apparent in coronary artery disease. *Circulation*. 2001;103:806–812.
42. Aronow WS, Ahn C. Circadian variation of death from congestive heart failure after prior myocardial infarction in patients >60 years of age. *Am J Cardiol*. 2003;92:1354–1355.
43. Fisher JT, Vincent SG, Gomeza J, Yamada M, Wess J. Loss of vagally mediated bradycardia and bronchoconstriction in mice lacking M2 or M3 muscarinic acetylcholine receptors. *FASEB J*. 2004;18:711–713.
44. Young ME. The circadian clock within the heart: potential influence on myocardial gene expression, metabolism, and function. *Am J Physiol*. 2006;290:H1–H16.

CLINICAL PERSPECTIVE

Clinical studies document an increased frequency of cardiovascular events such as unstable angina, myocardial infarction, sudden cardiac death, and thrombotic stroke during the morning hours, usually from 6 AM to noon. It is, however, not known whether this is primarily related to the diurnal variation of cardiovascular parameters and physical activities or controlled by the master clock that resides in the suprachiasmatic nuclei of the hypothalamus in mammals. In the present study, we show that mice with the mutation of the clock gene *Period2* (*Per2*) exhibit impaired endothelium-dependent relaxations due to decreased endothelial nitric oxide synthase activity and a decreased production of vasodilatory prostaglandin(s) in the aorta. The endothelium-dependent relaxation in response to acetylcholine is further decreased in the *Per2* mutant mice during transition from the inactive to the active phase, whereas it is increased in the wild-type littermates. Furthermore, an increase in cyclooxygenase-1 protein level and cyclooxygenase-derived vasoconstrictor production is observed in the *Per2* mutant mouse aorta. The endothelial dysfunction in the *Per2* mutant mice is not associated with hypertension or dyslipidemia. The results of the present study demonstrate that mutation of the *Per2* gene in mice is associated with endothelial dysfunction involving decreased production of nitric oxide and vasodilatory prostaglandin(s) as well as increased release of cyclooxygenase-1–derived vasoconstrictor(s). The results suggest a potential role of the *Per2* gene in maintenance of normal cardiovascular functions and may provide certain clues at the molecular level for the circadian pattern of cardiac events in clinical settings.

Appendix IV

Corticosterone levels before and after stress in wild-type and *Per2*^{Brdm1} mice

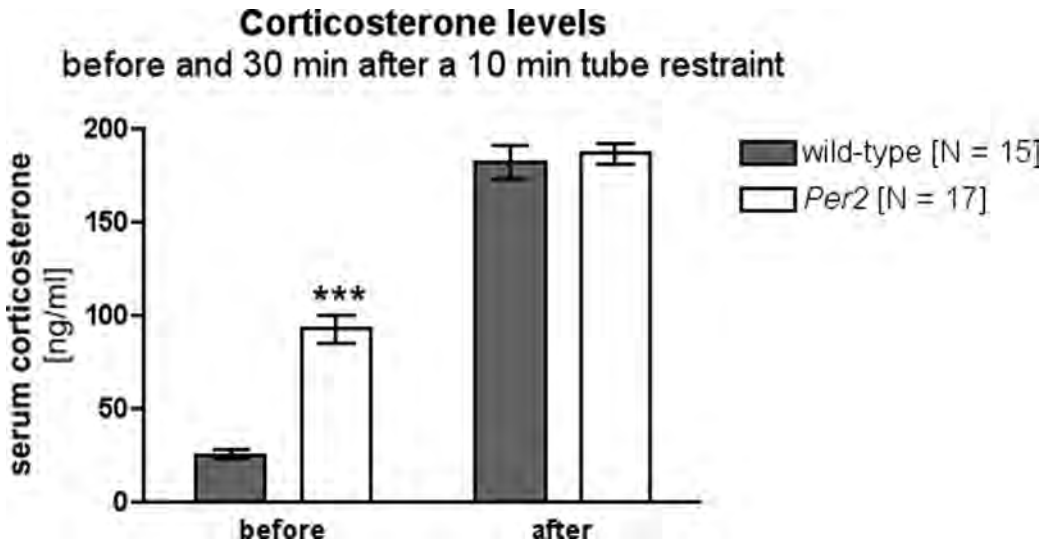

Fig. AIV-1: Serum corticosterone levels are significantly different between wild-type and *Per2*^{Brdm1} mice under normal conditions at ZT6. However, 30 min after a 10 min tube restraint the corticosterone levels are increased comparably in both genotypes. *** $p<0.0001$

Materials and Methods

Corticosterone determination

3 to 4 month old male mice are kept individually with food and water *ad libitum* for at least 1 day prior to blood sampling. Serum samples are collected around noon (ZT6) before and 30 min after a 10 min tube restraint. Mice are anesthetized using isoflurane (Attane^{TM} isoflurane, Provet, ATC vet code QN01AB06). A small horizontal incision is made close to the tail base on the ventral part of the tail. Blood is collected using a Microvette 100 (Sarstedt, cat # 20.1280) for serum preparation. Tubes are kept on ice until they are centrifuged at 6000 rpm and 4°C for 10 min. The serum is stored at -20°C. Corticosterone levels are determined using a radioimmunassay kit from MP Biomedicals (Corticosterone ^{3}H RIA kit for rats & mice, cat # 07-120002) according to the manufacturers instructions. 3 µl of serum are diluted in 1.5 ml of steroid diluent.